



**HAL**  
open science

# Early evolution of scalidophoran worms : fossil evidence from the lowermost Cambrian Kuanchuanpu Lagerstätte and lower Cambrian Chengjiang Lagerstätte, south China

Deng Wang

► **To cite this version:**

Deng Wang. Early evolution of scalidophoran worms : fossil evidence from the lowermost Cambrian Kuanchuanpu Lagerstätte and lower Cambrian Chengjiang Lagerstätte, south China. Paleontology. Université de Lyon, 2021. English. NNT : 2021LYSE1043 . tel-03727625

**HAL Id: tel-03727625**

**<https://theses.hal.science/tel-03727625v1>**

Submitted on 19 Jul 2022

**HAL** is a multi-disciplinary open access archive for the deposit and dissemination of scientific research documents, whether they are published or not. The documents may come from teaching and research institutions in France or abroad, or from public or private research centers.

L'archive ouverte pluridisciplinaire **HAL**, est destinée au dépôt et à la diffusion de documents scientifiques de niveau recherche, publiés ou non, émanant des établissements d'enseignement et de recherche français ou étrangers, des laboratoires publics ou privés.



N°d'ordre NNT :  
2021LYSE1043

## **THESE de DOCTORAT DE L'UNIVERSITE DE LYON**

opérée au sein de

**l'Université Claude Bernard Lyon 1**

**Ecole Doctorale N° ED 341**

**Evolution, Ecosystèmes, Microbiologie, Modélisation**

**Spécialité de doctorat** : Sciences de la Terre

**Discipline** : Paléontologie

Soutenue publiquement le 22/02/2021, par :

**Deng WANG**

---

# **Evolution précoce des scalidophores (Ecdysozoa) : apport des fossiles du Cambrien inférieur de Chine**

---

Devant le jury composé de :

MATTIOLI, Emanuela	Professeure	UCBL	Présidente
MA, Xiaoya	Professeure	University of Exeter	Rapporteure
HARVEY, Thomas	Lecturer	University of Leicester	Rapporteur
FOREL, Marie-Béatrice	Maître de conférence	MNHN Paris	Examinatrice
HAN, Jian	Professeur	Northwest University Xi'an	Co-directeur de thèse
VANNIER, Jean	Directeur de recherche	CNRS/UCBL	Co-directeur de thèse

## Acknowledgements

In the past two years, many kind persons helped me a lot in my research studies and everyday life. It is with sincere emotion that I thank them all here. My supervisors Jean Vannier and Jian Han guided me meticulously and taught me to have a cautious attitude in research and to be a better researcher. They also gave warm help in my life. I am lucky to have met them both. In addition, I want to thank the Chinese Scholarship Council (CSC) for financial support during my two-year stay in France and Northwest University for financial support during my 3-month-extension stay in France.

There are many people who gave me technical assistance. I thank Jie Sun, Yifei Sun who processed CT images; Meirong Cheng, Juan Luo, Xiaoguang Yang, Xing Wang, Xiaoyong Yao, Ping Liu, Qingqin Tang, Kaiyue He, Yanchun Yao, and Hujun Gong for technical help with fossil processing; Yao Du and Jinhua Yang who were for three-dimensional reconstructions; Lin Bai who for outreaching our published papers; Prof. Zhifei Zhang and Xinyi Ren for XRF and insightful discussions; Prof. Xingliang Zhang, Prof. Dongjing Fu (Northwest University, China) and Dr. Huaqiao Zhang (Nanjing Institute of Geology and Paleontology, Chinese Academy of Sciences, China) who kindly provided fossil images; Xiaoyu Yang (Yunnan University, China) for personal communications.

On the European and American side, I would like to thank Dr. Cédric Aria for teaching me various cladistic methods and insightful discussions on phylogeny. I am grateful to the staff of the Kristineberg Marine Research Station (Göteborg University), especially Bengt Lundve and Christian Lindberg for collecting live priapulids specimens and assistance in the lab during my stay in Sweden, and also to the staff of the Askö Laboratory (Stockholm University), especially Carl-Magnus Wiltén. I want to thank the ASSEMBLE-Plus Program for financial support to this research project in Sweden. Thank you to the Centre Technologique des Microstructures (CT $\mu$ ), Université Claude Bernard Lyon 1 for access to SEM facilities and technical assistance and also to Clémentine Fellah for SEM at the ENS Lyon; to Prof. Douglas Erwin and Mark Florence (Smithsonian National Museum of Natural History, Washington DC, USA) and Dr. J.B. Caron (Royal Ontario Museum, Toronto, Canada) for access to the Burgess Shale fossil collections and providing images; to Prof. Andreas Hejnol (University of Bergen, Norway), Prof. Andreas Schmidt-Rhaesa (Universität Hamburg, Germany), Dr. Ralf Janssen (Uppsala University, Sweden), Dr. Martin Vinther Sørensen (Natural History Museum of Denmark, Denmark), Dr. Neuhaus Birger (Museum für Naturkunde, Germany) for personal communications; Dr. Isabell Schumann (University of Leipzig, Germany) and Prof. Georg Mayer (Universität Kassel, Germany) for molecular data on ecdysis; to Tsuyoshi Komioya and his students (Tokyo University, Japan), and Kentaro Uesugi (Synchrotron Radiation Research Institute, Japan) for analysing fossils via Spring-8 Synchrotron radiation X-ray tomographic microscopy (SRXTM); to Prof. Heyo Van Iten (Hanover College, IN, USA), Prof. David J. Siveter (University of Leicester, UK) for reading our manuscripts and linguistic corrections; to Dr. Vincent Perrier for precious information on ostracods and images; to Colin Issartel from LEHNA (University Lyon 1) for photography of meiobenthic worms. I would also like to thank, Prof. Emanuela Mattioli, Prof Xiaoya Ma, Dr. Thomas Harvey, Dr. Marie-Béatrice Forel who kindly accepted to review my thesis and take part in my defense committee, and also the members of the doctoral school (E2M2) committee (Vincent Perrier, Frederic Quilleveré, Romain Amiot and Frédéric Thévenard) for guidance and advice. I want to thank Samuel Mailliot for printing the final version of my thesis and precious advice.

Finally, I want to thank my Chinese friends both in France (Pan Lu, Jihua Hao, Bomín Fu, Dandan Li, Yulan Peng, Xinke Wang, Wei Liao, Tian Jiang, Chenglong Ge) and China (Boxin Kang, Lu Cao, Jiale Qin, Jianchao Yang, Fan Liu, Yu Zhu), who gave me a lot of warmth during the last four years. I ought to thank the Chinese Government and the Health Department of Shaanxi for their kind support during the epidemic that affected China and the rest of the world in 2020. Last, but by no means least, I thank my family who is unique to me.

# Early steps in the evolution of Scalidophora: fossil evidence from the Cambrian of China

## Abstract

Ecdysozoans are among the most abundant animals (e.g. arthropods) on Earth and have an extremely long evolutionary history with a rich Cambrian fossil record. This thesis focusses on one of the major elements of the Cambrian ecdysozoan fauna, the scalidophoran worms. Our fossil material comes from: **1)** Small Shelly Fossil (SSF) assemblages from the basal Cambrian (Fortunian Stage) Kuanchuanpu Formation (Shaanxi Province, China; ca 535 Ma) and **2)** the early Cambrian (Stage 3) Chengjiang Lagerstätte (Yunnan Province, China; ca 518). Both localities yielded exceptionally preserved fossils that provide key information on the early evolutionary history of scalidophorans.

Our results are summarized as follows: **1-** The finding of exuviae (including those turned inside out) provide solid fossil evidence that ancestor ecdysozoan animals grew by moulting at least 535 million years ago, before the diversification of arthropods. This confirms that the scalidophoran worms from the Kuanchuanpu Formation are the oldest known true ecdysozoans. We hypothesize that ecdysis may have been selected as the most adequate solution to overcome mechanical constraints (growing with a rigid exoskeleton) and opened up new evolutionary perspectives. **2-** We also show that the external surface of the cuticle of scalidophoran worms from the Kuanchuanpu Formation (ca 535 Ma) bears a fine, micrometre-sized, hexagonal network that is interpreted as the faithful replica of the boundary between underlying epithelial cells. This interpretation is based on identical structures observed in extant priapulid worms. Cuticular reticulation in Ecdysozoa appears to be nothing more than an initial by-product of cell division during cuticle growth. Although this basic process remained unchanged since at least the basal Cambrian, many different variants evolved through time. During the course of evolution, the increased complexity of cuticular features (e.g. sclerotization, mineralization) associated with possible epidermal differentiation gave rise independently in almost all groups (except nematodes) to a great variety of patterns of reticulation (e.g. in arthropods). **3-** Based on exceptionally preserved specimens from the Chengjiang Lagerstätte (ca 518 Ma), the anatomy and lifestyle of *Selkirkia* are reexplored and more precisely the tube formation and relation to body. Fossil evidence indicate that the tube was probably secreted by trunk epithelial cells and renewed periodically via non-synchronous ecdysis. The tube of *Selkirkia* can be seen as a protective feature against physical damage and predation and may also have played a role in anchoring the animal to sediment. The moulting process of *Selkirkia* implies that the worm temporarily left its tube and probably remained buried in sediment until the renewal of its cuticle. Brachiopod epibionts also give precise information on the endobenthic habitat of *Selkirkia*, close to the water-sediment interface. *Selkirkia* may appear as the oldest unambiguous tube-dwelling ecdysozoan. **4-** Eggs preserved in situ within the internal cavity of *Selkirkia* from the Xiaoshi Lagerstätte (ca 514 Ma) and interpreted as oocytes (non-fertilized eggs) rather than early embryos, thus indicating that the general organization of female gonads in scalidophoran worms has remained virtually unchanged since the early Cambrian. These findings provide, for the first time, key information on the reproductive organs and pre-embryonic development of early ecdysozoans (Scalidophora). The relatively large size (possibly yolk-rich) and low number of oocytes suggest that the reproductive strategy of *Selkirkia* was comparable with that of modern meiobenthic priapulids and that energy invested by this Cambrian scalidophoran worm was possibly oriented towards quality rather than quantity. **5-** A new phylogeny of Scalidophora is proposed based on augmented morphological data, reassessment of characters and various cladistic methods. Maximum parsimony (Heuristic TBR, TNT, and TreeSearch), and maximum likelihood resolve topologies with extant priapulids forming a sister clade to *Selkirkia* and palaeoscolecids, and with Loricifera and Kinorhyncha branching off basally. By contrast, the unconstrained Bayesian runs converge on a basal *Selkirkia* sister group to Palaeoscolecida and Scalidophora. The strength of this model was tested by enforcing a backbone on the Bayesian analysis. The resulting topology bears overall similarity with the unweighted TreeSearch topology and yields on average slightly better harmonic means than the unconstrained model. A better treatment of inapplicable states helped parsimony converge with Bayesian inference, assuming a model with basal Loricifera and Kinorhyncha.

**Keywords:** Scalidophora, early Cambrian, China, ecdysis, cuticle, reproduction, phylogeny

# Evolution précoce des scalidophores (Ecdysozoa) : apport des fossiles du Cambrien inférieur de Chine

## Résumé

Les ecdysozoaires sont parmi les animaux les plus abondants (ex : les arthropodes) sur Terre et ont une histoire évolutive extrêmement longue avec un riche registre fossile au Cambrien. Cette thèse se concentre sur l'un des éléments majeurs de la faune ecdysozoaire cambrienne, les vers scalidophores. Le matériel fossile étudié provient : 1) d'assemblages de Small Shelly Fossils (SSF) du Cambrien basal (Fortunien) de la Formation de Kuanchuanpu (Province du Shaanxi, Chine ; env. 535 Ma) et 2) du Cambrien inférieur (Étage 3) du Lagerstätte de Chengjiang (Province du Yunnan), Chine ; env. 518 Ma). Ce sont des fossiles à préservation exceptionnelle qui fournissent des informations clés sur l'histoire évolutive précoce des scalidophores. Les principaux résultats sont les suivants : **1-** La découverte d'exuvies (y compris celles retournées en doigt de gant) montre que les premiers ecdysozoaires se développaient déjà par mues (ecdysis) successives il y a au moins 535 millions d'années, avant la diversification des arthropodes. Ceci confirme que les vers scalidophores de la Formation de Kuanchuanpu sont les plus anciens ecdysozoaires connus. L'ecdysis apparaît comme la solution la plus adéquate pour surmonter les contraintes mécaniques (grandir avec un exosquelette rigide) et semble avoir ouvert de nouvelles perspectives évolutives. **2-** Nous montrons également que la surface externe de la cuticule de ces vers du Cambrien basal porte un fin réseau hexagonal de taille micrométrique. Il est interprété comme la réplique fidèle des limites intercellulaires de l'épithélium sous-jacent, comme cela est observé chez les vers priapulidés actuels. La réticulation cuticulaire des ecdysozoaires n'est rien d'autre qu'un sous-produit initial de la division cellulaire pendant la croissance de la cuticule. Bien que ce processus de base soit resté inchangé depuis au moins le Cambrien basal, de nombreuses variantes ont évolué avec le temps. Au cours de l'évolution, la complexité accrue de l'ornementation cuticulaires (par exemple sclérotisation, minéralisation) associée à une éventuelle différenciation épidermique a donné lieu indépendamment dans presque tous les groupes (à l'exception des nématodes) à une grande variété de motifs réticulés (ex : arthropodes). **3-** Grâce à des spécimens des Lagerstätten de Chengjiang et Xiaoshiba (respectivement, env. 518 et 514 Ma), l'anatomie et le mode de vie de *Selkirkia* ont été ré-explorés et plus précisément la formation du tube et sa relation avec le corps de l'animal. Le tube était probablement sécrété par les cellules épithéliales du tronc et renouvelé périodiquement par ecdysis non-synchrone. Le tube de *Selkirkia* peut être considéré comme un élément de protection contre les dommages physiques et la prédation et peut également avoir joué un rôle dans l'ancrage de l'animal au sédiment. Le processus de mue de *Selkirkia* implique que le ver quittait temporairement son tube et restait enfoui dans le sédiment jusqu'au renouvellement de sa cuticule. Des brachiopodes épibiontes donnent également des informations précises sur l'habitat endobenthique de *Selkirkia*, sans doute proche de l'interface eau-sédiment. *Selkirkia* apparaît comme le plus ancien ecdysozoan tubulaire connu. **4-** Des œufs conservés *in situ* dans la cavité interne de *Selkirkia* sont interprétés comme des ovocytes (œufs non fécondés) plutôt que des embryons précoces. Ceci indique que l'organisation générale des gonades femelles chez les vers scalidophores est restée pratiquement inchangée depuis le début du Cambrien. Ces résultats fournissent, pour la première fois, des informations clés sur les organes reproducteurs et le développement pré-embryonnaire des ecdysozoaires ancestraux (Scalidophora). La taille relativement grande (abondantes réserves probables) et le faible nombre d'ovocytes suggèrent que la stratégie de reproduction de *Selkirkia* était comparable à celle des priapulidés méiobenthiques modernes et que l'énergie investie par ce ver cambrien était orientée vers la qualité plutôt que vers la quantité. **5-** Une nouvelle phylogénie des Scalidophora est proposée sur la base de données morphologiques augmentées, d'une réévaluation des caractères et de l'utilisation de diverses méthodes cladistiques. La parsimonie maximale (Heuristic TBR, TNT, and TreeSearch), and la plausibilité maximale résolvent des topologies dans lesquelles les priapulidés actuels forment un clade frère de *Selkirkia* et des paléoscolécidés, et où les Loricifera et Kinorhyncha se ramifient à la base. En revanche, les méthodes bayésiennes sans contrainte indiquent une position plus basale de *Selkirkia* (groupe frère de Palaeoscolécida + Scalidophora). La force de ce modèle est testée en imposant un squelette (backbone) lors de l'analyse bayésienne. La topologie résultante présente une similitude globale avec la topologie TreeSearch non pondérée et donne des moyennes harmoniques légèrement meilleures que le modèle sans contrainte. Un meilleur traitement des états inapplicables a permis à la parcimonie à converger avec la vraisemblance bayésienne, en supposant un modèle avec les Loricifera et Kinorhyncha en position basale.

**Mot-clés :** Scalidophora, Cambrien inférieur, Chine, ecdysis, cuticule, reproduction, phylogénie

# 华南寒武纪早期有吻突动物的演化

## 摘要

蜕皮动物是一类通过周期性蜕掉其坚硬外骨骼（表皮）而实现生长的原口动物。无论是化石还是现生的蜕皮动物，其数量庞大种类繁多，尤以节肢动物为最。蜕皮动物繁衍至今已有超过 5 亿年的演化历史，可追溯至寒武纪早期大量特异保存的化石。目前最早且可靠的化石来自寒武纪早期的陕南宽川铺组，距今大约 5.35 亿年前。这些化石躯体呈蠕形、发育吻部且无附肢，属于蜕皮动物中的一个子分支--有吻突动物。有吻突动物繁盛于寒武纪海洋，是当时海洋生态系统的重要组成，如在澄江动物群（约 5.18 亿年前）和布尔吉斯页岩动物群中。研究表明有吻突动物的身体结构可能多少保留了蜕皮动物祖先的特征。因此，本论文基于宽川铺生物群和澄江生物群的化石材料着重研究有吻突动物的蜕皮行为、表皮结构、繁殖器官以及其系统发生位置，并通过这些方面的研究探讨有吻突动物甚至蜕皮动物的演化历史。

结果总结如下：**(1)** 5.35 亿年前的宽川铺组中某些有吻突动物化石表皮整个以外翻的形式完整保存下来，表现为全部内指的骨板刺，这与正常的该类动物外指的骨板刺完全相反。这些特别的化石与某些现生有吻突动物的遗蜕极其相似，佐证了这些化石是有吻突动物蜕下的旧表皮（遗蜕）。因此，我们认为早在 5.35 亿年前就已经出现蜕皮行为并且该行为可能是为了解决束缚该类动物无法长大的坚硬外骨骼的问题。蜕皮行为是蜕皮动物重要的演化革新，为蜕皮动物的繁盛奠定基础。**(2)** 宽川铺组中某些有吻突动物化石表面保存毫米级的六边形或多边形网纹。经与现生有吻突动物对比，这些网纹一一对应其下表皮细胞的边界，并无其它特殊作用，仅仅是蜕皮-新表皮形成过程中的副产物。各种蜕皮动物表皮的形成机制基本类似，但网纹及表皮骨化、矿化在其各个分支变化很大。这说明大多数蜕皮动物（线虫动物除外）的网纹由于表皮的分化变得更加复杂，不再与其下表皮细胞边界具有一一对应关系。**(3)** 澄江动物群中的管栖动物 *Selkirkia* 可能具有特别的蜕皮方式，因此，我们重新研究了 *Selkirkia* 管的形成及其与躯干的关系。证据表明 *Selkirkia* 的管可能是躯干表皮经历非同步蜕皮且二次骨化形成的。管坚硬起保护作用，同时也可锚在沉积物中起固定作用。*Selkirkia* 管硬而重，导致移动能力较弱。腕足动物附着在管末端说明 *Selkirkia* 生活中水-沉积物界面附近。**(4)** 另外，我们首次报道了来自澄江动物群和小石坝动物群（约 5.14 亿年前）*Selkirkia* 的繁殖器官和胚胎之前的发育阶段。化石显示卵保存在雌性 *Selkirkia* 躯干靠后部分的体腔内部，分列肠道两侧。这种繁殖器官与现生有吻突动物并无二致，揭示了其保守演化特性。*Selkirkia* 的卵大但数量少，这与现生在间质中生活的有吻突动物的繁殖策略一样，可能反映寒武纪早期有吻突动物的繁殖策略是加强卵的质量降低卵的数量。**(5)** 最后，基于新编译的特征及其对应的数据集，我们使用多种分析方法重新研究了有吻突动物的系统发生。最大简约法（启发式 TBR，TNT 和 TreeSearch）以及最大似然法的结果整体上类似，都将大部分寒武纪的蜕皮类蠕虫（有吻突动物）解释为干群鳃曳动物。*Selkirkia* 是距离冠群鳃曳动物最近的一个分支，而古蠕虫类单独形成一个分支作为 *Selkirkia* +冠群鳃曳动物的姐妹群。不过，未加限定的贝叶斯算法显示大多数寒武纪蜕皮类蠕虫为有吻突动物的干群，*Selkirkia* 位于系统发生最低的位置，是古蠕虫类+冠群有吻突动物的姐妹群。然而，我们通过限定的贝叶斯算法来测试之前分析的强度，结果显示限定后拓扑结构的谐波均值的绝对值较小，意味着该结果比较可靠。由于化石的保存状况，很多形态学数据在数据集中以不确定或不可适用表示，导致分析结果不稳定。此次我们引入 TreeSearch 专门处理这些问题。其计算结果与限定后的贝叶斯算法结果大体相似，说明将大多数寒武纪的蜕皮类蠕虫解释为干群鳃曳动物的结果是比较可靠的。

**关键词：**有吻突动物、早寒武世、宽川铺组、澄江动物群、蜕皮、表皮、繁殖系统、系统发生

## Résumé étendu en français

Ce mémoire de thèse traite de l'histoire évolutive précoce d'un groupe important du règne animal : les Ecdysozoaires qui renferme des millions d'espèces actuelles parmi lesquelles les arthropodes (ex : crustacés, insectes), les onychophores, les tardigrades et plusieurs phyla d'organismes vermiformes (ex : nématodes, priapulidés). Cette question est abordée sous un angle paléontologique et plus particulièrement grâce à l'étude de gisements à préservation exceptionnelle de Chine, d'âge Cambrien inférieur, comme la Formation de Kuanchuanpu (Province du Shaanxi ; env. 535 Ma) et le Lagerstätte de Chengjiang Province du Yunnan ; env. 518 Ma). Deux types de fossiles sont étudiés : 1) des Small Shelly Fossils (SSFs) conservés en trois dimensions sous forme de phosphate de calcium et extraits par dissolution de la roche à l'acide acétique dilué (Kuanchuanpu) et 2) des macrofossiles conservés sous forme de compressions (Chengjiang). Les recherches ont porté essentiellement sur des vers scalidophores qui occupent souvent une position basale dans l'arbre phylogénétique des ecdysozoaires (ex : modèles basés sur des données moléculaires. En parallèle aux études paléontologiques, les scalidophores actuels ont été observés et récoltés (Suède) afin de fournir des données comparatives essentielles à l'interprétation de la morphologie et de l'écologie de leurs ancêtres du Cambrien. Sont détaillés ici les principaux résultats obtenus qui ont fait l'objet de publications scientifiques (travaux publiés en 2019 et 2020 et manuscrits soumis).

### 1- Origine de la mue

Les ecdysozoans, littéralement définis comme « les animaux qui muent », comprennent trois clades bien définis : les Scalidophora (Loricifera, Priapulida et Kinorhyncha), Nematoida (Nematoda et Nematomorpha) et Panarthropoda (Arthropoda, Tardigrada et Onychophora) Ensemble, ils forment ensemble une partie essentielle de la biodiversité actuelle avec des millions d'espèces vivant dans une très grande variété de milieux terrestres et aquatiques. Parmi eux, les crustacés et les insectes nous sont particulièrement familiers. Tous les ecdysozoaires sécrètent une cuticule qui doit être renouvelée périodiquement et remplacée par une plus grande, un processus appelé ecdysis. Pour permettre à n'importe quel crustacé et insecte d'augmenter de volume, son exuvie doit être éliminée et une enveloppe cuticulaire plus grande doit être synthétisée à partir des cellules épidermiques. Le rejet de l'ancienne cuticule (exuvie) est une autre étape vitale de ce processus qui est souvent associée à des comportements sophistiqués (par exemple chez les insectes). La mue est un processus complexe contrôlé et régulé par des hormones (ecdysone) et des gènes spécifiques. Les aspects biologiques de l'ecdysis ont été étudiés par des générations de scientifiques, et relativement récemment, des études génomiques et transcriptomiques ont mis en lumière les voies moléculaires impliquées dans ce processus complexe, ce qui a conduit à des scénarios évolutifs. Cependant, la plupart de ces études se sont focalisées sur les insectes et les crustacés. Le processus de mue chez les autres groupes d'ecdysozoaires tels que les scalidophores et les nématoides est beaucoup moins bien compris. Des données fossiles obtenues à partir d'arthropodes, typiquement les trilobites dont on sait que leur développement se faisait de façon discontinue et via la production d'exuvies, suggèrent que l'ecdysis a une origine très ancienne. Cependant, les preuves directes d'animaux cambriens « en train de muer » sont extrêmement rares et souvent discutables. Le but de cette étude était d'explorer l'origine de l'ecdysis en étudiant les vers scalidophores du Cambrien basal qui potentiellement, représentent un stade précoce de l'histoire évolutive des ecdysozoaires. Les minuscules vers

scolidophores extraits des roches carbonatées de la formation de Kuanchuanpu (535 Ma) ont été étudiés. Ils sont préservés en trois dimensions et caractérisés par une ornementation cuticulaire épineux (sclérites). Deux types de restes cuticulaires cylindriques ont été trouvés parmi ces assemblages de SSF. Le Type 1 possède un relief externe positif (sclérites pointant vers l'extérieur). Le Type 2 un relief négatif (de sclérites pointées vers l'intérieur. Ces fossiles interprétés comme des exuvies (mues correspondant au corps cylindrique du ver). Le type 2 résulte d'une inversion mécanique lors de la mue, l'exuvie fine et flexible ayant été retournée comme le doigt d'un gant. Ces interprétations sont étayées par des observations directes du comportement de mue des priapulidés actuels (Scalidophora) qui vivent encore dans certains environnements marins (par exemple en Suède et dans le nord de la Russie). Ces vers actuels fournissent de précieuses informations comparatives. L'exuvie de ces priapulidés modernes se sépare du corps le long du tronc et au moins une partie de l'exuvie (celle qui tapisse le pharynx) peut se retourner. Cette étude comparative a permis de reconstituer le processus de mue des vers scolidophores du Cambrien basal. Ces vers pouvaient soit s'extraire de leur ancienne cuticule en douceur, soit en retournant leur exuvie. Cette étude publiée dans les Proceedings of the Royal Society London B (2019) fournit des preuves solides permettant d'affirmer que certains ecdysozoaires primitifs, se développaient déjà par mues successives il y a au moins 535 millions d'années, avant la diversification des arthropodes. Les vers scolidophores de la Formation de Kuanchuanpu, en Chine, sont le plus anciens animaux ecdysozoaires connus. En parallèle, des échanges avec des biologistes travaillant sur les aspects moléculaires et évolutifs de l'ecdysis ont apporté un éclairage nouveau à ces découvertes. Ils suggèrent que l'évolution précoce de l'ecdysis a été associée une suite d'innovations moléculaires commençant par l'apparition de gènes précoces chez le dernier ancêtre commun des protostomiens et se poursuivant dans les trois clades d'ecdysozoaires (ex : acquisition du complexe EcR / USP et des gènes Halloween). Les données paléontologiques réunies ici fournissent un cadre chronologique à ce scénario évolutif proposé par les biologistes moléculaires et indique que des processus génétiques et physiologiques complexes associés à l'ecdysis étaient déjà opérationnels à une époque très reculée, celle de la transition Précambrien-Cambrien. Les scolidophores modernes diffèrent grandement des autres ecdysozoaires (par exemple les arthropodes) et semblent dépourvus d'éléments génétiques essentiels à la biosynthèse ecdystéroïde typique des arthropodes (par exemple les gènes d'Halloween). La voie moléculaire (20-hydroxyecdysone ou autres molécules) par laquelle les priapulidés, les kinorhynches et les loricifères effectue leur mue est pratiquement inconnue et doit être explorée. L'ecdysis apparaît comme une innovation clé et une condition préalable à la diversification et au succès des grands groupes d'animaux tels que les arthropodes. Nous émettons l'hypothèse que l'ecdysis a été sélectionnée comme la solution la plus adéquate pour surmonter les contraintes mécaniques (grandir avec un exosquelette rigide) et qu'elle a sans doute ouvert de nouvelles perspectives évolutives.

## **2- La cuticule des premiers scolidophores : origine épithéliale, diversité, fonctions et implications évolutives**

Cette étude est la suite logique des recherches centrées sur l'origine de la mue (voir chapitre L'épiderme est un tissu cellulaire fondamental présent chez tous les animaux. Il agit comme une interface entre le milieu externe et les tissus et organes internes. Il est constitué de cellules épithéliales et de matériel extracellulaire). Les cellules épithéliales forment un tissu grâce à



des systèmes complexes de jonctions intercellulaires et sécrètent deux types de substrats extracellulaires : à la base, la matrice extracellulaire (ECM) et, apicalement, le glycocalyx (couches de protéines et de sucre) et la cuticule. Les animaux dont la position est la plus basale, tels que les placozoaires et les cténophores, ont un épiderme (avec différents types de cellules) mais n'ont pas de glycocalyx qui, dans tous les autres groupes d'animaux, joue un rôle crucial en tant que matrice sur laquelle d'autres molécules extracellulaires (par exemple chitine, collagène) peuvent s'ancrer et former éventuellement une structure cuticulaire. Les ecdysozoans présentent une grande variété de structures cuticulaires fines et flexibles, sclérotisées ou biominéralisées, souvent associées à des organes sensoriels (ex : soies, récepteurs chimio-sensoriels, etc.). Le but de cette seconde étude était d'obtenir des informations sur la nature et le mode de formation de la cuticule des ecdysozoaires du Cambrien basal, à partir de vers scalidophores fossiles. L'acquisition d'une cuticule, c'est-à-dire d'une enveloppe protectrice à l'interface entre l'organisme et le sédiment, est apparue comme une étape fondamentale de l'évolution animale qu'il fallait explorer. Cette étude publiée dans *Proceedings of the Royal Society London B* en 2020, montre que la surface externe de la cuticule des vers scalidophores de la Formation de Kuanchuanpu (environ 535 Ma) porte un fin réseau hexagonal (taille micrométrique) interprété comme la réplique fidèle des limites entre les cellules épithéliales. Cette interprétation est basée sur des structures identiques observées dans les vers priapulidés actuels (réseau réticulé externe répliquant les limites des cellules polygonales sous-jacentes). Cette stricte correspondance de taille et de forme entre le réseau de cellules épidermiques et celui de la réticulation cuticulaire est fréquent chez d'autres ecdysozoaires actuels, en particulier les arthropodes. Avant la mue, les ecdysozoaires sécrètent des enzymes spécifiques qui brisent le contact entre la partie basale de l'ancienne cuticule et les cellules épidermiques. La croissance de l'épiderme par mitose donne de nouvelles cellules épidermiques relativement plus petites que lors de l'étape précédant la mue. Leur surface apicale d'apparence ondulée porte des microvillosités et commence à sécréter des plaques cuticulaires individuelles lesquelles fusionnent pour finalement former une nouvelle couche cuticulaire, alors que l'épiderme s'étire horizontalement. Nous émettons l'hypothèse qu'un processus comparable était responsable de la sécrétion de la cuticule des premiers ecdysozoaires. Bien que la nature du dernier ancêtre commun des ecdysozoans reste hypothétique, nous suggérons que cet animal avait une cuticule, croissait à travers des stades de mue successifs (voir partie 1 des résultats) et répliquaient fidèlement le pavage cellulaire épidermique pour former un réseau cuticulaire régulier. La réticulation cuticulaire chez les ecdysozoaires n'est autre qu'un sous-produit de la division cellulaire pendant la croissance de la cuticule. Bien que ce processus de base soit resté inchangé depuis au moins le Cambrien basal, de nombreuses variantes sont apparues au fil du temps. Au cours de l'évolution, la complexité accrue des structures cuticulaires (ex : sclérotisation, minéralisation) associée à une éventuelle différenciation épidermique, a donné lieu indépendamment dans presque tous les groupes (à l'exception des nématodes) à une grande diversité des patterns réticulés.

### **3- Paléobiologie du ver tubicole cambrien *Selkirkia* (Scalidophora)**

La radiation cambrienne a donné lieu à des nouveautés anatomiques remarquables et simultanément à une grande variété de modes de vie et de stratégies, qui illustrent comment la vie animale a rapidement colonisé de nouvelles niches et s'est adaptée avec succès à divers environnements en participant au fonctionnement d'écosystèmes marins de plus en plus

complexes. Ces recherches sont centrées sur les scalidophores qui constituent un élément faunique majeur des écosystèmes du Cambrien inférieur, en termes de diversité et d'abondance. Bien que la plupart de ces vers semblent avoir vécu à l'intérieur du sédiment (organismes endobenthiques fouisseurs), nous savons relativement peu de choses sur leur habitat exact, leurs niches écologiques et leur rôle dans les réseaux trophiques. Cette étude se concentre sur *Selkirkia* qui diffère nettement de tous les autres vers scalidophores fossiles et actuels par le fait que ce ver sécrétait et vivait dans un tube conique ouvert aux deux extrémités. L'objectif était ici de mieux comprendre la nature et la formation de cette structure cuticulaire très particulière et de discuter de ses implications écologiques. Sur la base de spécimens à préservation exceptionnelle du Lagerstätte de Chengjiang (environ 518 Ma), l'anatomie et le mode de vie de *Selkirkia* ont été analysés et tout particulièrement la formation du tube et sa relation avec le corps de l'animal. Les fossiles indiquent que le tube était probablement sécrété par les cellules épithéliales du tronc et renouvelé périodiquement par ecdysis non-synchrone. Le tube de *Selkirkia* peut être considéré comme un élément de protection contre les dommages physiques et la prédation et peut également avoir joué un rôle dans l'ancrage de l'animal au sédiment. *Selkirkia* avait un introvert (sorte de trompe invaginable et évaginable) fonctionnel bien développé qui lui aurait théoriquement permis de se déplacer à travers des sédiments boueux comme tous les autres vers scalidophores. Cependant, le tube est susceptible d'avoir engendré un surpoids pour l'animal, gênant ou limitant ainsi ses capacités à se déplacer dans son environnement (relativement aux autres vers non-tubicoles). Le processus de mue de *Selkirkia*, tel que supposé ici, implique que le ver quittait temporairement son tube et restait probablement enfoui dans le sédiment jusqu'au renouvellement de sa cuticule. Bien que non sédentaire, *Selkirkia* avait probablement des capacités limitées pour coloniser des régions éloignées. Un tel mode de vie serait compatible avec la présence de grandes concentrations d'individus trouvés dans certaines localités, et indiquant un possible comportement grégaire. De minuscules brachiopodes épibiontes ont également été trouvés chez de nombreux individus de *Selkirkia* (un seul brachiopode par ver), invariablement attachés à l'extrémité postérieure du tube. Nous avons émis l'hypothèse que de tels brachiopodes se nourrissaient de minuscules particules organiques en suspension libérées via les matières fécales à travers l'extrémité postérieure du tube de *Selkirkia*. Les brachiopodes auraient tiré avantage de leur hôte qui, en retour, ne demeurerait probablement pas affecté par cette interaction. Ces brachiopodes dont le mode d'alimentation était probablement généré par les cils de leur lophophore (comme chez toutes les espèces actuelles) devaient être en contact permanent avec l'eau en circulation. Ces contraintes écologiques et la localisation préférentielle des brachiopodes suggèrent que *Selkirkia* vivait relativement près de l'interface eau-sédiment. Le mode de vie tubicole supposé d'autres animaux du Cambrien est également analysé de façon critique, notamment chez les hémichordés, lobopodiens et les annélides. Il n'existe en fait chez aucun de ces groupes, de preuves solides permettant de dire d'affirmer que l'animal fabriquait un tube organique (cuticule) ou simplement consolidait un terrier via par exemple la production de mucus. Ainsi, *Selkirkia* semble apparaître comme le plus ancien ecdysozoaire tubicole connu. Ce trait évolutif qui offrait à l'animal une meilleure protection et un meilleur ancrage au sédiment, peut être considéré comme une réponse adaptative possible à une pression environnementale ou biologique croissante dans les écosystèmes marins cambriens. Le tube de *Selkirkia* illustre bien les capacités des ecdysozoaires à sécréter une remarquable variété d'éléments cuticulaires et apparaît comme

une innovation précoce au sein de ce groupe. Cependant, *Selkirkia* s'éteint au milieu du Cambrien (environ 508 Ma) et aucun autre ver scalidophore connu ne semble avoir adopté un tel mode de vie tubicole depuis lors, à l'exception d'une seule espèce méiobenthique actuelle : *Maccabeus tentaculatus*. D'autres stratégies endobenthiques favorisant une locomotion et un fouissage plus rapide semblent avoir prévalu au sein du groupe.

#### **4- Système reproducteur des vers scalidophores primitifs (Ecdysozoa)**

Cette étude également basée sur *Selkirkia* (voir partie 3 des résultats) et a été rendue possible grâce à la collaboration avec une équipe de recherche basée à Kunming (Université du Yunnan). Cette étude va bien au-delà de la description systématique de *Selkirkia* et aborde la question importante des organes reproducteurs et des stratégies des premiers animaux. Le matériel fossile provient du Lagerstätte de Xiaoshi (Chine ; env. 514 Ma) Malgré des résultats significatifs obtenus ces dernières années sur la paléobiologie des premiers animaux, de nombreux points d'interrogation demeurent concernant leurs modes de reproduction et de développement. Les fossiles des Lagerstätten cambriens tels que celui de Chengjiang et des schistes de Burgess révèlent des détails étonnant sur l'anatomie fonctionnelle et les modes de vie d'une grande variété d'animaux, mais livrent très peu d'information sur leurs organes de reproduction. Les œufs et les embryons trouvés dans les roches cambriennes fournissent des informations clé sur le développement embryonnaire des premiers animaux mais ne nous disent rien sur les étapes initiales de leur cycle de reproduction (gonades, œufs, fécondation). Certains arthropodes waptiidés ressemblant à des crevettes et fréquents dans les schistes de Burgess et le Lagerstätte de Chengjiang montrent des grappes d'œufs bien conservées disposées symétriquement de chaque côté du corps de la femelle, indiquant ainsi que ces animaux primitifs couvaient leurs œufs (brood care). Des travaux récents mettent également en évidence des différences de stratégies dans les soins parentaux et l'existence de compromis évolutifs. Chez *Selkirkia*, les œufs ont été conservés et fossilisés in situ dans la cavité interne du ver et sont interprétés comme des ovocytes (œufs non fécondés) plutôt que comme des embryons précoces. L'aspect cohérent de ces amas d'ovocytes (Fig. 44A-D) suggère qu'ils étaient maintenus dans une structure ovarienne unique ou plus complexe avant d'être libérés à l'extérieur via des canaux urogénitaux, comme cela est le cas chez les priapulidés actuels. Ces interprétations sont là encore basées sur des analogues actuels notamment des espèces macrobenthiques (par exemple Priapulid) récoltées en Suède et méiobenthiques (par exemple *Meiopriapulid fijiensis* ou *Maccabeus tentaculatus*). La taille relativement grande (associée à une grande abondance en matière nutritive) de ces ovocytes et leur nombre réduit, suggèrent que la stratégie de reproduction de *Selkirkia* était comparable à celle des priapulidés méiobenthiques modernes et que l'énergie investie par ce ver scalidophore cambrien était probablement orientée vers la qualité plutôt que vers la quantité, comme chez certains arthropodes waptiidés (voir ci-dessus). Cette étude indique également que l'organisation générale des gonades femelles chez les vers scalidophores est restée pratiquement inchangée depuis le début du Cambrien. Ces résultats fournissent, pour la première fois, des informations clé sur les organes reproducteurs et le développement pré-embryonnaire des ecdysozoaires primitifs (Scalidophora). La question de savoir si le dernier ancêtre commun des Ecdysozoa possédait des organes appariés et des modes de reproduction comparables ou non, reste une question ouverte qui doit être traitée avec une certaine prudence. En effet, les priapulidés actuels nous apprennent que les facteurs écologiques peuvent grandement influencer les

stratégies de reproduction (les espèces microbenthiques ont tendance à avoir un grand nombre de petits œufs contrairement aux espèces méiobenthiques). En gardant cela à l'esprit, le système reproducteur de *Selkirkia* peut ne pas représenter la condition ancestrale des scalidophores mais pourrait simplement résulter de son mode de vie particulier (voir partie 3 des résultats).

## 5- Phylogénie des Scalidophora

Les relations de parenté entre les espèces actuelles et éteintes peuvent être étudiées de deux façons : en comparant les génomes d'espèces actuelles (phylogénie moléculaires) ou en analysant les caractères morphologiques des espèces actuelles et fossiles. La phylogénie moléculaire alliée aux méthodes de l'horloge moléculaire permet de prédire à quel moment différentes lignées sont apparues par divergence. Les données fossiles permettent de calibrer ces modèles moléculaires. Plusieurs auteurs ont tenté de reconstituer la phylogénie des Scalidophora (Priapulida, Kinorhyncha, Loricifera) sur la base de l'analyse de caractères anatomiques ou moléculaires et certaines d'entre elles intègrent des données morphologiques obtenues à partir de fossiles. L'introvert réversible et son ornementation typique constituée de scalides (excroissances cuticulaires épineuses) est souvent considéré comme la principale synapomorphie des Scalidophora. De façon générale, les relations phylogénétiques entre et parmi les groupes de scalidophores sont mal résolues voire contradictoires. Par exemple, l'existence d'une larve portant une lorica, à la fois chez les Priapulida et les Loricifera a conduit certains auteurs à les considérer (regroupés sous le terme Vinctiplicata) comme le groupe frère des Kinorhyncha. Certaines phylogénies moléculaires indiquent que les Priapulida seraient le groupe frère des Kinorhyncha + Loricifera. D'autres suggèrent plutôt que les Loricifera forment le groupe frère des Nematomorpha ou encore que les Priapulida constituent le groupe frère de l'ensemble des sept phyla ecdysozoaires restants.

Le but de cette étude était de proposer une nouvelle phylogénie des Scalidophora, basée sur l'intégration de nombreuses nouvelles données fossiles obtenues récemment (incluant cette thèse), la réévaluation des caractères morphologiques utilisables et l'utilisation de différentes méthodes cladistiques permettant d'obtenir un arbre phylogénétique.

Méthodologie- Nos investigations sont basées sur des données morphologiques discrètes modifiées et augmentées à partir d'études précédentes. En construisant une nouvelle matrice, nous avons réalisé que beaucoup de caractères multi-états manquaient d'un caractère binaire « primaire » ou « souverain » correspondant. L'inclusion d'un état « absence » dans un caractère multi-états n'est justifiée que s'il y a des raisons de penser que la présence du caractère n'avait probablement pas une origine unique ; sinon, l'absence de caractère souverain représente une perte évidente de signal phylogénétique. Nous avons donc examiné l'optimisation des états de caractères pertinents avec Mesquite, mais avons constaté que, dans la plupart des cas, il n'existait pas de motif homoplasique fort justifiant l'omission de caractères binaires souverains. L'inclusion de tels caractères a ajouté un signal phylogénétique important à la matrice, mais a également abouti à des topologies moins bien résolues par la parcimonie : cela suggère que la matrice d'origine aurait pu être « adaptée » pour augmenter la résolution de l'arbre de consensus strict au prix d'un codage morphologique plus représentatif mais plus contradictoire, comme cela a également été observé dans un ensemble de données concernant les panarthropodes. Bien que l'objectif de la parcimonie soit de minimiser les étapes de transformation, les caractères homoplasiques peuvent toujours

conserver localement une valeur phylogénétique que les corrections basées sur l'homologie secondaire peuvent éliminer. À moins qu'une véritable convergence ne puisse être démontrée, au lieu du parallélisme, tout ensemble de données parfaitement « optimisé » de cette manière peut fournir de fausses reconstructions évolutives cachées derrière des topologies entièrement résolues et bien prises en charge. Des analyses de parcimonie ont été réalisées avec TNT ainsi qu'avec le package R \* TreeSearch qui utilise MorphyLib pour traiter les données inapplicables et des analyses bayésiennes avec MrBayes. *Lepidodermella squamata* (Gastrotricha) a été choisi comme « outgroup » et les caractères n'ont pas été ordonnés. En général, les nœuds supérieurs sont très mal pris en charge et atteindre la convergence dans n'importe quelle méthode (à l'exception de la reconnexion heuristique par bissection d'arbre (TBR)) nécessitait un nombre plus élevé qu'à l'accoutumé, de répliques / générations pour un ensemble de données de cette taille. Par souci de parcimonie, la TBR heuristique a été réalisée avec 1 000 arbres enregistrés pour 10 répliques. En raison du manque de gestion correcte des états inapplicables par TNT ou d'autres logiciels de parcimonie courants (heuristiques TBR et TNT traitant ici les entrées inapplicables comme des incertitudes), le package TreeSearch R \*, a été utilisé. Les recherches bayésiennes ont utilisé un modèle Mkv +  $\Gamma$  avec 4 essais chacun, avec 4 chaînes pour 10 000 000 générations. La recherche arborescente à maximum de vraisemblance a été menée dans IQ-TREE, et le support a été évalué à l'aide de la méthode de réplication bootstrap phylogénétique ultra-rapide pour exécuter 300 000 répétitions. Nous avons utilisé RogueNaRok pour rechercher des taxons déstabilisant l'arbre, mais nous n'en avons trouvé aucun ayant un impact significatif.

Résultats- Les résultats obtenus diffèrent considérablement de ceux qui ont été publiés auparavant, en raison de notre recodage et de l'implémentation extensifs de caractères primaires / souverains (voir ci-dessus). La TBR et le TNT heuristiques résolvent des topologies similaires avec les Priapulida actuels formant un clade sœur de *Selkirkia* et des paléoscolécidés, et avec les Loricifera et Kinorhyncha se ramifiant à la base. En revanche, les méthodes bayésiennes indiqueraient une position relativement basale de *Selkirkia* en tant que groupe frère des Palaeoscolecida et Scalidophora. Selon l'analyse TreeSearch non pondérée, les Loricifera et Kinorhyncha ont également une position basale, mais les groupes fossiles forment tous une longue série souche par rapport aux Priapulida actuels, avec *Selkirkia* et *Eximipriapulites* comme groupes frères les plus proches. Une position basale des Loricifera et Kinorhyncha avec un grand groupe total des Priapulida apparaissant systématiquement en parcimonie, nous avons testé la force de ce modèle en imposant une épine dorsale (backbone) lors de l'analyse bayésienne. La topologie résultante présente une similitude globale avec la topologie TreeSearch non pondérée et donne des moyennes harmoniques légèrement meilleures que le modèle sans contrainte. Un meilleur traitement des états inapplicables a donc aidé la parcimonie à converger avec la vraisemblance bayésienne, en supposant un modèle avec Loricifera basal et Kinorhyncha. L'arbre bayésien contraint apparaît donc comme le meilleur modèle évolutif pour les données utilisées. Dans ce scénario, la plupart des fossiles font partie d'un groupe souche (stem group) très peuplé au sein du groupe total des Priapulida, et *Selkirkia* est plus proche du groupe couronne (crown group) que les paléoscolécidés. Le crown-group des Priapulida comprend une forme du Carbonifère (*Priapulites konecniorum*), son groupe frère immédiat regroupant des formes du Cambrien inférieur comme *Paratubiluchus*, *Xiaoheiqingella* et *Yunnanpriapulites*, et *Sicyophorus* bifurque à la base vers ce groupe. Deux formes typiques de la faune de Kuanchuanpu, *Eokinorhynchus* et *Eopriapulites*

(voir parties 1 et 2 des résultats) sont en position intermédiaire entre *Sicyophorus* et *Selkirkia*. *Laojieella* (Lagerstätte de Chengjiang) apparaît comme un représentant précoce du clade *Selkirkia*, et les recherches bayésiennes montrent que *Markuelia* occupe également une position basale dans ce clade.

Table of Contents	
Acknowledgements .....	2
Abstract.....	3
Résumé .....	4
摘要.....	5
Chapter 1 General background .....	16
1.1 Introduction .....	16
1.2 Ecdysozoans: current knowledge and questions .....	18
1.3 Aims and steps .....	20
Chapter 2 Extant Ecdysozoa.....	21
2.1 What are ecdysozoans?.....	21
2.2 Body plan .....	23
2.3 Diversity .....	24
2.4 Phylogenetic relationships within Ecdysozoa.....	25
Chapter 3 Material and Methods of study.....	28
3.1 The Kuanchuanpu Formation .....	28
3.1.1 Geological setting.....	29
3.1.2 Palaeoenvironmental setting and taphonomy .....	33
3.1.3 Methods of study.....	34
3.2 The Chengjiang and other early Cambrian Lagerstätten .....	35
3.2.1 The Chengjiang Lagerstätte.....	35
3.2.2 Geological setting.....	36
3.2.3 Palaeoenvironment and taphonomy .....	38
3.2.4 Methods of study.....	40
3.2.5 The Xiaoshiba Lagerstätte.....	41
3.3 Comparative studies with extant priapulid worms .....	41
3.3.1 Material.....	41
3.3.2 Methods.....	43
3.4 Phylogenetic analyses .....	44
3.5 Work schedule.....	45
Chapter 4 Early ecdysozoans: review of previous work .....	46
4.1 Precambrian-Cambrian transition.....	46
4.2 Basal Cambrian: the oldest known ecdysozoans.....	49
4.2.1 Scalidophora .....	49
4.2.2 Panarthropoda.....	53
4.3 Early Cambrian: diversification of ecdysozoans exemplified by the Chengjiang Lagerstätte and coeval localities.....	53
4.3.1 Scalidophora .....	55
4.3.2 Panarthropoda.....	69
4.4 Diversity and disparity of ecdysozoans: a brief comparison between Kuanchuanpu and Chengjiang .....	73
Chapter 5 Results .....	75
5.1 Origin of ecdysis .....	75
5.2 The cuticle of early scalidophorans: epithelial origin, diversity and functions, evolutionary implications .....	96

5.3 Palaeobiology of the Cambrian tubicolous ecdysozoan <i>Selkirkia</i> : New insights from the Chengjiang Lagerstätte .....	117
5.4 Cambrian priapulid worms with oocytes shed light on the early evolution of reproductive systems.....	160
5.5 Phylogeny of scalidophorans .....	180
5.5.1 Previous work .....	180
5.5.2 New phylogenetic analysis of Scalidophora .....	183
Chapter 6 Conclusions and prospects .....	194
6.1 Conclusions .....	194
6.2 Future research and prospects .....	197
6.2.1 Postdoctoral research .....	197
6.2.2 Future research in China and international cooperation .....	201
References .....	202
Appendices .....	224



# Chapter 1 General background

## 1.1 Introduction

Metazoans (also called animals) are multicellular eukaryotic organisms (Fig. 1A) characterized by the ability to form organized tissues and organs through complex cell-cell junctions (e.g. epithelium). Even the most basal animals such as placozoans have a closely-knit epithelial layer that accommodates distinct cell types (Nielsen, 2012; Srivastava et al., 2008). All animals grow from a hollow sphere of cells, the blastula, during embryonic development (Brusca et al., 2016; Nielsen, 2012; Schmidt-Rhaesa, 2007). Another fundamental trait of animals with the exception of placozoans and acoels is to secrete a sub-epidermal extracellular matrix (ECM), typically made of collagen, fibronectin, and laminin, towards the inside of the body (Schmidt-Rhaesa, 2007). Distinct layers often occur within the ECM such as the basal lamina (e.g. bilaterians) which serves as the substrate on which epithelial cells can be organized (Nielsen, 2012; Schmidt-Rhaesa, 2007). Secretions towards the outside, exemplified by the cuticle (collagen or chitin such as in ecdysozoans) are equally important and act as an interface and protective layer between the epithelium and the surrounding medium. Animals are heterotrophic organisms that must acquire, digest, and metabolize food. They distribute usable products throughout their bodies and get rid of excreted. Most of them have a differentiated internal digestive system in which food is broken down by enzymes and assimilated.

Animal life is remarkable by its diversity with most probably millions of extant species but is amazingly expressed by a relatively limited number of body plans. In terms of symmetry, animals fall into three broad categories: those with a radial or bilaterian symmetry and those with no symmetry at all such as placozoans and sponges (Brusca et al., 2016). Basal groups such as cnidarians (e.g. jellyfish) have a central axis and a radial symmetry (e.g. tetra-radial) as shown by the arrangement of their internal organs such as gonads. A major proportion of animals have a bilaterian symmetry, i.e., having a left and a right side that are mirror images of each other. Bilateria is a huge clade generally subdivided into two groups, the Protostomia (Ecdysozoa, Lophotrochozoa) and Deuterostomia (e.g. Chordata, Ambulacraria) (Blair, 2009; Philippe et al., 2005). However, this classical subdivision is challenged by some authors (e.g. Brusca et al., 2016; Dunn et al., 2014; Fig. 1B) who introduced a third group represented by Xenacoelomorpha. Xenacoelomorphs are small, direct-developing (no larval stage), unsegmented, ciliated worm-like organisms. They have a midventral mouth and incomplete gut, lacking an anus (Brusca et al., 2016).

Bilaterians have both an antero-posterior and dorso-ventral polarity. The antero-posterior axis has led to the differentiation of a head and a tail, and to the cephalization that concentrates most sensory and feeding structures at anterior end of the animal and to locomotion modes oriented forwards (Brusca et al., 2016). The ventro-dorsal differentiation seems to have been a prerequisite condition to the evolution of functional legs and is also involved in locomotion processes. Most bilaterians also have a through gut -i.e open at both ends via the mouth and anus- a mesoderm and a complex network of circular and longitudinal muscles. However, some of them have lost these diagnostic features through evolution, in relation due to their peculiar lifestyle (e.g. blind gut of nematomorph; Brusca et al., 2016;

Schmidt-Rhaesa, 2014). Ecdysozoans are among the most diverse and prolific bilaterians on Earth (probably more than 1 million species, Brusca et al., 2016) and have rich fossil record over the last 500 million years or more. This animal group is the main focus of my thesis.

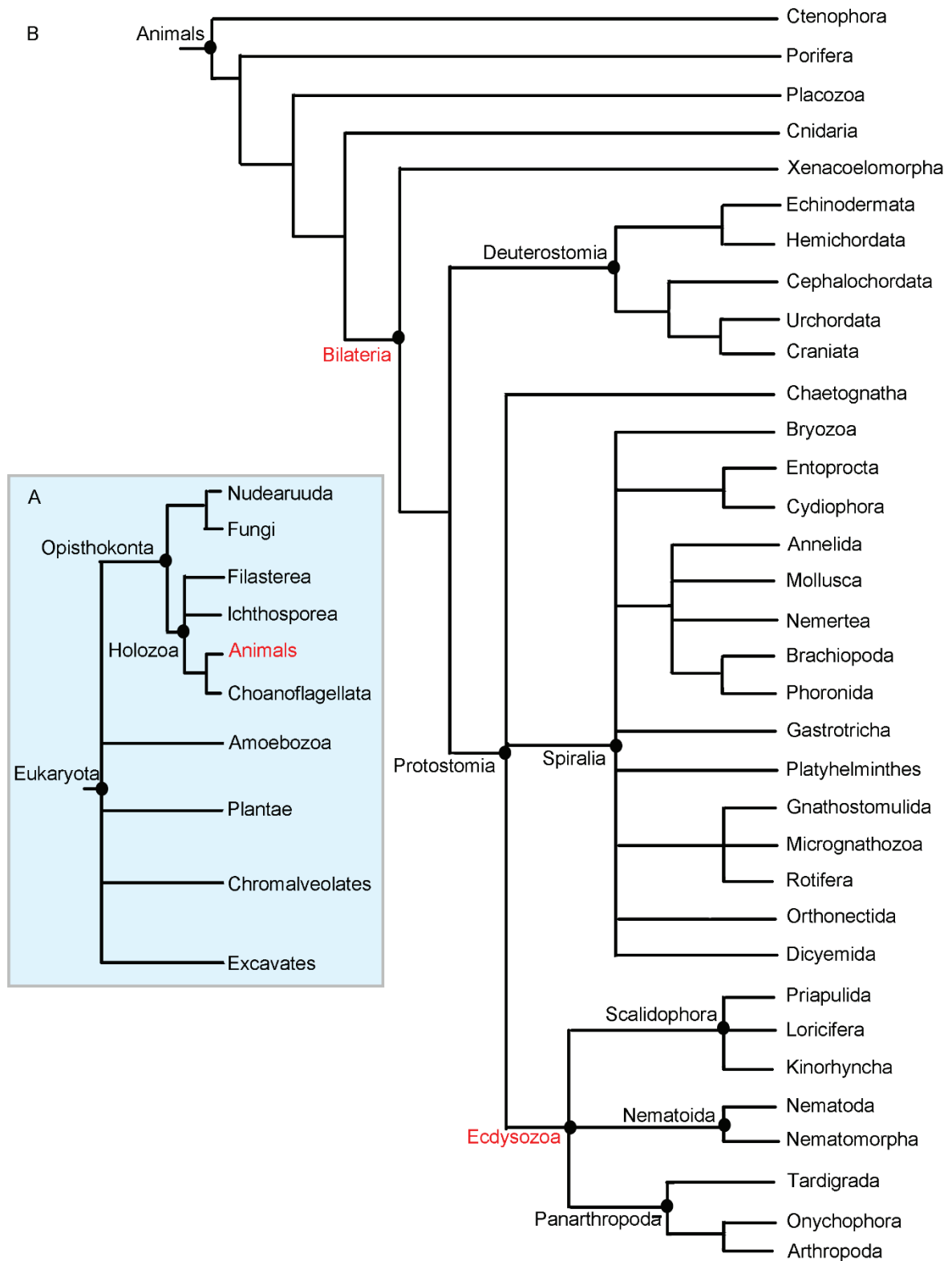


**Figure 1.** Phylogenetic tree showing the relation between animal groups. A. Position of animals within Eukaryota, modified from Dunn et al. (2014) and Bhattacharya et al. (2009). B. Position of Ecdysozoa within Bilateria, modified from Dunn et al. (2014).

## 1.2 Ecdysozoans: current knowledge and questions

Ecdysozoa encompasses Panarthropoda (Arthropoda, Onychophora, Tardigrada) and Cycloneuralia (Nematoda, Nematomorpha, Priapulida, Kinorhyncha, Loricifera; Aguinaldo et al., 1997; Nielsen, 2012; Schmidt-Rhaesa et al., 1998). Based on its fossil record, the group can be traced back to at least the basal Cambrian (e.g. Kuanchuanpu Formation, ca 535 Ma; Liu et al., 2014; Shao et al., 2019; Steiner et al., 2020; Zhang et al., 2015). However, its origin is most probably much older and deeply rooted into the Precambrian as suggested by molecular studies (Cunningham et al., 2017; Dunn et al., 2014; Dunn et al., 2008; Schmidt-Rhaesa et al., 1998; Telford et al., 2008; Fig. 2) and ichnology (Buatois and Gabriela Mángano, 2016).

As most animal groups, ecdysozoans have been extensively studied by generations of scientists since the 18<sup>th</sup> century (e.g. Linnaeus), who accumulated basic knowledge on their biology, ecology, and phylogeny. However, numerous puzzling and hot questions remain open concerning their origin and early evolutionary history such as 1) the origin of their segmentation pattern (Articulata vs. Ecdysozoa; Aguinaldo et al., 1997; Budd, 2001; Cuvier, 1817; Pilato et al., 2005; Schmidt-Rhaesa et al., 1998; Zhuravlev et al., 2011), 2) the arthropodization that led to complex articulated exoskeletons (e.g. arthropods; Garey, 2001; Giribet and Edgecombe, 2017; Neves et al., 2013; Telford et al., 2008; Yamasaki et al., 2015), 3), the evolutionary scenario through which major ecdysozoan lineages appeared and diversified during the early Palaeozoic (Dunn et al., 2014; Laumer et al., 2019; Lemburg, 1999) and 4) the nature and habitat of the last common ancestor of the group (Budd, 2001; Giribet and Edgecombe, 2017; Schmidt-Rhaesa, 1998; Schmidt-Rhaesa et al., 1998; Valentine and Collins, 2000). Recent progress in developmental biology (Martin-Duran et al., 2016; Wennberg et al., 2009), genetics (Chang and Mykles, 2011), and molecular phylogeny (Borner et al., 2014; Dunn et al., 2014; Laumer et al., 2019) based on the molecular clock theory have clarified some of these issues and led to models that propose a chronological framework to the early evolution of ecdysozoans. Palaeontology has a crucial role to play in this debate and especially fossils obtained from exceptional fossil sites discovered and exploited throughout the Cambrian over the last few decades (e.g. Chengjiang and Burgess Shale Lagerstätten), that provide a wealth of high-resolution information on the nature of ancestral ecdysozoans. Moreover, these fossils can be used to test and calibrate molecular models. Without fossils no realistic, accurate and vivid picture of early animal life can be obtained.

One of the hottest debates concerns the origin and divergence of the major ecdysozoan branches. The ancestral ecdysozoan is often represented as a relatively large, microannulated worm with a terminal mouth and small sclerites scattered over its body (Budd, 2001; Valentine and Collins, 2000), and an introvert bearing a circum-pharyngeal nerve ring (Eriksson et al., 2003; Telford et al., 2008). Whether the ancestral ecdysozoans bore segmentation is still open debate. There are still unresolved issues such as the appearance of segments of kinorhynchs (Müller and Schmidt-Rhaesa, 2003; Schmidt-Rhaesa and Rothe, 2006) and the similar deployment of homologous genes in arthropods and kinorhynchs (Telford et al., 2008). These hypothetical models often imply that ecdysozoans may originate from a relatively simple worm-like animal (Dzik and Krumbiegel, 1989; Valentine and Collins, 2000). This view is supported by the basal position of priapulids, a group of extant ecdysozoan worms with abundant Cambrian representatives, in most phylogenetic trees based on both molecular and morphological data (Dunn et al., 2014; Giribet and Edgecombe, 2017; Laumer et al., 2019;

Nielsen, 2012; Rota-Stabelli et al., 2013; Zhang et al., 2015; Fig. 2).

Although poorly supported by fossil evidence, an alternative scenario predicts that body plan of ancestral ecdysozoans resembled that of xenusian animals (e.g. *Xenusion*, Dzik and Krumbiegel, 1989; Zhuravlev et al., 2011), i.e. a worm-like animals with soft legs. This would imply that cycloneuralian worms (bearing a circum-pharyngeal nerve ring; Nielsen, 1995) had evolved from limb-bearing animals through the loss of legs (Xenusians-*Facivermis*-cycloneuralians). According to this model, xenusians would have given rise to arthropods (Zhuravlev et al., 2011), via arthropodization (sclerotization of the limbs) and arthrodization (sclerotization of the body).

Molecular models predict that ecdysozoans appeared in the Ediacaran (ca 600-million-year-old) several tens of thousands of years before than their first occurrence in the fossil record (e.g. Cunningham et al., 2017; Rota-Stabelli et al., 2013; Fig. 2). This apparent discrepancy is another puzzling question concerning the evolutionary history of the group. Indeed no solid fossil evidence supports the presence of ecdysozoans in the Precambrian, except complex burrow systems such as *Treptichnus pedum* found across the Precambrian-Cambrian boundary, most probably made by priapulid-like worms (see experimental studies in Kesidis et al., 2019; Vannier et al., 2010). Answering this issue would require testing two types of hypotheses: 1) either, the Precambrian fossil record of ecdysozoans is cryptic (e.g. represented by microscopic and/or soft-bodied organisms with extremely low potential to be fossilized (Liu et al., 2014) or 2) the group has no Precambrian ancestors and appeared across the Precambrian-Cambrian boundary, possibly driven by an exceptionally fast evolution rate.

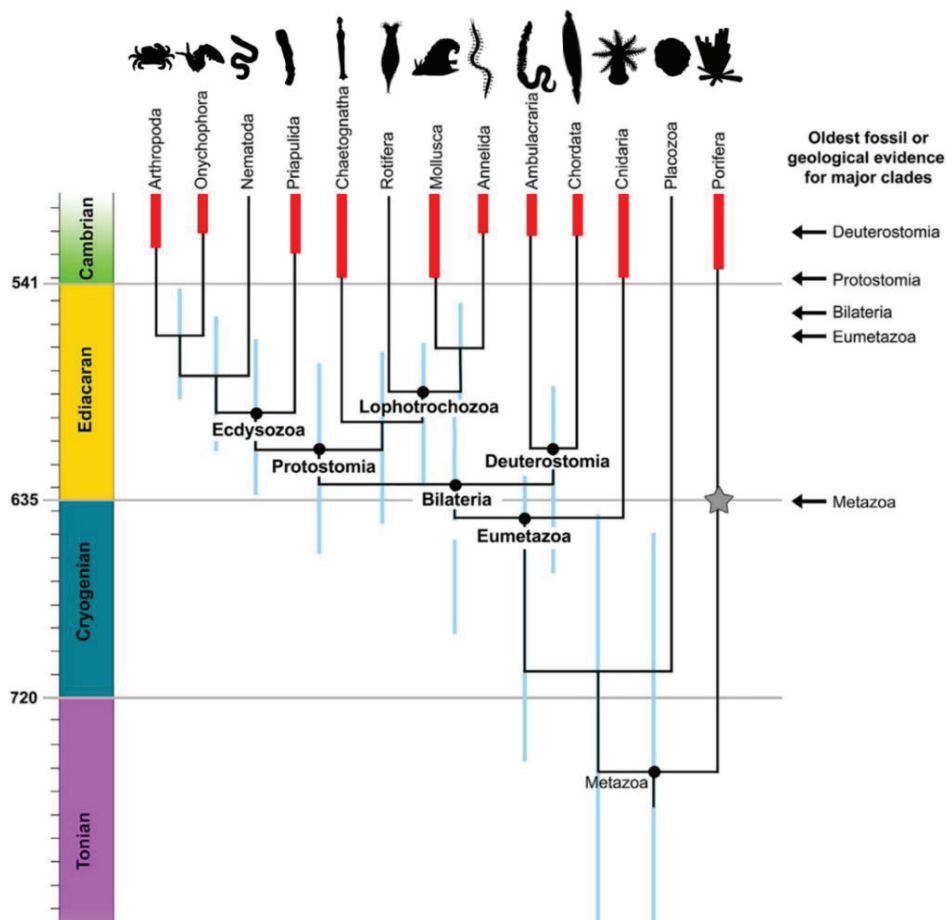


**Figure 2.** Phylogenetic tree showing the relation between animal groups (including Ecdysozoa) and their predicted chronology of divergence, modified from Cunningham et al. (2017). Bars indicate known fossil record for each group.

### 1.3 Aims and steps

The aim of my thesis is to provide answers to the puzzling question of the origin and diversification of ecdysozoans, especially the nature of their remote ancestors in terms of anatomy and ecology and the phylogenetic relationships between their major components such as scalidophorans, lobopodians and arthropods. I focused on scalidophorans.

I concentrated on two types of material: 1) Small Shelly Fossils (SSFs) from the Kuanchuanpu Formation dated from ca 535 Ma, that has yielded the oldest known ecdysozoans remains, mainly scalidophorans, 2) scalidophoran macrofossils from the Chengjiang Lagerstätte whose approximate age is ca 518 Ma.

These two evolutionary windows provide key information on the early evolution of several animal groups, including scalidophorans.

Scalidophorans are relatively abundant and diverse in both localities, due to the fact that their cuticle is more decay-resistant than the tissues of soft-bodied animals, and could be fossilized via various pathways such as secondary phosphatization (Kuanchuanpu; Bengtson and Yue, 1997; Liu et al., 2014) and pyritization (Chengjiang; Gabbott et al., 2004; Vannier et al., 2014; Zhu et al., 2005).

Cuticular fragments and complete specimens found in these localities display exquisite morphological details such as ornamented patterns at cellular level, that shed light on numerous aspects of the palaeobiology of ancient ecdysozoans such as their moulting process, locomotion, feeding mode, reproductive strategies, and lifestyles (e.g. tubicolous habits). These extremely rich sources of information also allowed me to re-explore the phylogeny of the group. The reassessment of morphological characters allowed me to perform new cladistic analyses in order to clarify the phylogenetic relations within Scalidophora and between Scalidophora and other ecdysozoans.

Contrasting with SSFs from the Kuanchuanpu Formation, the Chengjiang fossils reveal details of internal organs such as the digestive and reproductive systems (Caron and Vannier, 2016; Knaust, 2020; Ou et al., 2020; Peel and Rahman, 2017; Vannier et al., 2014). It was essential for me to study fossils from two different temporal and taphonomic contexts in order to have a more comprehensive view of the early diversification of scalidophorans.

To some extent, fossils are not sufficient to gain a comprehensive and integrated understanding of the palaeobiology and evolutionary history of animal groups. I had the chance to collect and study in lab modern representatives of scalidophorans via research stay at the Kristineberg Marine Station (Sweden).

These comparative studies had very positive and significant impact on how the Cambrian scalidophorans should be interpreted in terms of functional anatomy and palaeoecology.

## Chapter 2 Extant Ecdysozoa

### 2.1 What are ecdysozoans?

Ecdysozoa was first defined by Aguinaldo et al. (1997) as a clade encompassing seven protostome phyla (Arthropoda, Onychophora, Tardigrada, Nematoda, Nematomorpha, Priapulida and Kinorhyncha; Figs 3; 5), based on phylogenetic analyses using ribosomal DNA genes. Further molecular studies (e.g. Cunningham et al., 2017; Dunn et al., 2008; Laumer et al., 2019; Rota-Stabelli et al., 2013) also supported the Ecdysozoa as a clade to which Loricifera was added because of its moulting behaviour and cuticular features. Molecular data concerning loriciferans were not available at the time of Aguinaldo et al.'s pioneer studies (Schmidt-Rhaesa et al., 1998).

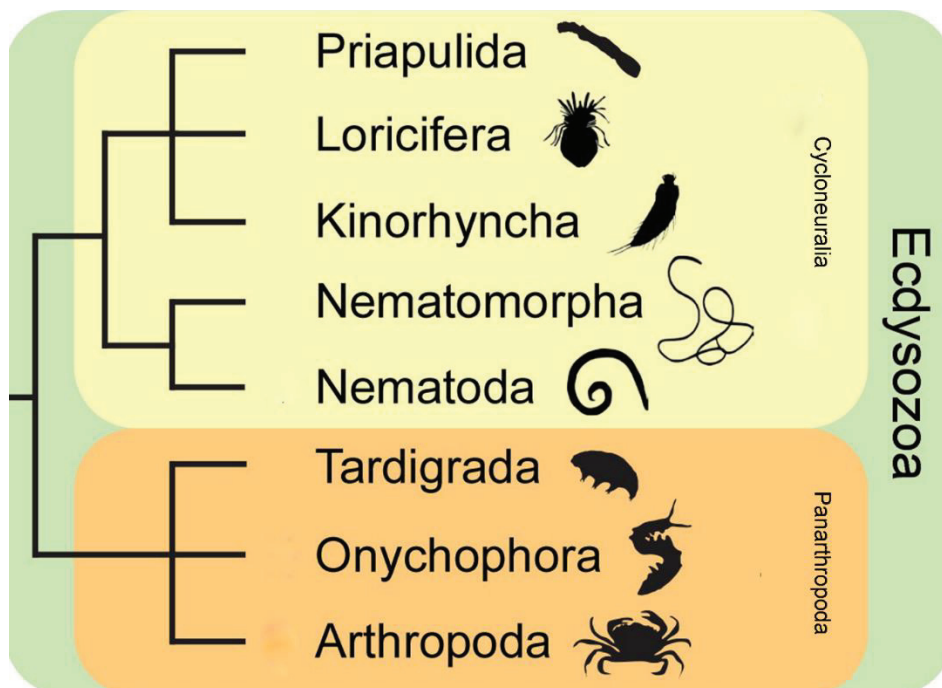


**Figure 3.** Phylogenetic relationships of the Ecdysozoa, modified from Borner et al. (2014) and Schumann et al. (2018).

There is a general consensus among scientists that ecdysozoans form a natural and monophyletic group (e.g. Laumer et al., 2019; Rota-Stabelli et al., 2013). This view is also supported by molecular studies and numerous morphological characters shared by the eight ecdysozoan phyla, such as development through successive moulting stages (ecdysis, Aguinaldo et al., 1997; Giribet and Edgecombe, 2017; Schmidt-Rhaesa et al., 1998; Telford et al., 2008). Ecdysozoa owes its name to this peculiar growth mode (ancient Greek ἑκδυσίς (ékdysis, “shedding”) plus ζῷον (zōon, “animal”). The Ecdysozoa concept challenged the Articulata hypothesis (Ax, 1996; Cuvier, 1817) that had been prevalent since the 19<sup>th</sup> century, according to which Arthropoda and Annelida had to be put together on account of their segmented body (Blair, 2008; Pilato et al., 2005). However, evolutionary developmental biology now shows that segmentation probably appeared independently at least three times

in the course of evolution, in Chordata, Annelida and Panarthropoda (Blair, 2008). The grouping proposed by Aguinaldo *et al.* (1997) is now almost universally accepted and replace the Articulata hypothesis that became obsolete.

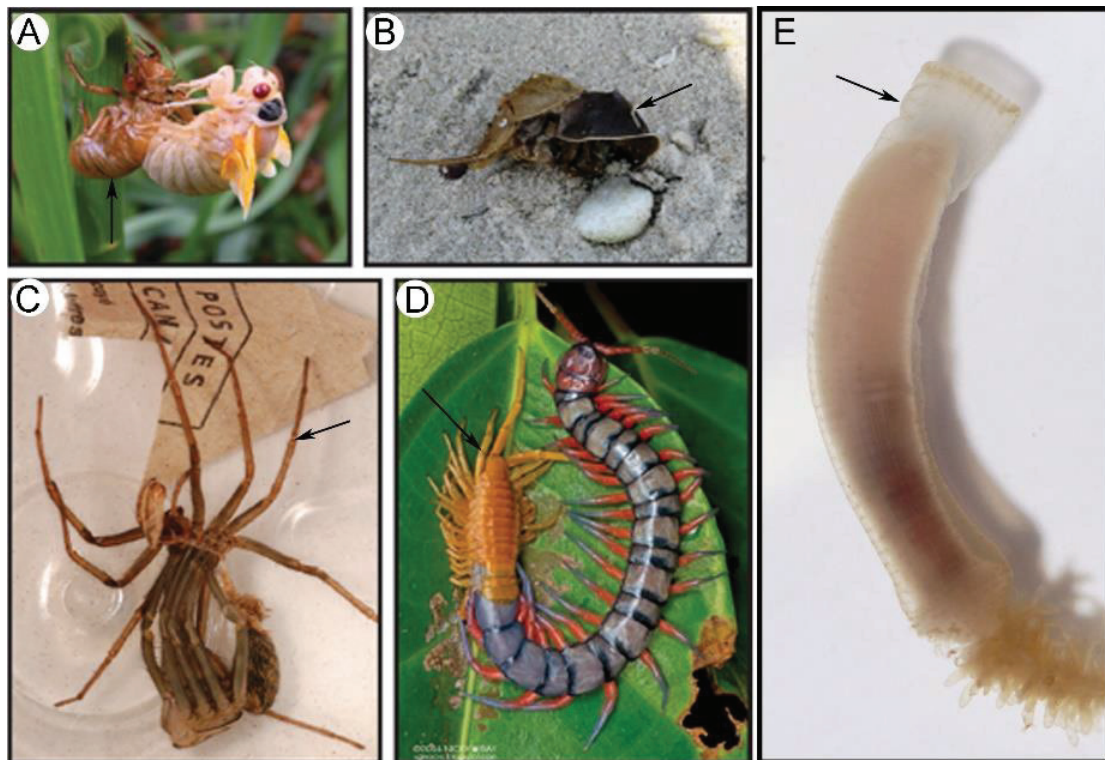


**Figure 4.** Ecdysis in extant ecdysozoans. A-D. Arthropoda. A. Cicada. B. Crab. C. Spider. E. Centipede. E. Moulting of *Priapulus caudatus* (Priapulida). Exuvia indicated by black arrows. A-D from [www.pinterest.com](http://www.pinterest.com). (E) courtesy J. Vannier.

Ecdysis is one of the most important diagnostic character of Ecdysozoa. Ecdysis is a process through which animals shed their whole old cuticle (exuvia; Fig. 4) and replace it by a new one. This process is regulated by ecdysteroid hormones (Brusca *et al.*, 2016; Schumann *et al.*, 2018). Ecdysis plays a crucial role in the metamorphosis of insects (Nijhout, 2013), and allows damaged tissue and missing limbs to be regenerated or substantially re-formed (Hopkins, 2001; Nijhout, 2013).

During the moulting process, the old exocuticle breaks along specific lines of weakness called ecdysial sutures where the exocuticle is particularly thin and can break apart very easily (Nijhout, 2013). Ecdysis is considered as a major autapomorphy for Ecdysozoa. Not all scientists share this opinion. Some of them argue that some non-ecdysozoan animals also moult (Paxton, 2005; Pilato *et al.*, 2005). For example, the jaws of polychaete annelids are renewed via a flaking process comparable to ecdysis. Gastrotrichs, a group of microscopic worm-like pseudocoelomate animals, also perform a partial shedding of their cuticle. However, flaking and partial shedding in these animals seem to differ markedly from ecdysis (as seen ecdysozoans) in important physiological aspects (Attout *et al.*, 2008; Bang-Berthelsen *et al.*, 2013; Bertolani *et al.*, 2009; Neuhaus, 2013; Nijhout, 2013; Paxton, 2005; Pilato *et al.*, 2005; Schmidt-Rhaesa, 2013; Wang *et al.*, 2019).

In addition to ecdysis, several important morphological and developmental traits unite

ecdysozoans. These are 1) the trilamellate structure of their epicuticle that is secreted from the tips of epidermal microvilli (Harvey et al., 2010; Lemburg, 1999; Schmidt-Rhaesa et al., 1998); 2) the lack of a primary (ciliated) larva with an apical organ; 3) the lack of spiral cleavage in embryos and 4) the lack of external epithelial cilia (Brusca et al., 2016; Schmidt-Rhaesa, 2007).

## 2.2 Body plan

All ecdysozoans have a bilateral symmetry exemplified by paired reproductive organs. However, their anatomy also displays a radial symmetry as exemplified by the pentaradial arrangement of cuticular spiny elements (scalids) along the introvert of priapulids (Fig. 5A). Ecdysozoans can be divided in a very simple way into two categories, those with legs (Panarthropoda) and those with a worm-like appearance (Cycloneuralia) (Fig. 5, blue and green rectangles). Panarthropoda (Nielsen, 1995) accommodates arthropods, onychophorans (velvet worms) and tardigrades (water bears or moss piglets). Most arthropods bear a hard cuticular exoskeleton (e.g. sclerotized, mineralized), a segmented body, and paired jointed appendages (Figs 4A-D; 5H, I). Tagmosis, defined as a specialized grouping of multiple segments or metameres into a coherently functional morphological unit, is also a characteristic feature of panarthropods. In contrast with arthropods, velvet worms and water bears, although segmented, lack jointed limbs and have “soft” legs (Fig. 5D, E). Their cuticle is thin and flexible.

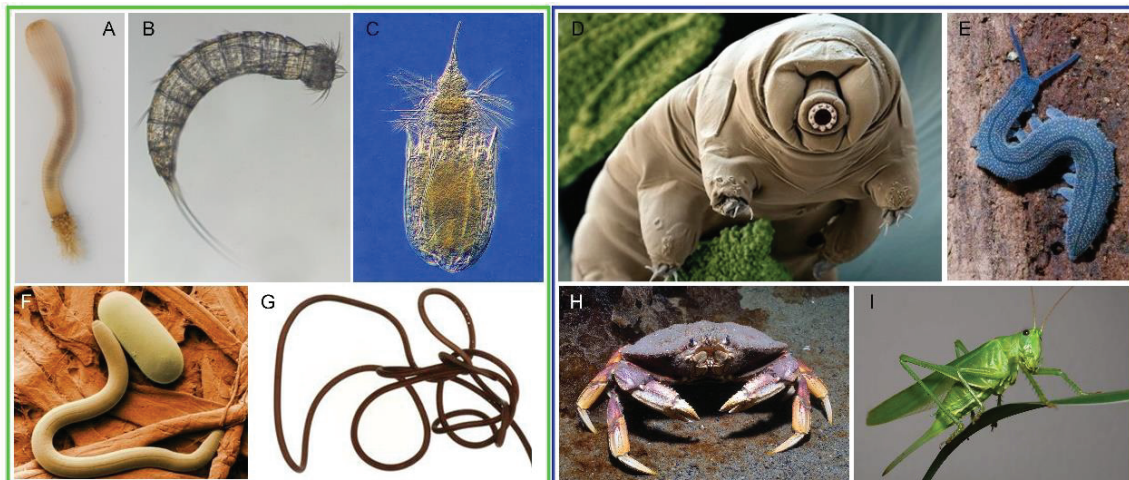


**Figure 5.** Diversity of extant ecdysozoans. A. Priapulida. B. Kinorhyncha, from Piper, (2013). C. Loricifera. D. Tardigrada. E. Onychophora. F. Nematoda. G. Nematomorpha. H. Arthropoda (Crustacean). I. Arthropoda (Insect). Rectangle in green and blue represent Cycloneuralia and Panarthropoda, respectively. (C-I) from [www.pinterest.com](http://www.pinterest.com).

In contrast, cycloneuralians are vermiform and lack appendages. They comprise the nematodes (roundworms, Fig. 5F), nematomorphs (horsehair worms or Gordian worms, Fig. 5G), priapulids (penis worms, Figs 4E;5A), kinorhynchs (mud dragons, Fig. 5B) and loriciferans (Fig. 5C). All cycloneuralians have an anterior mouth, a cylindrical pharynx and a collar-shaped, peripharyngeal brain (Ahrichs, 1995; Nielsen, 1995; Schmidt-Rhaesa, 2013; Fig. 5A-C, F, G). Their name comes from the specificity of their ring-like brain, (= *Introverta sensu*; Ahrichs,



1995; Nielsen, 1995). Cycloneurians distribute into two groups: the Scalidophora (Priapulida, Kinorhyncha, Loricifera) (Lemburg, 1995; Fig. 5A-C) and the Nematoida (Nematoda, Nematomorpha) (Ahlrichs, 1995; Schmidt-Rhaesa, 1996; Fig. 5F, G). Anatomical features of extant scalidophorans are given (see Chapter 4; Fig. 24).

Many nematodes and nematomorphs have specialized body features adapted to their parasitic lifestyles (e.g. specialized cuticular projections at head in the nematod *Acrobeles* sp.; Schmidt-Rhaesa, 2014). Scalidophorans are characterized by a well-developed eversible introvert (the anterior part of the animal that can be invaginated and unfolded). Although this feature also occur in nematomorph larvae (Schmidt-Rhaesa, 2013). The trunk of adult priapulids is annulated (Schmidt-Rhaesa, 2013), and priapulid larvae and loriciferans are encased within a specialized cuticular feature called the lorica that is devoid of annuli (Bang-Berthelsen et al., 2013). Kinorhynchs display a most peculiar exoskeleton made of externally segmented cuticular plates (Neuhaus, 2013; Fig. 5A-C). The posterior end of some priapulids bear a single or a pair of caudal appendages (Fig. 5A).

The body cavity of adult priapulids is spacious and extends into the caudal appendages (*Priapulus caudatus*, Fänge and Mattisson, 1961) or tail (*Tubiluchus corallicola*, Kirsteuer and van der Land, 1970; Schmidt-Rhaesa et al., 2017) when present. Except *Meiopriapulus fijiensis* (Storch et al., 1989), priapulids have a primary body cavity called the blastocoel (i.e. lined by extracellular matrix; McLean, 1984). Kinorhynchs also have a primary body cavity. The body cavity of loriciferans is very complex and variable, being absent or very small in larval and adult nanaloricids (Kristensen, 2002) and larger in pliciloricids (Kirstensen, 1991).

## 2.3 Diversity

The number of ecdysozoan species was estimated to be more than 5-10 million species (Ødegaard, 2000) possibly representing  $10^{18}$  individuals in total (Campbell, 1996). About 83% of present-day animal species known to science are arthropods and nematodes (Brusca et al., 2016). Arthropods have colonized a huge spectrum of ecological niches and are present in marine and freshwater habitats at various depths, as well as terrestrial and aerial environments, and some species can survive in extreme conditions (hydrothermal vent, cold seep; Botos, 2015; Tunnicliffe, 1991; Won, 2006). About fifty percent of nematode species (possibly more than one million extant species) are parasites of other animals including arthropods.

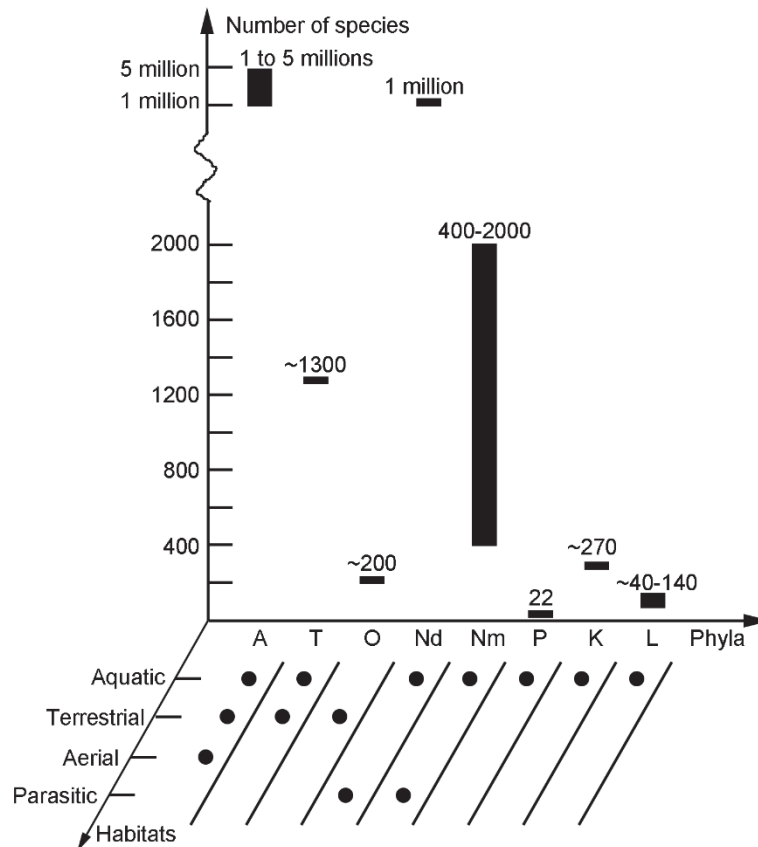


**Table 1.** Estimated diversity of ecdysozoans. Abbreviations: A, Arthropoda; T, Tardigrada; O, Onychophora; Nd, Nematoda; Nm, Nematomorpha; P, Priapulida; K, Kinorhyncha; L, Loricifera. Data from Brusca et al. (2016), Schmidt-Rhaesa (2013), and Schmidt-Rhaesa et al. (2017).

In contrast, the remaining ecdysozoans groups have a much lower diversity with probably less than 5,000 species in total, distributed among onychophorans (ca 200), tardigrades (ca 1300), kinorhynchans (ca 270), loriciferans (37 + ca 100 undescribed species), priapulids (22) and nematomorphs (less than 400) (Schmidt-Rhaesa, 2013; Schmidt-Rhaesa et al., 2017) (Table 1). The vast majority of scalidophorans are endobenthic animals.

## 2.4 Phylogenetic relationships within Ecdysozoa

Molecular data and morphological characters have been used by many scientists to study the phylogenetic relations with the group (Aguinaldo et al., 1997; Garey, 2001; Giribet and Edgecombe, 2017; Laumer et al., 2019; Lemburg, 1999; Telford et al., 2008; Fig. 6). Morphology-based analyses tend to distinguish two clades: the Cycloneuralia (limbless ecdysozoans with a collar-shaped brain) and Panarthropoda (forms with a segmented trunk and paired lateral legs) (Nielsen, 2012). Molecular methods also resolve Panarthropoda as a well-defined clade (Edgecombe, 2009; Giribet and Edgecombe, 2017; Fig. 6A, B, C, G). However, things become much more uncertain at a lower level. Some molecular analyses support Tardigrada as the sister group of Arthropoda + Onychophora (Dunn et al., 2014; Laumer et al., 2019; Piper, 2013). Other authors suggest that Onychophora is more likely the sister group of Arthropoda + Tardigrada, based on anatomical similarities (head, legs, and muscles; Howard

et al., 2020a; Mayer et al., 2013; Smith and Caron, 2015; Yang et al., 2015). These conflicting results demonstrate the urgent need to integrate both molecular and morphological data in a more coherent approach.

Similarly concerning the Cycloneuralia, the position of Nematoida and Loricifera are unstable (see molecular studies, Dunn et al., 2008; Hejnol et al., 2009; Laumer et al., 2015; Fig. 6D-F). The monophyly of Nematoida is generally well supported (Giribet and Edgecombe, 2017). In a few studies, however, tardigrades are surprisingly nested within nematoids (Borner et al., 2014; Hejnol et al., 2009; Fig. 6E). These results may be due to a long-branch attraction artifact (Rota-Stabelli et al., 2013). Morphologically, nematomorphs have larvae with an eversible introvert, resembling those of scalidophorans (Schmidt-Rhaesa, 2013). Nematodes have no such larval stage. For this reason, Petrov and Vladychenskaya (2005) suggested that Cycloneuralia may be a paraphyletic group.

The relation of Loricifera to other ecdysozoan groups is still debated. Loriciferans are grouped with scalidophorans, based on morphological features (Lemburg, 1995; Neuhaus, 1994; Neuhaus and Higgins, 2002; Fig. 4A, B, F). However, molecular analyses resolve them as the sister group of either Nematomorpha (Park et al., 2006; Sørensen et al., 2008; Fig. 6G), or Priapulida (Dunn et al., 2014; Laumer et al., 2015; Fig. 6B, F), or are placed within Panarthropoda (Yamasaki et al., 2015).

The phylogenetic position of Priapulida and Kinorhyncha varies according to the authors (Hejnol et al., 2009; Piper, 2013; Fig. 6C, E). In most cladistic trees Priapulida has a basal position within Ecdysozoa (Laumer et al., 2019; Petrov and Vladychenskaya, 2005; Webster et al., 2006; Fig. 6E, G).

However, Giribet and Edgecombe (2017) pointed out a number of uncertainties concerning the position of these two groups, and for Cycloneuralia as a whole, discrepancies between morphological and molecular results. Both the lack of lack detailed anatomical characters (typically in fossils) and limited molecular sampling (extant species) may account for this relatively poor resolution.

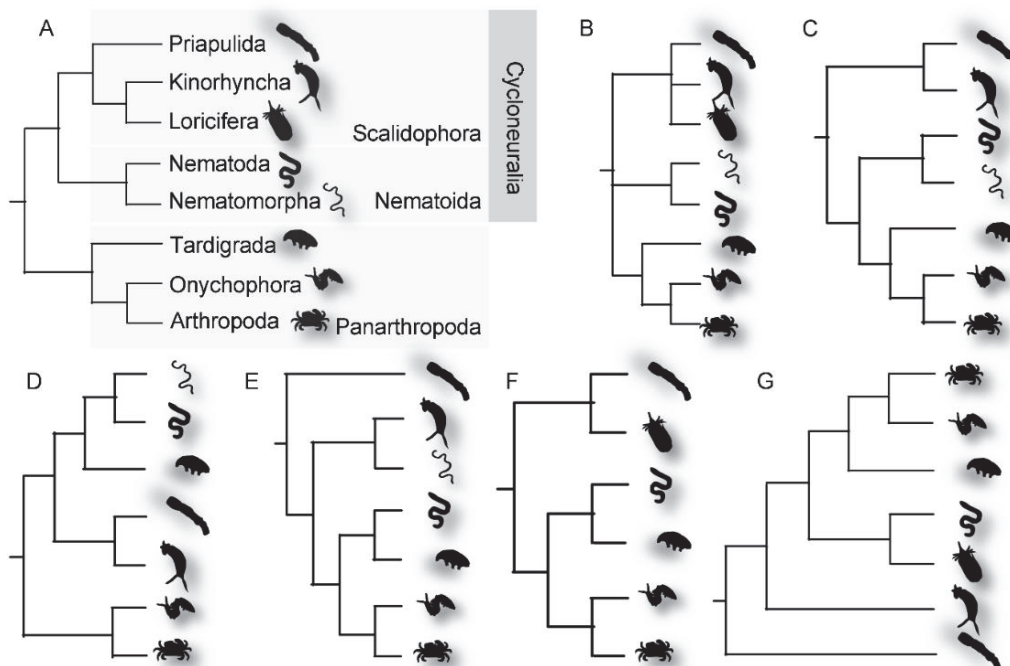


**Figure 6.** Summary of selected ecdysozoan phylogenies based on Giribet and Edgecombe (2017). A. Based on morphological characters, from Nielsen (2012). B-G. Based on molecular data. B. Compiled across multiple studies, from Dunn et al. (2014). C. Compiled across multiple studies, from Piper (2013). D. Based on expressed sequence tags (ESTs), from Dunn et al. (2008). E. Based on expressed sequence tags (ESTs), from Hejnol et al. (2009). F. Based on transcriptomes (nuclear protein-coding data), from Laumer et al. (2015). G. Based on transcriptome and genome data, from Laumer et al. (2019).

## Chapter 3 Material and Methods of study

The fossil material studied here was collected from 1) the Kuanchuanpu Formation (basal Cambrian, ca 535 Ma; southwestern Shaanxi Province) and 2) the Chengjiang Lagerstätte (early Cambrian, ca 518Ma; eastern Yunnan Province). The aim of this Chapter is to describe the geological background of both fossil sites (palaeogeographic framework, stratigraphy, palaeoenvironmental setting and preservation), and to present the methods I have been using to deal with these fossils. Comparative studies with extant animals, mainly priapulids from Sweden have also been performed during my PHD-thesis.

### 3.1 The Kuanchuanpu Formation

SSF assemblages from the Kuanchuanpu Formation and coeval localities from the eastern part of Yunnan, central and north Sichuan and west Hubei were first described by Qian (1977) in a Chinese paper (Qian, 1977). This pioneer study revealed an enigmatic and diverse animal world, unfamiliar to palaeontologists of that time (Fig. 7). Over the years the Kuanchuanpu Formation became a major palaeontological site where remarkably well-preserved fossils from diverse metazoan and non-metazoan groups were discovered such as bacteria (Yang et al., 2017; Fig. 7A), algae (Yang, 2018; Zheng et al., 2017; Fig. 7B), embryos (Yue and Bengtson, 1999; Fig. 7C), protoconodonts (e.g. *Protohertzina*, Qian, 1999; Fig. 7D), cnidarians (Han et al., 2016a; Han et al., 2010; Wang et al., 2017; Wang et al., 2020; Fig. 7I, J), molluscs (Qian, 1999; Steiner et al., 2004; Fig. 7F), slug-like halkieriids (Qian, 1999; Steiner et al., 2004), brachiopods (Jiang, 1980), echinoderms, scalidophoran worms (Liu et al., 2014; Shao et al., 2019; Zhang et al., 2015; see Fig. 25), lobopodians (unpublished information; see Fig. 27), and problematic fossils (Shao et al., 2015; Fig. 7G).

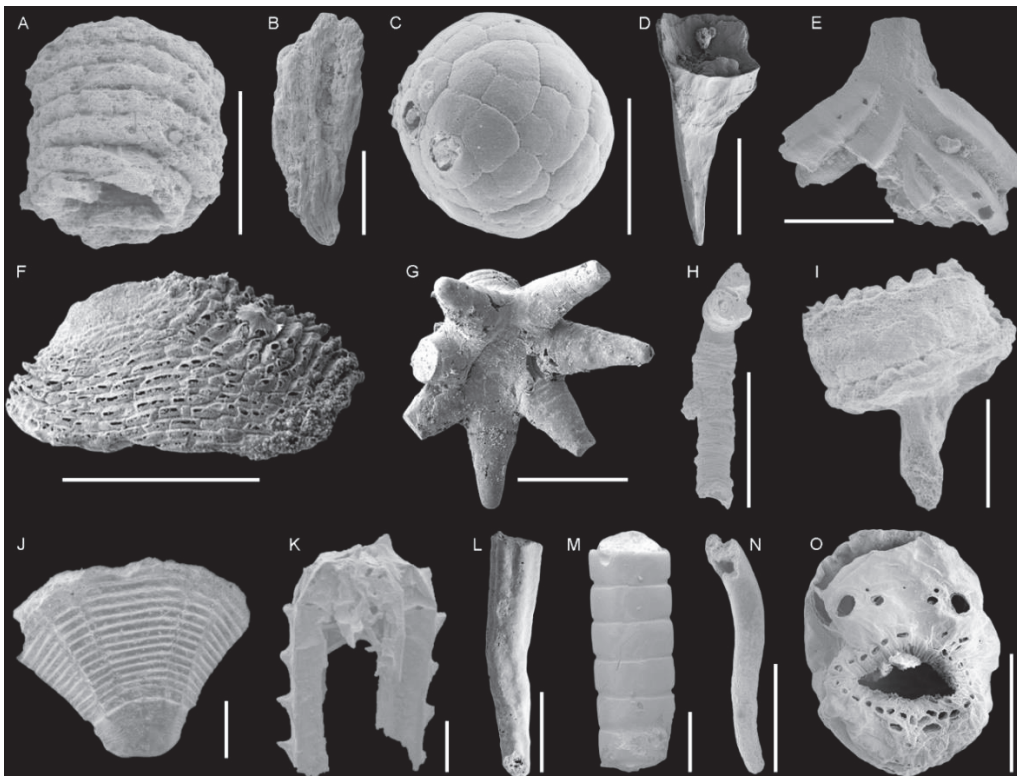


**Figure 7.** SEM images to show the diversity of the SSF assemblages from the Kuanchuanpu Formation (for scalidophorans, see Fig. 25). A. *Spirellus columnaris* Jiang in Luo et al., 1982, bacterial colony. B. *Cambriodidium capilloides* Jiang in Luo et al., 1982, algae. C. Undet. embryo. D. *Protohertzina anabarica* Missarzhevsky 1973. E. *Siphogonuchites triangularis* Qian, 1977. F. Mollusc shell. G. *Acanthocassis orthacanthus* Yang and He, 1984 and He and Xie, 1989, enigmatic fossil. H. *Feiyanella manica* Han et al., 2018, resembling *Cloudina*. I. *Eolympia pediculate* Han et al., 2010, cnidarian. J. *Hexaconularia* He and Yang, 1986, possible cnidarian. K. *Carinachites spinatus* Han et al., 2018, carinachitids. L. *Anabarites trisulcatus* Missarzhevsky in Voronova & Missarzhevsky, 1969. M. *Hyalithellus* Billings, 1871. N. *Conotheca* Rozanov et al. 1969. O. *Saccorhytus coronarius* Han et al., 2017. Scale bars: 1 mm (B, D, F, L, N), 500  $\mu\text{m}$  (A, E, G, J, K, M, O), 400  $\mu\text{m}$  (H), 200  $\mu\text{m}$  (C, I). (A-O) courtesy J. Han.

These Small Shelly Fossils (SSF) preserved in calcium phosphate, are a precious source of information to study the early stage of animal diversification and to better characterize the morphology of the remote ancestors of several major extant animal groups such as cnidarians and bilaterians, exemplified here by ecdysozoans.

### 3.1.1 Geological setting

The Kuanchuanpu Formation is exposed at various localities in the southern part of the Shaanxi Province (e.g. Xixiang and Zhangjiagou sections; Steiner et al., 2007) and the northern part of the Sichuan Province (Xinli section; Yang et al., 1983). Stratigraphical horizons of virtually the same age (basal Cambrian, ca 535 Ma) occur in the Zhujiaping Formation (eastern Yunnan Province), Maidiping Formation (central Sichuan Province), and Yanjiahe Formation (west Hubei Province) (see Fig. 10). Current research has mainly focused on the Zhangjiagou section (near Hanzhong City, southern part of the Shaanxi province) (Fig. 8C, D). All these localities belong to the South China block which crossed the palaeoequator during the Fortunian (earliest Cambrian, 541-529 Ma) and the late Neoproterozoic, and was close to the Australia block (Torsvik and Cocks, 2013; Fig. 8A). The Yangtse platform was the main sedimentary area of the South China block, in which the Kuanchuanpu Formation was deposited during the Fortunian (basal part of Cambrian, 541-529 Ma; Fig. 8B) (Qian et al., 1999; Steiner et al., 2014).

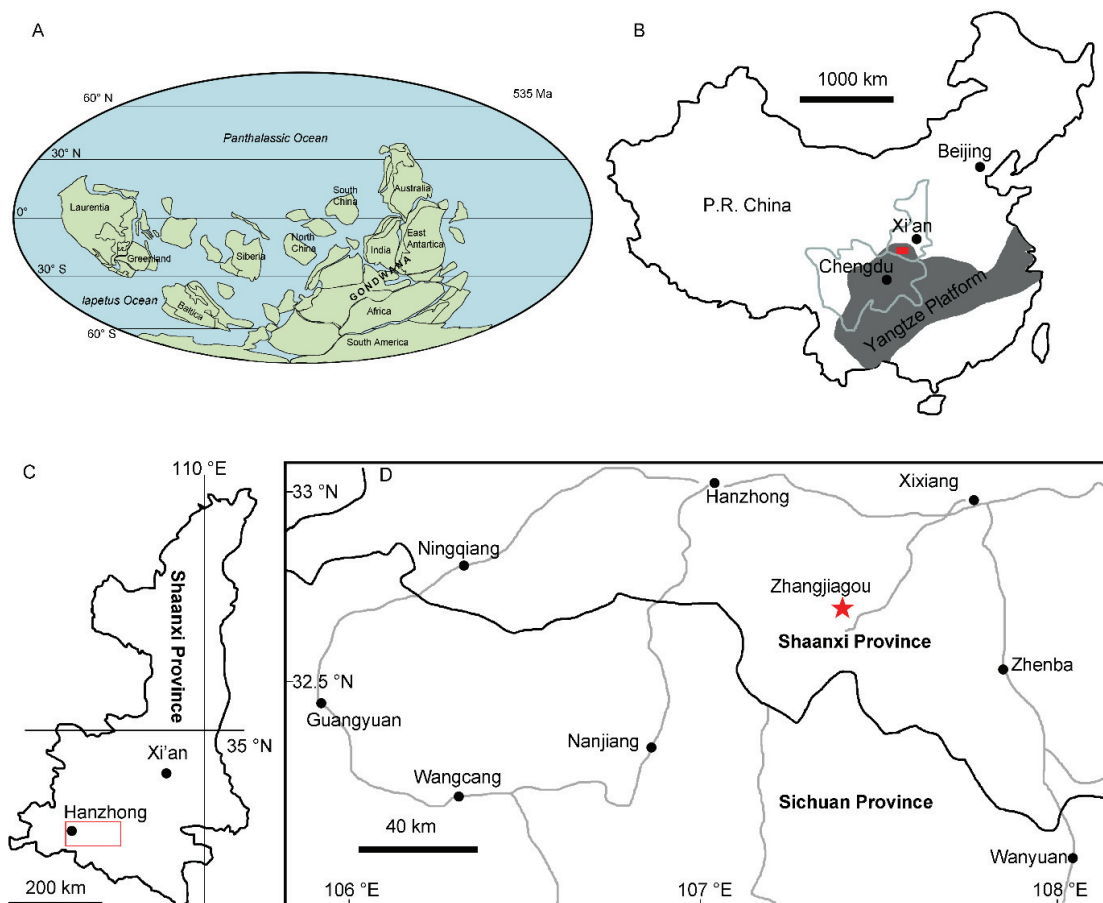


**Figure 8.** Main fossil localities where the Kuanchuanpu Formation is exposed. A. Palaeogeographic setting of the South China Block ca 535-million years ago (Ma), re-drawn from Torsvik and Cocks (2013). B-D. location maps of main fossil sites, along the Yangtze platform (dark gray), modified from Steiner et al. (2014), in the Shaanxi Province and near Zhangjiagou section, modified from Liu et al. (2014) and Wang (2018).

The Kuanchuanpu Formation unconformably overlays the Neoproterozoic Dengying Formation and underlays the Cambrian Guojiaba Formation (Fig. 9A). Its lower part consists of phosphatic limestones with thick interlayers of cherts and shales. SSFs are found in limestones within the middle-upper part (Fig. 9). The uppermost part of the formation is made of 10-m-thick clastic limestones containing breccia beds and conglomerates (Steiner et al., 2004; Steiner et al., 2020).

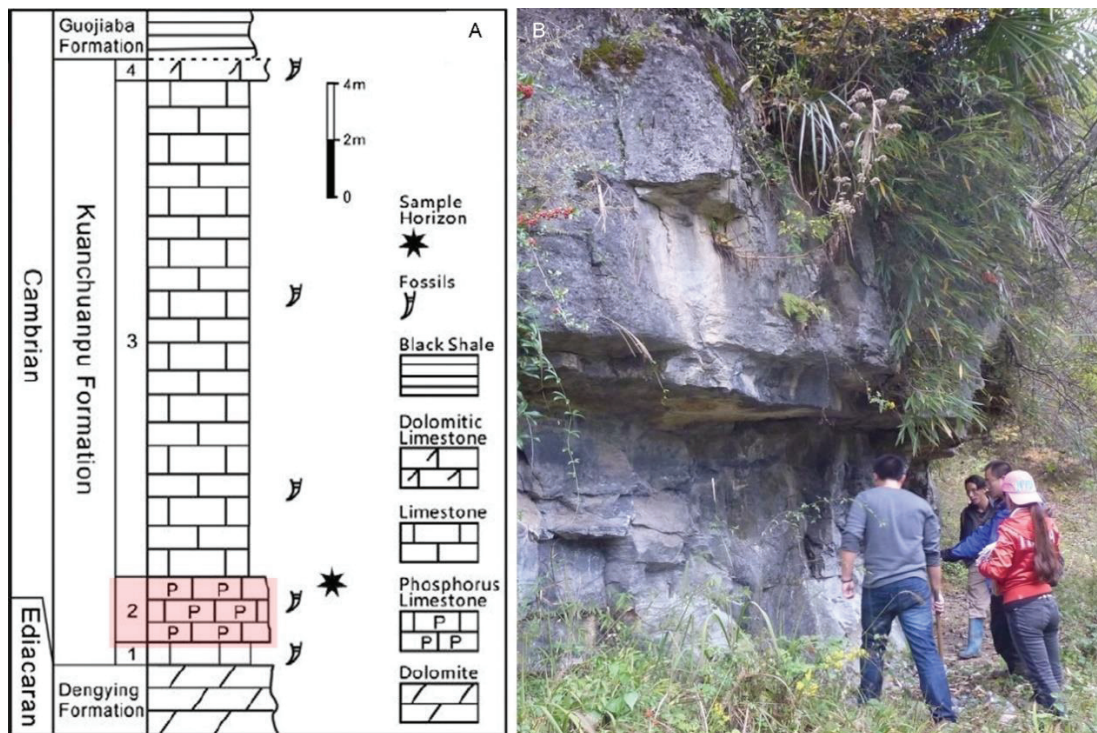


**Figure 9.** The Kuanchuanpu Formation at the Zhangjiagou section. A. Simplified log showing lithological succession, modified from Yang (2018); fossil-rich beds highlighted in red. B. Outcrop showing Bed 2 of the Kuanchuanpu Formation, that yielded most studied fossils.

These SSFs occur in an approximately 15-m-thick layer of phosphatic limestones that corresponds to *Anabarites trisulcatus*-*Protohertzina anabarica* biozone defined from the phosphorites of the lower Meishucunian (equivalent of Fortunian Stage) of the Yunnan Province, China (Steiner et al., 2004). The age of the Meishucunian phosphorites is  $536.5 \pm 2.5$  Ma (Sawaki et al., 2008). The approximate age of the Kuanchuanpu Formation (535 Ma) is given via correlations (Steiner et al., 2014).

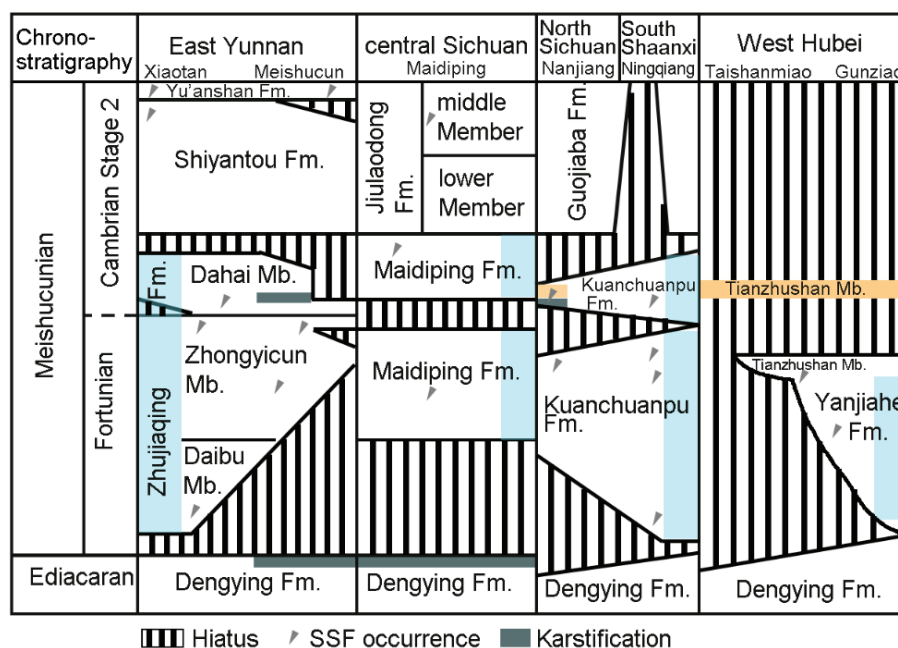




**Figure 10.** The Kuanchuanpu Formation and contemporaneous strata in the Yangtze platform (blue bars), modified from Steiner et al. (2020). Horizons with reworked fossils are indicated in orange.

When observed with a hand-lens, the weathered surface of limestones (Bed 2) often shows randomly scattered tiny fossils with a consistent black colour (Fig. 11A). These abundant SSFs can be released from rock samples through maceration in diluted acetic acid (methods see below). Most of these tiny fossils are fragments of tubular or vermiform organisms, or isolated spines and sclerites. Their average size is most frequently below 2 mm, except some tubular hyoliths that may reach more than 5 mm in length. These fossils and their preservational mode recall those from the Orsten-type Lagerstätten from Sweden (Maas et al., 2006; Müller, 1979) but do not contain any arthropod remains. Most SSFs from the Kuanchuanpu Formation are decay-resistant exoskeletal elements such as shells, tubes, and cuticular integument (Fig. 11B, C). A relatively small proportion of them are complete or incomplete soft-bodied animals such as cnidarian embryos (Fig. 7I) which display very fine and 3D-preserved details of their internal structure. Elemental analysis indicate that these exoskeletal and soft tissue remains were secondarily phosphatized, the most abundant chemical elements being O, C, Ca, and P (Fig. 11E).

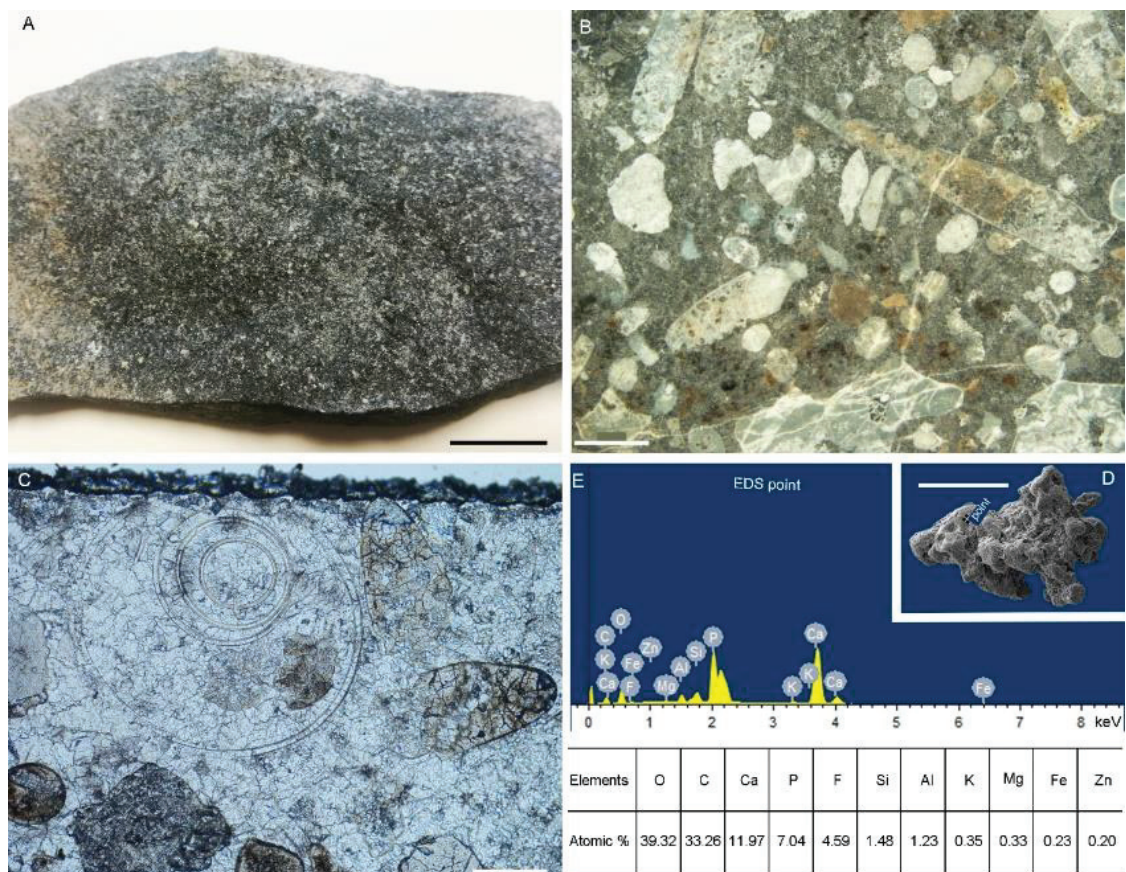


**Figure 11.** Small Shelly Fossils from the Kuanchuanpu Formation. A. As they appear on the surface of rock (tiny black spots). B. Slab of hand specimen, showing SSFs arranged irregularly (unweathered part, SSFs in white or gray). C. Thin section showing a coiled form and other fossil fragments. D. Fragment of SSF extracted from rock after acid maceration. E. Chemical composition of (D), showing enrichment in oxygen, carbon, calcium and phosphorus. Scale bars: 2 cm (A), 200  $\mu$ m (B, C), 500  $\mu$ m (D). (B, C) courtesy X.-G. Yang.

### 3.1.2 Palaeoenvironmental setting and taphonomy

It is a difficult task to characterize the depositional environment of the Kuanchuanpu Formation because of tectonic disturbances in the rock succession across the late Ediacaran-Cambrian transition. Rare scientists have tried to tackle the problem (Cui et al., 2020; Li, 1984; Steiner et al., 2004). In the Xixiang area (Zhangjiagou section), the presence of photosynthetic cyanobacteria suggests that marine communities lived within the photic zone (Vogel and Marinovich Jr., 2004; Yang, 2018; Yang et al., 2017) in a relatively shallow-water environment. This opinion is also supported by sedimentary features such as low-angled (ca. 8°) hummocky cross-stratification (HCS), which normally characterize depositional environments somewhere below the fair-weather wave base and above the storm-weather wave base (Wang, 2018). Further, tubular SSFs are often abraded, suggesting interactions with coarser grains in a possible fluctuating tidal environment (Cui et al., 2020; Steiner et al., 2001).

SSFs found in concentration layers and associated with HCS might indicate that they have been transported by currents (allochthonous burial; Wang, 2018). Indeed, complete organisms are extremely rare, exemplified by scalidophoran worms that are mainly represented by trunk fragments (Liu et al., 2014; Zhang et al., 2015). However, the relatively low sorting of the SSFs (Fig. 11B) would indicate that transportation operated over a relatively short distance. Lithoclasts and phosphatic grains in SSFs-bearing limestone suggest that both SSFs and host-sediment may have been reworked during early diagenesis, possibly via the action of relatively high-energy current (e.g. tidal environment). Several authors (Cui et al., 2020; Steiner et al., 2014) suggested that most faunal elements had been redeposited before secondarily phosphatization and calcareous cementation took place.

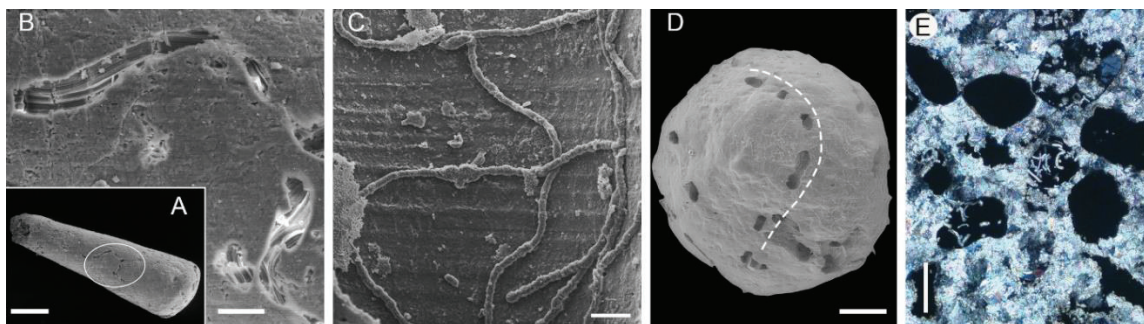


**Figure 12.** Micro-structures as indicators of preservation mode, taphonomy and diagenesis of SSFs. A, B. Ambient inclusion trails (AITs) on the tube of *Conotheca*, general view, and close-up showing details of AITs. C. SEM images of euendolithic cyanobacteria (*Endoconchia lata*) on the tube of *Conotheca*. D. Continuous AITs in embryo-like fossil. E. Thin section (crossed polarization) with AITs. Note that AITs do not extend into the calcareous cement. Scale bars: 500  $\mu\text{m}$  (E), 200  $\mu\text{m}$  (D), 100  $\mu\text{m}$  (A), 30  $\mu\text{m}$  (B, C). (A-E) courtesy X.-G. Yang.

Microbe traces closely associated to SSFs can also give clues on the chronological sequence of early taphonomic and diagenetic processes.

Euendolithic cyanobacteria (*Endoconchia lata*) specifically lived on the surface of rock or organisms and produced unbranched microborings. Some of them can be seen as internal moulds on the surface of SSFs (Bengtson et al., 1990; Runnegar, 1985; Fig. 12C). This suggests that these unbranched microborings were made when the host organism was still alive (Golubic S., 1975). Ambient inclusion trails (AITs) are hollow and form irregular micro-tunnels.

They are formed by the migration of small grains (e.g. diagenetic pyrite) that were propelled by gases (e.g. CH<sub>4</sub> and CO<sub>2</sub> released through the degradation of organic matter), resulting in microborings through the shells (Xiao and Knoll, 1999; Yang et al., 2017; Fig. 12A, B). AITs found in the Kuanchuanpu microfossils most probably appeared after the early phosphatization of sediment and animal remains (McLoughlin et al., 2007; Wang et al., 2017). AITs never occur within the internal calcareous infilling of SSFs (Yang et al., 2017; Fig. 12E), suggesting that calcareous cementation took place after AITs were formed. These micro-structures allow to reconstruct important chronological steps in the taphonomy and diagenesis of the SSFs from the Kuanchuanpu Formation (Wang et al., 2017).

### 3.1.3 Methods of study

Extracting SSFs from rock requires several steps and specific methods. Our method is that of Müller (1962). Phosphatic limestone are broken into walnut pieces and then put into 8%-10% acetic acid in buckets (Fig. 13A, B). It takes two or three days before the calcareous matrix is dissolved, and the SSFs released as insoluble residues (Fig. 13C). The residues are rinsed softly under taper water in order to clean out the residual acetic acid. Residues are air dried naturally and microfossils are picked up under a binocular microscopy (Fig. 13D).

Recently, the Northwest University colleagues (Prof. Jian Han's team) collaborated with Chinese engineers in order to apply artificial intelligence (AI) to pick and sort microfossils (Zhang et al., 2019). First, numerous and diverse types of images of SSFs (> 5000) were stored into the system as a database for AI recognition. These images were standardized in resolution, brightness, and magnification. A specific algorithm was designed using Python 3.6. This new system is currently able to distinguish tubular and spherical SSFs but cannot make the difference between tubular shelly fossil and a cylindrical worm fragment. More information (e.g. micro-ornament) still needs to be added to the database. This method has great potential to improve the efficiency of sorting SSFs and can be operated in automatic mode 24 hours a day and 7 days a week, thus reducing working costs and work arduousness. Fossil extraction and picking was performed during my first year at Northwest University under the supervision of my Chinese supervisor, Prof. Jian Han.



**Figure 13.** Successive steps from rock sampling to sorting and observing microfossils. A. Phosphatic limestone. B. Technical lab for fossil maceration in acid. C. Residues. D. Picking microfossils under the binocular microscopy. E-G. Scanning electron microscopy (SEM), X-ray microtomography (microCT, Northwest University, Xi'an) and synchrotron radiation X-ray tomographic microscopy (SRXRTM, Japan), respectively. scale bars: 2 cm (A), 3 cm (C).

Most phosphatic SSFs from the Kuanchuanpu Formation are devoid of mineralized internal tissues. The SSFs studied here were imaged by using scanning electron microscopy (SEM) both in China (FEI Quanta 400 FEG, secondary electron modes, Northwest University) and France (Zeiss Merlin compact, CT $\mu$ , University Claude Bernard Lyon 1). This method allowed high-resolution images of key external micro-ornament (e.g. worm cuticle) to be obtained (Fig. 13E). X-ray microtomography (microCT, Northwest University, China) and synchrotron radiation X-ray tomographic microscopy (SRXTM, Spring-8, Japan) were used in specimens with remnants of soft tissues or to reveal the 3D aspect of some morphological features with more accuracy (Fig. 13F, G). CT scans were assembled and processed with Dragonfly 4.0 software. Lithological slabs and thin sections through SSFs and the surrounding matrix were also made in order to study the microstructure and mineralization of cuticular elements (Fig. 11B, C).

## 3.2 The Chengjiang and other early Cambrian Lagerstätten

In parallel with the study of SSFs from the Kuanchuanpu Formation, I also focused on macrofossils from the early Cambrian Chengjiang Lagerstätte and comparable Chinese localities. These fossils were collected during successive field campaigns led by the Northwest University colleagues in the Yunnan Province, in which I took part as a first-year PhD-student. In contrast to SSFs, these macrofossils are preserved in compression and do not require specific chemical processing. They are obtained by splitting siltstone slabs and through careful preparation work under the binocular microscope using tiny needles, blades, brushes with soft hairs.

### 3.2.1 The Chengjiang Lagerstätte

The Chengjiang Lagerstätte owes its renown to the exceptional quality of its fossils and the very high diversity of its faunal assemblages. Since its discovery in 1984, ca 262 species have been described by scientists, that reveal the extraordinary beauty and complexity of early animal life exemplified by arthropods and scalidophorans (Hou et al., 2017). The Chengjiang Lagerstätte encompasses several localities and exposures in the Yunnan Province (Chen et al., 2002; Hou et al., 2017; Luo et al., 1999; Fig. 14B, C). It is now part of the world's natural heritage (UNESCO) and a highly protected area. Key faunal elements such as sponges (Rigby and Hou, 1995), cnidarians (Han et al., 2016b; Zhao et al., 2019), ctenophores (Ou et al., 2015), lobopodians (Liu et al., 2011; Ma et al., 2014; Ou et al., 2011; Ou and Mayer, 2018), brachiopods (Zhang et al., 2011), molluscs (Zhao, 2015), arthropods (Vannier et al., 2007; Zeng et al., 2020; Zhang et al., 2007), vetulicolians (Chen et al., 2003a; Ou et al., 2012; Shu et al., 2001), and chordates (Chen et al., 2003b; Shu et al., 1999) have been described in numerous scientific papers and textbooks (Chen et al., 2002; Hou et al., 2017; Luo et al., 1999).

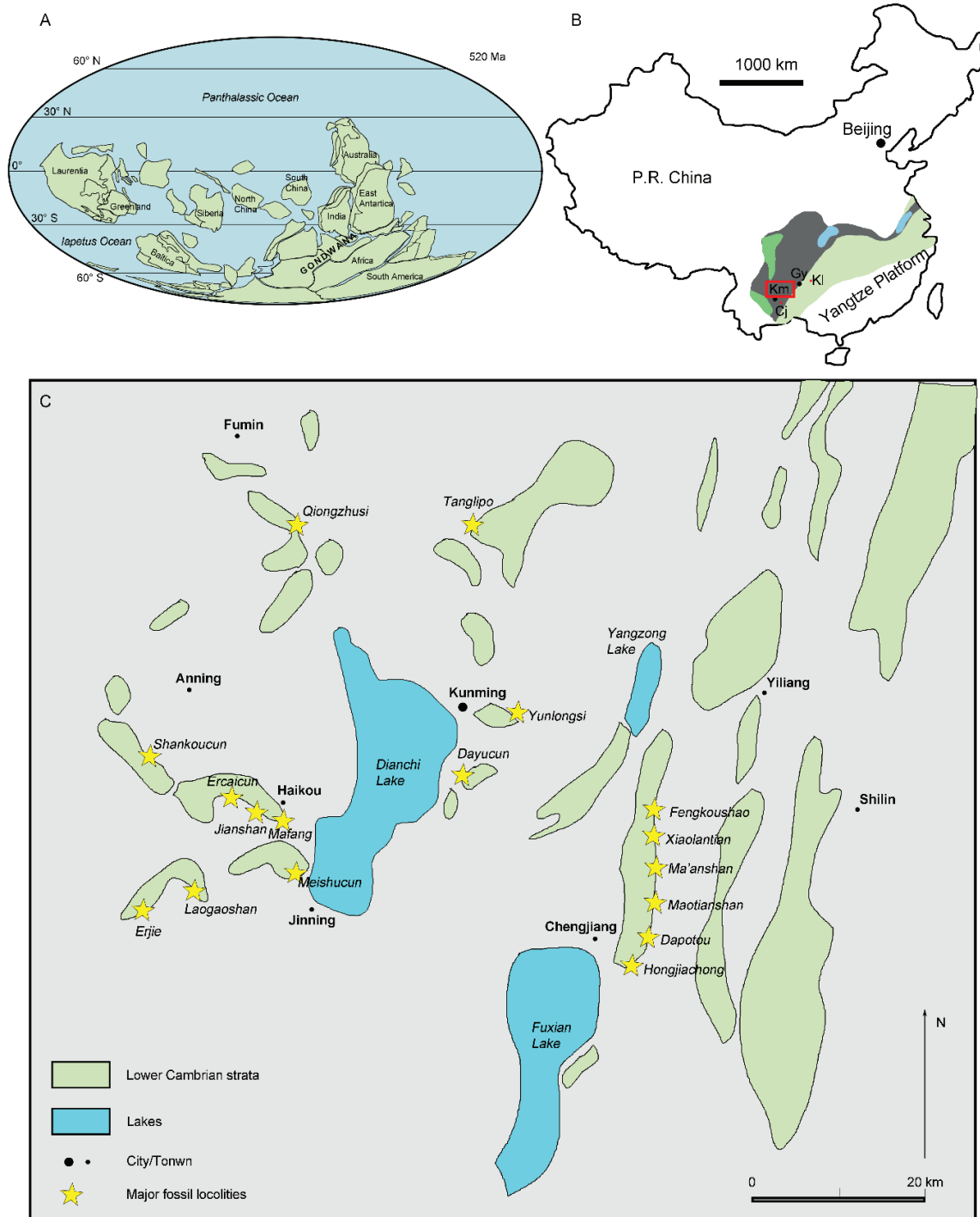


**Figure 14.** The Chengjiang Lagerstätte: main fossil localities. A. Palaeogeographic setting of the Yangtze platform during Cambrian Stage 3 (ca 518 Ma), modified from Torsvik and Cocks (2013). B. Distribution of sedimentary facies in the Yangtze platform during Cambrian Stage 3, modified from Zhang et al. (2008). Green colour in A and B represents plates and emerged land, respectively; light blue, light green, and grey colour represent carbonate platform, basin slope (mudstones), and clastic platform, respectively. C. Location map of the main fossil localities, modified from Hu (2005). Abbreviations: Km, Kunming; Gy, Guiyang; Cj, Chengjiang.

### 3.2.2 Geological setting

The palaeogeography in early Cambrian times differed markedly from that of present-day

and was dominated by the Gondwana supercontinent (Fig. 14A). South China formed a discrete continental block in the western part of Gondwana, possibly adjacent to the Indian block (Cocks & Torsvik 2013). Sediment deposition along the southwestern part of the Yangtze platform was almost continuous during the Fortunian Stage to the Stage 4 interval deposited (Fig. 14B). During the Cambrian, the Yangtze area seems to have been an epicontinental sea dominated by carbonate and clastic deposition in the SW regions, and by mudstones along the deep shelf to basin slope SE areas. The Chengjiang Lagerstätte was deposited along the shelf platform and is dominated by clastic facie. Chengjiang fossils come from several localities in the central and eastern Yunnan (Fig. 14B, C), such as Chengjiang, Jinning, Anning, Wuding, Yilang, Malong and Qujing counties and the Kunming District (Hou et al., 2017; Steiner et al., 2005; Zhang et al., 2008). The best-preserved fossils were collected from the eastern part of the Chengjiang County (Maotianshan, Ma'anshan, and Xiaolantian), and in the Haikou areas (Dianchi Lake, as at Ercaicun, Jianshan, Mafang).

The Chengjiang Lagerstätte occurs in the mudstone-dominated Yu'anshan Formation and corresponds with the *Eoredlichia-Wuyangaspis* trilobite biozone, Nangaoan Stage (Cambrian Stage 3), early Cambrian (Hou et al., 2017; Fig. 15). In most localities of the studied area the succession starts with the upper Ediacaran Dengying Formation, followed by the Zhujiaping, Shiyantou and the Yu'anshan Formation (Fig. 15). The fossil-bearing horizons of the Yu'anshan Formation, as they appear in outcrops, are often strongly weathered, and have a typical yellowish and beige colour. However, deeper excavations show that the original colour of these mudstones is light or dark gray. The most common fossils are trilobites and other arthropods that have a typical reddish colour (iron oxides) that sharply contrasts with the matrix.

The Yu'anshan Formation consists of four informal lithological units (Zhu et al., 2001). The lowermost strata consist of dark-grey siltstones containing the earliest known trilobites of eastern Yunnan as well as abundant bradoriid arthropods such as *Hanchiangella*, *Liangshanella*, and *Nanchengella*. These fossils belong to the *Hupeidiscus-Sinodiscus* biozone defined in south China (Hou et al., 2017). Just above this unit are yellowish or greenish mudstones interbedded with 10-20 cm of siltstones and sandstones, which have yielded the majority of the Chengjiang soft-bodied and lightly sclerotized fossils, such as arthropods, lobopodians, eldoniids, worms, and sponges. Altogether this second unit is ca. 40-50 m thick. The top part of the Yu'anshan Formation is represented by about 113 m of yellowish silty sandstones with sparse fossils mainly trilobites such as *Eoredlichia* and *Yunnanocephalus*. The most recent given age for the Yu'anshan Formation is ca. 518 Ma (Yang et al., 2018).

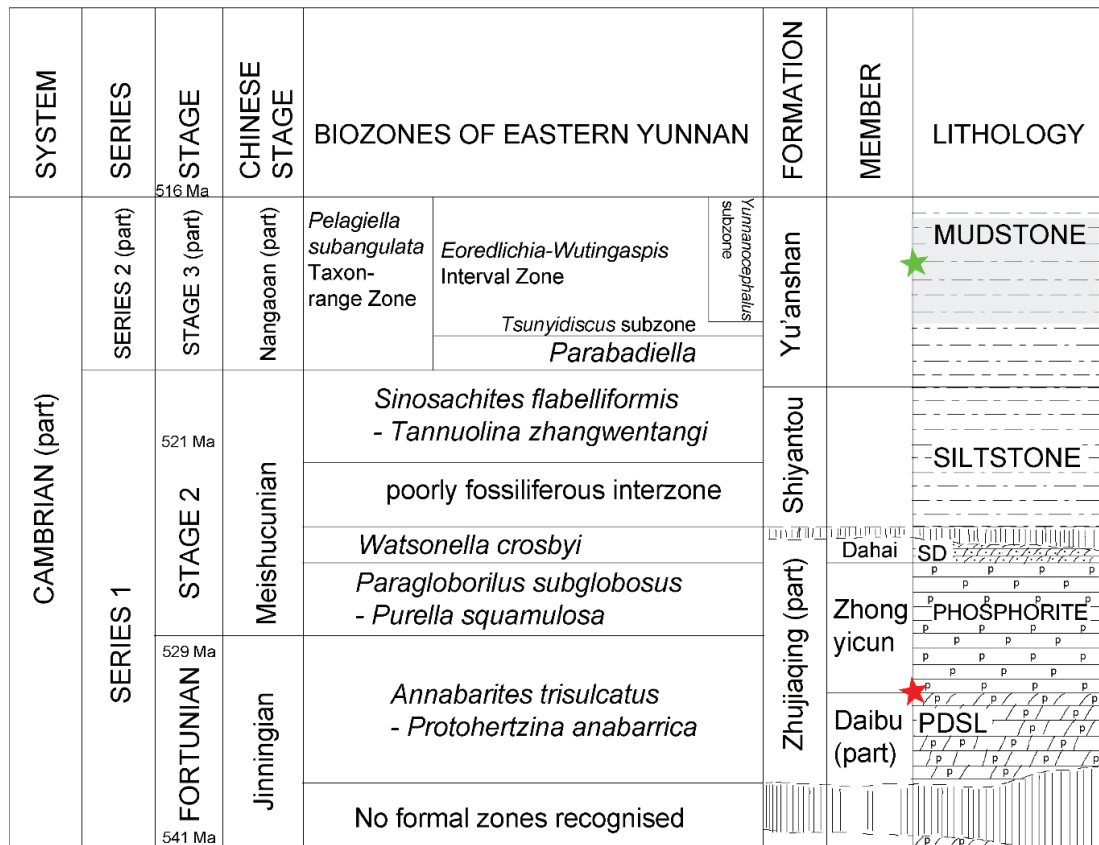


**Figure 15.** Lower Cambrian stratigraphy in the eastern part of the Yunnan Province. Green and red star indicate the stratigraphic position of the Chengjiang Lagerstätte (ca 518 Ma) and the oldest known SSF assemblages, respectively. Data from Hou et al. (2017) and the National Commission on Stratigraphy of China, (2015). SD, sandy dolomite; PDSL, phosphatic dolomite with thin siliceous layers.

### 3.2.3 Palaeoenvironment and taphonomy

The Chengjiang Lagerstätte was deposited in a relatively shallow, gently eastwardly sloping epeiric shelf environment dominated by mud and sand deposition (Hu, 2005; Zhang et al., 2008). The depositional environment is most probably deeper than the intertidal zone as hypothesized by Babcock et al., (2001).

One of the most typical sedimentary features of the host rocks of the Chengjiang Lagerstätte are intercalated background and event beds (Hu, 2005) which often form a rhythmic succession. Background beds dominantly comprise organic-rich laminae containing abundant algal fragments, small shells, and animal exuviae (Chen et al., 1996; Steiner et al., 2005). Event beds have a sharp base that show erosional sedimentary structures when interbedded with the background beds (Zhu et al., 2001). Most of the exceptionally preserved fossils (including those studied in my thesis) occur in such event beds. The quality of preservation of most fossils (e.g. complete arthropods with delicate appendages still attached to the body) and the alternation of background and event layers both suggest that most Chengjiang organisms were suddenly buried in situ by sediment inputs (hypautochthonous burial with almost no post-mortem transportation) resulting from the effect of periodical storms (Hu, 2005).

Comparable scenarios have been proposed for other Burgess-Shale-type (BST) Lagerstätten (Gaines et al., 2008), in which animal communities living at or near that water-sediment

interface were periodically affected by storm disturbances (Zhang et al., 2008) which implied the frequent recolonization. Hypoxic or anaerobic conditions are often seen as one the prerequisite conditions to the post-burial preservation of organisms in sediment. Burial in such low-oxygenated environments probably limited decay processes and kept carcasses away from potential scavengers (Allison and Briggs, 1993; Orr et al., 2003). The worms studied in my thesis were most likely endobenthic animals that have been exposed to the same sedimentary dynamics and taphonomic processes as other members of marine communities.

In contrast with the fossil material from the Kuanchuanpu Formation (see Fig. 7 and Chapter 4.1), that from Chengjiang is flat (two-dimensional compression) with exception of structures or organs that retain low three-dimensional relief (tube and pellets in *Selkirkia*, Fig. 16A; 17A, B; digestive glands of *Naraoia*, Vannier and Chen, 2002). Chengjiang fossils are characterized by the remarkable preservation of extremely labile anatomical features such as the tentacles of jellyfish (Han et al., 2016b; Zhao et al., 2019), the gills of possible deuterostomes (Shu et al., 2001), the appendages of arthropods (e.g. podomeres, setae; Fu et al., 2014) and more specifically here the micro-ornament of scalidophoran worms (e.g. scalids on introvert, pharyngeal teeth; see Chapter 5.3).

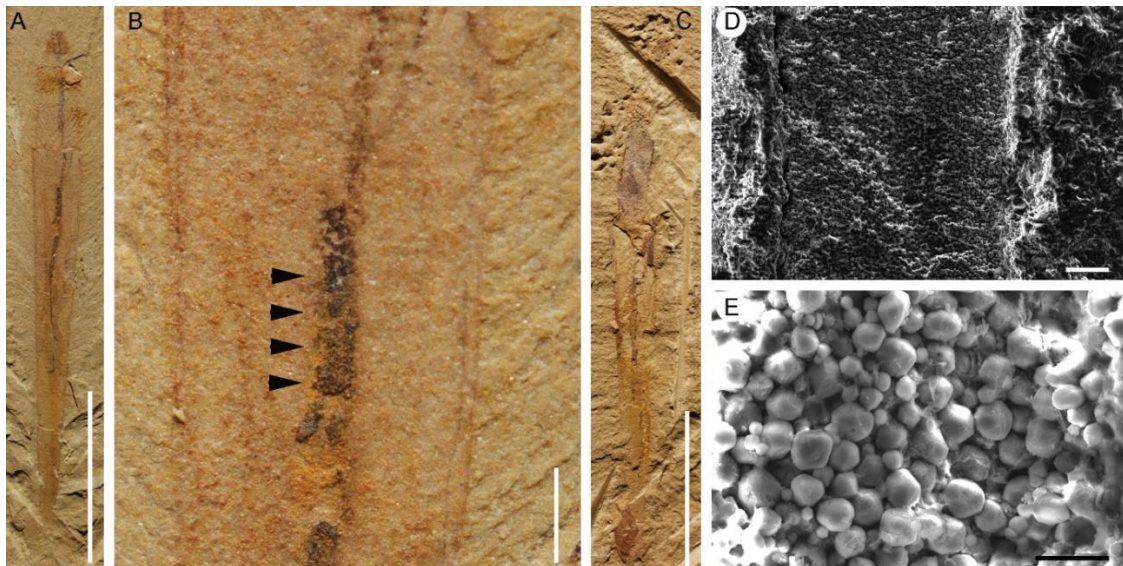


**Figure 16.** Preservation mode of Chengjiang fossils exemplified by *Selkirkia sinica* (Scalidophora). A, B. General view of *S. sinica*, close-up of gut content with organic remains (carbon film) and iron oxides (black arrowheads). C, D. General view of *S. sinica*, SEM image of tube wall filled with iron oxides. Scale bars: 5 mm (A, C), 400  $\mu\text{m}$  (B), 40  $\mu\text{m}$  (D), 10  $\mu\text{m}$  (E).

Elemental analyses indicate that most Chengjiang fossils contain aluminosilicates (Al, Si, O) and are locally enriched in elements such as Fe, S, P and C (see Fig. 17). Remains of soft tissues or gut contents are sometimes preserved as small patches of carbon films (Fig. 16B). The outline of most anatomical features is underlined by iron oxides (Gabbott et al., 2004; Zhu et al., 2005; Fig. 16E).

These iron oxides result from the oxidation of pyrite that coated the surface of animal carcasses. Pyrite is considered to be the product of bacterial sulphate reduction (BSR), through which bacteria obtain energy by oxidizing organic matter below the oxic–anoxic interface (Bernier, 1970; Vannier et al., 2014). In modern sediments (Bernier, 1984), precipitation of



pyrite takes place immediately following the precipitation of phosphate in the sulphate reduction zone below the redox boundary. As is the case for other Palaeozoic Lagerstätten (e.g. Fezouata; Kouraiss et al., 2018), diagenesis and weathering are responsible for the loss of sulphur and the transformation of pyrite into iron oxides (Gabbott et al., 2004; Fig. 16E).

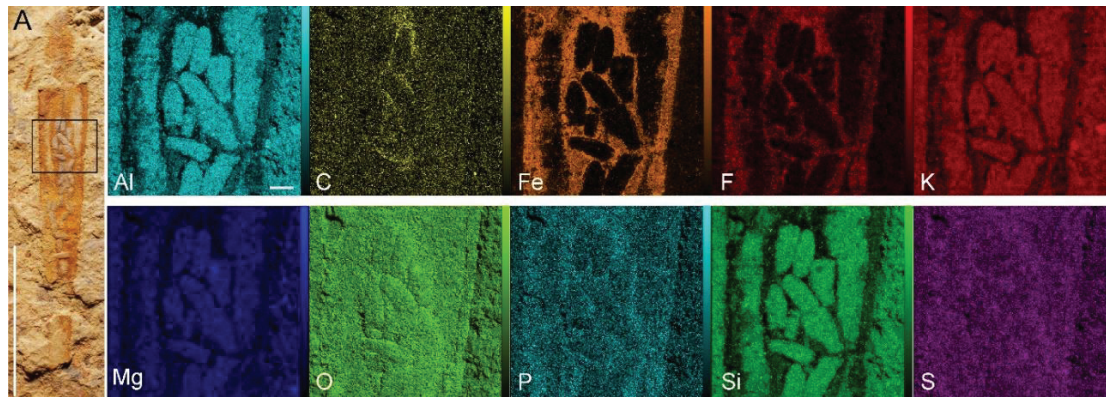


**Figure 17.** Elemental composition of Chengjiang fossils exemplified by *Selkirkia sinica* (Scalidophora). Scale bars: 5 mm (A), 200 µm (same scale for all maps).

Experimental taphonomy performed with various animal groups establishes a sequence of decay and indicates which anatomical features decay and disappear first, and how the overall appearance and internal organs of organisms often change dramatically through decay (Briggs, 2003; Murdock et al., 2014; Sansom, 2016). Although relatively limited in Chengjiang fossils, the effect of decay must be taken into consideration in order to avoid erroneous morphological interpretations. It was essential for me to observe numerous fossil specimens in order to make clear distinction between original biological features and artefacts due to decay.

Decay experiment conducted with the *Priapulid caudatus* (Scalidophora, Priapulida) reveals strong heterogeneity in decay processes such as the rapid loss of internal non-cuticular anatomy and the conservation of recalcitrant cuticular structures (Sansom, 2016). These interesting experiments indicate that a significant proportion of internal tissues are unlikely to be faithfully fossilized. This is precisely what we observed in scalidophoran worms from the Chengjiang Lagerstätte. Their cuticular ornament and digestive tract (gut contents such as pellets) are generally well-preserved. Almost no internal tissues are preserved with exception of possible oocytes (*Selkirkia*, see Chapter 5.4) and assumed retractor muscles (also, *Selkirkia*, see Chapter 5.3). Numerous scalidophoran worms from Chengjiang still display the original shape of their introvert, allowing relatively accurate reconstruction of their body and lifestyles.

### 3.2.4 Methods of study

The scalidophorans from the Chengjiang Lagerstätte were observed under the binocular microscope and prepared when necessary. Most specimens belong to the collections of Northwest University and were studied both in Xi'an and Lyon. Specimens of interest were photographed with a Canon EOS 5D Mark IV (University of Lyon 1) and Canon EOS 5DS R (Northwest University, Xi'an; Fig. 18B) digital camera. SEM was used to image fine anatomical details and microstructures, both in China (FEI Quanta 400 FEG, Northwest University, China;

Zeiss Merlin compact) and France (CT $\mu$ , University Claude Bernard Lyon 1, France; Fig. 20E). Back-scattered Electron Detector (MEB, FEI Quanta 250 FEG, University Claude Bernard Lyon 1, France) and X-ray Fluorescence (XRF, Northwest University, Zeiss Merlin compact; Fig. 18C) were used for elemental mapping. MicroCT was used to explore the internal structure of some fossil specimens (Fig. 13F). The Dragonfly 4.0 software was used to process CT data and make 3D-reconstructions.



**Figure 18.** Methods of study applied to the Chengjiang fossils. A. Fieldwork in the eastern part of the Yunnan Province near Erjie village. B. Photography with digital camera. C. X-ray Fluorescence (XRF).

### 3.2.5 The Xiaoshiba Lagerstätte

I also examined early Cambrian fossils from the Xiaoshiba Lagerstätte which lies in the lower part of the mudstone-dominated Hongjingshao Formation and belongs to the *Yunnanocephalus-Chengjiangaspis-Hongshiyanaspis* biozone (Cambrian Series 2, Stage 3; Yang et al., (2013); Fig. 15). This Lagerstätte has yielded numerous arthropods such as *Fuxianhuia* (Yang et al., 2013) and scalidophorans such as *Mafangscoplex cf. yunnanensis* (Yang et al., 2020) and *Selkirkia sinica* (Lan et al., 2015) described in my thesis. I took part in a joint research project with colleagues from the Yunnan University, that concentrated on the reproduction mode of Cambrian scalidophorans (Chapter 5.4).

## 3.3 Comparative studies with extant priapulid worms

### 3.3.1 Material

Scalidophorans (see Table 2) have extant microbenthic and meiobenthic representatives in modern marine ecosystems and can easily be observed and collected in several localities of northern Europe (e.g. Sweden and the White Sea in Russia) and North America (Trott, 2017; van der Land, 1970) such as the iconic species *Priapulus caudatus* that preferentially lives in cold and poorly oxygenated waters. Detailed observations of the morphology and behaviour of extant priapulids were essential to my research work and allowed better to argument interpretations of fossil species.

Ten specimens of *Priapulus caudatus* were collected from the Gullmarsfjord (58°15'3"-58°16'39"N; 11°25'36"-11°26'34"E; depth ca 40 m; salinity ca 33 PSU [Practical Salinity Unit]), near the Kristineberg Marine Research Station (KMRS; Göteborg University) and sixty-three specimens *Halicryptus spinulosus* were collected from the brackish waters of the Baltic Sea (at

58°50'53"-58°50'48"N;17°32'22"-17°32'32"E; depth ca 16 m; salinity ca 7 PSU), near the Askö Laboratory, Baltic Sea Centre, (Stockholm University) (Fig. 19C, E). This research travel and a one-month-stay at the Kristineberg Marine Station (September 2019) was part of a research project supported by ASSEMBLE Plus. Additional specimens of *P. caudatus* collected by Jean Vannier near the White Sea Biological Station (northern part of Russia; University of Moscow) were also studied.

*Maccabeus tentaculatus* (Fig. 19F) is a rare meiobenthic species that rarely exceeds 3 mm long. Some specimens were obtained on loan from the zoological collections of the Hebrew University in Jerusalem, Israel. This priapulid secretes mucus from glandular scalids, that is used to cement around particles and form a protective tube (Por and Bromley, 1974). These specimens also allowed detailed comparisons with Cambrian ones, especially concerning reproductive organs and strategies.



**Figure 19.** Extant priapulids. A-E. Sampling work in Sweden. A. Location of sampling spots (image from Google map). B, C. Askö Laboratory in the background where *Halicryptus spinulosus* (live specimen) was collected. D, E. Sampling of *Priapulus caudatus* near the Kristineberg Marine Station (live specimen). F. *Maccabeus tentaculatus* Por and Bromley (1974), a microbenthic priapulid from Cyprus (specimen in alcohol, provided by the Hebrew University, Israel). Scale bars: 3 cm (E), 1 cm (C), 200 µm (F).

### 3.3.2 Methods

Freshly collected priapulids (*P. caudatus* and *H. spinulosus*) were stored in a room at 10 °C (KMRS). This temperature is comparable with that of their natural environment. As *P. caudatus* is relatively large and has cannibalistic habits, each individual was kept in a separate plastic box (ca 20 cm) filled with sea water and black mud from their respective habitats. *H. spinulosus* is relatively smaller than *P. caudatus* and the collected specimens were placed into three tanks (10 cm x 17 cm) filled with seawater and mud from their natural brackish environment (Askö). Seawater was changed every two days after being oxygenated (bubble pumps, 2 hours). Animals were fed with tiny fragments of mussel soft tissues. *P. caudatus* and *H. spinulosus* are active burrowers and generally dig into the sediment immediately after being deposited on mud and remain concealed in sediment. Animals were repeatedly taken from mud for various laboratory observations (e.g. locomotion, moulting process). Photographs and videos of several specimens were taken (Fig. 20A, B). After taking the photos, animals were returned to the cold room.

Specimens of both species were eventually fixed (glutaraldehyde) (Appendix 1), kept in 70% Ethanol and desiccated (Leica Critical Point Dryer; CT $\mu$ , University of Lyon) for microscopic observations under the SEM. *P. caudatus* and *H. spinulosus* secrete mucus which traps sedimentary particles and detritus along their body surface (Oeschger and Janssen, 1991), thus preventing clear observation of cuticular ornament. Fine cuticular features were best observed in freshly moulted specimens and exuviae. Images of dissected and whole specimens were taken with a ZEISS Merlin Compact Scanning Electron Microscope (SEM) at the Centre Technologique des Microstructures (CT $\mu$ , University Claude Bernard Lyon 1; Fig. 20C, D) and Leica binocular microscope.

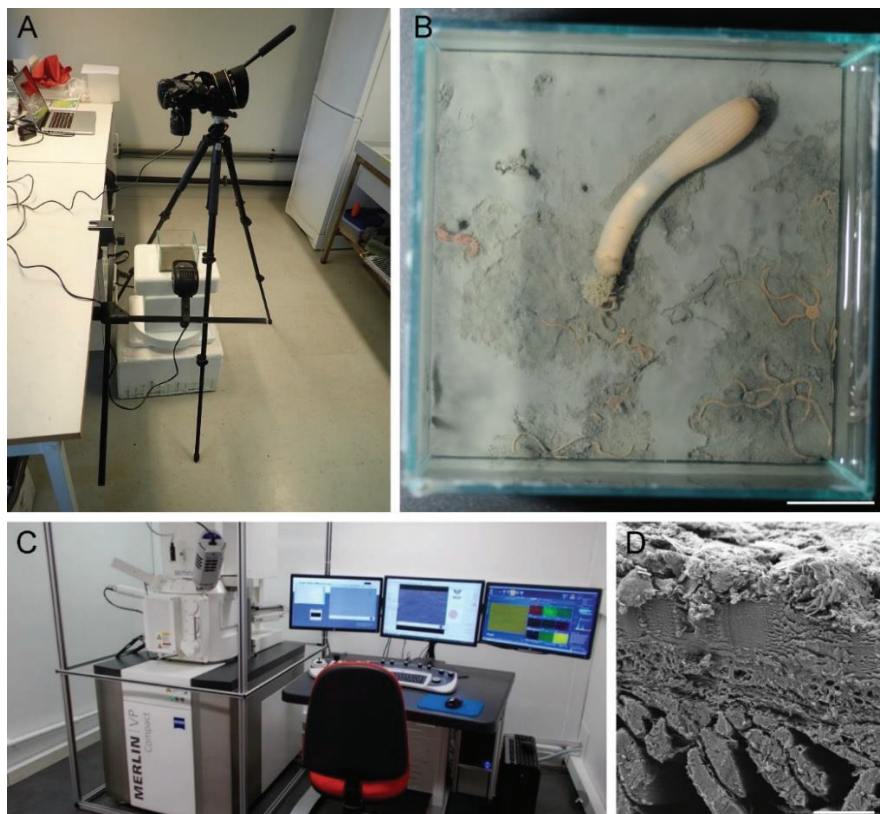


**Figure 20.** Extant priapulids: methods of study. A. Digital camera with a tripod to take photos and videos of living specimens. B. Photo of a live specimen in a tank (KRMS, Sweden). C. Scanning Electron Microscope (CTμ, Lyon). D. SEM image showing section through cuticle (*P. caudatus*, after preparation and desiccation). Scale bars: 3 cm (B), 4 μm (D).

Some specimens of *P. caudatus* and *H. spinulosus* were embedded in resin (EPON), sliced (Ultramicrotome Reichert Ultracut S; CTμ, Lyon) and stained with Toluidine blue for observation of cellular and cuticular features using optical microscopy (Fig. 21).

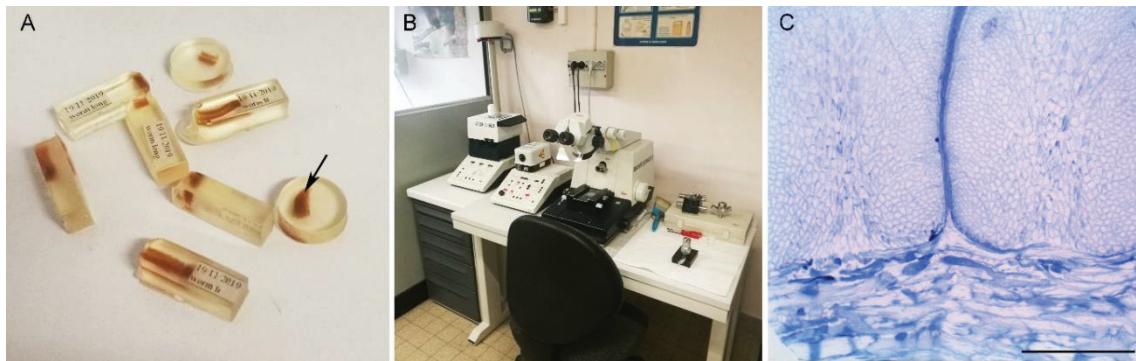


**Figure 21.** Biological cross-sections. A. Specimens (arrow) embedded in resin. B. Ultramicrotome for slicing embedded specimens. C. Section through the cuticle of *P. caudatus* (optical microscopy). Scale bar: 250 μm (C).

### 3.4 Phylogenetic analyses

Numerous extinct and extant scalidophoran species have been described by scientists (Conway Morris, 1977a; Fu et al., 2019; Peel, 2010a, b; Schmidt-Rhaesa, 2013; van der Land, 1970). However, there are still important uncertainties concerning their phylogenetic relationships and the origin and chronology of divergence of major subgroups (Han et al., 2004a; Maas et al., 2007a; Wills et al., 2012). I found it important to use several phylogenetic methods in order to analyse the phylogenetic relation among cycloneuralian taxa including maximum parsimony (MP; Farris, 1970; Fitch, 1971), maximum-likelihood (ML; Nguyen et al., 2015) and Bayesian inferences (Huelsenbeck and Ronquist, 2001; Ronquist et al., 2012).

Under MP criterion, optimal tree will minimize the amount of homoplasy (i.e., convergent evolution, parallel evolution, and evolutionary reversals). However, if the selected taxa have experienced convergent evolution or parallel evolution, the results will not be good. A new method TreeSearch package in R\* is based on single-character parsimony algorithm (Brazeau et al., 2019). It was designed for analysing data set based on morphological traits of fossils, which had many missing or inapplicable characters (Brazeau et al., 2019; Smith, 2018). ML stresses on the maximum similarity of morphological characters. The problem of ML is long-branch attraction artefacts (Laumer et al., 2015). Bayesian inference is statistics method based on posterior probability, which can control for the potential systematic artefacts (Laumer et al., 2015).

The three algorithms correspond to four software. TNT v.1.5 (<http://www.lillo.org.ar/phylogeny/tnt/>; Goloboff and Catalano, 2016) and TreeSearch package in R\* v.0.4.3 (<https://github.com/ms609/TreeSearch>; Smith, 2018) are based on MP. Visualization of results of TreeSearch was by the Inapp package

(<https://github.com/TGuillerme/Inapp>; Guillerme et al., (2018). In TreeSearch, MorphyLib was used to handle inapplicable data (Brazeau et al., 2017). MrBayes 3.2.6a is based on Bayesian inference (<http://nbisweden.github.io/MrBayes/>). IQ-TREE 1.6.12 is based on ML (<http://www.iqtree.org/#download>).

The dataset, focusing on cycloneuralian relationships, is based on discrete morphological characters modified from Harvey et al., (2010) and Zhang et al., (2015). The updated dataset re-considered the morphological characters and corresponding codes (see Appendices 2, 3).

The dataset was analyzed by the four software. The results were compared with each other. Mesquite v.3.61 was used to scrutinize the optimization of relevant character states (Maddison and Maddison, 2019). RogueNaRok was to search for rogue taxa destabilizing the tree (Aberer et al., 2013).

### **3.5 Work schedule**

The first year of my PhD (June 2017 to November 2018) was carried out at Northwest University, Xi'an, China in Prof. Jian Han's laboratory. This period was devoted to field work (several times), rock sampling (ca 500 kg) and extracting SSFs from rock through maceration in diluted acetic acid. In parallel, I focused on reading many scientific papers and textbooks on ecdysozoans, especially cycloneuralians, in order to acquire basic knowledge on both fossil and present-day animals. At the same time, I learned how to recognize various Chengjiang and Kuanchuanpu fossils.

After my first year I moved to Lyon (December 2018 to February 2021) as a PhD-student supported by the China Scholarship Council (CSC) and the Northwest University (during a 3-month extension due to the Covid19-situation in Europe). During this period, I studied at the Laboratoire de Géologie de Lyon: Terre, Planètes, Environnement (LGLTPE) based at the University Claude Bernard Lyon 1, under the supervision of Jean Vannier. In 2019, I took part in a summer school in the Azores Islands (Portugal) in order to learn about meiofaunal organisms (including microbenthic scalidophorans). I also went to Sweden (September 2019) for collecting macrobenthic priapulids in the framework of an ASSEMBLE Plus project.

# Chapter 4 Early ecdysozoans: review of previous work

## 4.1 Precambrian-Cambrian transition

Most evolutionary scenarios based on molecular data and calibrated by (sometimes questionable) fossil occurrence predict a remote origin for Ecdysozoa, deeply rooted into the Ediacaran (Cunningham et al., 2017; Paterson et al., 2019; Schumann et al., 2018; Fig. 22). However, no solid fossil evidence has been presented so far that supports this prediction (Fig. 2). Numerous uncertainties remain concerning possible ecdysozoan candidates in the Precambrian. The oldest unambiguous ecdysozoans are those found in the lowermost Cambrian of the Kuanchuanpu Formation and represented by a great variety of scalidophoran worms (Liu et al., 2018; Liu et al., 2014; Zhang et al., 2018; Zhang et al., 2015; Fig. 25) and lobopodians (unpublished information; Fig. 27).

Iconic fossils from the Ediacaran of Australia and Russia such as *Parvancorina minchami* and *Spriggina floundersi* (ca 555 Ma; (Glaessner, 1958; Fig. 22A, B) do resemble arthropods in their overall shape, segmented body and clear antero-posterior polarity that might suggest some kind of “proto-cephalization”. However, *Spriggina* has a glide symmetry (e.g. anterior shield-like structure) that typifies numerous Ediacaran organisms such as rangeomorphs (Laflamme et al., 2018) and *Dickinsonia* (Evans et al., 2015). The shield-like anterior part of its body has no direct counterpart in arthropods either. The morphology of *Parvancorina* is very simple and lacks any multisegmented pattern. Possible affinities with molluscs instead of arthropods have been proposed by Naimark and Ivantsov, (2009) based on its growth mode and resemblances *Temnoxa* (Ivantsov et al., 2004).

*Yilingia* is an intriguing fossil recently described from terminal Ediacaran Dengying Formation (basal part of Shibantan Member) in south China that appears to be an elongate and segmented bilaterian with an assumed trilobate structure (central lobe flanked by posteriorly pointing lateral lobes; Chen et al., 2019; Fig. 22C). These body fossils are often associated with a long and continuous trail that the animal is supposed to have made in sediment. Chen et al. (2019) suggest that this enigmatic animal might be related to annelids or ecdysozoans (possibly panarthropods). However, this hypothesis was questioned by Shu and Han (2020) based on the lack of mouth and gut in the fossils.

*Vittatusivermis annularius* is another an enigmatic worm-like organism from the lowermost Cambrian of South China (ca 535 Ma) that is also associated with possible trails and burrows (Zhang et al., 2017; Fig. 22F). It bears clear external annulations. Zhang et al. (2017) suggested that this relatively large animal (8 to 18 mm in width, 260 mm in maximum length) had a hydrostatic skeleton and moved through its environment via peristaltic contractions as do modern priapulid worms. This option cannot be excluded and *Vittatusivermis* may have been one of the numerous potential makers of trace fossils found across the Precambrian-Cambrian boundary. However, these findings do not significantly contribute to resolving the origin of ecdysozoans since unambiguous and well-preserved scalidophorans do occur in other Cambrian localities of virtually the same age (Kuanchuanpu Formation, 535 Ma; see *Eopriapulites* and *Eokinorhynchus* (< 2mm in length; Liu et al., 2014; Zhang et al., 2015). *Vittatusivermis* may represent another type of ecdysozoans that did not occur in the Kuanchuanpu biota. Zhang et al. (2017) noted that the annulated structure of *Vittatusivermis*

resembled that of *Wutubus annularius* (Chen et al., 2014; Fig. 22E) a problematic fossil from the late Ediacaran. However, *W. annularius* resembles tubular animals such as *Cloudina* or *Conotubus* (Chen et al., 2014) and should not be considered as a worm. External “annulations” do not necessarily indicate ecdysozoan affinities as numerous animals such as deuterostome enteropneusts and annelids (Brusca et al. 2016) have an annulated and fluid-filled body (Zhang et al., 2017).

*Treptichnus pedum* are index trace fossils found across the Ediacaran-Cambrian boundary which are subhorizontal burrow systems produced in the subsurface (Vannier et al., 2010; Fig. 22D). Experimental ichnology with *Priapulid caudatus* (Scalidophora, Priapulida; Vannier et al. (2010) suggest that these complex burrow systems may be produced by priapulid-like animals that used their introvert, muscles and hydrostatic skeleton to dig into the sediment in a multi-directional manner. In addition, fine longitudinal structures observed along the burrow casts of *Treptichnus* suggest that the trace maker had a scolid-bearing introvert probably very similar with that of extant *Priapulid caudatus* (Kesidis et al., 2019). Although the makers are absent, these trace fossils strongly suggest the ecdysozoan clade had scalidophoran-like ancestors in the late Ediacaran (Kesidis et al., 2019).

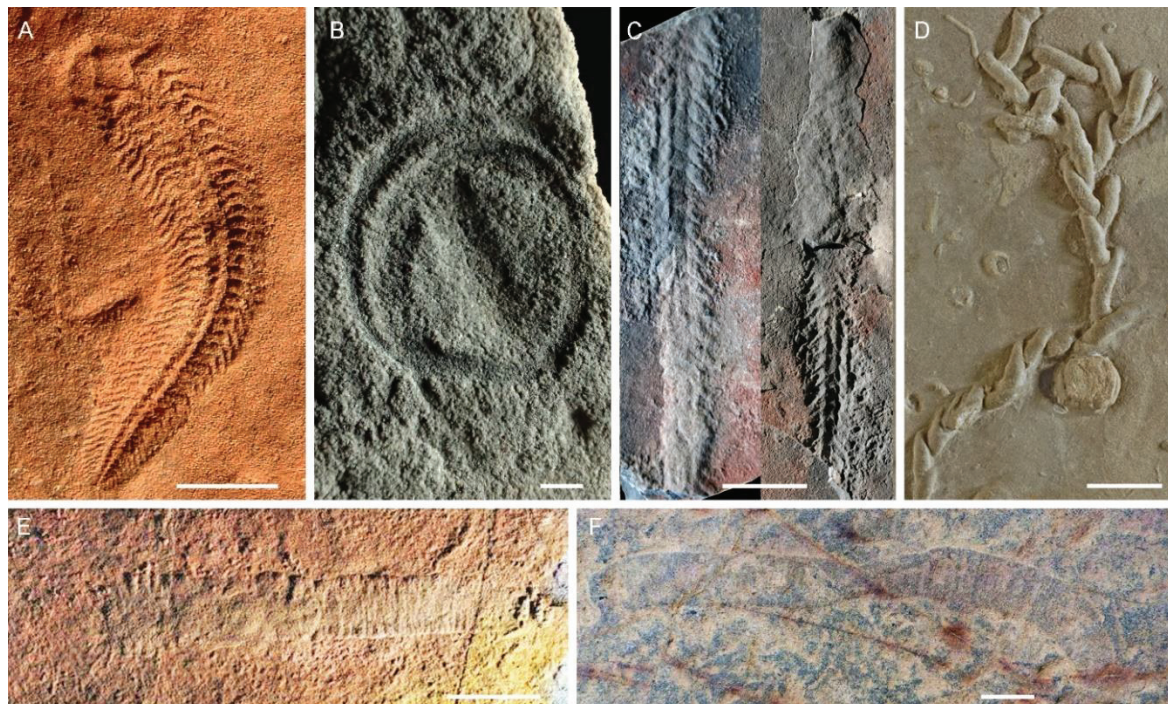


**Figure 22.** Supposed ecdysozoans from Precambrian or Precambrian-Cambrian boundary. A. *Spriggina flouderesi* Glaessner, 1958. B. *Parvancorina minchami* Glaessner, 1958. C. *Yilingia spiciformis* Chen et al., 2019. D. *Treptichnus pedum* Vannier et al., 2010. E. *Wutubus annularius* Chen et al., 2014. F. *Vittatusivermis annularius* Zhang et al., 2017. Scale bars: 2 cm (C, E), 1 cm (A, D, F), 1 mm (B). (A, B) from Glaessner (1958). (C) from Chen et al. (2019). (D) courtesy Jean Vannier. (E) from Chen et al. (2014). (F) from Zhang et al. (2017).

Cambrian Lagerstätten and other types of exceptional fossil localities provide abundant and accurate fossil evidence that ecdysozoans were present in the early Cambrian and diversified throughout the Cambrian period (Fig. 23). They played a major role in marine ecosystems as bioturbators, predators and recyclers.

Over the last few decades, a huge amount of scientific papers revealed the extraordinary



variety of ecdysozoans found in numerous early and mid-Cambrian Lagerstätten such as those of Chengjiang, Qingjiang, Guanshan, Kaili, south China (Fu et al., 2019; Hou et al., 2017; Hu et al., 2013; Zhao, 2011), Sirius Passet, Greenland (Conway Morris et al., 1987; Peel, 2010a), Sinsk, Russia (Ivantsov et al., 2005), Emu Bay, Australia (Paterson et al., 2016), and the Burgess Shale, Canada (Briggs et al., 1994). Arthropods are particularly well represented and seem to have been the dominant animal group in most marine ecosystems (Aria et al., 2015; Daley and Legg, 2015; Vannier et al., 2018; Yang et al., 2013; Zeng et al., 2020). Compared to soft-bodied animals (e.g. jellyfish, ctenophores, worms), arthropods possess a stiff cuticular exoskeleton that has a relatively high potential to be fossilized by various pathways (e.g. phosphatization, preservation as small carbonaceous fossils (SCF), aluminosilicate replication), which might partly explain their over-representation in the fossil record (taphonomic bias). The purpose of this chapter is not to review the abundant literature on Cambrian ecdysozoans as a whole but to concentrate on basal groups, essentially scalidophorans.

As already mentioned above, the earliest known unambiguous ecdysozoans are those from the lowermost Cambrian Kuanchuanpu Formation, south China. They almost exclusively consist of scalidophoran worms (Liu et al., 2014; Zhang et al., 2015) and rare lobopodians (unpublished information, see below).

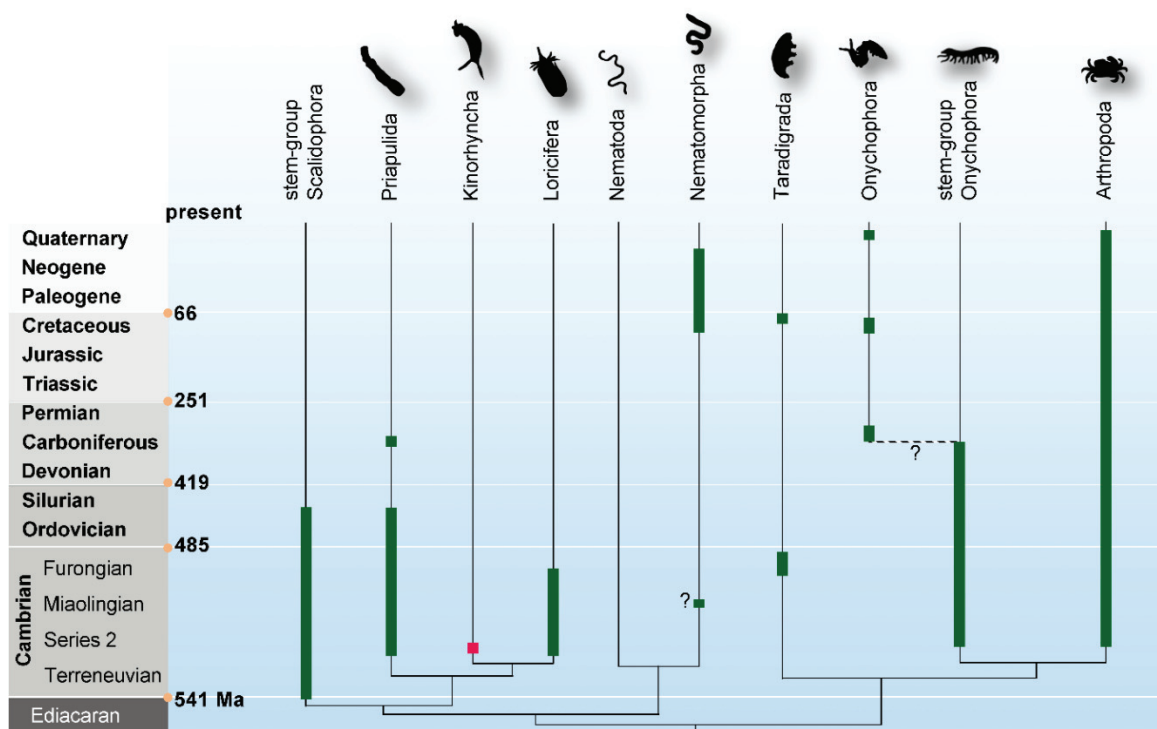


**Figure 23.** Distribution of fossil ecdysozoans through geological times, modified from Wang et al. (2020). Green and red bars represent attested and possible fossil occurrences, respectively. Lobopodians form an informal category that accommodates various panarthropods; some of them are tentatively placed here with the stem-group Onychophora as suggested by some authors (e.g. Caron and Aria, 2017; Yang et al., 2015). Question mark with dotted line indicate uncertainties concerning the divergence time of Onychophora.

## 4.2 Basal Cambrian: the oldest known ecdysozoans

### 4.2.1 Scalidophora

Fossils from the Kuanchuanpu Formation provide very detailed information on scalidophoran diversity at 535-million-years-ago. Although complete specimens are relatively rare, six different species have been recognized by previous authors and twelve unnamed forms are awaiting to be described (Liu et al., 2018; Shu and Han, 2020; Wang et al., 2019; Zhang et al., 2018; Fig. 25A-F). Most of these scalidophoran worms have been tentatively assigned to the stem-group Priapulida, a smaller percentage of them to the stem-group Kinorhyncha. Anatomical features of extant scalidophorans are given in Figure 24.

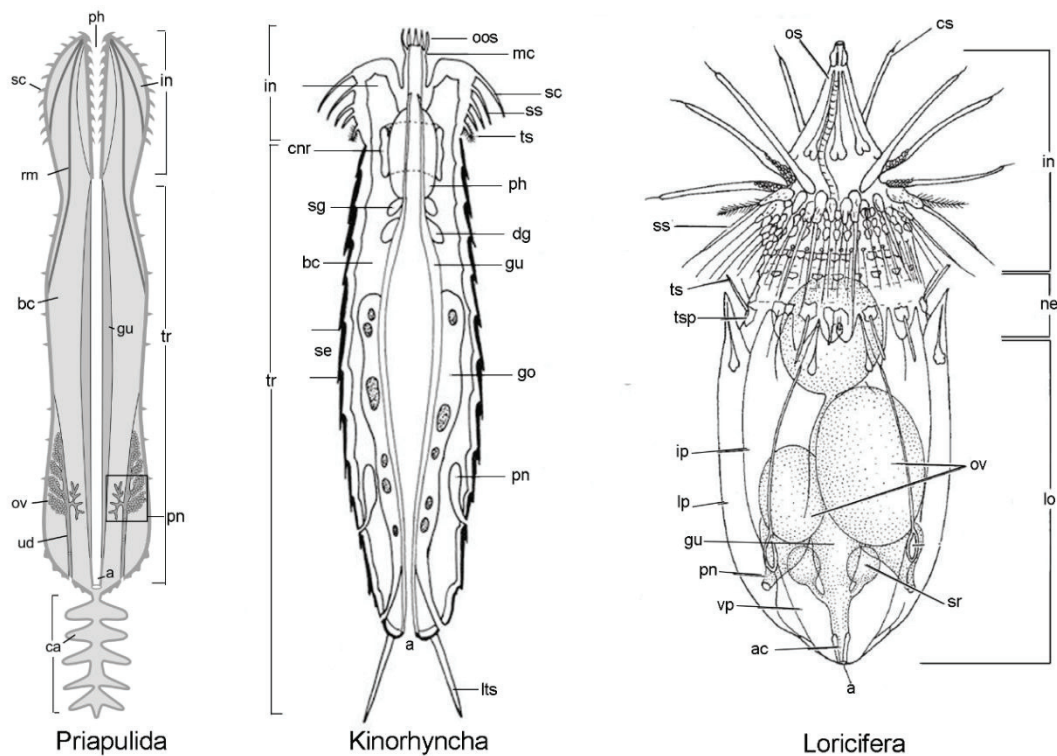


**Figure 24.** General body plan of extant scalidophorans. A. Priapulida. B. Kinorhyncha. C. Loricifera. Abbreviations: a, anus; ac, anal cone; bc, body cavity; ca, caudal appendage; cnr, circum-pharynx nerve ring; cs, clavoscalid; dg, digestive gland; go, genital gland; gu, gut; in, introvert; ip, intermediate plate; lo, lorica; lp, lateral plate; lts, lateral terminal spine; mc, mouth cone; ne, neck; oos, outer oral style; os, oral stylet; ov, ovary; ph, pharynx; pn, protonephridium; rm, retractor muscle; sc, scalid; se, segment; sg, salivary gland; sr, seminal receptacle; ss, spinoscalid; tr, trunk; ts, trichoscalid; tsp, trichoscalid plate; ud, unogenital duct; vp, ventral plate. (A) courtesy J. Vannier. (B) from Neuhaus (2013). (C) modified from Neves et al. (2013). Drawings not to scale.

#### 4.2.1.1 Priapulida

*Eopriapulites sphinx* is a scalidophoran worm characterized by an introvert armed with scalids, a pharyngeal area with hexaradially arranged teeth and an annulated trunk devoid of cuticular outgrowths such as sclerites (Liu et al., 2014; Shao et al., 2016; Shao et al., 2019; Fig.

25A). It resembles extant priapulids in overall morphology (e.g. subdivision of introvert; see *Priapulid*, van der Land, 1970), circumorally coronal scalid (*Maccabeus*, Por and Bromley, 1974), and caudal projection (*Maccabeus*, Salvini-Plawen, 1974). However, the hexaradial symmetry of the pharyngeal teeth of *Eopriapulites* has no equivalent in extant scalidophorans (e.g. priapulids typically have pharyngeal teeth arranged in a pentaradial manner) but occurs in nematoids (Adrianov and Malakhov, 2001; Schmidt-Rhaesa, 2013). Thus, Shao et al. (2019) considered *E. sphinx* as a possible member of the stem-group Cycloneuralia. However, *E. sphinx* has many more similarities with Priapulida than any other ecdysozoan groups. The significance of variations in the symmetry modes exemplified by pharyngeal teeth and scalids requires further investigation.

#### 4.2.1.2 Kinorhyncha

Extant kinorhynchs are all meiofaunal species with total body length ranging from 0.13 to 1.04 mm. Their main diagnostic features are an introvert with a protrusible mouth cone, a neck and 11 trunk “segments” (zonites). The introvert bears pentaradially arranged scalids of various types. Kinorhynchs also have a pair of lateral terminal spines (Neuhaus, 2013; Fig. 4B).

Overall resemblances with modern representatives of the group have led several authors to consider *Eokinorhynchus rarus* (Zhang et al., 2015; Fig. 25B) and *Zhongpingscolex qinensis* (Shao et al., 2020; Fig. 25C) from the Kuanchuanpu Formation as ancestral kinorhynchs and the earliest known species of the group. *E. rarus* bears an introvert, a neck, and a trunk. Both introvert and neck are annulated. The first two series of scalids distribute in 25 longitudinal rows, the third to fifth ones in 10 rows. At least two paired large sclerites occur bilaterally along at the assumed ventral side (Zhang et al., 2015). The external surface of the trunk bears unusually broad annulations (macroannulation), compared with the closely-spaced microannulations of most Cambrian scalidophorans. These macroannulations vaguely recall the “segments” of extant kinorhynchs. However, most of the complex features that characterize the kinorhynch “segments” cannot be found in *E. rarus*. For example, the “segment” of extant kinorhynchs typically consists of one to three ventral and one dorsal cuticular plates (Neuhaus, 2013). This character is not found in *Eokinorhynchus*. In addition, *E. rarus* bears neither an oral style, nor spinoscalids and trichoscalids that are diagnostic features of extant kinorhynchs. Whether *Eokinorhynchus rarus* is a kinorhynch or not thus remains questionable.



**Figure 25.** Scaldiphoran worms from the early Cambrian Kuanchuanpu Formation. A. *Eopriapulites sphinx* Liu et al., 2014. B. *Eokinorhynchus rarus* Zhang et al., 2015, a kinorhynch-like scaldiphoran worm. C. *Zhongpingscolex qinensis* Shao et al., 2020. D. *Qinscolex spinosus* Liu et al., 2018. E. *Shanscolex decorus* Liu et al., 2018. F. *Dahecolex kuanchuanpuensis* Shao et al., 2019. G-J. Unpublished scaldiphorans (ELI collections). G. ELIXX87-355 showing different types of sclerites along trunk. H. ELIXX73-300 showing sparse small sclerites on each annulated ring. I. ELIXX25-1 showing microfolded trunk with presumably closely-spaced annulations and no sclerites. J. ELIXX102-310, possible loriciferan showing longitudinal ridges (lorica). Scale bars: 1 mm (E-I), 500  $\mu$ m (B-D, J), 200  $\mu$ m (A). (A, C-F) reproduced here with the permission from Elsevier. (B) courtesy H.-Q. Zhang.

#### 4.2.1.3 Loricifera or loricate larvae of Priapulida

Loriciferans and the loricate larvae of priapulids (Kirstensen, 1983; van der Land, 1970) have their body (except introvert) encased within a lorica (e.g. *Maccabeus tentaculatus*; Por and Bromley, 1974; Salvini-Plawen, 1974; Fig. 26). The lorica is formed by the regional thickening of the cuticle and consists of several plates connected by a thinner and flexible cuticular layer (Bang-Berthelsen et al., 2013).

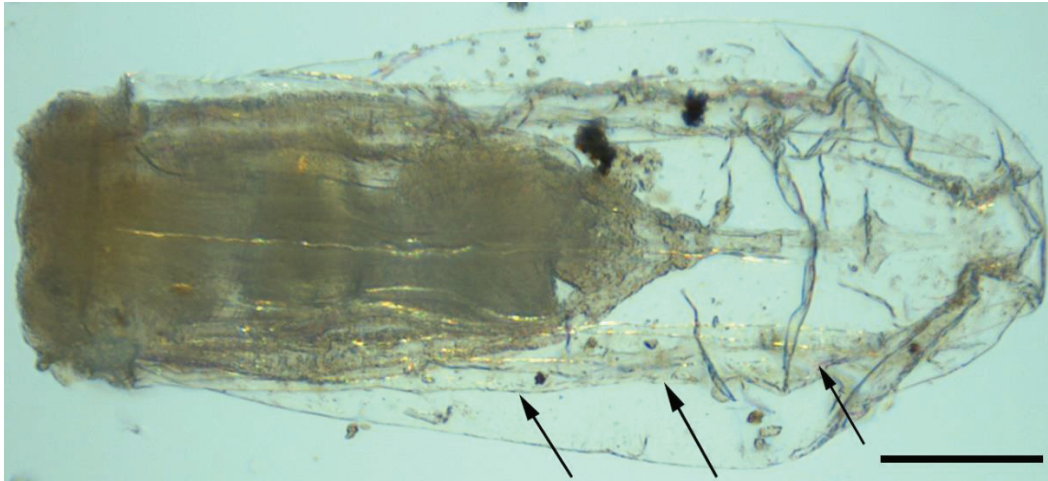


**Figure 26.** Lorica of *Maccabeus tentaculatus* Por and Bromley (1974), from Cyprus, seen in transmitted light. Cuticular ridges indicated by black arrows. Scale bar: 100  $\mu\text{m}$ .

Only one specimen (Fig. 25J) from our ELI collections displays longitudinal features with a sharp relief that closely resemble the typical longitudinal ridges of loricae (e.g. *Pliciloricus pedicularis*, Gad, 2005) and larval priapulids (e.g. *Tubiluchus corallicola*, Schmidt-Rhaesa, 2013; van der Land, 1968). Resemblances with the mid-Cambrian loricated larvae *Orstenoloricus shergoldii* (Maas et al., 2009) should also be noted. The anterior part of this undescribed form shows holes arranged longitudinally but neither a mouth cone nor oral stylets. The longitudinal ridges (Fig. 25J) may represent original biological features or may alternatively result from the post-mortem radial shrinkage of a smooth lorica as suggested by Maas et al. (2009) for *O. shergoldii*. A single specimen is definitely not sufficient to confirm the presence of loriciferans or loricated larvae of priapulids in the Kuanchuanpu fauna.

#### 4.2.1.4 Scalidophorans of uncertain affinity

Three scalidophoran species, namely *Dahesclex kuanchuanpuensis* (Shao et al., 2019), *Shanscolex decorus* (Liu et al., 2018) and *Qinscolex spinosus* (Liu et al., 2018) have been established, based on incomplete and relatively poorly preserved specimens (e.g. showing a small part of introvert or trunk). Although these forms most probably belong to Scalidophora, the lack of visible diagnostic features makes their placement within Priapulida or any other group, uncertain.

Similarly, our collections contain numerous undetermined more or less complete fragments (e.g. well-preserved trunk, incomplete or missing introvert) that could potentially represent new species (Fig. 25G-I). For example, one specimen shows two types of sclerites of its trunk (Fig. 25G) and has six anterior rows of sclerites with an elliptical basis and four posterior ones with a more rectangular shape. Another specimen represented by a trunk fragment (diameter ca 1 mm; Fig. 25H) shows annulated rings bearing a large sclerite and much smaller ones (ca 16). These fine cuticular details are unfortunately unable to tell us to which scalidophoran group these specimens may belong.

In summary, eighteen scalidophoran species have been established and three additional forms are still undetermined. Based on their cuticular ornament, two types of scalidophoran worms may be distinguished, those with no cuticular outgrowths on their trunk, such as

*Eopriapulites sphinx* (e.g. sclerites, Figs 25I) and those bearing both small and larger sclerites such as *Eokinorhynchus rarus* (Fig. 25B-H).

## 4.2.2 Panarthropoda

Rare undescribed specimens collected over the last ten years from the Kuanchuanpu Formation seem to represent lobopodian fragments (Fig. 27). They consist of a roughly cylindrical, segmented body on which regularly spaced paired conical structures are attached (Fig. 27A, C). These structures strongly recall the paired legs of Cambrian lobopodians such as *Paucipodia* (Chen et al., 1995) and *Antennacanthopodia* (Ou et al., 2011). However, no claws have been found at the tip of these assumed legs (see for example in Smith and Ortega-Hernández, 2014; Vannier and Martin, 2017). The anterior part of the body may be incomplete. Although no paired dorsal sclerites (e.g. *Microdictyon*, Chen et al., 1989; *Cardiodictyon*, Hou et al., 1991) can be seen, the trunk and limbs of these assumed lobopodians display a relatively well-preserved reticulated network made of five-to-seven-sided polygons. This pattern is known in some Cambrian lobopodians such as *Microdictyon* (Chen et al., 1989) and scalidophoran worms (Wang et al., 2020). Such micro-reticulated networks have been recently interpreted as replicating the boundaries between the epidermal cells that secrete the cuticle.

Up to now, the only ecdysozoans remains found in the Kuanchuanpu fauna are worms (Scalidophora) and lobopodians (Panarthropoda). None of the hundred residues so far extracted from rocks has yielded any arthropod cuticular fragment (e.g. part of jointed appendage, setae, cuticular sensory features typical of arthropods). In contrast, typical Orsten-type faunas (e.g. Sweden, Maas et al., 2006; Sichuan in south China, Dong et al., 2004) display a great variety of arthropod remains such as tiny larval stages and countless cuticular fragments (e.g. appendages, setae). Since the preservation mode (secondary phosphatization) of the Kuanchuanpu fossils is comparable with those of Orsten-type deposits, it would be natural to find arthropod remains if they had been present. Two options may be considered: 1) arthropods had not yet emerged 535 million years ago; 2) arthropods, if present lived in a different type of environment, i.e., different from that occupied by scalidophoran worms and lobopodians.

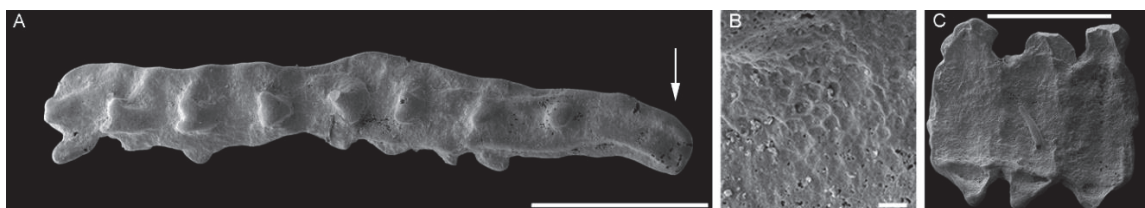


**Figure 27.** Lobopodian fossils from Kuanchuanpu Formation. A. Complete specimen showing head (white arrow) and trunk with paired, bud-like limbs. B. Close-up of limb in (A) showing cuticular reticulation. C. Trunk fragment showing clear segments with paired limbs. Scale bars: 1 mm (A, C), 20  $\mu\text{m}$  (B).

## 4.3 Early Cambrian: diversification of ecdysozoans exemplified by the Chengjiang Lagerstätte and coeval localities

As already mentioned above, ecdysozoans are arguably the most dominant animal group of the Cambrian period as exemplified by early Cambrian Lagerstätten such as those of

Chengjiang, Qingjiang, Guanshan, Shipai, Balang in south China (Fu et al., 2019; Hou et al., 2017; Hu et al., 2013; Peng et al., 2015; Yang and Zhang, 2016a, b), Sirius Passet in Greenland (Budd, 1999; Conway Morris and Peel, 2010; Peel, 2010a, b), Emu bay in Australia (García-Bellido et al., 2013; Paterson et al., 2016) and Sinsk in Siberia (Ivantsov and Wrona, 2004)(Fig. 28). A great variety of arthropods, lobopodians, and scalidophorans prevail in these Lagerstätten. Scalidophorans are mainly represented by priapulid-like worms. By contrast, kinorhynchs and loriciferans are relatively rare whereas nematoids and tardigrades seem to be absent (Tables 2, 3).

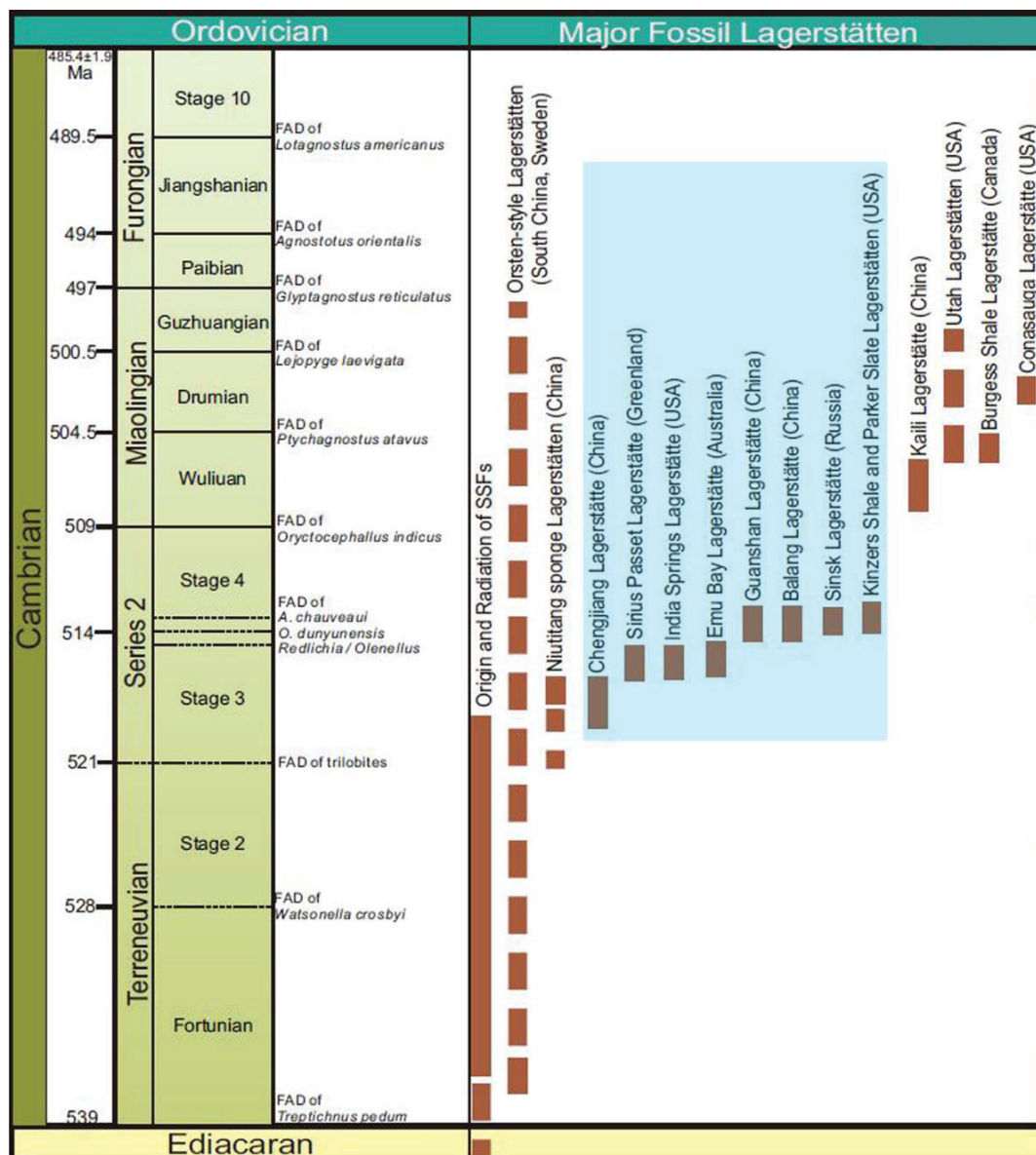


**Figure 28.** Major Cambrian Lagerstätten from Zhu et al. (2019). Blue area indicates major early Cambrian Burgess-Shale-type (BST) Lagerstätten.

## 4.3.1 Scalidophora

### 4.3.1.1 Kinorhyncha

Kinorhynch fossils are extremely rare. However, well-preserved specimens have been recently discovered from the early Cambrian Qingjiang Lagerstätte (Fu et al., 2019), which are awaiting to be described in details. One of them is ca 2 cm long- i.e., 20 to 200 times larger than extant representatives of the group (0.13-1.03 mm, Neuhaus 2013; Fig. 4B). It shows an introvert and a trunk with possibly 16 segments that may correspond in number and shape to the zonites of modern kinorhynchs. These segments clear differ from the annulations seen in other Cambrian scalidophorans, which are usually more closely spaced. (e.g. palaeoscolecsids, Hou and Bergström, 1997; *Tylotites*, Han et al., 2007b). No cuticular ornament is visible on these external segments. Part of the three-dimensional gut is exposed in the anterior part anterior of the trunk. More importantly, paired lateral terminal spines directed posteriorly occur at the trunk end. These features (segmented body, lateral spines) are typical of modern kinorhynchs.

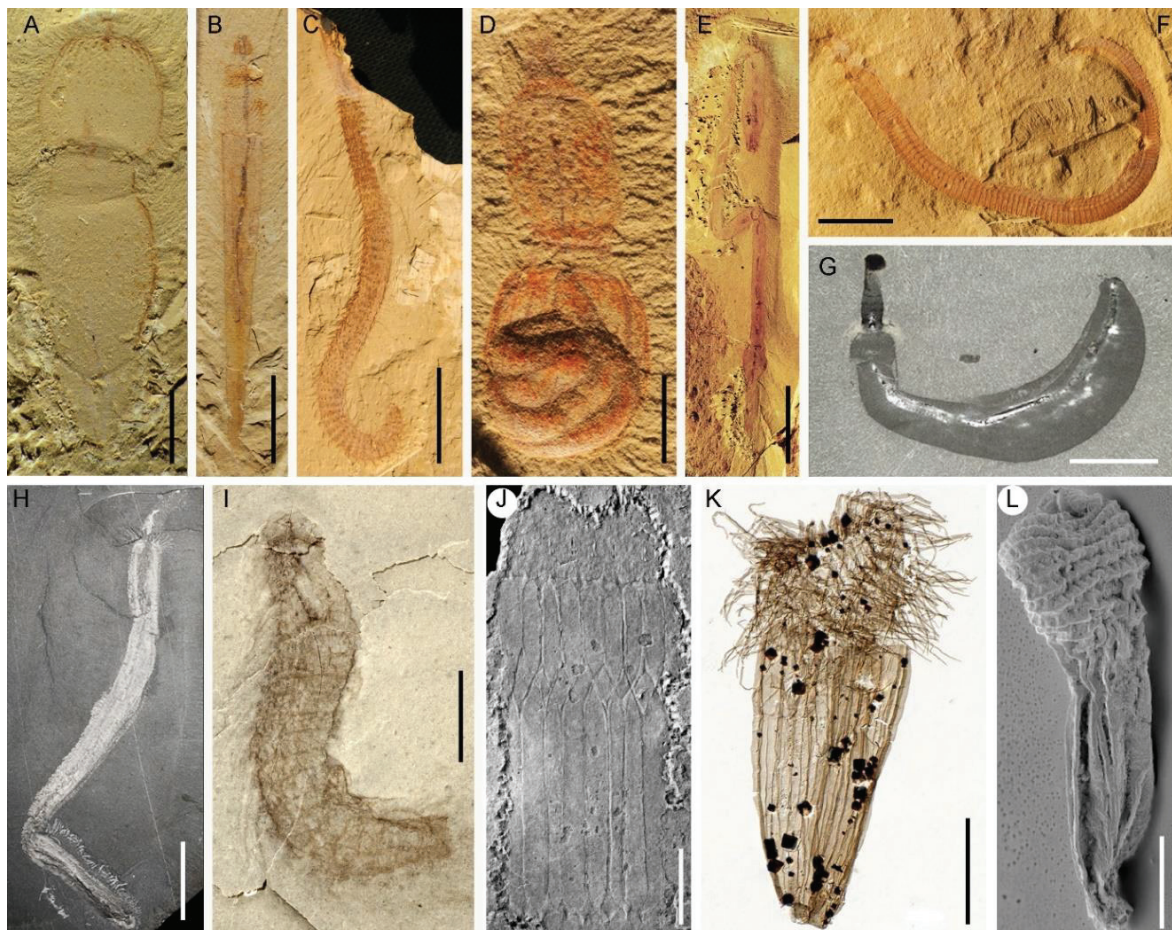




**Figure 29.** Cambrian Scalidophora. A-H. Possible stem group priapulids. A. *Paratubiluchus bicaudatus* Han et al., 2004 (early Cambrian). B. *Selkirkia sinica* Luo and Hu in Luo et al., 1999 (early Cambrian). C. *Tylotites petiolaris* Luo and Hu in Luo et al., 1999 (early Cambrian). D. *Sicyophorus rara* Luo and Hu in Luo et al., 1999 (early Cambrian). E. *Laojieella thecata* Han et al., 2006 (early Cambrian). F. *Cricocosmia jinningensis* Hou and Sun, 1988 (early Cambrian). G. *Ottoia prolifica* Conway Morris, 1977a and Walcott, 1911 (mid-Cambrian). H. *Louisella pedunculata* Conway Morris, 1977a and Walcott, 1911 (mid-Cambrian). I. Undescribed kinorhynch Fu et al., 2019 from Qingjiang biota (early Cambrian). J-L. Loriciferans, *Sirilorica carlsbergi* Peel, 2010a (early Cambrian), *Eolorica deadwoodensis* Harvey and Butterfield (late Cambrian), 2017, *Orstenoloricus shergoldii* Maas et al., 2009 (late Cambrian), respectively. Scale bars: 4 cm (G, H), 2 cm (C), 1 cm (E, F, J), 5 mm (I), 3mm (B), 2 mm (A), 1 mm (D), 200  $\mu$ m (L), 50  $\mu$ m (K). (A, C, E, F) courtesy J. Han. (G, H) downloaded from Burgess Shale official website: [burgess-shale.rom.on.ca](http://burgess-shale.rom.on.ca). (I) courtesy D.-J. Fu. (J) from Peel (2010a). (K) from Harvey and Butterfield (2017). (L) from Maas et al. (2009).

### 4.3.1.2 Loricifera

Loriciferans occur in the middle Cambrian of Mt. Murray, Georgina Basin, Australia (*Orstenoloricus shergoldii*, Maas et al., 2009; Fig. 29L), the late Cambrian Deadwood Formation, western Canada (*Eolorica deadwoodensis*, Harvey and Butterfield, 2017) and the early Cambrian Sirius Passet Lagerstätte, Greenland (Peel, 2010a, b; Peel et al., 2013). Except *Sirilorica carlsbergi* and *Sirilorica pustulosa* (>2 cm in length), *Orstenoloricus* and *Eolorica* are below 1mm. All of them closely resemble extant loriciferans in size, general morphology (e.g. specialized scalids of introvert) and the presence of a loricate trunk (Bang-Berthelsen et al., 2013; Harvey and Butterfield, 2017; Maas et al., 2009).

*Orstenoloricus* was interpreted as a possible larval loriciferan (0.5-1 mm in length). Its most obvious features are: a folded neck, 20 longitudinal plates (lorica) and terminal paired setae (Maas et al., 2009). *Eolorica* is a wonderfully well-preserved loriciferan obtained from Small Carbonaceous fossils (SCFs) residues. It about 180 to 300  $\mu$ m long, has about 20 spinoscalids, trichoscalids, clavoscalids from proximal to distal and 20 longitudinal strip-like plicae (Harvey and Butterfield, 2017). In *Sirilorica* the loricate trunk has seven well-marked longitudinal plates (loricae) connected by hinge zones (*Sirilorica*, Peel, 2010a, b). Distally, individual plates carry one to three short spines. A circle of sclerotized denticles lies at the base of introvert.

The size of *Orstenoloricus* and *Sirilorica* indicates that early to late Cambrian loriciferans were larger than extant representatives of the group, suggesting that the group may have evolved towards miniaturization since the middle Cambrian onwards (Harvey and Butterfield, 2017).

### 4.3.1.3 Other scalidophorans

Apart from kinorhynchs and loriciferans, the majority of Cambrian scalidophorans consist of species and genera whose exact affinities are still unclear. However, a majority of them (e.g. the Chengjiang Lagerstätte) show obvious external resemblances with modern priapulids, such an annulated trunk (Harvey et al., 2010; Maas, 2013), eversible introvert with hooks and spines (Conway Morris, 1977a; Ma et al., 2014a), pharynx lined with multispinose teeth (Conway Morris, 1977a; Smith et al., 2015), and caudal appendages (Han, 2002; Han and Hu, 2006; Han et al., 2004a, b; Han et al., 2006; Huang, 2005; Huang et al., 2006; Huang et al.,

2004a, b; Ma et al., 2010; Maas et al., 2007a). Other scolidophoran fossils such as *Laojieella*, *Sicyophorus*, *Selkirkia* (Cheng, 2019; Han et al., 2006; Yang, 2016) and palaeoscolecid share less characters with extant scolidophorans and their exact affinities are debated (Harvey et al., 2010; Ma et al., 2010; Whitaker et al., 2020).

	Family	Genus	Species	Source	Lagerstätte	Chronostratigraphy
1	Maotianshaniiidae	<i>Maotianshania</i>	<i>M. cylindrica</i>	Sun & Hou 1987	Chengjiang (south China)	Cambrian Stage 3
2	Cricocosmiidae	<i>Cricocosmia</i>	<i>C. jinningensis</i>	Hou & Sun 1988		
3	Tabelliscolecidae	<i>Tabelliscolex</i>	<i>T. hexagonus</i>	Han 2002; Han et al. 2003		
4			<i>T. maanshanensis</i>	Han et al. 2007		
5	Palacoscolecidae	<i>Mafangsclex</i>	<i>M. sinensis</i>	Hou & Sun 1988; Hu 2005; Huang 2005		
6		<i>Houscolex</i>	<i>H. lepidotus</i>	Zhang & Pratt 1996	Zhenping (south China)	
7		<i>Sanxiascolex</i>	<i>S. papillogyrus</i>	Yang & Zhang 2016b	Shipai (south China)	Cambrian Stage 4
8		<i>Wronascolex</i>	<i>W. yichangensis</i>	Yang & Zhang 2016a		
9			<i>W. iacoborum</i>	García-Bellido et al. 2013	Emu bay (Australia)	
10			<i>W. antiquus</i>	Glaessner 1979; García-Bellido et al. 2013		
11			<i>W. geyiensis</i>	Peng et al. 2015	Balang (south China)	
12		<i>Sahascolex</i>	<i>S. labyrinthus</i>	Ivantsov & Wrona 2004	Sinsk (Russia)	
13		<i>Palaeoscolex</i>	<i>P. lubovae</i>	Ivantsov & Wrona 2004		
14			<i>P. spinosus</i>	Ivantsov & Wrona 2004		
15			<i>P. huainanensis</i>	Lin 1995	Huainan (north China)	
16			<i>P. xinglongensis</i>	Liu et al. 2016	Guanshan (south China)	
17		<i>Guanduscolex</i>	<i>G. minor</i>	Hu et al. 2008		
18		<i>Yunnanoscolex</i>	<i>Y. magnus</i>	Hu et al. 2012		
19		<i>Wudingscolex</i>	<i>W. sapushanensis</i>	Hu et al. 2012		
20		<i>Paramaotianshania</i>	<i>P. zijunia</i>	Hu et al. 2012		
21		<i>Shaanxiscolex</i>	<i>S. xixiangensis</i>	Yang et al. 2017	Xixiang (south China)	
22	Chalazoscolecidae	<i>Chalazoscolex</i>	<i>C. pharkus</i>	Conway Morris & Peel 2010	Sirius Passet (Greenland)	Cambrian Stage 3
23		<i>Xystoscolex</i>	<i>X. boreogyrus</i>	Conway Morris & Peel 2010	Qingjiang (south China)	
24			Unnamed palaeoscolecid	Fu et al. 2019		
25	Priapulidae	<i>Xiaoheiqingella</i>	<i>X. peculiaris</i>	Hu in Chen et al. 2002; Gosse 1855	Chengjiang (south China)	
26		<i>Yunnanpriapulid</i>	<i>Y. halteriformis</i>	Huang et al. 2004		
27		<i>Xiaolantianella</i>	<i>X. longibicaudatus</i>	Guo et al. 2016		
28	Tubiluchidae	<i>Paratubiluchus</i>	<i>P. bicaudatus</i>	Han et al. 2004; van der Land 1970		
29		<i>Cambropriapulid</i>	<i>C. sinicum</i>	Huang 2005		
30		<i>Eximipriapulid</i>	<i>E. globocaudatus</i>	Ma et al. 2014		
31		<i>Singuuriquia</i>	<i>S. simoni</i>	Peel 2017	Sirius Passet (Greenland)	
32			Unnamed priapulid	Fu et al. 2019	Qingjiang (south China)	
33	Sicyophoridae	<i>Sicyophorus</i> *	<i>S. rara</i>	Luo & Hu 1999	Chengjiang (south China)	
34			<i>S. sp.</i>	Dong et al. 2018	Guanshan (south China)	Cambrian Stage 4
35	Tylotitidae	<i>Tylotites</i>	<i>T. petiolaris</i>	Luo & Hu 1999; Han 2002	Chengjiang (south China)	Cambrian Stage 3
36	Corynetidae	<i>Corynetis</i>	<i>C. brevis</i>	Luo & Hu 1999		
37			<i>C. fortis</i>	Hu et al. 2012		
38	Anningidae	<i>Anningvermis</i>	<i>A. multispinosus</i>	Huang et al. 2004		
39		<i>Xianjiella</i>	<i>X. lubrica</i>	Huang 2005		
40	Laojieellidae	<i>Laojieella</i>	<i>L. thecata</i>	Han et al. 2006		
41	Selkirkiidae	<i>Selkirkia</i>	<i>S. sinica</i>	Luo & Hu 1999		
42			<i>S. transita</i> sp. nov.	Wang et al. in review		
43		<i>Sullulika</i>	<i>S. broenlundi</i>	Peel & Willman 2018	Sirius Passet (Greenland)	
44		<i>Sirilorica</i>	<i>S. carlsbergi</i>	Peel 2010a		
45			<i>S. pustulosa</i>	Peel 2010b		
46			Unnamed kinorhynch	Fu et al. 2019	Qingjiang (south China)	

**Table 2.** Early Cambrian scalidophorans. Palaeoscolecida highlighted in blue, Priapulomorpha in yellow, loriciferans in green and kinorhynchans in grey. \*, *Palaeopriapulites parvus* Hou et al., 1999 is a possible synonym of *Sicyophorus rara* Luo & Hu in Luo et al., 1999 (= *Protopriapulites haikouensis* Hou et al., 1999) (Hu in Chen et al., 2002; Cheng, 2019; Han, 2002).

A brief review of published articles identifies a total of at least 46 scalidophoran species in the early Cambrian as a whole (Table 2). Twenty of them are from the Chengjiang Lagerstätte that altogether account for about 43% of the animal diversity. These 20 species fall into 17 genera and 11 families (Table 2). Problematic or poorly defined species such as *Selkirkia? elongata* (Luo et al., 1999), *Archotuba conoidalis* (Hou et al., 1999), *Lotuba chengjiangensis* (Chen et al., 1996; Huang, 2005), *Acosmia maotiania* (Chen and Zhou, 1997; Han, 2002; Howard et al., 2020a; Huang, 2005) and *Lagenula striolata* (Luo et al., 1999) are not included in our inventory (Table 2).

Diversity is great among these worms and is expressed by a wide range of morphological variations of body shape and external ornament (e.g. trunk and introvert). Previous authors have created numerous subordinal categories (Huang, 2005; Maas et al., 2007a) to accommodate these scalidophorans, that are often neither justified nor necessary (e.g. monogeneric families), and no reliable indicators of their actual morphological disparity.

### ***Palaeoscolecida***

Palaeoscolecids are important member of scalidophorans, they were interpreted as stem-group Priapulida based on resemblances of annulated trunk and scalid-bearing introvert to modern priapulids. However, their trunk ornamentation, uniform body width and paired caudal spines show remarkable differences with extant priapulids (Conway Morris and Peel, 2010; García-Bellido et al., 2013; Harvey et al., 2010).

Typical representatives of the group (*Palaeoscolecida sensu stricto*) are characterized by a very elongated body and a unique ornamented pattern made of polymorphic tessellating plates regularly distributed around the trunk annuli (e.g. *Sahascolex*, Ivantsov and Wrona 2004; Conway Morris and Robinson 2010; García-Bellido et al. 2013). Other elongated forms with no tessellating plates have been added to the group (e.g. *Maotianshania*, Sun and Hou, 1987; *Cricocosmia*, Hou and Sun, 1988). Palaeoscolecids have rich fossil record in the early Palaeozoic (early Cambrian to late Silurian, ca 520-418 Ma; Harvey et al., 2010).

Although most scientists consider them as probable members of Cycloneuralia (Maas et al., 2007; Budd, 2001), uncertainties remain concerning their relation to particular cycloneuralian groups such as Priapulida (García-Bellido et al., 2013; Harvey et al., 2010), Nematomorpha (Hou and Bergstrom, 1994) or Scalidophora (Harvey et al., 2010; Wills et al., 2012; Zhang et al., 2015). Some authors have suggested that palaeoscolecids had the potential to provide key information on the nature of the ancestral ecdysozoans (Budd, 2003; Conway Morris and Peel, 2010) and that the group may represent a key step in the evolutionary emergence of panarthropods (Dzik and Krumbiegel, 1989). However detailed studies (Harvey et al., 2010) do not support the view that ecdysozoans occupy such a deeper position in the evolutionary history of Ecdysozoa and consider them as possible stem-group Priapulida (García-Bellido et al., 2013).

The Class Palaeoscolecida (Conway Morris and Robison, 1986) is divided into two families,

the Palaeoscolecidae (Whittard, 1953) and the Chalazoscolecidae (Conway Morris and Peel 2010). Palaeoscolecids *sensu stricto* contain numerous fossil species (e.g. *Mafangsclex*, Fig. 30A; *Wronascolex yichangensis*, Fig. 30B-D; *Palaeoscolex*, Fig. 30E, F; Table 2) that can be distinguished by their overall shape, the number, and arrangement of their plates, platelets, microplates along their trunk.

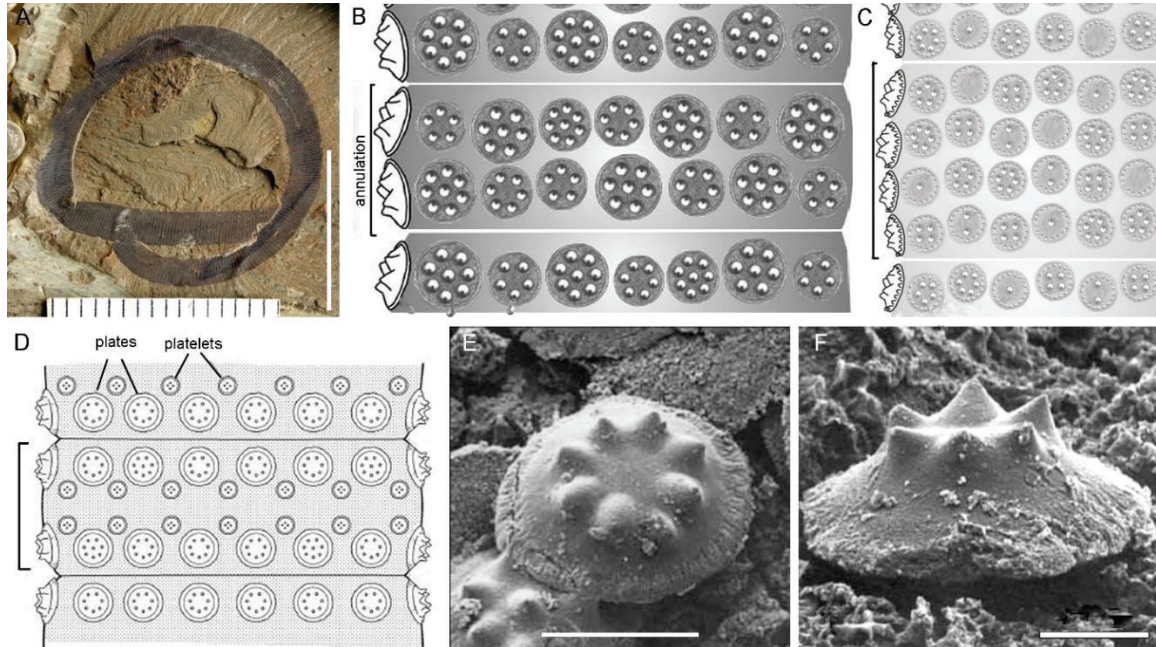


**Figure 30.** External ornament of palaeoscolecids *sensu stricto* from the early Cambrian. A. *Mafangsclex yunnanensis* Luo and Zhang, 1986, general view of a coiled specimen. B-D. Diagrams showing plate and platelet ornament in *Wronascolex yichangensis* (Yang and Zhang, 2016a), *Sanxiascolex papillogyrus* Yang and Zhang, 2016), and *Palaeoscolex lubovae* Ivantsov and Wrona, 200), respectively. E, F. Details of individual plates bearing nodes in *Palaeoscolex lubovae* Ivantsov and Wrona, 2004 and *Wronascolex spinosus* Ivantsov and Wrona, 2004. Scale bars: 1 cm (A), 50 µm (E), 20 µm (F). (B) from Yang and Zhang (2016a). (C) from Yang and Zhang (2016b). (D-F) from Ivantsov and Wrona (2004).

Although devoid of tessellating ornament, other taxa with a very slender body, a conspicuously uniform body width and paired caudal hooks have been assigned to Palaeoscolecida (Han et al., 2007b; Harvey et al., 2010; Hou and Bergstrom, 1994). These are the early Cambrian *Maotianshania*, *Cricocosmia*, *Tabelliscolex*, *Tylotites* (Han, 2002; Hou and Sun, 1988; Sun and Hou, 1987; Luo and Hu in Luo et al., 1999; Han, 2002; Table 2 in blue colour; Fig. 31), and mid-Cambrian *Louisella* (Conway Morris 1977a; Fig. 29H). Four families have been established to accommodate these ‘untypical’ palaeoscolecids from Chengjiang biota (*Maotianshaniidae*, *Cricocosmiidae*, *Tabelliscolecidae*, and *Tylotitidae*, respectively).

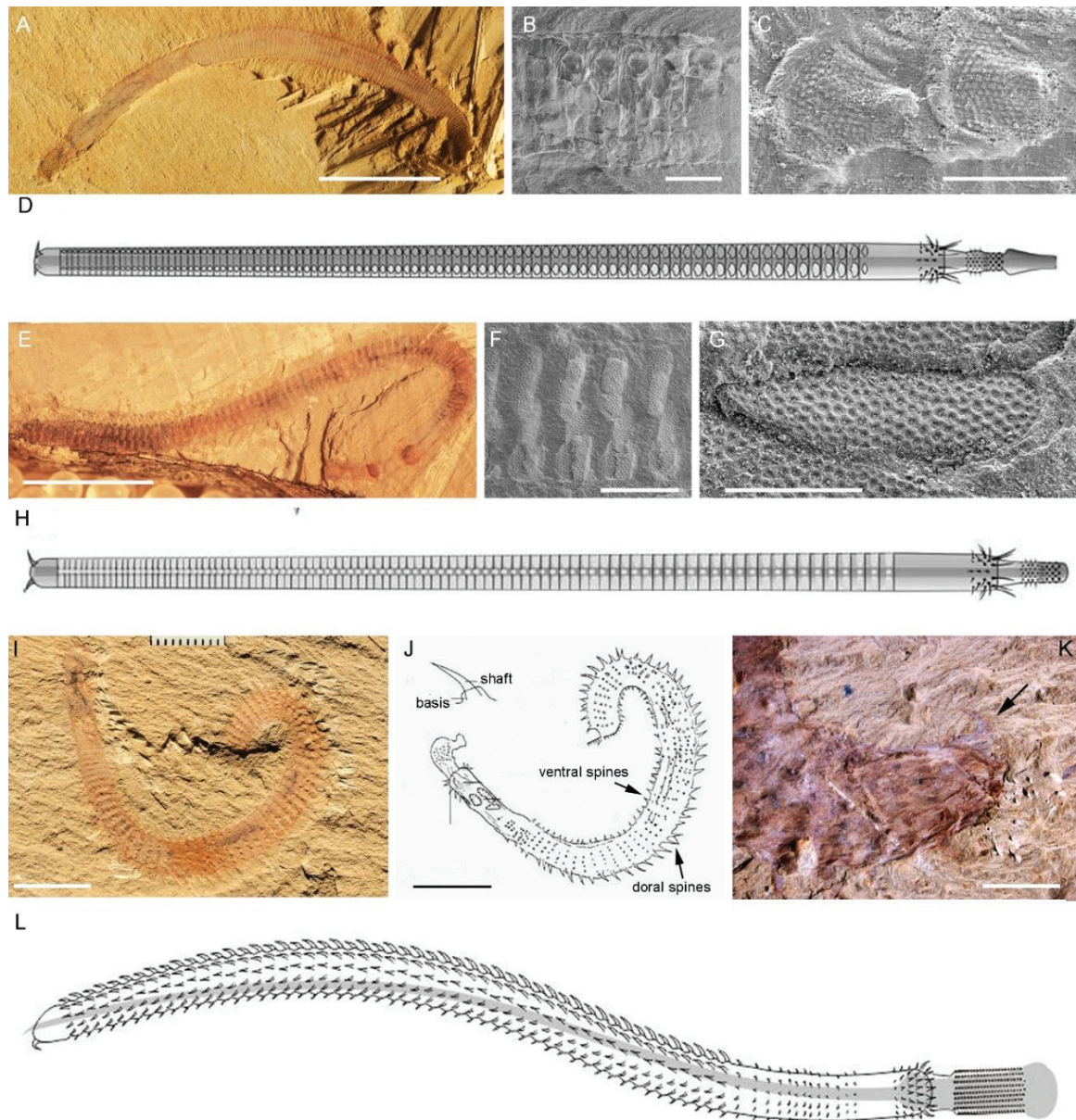


**Figure 31.** External ornament of palaeoscolecids from early Cambrian the Chengjiang Lagerstätte, that do not have tessellating plates. A-D. *Crilocosimia jinningensis* Hou and Sun, 1988, general view and SEM images showing plates with a rounded base and a central spine. E-H. *Tabelliscolex hexagonus* Han et al., 2003, general view and SEM images showing elliptical plates with reticulation but no nodes. I-L. *Tylotites petiolaris* Luo and Hu in Luo et al. 1999, general view and details of trunk spines. Scale bars: 1 cm (A, E, I, J), 5 mm (K), 1 mm (B, F), 500  $\mu\text{m}$  (G), 300  $\mu\text{m}$  (C). D, H, L, drawings not to scale. (A-H) from Han et al. (2007a). (I-L) from Han et al. (2007b). (A-L) courtesy J. Han.

### ***Priapulomorpha***

The Order Priapulimorpha (Salvini-Plawen, 1974) or Priapulomorpha (Adrianov & Malakhov, 2001) accommodates the Priapulidae and the Tubiluchidae based on characters shared by these two families (scalids arranged in 25 longitudinal rows and caudal appendages) (Salvini-Plawen, 1974; Adrianov & Malakhov, 2001).

Three Cambrian forms, *Xiaoheiqingella*, *Yunnanpriapululus* (Luo and Hu in Luo et al., 1999;

Huang et al., 2004b) and *Paratubiluchus* (Han et al., 2004a; Fig. 32) that all bear 25 longitudinal rows of scalids (introvert) and paired caudal appendages, have been reasonably assigned to Priapulomorpha (Huang 2004b; Han et al. 2004a). *Xiaoheiqingella* and *Yunnanpriapulidus* were tentatively placed within the Priapulidae (Huang et al. 2004b; Huang et al. 2006). Although *Paratubiluchus* has trunk annulations and papillae as in modern Tubiluchidae (Han et al., 2004a), its general morphology remains atypical of this group. Diagnostic characters such as pectinate pharyngeal teeth, the presence of polythyridium and a neck (van der Land, 1970; Schmidt-Rhaesa, 2013) that could support close affinities with Tubiluchidae, but these are lacking in *Paratubiluchus*. Clear affinities between *Paratubiluchus* and modern Tubiluchidae (as suggested by Han et al. 2004a) are difficult to establish (Huang et al. 2006).

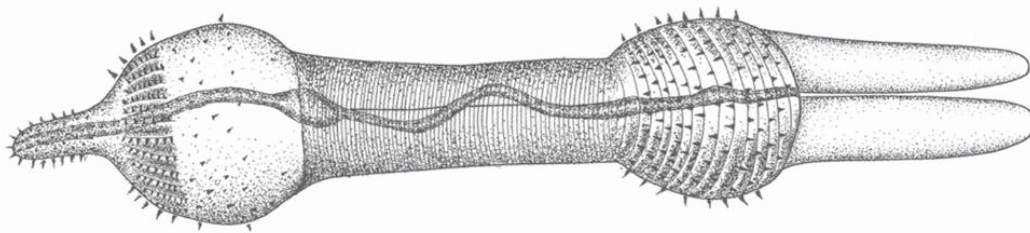


**Figure 32.** *Paratubiluchus bicaudatus* Han et al., 2004a from the early Cambrian Chengjiang Lagerstätte. Courtesy J. Han.

### **Other taxa**

Sicyophoridae is a monogeneric family with two species and one undetermined form: *Sicyophorus rara* (Luo and Hu in Luo et al., 1999) and *S. sp.* (Dong et al., 2018) from the early Cambrian Chengjiang and Guanshan Lagerstätten, respectively, and *S. guizhouensis* from mid-Cambrian Kaili Lagerstätte (Yang, 2016). *S. rara* has a peculiar gourd shape. Adult specimens are characterized by an introvert with 25-30 longitudinal rows of scalids at anterior part, a constricted neck, a trunk lined with 25-30 longitudinal rows of plates (Cheng, 2019; Fig. 33B), and a coiled or straight gut.

*S. sp.* bears 20 longitudinal rows of scalids along the whole introvert and 15 longitudinal rows of plates (Dong et al., 2018). The length of the trunk of *S. sp.* is twice as long its introvert. However, it is a poorly defined form with a single specimen that possibly represents one of the different developmental stages of *S. rara* (Cheng, 2019).

*S. guizhouensis* has 20 longitudinal rows of scalids at anterior part of its introvert, 50 longitudinal rows of plates, and a caudal projection (Yang, 2016) only seen in the holotype. It is actually unclear whether this feature has a biological origin (trunk end) or is a strand of feces material. The original figures show an obvious gap between the assumed caudal projection and the trunk end (Yang, 2016).

Anningiidae and Corynetidae were established by Huang et al., (2004a) to accommodate species that actually differ from each other by only very few characters. This questions the need to maintain two distinct families (Dong et al., 2005; Ma et al., 2010). The members of these two families all have an eversible introvert (smooth basal part, circlet of circumorally scalids pointing anteriorly or outwardly), a slim and eversible pharynx armed with spiny pharyngeal teeth, a spiny trunk and a caudal structure (Huang et al., 2004a; Fig. 33C, D). *Anningvermis* has a long caudal structure (caudal appendage) and a short collar (Huang et al.,

2004a), whereas *Corynetis* bears a very short caudal projection and a long collar (Huang et al., 2004a). The morphological differences between the two species may result from preservation, which led some authors (Dong et al., 2005; Ma et al., 2010) to suggest *Anningvermis* and *Corynetis* may be synonymous.

Laojieellidae accommodates a single species, *Laojieella thecata*, described by Han et al., (2006), from a complete specimen (holotype) and a trunk fragment, both bearing an assumed “theca” at the posterior part of the trunk (Fig. 29E). However, the nature of this unusual feature (possibly sclerotized plate) is still unclear. Similarly, the number and arrangement of cuticular elements along the introvert and pharynx of *L. thecata* are uneasy to characterize. The trunk of *L. thecata* is smooth and bears paired caudal appendage, although their exact outline is hardly visible in the original figure (Han et al., 2006). The paired caudal appendage recalls those of extant priapulids (e.g. *Priapulopsis bicaudatus*, van der Land, 1970).

Selkirkiidae secrete an annulated conical tube around their trunk and have a relatively complex introvert subdivided into different zones each bearing a specific ornamented pattern (e.g. *Selkirkia sinica*, Luo and Hu in Luo et al., 1999; Fig. 33A). Their tubicolous habit make them unique among scalidophoran worms. Detail concerning the morphology, ecology, and phylogeny of *Selkirkia* are given in Chapter 5.3 to 5.5.

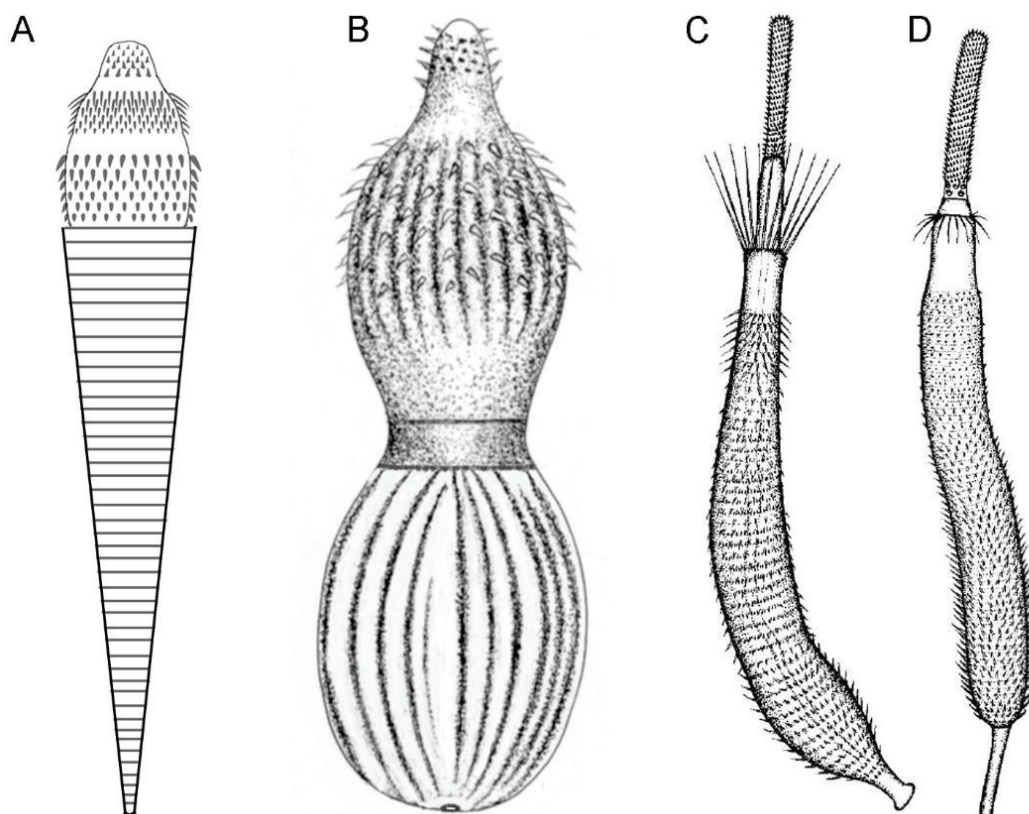


**Figure 33.** Diagram to show extreme morphological variations among early Cambrian scalidophorans, exemplified by species from the Chengjiang Lagerstätte. A. *Selkirkia transitia* sp. nov. B. *Sicyophorus rara* Luo and Hu in Luo et al., 1999. C. *Corynetis brevis* Luo and Hu in Luo et al., 1999. D. *Anningvermis multispinosus* Huang et al. 2004a. (B) Unpublished data. (C, D) from Huang et al. (2004a). Drawings not to scale.



### 4.3.1.4 Palaeoecology of early Cambrian scalidophoran worms

#### *Locomotion and relation to sediment*

The overall morphology of Cambrian scalidophoran worms as seen from fossil specimens preserved in various attitudes (e.g. *Xiaoheiqingella* and *Sicyophorus*; Han et al., 2007D; Han, 2002; Huang, 2005) show that their introvert had capabilities to extend (eversion process) and therefore to dig into soft sediment. Inflated or contracted shapes strongly suggest that these worms had a hydrostatic skeleton controlled by a complex system of circular, longitudinal and retractor muscles. However, muscles are very rarely preserved in BST-type fossils (e.g. Chengjiang Lagerstätte). Extant macrobenthic priapulids such as *Priapulid* and *Halicryptus* are the best models to understand how Cambrian scalidophorans may have moved through their environment.

The whole locomotion process of *Priapulid* has been described and reconstructed in details by previous authors (Elder and Hunter, 1980; Hammond, 1970; Vannier et al., 2010; Vannier and Martin, 2017). I had the chance to observe the behaviour of *Priapulid* and *Halicryptus* in laboratory conditions during my stay in Sweden. Locomotion is performed via peristaltic contractions. via pressure variations induced by longitudinal, circular cuticular muscles and retractor muscles (Storch, 1991). These muscles exert pressure on the body cavity filled with fluid (hydrostatic skeleton), allowing the introvert and pharynx to invaginate or project outside (Vannier et al., 2010; Vannier, 2012; Vannier and Martin, 2017). There are four successive steps: 1) trunk contraction (Fig. 34A, B), 2) introvert invagination (Fig. 34C-E), 3) powerful eversion (Fig. 34F-H), and 4) club-shape inflation of the introvert (Fig. 34I).

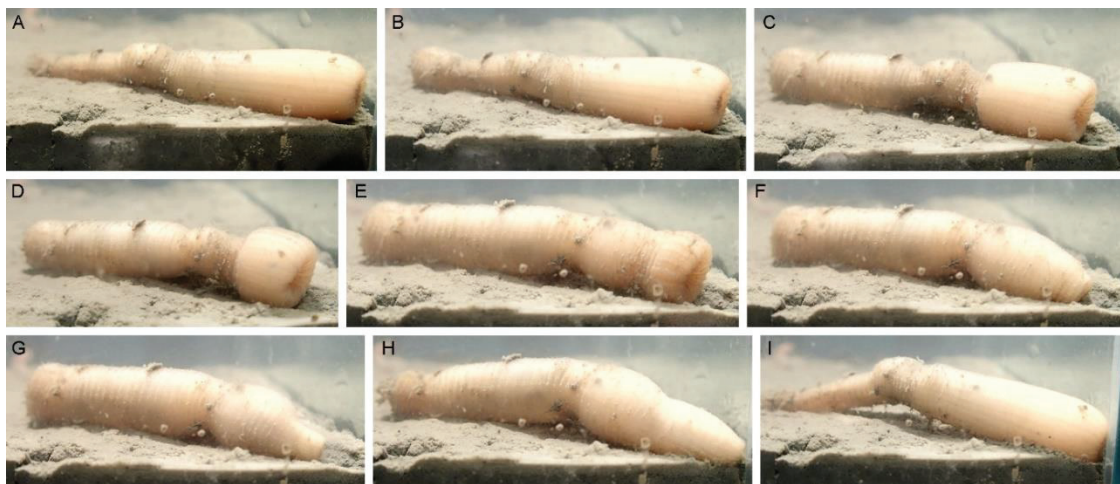


**Figure 34.** Sequence showing successive steps in the peristaltic contractions of *Priapulid caudatus* from Sweden. Observation of live specimen in aquarium. A-B. Trunk contraction. C-E. Introvert invagination. F-H. Introvert eversion and attempt to dig into sediment. I. Introvert full eversion and trunk relaxation. Worm length is approx. 12 cm in (A).

The wide range of morphologies seen in Cambrian scalidophorans suggest that these animals may have performed locomotion through various ways. For example, *Mafangscplex* often displays a snake-like, twisting shape, that probably implies some kind of sidewinding locomotion (Fig. 36A, B). The trunk of *Cricocosmia* is lined with paired lateral plates, which

may have helped the worm to move by crawling on the sediment surface (Huang et al., 2014; Fig. 36C-E). Similarly, *Tylotites* bears many long spines on the assumed dorsal and lateral part of its trunk and shorter ones ventrally, which may play a role in epibenthic crawling (Han et al., 2007b; Fig. 31I-L). However, no locomotion traces possibly made by *Tylotites* and *Cricocosmia* have been found so far. Locomotion via ventral spines or lateral plates should be considered cautiously.

Body fossils of *Sicyophorus* have been found associated with striated traces, suggesting that the animal dragged its loricate trunk forwards (Han et al., 2007d; Fig. 36F). These specimens also show that the introvert of *Sicyophorus* stretched and became narrower when moving. A very similar movement behaviour has been observed in extant loricate priapulid larvae (Hammond, 1970). Moreover, the trace left by *Sicyophorus* runs across several bedding planes, indicating that this worm had the ability to move obliquely through sediment.

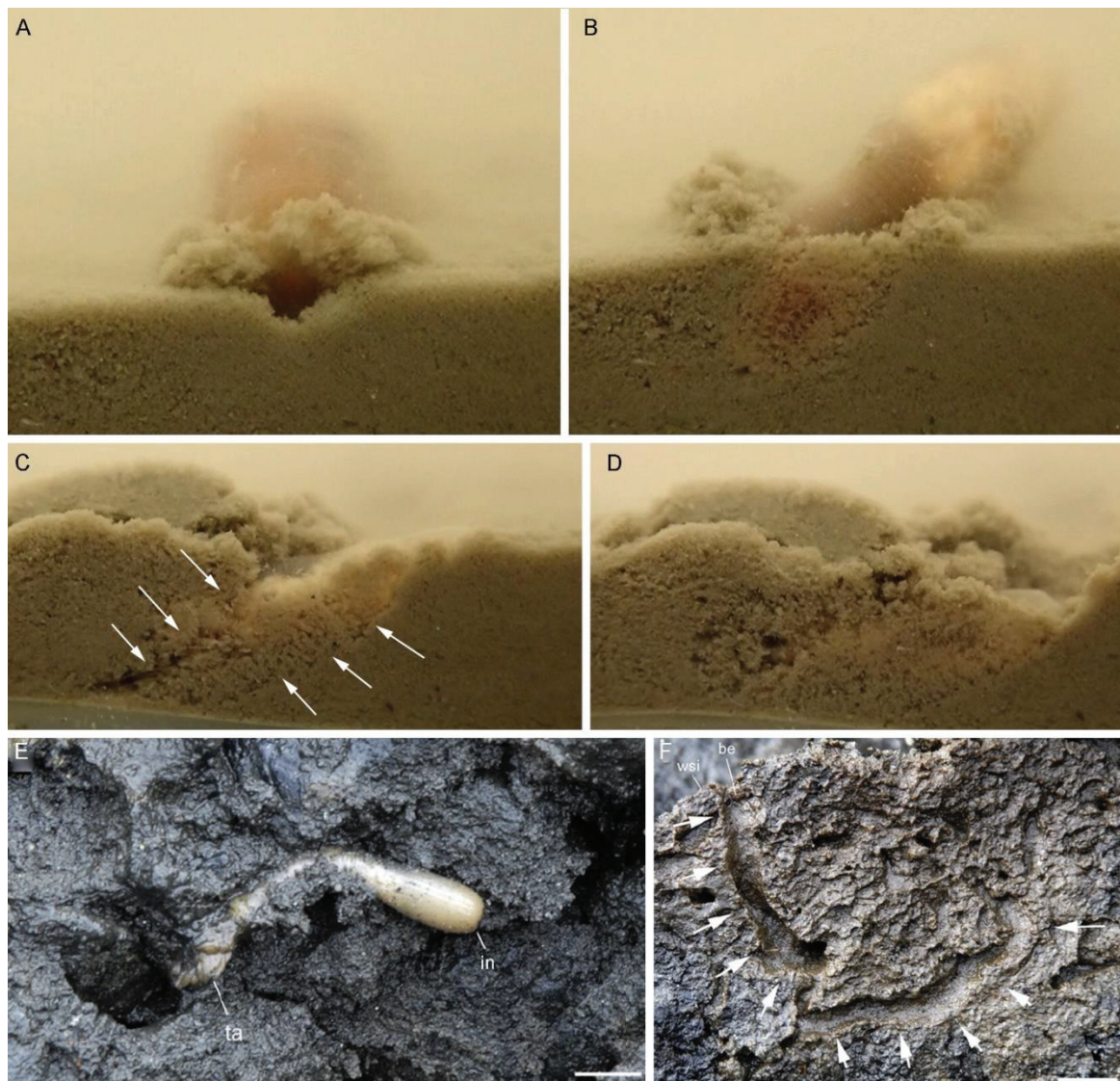


**Figure 35.** Burrowing of extant macrobenthic Priapulida. A-D. *Halicyptus spinulosus*, oblique digging in mud observed in laboratory (Sweden), white arrows indicate burrow. E, F. *Priapulid caudatus* within mud (intertidal environment, White Sea, Russia) and empty burrows left by the animal a few centimetres below the water-sediment interface (burrows underlined by white arrows). Abbreviations: be, burrow entrance; in, introvert; ta, tail; wsi, water-sediment interface. Scale bars: 1 cm (E, F). (E, F) from Vannier and Martin (2017).

Extant priapulid worms live in burrows (Fig. 35). *Priapulid* and *Halicryptus* when deposited on the surface of mud, dig into it relatively rapidly (a few minutes or less) and remain concealed with the sediment (Vannier and Martin, 2017; *Halicryptus*, Fig. 35A-D; *Priapulid*, Fig. 35E, F). These burrows display various shapes and orientation (from subhorizontal to almost vertical) but do not form a U-shaped structure as seen in other marine worms (e.g. annelids, sipunculans). Although it is almost certain that most Cambrian scalidophorans were endobenthic burrowers such as *Xiaoheiqingella* (Huang et al., 2004b), *Ottoia* (Conway Morris, 1977a), *Corynetis* and *Anningvermis* (Huang et al., 2004a), *Sicyophorus* (Luo and Hu in Luo et al., 1999) and certain palaeoscolecs *Mafangsclex* (Zhang et al., 2006), *Cricocosmia* (Huang et al., 2014), direct evidence for burrows are relatively rare.

Burrows associated with their makers have been described in *Mafangsclex* (Zhang et al., 2006) and *Cricocosmia* (Huang et al., 2014). The cylindrical burrows of these two palaeoscolecs seem to have been consolidated by mucus secretions and always lie in a subhorizontal position relative to the water-sediment interface (Huang et al., 2014). These burrows are elongate, tubular, clearly wider than the worm, and probably open at both ends (Fig. 36A-D). There is no convincing evidence of U-shaped burrows in any Cambrian scalidophoran worms (Huang et al., 2014; Zhang et al., 2006).

*Selkirkia* differ markedly from all other Cambrian scalidophoran worms in that they lived within a conical tube open at both ends (Fig. 29B). Previous authors thought that *Selkirkia* may have stood vertically within the sediment (Conway Morris 1977a). However, our study presented in Chapter 5.3 shows that a brachiopod often attached near the posterior opening of the tube. Since the brachiopod feeding mode is generated by lophophoral cilia and requires constant contact with circulating water (Brusca et al., 2016), its preferential location near the posterior end of *Selkirkia*'s tube would suggest that *Selkirkia* probably lived relatively close to the water-sediment interface, possibly lying in a subhorizontal or slightly tilted position, and maintaining contact with free water via the posterior tip of its tube (see Chapter 5.3 for details).

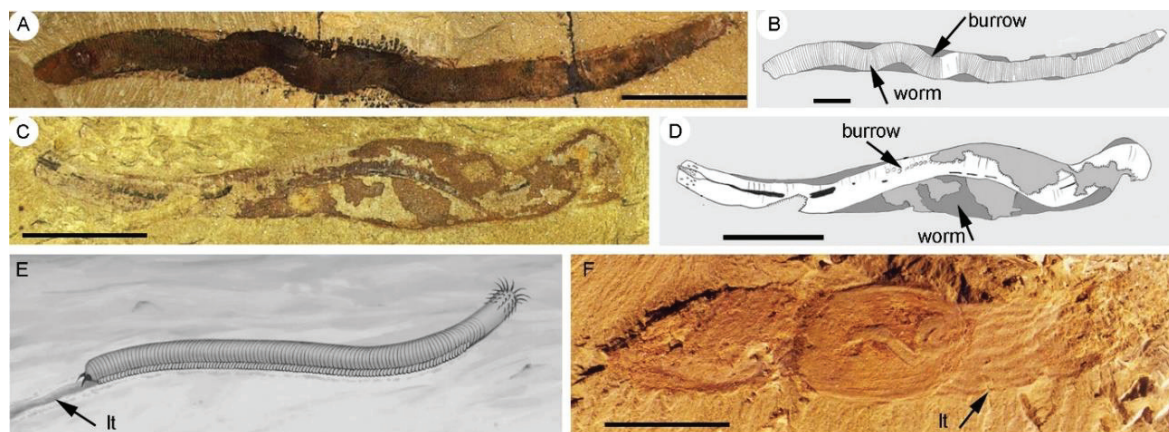


**Figure 36.** Locomotion and burrows in scalidophorans from the early Cambrian. A, B. *Mafangsclex yunnanensis* Luo and Zhang, 1986 and Hu, 2005, general view and line drawing. C-E. *Cricocosmia jinningensis* Hou and Sun, 1988, general view, line drawing and reconstruction. F. *Sicyophorus rara* showing locomotion trace from Han et al., (2007d). Abbreviation: lt, locomotion trace. Scale bars: 1 cm (A), 5 mm (B-D, F). (A-E) from Huang et al. (2014). (F) courtesy J. Han.

### ***Possible gregarious habits***

Most Cambrian scalidophorans are found as individual specimens on the surface of bedding planes, implying that they did not live-in groups (e.g. *Xiaoheiqingella*, *Tylotites*). However, some of them might have been gregarious as suggested by large concentrations of conspecific individuals as seen in *Selkirkia sinica* (Fig. 37A, B), *Maotianshania*, *Cricocosmia* (Fig. 37C, D), *Sicyophorus* (Fig. 37E), and *Ottoia* (Fig. 37F).

Relatively large concentration of *Selkirkia sinica* have been found on several bedding planes (Fig. 37B) and usually shows directional polarity. Fossil assemblages dominated by *Cricocosmia* and *Mafangsolex* also contain lobopodians and arthropod remains (Vannier and Martin, 2017). These associations may indicate gregarious habits, but other options should be considered. They may either result from post-mortem transportation and accumulation (Fig. 37A) or alternatively may have been triggered by attraction to a possible food sources (e.g. possibly sediment enriched in decaying material). This feeding behaviour is frequent in present marine animals and has been suggested to explain large concentrations of worms in the Burgess Shale-type Lagerstätten (*Ottoia*, Bruton, 2001; Vannier, 2012).

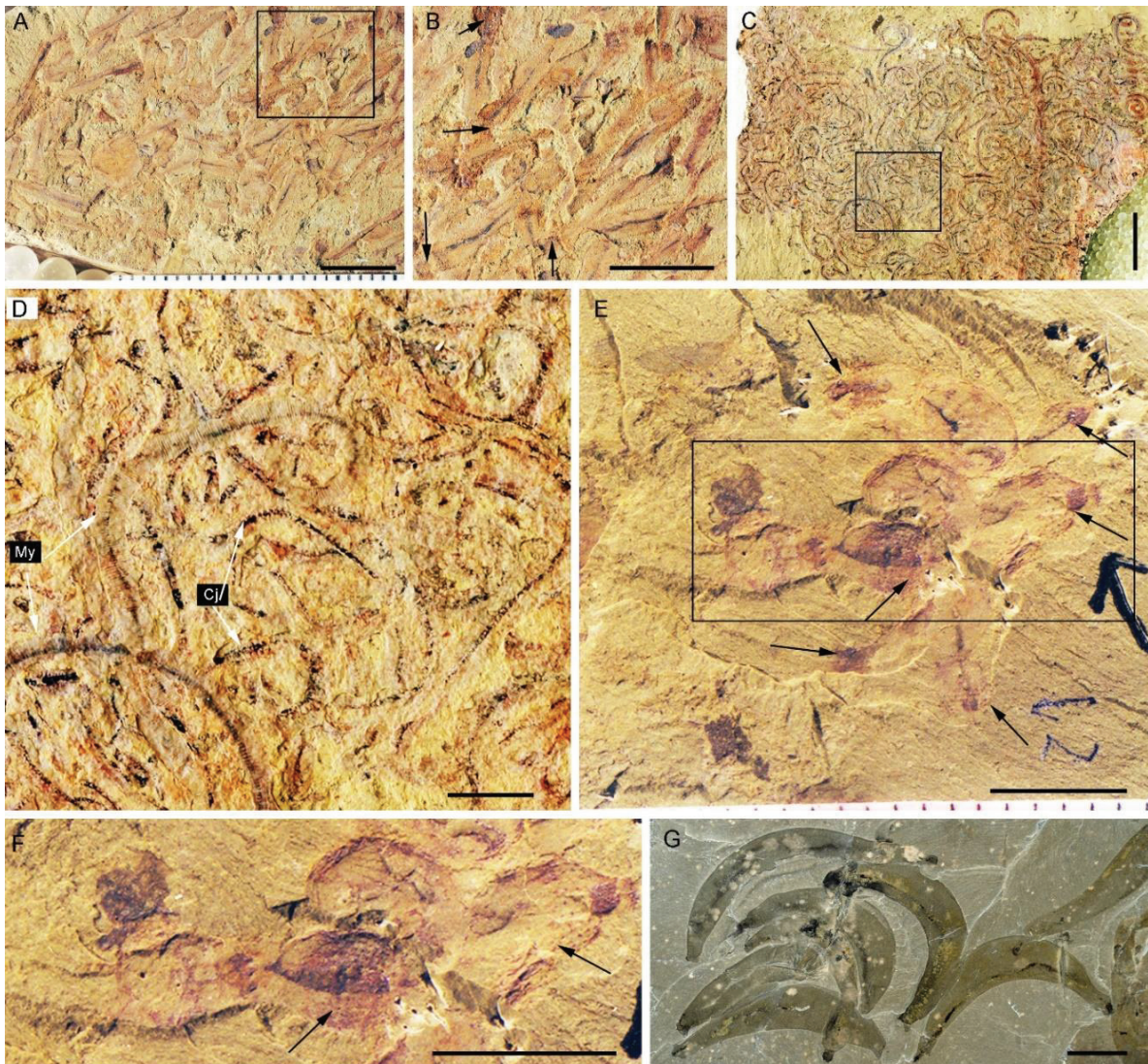


**Figure 37.** Fossil assemblages suggesting gregarious habits in scalidophoran worms from various Cambrian BST Lagerstätten. A-E. Scalidophoran worms from the early Cambrian Chengjiang Lagerstätte. F. *Ottoia prolifica* Conway Morris, 1977a and Walcott 1911. from the mid-Cambrian Burgess Shale Lagerstätte. A, B. *Selkirkia sinica* Luo and Hu in Luo et al., 1999 and Hou et al., 1999, showing general view of the concentration and close-up. C, D. The large concentration of *Mafangscotlex yunnanensis* Luo and Hu in Luo et al., 1999 and Hu, 2005, *Cricocosmia jinningensis* Hou and Sun, 1988, and close-up. E, F. Concentration in *Sicyophorus rara* Luo and Hu in Luo et al., 1999, and close-up; black arrows indicate the introvert. G. *Ottoia prolifica* on a large rock slab; from Vannier (2012). Abbreviations: My, *Mafangscotlex yunnanensis*; Cj, *Cricocosmia jinningensis*. Scale bars: 2 cm (C, G), 5 mm (A, B, D-F). (G) courtesy J. Vannier.

### **Feeding behaviour and diet**

Our interpretations of the possible feeding modes of Cambrian scalidophorans almost entirely rely on the way modern priapulids feed and the morphology of their feeding apparatus (Fig. 38F). For example, *Priapulid* has well-developed pharyngeal teeth (Fig. 38F; Vannier, 2012) that are used to grasp food (prey such as other worms and other elements) and draw it into the gut through the invagination of introvert. Indeed, some Cambrian worms do have identical teeth and pharynx structure, suggesting that they may have had comparable feeding habits, as exemplified by *Ottoia*, *Selkirkia* and others (see also Chapter 5.3).

Undigested skeletal remains found in the gut of *Ottoia prolifica* provide direct evidence for predation or scavenging (Bruton, 2001; Vannier, 2012; Vannier et al., 2014). Rare worms from the Chengjiang Lagerstätte such *Laojieella* sp. (Han et al., 2006) reveal comparable details. The presence of *Archotuba* in the gut of *Laojieella* sp. indicates possible predation (Han et al., 2007c; Fig. 38A-C). The fact that *Archotuba* is not disarticulated suggests that prey was swallowed whole and that the pharyngeal teeth of *Laojieella* sp. were not powerful enough to break the tube of *Archotuba*. Although *Selkirkia* bears sharp pharyngeal teeth, no strong fossil evidence indicates a predatory feeding habit. Instead *Selkirkia*, *Sicyophorus*, *Xiaoheiqingella* may be mud-eaters as indicated by numerous pellets were found in their gut (Huang et al., 2004b; Lan et al., 2015; Peel, 2017; Fig. 38D, E).

The pharynx of *Corynetis* and *Anningvermis* is lined with numerous teeth. Their small size suggests potential abilities to grasp small meiobenthic organisms (Huang et al. 2004a) or simply organic detritus found within the sediment or at the water-sediment interface. Vannier and Martin (2017) suggested that these worms may have been mud-eaters. Feeding habits of most palaeoscolecid *sensu stricto* is hypothetical (Han et al., 2004a; Vannier et al., 2012). Their sharp pharyngeal teeth may indicate predation (Han et al., 2004b) as in *Corynetis* (Huang et al. 2004a).

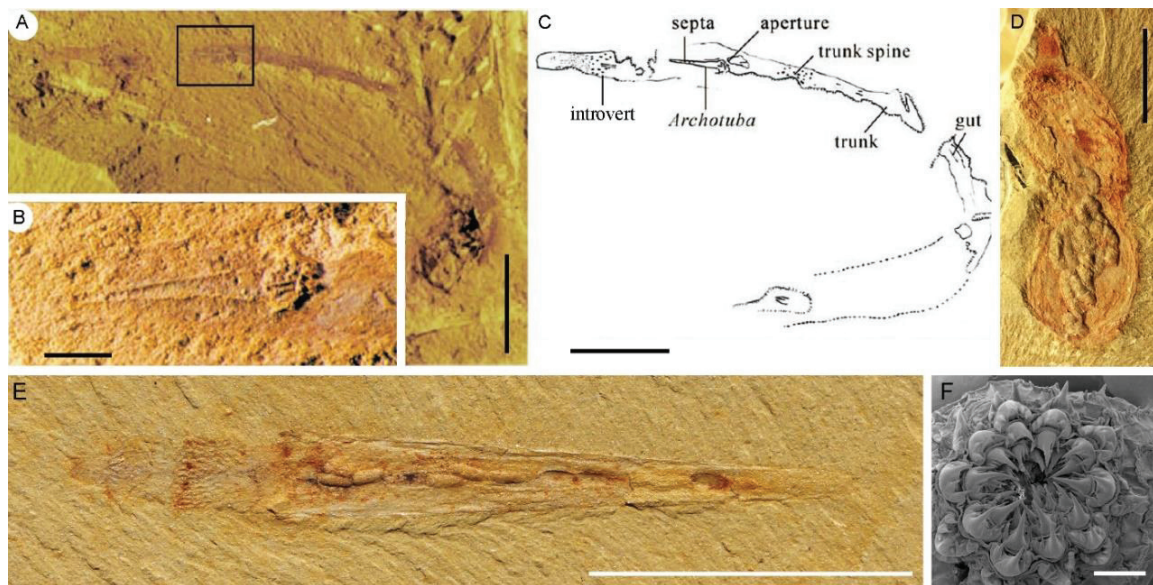


**Figure 38.** Feeding habits and diet of early Cambrian scalidophorans. A, C. *?Laojieella* sp. from Han et al., 2006, general view and line drawing (in scale). B. Close-up of *Archotuba* inside the gut of *?Laojieella* sp. (see location in A). D. *Sicyophorus rara* showing mud-filled gut. E, Pellets in *Selkirkia sinica*. F, Pharyngeal teeth of the extant priapulid *Priapulius caudatus*. Scale bars: 5 mm (A, C, E), 2 mm (D), 1 mm (B, F). (A-C) courtesy J. Han. (F) courtesy J. Vannier.

## 4.3.2 Panarthropoda

### 4.3.2.1 Arthropoda and Tardigrada

Panarthropods consist of three extant groups: Arthropoda, Tardigrada, and Onychophora. They are well represented in Cambrian marine ecosystems with extinct iconic groups such as radiodontans (e.g. anomalocaridids, Cong et al., 2017; Daley et al., 2009; Van Roy et al., 2015), trilobites, and the possible remote ancestors of crustaceans and chelicerates (e.g. Briggs et al., 1994; Hu et al., 2013; Ortega-Hernández, 2016; Vannier et al., 2018; Vinther et al., 2014; Fig. 39A-C). Arthropods have colonized a spectrum of ecological niches greater than other ecdysozoans groups (e.g. scalidophorans; see above), with both epibenthic and free-swimming members. They are characterized by a segmented body and jointed legs (podomeres) (e.g. Brusca et al., 2016; Daley and Antcliffe, 2019; Mayer et al., 2013; Paterson et al., 2019).

Since the 1980's Cambrian Lagerstätten have been providing a huge amount of information on the morphology, phylogeny and palaeoecology of early arthropods (e.g. Aria et al., 2015; Budd and Telford, 2009; Daley and Legg, 2015; Glaessner, 1979; Hou et al., 2017; Ivantsov et al., 2005; Skovsted et al., 2006; Vannier et al., 2018; Yang et al., 2013; Zeng et al., 2020; Zhang et al., 2008). The purpose of my thesis is not to review this prolific literature but to concentrate on more basal ecdysozoan groups, essentially scalidophorans (Chapter 4.4.1).

The fossil record of Tardigrada is extremely patchy. These tiny panarthropods occur in the mid-Cambrian Kuonamka Formation of Siberia (Müller et al., 1995; Fig. 39D) but have no representatives in any early Cambrian Lagerstätten or Orsten-type SSF assemblages.

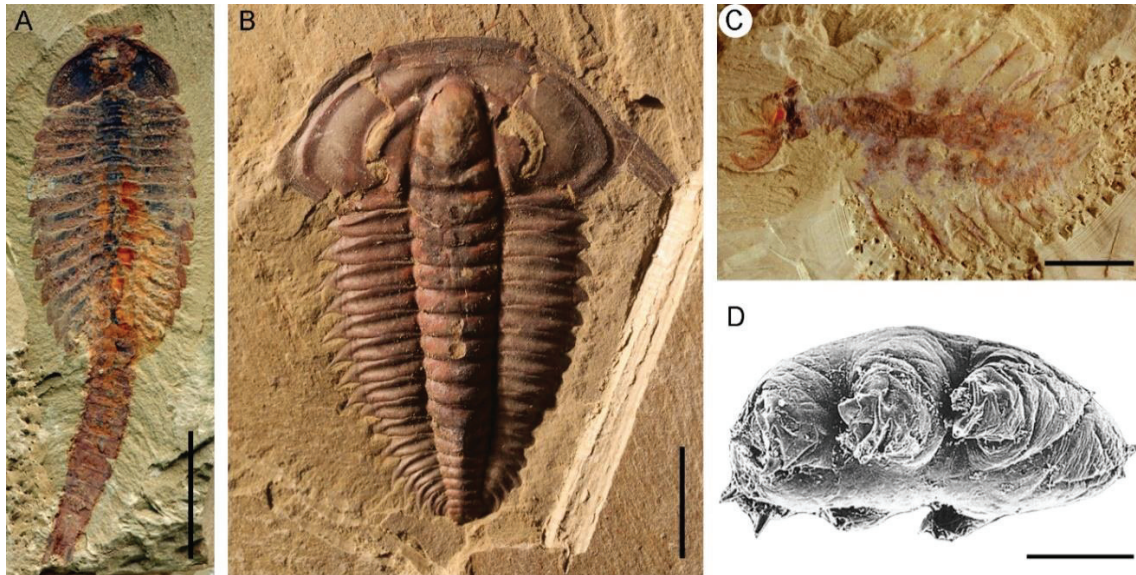


**Figure 39.** Cambrian Panarthropoda. A-C. Arthropods, *Fuxianhuia* Hou, 1987 (stem-group euarthropod), *Eoredlichia* Zhang, 1950 (Trilobita), *Lyrarapax* Cong et al., 2014 (stem-group arthropod), respectively. D. Tardigrade from the mid-Cambrian Kuonamka Formation of Siberia. Scale bars: 1 cm (A), 5 mm (B, C), 100  $\mu$ m (D). (D) from Müller et al. (1995).

#### 4.3.2.2 Lobopodia

Panarthropods with soft (non-jointed) appendages are abundantly represented in several early and mid-Cambrian Lagerstätten (e.g. Bergström and Hou, 2001; Budd, 1993; Dzik, 2003; Maas et al., 2007b; Smith and Caron, 2015; Fig. 40) and are often referred to as “lobopodians” although this category remains informal (Ortega-Hernandez, 2015; Yang et al., 2015). Lobopodians form a paraphyletic group (Caron and Aria, 2020; Ou, 2020). Twenty-five lobopodian species have been described from several early Cambrian Lagerstätten (Table 3) with fourteen of them (ca 38%) originating from the Chengjiang Lagerstätte (Table. 3; Fig. 40C-I).

Most lobopodians (<10 cm in length) have a segmented vermiform trunk with a terminal mouth, a series of paired ventrolateral unjointed legs, and differ from each other by various features such as their cuticular ornament (e.g. dorsal spines and plates) and the shape of their anterior appendages. For example, *Aysheaia* from the Burgess Shale bears spiny anterior appendages and claws at end of unjointed legs (e.g. Whittington, 1978; Fig. 40B-E). *Luolishania* (Hou and Chen, 1989a; Fig. 40E) and *Ovatiovermis* (Caron and Aria, 2017) have a well-differentiated head with specialized antenniform appendages. *Hallucigenia* (Conway Morris, 1977b; Hou and Bergström, 1995; Fig. 40D), *Collinsovermis* (Caron and Aria, 2020), and *Collinsium* (Yang et al., 2015) bear dorsally elongated spines. Cirriform appendicules are found at the posterior end of the trunk of *Antennacanthopodia* (Ou et al., 2011; Fig. 40F). *Diania* (Liu et al., 2011; Ma et al., 2014b; Fig. 40G) and *Microdictyon* (Chen et al., 1989; Fig. 40C) are armoured with stiff sclerites along their trunk, whereas *Paucipodia* (Chen et al., 1995; Fig. 40H) and *Lenisambulatrix* (Ou and Mayer, 2018; Fig. 40I) have a naked body without any cuticular thickenings.

Recent studies indicate that some lobopodians may belong to the stem-group Onychophora (velvet worms). The claws and dorsal spines of *Hallucigenia sparsa* from the Burgess Shale are

characterized by a stacked structures (Caron et al., 2013; Smith and Ortega-Hernández, 2014), which have direct counterparts in extant onychophorans (Oliveira et al., 2013; Robson, 1964; Oliveira and Mayer 2013; Robson 1964). Such microstructures have not been observed in the Chengjiang lobopodian *Hallucigenia fortis* (Fig. 40D). *Collinsium ciliosum* from the Xiaoshiba Lagerstätte (Yang et al., 2015) is equipped with supernumerary dorsal spines and specialized limbs for filter feeding. It is also resolved as a stem-group Onychophora based on a well-supported phylogeny (Yang et al., 2015). A very recent phylogenetic study that integrates new morphological characters (e.g. paired eyes and a tube) resolves *Facivermis yunnanicus* as a possible stem-group onychophoran (Howard et al. 2020a).

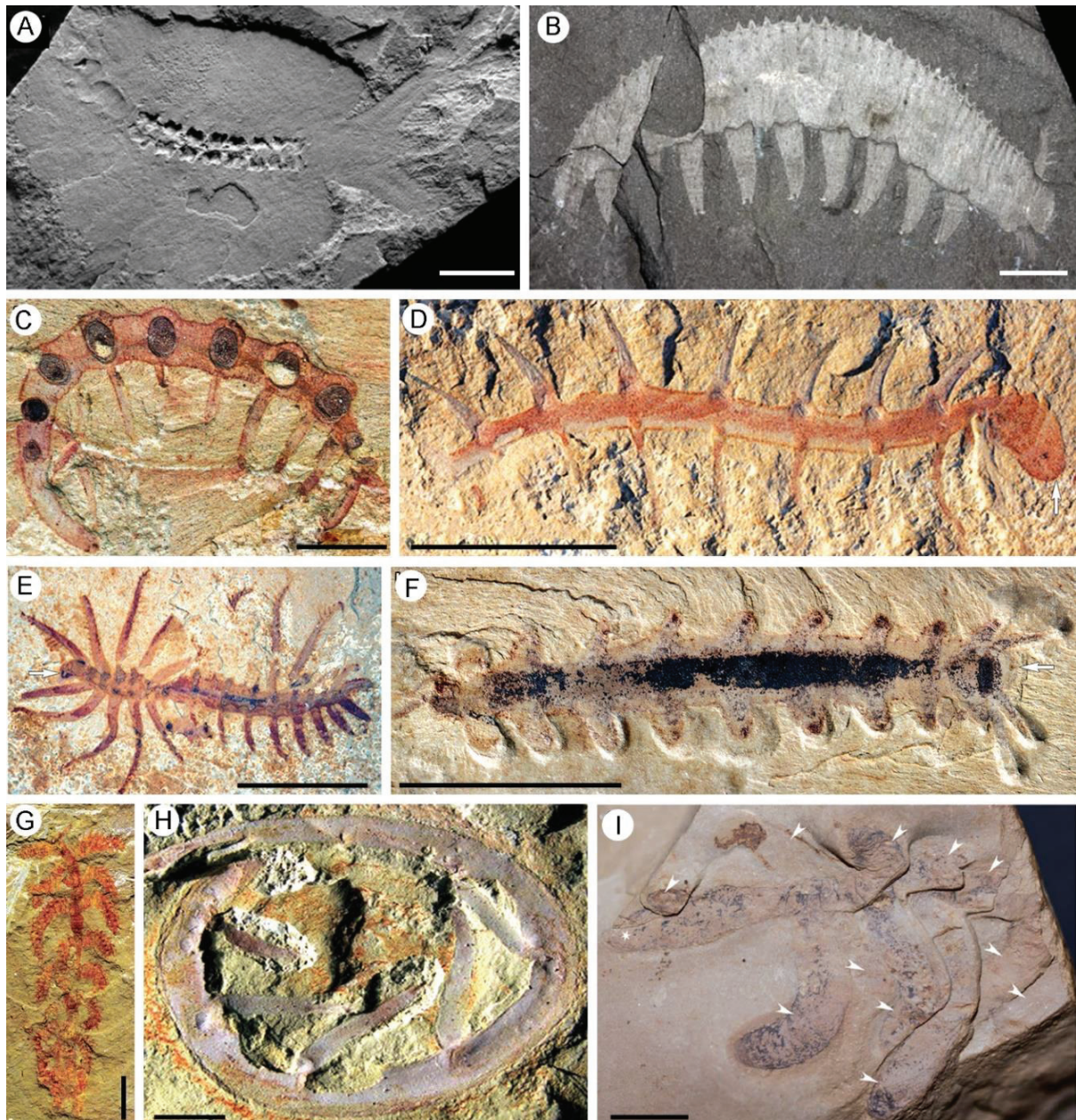




**Figure 40.** Lobopodians from the early Cambrian. A. *Kerygmachela kierkegaardi* Budd, 1993. B. *Aysheia pedunculata* Whittington, 1978. C. *Microdictyon sinicum* Chen et al., 1989. D. *Hallucigenia fortis* Hou and Bergström, 1995, arrow indicates head. E. *Luolishania longicuris* Hou and Chen, 1989a. F. *Antennacanthopodia gracilis* Ou et al., 2011, arrow indicates head. G. *Diania cactiformis* Liu et al., 2011. H. *Paucipodia inermis* Chen et al., 1995. I. *Lenisambulatrix humboldti* Ou et al., 2018, asterisk indicates a body terminus interpreted as the anterior end, arrowheads indicate thick legs. Scale bars: 1 cm (G), 5 mm (A-F, H, I). (A, B) from Ortega-Hernández (2014). (C-F, H, I) courtesy Q. Ou.

Other early Cambrian lobopodians are relatively large in size (more than 15 cm long) such as *Jianshanopodia* (Liu et al., 2006), *Megadictyon* (Liu et al., 2007), and *Kerygmachela* (Budd, 1998; Fig. 40A). They have powerful frontal appendages, paired digestive glands (*Megadictyon* and *Jianshanopodia*, Vannier et al., 2014; *Kerygmachela*, Fig. 40A), sclerotized mouthparts and some species have flaps on each trunk segment (*Kerygmachela*, Budd, 1998).

The lateral flaps of *Kerygmachela* are often considered as being homologous to the dorsal flaps of radiodontans and the exopods of Euarthropoda (Budd, 1998; Van Roy et al., 2015). In many recent phylogenetic trees these large lobopodians (*Jianshanopodia*, *Kerygmachela*) are resolved as basalmost stem-group arthropods (Caron and Aria, 2017; Howard et al., 2020b; Smith and Caron, 2015).

	Species	Source	Lagerstätte	Chrono-stratigraphy
1	<i>Xenusion auerswaldae</i>	Dzik & Krumbiegel 1989	Kalmarsund Sandstone (Hiddensee)	Cambrian Stage 2 to 3
2	<i>Microdictyon sinicum</i>	Chen et al. 1989; Chen et al. 1995	Chengjiang (south China)	Cambrian Stage 3
3	<i>Facivermis yunnanicus</i>	Hou & Chen 1989a; Howard et al., 2020		
4	<i>Luolishania longicuris</i>	Hou & Chen 1989b; Ma et al. 2009		
5	<i>Cardiodictyon catenulum</i>	Hou et al. 1991		
6	<i>Onychodictyon ferox</i>	Hou et al. 1991; Ramsköld & Hou 1991		
7	<i>Paucipodia inermis</i>	Chen et al. 1995; Hou et al. 2004		
8	<i>Hallucigenia fortis</i>	Hou & Bergström 1995		
9	<i>Megadictyon haikouensis</i>	Luo et al. 1999; Liu et al. 2007		
10	<i>Miraluolishania haikouensis</i>	Liu et al. 2004		
11	<i>Jianshanopodia decora</i>	Liu et al. 2006		
12	<i>Onychodictyon gracilis</i> <sup>1</sup>	Liu et al. 2008		
13	<i>Antennacanthopodia gracilis</i>	Ou et al. 2011		
14	<i>Diania cactiformis</i>	Liu et al. 2011; Ma et al. 2013		

15	<i>Lenisambulatrix humboldti</i>	Ou & Mayer 2018		
16	Unnamed lobopodian	Fu et al. 2019	Qingjiang (south China)	
17	<i>Collinsium ciliosum</i>	Yang et al. 2015	Xiaoshiba (south China)	
18	<i>Tritonychus phanerosarkus</i>	Zhang et al. 2016	Chengjiang (south China) *	
19	<i>Hadranax augustus</i>	Budd & Peel 1998	Sirius Passet (Greengland)	
20	<i>Kerygmachela kierkegaardi</i>	Budd 1993, 1998		
21	<i>Pambdelurion whittingtoni</i>	Budd 1998		
22	<i>Siberion lenaicus</i>	Dzik 2011	Sinsk (Russia)	
23	<i>Hallucigenia hongmeia</i>	Steiner et al. 2012	Guanshan (south China)	Cambrian Stage 4
24	<i>Collinsium</i> sp.	Jiao et al. 2016		
25	Unnamed “Collins” monster	García-Bellido et al. 2013	Emu Bay (Australia)	

**Table 3.** Lobopodian species from the early Cambrian. Modified from Ou (2020). \*, microfossils extracted from black shales (Yu’anshan Formation, south China).

#### 4.4 Diversity and disparity of ecdysozoans: a brief comparison between Kuanchuanpu and Chengjiang

The ecdysozoan fauna from the Kuanchuanpu Formation and the Chengjiang Lagerstätte differ from each other in terms of diversity and composition (Table 4). The Chengjiang biota is clearly dominated by arthropods whereas that of Kuanchuanpu biota consists of scalidophoran worms and lobopodians and lacks arthropod elements. These differences must be cautiously interpreted in the light of various possible factors (taphonomy, evolution).

Secondary phosphatization tends to favour the fossilization of tiny, often sub-millimetric fossils (Maas et al., 2006). Phosphatized SSF from the Kuanchuanpu Formation (ca 535 Ma) are indeed rarely larger than two millimetres. The lack of larger organisms, if present in original animal communities, may largely result from taphonomy. Although scalidophorans and lobopodians are represented by more or less complete specimens or cuticular fragments, it is worth noting that arthropod elements are absent. Not even a tiny fragment of jointed appendage (or any typical element of arthropod exoskeleton) has been found in any of the hundreds of residues obtained so far by our research team. Provisional comparative diagrams are given in Table 4.

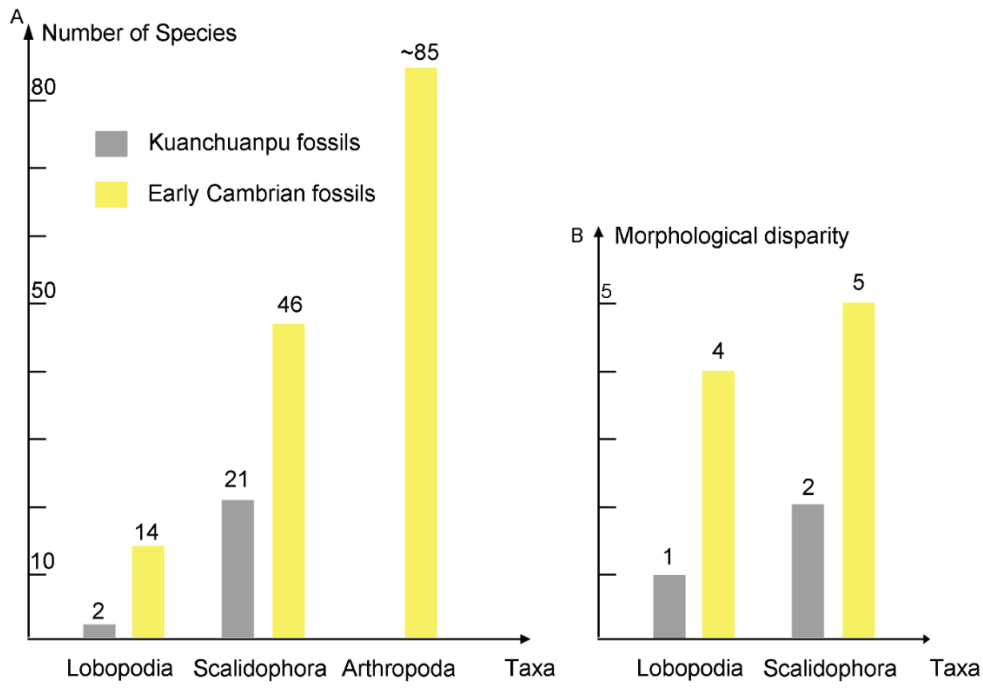


**Table 4.** Ecdysozoan composition of the Kuanchuanpu and other early Cambrian faunas. A, Showing species diversity. B, Showing morphological disparity. Note that morphological disparity means significant differences of body plan (see Chapter 4.2.1.4 and 4.3.1.3).

# Chapter 5 Results

## 5.1 Origin of ecdysis

Ecdysozoans, literally defined as “the moulting animals”, include three well-supported clades: the Scalidophora (Loricifera, Priapulida and Kinorhyncha), the Nematoida (Nematode and Nematomorpha) and the Panarthropoda (Arthropoda, Tardigrada and Onychophora) (Aguinaldo et al., 1997; Schmidt-Rhaesa et al. 1998; Giribet and Edgecombe, 2017), and altogether form an essential part of the present-day biodiversity (Brusca et al., 2016; Daley and Drage, 2016) with millions of species living in terrestrial and aquatic environments. Among them, crustaceans and insects are particularly familiar to us. All ecdysozoans secrete a cuticle which must be moulted periodically and replaced by a larger one (Nielsen, 2012; Purves et al., 2004), a process called ecdysis. For allowing any crustacean and insect to increase in volume, its cuticle must be shed periodically and a larger one must be synthesized from epidermal cells. The shedding of the old cuticle is another vital step of this process that is often associated with sophisticated behaviours (e.g. insects). Moulting is a complex process controlled and regulated by hormones (ecdysone) and specific genes. Various biological aspects of ecdysis have been studied by generations of scientists, and relatively recently genomic and transcriptomic studies have brought light on the molecular pathways involved in this complex process and led to evolutionary scenarios. However, most of these studies focus on insects and crustaceans. The moulting process of other ecdysozoans groups such as scalidophorans and nematoids is much less well understood. Fossil evidence from the discontinuous developmental mode of numerous fossil arthropods, exemplified by Cambrian trilobites (Drage et al., 2018; Wang et al., 2020) suggest that ecdysis has a very ancient origin. However, direct evidence of Cambrian animals “in the act of moulting” is extremely rare and often questionable. The aim of my study was to explore the origin of ecdysis by studying ecdysozoans worms from the basal Cambrian which potentially represent an early stage in the evolutionary history of moulting animals. Tiny fossil scalidophoran worms from the 535-million-year-old Kuanchuanpu Formation from China (basal Cambrian; Shaanxi Province). These worms are 3D-preserved in calcium phosphate and are often characterized by a spiny cuticular ornament (sclerites).

We found two types of cylindrical cuticular remains (Fig. 41A, C) among the SSFs from the Kuanchuanpu Formation. Type 1 with a positive external relief (spines of sclerites outwards pointing; Fig. 41A); Type 2 with a negative relief (spines of sclerites pointed inwards; Fig. 41C). We interpreted these fossils as exuviae. Type 2 results from mechanical inversion during moulting (Fig. 41B), the thin and flexible exuvia being turned inside out like the finger of a glove. These interpretations are congruent with direct observations of the moulting behaviour of extant priapulids (Scalidophora) that still live in present-day marine environments (e.g. Sweden, Russia) and provide precious comparative information (Fig. 41D-F). The old cuticle of these modern priapulids separates from the body along the trunk and at least one part of the exuvia (that lining the pharynx) can evaginate (Fig. 41E). This comparative study allowed us to reconstruct the moulting process of early Cambrian scalidophoran worms. It implies that these animals were capable of extricating themselves from their old cuticle either smoothly (Fig. 41A) or by turning their exuvia inside out (Fig. 41B, C).

Our study published in the Proceedings of the Royal Society London B (2019) provide solid fossil evidence that basal ecdysozoans animals grew by moulting at least 535 million years ago, before the diversification of arthropods, and shed light on mechanical aspect of their moulting. Scalidophoran worms from the Kuanchuanpu Formation, China are the oldest known record of moulting in ecdysozoans. In order to understand the molecular and evolutionary background of ecdysis, we collaborated with biologists (Isabell Schumann at Georg Mayer's lab in the University of Kassel, German). Their studies suggest that the early evolution of ecdysis included a suite of molecular innovations starting with the occurrence of Early genes in the last common ancestor of protostomes and continuing throughout the three ecdysozoan clades (acquisition of the EcR/USP complex and Halloween genes). Our study provides a chronological framework to this evolutionary scenario proposed by molecular biologists and indicates that complex genetical and physiological processes associated to ecdysis were already operating close to the Precambrian-Cambrian boundary. Modern scalidophorans greatly differ from other ecdysozoans (e.g. arthropods) and seem to lacking genetic elements essential to the ecdysteroid biosynthesis of arthropods and their relatives (e.g. Halloween genes). The molecular pathway (20-hydroxyecdysone or other molecules) through which priapulids, kinorhynchs and loriciferans achieve their moulting is virtually unknown and needs to be explored (see perspectives in Chapter 6.2).

Ecdysis appears as a key innovation and prerequisite condition to the diversification and success of major ecdysozoan groups such as arthropods. We hypothesize that ecdysis may have been selected as the most efficient solution to overcome mechanical constraints (growing with a rigid exoskeleton) and may have opened up new evolutionary perspectives.

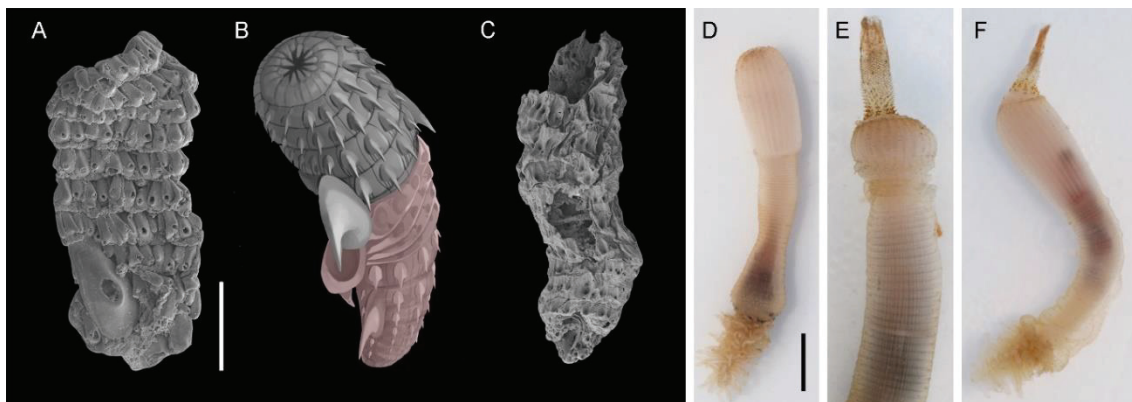


**Figure 41.** Moulting in early Cambrian and extant scalidophorans. A, C. Fossil exuviae of type 1 and type 2, respectively. B. Reconstruction showing exuvia (in pink) being turned inside out like the finger of a glove. D-F. Moulting in *Priapulus caudatus* from Sweden, showing everted pharyngeal cuticle. Scale bars: 5 mm (D-F), 500  $\mu$ m (A, C).

## Research



**Cite this article:** Wang D, Vannier J, Schumann I, Wang X, Yang X-G, Komiya T, Uesugi K, Sun J, Han J. 2019 Origin of ecdysis: fossil evidence from 535-million-year-old scalidophoran worms. *Proc. R. Soc. B* **286**: 20190791.  
<http://dx.doi.org/10.1098/rspb.2019.0791>

Received: 4 April 2019  
 Accepted: 17 June 2019

**Subject Category:**  
 Palaeobiology

**Subject Areas:**  
 palaeontology, ecology, evolution

**Keywords:**  
 Ecdysozoa, Scalidophora, moult, Cambrian, Kuanchuanpu Formation, South China

**Author for correspondence:**  
 Jian Han  
 e-mail: [elihanj@nwu.edu.cn](mailto:elihanj@nwu.edu.cn)

Electronic supplementary material is available online at <https://dx.doi.org/10.6084/m9.figshare.c.4552649>.

# Origin of ecdysis: fossil evidence from 535-million-year-old scalidophoran worms

Deng Wang<sup>1,2</sup>, Jean Vannier<sup>2</sup>, Isabell Schumann<sup>3,4</sup>, Xing Wang<sup>5</sup>,  
 Xiao-Guang Yang<sup>1</sup>, Tsuyoshi Komiya<sup>6</sup>, Kentaro Uesugi<sup>7</sup>, Jie Sun<sup>1</sup> and Jian Han<sup>1</sup>

<sup>1</sup>State Key Laboratory of Continental Dynamics, Shaanxi Key Laboratory of Early Life and Environments, Department of Geology, Northwest University, Xi'an 710069, People's Republic of China

<sup>2</sup>Laboratoire de Géologie de Lyon: Terre, Planètes, Environnement (CNRS-UMR 5276), Université Claude Bernard Lyon 1, Villeurbanne Cedex 69622, France

<sup>3</sup>Department of Genetics, and <sup>4</sup>Molecular Evolution & Animal Systematics, Institute of Biology, University of Leipzig, Talstraße 33, 04103 Leipzig, Germany

<sup>5</sup>Qingdao Institute of Marine Geology, China Geological Survey, Qingdao 266071, People's Republic of China

<sup>6</sup>Department of Earth Science and Astronomy, Graduate School of Arts and Sciences, University of Tokyo, Tokyo 153-8902, Japan

<sup>7</sup>Japan Synchrotron Radiation Research Institute (JASRI), 1-1-1 Kouto, Sayo-cho, Sayo-gun, Hyogo, Japan

DW, 0000-0002-4464-9632; JV, 0000-0003-0998-1231; IS, 0000-0001-8354-2523; JH, 0000-0002-2134-4078

With millions of extant species, ecdysozoans (Scalidophora, Nematoida and Panarthropoda) constitute a major portion of present-day biodiversity. All ecdysozoans secrete an exoskeletal cuticle which must be moulted periodically and replaced by a larger one. Although moulting (ecdysis) has been recognized in early Palaeozoic panarthropods such as trilobites and basal groups such as anomalocaridids and lobopodians, the fossil record lacks clear evidence of ecdysis in early scalidophorans, largely because of difficulties in recognizing true exuviae. Here, we describe two types of exuviae in microscopic scalidophoran worms from the lowermost Cambrian Kuanchuanpu Formation (*ca* 535 Ma) of China and reconstruct their moulting process. These basal scalidophorans moulted in a manner similar to that of extant priapulid worms, extricating themselves smoothly from their old tubular cuticle or turning their exuviae inside out like the finger of a glove. This is the oldest record of moulting in ecdysozoans. We also discuss the origin of ecdysis in the light of recent molecular analyses and the significance of moulting in the early evolution of animals.

## 1. Introduction

Ecdysozoans, defined literally as 'the moulting animals', comprise three well-supported clades, namely Scalidophora (Loricifera, Priapulida and Kinorhyncha), Nematoida (Nematoda and Nematomorpha) and Panarthropoda (Arthropoda, Tardigrada and Onychophora) [1–8]. Together, these groups form an essential part of the present-day biodiversity [9,10], with millions of species living in terrestrial and aquatic environments. Ecdysozoans secrete an exoskeletal cuticle which must be shed during growth and replaced by a larger one [11,12], a process called ecdysis. Periodic moulting occurs in all extant representatives of Ecdysozoa and is a key diagnostic feature of the group [10]. Most previous studies on ecdysis focus on physiological and mechanical aspects such as secretion and hardening (e.g. tanning and biomineralization) of new cuticle, as well as shedding of exuvia [13–17] and the neuroendocrine process responsible for it [18]. Recently, genomic and transcriptomic studies have shed new light on the molecular pathways involved in ecdysis, which development has paved the way for the formulation of detailed evolutionary scenarios [18,19]. The two critical steps of ecdysis are separation of the old cuticle from the underlying epidermal cells and splitting of the cuticle along predetermined lines of weakness, a process which allows the animal to extricate itself from its old exoskeleton. In contrast to moulting in arthropods (e.g. crustaceans and insects), the moulting process in other ecdysozoan

groups such as scalidophorans and nematoidans is much less well understood, except for certain parasitic nematoidan worms of the human body [20–24] and the larval stages of some scalidophorans [25–28]. Ecdysis is relatively well documented in early Palaeozoic panarthropods such as trilobites [10,29–31], and has also been recognized in more basal groups such as anomalocaridids [32] and lobopodians [33]. A recent study describes the apparent moulting process of a fuxianhuid euarthropod from the early Cambrian Xiaoshiba Lagerstätte of China [34].

Scalidophoran worms (Priapulida, Kinorhyncha and Loricifera) occur in several exceptional fossil deposits of Cambrian age, either as complete body fossils, incomplete fragments or isolated cuticular sclerites [35–39]. Although some of these cuticular remains have been interpreted provisionally as exuviae [36,40,41] (electronic supplementary material, table S2), uncertainty remains as to whether such fossils are true exuvial fragments discarded by the animal after moulting or incomplete decayed body fossils [3,35,42–44]. Convincing evidence for ecdysis in early Cambrian scalidophorans is provided by a nearly complete specimen of a stem-group loriciferan from the Sirius Passet Lagerstätte that is closely associated with a deformed lorica interpreted as its exuvia [41]. Especially, in macrobenthic scalidophorans [26], the cuticle of modern scalidophoran worms is extremely thin [45] compared with that of arthropods and is prone to mechanical alteration (e.g. tearing, folding, wrinkling and scattering of fragments) after being discarded. This characteristic probably contributed to the scarcity and poor preservation of fossil exuviae and to difficulty in recognizing them. Here, we describe two types of exuviae in scalidophoran worms from the Lower Cambrian Kuanchuanpu Formation (Fortunian Stage, Terreneuvian Series) of Shaanxi Province [46,47], China. These fossils provide the earliest evidence of moulting in ecdysozoans.

## 2. Material and methods

Specimens examined in the present study were collected from Bed 2 of the Kuanchuanpu Formation in the Zhangjiagou Section near Kuanchuanpu, Xixiang County [47–49]. The fossil-bearing bed belongs to the *Anabarites trisulcatus*-*Protohertzina anabarica* Assemblage zone [48], which correlates with the Nemakit-Daldynian interval in Siberia [48]. The absolute age of this bed is estimated to be about 535 Ma [46,50]. Phosphatic fossils were obtained by digesting rock samples in 8–10% acetic acid [51] followed by picking under a binocular microscope. The most common elements are globular spherical microfossils, specifically olivoids [46,52], metazoan embryos [47], cnidarians [53,54], bacteria [55], possible deuterostomes [51] and problematic fossils [56]. Ecdysozoans are rare and consist of scalidophoran remains, most of which are deformed, cylindrical cuticular fragments secondarily mineralized in calcium phosphate; the rest consist of nearly complete specimens [37,38,57]. External ornament is preserved in three dimensions (e.g. sclerites) with remarkable fidelity.

The 13 best-preserved specimens (ELIXX86-112, ELIXX63-29, ELIXX94-84, ELIXX99-492, ELIXX40-125, ELIXX85-284, ELIXX90-221, ELIXX85-429, ELIXX57-467, ELIXX98-179, ELIXX78-205, ELIXX85-16 and ELIXX85-120) were mounted on stubs, coated with gold and imaged with a scanning electron microscope (SEM) (FEI Quanta 400 FEG, high vacuum, secondary electron modes). Synchrotron radiation X-ray tomographic microscopy (SRXTM) was conducted at SPring-8 in Hyogo, Japan (23 KeV,  $0.51 \times 0.51 \times 0.51 \mu\text{m}^3 \text{pixel}^{-1}$ ) to study the internal anatomy of

two specimens (ELIXX85-429 and ELIXX90-221). SRXTM data were processed with DRAGONFLY 4.0 software for microtomographic analysis and three-dimensional (3D) visualization. Specimens of *Ottoia prolifica* Walcott, 1911 from the middle Cambrian Burgess Shale were examined in the National Museum of Natural History (Smithsonian Institution), Washington, DC, USA and the Royal Ontario Museum, Toronto, Canada, and photographed using a NIKON D3X digital SLR camera fitted with a macro lens under polarized light. Live specimens of *Priapulius caudatus* were collected near the Kristineberg Marine Station, Sweden (see details of locality in [58,59]), observed in the laboratory and photographed. All fossil specimens from the Kuanchuanpu Formation are deposited in the palaeontological collections of the Shaanxi Key Laboratory of Early Life and Environments, Northwest University, Xi'an, China (ELIXX numbers). Specimens from the Burgess Shale are housed in the collections of the National Museum of Natural History, Washington DC (USNM numbers) and the Royal Ontario Museum, Toronto, Canada (ROMIP numbers).

## 3. Results

### (a) Cuticular fragments showing positive or negative relief

We describe here two types of ornamented cuticular remains from the Kuanchuanpu Formation, based on 73 3D preserved specimens. The first type ( $n = 66$ ) consists of crumpled and compressed cylindrical fragments exhibiting positive external relief (PER). Their length and diameter range from approximately 800  $\mu\text{m}$  to 3000  $\mu\text{m}$  and 600  $\mu\text{m}$  to 1200  $\mu\text{m}$ , respectively. They display up to 14 evenly spaced annuli (longitudinal length approx. 140  $\mu\text{m}$  to 360  $\mu\text{m}$ ) separated by a deep furrow (figure 1*a,b,e,f*; electronic supplementary material, figure S4*(h)-(i)* and table S5). The annuli bear numerous small, evenly distributed sclerites having a broadly rounded or elliptical base extending into a strong apical hollow spine which is often broken. The length and width of the sclerites range from approximately 100 to 290  $\mu\text{m}$  and approximately 30–140  $\mu\text{m}$ , respectively. Sclerites are distributed radially and are slightly curved (figure 1*a,b,e,f*; electronic supplementary material, figure S4*(a)-(i)* and table S5). Each annulus bears between eight and 24 closed-packed sclerites separated by a very narrow gap occupied by crumpled cuticular material (electronic supplementary material, table S5). The small sclerites are not aligned in longitudinal columns but instead display a staggered arrangement. Most PER fragments exhibit at least one or two much larger (approx. 500  $\mu\text{m}$  long) sclerites with a circular or elliptical base of the same size. These stout sclerites extend over three or four adjacent annuli and seem to have been symmetrically distributed in pairs around the tubular structure (figure 1*a,b,e,f*; electronic supplementary material, figure S4*(a)-(d)*, *(f)-(i)* and table S5). Both sclerite types and other cuticular areas display a fine reticulated ornament with a mesh size varying from approximately 4  $\mu\text{m}$  to 16  $\mu\text{m}$  (electronic supplementary material, table S5). This ornament is particularly well developed in the proximal half of the sclerites (figure 1*c,d*), but elsewhere it has a wrinkled and more irregular appearance (electronic supplementary material, figure S4*(e)*). PER fragments display the same external morphology as that of 3D-preserved scalidophoran worms described from the same biota by previous authors (especially Indeterminate Form 1) and consisting of an annulated trunk lined with small and large scalds, a proboscis, a mouth opening and a tail part [38,60].

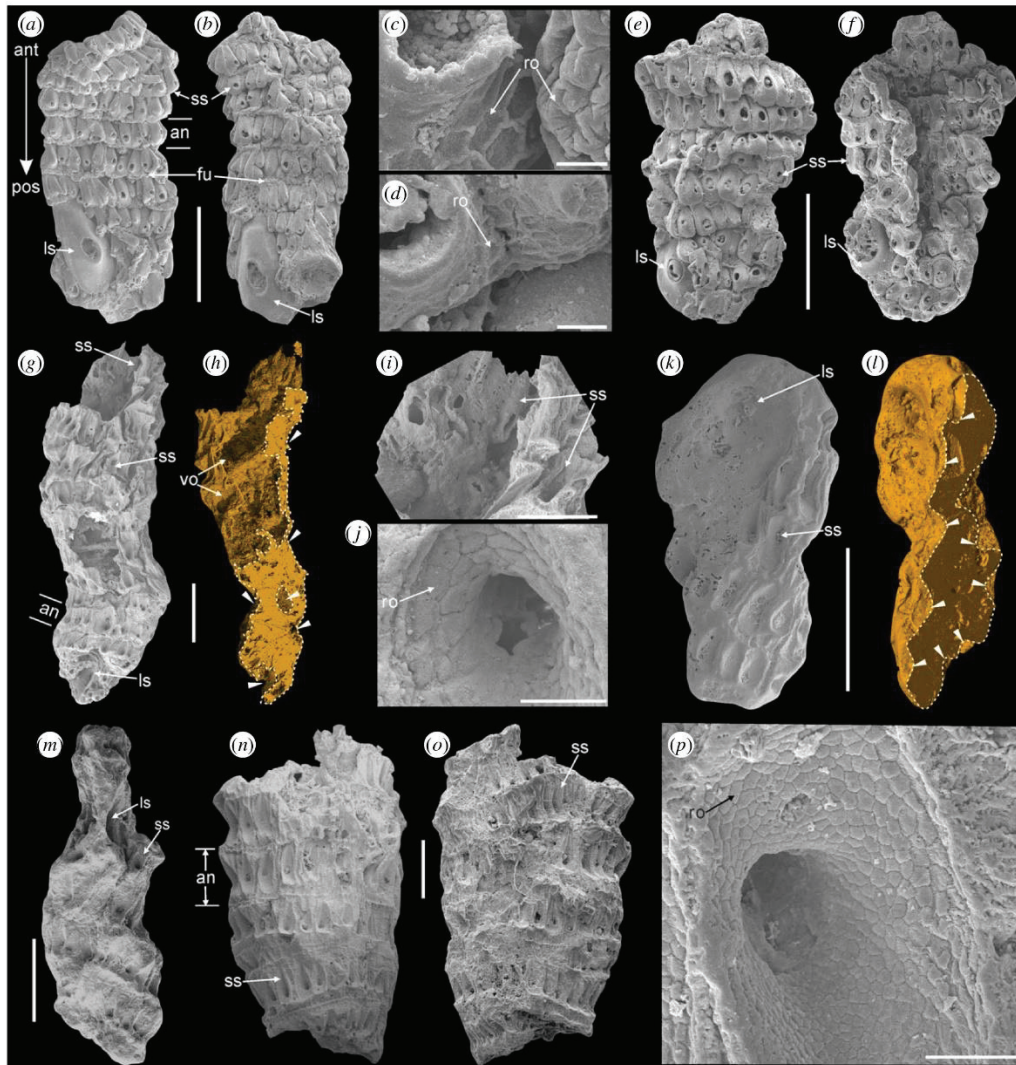


**Figure 1.** Scaldiphoran cuticular fragments from the lowermost Cambrian Kuanchuanpu Formation, Shaanxi Province, China. (a–f) Specimens with positive external relief (PER; see explanations in text). (g–p) Specimens with negative external relief (NER). (a–m) Specimens assigned to Indeterminate Form 1 (see the electronic supplementary material, S3). (n–p) A specimen assigned to Indeterminate Form 2 (electronic supplementary material, S3). (a–c) ELIXX86–112, general views from two opposite sides showing small sclerites on annuli and a large sclerite, and details of reticulated ornament along basal part of a sclerite (c). (d–f) ELIXX63–291, reticulated ornament (d) and general views from two opposite sides showing sclerites on annuli. (g–j) ELIXX90–221, general view showing sclerites pointing inwards towards the longitudinal axis of the tubular structure, longitudinal virtual section (microtomographic image) showing sclerites with hollow conical structure (white triangle), details of upper part with sclerites pointing inwardly and outwardly, and reticulated micro-ornament along the inner surface of a sclerite. (k–l) ELIXX85–429, general view and oblique virtual section showing sclerites pointing inwards (white triangle). (m) ELIXX85–16, compressed fragment with elongated end. (n–p) ELIXX85–120, general view from two opposite sides showing small spinose sclerites on annuli, pointing inwards, and details of reticulated ornament of inner surface of a sclerite. All SEM images except (h) and (l) obtained by using synchrotron radiation X-ray tomographic microscopy. Anterior–posterior orientation based on complete specimens described by *Eopriapulites sphinx* [37], *Eokinorhynchus rarus* [38], *Qinscolex spinosus* and *Shanscolex decorus* [60]. an, annulus; ant, anterior part; fu, furrow between annuli; ls, large spinose sclerite; pos, posterior part; ro, reticulated ornament; ss, small spinose sclerite; vo, void. Scale bars: 500  $\mu\text{m}$  (a,b,e,f,g–i,k–o); 10  $\mu\text{m}$  (c); 20  $\mu\text{m}$  (d) and (j); and 50  $\mu\text{m}$  (p). (Online version in colour.)

The remaining fragments ( $n = 6$ ) exhibit the same size, crumpled cylindrical shape, small and large sclerites and reticulated ornament as PER fragments, but differ from them in showing inverted relief. Sclerites, instead of projecting outwards, point inwards radially, thus exposing the hollow interior (figure 1g–m); electronic supplementary material, figure S4(j)–(o)). Negative external relief (NER) and PER

fragments possess the same type of small and large sclerites and the same reticulated micro-ornament (electronic supplementary material, S3 and table S5). The NER type appears to be an invaginated version of the PER type, having resulted from the inward folding of a flexible, cylindrical cuticular structure about its longitudinal axis, in a manner similar to the reversal of a glove finger.



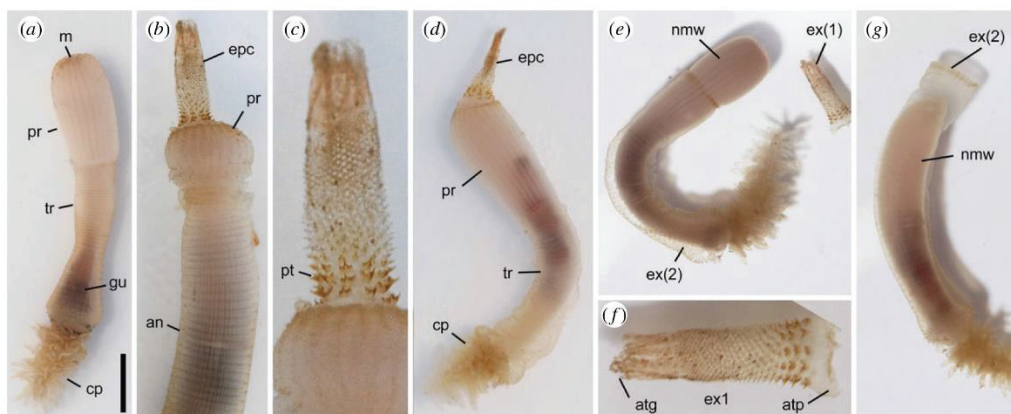


**Figure 2.** Moulting process in the extant priapulid worm *Priapulus caudatus* from Sweden, as observed under laboratory conditions (no sediment). (a) Before moulting. (a–c) Evaginated pharyngeal cuticle, general view and details (showing pharyngeal teeth pointing upwards). (d) Folded pharyngeal cuticle still attached to proboscis. (e–f) Exuvia split into two parts (pharyngeal cuticle discarded) and newly moulted worm protruding beyond its old cuticle; general view and details of pharyngeal cuticle. (g) Newly moulted worm retracted into its old cuticle. Light photographs of live specimen in seawater. an, annulation; atg, attachment to gut; atp, attachment to proboscis; cp, caudal process; epc, evaginated pharyngeal cuticle; ex(1) anterior part of exuvia; ex(2) posterior part of exuvia; gu, gut; m, mouth; nmw, newly moulted worm; pr, proboscis; pt, pharyngeal teeth; tr, trunk. Scale bars: 5 mm. (Online version in colour.)

Both NER and PER cuticular fragments undoubtedly belong to scalidophorans; however, their fragmentary nature allows neither generic nor specific determination. At least four virtually complete scalidophoran worms (*Eopriapulites sphinx* [37,57], *Eokinorhynchus rarus* [38], *Qinscolex spinosus* and *Shanscolex decorus* [60]) and 12 unnamed forms [38,43,60] have been reported from the Kuanchuanpu Formation. Our specimens may represent two distinct forms, predominantly Indeterminate Form 1 and Indeterminate Form 2 (figure 1*n–p*; electronic supplementary material, figure S3 and table S5).

## 4. Discussion

### (a) Evidence for exuviae in the lowermost Cambrian

It is generally difficult to distinguish moults (exuviae) from carapaces unless the animal is preserved in the act of shedding its old exoskeleton [34,41]. Suggested criteria for the identification of fossil moults are mainly applicable to arthropods having a relatively hard carapace such as trilobites [10], and include the presence of suture lines as well as repetitive associations and configurations of specific exoskeletal elements [10].

Unlike the cuticle of arthropods, that of modern scalidophoran worms is extremely thin and fragile (electronic supplementary material, figure S1(a)–(g)) [59]. Exuviae are, therefore, prone to dispersal, tearing, folding and (eventually) decay, thus greatly reducing their preservation potential. Certain cuticular fragments from Cambrian and younger strata have been interpreted as possible exuviae (electronic supplementary material, table S2). Potential criteria for positive identification of exuviae (versus decayed body fossils) include: (i) a highly distorted and folded appearance [3,35,42,43]; (ii) the absence of remains of internal tissues and organs [41,44]; and (iii) dislocation of cuticle elements (e.g. isolated proboscis and trunk fragments detached from the proboscis) [36,41]. However, worm bodies (e.g. *Priapulus*) that have undergone selective decay (e.g. cuticle versus soft tissues) [61], post-mortem transportation and disarticulation [10] may exhibit configurations similar to those observed in putative fossil

exuviae [61]. For example, *Ottoia prolifica*, from the middle Cambrian Burgess Shale is represented both by complete body fossils with a typical swollen shape (electronic supplementary material, figure S6) and preserved intestine, and by a variety of distorted and incomplete specimens produced by more or less advanced decomposition [36]. A very small percentage of these incomplete specimens, though folded, exhibit distinct outlines and seem to represent compressed, empty cuticular envelopes that may confidently be interpreted as exuviae (electronic supplementary material, figure S6). Another example is a single loriferan from the lower Cambrian Sirius Passet Lagerstätte that appears to be preserved in the process of emerging from its empty exuvia (loricae, [41]). Similarly, Müller & Hinz-Schallreuter [40] interpreted palaeoscolecid cuticular fragments with double-layer ornamentation as belonging to worms buried shortly before ecdysis. Aside from these rare cases, the identification of fossil exuviae is uncertain [3,42–44]. Indeed, PER fragments from the Kuanchuanpu Formation may represent either exuviae or body fragments in which soft parts are entirely decomposed. The same is definitely not true, however, for NER fragments (figure 1*g–p*; electronic supplementary material, figure S4(*j–n*)), which as argued above resulted from the invagination of a flexible, tube-like cuticular envelop. Such specimens could not have been produced by simple disarticulation or by external physical forces such as bottom currents. We conclude therefore that NER fragments are exuviae that underwent mechanical inversion during moulting. These unusual tubular fossils with inverted relief provide the solid confirmation of ecdysis in fossil scalidophorans, and extend the origin of moulting back to the lowermost Cambrian (*ca* 535 Ma).

### (b) Moulting process in extant scalidophorans

The moulting process in extant scalidophorans was described by Lang [62] from *Priapulus caudatus*, which undergoes separation of the cuticle from the epidermis and breakup of the old cuticle in the oral region, allowing the worm to emerge from its exuvia through undulating movements and repeated friction with sediment [25,26,62]. Recent observations on *Priapulus caudatus* under laboratory conditions [62] (J.V.,

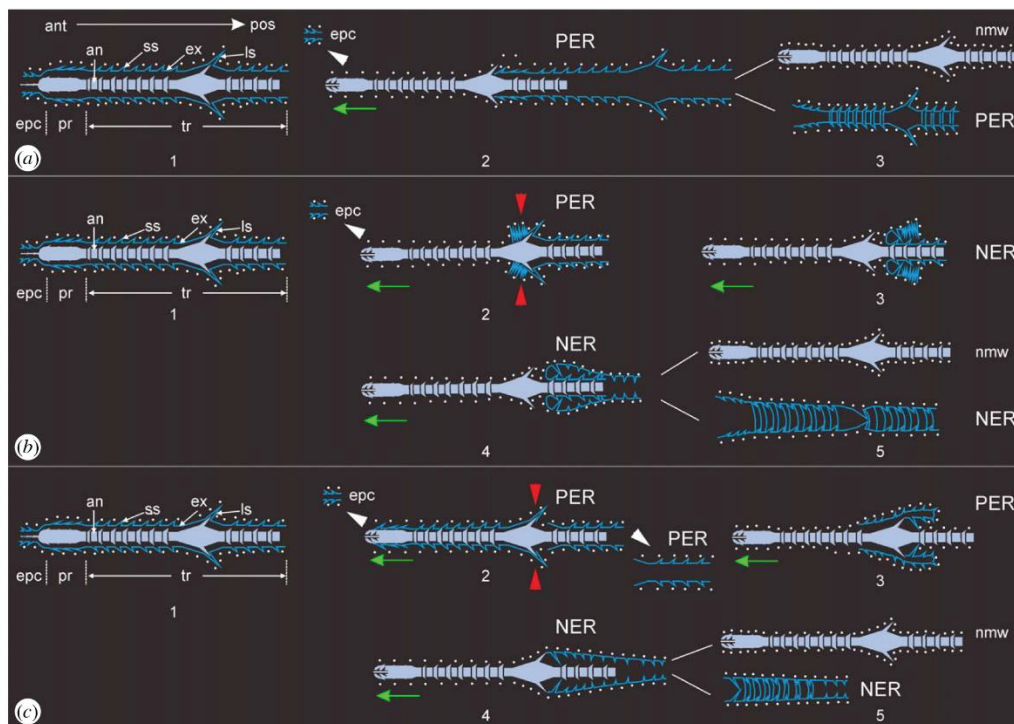


**Figure 3.** Hypothesized moulting processes in scalidophoran worms from the lowermost Cambrian Kuanchuanpu Formation, Shaanxi Province, China. Worm body and exuvia represented in light and dark blue, respectively. (a) Ecdysis of type 1 (PER); (1) the old cuticle detaches from body, (2) the worm extricates itself from its tubular exuvia via muscular contractions and (3) has shed its old cuticle which shows positive relief (expressed by sclerites pointing outwards). (b) Ecdysis of type 2 (NER); (1) friction or local anchoring to sediment (red arrows) cause the cuticle to withdraw and fold up posteriorly, (2) to be eventually evaginated (3 and 4) as the worm moves forwards (green arrows), leading to the exuvia being turned inside out (5). (c) Ecdysis with both types (PER and NER); (1) the cuticle remains attached locally (e.g. sclerite) to the body and breaks apart (owing to straining forces), (2) the posterior part is released as a PER exuvia whereas the anterior portion is dragged along and invaginated as the worm goes forward (3 and 4), leading to a NER exuvia (5). an, annulus; ant, anterior part; epc, evaginated pharyngeal cuticle; ex, exuvia; ls, large spinose sclerite; NER, negative external relief; nmw, newly moulted worm; PER, positive external relief; pos, posterior part; pr, proboscis; ss, small spinose sclerite; tr, trunk; white dots represent sediment. Not to scale. (Online version in colour.)

figure 2) revealed the operation of three successive steps: (i) gradual separation of the old cuticle from the body along the trunk (figure 2b); (ii) detachment of the cuticle lining the pharynx from the anteriormost part of the gut followed by evagination of this cuticle to form an empty, fragile envelope which remains attached to the proboscis temporarily (figure 2b–d); and (iii) splitting of the old cuticle into two parts around the proboscis, allowing the pharyngeal cuticle to detach (figure 2e,f). During the final stage, the worm is in the process of hardening a new cuticle and is able to extend and retract its proboscis within the tubular structure formed by the exuvia (figure 2g). How the newly moulted worm eventually extricates itself completely from its exuvia could not be observed. Nevertheless, we now know that at least one part of the exuvia (pharynx) can evaginate. Also, exuviae exhibiting negative relief similar to NER type in fossil worms (figure 1) were not observed under laboratory conditions (Petri dish with seawater [26–28,62] and present paper). More detailed studies comparing the moulting process of *Priapulius* with that of other priapulid worms such *Halicryptus* are needed to confirm these preliminary observations, and such observations must take into account the role of sediment in ecdysis (e.g. friction, anchoring and pressure exerted by sediment in burrows).

### (c) Moulting process in lowermost Cambrian scalidophorans

Two types of scalidophoran exuviae coexist in the Kuanchuanpu biota. The most frequent type is represented by a deformed, cylindrical cuticular structure showing PER expressed by pointed sclerites (figure 1a,b,e,f; electronic supplementary material, figure S4(a)–(i)). We hypothesize that this type resulted from the uniform separation of the new cuticle, allowing the newly moulted worm to leave its old cuticle smoothly (figure 3a). The external cuticular ornament (e.g. scalds), by promoting friction and anchoring to sediment, may have helped the worm to withdraw from its exuvia, assuming that ecdysis occurred within the sediment (infaunal lifestyle as in extant priapulids). The second type has a comparable cylindrical shape but an NER expressed by sclerites pointing inwardly (figure 1g–p; electronic supplementary material, figure S4(j)–(o)). Two different mechanical processes may explain NER exuviae: (i) frictional forces between the cuticular ornament (e.g. sclerites) and sediment causing the cuticle to evaginate as the worm moves forwards (figure 3b); or (ii) local attachment of the cuticle to the body plus pressure from surrounding sediment causing the cuticle to break apart, with the posterior portion being released and the anterior part remaining attached to the

body, invaginating, and then being dragged along as the worm moves forwards (figure 3c). Both mechanisms are capable of producing an exuvia exhibiting negative relief. PER and NER moulting processes have analogues in extant scalidophorans (figure 2) [26]. The PER type clearly corresponds to the moulting of the trunk of *Priapulius* (the newly moulted worm extricates itself smoothly from the old cuticle when loosened), while the NER type strongly recalls the evagination of the pharyngeal cuticle (figure 2b–f). An interesting analogue of cuticular invagination is also found in snakes (electronic supplementary material, figure S7—compare with figure 3b), in which the external layer of the skin is peeled away. The snake crawls out of it, turning it inside out and thus exposing scales with inverted relief. As in Cambrian scalidophorans, this process is initiated by local attachments of the old skin to the body and is associated with the splitting of the exuvia into tubular sections of various lengths.

#### (d) Origin and evolution of ecdysis

Molecular phylogenies suggest that ecdysozoans have a very remote origin and ramified during the Ediacaran Period (approx. 635–543 Ma) [4,63–66]. However, uncertainties remain concerning the chronology of divergence of the major ecdysozoan clades (Nematoida, Scalidophora and Panarthropoda) and the phylogenetic relationships between subgroups (e.g. Priapulida, Kinorhyncha and Loricifera for Scalidophora). Alternative evolutionary hypotheses require proper testing using fossil data, more accurate calibration (e.g. [67]) and a critical approach to molecular clock dating (e.g. [66]).

Although scalidophorans and a variety of panarthropods including lobopodians [68] and iconic arthropods such as trilobites [69] are abundantly represented in early Cambrian marine communities (e.g. the 520-Ma-old Chengjiang biota [70] and the 518-Ma-old Qingjiang biota [39]), no ecdysozoan fossils have been found thus far in late Precambrian (Ediacaran) rocks [65]. Burrow systems attributed to priapulid-like worms are used to define the Precambrian–Cambrian boundary [58,71,72], but they are not associated with their assumed trace-makers. The oldest confirmed occurrence of ecdysozoans in the lowermost Cambrian (Fortunian Stage, ca 535 Ma) is the complete body fossils [37,38,57] and exuviae (this paper) of scalidophorans from the Kuanchuanpu Formation. Our findings also corroborate hypotheses based on fossil evidence that younger Cambrian scalidophorans such as *Ottoia prolifica* (electronic supplementary material, figure S6) and other forms [3,35] shed their cuticle during growth.

The occurrence of moulting in early scalidophorans suggests that these animals had already acquired a genetic tool-kit and possibly a neuroendocrine system to achieve ecdysis. Although little is known about the molecular control of moulting in scalidophoran worms, a recent molecular study has shed light on key evolutionary aspects of ecdysis [18]. Scalidophorans possess genes that are known to play a key role in the moulting process of other ecdysozoan taxa (e.g. homologues of Early genes and Receptor genes (*EcR*, *USP/RXR*) [18]), but they lack genetic elements essential to the ecdysteroid biosynthesis of arthropods and their relatives (e.g. Halloween genes [18]). This raises the question of whether priapulids, kinorhynchs and loriciferans use steroid hormones such as 20-hydroxyecdysone (20E) or other molecules (e.g. daferochronic acid in free-living nematodes [73]) for moulting. The moulting hormone 20E also occurs in non-ecdysozoan

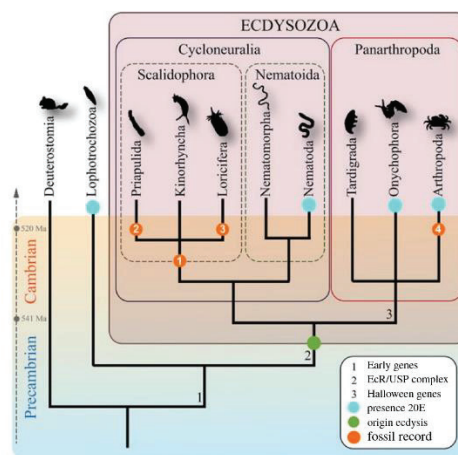


**Figure 4.** Evolution of moulting. Simplified tree showing phylogenetic relationships of the major bilaterian taxa, including ecdysozoans, lophotrochozoans and deuterostomes (modified after [18,19,78]). Numbers at nodes represent possible genetic innovations in the early evolution of ecdysis. Blue dots indicate the presence of the moulting hormone 20-hydroxyecdysone (20E), which is present in parasitic nematodes and has been not found in free-living forms to date. Green dot indicates the origin of ecdysone-induced moulting. Orange dots with white numbers indicate the early fossil record of ecdysis in basal scalidophorans (1; this paper, priapulids (2; [36,40]), loriciferans (3; [41]), and arthropods (4; fuxianhuids, [34]). (Online version in colour.)

animals (e.g. platyhelminthes, annelids and molluscs) and may have been present in the last common ancestor (LCA) of protostomes [18,74–77]. This set of recent molecular data suggests that the early evolution of ecdysis includes a suite of molecular innovations possibly starting with the occurrence of Early genes in the LCA of protostomes and continuing throughout the three ecdysozoan clades (acquisition of the *EcR*/*USP* complex and Halloween genes; figure 4).

Fossil evidence confirms that several groups of moulting animals, including scalidophorans (this paper), loriciferans [41] and various panarthropods (e.g. stem-group arthropods, [34]), were present in the early Cambrian. The time of origin (whether Ediacaran or later) and general morphology of the first moulting animal remain an open question. We here hypothesize that this animal was a worm-like, possibly infaunal organism with a hydrostatic skeleton [79], the forces governing locomotion having been transmitted not through rigid skeletal elements but rather through internal pressure controlled by muscle contractions and relaxation as in extant priapulid worms [59]. The scalidophorans from the Kuanchuanpu Formation have high-relief sclerites, suggesting that thicker and more complex cuticular features developed among early ecdysozoans for greater protection against abrasion, and/or predation, or for more efficient locomotion (e.g. anchoring features for burrowing [7,68]). This set of innovations may have been of major importance in the rise of ecdysis, as an ornamented and relatively rigid exoskeleton is hardly compatible with continuous growth (e.g. extant crustaceans) and must be replaced by a larger one. Thus, ecdysis may have been selected as the most adequate solution to overcome these mechanical constraints, and may have opened up new evolutionary opportunities. Ecdysis implies molecular innovations probably inherited from genetic elements were already present in non-moulting ancestors (figure 4), an

**Table 1.** Ecdysis in extant Ecdysozoa and Annelida: relationships between body plan and moulting process. (\*1: some parasitic nematodes have a reduced cuticle or no cuticle at all. \*2: external segmental cuticular elements. \*3: a stiff cuticular case with plate-like elements. \*4: parapodia act as limbs in most polychaetes. \*5: moult in pre-adult stages and females (e.g. *Panagrellus silusiae*). \*6: moulting in adult males (e.g. *Panagrellus silusiae*). \*7: friction with sediment may facilitate ecdysis. \*8: observed in Polychaeta (e.g. *Lumbrineris crosslandi*; *Marphysa sanguinea*; *Nereis diversicolor*). \*9: observed in jaws from some Polychaeta (e.g. *Diopatra aciculata*).

clade	taxa	body plan	moulting process	refs
Panarthropoda	Arthropoda	articulated chitinous exoskeleton; jointed limbs	exuvia splits open through various ways, where cuticle is thinner	[80]
	Onychophora	unarticulated chitinous cuticle; unjointed limbs	ecdysis starts from mid-dorsal split line	[81]
	Tardigrada	unarticulated chitinous cuticle; unjointed limbs	ecdysis starts from anterior end	[15]
	Nematomorpha	worm-shaped; no limbs; no circular muscles	ecdysis starts from anterior end	[82]
Nematoida	Nematoda (free-living)	worm-shaped; no limbs; cuticle with collagen; no circular muscles	cuticle sheds in tatters (*5) or peels off from anterior end (*6)	[83]
	Nematoda (parasitic)	worm-shaped; no limbs; cuticle (*1) with collagen; no circular muscles	ecdysis starts from anterior end	[84]
	Priapulida	worm-shaped; no limbs; thin chitinous cuticle; circular and longitudinal muscles	ecdysis starts from anterior end; friction with sediment (*7)	[26,62]
Scalidophora	Kinorhyncha	worm-shaped; no limbs; segmented trunk (*2); thin chitinous cuticle; circular and longitudinal muscles	ecdysis starts from anterior end	[28]
	Loricifera	no limbs; trunk covered by lorica (*3); thin chitinous cuticle; circular and longitudinal muscles	ecdysis starts from anterior end	[27,85]
Lophotrochozoa	Annelida	segmented body; cuticle with collagen; parapodia (*4)	cuticle sheds in flakes (*8) or partial ecdysis (*9)	[74,86]

epidermal structure compatible with ecdysis, and close correlations between body plans and the moulting process (table 1). Ecdysis seems to have appeared in the context of the profound environmental changes that characterized the Precambrian–Cambrian transition, including increasing oxygen levels [87–89] and interactions among animals [90–92], and thus the onset of more complex marine ecosystems (e.g. food webs and colonization of infaunal niches [90,91]).

**Data accessibility.** All fossil specimens from the Kuanchuanpu Formation are deposited in the collections of the Shaanxi Key Laboratory of Early Life and Environments, Northwest University, Xi'an, China (ELIXX numbers), those from the Burgess Shale, in the collections of the National Museum of Natural History, Washington DC (USNM numbers) and the Royal Ontario Museum, Toronto, Canada (ROMIP numbers).

**Authors' contributions.** J.H. conceived the project. D.W., J.H. and J.V. interpreted the fossil material; T.K. and K.U. conducted the microtomographic analyses (synchrotron). J.S. reconstructed the microtomographic data. D.W., J.H., J.V. and I.S. wrote the paper

with input from the other authors. All authors read and approved the final manuscript.

**Competing interests.** We declare we have no competing interests.

**Funding.** This work was supported by the Strategic Priority Research Program of Chinese Academy of Sciences (grant no. XDB26000000), Natural Science Foundation of China (nos. 41621003, 41772010, 41672009, 41720104002), Ministry of Science and 111 project of Ministry of Education of China (no. D17013), the Most Special Fund from the State Key Laboratory of Continental Dynamics, Northwest University, China (BJ11060) and Northwest University Graduate Innovation and Creativity Funds (no. YZZ17195).

**Acknowledgements.** We thank Long Pang, Juan Luo and Meirong Cheng (State Key Laboratory for Continental Dynamics, Northwest University, Xi'an, China) for their assistance in both field and laboratory work. We also thank the Kristineberg Marine Station for assistance with extant priapulid worms, D. Erwin and M. Florence (Smithsonian National Museum of Natural History, Washington DC) and J.B. Caron (Royal Ontario Museum) for access to the Burgess Shale Fossil collections, J. Sundukova for photographs, H. Van Iten (Hanover College, IN, USA) for linguistic corrections and the two referees.

## References

1. Aguinaldo AMA, Turbeville JM, Linford LS, Rivera MC, Garey JR, Raff RA, Lake JA. 1997 Evidence for a clade of nematodes, arthropods and other moulting animals. *Nature* **387**, 489–493. (doi:10.1038/387489a0)
2. García-Bellido C. 2004 Moulting arthropod caught in the act. *Nat. Brief Commun.* **429**, 02587. (doi:10.1038/429040a)
3. García-Bellido DC, Paterson JR, Edgecombe GD. 2013 Cambrian palaeoscolecid (Cycloneuralia) from Gondwana and reappraisal of species assigned to *Palaeoscolex*. *Gondwana Res.* **24**, 780–795. (doi:10.1016/j.gr.2012.12.002)
4. Giribet G, Edgecombe GD. 2017 Current understanding of Ecdysozoa and its internal phylogenetic relationships. *Integr. Comp. Biol.* **57**, 455–466. (doi:10.1093/icb/ix072)

5. Haug JT, Haug C. 2014 A new cycloneuralian from the Burgess Shale with a palaeoscolecid-type terminal end. *Neues Jahrbuch für Geologie und Paläontologie - Abhandlungen* **274**, 73–79. (doi:10.1127/njgpa/2014/0441)
6. Schmidt-Rhaesa A. 1998 Phylogenetic relationships of the nematomorpha: a discussion of current hypotheses. *Zoologischer Anz.-J. Comp. Zool.* **236**, 203–216.
7. Valentine JW, Collins AG. 2000 The significance of moulting in ecdysozoan evolution. *Evol. Dev.* **2**, 152–156. (doi:10.1046/j.1525-142x.2000.00043.x)
8. Ax P. 2003 *Multicellular animals: order in nature-system made by Man*, pp. 1–41. Berlin, Germany: Springer.
9. Brusca RC, Moore W, Shuster SM. 2016 *Invertebrates*, 3rd edn, pp. 639–910. Sunderland, MA: Sinauer Associates.
10. Daley AC, Drage HB. 2016 The fossil record of ecdysis, and trends in the moulting behaviour of trilobites. *Arthropod. Struct. Dev.* **45**, 71–96. (doi:10.1016/j.asd.2015.09.004)
11. Nielsen C. 2012 *Animal evolution: interrelationships of the living phyla*, 3rd edn, pp. 238–310. Oxford, UK: Oxford University Press.
12. Purves WK, Sadava D, Orians GH, Heller HC. 2004 *Life the science of biology*, 7th edn, pp. 641–654. Sunderland, MA: Sinauer Associates.
13. Arakane Y, Li B, Muthukrishnan S, Beeman RW, Kramer KJ, Park Y. 2008 Functional analysis of four neuropeptides, EH, ETH, CCAP and burscion, and their receptors in adult ecdysis behavior of the red flour beetle, *Tribolium castaneum*. *Mech. Dev.* **125**, 984–995. (doi:10.1016/j.mod.2008.09.002)
14. Ayali A. 2009 The role of the arthropod stomatogastric nervous system in moulting behaviour and ecdysis. *J. Exp. Biol.* **212**, 453–459. (doi:10.1242/jeb.023879)
15. Bertolani R, Altiero T, Nelson DR. 2009 Tardigrada (water bears). In *Encyclopaedia on inland water* (ed. GE Likens), pp. 443–455. Oxford, UK: Elsevier.
16. Chang ES, Mykles DL. 2011 Regulation of crustacean molting: a review and our perspectives. *Gen. Comp. Endocrinol.* **172**, 323–330. (doi:10.1016/j.ygcen.2011.04.003)
17. Chung JS, Webster SG. 2003 Moulting cycle-related changes in biological activity of moulting-inhibiting hormone (MIH) and crustacean hyperglycaemic hormone (CHH) in the crab, *Carcinus maenas*. From target to transcript. *Eur. J. Biochem.* **270**, 3280–3288. (doi:10.1046/j.1432-1033.2003.03720.x)
18. Schumann I, Kenny N, Hui J, Hering L, Mayer G. 2018 Halloween genes in panarthropods and the evolution of the early moulting pathway in Ecdysozoa. *R. Soc. open sci.* **5**, 180888. (doi:10.1098/rsos.180888)
19. Borner J, Rehm P, Schill RO, Ebersberger I, Burmester T. 2014 A transcriptome approach to ecdysozoan phylogeny. *Mol. Phylogenet. Evol.* **80**, 79–87. (doi:10.1016/j.ympev.2014.08.001)
20. Panesar TS. 1989 The moulting pattern in *Trichuris muris* (Nematoda: Trichuroidea). *Can. J. Zool.* **67**, 2340–2343. (doi:10.1139/z89-330)
21. Bird AF. 1983 Growth and moulting in nematodes: changes in the dimensions and morphology of *Rotylenchulus reniformis* from start to finish of moulting. *Int. J. Parasitol.* **13**, 201–206. (doi:10.1016/0020-7519(83)90013-9)
22. Wilson PAG. 2010 Nematode growth patterns and the moulting cycle: the population growth profile. *Proc. Zool. Soc. Lond.* **179**, 135–151. (doi:10.1111/j.1469-7998.1976.tb03231.x)
23. Ondrovics M, Gasser RB, Joachim A. 2016 Recent advances in elucidating nematode moulting: prospects of using *Oesophagostomum dentatum* as a model. *Adv. Parasitol.* **91**, 233. (doi:10.1016/bs.apar.2015.09.001)
24. Stepek G, McCormack G, Birnie AJ, Page AP. 2011 The astacin metalloprotease moulting enzyme NAS-36 is required for normal cuticle ecdysis in free-living and parasitic nematodes. *Parasitology* **138**, 237–248. (doi:10.1017/S00331182010001113)
25. Wennberg SA, Janssen R, Budd GE. 2009 Hatching and earliest larval stages of the priapulid worm *Priapulius caudatus*. *Invert. Biol.* **128**, 157–171. (doi:10.1111/j.1744-7410.2008.00162.x)
26. Trott TJ. 2017 Feeding by *Priapulius caudatus* (Cephalorhyncha: Priapulidae): observations of the effects of seasonal temperature change and molting. *Mar. Freshwater Behav. Physiol.* **50**, 55–65. (doi:10.1080/10236244.2017.1304153)
27. Higgins RP, Kristensen RM. 1986 New Loricifera from southeastern United States coastal waters. *Smithson. Contrib. Zool.* **438**, 1–70. (doi:10.5479/si.00810282.438)
28. Neuhaus B, Sørensen MV. 2013 Populations of *Campyloides* sp. (Kinorhyncha, Cyclorhagida): one global species with significant morphological variation? *Zoologischer Anz.* **252**, 48–75. (doi:10.1016/j.jcz.2012.03.002)
29. Budil P, Bruthansova J. 2005 Moulting in Ordovician dalmanitoid and acastoid trilobites of the Prague Basin. Preliminary observation. *Geol. Acta* **3**, 373–383.
30. Tettie OE, Brandt DS, Briggs DE.G. 2008 Ecdysis in sea scorpions (Chelicerata: Eurypterida). *Palaeogeogr. Palaeoclimatol. Palaeoecol.* **265**, 182–194. (doi:10.1016/j.palaeo.2008.05.008)
31. Drage HB, Holmes JD, García-Bellido DC, Daley AC. 2018 An exceptional record of Cambrian trilobite moulting behaviour preserved in the Emu Bay Shale, South Australia. *Lethaia* **51**, 473–492. (doi:10.1111/let.12266)
32. Daley AC, Budd GE, Caron J-B. 2013 Morphology and systematics of the anomalocaridid arthropod *Hurdia* from the Middle Cambrian of British Columbia and Utah. *J. Syst. Paleontol.* **11**, 743–787. (doi:10.1080/14772019.2012.732723)
33. Caron J-B, Smith MR, Harvey THP. 2013 Beyond the Burgess Shale: Cambrian microfossils track the rise and fall of hallucigeniid lobopodians. *Proc. R. Soc. B* **280**, 20131613. (doi:10.1098/rspb.2013.1613)
34. Yang J, Ortega-Hernandez J, Drage HB, Du KS, Zhang XG. 2019 Ecdysis in a stem-group euarthropod from the early Cambrian of China. *Sci. Rep.* **9**, 5709. (doi:10.1038/s41598-019-41911-w)
35. Han J, Zhang XL, Zhang ZF, Shu DG. 2003 A new platy-armored worm from the early Cambrian Chengjiang Lagerstätte, South China. *Acta Geol. Sinica* **77**, 1–6. (doi:10.1111/j.1755-6724.2003.tb00103.x)
36. Conway MS. 1977 Fossil priapulid worms. *Special Papers Palaeontol.* **20**, 1–95.
37. Liu YH, Xiao SH, Shao TQ, Broce J, Zhang HQ. 2014 The oldest known priapulid-like scalidophoran animal and its implications for the early evolution of cycloneuralians and ecdysozoans. *Evol. Dev.* **16**, 155–165. (doi:10.1111/ede.12076)
38. Zhang HQ, Xiao SH, Liu YH, Yuan XL, Wan B, Muscente AD, Shao TQ, Gong H, Cao GH. 2015 Armored kinorhynch-like scalidophoran animals from the early Cambrian. *Sci. Rep.* **5**, 16521. (doi:10.1038/srep16521)
39. Fu DJ et al. 2019 The Qingjiang biota: a Burgess shale-type fossil Lagerstätte from the early Cambrian of South China. *Science* **363**, 1338–1342. (doi:10.1126/science.aau8800)
40. Müller KJ, Hinz-Schallreuter I. 1993 Palaeoscolecid worms from the middle Cambrian of Australia. *Palaeontology* **36**, 549–592.
41. Peel JS, Stein M, Kristensen RM. 2013 Life cycle and morphology of a Cambrian stem-lineage loriciferan. *PLoS ONE* **8**, e73583. (doi:10.1371/journal.pone.0073583)
42. Han J, Liu JN, Zhang ZF, Zhang XL, Shu DG. 2007 Trunk ornament on the palaeoscolecid worms *Cricocosmia* and *Tabelliscolex* from the Early Cambrian Chengjiang deposits of China. *Acta Palaeontologica Polonica* **52**, 423–431.
43. Zhang HQ, Maas A, Waloszek D. 2018 New material of scalidophoran worms in Orsten-type preservation from the Cambrian Fortunian Stage of South China. *J. Paleontol.* **92**, 14–25. (doi:10.1017/jpa.2017.39)
44. Ma XY, Aldridge RJ, Siveter DJ, Siveter DJ, Hou XG, Edgecombe GD. 2014 A new exceptionally preserved Cambrian priapulid from the Chengjiang Lagerstätte. *J. Paleontol.* **88**, 371–384. (doi:10.1666/13-082)
45. Lemburg C. 1998 Electron microscopical localization of chitin in the cuticle of *Halicryptus spinulosus* and *Priapulius caudatus* (Priapulida) using gold-labelled wheat germ agglutinin: phylogenetic implications for the evolution of the cuticle within the Nemathelminthes. *Zoomorphology* **118**, 137–158. (doi:10.1007/s004350050064)
46. Steiner M, Qian Y, Li GX, Hagadorn JW, Zhu MY. 2014 The developmental cycles of early Cambrian Olivoidae fam. nov. (Cycloneuralia) from the Yangtze Platform (China). *Palaeogeogr. Palaeoclimatol. Palaeoecol.* **398**, 97–124. (doi:10.1016/j.palaeo.2013.08.016)
47. Bengtson S, Yue Z. 1997 Fossilized metazoan embryos from the earliest Cambrian. *Science* **277**, 1645–1648. (doi:10.1126/science.277.5332.1645)
48. Steiner M, Li GX, Qian Y, Zhu MY. 2004 Lower Cambrian small shelly fossils of northern Sichuan and southern Shaanxi (China), and their biostratigraphic importance. *Geobios* **37**, 259–275. (doi:10.1016/j.geobios.2003.08.001)
49. Li ZP. 1984 The discovery and its significance of early Cambrian small shell fossils in Hexi area Xixiang Shaanxi. *Geol. Shaanxi* **2**, 73–78.

50. Sawaki Y *et al.* 2008 Internal structures and U–Pb ages of zircons from a tuff layer in the Meishucunian Formation, Yunnan Province, South China. *Gondwana Res.* **14**, 148–158. (doi:10.1016/j.gr.2007.12.003)
51. Han J, Conway Morris S, Ou Q, Shu DG, Huang H. 2017 Meiofaunal deuterostomes from the basal Cambrian of Shaanxi (China). *Nature* **542**, 228–231. (doi:10.1038/nature21072)
52. Liu YH, Li Y, Shao TQ, Zhang HQ, Wang Q, Qiao JP. 2014 *Quadruprygites* from the lower Cambrian of South China: growth pattern, post-embryonic development, and affinity. *Chin. Sci. Bull.* **59**, 4086–4095. (doi:10.1007/s11434-014-0481-5)
53. Shao TQ, Tang HH, Liu YH, Waloszek D, Maas A, Zhang HQ. 2018 Diversity of cnidarians and cycloneuralians in the Fortunian (early Cambrian) Kuanchuanpu Formation at Zhangjiagou, South China. *J. Paleontol.* **92**, 115–129. (doi:10.1017/jpa.2017.94)
54. Wang X, Han J, Vannier J, Ou Q, Yang XG, Uesugi K, Sasaki O, Komiya T, Sevastopulo G. 2017 Anatomy and affinities of a new 535-million-year-old medusozoan from the Kuanchuanpu Formation, South China. *Palaeontology* **60**, 853–867. (doi:10.1111/pala.12320)
55. Yang XG, Han J, Wang X, Schifftbauer JD, Uesugi K, Sasaki O, Komiya T. 2017 Euendoliths versus ambient inclusion trails from Early Cambrian Kuanchuanpu Formation, South China. *Palaeogeogr. Palaeoclimatol. Palaeoecol.* **476**, 147–157. (doi:10.1016/j.palaeo.2017.03.028)
56. Shao TQ *et al.* 2015 New small shelly fossils (*Acanthocassis* and *Xinlispinga* gen. nov.) from the Fortunian stage (early Cambrian) in southern China. *Acta Geologica Sinica (English Edition)* **89**, 1470–1481. (doi:10.1111/1755-6724.12558)
57. Shao TQ, Liu YH, Wang Q, Zhang HQ, Tang HH, Li Y. 2016 New material of the oldest known scalidophoran animal *Eopriapulites sphinx*. *Palaeoworld* **25**, 1–11. (doi:10.1016/j.palwor.2015.07.003)
58. Vannier J, Calandra I, Gaillard C, Żylińska A. 2010 Priapulid worms: pioneer horizontal burrowers at the Precambrian–Cambrian boundary. *Geology* **38**, 711–714. (doi:10.1130/g30829.1)
59. Vannier J, Martin E.L.O. 2017 Worm-lobopodian assemblages from the Early Cambrian Chengjiang biota: insight into the ‘pre-arthropodan ecology’? *Palaeogeogr. Palaeoclimatol. Palaeoecol.* **468**, 373–387. (doi:10.1016/j.palaeo.2016.12.002)
60. Liu YH *et al.* 2019 New armoured scalidophorans (Ecdysozoa, Cycloneuralia) from the Cambrian Fortunian Zhangjiagou Lagerstätte, South China. *Papers Palaeontol.* **5**, 241–260. (doi:10.1002/spp2.1239)
61. Sansom RS. 2016 Preservation and phylogeny of Cambrian ecdysozoans tested by experimental decay of *Priapulites*. *Sci. Rep.* **6**, 32817. (doi:10.1038/srep32817)
62. Lang K. 1948 On the morphology of the larva of *Priapulites caudatus* Lam. *Arkiv för zoologi* **41**, 1–8.
63. Rota-Stabelli O, Daley AC, Pisani D. 2013 Molecular timetrees reveal a Cambrian colonization of land and a new scenario for ecdysozoan evolution. *Curr. Biol.* **23**, 392–398. (doi:10.1016/j.cub.2013.01.026)
64. Erwin DH, Laffamme M, Tweedt SM, Sperling EA, Pisani D, Peterson KJ. 2011 The Cambrian conundrum: early divergence and later ecological success in the early history of animals. *Science* **334**, 1091–1097. (doi:10.1126/science.1206375)
65. Cunningham JA, Liu AG, Bengtson S, Donoghue PCJ. 2017 The origin of animals: can molecular clocks and the fossil record be reconciled? *Bioessays* **39**, 1–12. (doi:10.1002/bies.201600120)
66. dos Reis M, Thawornwattana Y, Angelis K, Telford MJ, Donoghue PC, Yang Z. 2015 Uncertainty in the timing of origin of animals and the limits of precision in molecular timescales. *Curr. Biol.* **25**, 2939–2950. (doi:10.1016/j.cub.2015.09.066)
67. Wolfe JM. 2017 Metamorphosis is ancestral for crown Euarthropods, and evolved in the Cambrian or earlier. *Integr. Comp. Biol.* **57**, 499–509. (doi:10.1093/icb/ix039)
68. Ortega-Hernández J. 2015 Lobopodians. *Curr. Biol.* **25**, R873–R875. (doi:10.1016/j.cub.2015.07.028)
69. Paterson JR, Edgecombe GD, Lee MS.Y. 2019 Trilobite evolutionary rates constrain the duration of the Cambrian explosion. *Proc. Natl Acad. Sci. USA* **116**, 4394–4399. (doi:10.1073/pnas.1819366116)
70. Hou XG, Siveter DJ, Siveter DJ, Aldridge RJ, Cong PY, Gabbott SE, Ma XY, Pumell MA, Williams M. 2017 *The Cambrian fossils of Chengjiang, China: the flowering of early animal life*, 2nd edn, pp. 98–270. Hoboken, NJ: Wiley Blackwell.
71. Mángano MG, Buatois LA. 2017 The Cambrian revolutions: trace-fossil record, timing, links and geobiological impact. *Earth Sci. Rev.* **173**, 96–108. (doi:10.1016/j.earscirev.2017.08.009)
72. Kesidis G, Slater BJ, Jensen S, Budd GE. 2019 Caught in the act: Priapulid burrowers in early Cambrian substrates. *Proc. R. Soc. B* **286**, 20182505. (doi:10.1098/rspb.2018.2505)
73. Sommer RJ, Ogawa A. 2011 Hormone signaling and phenotypic plasticity in nematode development and evolution. *Curr. Biol.* **21**, R758–R766. (doi:10.1016/j.cub.2011.06.034)
74. Paxton H. 2005 Molting polychaete jaws: Ecdysozoans are not the only molting animals. *Evol. Dev.* **7**, 337–340. (doi:10.1111/j.1525-142X.2005.05039.x)
75. Mendis A.H.W, Rees HH, Goodwin TW. 1984 The occurrence of ecdysteroids in the cestode, *Moniezia expansa*. *Mol. Biochem. Parasitol.* **10**, 123–138. (doi:10.1016/0166-6851(84)90001-X)
76. Nolte A, Koolman J, Dörflöcher M, Straub H. 1986 Ecdysteroids in the dorsal bodies of pulmonates (Gastropoda): synthesis and release of ecdysone. *Comp. Biochem. Physiol. A* **84**, 777–782. (doi:10.1016/0300-9629(86)90405-6)
77. García M, Gharbi J, Girault J.-P., Hetru C, Lafont R. 1989 Ecdysteroid metabolism in leeches. *Invert. Reprod. Develop.* **15**, 57–68. (doi:10.1080/07924259.1989.9672022)
78. Martín-Durán JM, Hejnol A. 2015 The study of *Priapulites caudatus* reveals conserved molecular patterning underlying different gut morphogenesis in the Ecdysozoa. *BMC Biol.* **13**, 29. (doi:10.1186/s12915-015-0139-z)
79. Kier WM. 2012 The diversity of hydrostatic skeletons. *J. Exp. Biol.* **215**, 1247–1257. (doi:10.1242/jeb.056549)
80. Nijhout HF. 2013 Arthropod developmental endocrinology. In *Arthropod biology and evolution* (eds A Minelli, G Boxshall, G Fusco), pp. 123–148. Berlin, Germany: Springer.
81. Robson EA. 1964 The cuticle of *Peripatopsis moseleyi*. *J. Cell Sci.* **105**, 281–299.
82. Schmidt-Rhaese A, Thomas F, Poulin R. 2000 Redescription of *Gordius paramensis* Cameron, 1892 (Nematomorpha), a species new for New Zealand. *J. Nat. Hist.* **34**, 333–340. (doi:10.1080/002229300299516)
83. Samoiloff MR, Pasternak J. 1969 Nematode morphogenesis: fine structure of the molting cycles in *Panagrellus silusiae* (de Man 1913) Goodey 1945. *Can. J. Zool.* **47**, 639–651. (doi:10.1139/z69-109)
84. Attout T, Martin C, Babayan SA, Kozek WJ, Bazzocchi C, Oudet F, Gallagher IJ, Specht S, Bain O. 2008 Pleural cellular reaction to the filarial infection *Litomosoides sigmodontis* is determined by the molting process, the worm alteration, and the host strain. *Parasitol. Int.* **57**, 201–211. (doi:10.1016/j.parint.2008.01.001)
85. Heiner I, Neuhaus B. 2007 Loricifera from the deep sea at the Galápagos Spreading Center, with a description of *Spinoloricus turbatio* gen. et sp. nov. (Nanaloricidae). *Helgol. Mar. Res.* **61**, 167–182. (doi:10.1007/s10152-007-0064-9)
86. Pilato G *et al.* 2005 The clade Ecdysozoa, perplexities and questions. *Zoologischer Anz.-J. Comp. Zool.* **244**, 43–50. (doi:10.1016/j.jcz.2005.04.001)
87. Williams M, Vannier J, Corbari L, Massabuau J.-C. 2011 Oxygen as a driver of early arthropod microbenthos evolution. *PLoS ONE* **6**, e28183. (doi:10.1371/journal.pone.0028183)
88. Wei HM, Wang XQ, Shi XY, Jiang GQ, Tang DJ, Wang LJ, An ZZ. 2019 Iodine content of the carbonates from the Doushantuo formation and shallow ocean redox change on the Ediacaran Yangtze Platform, South China. *Precambrian Res.* **322**, 160–169. (doi:10.1016/j.precamres.2019.01.007)
89. Chen X *et al.* 2015 Rise to modern levels of ocean oxygenation coincided with the Cambrian radiation of animals. *Nat. Commun.* **6**, 7142. (doi:10.1038/ncomms8142)
90. Bambach RK, Bush AM, Erwin DH. 2007 Autecology and filling of ecospace: key metazoan radiations. *Palaeontology* **50**, 1–22. (doi:10.1111/j.1475-4983.2006.00611.x)
91. Dunne JA, Williams RJ, Martinez ND, Wood RA, Erwin DH. 2008 Compilation and network analyses of Cambrian food webs. *PLoS Biol.* **6**, e102. (doi:10.1371/journal.pbio.0060102)
92. Vannier J. 2012 Gut contents as direct indicators for trophic relationships in the Cambrian marine ecosystem. *PLoS ONE* **7**, e52200. (doi:10.1371/journal.pone.0052200.g001)

## **Supplementary materials**

### **Origin of ecdysis: fossil evidence from 535-million-year-old scalidophoran worms**

Deng Wang, Jean Vannier, Isabell Schumann, Xing Wang, Xiaoguang Yang, Tsuyoshi Komiya, Kentaro Uesugi, Jie Sun, and Jian Han

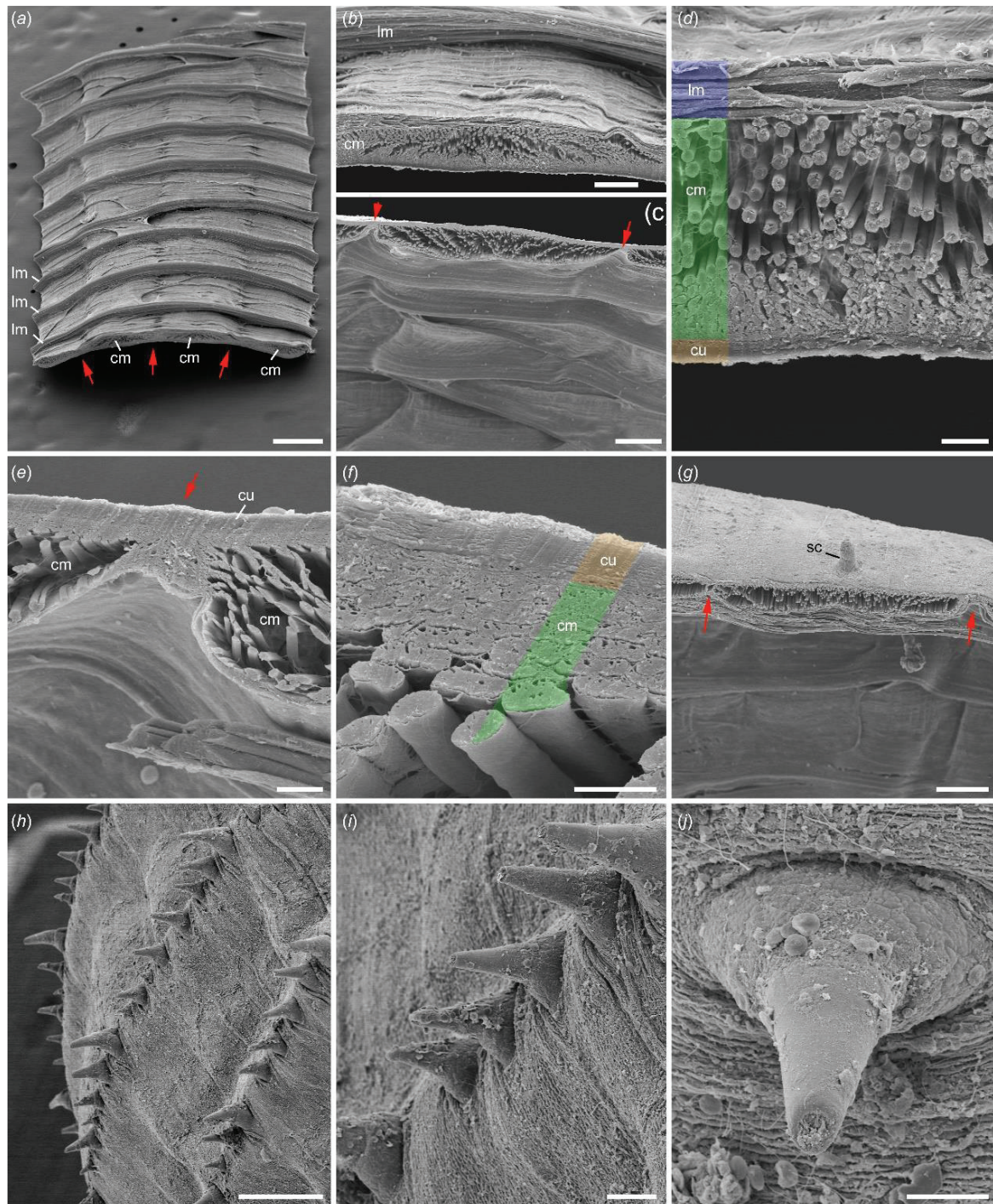


**Figure S1. Cuticle and associated muscles in *Priapulidae* from Sweden [s1].** (A), fragment of body wall showing circular and longitudinal muscles. (B, C), transverse sections through circular muscles. (D), transverse section showing the cuticle (orange), fibres of circular muscles (green) and fibres of longitudinal muscles (blue). (E, F), transverses section showing details of chitinous cuticle and underlying muscle fibres. (G), transverse section near scalid. (H-J), scalids distributed in longitudinal rows along the proboscis and details of conical scalid. Red arrows represent boundaries between adjacent annuli. All SEM images. cm, circular muscles; cu, cuticle; lm, longitudinal muscles; sc, scalids. Scale bars: 500 µm (A, H); 200 µm (C, G), 100 µm (B, I); 50 µm (J); 20 µm (D, E); 10 µm (F).



Species	References	Syst. position	Stratigraphy	Age	Preservation	Description
<i>Schistoscolex umbilictus</i>	[S2], fig.12b	Palaeoscolecida	Monastery Creek Fm.	Cambrian (Ser.3, St.5)	3D, phosphatized	Double layered cuticular structure
<i>Tabelliscolex hexagomus</i>	[S3], pl.1, fig.2a,b [S9], fig.1	Palaeoscolecida	Heilimpu Fm.	Cambrian (Ser.2, St.3)	BST (compression)	Strongly distorted cuticle
<i>Wronascolex antignus</i>	[S10], fig.3d,e	Palaeoscolecida	Murero Fm.	Cambrian (Ser.3, St.5)	BST (compression)	Weakly expressed annulations; wrinkles
<i>Exinipriatulus globocaudatus</i>	[S5], figs 1-5	Priapulida	Heilimpu Fm.	Cambrian (Ser.2, St.3)	BST (compression)	Contracted/distorted shape; no internal organ
<i>Ottoia prolifca</i>	[S11], fig.4	Priapulida	Burgess Shale Fm.	Cambrian (Ser.3, St.5)	BST (compression)	Body wall detached from cuticle; no internal organs; proboscis incomplete
<i>Siriloricapustulosa</i>	[S7], figs 6, 7	Loricifera	Buen Fm.	Cambrian (Ser.2, St.3)	BST (compression)	Molted individual emerging from lorica
Undet. Form D	[S8], fig.7.3	Scalidophora	Kuanchuanpu Fm.	Cambrian (Fortunian St.)	3D, phosphatized	Strongly distorted cuticle

**Table S2.** Cambrian scalidophoran worms with assumed exuviae. Abbreviations are as follows: BST, Burgess-Shale-type preservation; Fm, Formation; Ser., Series; St., Stage; 3D, three-dimensions.

**Text S3. Morphological description of the two indeterminate forms (scalidophoran worms) described in the present paper (see Figures 1, 3), both from the lowermost Cambrian Kuanchuanpu Formation, Shaanxi Province, China.**

Scalidophora Lemburg, 1995

**Indeterminate Form 1**

2015 *Eokinorhynchus rarus*, Zhang et al., fig. 3h–i.

2015 Unnamed Form I, Zhang et al., fig. 4a, b.

2018 Unnamed Form B, Zhang et al., fig. 5.1–3.

2018 Indeterminate Form 1, Liu et al., fig. 9A–B.

**Material.** Twelve specimens: ELIXX86-112, ELIXX63-29, ELIXX94-84, ELIXX99-492, ELIXX40-125, ELIXX85-284, ELIXX90-221, ELIXX85-429, ELIXX57-467, ELIXX98-179, ELIXX78-205 and ELIXX85-16; all from Bed 2 [16] of the Lower Cambrian Kuanchuanpu Formation (Fortunian Stage, Terreneuvian Series) at the Zhangjiagou Section of Xixiang County, Shaanxi Province South China. ELIXX86-112, ELIXX63-29, ELIXX94-84, ELIXX99-492, ELIXX40-125, ELIXX85-284, ELIXX90-221, ELIXX85-429 and ELIXX85-16 display a positive relief (PER; see explanation in text). ELIXX98-179, ELIXX78-205 and ELIXX57-467 display a negative relief (NER see explanation in text).

**Measurements.** See Table S5.

**Description.** Annulated trunk fragments armoured with small and large spinose sclerites. Small sclerites, tightly juxtaposed around annuli, each with an expanded elliptical base and a spinose projection, not aligned in longitudinal columns but forming a staggered pattern. Large sclerites with a base extending over 3 or 4 annuli and a stout spinose projection. Base of small and large sclerites and other cuticular areas with well-defined reticular ornament.

**Comparisons.** These specimens show overall similarities with the trunk of three species and one indeterminate form of scalidophoran worms from the same biota. They resemble *Eokinorhynchus rarus* in bearing closely packed small sclerites around annuli. However, the small sclerites of *Eokinorhynchus rarus* have a sub-quadrangular basis and do not bear a spine. The trunk of *Qinscolex spinosus* has five large spinose sclerites whereas the present indeterminate form has only two. The small spinose sclerites are in close contact with each other and are about the same length as the annulus in Indeterminate Form 1 (this paper), whereas they do not reach the annulus margin and are more widely interspaced in *Shanscolex decorus*. Our specimens best resemble “Unnamed Form 1” described by Zhang et al. 2018 in most important aspects of their morphology (e.g. shape and distribution of sclerites). Both forms have a spinose sclerite three times wider than the small ones although inserted within a single annulus (Figure 1G and [S12] text-fig. 9A–B).

**Orientation.** Comparisons with complete specimens of scalidophoran worms from the Kuanchuanpu Formation [8, 12–14] allow us to determine the antero-posterior polarity of the

trunk fragments of Indeterminate Form 1 (this paper). Sclerites project radially with their main axis pointing posteriorly.

## **Indeterminate Form 2**

2018 Indeterminate Form 1 Liu et al., fig. 9C.

**Materials.** ELIXX85-120 with a negative external relief (NER; see explanation in text) from the same bed as Indeterminate Form 1 (see above).

**Measurements.** See Table S5.

**Description.** Single trunk fragment with a cylindrical shape and six annuli. Small spinose sclerites in a central position along each annulus with a basis of about two-thirds the length of annulus, characterized by a spoon-shaped basis and a central conical spine. Sclerites do not contact along annuli. Base of sclerites and other cuticular areas with well-defined reticular ornament. This fragment has only one type of (small) sclerites.

**Comparison.** This specimen resembles the trunk of *Qinscolex spinosus* and *Shanscolex decorus* in having well-separated sclerites along annuli. However, its unusual spoon-shaped sclerites has no equivalent in *Qinscolex spinosus* (round), *Shanscolex decorus* (narrow elliptical) and other scalidophoran from the Kuanchuanpu Formation, including Indeterminate Form 1 (this paper; see above) which develops large spinose sclerites. Although preserved in negative relief, this specimen closely resembles Indeterminate Form 1 described by Liu et al. 2018 ([12] text-fig. 9C).

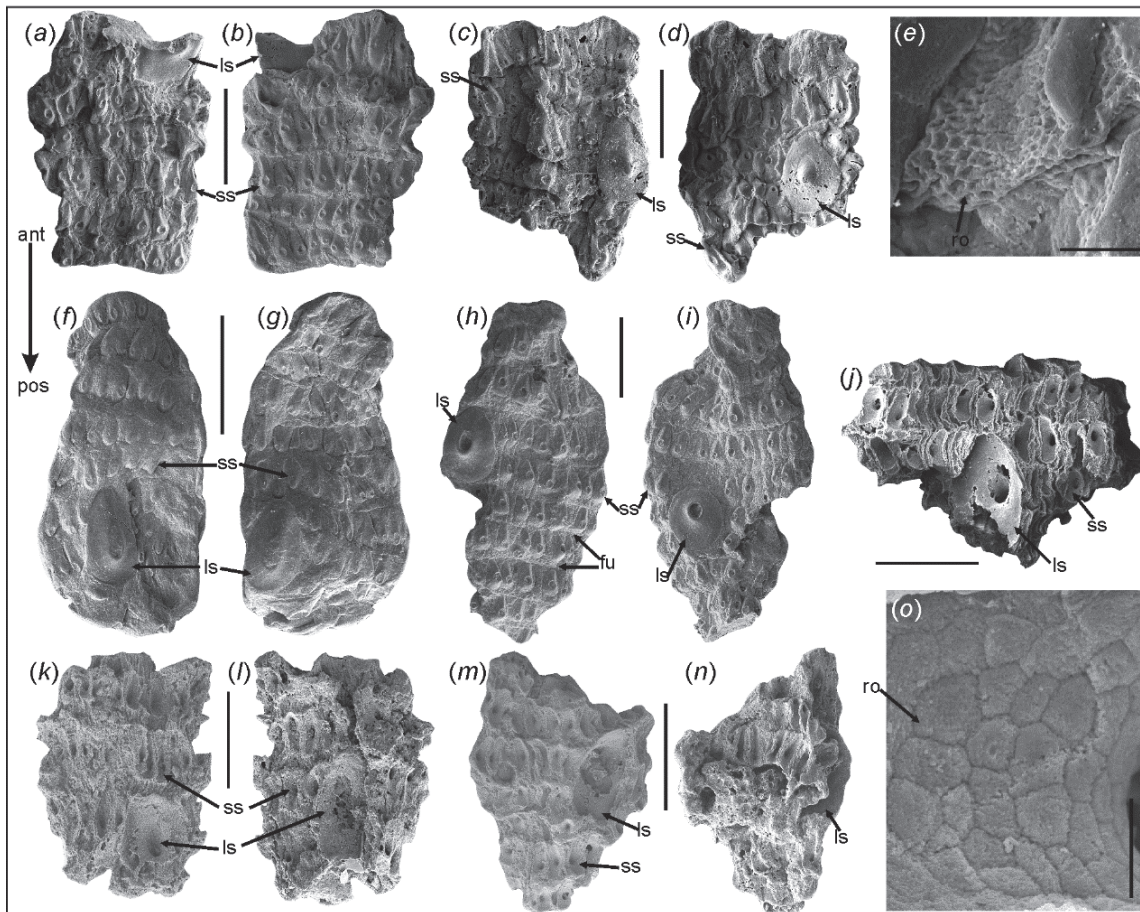


**Figure S4. Additional specimens of Indeterminate Form 1 (see description in S3) from the lowermost Cambrian Kuanchuanpu Formation, Shaanxi Province, China.** (A-I) specimens with a positive external relief (PER; see explanation in text). (J-O) specimens with a negative external relief (NER; see explanation in text). (A, B), ELIXX85-284, general views from two opposite sides showing small and a large sclerite. (C-E), ELIXX40-125, general views from two opposite sides showing small sclerites on annuli and a large sclerite and details of reticulated ornament along basal part of sclerite. (F, G), ELIXX94-84, general views from two opposite sides showing small and large sclerites. (H, I), ELIXX99-492, general views from two opposite sides showing small and large sclerites. (J, O), ELIXX78-205, wrinkled trunk fragments showing small and large sclerites and details of reticulated ornament along the basal part of the inner surface of a sclerite. (K, L), ELIXX57-467 general views from two opposite sides showing small and large sclerite. (M, N), ELIXX98-179, general views from two opposite sides showing small and large sclerite. All SEM images. Abbreviations are as follows: ant, anterior part; fu, furrow between annuli; ls, large spinose sclerite; pos, posterior part; ro, reticulated ornament; ss, small spinose sclerite. Scale bars: 500  $\mu\text{m}$  (A-D), (F-N), 50  $\mu\text{m}$  (E, N).

Species/Form	Coll. number	TRUNK			ANNULUS			SMALL SCLERITES			LARGE SCLERITES			ORNAMENT			
		L (µm)	W (µm)	shape	L (µm)	nss/a	N	L (µm)	W (µm)	basis	L (µm)	W (µm)	N		nss	basis	D (µm)
Undet. XXI (this paper)	ELIXX86-112	1636	680-750	flat	160-204	16-24	11	100-165	44-88	elliptical	close	242-264	2	4	elliptical	4-11	
	ELIXX63-291	1269	631-718	flat	185-222	16-20	10	130-218	74-111	elliptical	close	188-236	2	3	elliptical	6-9	
Undet. Form B sensu [S8] Undet. Form Ia sensu [S13]	ELIXX94-84	1441	603-695	flat	152-202	16-22	11	131-175	54-86	elliptical	separated	415-428	2	3	elliptical	8-12	
	ELIXX99-492	2166	894-1061	flat	196-347	14-18	10	166-241	76-136	elliptical	separated	422-483	2	2-3	elliptical	9-12	
	ELIXX40-125	1486	992-1039	flat	243-364	20-24	6	189-271	68-85	elliptical	close	337-432	2	3	elliptical	12-16	
	ELIXX85-284	1375	883-937	flat	175-287	14-22	7	100-287	62-100	elliptical	close	275	1	2	elliptical	nm	
	ELIXX90-221	3015	953-987	cylindrical	178-321	16-20	14	107-285	71-108	elliptical	close	250-464	nm	2	1-3	elliptical	5-10
	ELIXX85-429	1212	529-604	flat	227-302	8-10	6	182-242	76-91	elliptical	close	302	1	3	elliptical	nm	
	ELIXX57-467	1275	904-937	flat	287-352	16-18	4	212-275	63-100	elliptical	close	462-562	2	2	elliptical	nm	
	ELIXX78-205	833	1084-1169	crumpled	193-210	20-24	4	104-174	52-87	elliptical	close	272	1	3	elliptical	6-13	
	ELIXX98-179	1214	712-836	flat	143-210	12-18	7	110-164	52-67	elliptical	close	442	2	3	elliptical	7-8	
	ELIXX85-16	2018	367-702	flat	161-362	16-18	8	101-209	33-57	elliptical	close	215	nm	2	2	elliptical	nm
Undet. XX2 (this paper)	ELIXX85-120	2742	1072-1494	cylindrical	426-491	20-24	6	168-354	58-137	spoon-shaped	separated	na	na	na	na	7-13	
Undet. Form B sensu [S8]	NINGP 160438-41	607-1163	986-1527	flat	130-250	20-40	3-8	130-250	30-100	elliptical	close	500	340	1	4	elliptical	10-13
Undet. Form Ia sensu [S13]	XXDW 001	1421	1125-1314	flat	180-300	20-40	10	180	110	rectangular	close	330-410	390	3	2-3	elliptical	nm
<i>Eobithyvelus rarus</i>	NINGP 160400	756-1260	158-308	cylindrical	20-60	20-40	-20	32-100	23	rectangular	separated	180	90-190	15	2-3	elliptical	nm
<i>Quisculex spinosus</i>	UMCU16CHD 0618-006	1800	1130	crumpled	34-160	40-50	10	35-150	29-60	elliptical	separated	340	300	1	2	rounded	nm
<i>Stanscolex decorus</i>	UMCU15CHD 0819-009	3250	1310	flat	143-428	22-24	12	70-300	56-100	rectangular	separated	434-480	360-480	5	2	elliptical/	nm
Undet. Form 1 sensu [S12]	UMCU16CHD 0102-001,002	1140-1340	1180-1300	flat	45-110	24-28	7-9	119-210	45-189	elliptical	close	380	314	2	2	rounded	nm
Undet. Form 2 sensu [S12]	UMCU16CHD 0306-003	1440	1440	flat	340	18-22	5	238	120	spoon-shaped	separated	na	na	na	na	na	nm

**Table S5. Measurements of scaldiphoran specimens described in the present paper and previous works, all from the lowermost Kuanchuanpu Formation, China. D, diameter of ornamented pentagonal cell; L, length; n, number; Coll., Collections; na, not applicable; nss, number of annuli straddled by large sclerites; nm, not measured due to poor preservation; nss/a, number of small sclerites per annulus; W, width.**

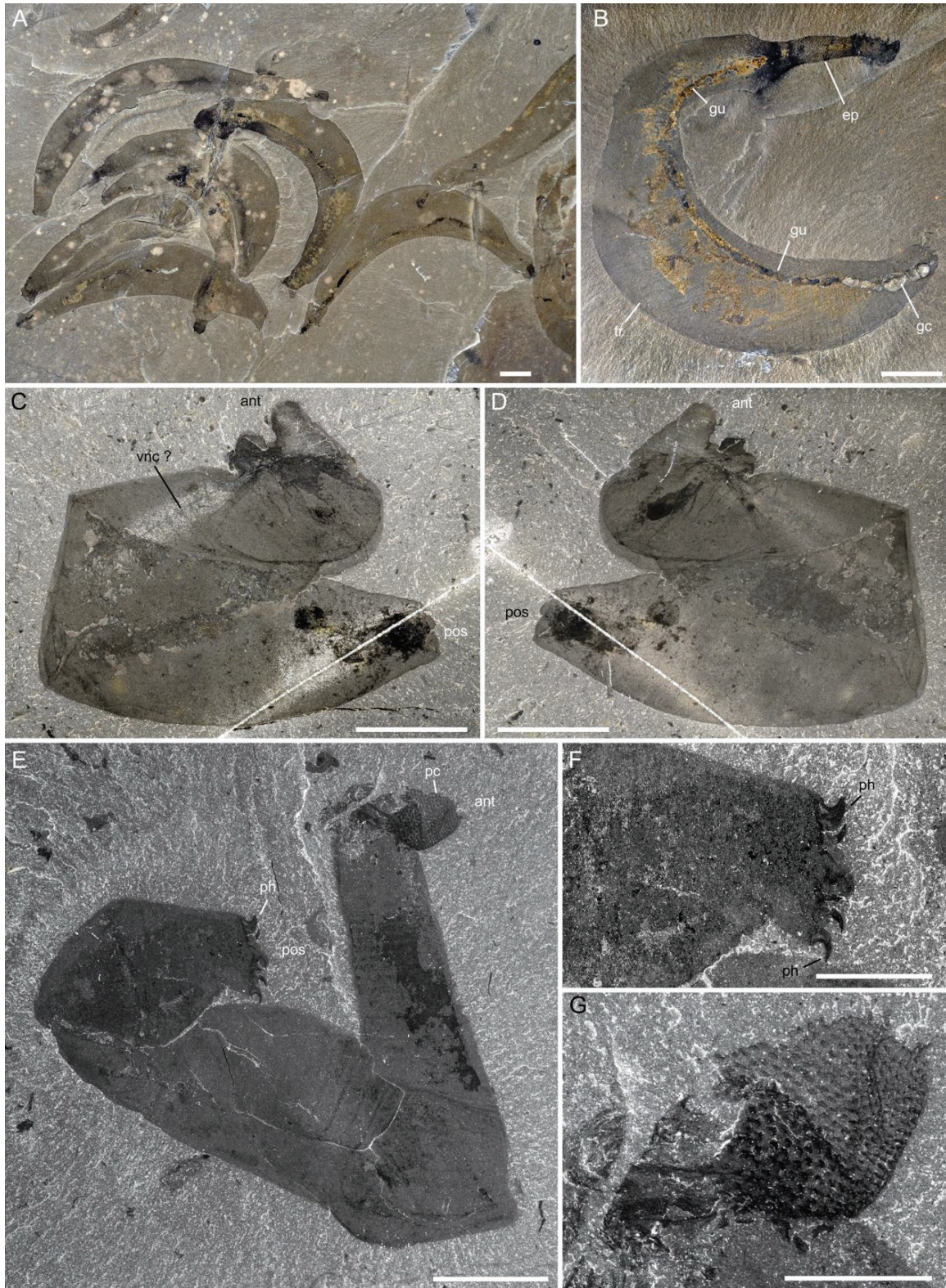


**Figure S6. *Ottoia prolifica* from the middle Cambrian Burgess Shale, Canada.** (a) ROMIP 61780, clustered specimens (body fossils). (b) ROMIP 61779 showing gut tract and gut contents (small brachiopods). (c) and (d) WQ94-0014, presumed exuvia, part and counterpart. (e) USNM 188637, presumed exuvia. All photographs in polarized light. Abbreviations are as follows: ant, anterior part of exuvia; ep, everted pharynx; gc, gut content (small brachiopods); gu, gut; pc, pharyngeal cuticle; ph, posterior hook; pos, posterior part of exuvia; tr, trunk; vnc?, ventral nerve chord?. Scale bars: 1cm (A-E), 5 mm (F, G).

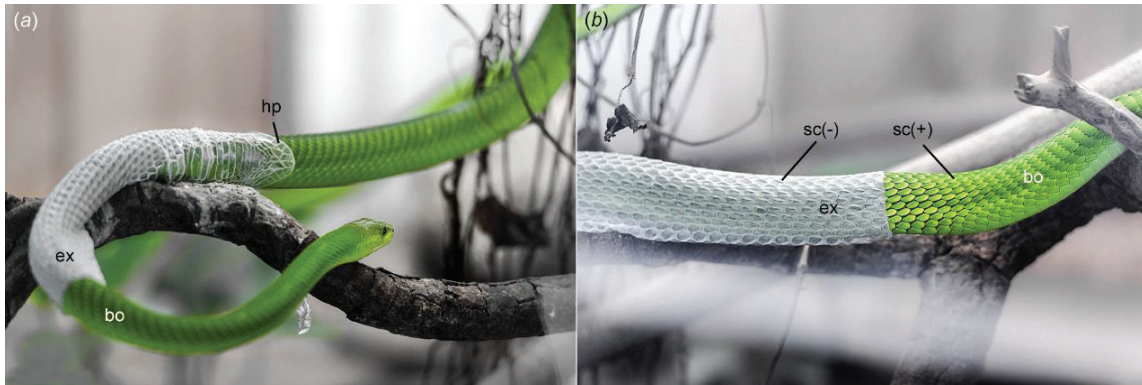


**Figure S7. Moulting in a mamba snake.** (A) Snake crawling out of its exuvia and turning it inside out. (B) The external surface of the exuvia shows a negative relief. Abbreviations are as follows: bo, body; ex, exuvia; hp, head part of exuvia; sc(+) and sc(-), scales with a positive (body) and negative relief (exuvia). Courtesy Julia Sundukova.

## Supplementary references

- S1. Vannier J., Martin E.L.O. 2017 Worm-lobopodian assemblages from the Early Cambrian Chengjiang biota: Insight into the “pre-arthropodan ecology”? *Palaeogeography, Palaeoclimatology, Palaeoecology* **468**, 373-387. (doi:10.1016/j.palaeo.2016.12.002).
- S2. Müller K.J., Hinz-Schallreuter I. 1993 Palaeoscolecid worms from the middle Cambrian of Australia. *Palaeontology* **36**(3), 549-592.
- S3. Han J., Zhang X.L., Zhang Z.F., Shu D.G. 2003 A new platy-armored worm from the Early Cambrian Chengjiang Lagerstätte, South China. *Acta Geologica Sinica* **77**(1), 1-6.
- S4. Glaessner M.F. 1979 Lower Cambrian Crustacea and annelid worms from Kangaroo Island, South Australia. *Alcheringa: An Australasian Journal of Palaeontology* **3**(1), 21-31. (doi:10.1080/03115517908565437).
- S5. Ma X.Y., Aldridge R.J., Siveter D.J., Siveter D.J., Hou X.G., Edgecombe G.D. 2014 A new exceptionally preserved Cambrian priapulid from the Chengjiang Lagerstätte. *Journal of Paleontology* **88**(2), 371-384.
- S6. Walcott C.D. 1911 Middle Cambrian Annelids, *Cambrian Geology and Paleontology II. Smithsonian Miscellaneous Collections* **57**(5), 110-144.
- S7. Peel J.S. 2010 A Corset-like Fossil From The Cambrian Sirius Passet Lagerstätte of North Greenland and its Implications For Cycloneuralian Evolution. *Journal of Palaeontology* **84**(2), 332-340.
- S8. Zhang H.Q., Maas A., Waloszek D. 2018 New material of scalidophoran worms in Orsten-type preservation from the Cambrian Fortunian Stage of South China. *Journal of Paleontology* **92**(01), 14-25. (doi:10.1017/jpa.2017.39).
- S9. Han J., Liu J.N., Zhang Z.F., Zhang X.L., Shu D.G. 2007 Trunk ornament on the palaeoscolecid worms *Cricocosmia* and *Tabelliscollex* from the Early Cambrian Chengjiang deposits of China. *Acta Palaeontologica Polonica* **52**(2), 423-431.
- S10. García-Bellido D.C., Paterson J.R., Edgecombe G.D. 2013 Cambrian palaeoscolecids (Cycloneuralia) from Gondwana and reappraisal of species assigned to *Palaeoscolex*. *Gondwana Research* **24**(2), 780-795. (doi:10.1016/j.gr.2012.12.002).
- S11. Conway Morris S. 1977 Fossil priapulid worms. *Special Papers in Palaeontology* **20**, 1-95.
- S12. Liu Y.H., Qin J.C., Wang Q., Maas A., Duan B.C., Zhang Y.N., Zhang H., Shao T.Q., Zhang H.Q., Zhang X.G. 2018 New armoured scalidophorans (Ecdysozoa, Cycloneuralia) from the Cambrian Fortunian Zhangjiagou Lagerstätte, South China. *Papers in Palaeontology*, 1-20. (doi:10.1002/spp2.1239).
- S13. Zhang H.Q., Xiao S.H., Liu Y.H., Yuan X.L., Wan B., Muscente A.D., Shao T.Q., Gong H., Cao G.H. 2015 Armored kinorhynch-like scalidophoran animals from the early Cambrian. *Scientific Reports* **5**, 16521. (doi:10.1038/srep16521).
- S14. Liu Y.H., Xiao S.H., Shao T.Q., Broce J., Zhang H.Q. 2014 The oldest known priapulid-like scalidophoran animal and its implications for the early evolution of cycloneuralians and ecdysozoans. *Evolution & Development* **16**(3), 155-165. (doi:10.1111/ede.12076).
- S15. Vannier J. 2012 Gut contents as direct indicators for trophic relationships in the Cambrian marine ecosystem. *PLoS One* **7**(12), e52200. (doi:10.1371/10.1371/journal.pone.0052200.g001).



## 5.2 The cuticle of early scalidophorans: epithelial origin, diversity and functions, evolutionary implications

This study is the logical follow-up to my research on the origin of moulting (see Chapter 5.1) and focusses on the cuticle of early ecdysozoans, based on fossil evidence.

The epidermis is a fundamental cellular tissue of all animals (Gibson and Gibson, 2009), which acts as an interface between the external medium and the internal tissues and organs. It is made of epithelial cells and extracellular material (Schmidt-Rhaesa, 2007). Epithelial cells form a tissue with complex junction systems and secrete two types of extracellular substrates: basally, the extracellular matrix (ECM) and, apically, the glycocalyx (layers of proteins and sugar) and the cuticle (Schmidt-Rhaesa, 2007). Basal animals such as placozoans and ctenophores do have an epidermis (with various cell types) but lack a glycocalyx that, in all other animal groups, plays a crucial role as a matrix on which other extracellular molecules (e.g. chitin, collagen) can anchor and eventually form a cuticular structure (Schmidt-Rhaesa, 2007). Ecdysozoans display a great variety of soft, sclerotized or biomineralized cuticular structures often associated with sensory organs (e.g. setae, chemo-sensory receptors). The aim of this second study was to obtain information of the nature and mode of formation of the cuticle of early Cambrian ecdysozoans, exemplified by scalidophorans. The acquisition of a cuticle, i.e. a protective envelope at the interface between the organism and the sediment appeared to me as a fundamental step in animal evolution (Bereiter-Hahn et al., 1984; Schmidt-Rhaesa, 2007) that needed to be explored.

Our study shows that the external surface of the cuticle of scalidophoran worms from the Kuanchuanpu Formation (ca 535 Ma) bears a fine hexagonal network (micrometre-size, Fig. 42A-C) that is interpreted as the faithful replica of the boundary between underlying epithelial cells. This interpretation is based on identical structures observed in extant priapulid worms (Fig. 42D-F), that effectively correspond to polygonal cell boundaries. This strict correspondence in size and shape between the network of epidermal cells and that of the cuticular reticulation also occur in various extant ecdysozoans, especially arthropods. Prior to moulting, ecdysozoans secrete specific enzymes that loosen contact between the basal part of the old cuticle and the epidermal cells (Chapman, 2013; Lemburg, 1998). The growth of epidermis via mitosis results in new epidermal cells relatively smaller than in their pre-moult state (Bennet-Clark, 1971; Wigglesworth, 1973). Their apical surface characterized by a wavy appearance (Gibson et al., 2006) bears microvilli and starts to secrete individual cuticular patches (Lemburg, 1998; Wigglesworth, 1973) which fuse together to eventually form a new cuticular layer as the epidermis stretches horizontally (Fig. 42G).

We hypothesize that a comparable process was responsible for the secretion of the cuticle of earliest representatives of Ecdysozoa. Although the nature of the last common ancestor of ecdysozoans remains hypothetical, we suggest that this animal had a cuticle, grew through successive moulting stages (ecdysis see Chapter 5.1) and replicated its epidermal cellular pavement to form a regular cuticular network. Cuticular reticulation in Ecdysozoa appears to be nothing than an initial by-product of cell division during cuticle growth. Although this basic process remained unchanged since at least the basal Cambrian, many different variants evolved through time. During the course of evolution, the increased complexity of cuticular features (e.g. sclerotization, mineralization) associated with possible epidermal differentiation

gave rise independently in almost all groups (except nematodes) to a great variety of patterns of reticulation.

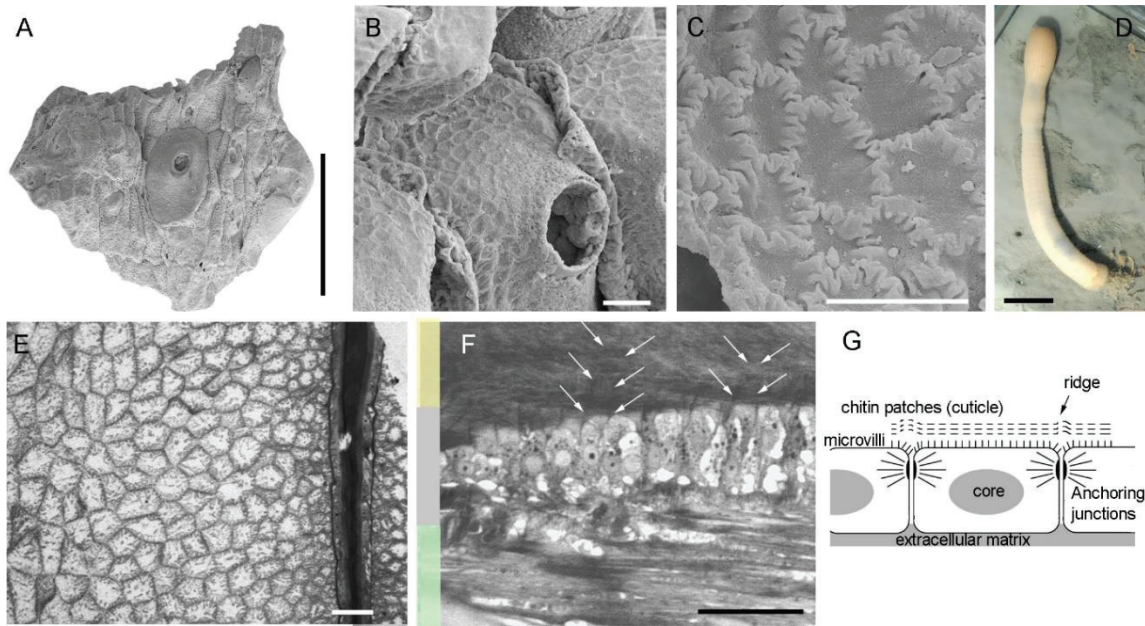


**Figure 42.** Cuticular reticulation and its epithelial origin. A-C. Two types of reticulated pattern on the external surface of the cuticle of scalidophorans from the early Cambrian Kuanchuanpu Formation. D-F. Cuticular reticulation in *Priapulid caudatus* (general view of live specimen in D) showing correspondence between the boundaries of epidermal cells and the walls of cuticular reticulation (arrows). G. Sketch to summarize epidermis secretion. Yellow, grey, and green bars represent the cuticle, single epidermal layer, and circular muscles, respectively. Scale bars: 2 cm (D), 500  $\mu\text{m}$  (A), 25  $\mu\text{m}$  (B), 20  $\mu\text{m}$  (C, E, F). (G) modified from Lemburg (1998) and Schmidt-Rhaesa (2007).

## Research



**Cite this article:** Wang D, Vannier J, Yang X-guang, Sun J, Sun Y-f, Hao W-jing, Tang Q-qin, Liu P, Han J. 2020 Cuticular reticulation replicates the pattern of epidermal cells in lowermost Cambrian scalidophoran worms. *Proc. R. Soc. B* **287**: 20200470. <http://dx.doi.org/10.1098/rspb.2020.0470>

Received: 3 March 2020

Accepted: 9 April 2020

**Subject Category:**

Palaeobiology

**Subject Areas:**

palaeontology, cellular biology, evolution

**Keywords:**

reticulation, epidermis, cuticle, Scalidophora, Cambrian, China

**Authors for correspondence:**

Jean Vannier

e-mail: [jean.vannier@univ-lyon1.fr](mailto:jean.vannier@univ-lyon1.fr)

Jian Han

e-mail: [elihanj@nwu.edu.cn](mailto:elihanj@nwu.edu.cn)

Electronic supplementary material is available online at <https://doi.org/10.6084/m9.figshare.c.4944831>.

THE ROYAL SOCIETY  
PUBLISHING

# Cuticular reticulation replicates the pattern of epidermal cells in lowermost Cambrian scalidophoran worms

Deng Wang<sup>1,2</sup>, Jean Vannier<sup>2</sup>, Xiao-guang Yang<sup>1</sup>, Jie Sun<sup>1</sup>, Yi-fei Sun<sup>1</sup>, Wen-jing Hao<sup>1</sup>, Qing-qin Tang<sup>1</sup>, Ping Liu<sup>1</sup> and Jian Han<sup>1</sup>

<sup>1</sup>State Key Laboratory of Continental Dynamics, Shaanxi Key Laboratory of Early Life and Environments, Department of Geology, Northwest University, Xi'an 710069, People's Republic of China

<sup>2</sup>Univ Lyon, Univ Lyon 1, ENSL, CNRS, LGL-TPE, F-69622, Villeurbanne, France

DW, 0000-0002-4464-9632; JV, 0000-0003-0998-1231; JH, 0000-0002-2134-4078

The cuticle of ecdysozoans (Panarthropoda, Scalidophora, Nematoida) is secreted by underlying epidermal cells and renewed via ecdysis. We explore here the relationship between epidermis and external cuticular ornament in stem-group scalidophorans from the early Cambrian of China (Kuanchuanpu Formation; *ca* 535 Ma) that had two types of microscopic polygonal cuticular networks with either straight or microfolded boundaries. Detailed comparisons with modern scalidophorans (priapulids) indicate that these networks faithfully replicate the cell boundaries of the epidermis. This suggests that the cuticle of early scalidophorans formed through the fusion between patches of extracellular material secreted by epidermal cells, as observed in various groups of present-day ecdysozoans, including arthropods. Key genetic, biochemical and mechanical processes associated with ecdysis and cuticle formation seem to have appeared very early (at least not later than 535 Ma) in the evolution of ecdysozoans. Microfolded reticulation is likely to be a mechanical response to absorbing contraction exerted by underlying muscles. The polygonal reticulation in early and extant ecdysozoans is clearly a by-product of the epidermal cell pavement and interacted with the sedimentary environment.

## 1. Introduction

The epidermis is a fundamental cellular tissue of Metazoa [1] which acts as an interface between the external medium and the body interior [2]. It includes epithelial cells and extracellular material. Epithelial cells form a tissue with complex junction systems and secrete two types of extracellular substrates: basally, the extracellular matrix (ECM), and apically, the glycocalyx (layers of proteins and sugar) and the cuticle [2]. Although absent in placozoans and ctenophores, the glycocalyx plays a crucial role as a matrix on which other extracellular molecules (e.g. chitin, collagen) can anchor and eventually form a cuticular structure. A cuticle occurs in all present-day ecdysozoans (Nematoida, Scalidophora, Panarthropoda), with a consistent three-layered structure [2,3]. Ecdysozoans display a great variety of cuticular structures often associated with sensory organs (e.g. setae). Cuticular moulting is common to all extant representatives of Ecdysozoa and is a key diagnostic feature of the group. Exuviae found in early Cambrian scalidophoran worms from China (*ca* 535 Ma [4]) suggest that ecdysis has a very ancient origin and evolves through a suite of genetic innovations in the three ecdysozoans clades (Scalidophora, Nematoida, Panarthropoda [4,5]).

Cambrian scalidophorans have very diverse cuticular features that are best preserved in Burgess Shale-type Lagerstätten [6,7] and small carbonaceous fossil (SCF) [8] and small shelly fossil (SSF) [9,10] assemblages in which (SSF) scalids, platelets and pharyngeal teeth are preserved in three dimensions as exemplified by stem-group scalidophorans such as *Eopriapulites*, *Eokinorhynchus* [9,10] and palaeoscoleids [11–14]. These microscopic cuticular elements have been studied

in detail in various groups of early Cambrian scalidophorans and provide diagnostic characters useful to their classification. Recently, Wang *et al.* [4] found a new type of micro-ornament in scalidophoran worms from the early Cambrian Kuanchuanpu Formation (*ca* 535 Ma). It consists of very fine reticulation on both the external and internal surface of exuviae. The relationships between the external cuticular features and the underlying epidermal tissues of ancient animals have been largely overlooked. In extant arthropods such as centipedes, the polygonal surface pattern of the cuticle faithfully reproduces the geometry of the underlying epidermal cells [15]. A comparable epidermis-to-cuticular correspondence has been established in crustaceans such as ostracods [16,17], isopods [18] and decapods [19], but has never been observed in other ecdysozoans groups such as the Scalidophora and the Nematoida. Here, we describe two types of micro-reticulate cuticular patterns in lowermost Cambrian scalidophoran worms from the Kuanchuanpu Formation, which have direct counterparts in extant priapulid worms such as *Priapulus caudatus* and *Halicryptus spinulosus*, suggesting that the reticulation observed on the external surface of the Cambrian worms is the direct expression of the epidermis cellular pavement. Our results provide key information on the cuticle formation of basal ecdysozoans that complement recent studies on their moulting process [4].

## 2. Material and methods

### (a) Fossil material

The studied specimens were collected from Bed 2 of the early Cambrian Kuanchuanpu Formation (Fortunian Stage, Terreneuvian Series) at the Zhangjiagou Section near Dahe town, Xixiang County, Shaanxi Province [20]. The Xixiang area was palaeogeographically located on the northwestern margin of the Yangtze Platform during the Ediacaran and Cambrian periods. The fossil-bearing horizon correlates to the *Anabarites trisulcatus*–*Protohertzina anabarica* assemblage biozone [21], which indicates the Meishucunian Stage (equivalent to the Fortunian Stage). U–Pb dating of zircons from tuff layers (Meishucun Section, Yunnan Province) gives an estimated age of  $536.5 \pm 2.5$  Ma [22]. Several horizons of the Kuanchuanpu Formation have yielded abundant secondarily phosphatized SSFs that are extracted from calcareous rocks through digestion in 8–10% acetic acid [23] and picked out from residues under a binocular microscope. These SSF assemblages contain abundant fossils with cnidarian affinities [24,25], possible deuterostomes [26], diverse scalidophoran worms [9,10,27,28], cyanobacteria [29] and problematic forms [30]. Our study is based on 22 specimens in which cuticular ornament is particularly well preserved. All specimens are deposited in the collections of the Early Life Institute of Northwest University, Xi'an, China (see electronic supplementary material, table S1). These specimens were mounted on stubs, coated with gold and observed under a FEI Quanta 400 FEG Scanning Electron Microscope (SEM; high vacuum and 20 kV) at the State Key Laboratory of Continental Dynamics (SKLCD), Northwest University, China. X-ray microtomography (MicroCT) was performed at SKLCD in order to reconstruct the three-dimensional morphology of the reticulate microstructures of two specimens (ELIX93-335 and ELIX95-85). MicroCT images were processed with 'Dragonfly 4.0' software.

### (b) Biological material

*Priapulus caudatus* was collected from the Gullmarsfjord ( $58^{\circ}15'3''$ – $58^{\circ}16'39''$  N;  $11^{\circ}25'36''$ – $11^{\circ}26'34''$  E; depth approx. 40 m; salinity approx. 33 PSU (practical salinity unit)), near the Kristineberg

Marine Research Station (KMRS; Göteborg University), Sweden, and *H. spinulosus* from the brackish waters of the Baltic Sea (at  $58^{\circ}50'53''$ – $58^{\circ}50'48''$  N;  $17^{\circ}32'22''$ – $17^{\circ}32'32''$  E; depth approx. 16 m; salinity approx. 7 PSU), near the Askö Laboratory, Baltic Sea Centre (Stockholm University). *Priapulus caudatus* was dredged from muddy, poorly oxygenated sediments and kept in tanks at low temperature before being fixed (glutaraldehyde) and desiccated (Leica Critical Point Dryer) for microscopic observations. *Halicryptus spinulosus* was prepared via comparable standard methods. *Priapulus caudatus* and *H. spinulosus* secrete mucus which sticks sedimentary particles and detritus to the external surface of the trunk [31], thus preventing clear observation of the cuticular microstructures. Fine cuticular structures were best observed in freshly moulted specimens and exuviae. Images of dissected and whole specimens were taken with a Zeiss Merlin compact scanning electron microscope (SEM) at the Centre Technologique des Microstructures (CTμ, University Claude Bernard Lyon 1). Some specimens were embedded in resin (EPON), sliced (Ultramicrotome Reichert Ultracut S) and stained with Toluidine blue for observation of cellular and cuticular features using optical microscopy.

## 3. Results

### (a) Cuticular reticulation in early scalidophorans

Scalidophoran worms are frequent elements of SSF assemblages from the early Cambrian Kuanchuanpu Formation, and are represented by at least five different species and more than nine unnamed forms [9,10,28,32]. They consist of relatively rare complete specimens and more frequent fragmentary tubular remains, all secondarily preserved in calcium phosphate and showing very fine external details of cuticular features (e.g. sclerites, scalids and pharyngeal teeth). Some of these tubular elements are exuviae which display either a positive or a negative relief (figure 1*d,m*), indicating that these worms were able to turn their flexible cuticle inside out during ecdysis in a manner similar to that of extant priapulids [4]. SEM observations have revealed very fine reticulate ornament over the entire external surface of the cuticle, characterized by a polygonal network with interconnected narrow ridges or furrows (figure 1*c,f*). This micro-ornament may be locally less well defined due to factors of preservation (figure 1*b,g*). A second type of reticulate pattern, characterized by wavy ridges, occurs on the inner surface of exuviae (figure 1*n,o*).

#### (i) Reticulation on sclerites

Reticulation is well defined in the two types of exuviae, especially around the basal part of sclerites. In exuviae with a positive relief, it consists of five- to seven-sided polygons delimited by straight interconnected ridges (SIR), which form a rather regular network. In some cases, elongate polygons or polygons with a more irregular shape are evident. SIR relief decreases towards the apex of the sclerites. Measurements of more than 200 polygons were made in 10 different specimens (electronic supplementary material, table S1). The diameter of the polygons ranges from 4 to 12  $\mu\text{m}$ , their perimeter length is from 14 to 31  $\mu\text{m}$  and SIR width varies from 1.3 to 2.0  $\mu\text{m}$  (figure 1*b,c*; electronic supplementary material, table S1). The exact counterpart of this polygonal network was observed in exuviae with a negative relief (i.e. sclerites pointing inwards instead of outwards) in which SIR faithfully correspond to interconnected furrows (SIF). SIF encircle

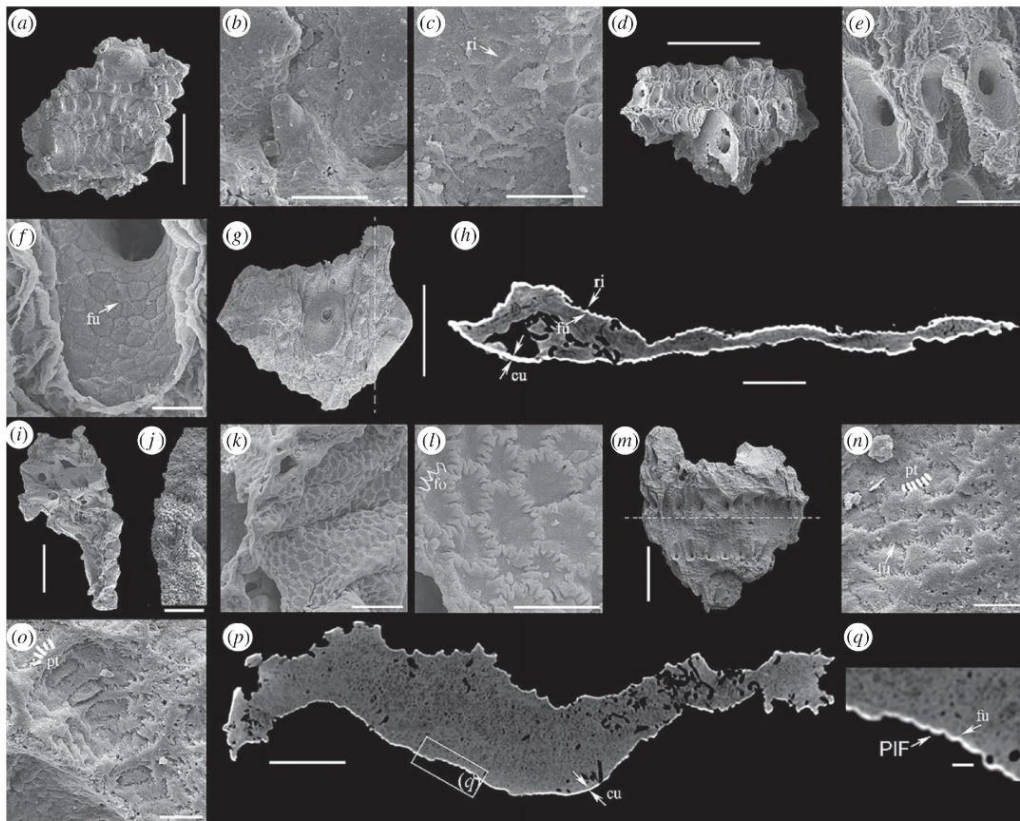


**Figure 1.** Reticulation in scaldiphoran worms from the early Cambrian Kuanchuanpu Formation, China. (a–c) Reticulation on the external surface of sclerites; ELIXX106-520, general view and close-ups showing polygons with SIR. (d–f) Reticulation on the internal surface of sclerites; ELIXX78-205, general view and close-ups showing polygons with SIF. (g,h) ELIXX93-335, general view and microCT image of a virtual section through the specimen (dotted line); each ridge on the outer surface corresponds to a furrow on the inner surface. (i–l) ELIXX73-212, reticulation on the external surface of flexible cuticle; (i) general view and close-ups showing reticulation with MIR (9–26 V-shaped microfolds); (j) a broken part of phosphatized cuticle with no visible microstructures. (m–q) ELIXX95-85, general view and close-ups showing reticulation with PIF (10–22 pits) and elongated PIF between sclerites (external surface of an inverted exuvia; see Wang *et al.* [4]); (p,q) microCT images of a virtual section through the specimen (dotted line in e). cu, cuticle; fo, fold; fu, furrow; PIF, punctuated interconnected furrows; pt, pit; ri, ridge. Scale bars represent: 500  $\mu\text{m}$  (a,e,g,i,m), 200  $\mu\text{m}$  (p), 100  $\mu\text{m}$  (e,h), 50  $\mu\text{m}$  (b,k), 20  $\mu\text{m}$  (c,f,l,n,o,q), 4  $\mu\text{m}$  (j).

slightly convex polygonal areas. Measurements of about 200 of these polygons in 5 specimens give values similar to those obtained from sclerites with a positive relief (polygon diameter and perimeter, 4–15 and 20–43  $\mu\text{m}$ , respectively; electronic supplementary material, table S1; figure 1e,f). Virtual tomographic sections show that SIR are the exact counterparts of SIF (figure 1h).

### (ii) Reticulation on flexible parts of the cuticle

A different type of reticulate pattern is evident in areas where the cuticle is devoid of sclerites and supposedly more flexible. It is characterized by strongly microfolded interconnected ridges (MIR) (figure 1k,l) which contrast with the straight outline of SIF (figure 1c). These ridges bear tiny V-shaped, evenly distributed microfolds (figure 1l). The diameter of these polygons ( $n = 130$  in 7 different specimens) ranges from 5 to 19  $\mu\text{m}$  with a wall thickness of 0.4–2.0  $\mu\text{m}$ . Their perimeter varies from 19 to 47  $\mu\text{m}$ . Individual polygons have 9 to 26 microfolds (microfold length between 3.0 and 4.6  $\mu\text{m}$ ; see electronic supplementary material, table S1).

Exuviae with a negative relief show a reticulate pattern characterized by punctuated interconnected furrows (PIF) around polygonal areas (figure 1n,o). As for SIR and SIF (observed on sclerites), PIF are the inverted counterparts of MIR. The smooth microfolded walls of MIR match exactly with the punctuated outline of PIF as confirmed by measurements ( $n = 100$ ; polygon diameter: 5–15  $\mu\text{m}$ ; number of pits: 10–22) and tomographic cross-sections (figure 1p,q). Some polygonal areas seem to be stretched in one direction (figure 1o).

### (b) Reticulation and cuticle structure in extant priapulid worms

In *P. caudatus* (figure 2a,b), reticulation occurs along both the trunk (figure 2c–e) and the proboscis (figure 2f,g), with polygonal diameters of 9–14 and 10–21  $\mu\text{m}$ , respectively (electronic supplementary material, table S1). The three to five-sided polygons observed on the trunk are delimited by straight weakly elevated interconnected ridges and form a rather regular network (figure 2c,d). Microfolded polygons (resembling the MIR-type in fossils) preferentially occur in

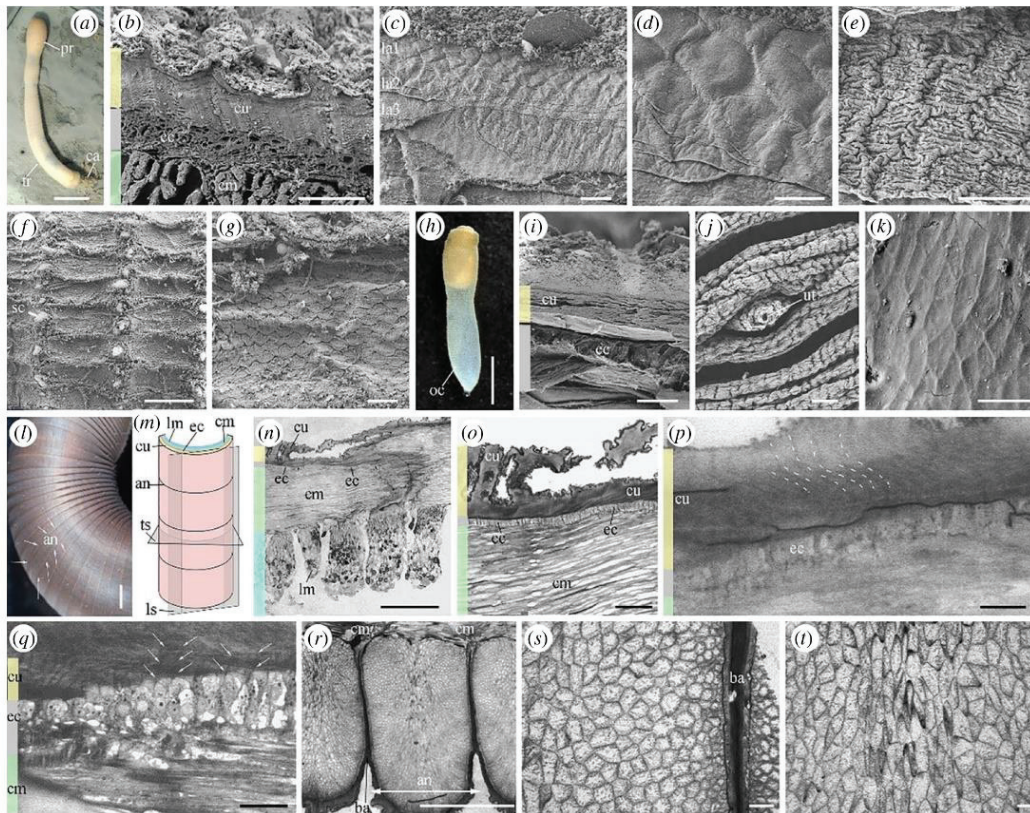


**Figure 2.** Reticulation and epidermal cells in *Priapulus caudatus* and *H. spinulosus* from Sweden. (a–g) *Priapulus caudatus*. (a) General view of a live specimen on sediment. (b) Transverse section through the cuticle (details of epicuticle surface obscured by sediment particles and debris). (c,d) Oblique section showing the layered structure of the cuticle (each layer with reticulate network); general view and close-up. (e) Reticulate surface affected by microfolds (on both ridges and the floor of the polygons). (f) Scaly reticulation on the proboscis. (g) Close-up of f. (h–k) *H. spinulosus*. (h) General view of a moulting specimen with old cuticle partly detached from the body. (i) Transverse section through trunk showing cuticle epidermal cells and circular muscles. (j) Newly moulted cuticle with reticulation and unsclerotized tubuli. (k) Reticulation along the internal surface of an exuvia. (l–t) *Priapulus caudatus* from Sweden; microtome sections of specimens embedded in resin (toluidine blue staining). (l) Trunk annuli of *Priapulus caudatus*. (m) Simplified diagram of trunk to show location of transverse and longitudinal sections. (n) Transverse section through trunk cuticle (cuticle, epidermal cells, circular muscles, longitudinal muscles in light grey, red green and white, respectively). (o) Transverse section showing epidermis (single layer) between cuticle and circular muscle. (p,q) Sections showing correspondence between the boundaries of epidermal cells and the walls of cuticular reticulation. (r–t) Intermediate section showing boundaries between annuli (dark blue lines) and reticulation within annuli; general view and details showing subhexagonal network near the boundaries and more elongated one in central part of annulus. an, annulus; ba, boundaries of annuli; ca, caudal appendage; cm, circular muscle; cu, cuticle; ec, epidermal cells; la, layer; lm, longitudinal muscles; ls, longitudinal section; pr, proboscis; tr, trunk; ts, transverse section; ut, unsclerotized tubuli. Light grey, purple and light green colours represent the cuticle, epidermal cells and circular muscles, respectively. Scale bars represent: 2 cm (a), 500  $\mu\text{m}$  (n,r), 100  $\mu\text{m}$  (o), 20  $\mu\text{m}$  (c,g,i,j,k,p,q,s,t), 10  $\mu\text{m}$  (b,d,e) and 5  $\mu\text{m}$  (h). (Online version in colour.)

the strongly contracted areas of the trunk (figure 2e). Their diameter and thickness are 7–11  $\mu\text{m}$  and 1.2–1.6  $\mu\text{m}$ , respectively. Microfolds are evident both on the walls and inner areas of the polygons (figure 2e).

Transverse sections observed under the SEM show that the cuticle of *P. caudatus* sits above the epidermal cells and is made of numerous, densely packed laminated layers (figure 2b,c). The cuticle thickness varies from 4.7 to 10  $\mu\text{m}$  (see also [33]). However, clear subdivisions (e.g. exocuticle, endocuticle) could not be observed in SEM. Reticulation seems to affect the most superficial part of the cuticle, presumably the epicuticle (figure 2c). Sections through embedded specimens reveal the configuration of epidermal cells and also the relation between the epidermis and the cuticle. Transverse sections show that the epidermis has a

single layer of subrectangular cells (figure 2b,o,q). However, the height (10–20  $\mu\text{m}$ ) and width (approx. 10  $\mu\text{m}$ ) of these cells depend on the location and orientation of the microtome sections (figure 2m,o–q) and therefore show some variations. The boundaries between epidermal cells correspond to the external polygonal ridges observed on the external surface of the cuticle. Longitudinal sections through the epidermal layer show that the layer of epidermal cells forms a well-defined pentagonal and hexagonal network (cell size between 8 and 25  $\mu\text{m}$  in diameter; figure 2r–t).

A comparable reticulation was observed (SEM) in freshly moulted specimens of *H. spinulosus* (figure 2h–j), the diameter of polygons (7–16  $\mu\text{m}$ ) being virtually the same as in *P. caudatus*. The strongly wrinkled appearance of the cuticle is probably due to its extreme thinness and disappears after

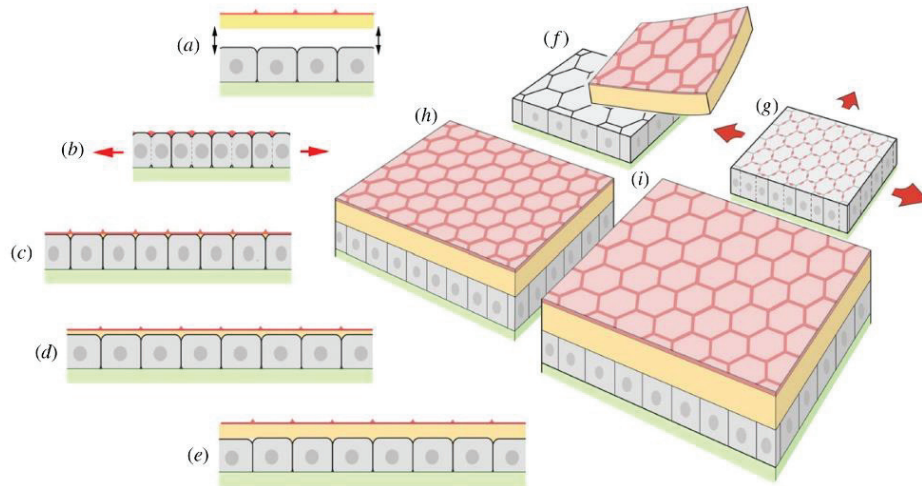


**Figure 3.** Idealized diagram to explain cuticular reticulation in Cambrian scalidophoran worms, based on analogues in extant priapulids (*Priapululus*, *Halicryptus*; see text for details). (a–e) Successive steps in cuticle formation: (a) old cuticle splitting from the epidermis layer (ecdysis); (b) mitosis within epidermis (dividing cells) and formation of small cuticle patches at the boundary between cells; (c) epicuticle layer is formed and bears external reticulation; underlying cuticular layer starts growing; (d) intermediate step; (e) whole cuticle is formed. (f–i) Block diagrams successively showing ecdysis, cell division and initial step of cuticle secretion (as in figure 2) and expansion (red arrows) of epidermal layer and cuticle, leading to final reticulate pattern (polygons have the same size in f and i). Epicuticle is depicted in red/pink; undifferentiated exo- and endocuticle in yellow; epidermal cells in grey; and circular muscles in light green. (Online version in colour.)

a few days following ecdysis (figure 2i). In *H. spinulosus*, reticulation also occurs along the inner surface of fresh exuviae (figure 2k), with five- to seven-sided polygons of 5–16  $\mu\text{m}$  and 0.8–1.3  $\mu\text{m}$  in size and wall thickness, respectively (electronic supplementary material, table S1).

## 4. Discussion

### (a) Polygons replicate epidermal network

SIR/SIF and MIR/PIF clearly represent the positive/negative expressions of two types of cuticular micro-ornament. The consistent size range of polygons (4–19  $\mu\text{m}$ ; see electronic supplementary material, table S1) overlaps with that of epidermal cells in *Priapululus* (8–25  $\mu\text{m}$ ). Moreover, as seen in *Priapululus*, epidermal cells form a regular polygonal network in which cell boundaries match with the walls of the reticulation (figure 2o–q; electronic supplementary material, table S1). These comparative studies with modern priapulids suggest that the reticulation evident on the cuticle of Cambrian scalidophorans similarly replicates the pavement of underlying epidermal cells from which the cuticle was secreted.

In present-day ecdysozoans, epidermal cells secrete a cuticle characterized by three distinct layers: a basal layer with chitin, a middle layer of homogeneous structure and an apical layer having three very thin lamellae [2,3,34], establishing a faithful correspondence in size and shape between the network of epidermal cells and that of the cuticular reticulation. A typical example is in the case of centipedes which display a regular hexagonal network over the external surface of their cuticle. In these myriapods, reticulation appears on the epicuticle and clearly replicates the epidermal cell pavement evident at the beginning of moulting [15]. A comparable geometrical replication occurs in crustacean ostracods and other extant arthropod groups [16,19]. Prior to moulting, ecdysozoans secrete specific enzymes that loosen contact between the

basal part of the old cuticle and the epidermal cells [33,35] (figure 3a,e). The growth of epidermis via mitosis (e.g. [36,37]) results in new epidermal cells relatively smaller than in their pre-moult state (figure 3b,c,f). Their apical surface characterized by a wavy appearance [38] bears microvilli and starts to secrete individual cuticular patches [33,36] (figure 3b) which fuse together to eventually form a new cuticular layer as the epidermis stretches horizontally (figure 3c,d,g).

The accumulation of material secreted by microvilli at the boundary between adjacent epidermal cells [39,40] most probably induces the formation of cuticular ridges in this particular boundary area (figure 3d–i). This process leads to an exact correspondence between the epidermal and the cuticular reticulate networks (figure 3d,h). Although our fossil material does not show details of the cuticle ultrastructure (figure 1j) and underlying epidermal cells (figure 1h,j), we hypothesize that the cuticle of early Cambrian scalidophoran worms was formed through a comparable process. Thus, fundamental aspects of ecdysis [4] and cuticle formation (this study) seem to have been established early in the evolution of ecdysozoans (at least not later than 535 Ma), possibly before the rise and major diversification of arthropods.

### (b) Microfolds in reticulation

We suggest that the microfolds associated with the reticulation of the cuticle of Cambrian worms may be original features. The cuticle of extant scalidophorans such as *P. caudatus* and *H. spinulosus* is very thin (approx. 4.7–10  $\mu\text{m}$ ) and responds in a flexible manner to the contraction and relaxation of circular and longitudinal muscles [33] by creating transverse microfolds, parallel to annuli. The reaction of worms to fixing chemicals (e.g. glutaraldehyde, formaldehyde) often results in extreme body contraction and cuticular folding which, when exerted on reticulate structures, generate microfolds along the walls of the polygons (figure 2e). The microfolded features observed on the cuticle of Cambrian worms,

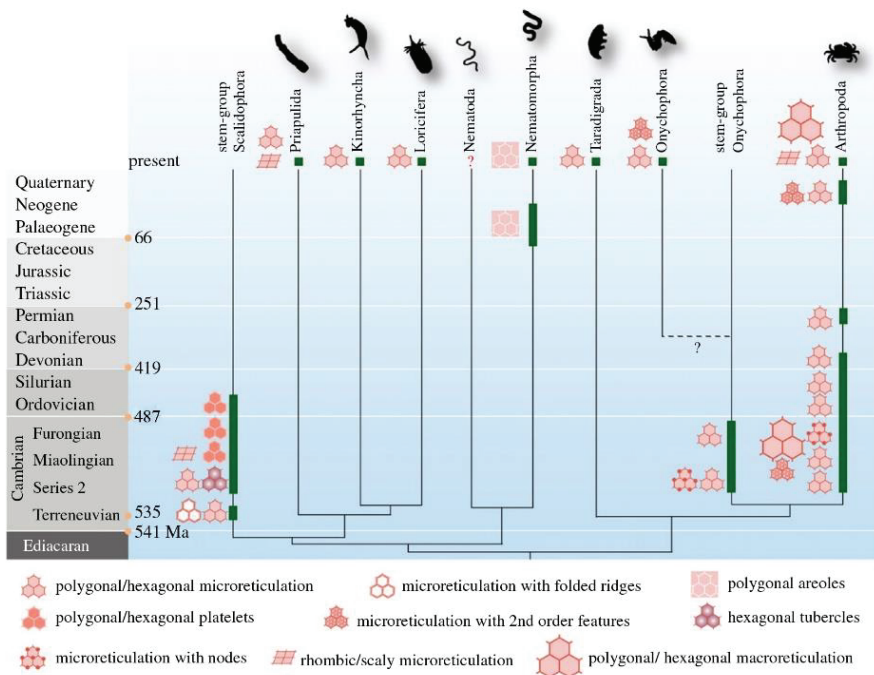


**Figure 4.** Occurrences of cuticular patterns of reticulation plotted on a phylogenetic tree of Ecdysozoa based on Nielsen's phylogeny (supported by morphological characters, see [34]) showing two sister groups (Cycloneuralia and Panarthropoda). For alternative phylogenies based on molecular data, see [44]. The stem-group Scalidophora to which the present fossil material belongs and the stem-group Onychophora (lobopodian panarthropods) are added to the tree. The scalidophoran fossil record goes back to the lowermost Cambrian (e.g. body fossils from the Kuanchuanpu Formation, Terreneuvian) but may extend to the Precambrian–Cambrian boundary as exemplified by trace fossils probably made by stem-group scalidophoran worms (e.g. *Treptichnus* [45,46]). Black question mark and dotted lines represent the first fossil record crown Onychophora [47]. Some lobopodian panarthropods (e.g. *Hallucigenia*) are likely to belong to the stem-group Onychophora [48,49]. Whether onychophorans from the Carboniferous Mazon Creek and Montceau-les-Mines Lagerstätten belong to the crown-group Onychophora or not is currently debated [47,50,51]. The chronology of divergence between groups below the basal Cambrian is hypothetical. Reticulation of the cuticle is found in all ecdysozoan clades except Nematoda (red question mark) and may be present in the last common ancestor of ecdysozoans (see text). Green bars represent the appearance of reticulation. Microreticulation corresponds to polygon size of 10–60  $\mu\text{m}$  that replicates epidermal cell boundaries; macroreticulation to polygons of larger size that may result from more complex cellular processes. (Online version in colour.)

exemplified by MIR/PIF, may be similarly explained by muscular contractions, possibly induced by environmental stress that caused the animal's death. However, these microfolds are not seen in the inner areas (floors) of the polygons. In addition, the V-shaped microfolds observed along the polygonal ridges have a consistent amplitude and a virtually constant number (figure 1*l*). By contrast, the microfolds seen in extant priapulids are distributed more irregularly and seem to affect the whole cuticular structure (figure 2*e*). We suggest that the microfolds associated with the cuticle reticulation evident in Cambrian worms may be original features. They may characterize freshly moulted worms in which the cuticle is extremely thin and wrinkled as seen in extant *H. spinulosus* (figure 2*k*), or result from unknown external or internal factors. Interestingly, MIR/PIF are mostly found in areas where the cuticle is supposed to be thinner and flexible, whereas SIR/SIF preferentially occur around thick sclerites. Microfolds may be seen as a physical solution to absorb plastic deformation due to muscular contractions, especially where the cuticle is thin. That would explain why non-deformable sclerites lack such wavy appearance. Similarly, *Eopriapulites sphinx*, another scalidophoran worm from the Kuanchuanpu Formation, shows a complex wrinkled cuticular pattern with closely spaced annuli and short longitudinal folds running across each

annulus [27]. This pattern may represent another solution to absorb contraction exerted by both circular and longitudinal muscles. An alternative third hypothesis is that the microfolded walls of polygons might be the external replica of interdigitated junctions between epidermal cells. Such junctions might have strengthened contacts between cells in body areas subjected to frequent contractions [41–43].

In summary, both reticulation types (SIR/SIF and MIR/PIF) support the hypothesis that early Cambrian scalidophorans secreted their cuticle in a similar way to that of modern ecdysozoans, that is: (i) that individual epidermis cells served as a matrix for the deposition of molecules such as chitin, which resulted in the formation of the cuticular layer; and (ii) that the reticulate pattern of the cuticle replicate the boundaries between epidermal cells. SIR/SIF seem to be mainly associated with relatively thick cuticular structures, typically trunk sclerites, whereas MIR/PIF preferentially occur in areas where the cuticle is thinner and more flexible. MIR/PIF may result from the absorption of body contraction exerted by underlying muscles, cuticular shrinkage during the early step of cuticle formation or (more improbably) from a special type epidermal cell junctions. Reticulation also appears in other ecdysozoan groups (e.g. palaeoscoleids, panarthropods; figure 4; electronic supplementary material, table S1).



### (c) Evolutionary significance

The oldest known body fossil record of ecdysozoans is at ca 535 Ma, as exemplified by the diverse stem-group scaldiphoran worms from the Kuanchuanpu Formation. No other ecdysozoan group (e.g. panarthropods) is known from this early Cambrian (Terreneuvian) biota. This suggests that scaldiphorans diverged early in the evolutionary history of ecdysozoans and that the last common ancestor of ecdysozoans has yet to be found in the Precambrian. Various phylogenies based on genomic and morphological data have been proposed over the recent years and reveal important uncertainties and controversies [52] in the divergence pattern and relationships of major ecdysozoan lineages. The simplified phylogenetic tree used here (figure 4) to plot the occurrence of reticulate patterns of the cuticle through geological times is that of Nielsen [34], in which Panarthropoda (Arthropoda, Onychophora, Tardigrade) and Cycloneuralia (Scaldiphora, Nematoda, Nematomorpha) are sister groups. The stem-group Scaldiphora which accommodates various worm categories (e.g. palaeoscolideans and taxa from the Kuanchuanpu biota) and the stem-group Onychophora (lobopodian panarthropods) were added to the tree. It is evident that various types of cuticular patterns developed during the Cambrian period within both the Scaldiphora and the Panarthropoda (e.g. arthropods and lobopodian stem-group onychophorans; figure 4; electronic supplementary material, table S3). The oldest known types of reticulation occur in scaldiphorans from the Kuanchuanpu Formation and consist of simple hexagons and other polygons with either straight (SIR/SIF) or microfolded (MIR/PIF) walls. Although the nature of the last common ancestor of ecdysozoans remains to be defined, we suggest that this animal had a cuticle, grew through successive moulting stages (ecdysis [4]) and replicated its epidermal cellular pavement to form a regular cuticular network. Cuticular reticulation in Ecdysozoa appears to be nothing than an initial by-product of cell division during cuticle growth. However, this basic process evolved to produce many different variants through time. An ancient differentiation may have occurred when cuticles became more complex and thicker (e.g. strengthening features) as

exemplified by the SIR/SIF and MIR/PIF types (Kuanchuanpu scaldiphorans) found in the rigid and flexible cuticular areas, respectively. During the course of evolution, the increased complexity of cuticular features (e.g. sclerotization, mineralization) associated with possible epidermal differentiation [53–55] gave rise independently in almost all groups (except nematodes) to a great variety of patterns of reticulation. In contrast with arthropods, the cuticular ornament of scaldiphoran worms has remained virtually unchanged and poorly diversified since the early Cambrian.

**Data accessibility.** All fossil specimens from the Kuanchuanpu Formation are deposited in the collections of the Shaanxi Key Laboratory of Early Life and Environments, Northwest University, China. Extant *P. caudatus* and *H. spinulosus* were collected from Kristineberg Marine Research Station and Baltic Sea, respectively. Some figures, tables and text have been uploaded as electronic supplementary material.

**Authors' contributions.** J.H. conceived the project. D.W., J.H. and J.V. interpreted the fossil material and wrote the paper with input from the other authors. J.S. and Y.-f.S. reconstructed the microtomographic data. All authors read and approved the final manuscript.

**Competing interests.** We declare we have no competing interests.

**Funding.** Financial support was provided by the Strategic Priority Research Program of Chinese Academy of Sciences (grant no. XDB26000000), Natural Science Foundation of China (grant nos. 41621003, 41772010, 41672009, 41720104002), the Ministry of Science and 111 project of Ministry of Education of China (grant no. D17013), the Most Special Fund from the State Key Laboratory of Continental Dynamics, NWU, China (grant no. BJ11060), the China Scholarship Council (CSC, grant no. 201806970013) for D.W.'s 2-year research stay at UCBL, the ASSEMBLE programme, CNRS (France) and NSFC (China) for a PRC cooperation grant, and Pack Ambition International (UCBL and Région Auvergne-Rhône-Alpes).

**Acknowledgements.** We thank Long Pang, Juan Luo, Meirong Cheng (State Key Laboratory for Continental Dynamics, Northwest University (NWU), Xi'an, China) for assistance in the field and laboratory work, the CTμ (Centre Technologique des Microstructures, Université Lyon 1 (UCBL) for SEM facilities and assistance, Vincent Perrier (UCBL) and Jean-Bernard Caron (Royal Ontario Museum) for photographs, the staff of the Kristineberg Marine Research Station and Askö Laboratory (Sweden) during J.V. and D.W.'s research stay, and David J. Siveter (University of Leicester) for linguistic corrections and insightful remarks and two anonymous referees.

### References

- Gibson WT, Gibson MC. 2009 Cell topology, geometry, and morphogenesis in proliferating epithelia. *Curr. Top. Dev. Biol.* **89**, 87–114. (doi:10.1016/s0070-2153(09)89004-2)
- Schmidt-Rhaesa A. 2007 *The evolution of organ systems*, pp. 54–73. Oxford, UK: Oxford University Press.
- Brusca RC, Moore W, Shuster SM. 2016 *Invertebrates*, pp. 639–910, 3rd edn. Sunderland, MA: Sinauer Associates.
- Wang D, Vannier J, Schumann I, Wang X, Yang XG, Komiya T, Uesugi K, Sun J, Han J. 2019 Origin of ecdysis: fossil evidence from 535-million-year-old scaldiphoran worms. *Proc. R. Soc. B* **286**, 20190791. (doi:10.1098/rspb.2019.0791)
- Schumann I, Kenny N, Hui J, Hering L, Mayer G. 2018 Halloween genes in panarthropods and the evolution of the early moulting pathway in Ecdysozoa. *R. Soc. Open Sci.* **5**, 180888. (doi:10.1098/rsos.180888)
- Smith MR, Harvey THP, Butterfield NJ, Kouchinsky A. 2015 The macro- and microfossil record of the Cambrian priapulid *Ottoia*. *Palaeontology* **58**, 705–721. (doi:10.1111/pala.12168)
- Conway Morris S. 1977 Fossil priapulid worms. *Spec. Pap. Palaeontol.* **20**, 1–95.
- Harvey THP, Butterfield NJ. 2017 Exceptionally preserved Cambrian *loriciferans* and the early animal invasion of the meiobenthos. *Nat. Ecol. Evol.* **1**, 22. (doi:10.1038/s41559-016-0022)
- Liu YH, Xiao SH, Shao TQ, Broce J, Zhang HQ. 2014 The oldest known priapulid-like scaldiphoran animal and its implications for the early evolution of cycloneuralians and ecdysozoans. *Evol. Dev.* **16**, 155–165. (doi:10.1111/ede.12076)
- Zhang HQ, Xiao SH, Liu YH, Yuan XL, Wan B, Muscente AD, Shao TQ, Gong H, Cao GH. 2015 Armored kinorhynch-like scaldiphoran animals from the early Cambrian. *Sci. Rep.* **5**, 16521. (doi:10.1038/srep16521)
- Müller KJ, Hinz-Schallreuter I. 1993 Palaeoscolicid worms from the middle Cambrian of Australia. *Palaeontology* **36**, 549–592.
- Han J, Zhang XL, Zhang ZF, Shu DG. 2003 A new platy-armored worm from the early Cambrian Chengjiang Lagerstätte, South China. *Acta Geol. Sin.* **77**, 1–6. (doi:10.1111/j.1755-6724.2003.tb00103.x)
- Han J, Liu JN, Zhang ZF, Zhang XL, Shu DG. 2007 Trunk ornament on the palaeoscolicid worms *Cricocosmia* and *Tabelliscolex* from the Early Cambrian Chengjiang deposits of China. *Acta Palaeontol. Pol.* **52**, 423–431.

14. Conway Morris S. 1997 The cuticular structure of the 495-Myr-old type species of the fossil worm *Palaeoscolex, P. piscatorum* (? Priapulida). *Zool. J. Linn. Soc.* **119**, 69–82. (doi:10.1111/j.1096-3642.1997.tb00136.x)
15. Fusco G, Brena C, Minell A. 2000 Cellular processes in the growth of lithobiomorph centipedes (Chilopoda: Lithobiomorpha). A cuticular view. *Zool. Anz.* **91**, 91–102.
16. Okada Y. 1982 Structure and cuticle formation of the reticulated carapace of the ostracode *Bicornucythere bisanensis*. *Lethaia* **15**, 85–101. (doi:10.1111/j.1502-3931.1982.tb01124.x)
17. Okada Y. 1981 Development of cell arrangement in ostracod carapaces. *Paleobiology* **7**, 276–280. (doi:10.1017/S009483730000405X)
18. Schmalfuss H. 1978 Morphology and function of cuticular micro-scales and corresponding structures in terrestrial isopods (Crust., Isop, Oniscoidea). *Zoomorphologie* **91**, 263–274. (doi:10.1007/BF00999815)
19. Giraud-Guille M-M. 1984 Calcification initiation sites in the crab cuticle: the interprismatic septa—an ultrastructural cytochemical study. *Cell Tissue Res.* **236**, 413–420. (doi:10.1007/bf00214245)
20. Li ZP. 1984 The discovery and its significance of early Cambrian small shell fossils in Hexi area Xixiang Shaanxi. *Geol. Shaanxi* **2**, 73–78.
21. Steiner M, Li GX, Qian Y, Zhu MY. 2004 Lower Cambrian small shelly fossils of northern Sichuan and southern Shaanxi (China), and their biostratigraphic importance. *Géobios* **37**, 259–275. (doi:10.1016/j.geobios.2003.08.001)
22. Sawaki Y *et al.* 2008 Internal structures and U–Pb ages of zircons from a tuff layer in the Meishucunian formation, Yunnan Province, South China. *Gondwana Res.* **14**, 148–158. (doi:10.1016/j.gr.2007.12.003)
23. Müller KJ. 1962 Aus der Praxis—Ein einfacher behelf für die listungstechnik. *Paläontol. Z.* **36**, 265–267. (doi:10.1007/BF02986978)
24. Wang X, Han J, Vannier J, Ou Q, Yang XG, Uesugi K, Sasaki O, Komiya T, Sevastopulo G. 2017 Anatomy and affinities of a new 535-million-year-old medusozoan from the Kuanchuanpu Formation, South China. *Palaeontology* **60**, 853–867. (doi:10.1111/pala.12320)
25. Shao TQ, Tang HH, Liu YH, Waloszek D, Maas A, Zhang HQ. 2018 Diversity of cnidarians and cycloneuralians in the Fortunian (early Cambrian) Kuanchuanpu Formation at Zhangjiagou, South China. *J. Paleontol.* **92**, 115–129. (doi:10.1017/jpa.2017.94)
26. Han J, Conway Morris S, Ou Q, Shu DG, Huang H. 2017 Meiofaunal deuterostomes from the basal Cambrian of Shaanxi (China). *Nature* **542**, 228–231. (doi:10.1038/nature21072)
27. Shao TQ, Liu YH, Wang Q, Zhang HQ, Tang HH, Li Y. 2016 New material of the oldest known scalidophoran animal *Eopriapulites sphinx*. *Palaeoworld* **25**, 1–11. (doi:10.1016/j.palwor.2015.07.003)
28. Shao TQ *et al.* In press. New macrobenthic cycloneuralians from the Fortunian (lowermost Cambrian) of South China. *Precambrian Res.* 105413. (doi:10.1016/j.precamres.2019.105413)
29. Yang XG, Han J, Wang X, Schifbauer JD, Uesugi K, Sasaki O, Komiya T. 2017 Euendoliths versus ambient inclusion trails from Early Cambrian Kuanchuanpu Formation, South China. *Palaeogeogr. Palaeoclimatol. Palaeoecol.* **476**, 147–157. (doi:10.1016/j.palaeo.2017.03.028)
30. Shao TQ *et al.* 2015 New small shelly fossils (*Acanthocassis* and *Xinlispina* gen. nov.) from the Fortunian stage (early Cambrian) in southern China. *Acta Geol. Sin. (English Ed.)* **89**, 1470–1481. (doi:10.1111/1755-6724.12558)
31. Oeschger R, Janssen HH. 1991 Histological studies on *Halicryptus spinulosus* (Priapulida) with regard to environmental hydrogen sulfide resistance. *Hydrobiologia* **222**, 1–12. (doi:10.1007/BF00017494)
32. Liu YH *et al.* 2018 New armoured scalidophorans (Ecdysozoa, Cycloneuralia) from the Cambrian Fortunian Zhangjiagou Lagerstätte, South China. *Pap. Palaeontol.* **5**, 241–260. (doi:10.1002/spp2.1239)
33. Lemburg C. 1998 Electron microscopical localization of chitin in the cuticle of *Halicryptus spinulosus* and *Priapulus caudatus* (Priapulida) using gold-labelled wheat germ agglutinin: phylogenetic implications for the evolution of the cuticle within the Nematelminthes. *Zoomorphology* **118**, 137–158. (doi:10.1007/s004350050064)
34. Nielsen C. 2012 *Animal evolution: interrelationships of the living phyla*, pp. 238–310, 3rd edn. Oxford, UK: Oxford University Press.
35. Chapman RF. 2013 *The insects—structure and function*, pp. 463–498, 5th edn. Cambridge, UK: Cambridge University Press.
36. Wigglesworth VB. 1973 The role of the epidermal cells in moulding the surface pattern of the cuticle in *Rhodnius* (Hemiptera). *J. Cell Sci.* **12**, 683–705.
37. Bennet-Clark HC. 1971 The cuticle as a template for growth in *Rhodnius prolixus*. *J. Insect Physiol.* **17**, 2421–2434. (doi:10.1016/0022-1910(71)90089-8)
38. Gibson MC, Patel AB, Nagpal R, Perrimon N. 2006 The emergence of geometric order in proliferating metazoan epithelia. *Nature* **442**, 1038–1041. (doi:10.1038/nature05014)
39. Locke M. 1966 The structure and formation of the cuticulin layer in the epicuticle of an insect, *Calpodes ethlius* (Lepidoptera, Hesperidae). *J. Morphol.* **118**, 461–494. (doi:10.1002/jmor.1051180403)
40. Botting JP, Muir LA, Van Roy P, Bates D, Upton C. 2012 Diverse middle Ordovician palaeoscolecidan worms from the Buihth-Llandrindod Inlier of central Wales. *Palaeontology* **55**, 501–528. (doi:10.1111/j.1475-4983.2012.01135.x)
41. Moritz K. 1972 Zur Feinstruktur integumentaler Bildungen bei Priapuliden (*Halicryptus spinulosus* und *Priapulus caudatus*). *Z. Morphol. Tiere* **72**, 203–230. (doi:10.1007/BF00391552)
42. Higgins RP, Storch V. 1989 Ultrastructural observations of the larva of *Tubiluchus corallicola* (Priapulida). *Helgoländ Mar. Res.* **43**, 1–11. (doi:10.1007/BF02365545)
43. Higgins RP, Storch V, Shirley TC. 1993 Scanning and transmission electron microscopical observations on the larvae of *Priapulus caudatus* (Priapulida). *Acta Zool.* **7**, 301–319. (doi:10.1111/j.1463-6395.1993.tb01245.x)
44. Borner J, Rehm P, Schill RO, Ebersberger I, Burmester T. 2014 A transcriptome approach to ecdysozoan phylogeny. *Mol. Phylogenet. Evol.* **80**, 79–87. (doi:10.1016/j.ympev.2014.08.001)
45. Vannier J, Calandra I, Gaillard C, Žylińska A. 2010 Priapulid worms: pioneer horizontal burrowers at the Precambrian-Cambrian boundary. *Geology* **38**, 711–714. (doi:10.1130/g30829.1)
46. Kesidis G, Slater BJ, Jensen S, Budd GE. 2019 Caught in the act: priapulid burrowers in early Cambrian substrates. *Proc. R. Soc. B* **286**, 20182505. (doi:10.1098/rspb.2018.2505)
47. Thompson I, Jones DS. 1980 A possible onychophoran from the middle Pennsylvanian Mazono Creek beds of northern Illinois. *J. Paleontol.* **54**, 588–596.
48. Smith MR, Ortega-Hernández J. 2014 *Hallucigenia's* onychophoran-like claws and the case for Tactopoda. *Nature* **514**, 363–366. (doi:10.1038/nature13576)
49. Yang J, Ortega-Hernández J, Gerber S, Butterfield NJ, Hou JB, Lan T, Zhang XG. 2015 A superarmored lobopodian from the Cambrian of China and early disparity in the evolution of Onychophora. *Proc. Natl Acad. Sci. USA* **112**, 8678–8683. (doi:10.1073/pnas.1505596112)
50. Murdock DJ, Gabbott SE, Purnell MA. 2016 The impact of taphonomic data on phylogenetic resolution: *Helenedora inopinata* (Carboniferous, Mazon Creek Lagerstätte) and the onychophoran stem lineage. *BMC Evol. Biol.* **16**, 1–14. (doi:10.1186/s12862-016-0582-7)
51. Garwood RJ, Edgecombe GD, Charbonnier S, Chabard D, Sotty D, Giribet G. 2016 Carboniferous Onychophora from Montceau-les-Mines, France, and onychophoran terrestrialization. *Invertebr. Biol.* **135**, 179–190. (doi:10.1111/ivb.12130)
52. Giribet G, Edgecombe GD. 2017 Current understanding of Ecdysozoa and its internal phylogenetic relationships. *Integr. Comp. Biol.* **57**, 455–466. (doi:10.1093/icb/ix072)
53. Waku Y. 1978 Fine structure and metamorphosis of the wax gland cells in a psyllid insect, *Anomoneura mori* Schwartz (Homoptera). *J. Morphol.* **158**, 243–274. (doi:10.1002/jmor.1051580302)
54. Neil JV. 2000 Factors influencing intraspecific variation and polymorphism in marine podocopic Ostracoda, with particular reference to tertiary species from southeastern Australia. *Hydrobiologia* **419**, 161–180. (doi:10.1023/A:1003983918339)
55. Guillot C, Lecuit T. 2013 Mechanics of epithelial tissue homeostasis and morphogenesis. *Science* **340**, 1185–1189. (doi:10.1126/science.1235249)

## **Supplementary materials**

### **Cuticular reticulation replicates the pattern of epidermal cells in lowermost Cambrian scalidophoran worms**

Deng Wang, Jean Vannier, Xiao-guang Yang, Jie Sun, Yi-fei Sun, Wen-jing, Hao, Qing-qin Tang, Ping Liu, Jian Han

## Text S1

### Function of reticulate ornament in scalidophorans

Early scalidophorans display a great variety of cuticular features such as sclerites, scalids, platelets and reticulation, which raises the question of their possible function. Overall similarities with modern priapulids suggest that these ancient worms had a hydrostatic skeleton [1, 2]; that is that force is transmitted by the internal pressure of their coelomic fluid and the role of their circular and longitudinal muscles is to deform this hydrostatic skeleton resulting in local contractions, retractions and extensions of their body. This system would have allowed Cambrian worms to move through sediment and capture food (e.g. pharynx evagination) as observed in modern priapulids. Their cuticle directly interacted with sediment involving frictional forces, and at the same time protected the body of the worm from interactions with sediment particles (e.g. when burrowing). Scalids may have played a role in anchoring [3] and/or housed sensory organs [4]. Although mounted on extensible stretchable annuli the closely spaced sclerites of *Eokinorhynchus rarus* [5], *Tabelliscolex hexagonus* [6] and allied forms also had an evident protective role but are likely to have limited the flexibility of the animal [7, 8]. The possible function of reticulation is more uncertain. Although it interacted with small particles (e.g. clay minerals), it is difficult to determine if tiny polygons (4-12  $\mu\text{m}$ ) actually played a significant role in friction and locomotion. It has been argued that reticulation, even in millimetre size animals, acted as a strengthening feature (e.g. in arthropods with a relatively thin cuticle, such as Cambrian agnostids; see [9]) or represented an economical solution to reduce mass while ensuring optimal exoskeletal strength (e.g. ostracods, [10]). These are open options that require testing.

Palaeoscolecids are worms characterized by a great variety of complex micro-ornament (e.g. cuticular platelets) and are common elements of Cambrian-Ordovician marine communities. Reticulate networks frequently occur along their trunk and form various structures such as polygonal platelets or hexagonal pits. They are present both on the surface of sclerites (2-40  $\mu\text{m}$ ) (e.g. *Tabelliscolex*, *Cricocosmia*; [6, 11]; Fig. S1) and in the interspace between them, where the cuticle was probably thin and flexible (e.g. *Wernia eximia* and *Houscolex lepidotus* in [12, 13], Table S2). Polygons in *H. lepidotus* are usually small (1-15  $\mu\text{m}$ ) but may reach up to 20-40  $\mu\text{m}$  in diameter (Table S2). This type of reticulation strongly recalls that of the scalidophorans from the Kuanchuanpu Formation in shape and size and may similarly replicate underlying epidermal structures.

Extant loriciferans and kinorhynchs also display reticulation (polygon diameter, 0.3-2.0  $\mu\text{m}$  and 0.6-4.3  $\mu\text{m}$ ; Table S2), respectively. The scalids of these tiny worms are likely to increase friction with sediment. However, the frictional effect of their cuticular reticulation is hypothetical.

### Reticulation in other ecdysozoan groups

In extant ecdysozoans reticulation is chiefly expressed in the most external layer of the cuticle (epicuticle). Although the three-layered structure is common to the vast majority of ecdysozoans [14, 15], important differences appear within the clade.

#### *Arthropods*

The cuticle of arthropods shows a great variety of sclerotized or calcified layers. Some

crustaceans have a clearly defined calcified exocuticle and chitinous endocuticle [14]. Fossil and extant arthropod cuticle display a huge variety of external patterns of reticulation. Their extensive revision is beyond the scope of the present paper, in which the main focus is the relationship between reticulation and epidermis. Several studies (e.g. [9, 16-19]; Table S3) clearly show a close correspondence in size and shape between reticulation and epidermal cells, in various arthropod groups (e.g. ostracods, myriapods, decapods; Fig. S2 A-E, G-I). Although the mesh size of these polygonal structures usually falls within a consistent range (10-25  $\mu\text{m}$  in diameter in most extant and fossil species; Table S3), larger values frequently occur (e.g. 40-60  $\mu\text{m}$ ; [16, 20]). There are also innumerable examples of much larger polygonal patterns such as in the Cambrian arthropod *Tuzoia* (1-3 mm in diameter [21] and Fig. S2 F) or the trilobite-like *Retifacies* [22]. This large scale reticulation is unlikely to have resulted from a strict replication of individual cell boundaries and probably involved more complex processes such the possible formation of cell clusters within the epidermis [23, 24] or cell differentiation [25].

#### *Lobopodians and onychophorans*

The cuticle of onychophorans is soft, thin, flexible and very permeable [14]. Reticulation in the onychophoran cuticle consists of tiny polygons (10-17  $\mu\text{m}$  in diameter), which correspond to the size of epidermal cells ([26] and Table S3). They are often filled with smaller secondary features (0.7-2  $\mu\text{m}$  in diameter). Lobopodians, a group of extinct soft-bodied non-articulated panarthropods (e.g. [27]), probably phylogenetically close to onychophorans [28], have a cuticle locally reinforced by dorsal paired plates (e.g. *Microdictyon*; [29, 30]; Fig. S2 J, K) or spines (e.g. *Hallucigenia*; [31]). These elements often bear a polygonal micro-ornament (mesh size from 4.5 to 13  $\mu\text{m}$ ; Table S2) which possibly replicated the epidermal pavement [29, 32]. Tiny nodes are associated with the hexagonal reticulation (plates) of *Microdictyon* as in some Cambrian arthropod bradoriids [33].

#### *Tardigrades*

The cuticle of tardigrades is thin and non-mineralized [14]. Reticulation is found on the cuticle of extant species (0.7-3.5  $\mu\text{m}$ ; [34] and Table S3) but has not been observed in fossil representatives of the group [35, 36].

#### *Nematoids*

The cuticle of nematodes is secreted by a cellular or syncytial epidermis and lacks chitin, being mainly composed of collagen. That of nematomorphs typically consists of a lamellate, fibrous inner layer (proteins) overlain by an homogeneous outer one [15]. Extant nematomorph cuticle displays polygonal microstructures termed megareoles (17-65  $\mu\text{m}$  in diameter), areoles (6-30  $\mu\text{m}$ ) and microareoles (2-8  $\mu\text{m}$ ; see Table S4). Their possible relationship with epidermal cells (e.g. [37]) remains unclear. Fossil forms attributed to nematomorphs have comparable areoles (Table S4) which are columnar, variable in height but at least three times as high as wide, and with a diameter of 3-5  $\mu\text{m}$ . Reticulation seems to be absent in extant and fossil nematodes [38, 39] perhaps due to the acellular nature of their cuticle [39].

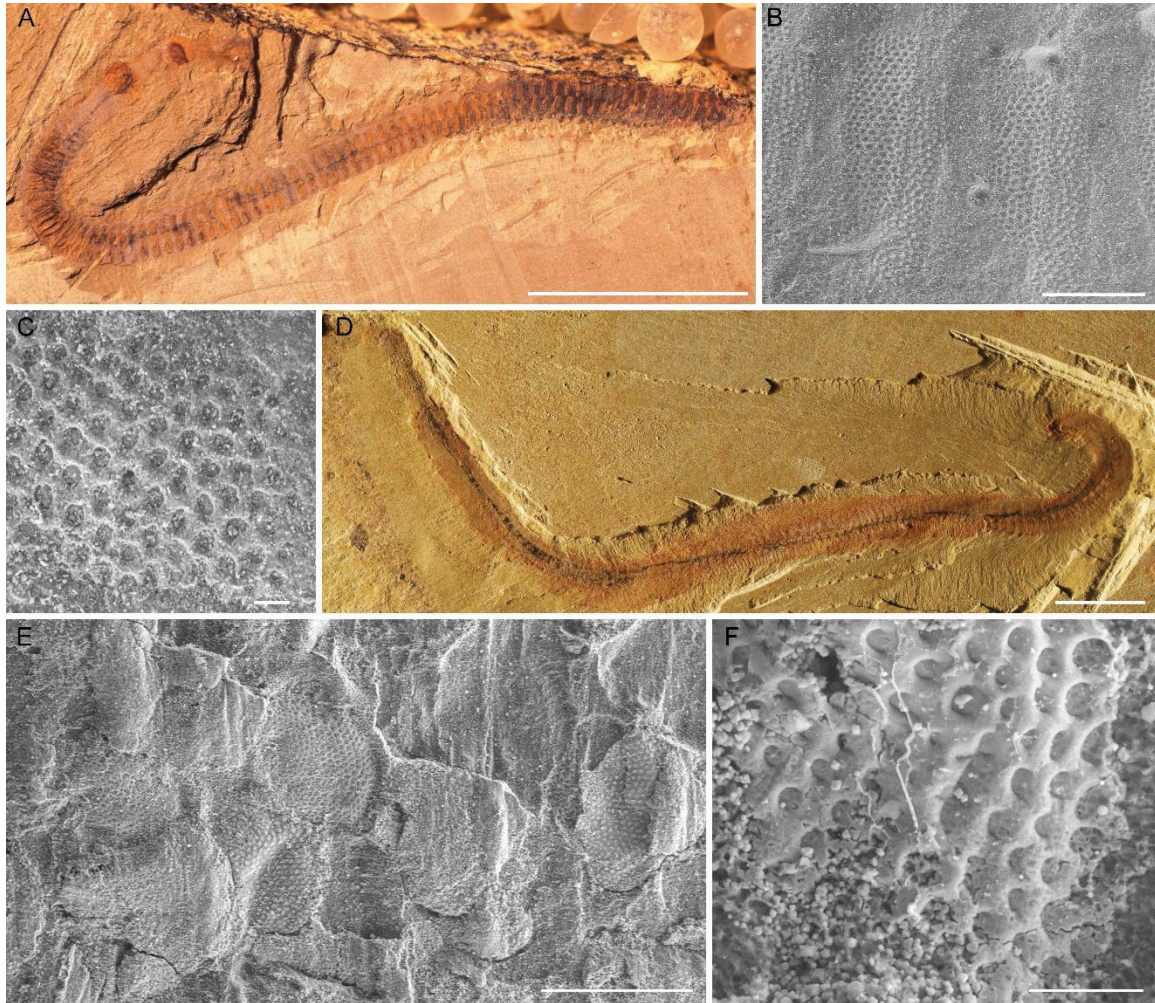


**Figure S1.** Reticulation on the cuticle of fossil palaeoscolecids from early Cambrian Chengjiang biota, south China. A-C. *Tabelliscolex hexagonus* (ELI-0001218). D-F. *Cricocosmia jinningensis* (ELI-0001402). Scale bars represent: 5 mm (D), 1 mm (A), 500  $\mu$ m (B, E) and 50  $\mu$ m (C, F).

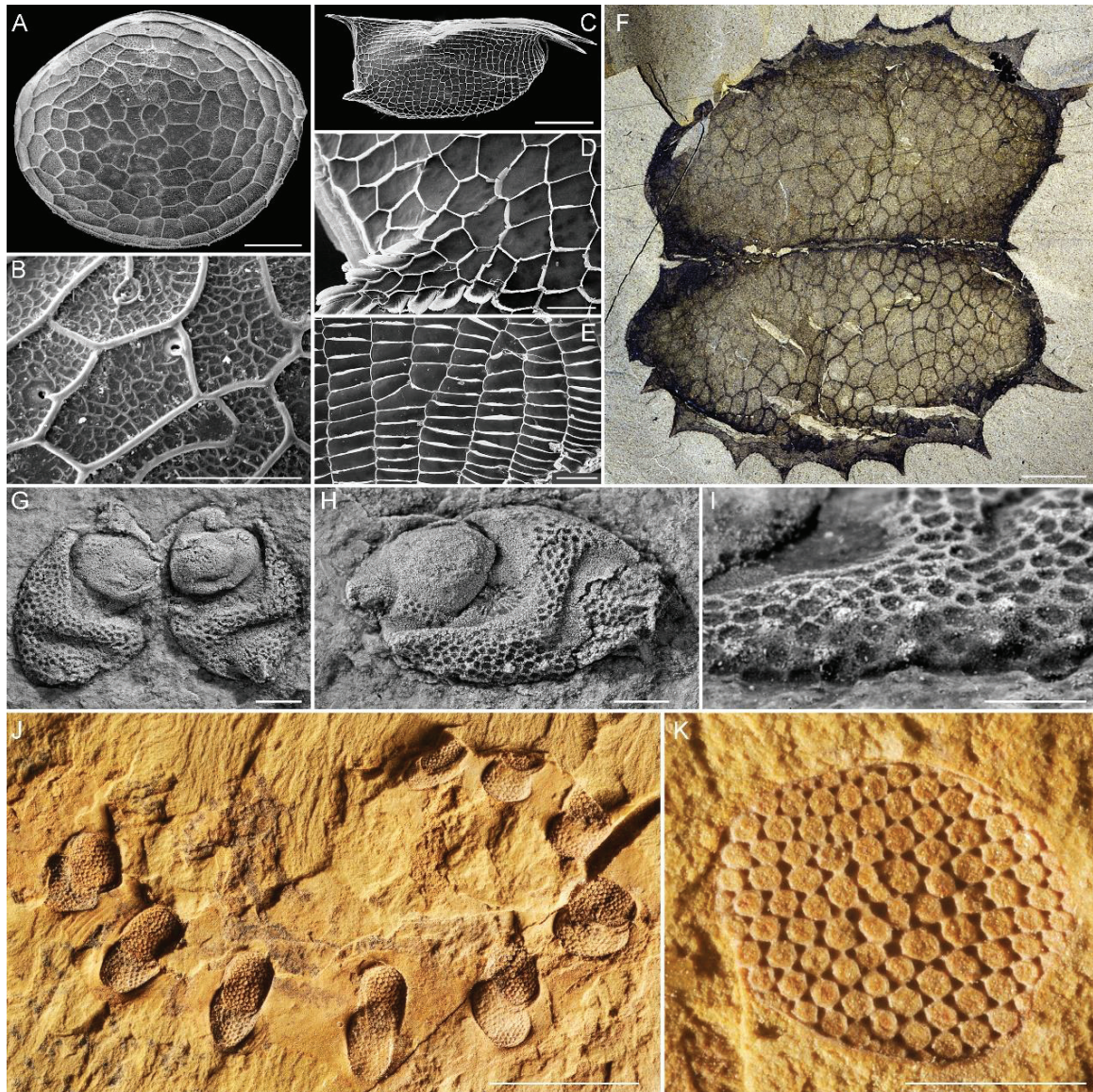


**Figure S2.** Reticulation on the cuticle of extant and fossil bivalved arthropods and lobopodians. A, B. *Polycope reticulata* (Cladocopina, Ostracoda, Crustacea) from the Mediterranean Sea; lateral view and detail of primary (ca 30-60  $\mu\text{m}$ ) and secondary reticulation (ca 2.8-6.2  $\mu\text{m}$ ). C-E. *Conchoecia imbricata* (Halocypridina, Ostracoda, Crustacea) from the Pacific Ocean near Japan; right lateral view and details of polygonal (ca 20-67  $\mu\text{m}$ ) and sub-rectangular reticulation (ca 7.7-18.5  $\mu\text{m}$ ). F. *Tuzoia canadensis* from the Middle Cambrian Burgess Shale (USNM 80488). G-I. *Parabolbozoe bohémica* (Myodocopida, Ostracoda, Crustacea) from the Silurian (ca 120-160  $\mu\text{m}$ , courtesy Vincent Perrier). J, K. *Microdictyon* (Lobopodia) from the early Cambrian Chengjiang biota (ELI-0002001), South China; general view and detail of polygons on the surface of a sclerite (ca 150-270  $\mu\text{m}$ ). Scale bars represent 1 cm (F), 4 mm (J), 1 mm (C, G-I, K), 100  $\mu\text{m}$  (A), 50  $\mu\text{m}$  (B, D) and 25  $\mu\text{m}$  (E). Credit: Vincent Perrier, Université Lyon 1 (G-I) and Jean-Bernard Caron, Royal Ontario Museum (F).

Species / Specimens	Reticulation type	ns	Reticulated polygons			Rt (μm)	Microfolds			Pits		
			D (μm)	P (μm)	N		Shape	L (μm)	n	Shape	L (μm)	np
<b>CAMBRIAN</b>												
unnamed form - ELIXX31-95	SIR	5-7	3.8-8.4	15-21	14	1.1-1.9						
unnamed form - ELIXX41-148	SIR	5-7	4.2-7.0	15-22	10	1.6-2.3						
unnamed form - ELIXX57-320	SIR	5-7	5.0-8.3	15-20	10	1.8-2.3						
unnamed form - ELIXX63-291	SIR	5-7	5.4-9.8	15-27	10	1.3-1.7						
unnamed form - ELIXX66-173	SIR	5-7	2.8-12	19-31	10	1.4-2.0						
unnamed form - ELIXX86-112	SIR	5-7	3.3-8.6	19-26	50	0.5-1.5						
unnamed form - ELIXX87-201	SIR	5-7	3.0-9.7	20-29	50	1.8-2.6						
unnamed form - ELIXX90-295	SIR	5-7	3.7-7.5	17-21	20	1.4-2.1						
unnamed form - ELIXX98-278	SIR	5-7	3.6-8.3	19-21	5	1.6-2.2						
unnamed form - ELIXX106-520	SIR	5-7	3.3-9.3	14-27	30	0.9-1.5						
unnamed form - ELIXX78-205	SIF	5-7	4-12	25-35	40							
unnamed form - ELIXX85-118	SIF	5-7	6.7-15	21-43	100							
unnamed form - ELIXX90-221	SIF	5-7	5-12.5	21-38	40							
unnamed form - ELIXX95-85	SIF	5-7	5.7-12.5	23-35	30							
unnamed form - ELIXX98-179	SIF	5-7	5.5-12.5	20-35	40							
unnamed form - ELIXX25-169	MIR	5-7	7.3-9.6	30-32	3	0.9-1.5	V	3.6-4.6	16-17			
unnamed form - ELIXX63-3	MIR	5-7	5-10.8	19-30	10	0.9-1.9	V	3.7-4.0	9-17			
unnamed form - ELIXX73-212	MIR	5-7	4.4-16.0	21-34	60	0.4-1.2	V	3.1-5.1	14-24			
unnamed form - ELIXX73-300	MIR	5-7	6.4-18.8	29-47	8	0.6-2.0	V	2.9-3.9	21-26			
unnamed form - ELIXX95-158	MIR	5-7	4.4-11.1	19-31	15	0.6-1.7	V	2.1-4.0	11-16			
unnamed form - ELIXX96-45	MIR	5-7	4.5-14.3	22-37	20	0.9-1.3	V	2.7-4.6	16-22			
unnamed form - ELIXX98-243	MIR	5-7	4.9-15.4	27-39	16	0.5-1.4	V	2.7-6.1	16-24			
unnamed form - ELIXX85-118	PIF	5-7			8					linear	4.5-8.0	10-22
unnamed form - ELIXX95-85	PIF	5-7	4.9-14.6	25-41	100					polygonal	3.4-5.7	12-20
unnamed form - ELIXX95-85	PIF				10					linear	8.2-9.2	16-20
<b>EXTANT</b>												
<i>Priapulus caudatus</i> (trunk)	SIR-like	3-5	8.6-13.5	34-44	15							
<i>Priapulus caudatus</i> (trunk)	MIR-like	5-7	6.5-11.2	21-23	30	1.2-1.6						
<i>Priapulus caudatus</i> (proboscis)	SIR-like	3-5	9.6-21	37-51	50							
<i>Halicryptus spinulosus</i> (new moulted trunk)	SIR-like	5-7	7.4-15.4	39-43	20	~2						
<i>Halicryptus spinulosus</i> (Inner surface, exuvia, trunk)	SIR-like	5-7	5.0-15.9	27-35	30	0.8-1.3						
<b>EPIDERMAL CELLS (<i>Priapulus caudatus</i>)</b>												
location	location	ns	H/W (μm)	P (μm)	N	Rt (μm)						
longitudinal section (trunk)	Trunk	4	10-20/ ~10		50							
transverse section (trunk)	Trunk	4-7	8-25	42-72	50	-1.5						

**Supplementary Table S1.** Measurements of reticulation in scalidophoran worms from the early Cambrian Kuanchuanpu Formation, China. Four reticulation types are recognized: SIR (Straight Interconnected Ridges), SIF (Straight Interconnected Furrows), MIR (Microfolded Interconnected Ridges) and PIF (Punctuated Interconnected Furrows). Measurements of epidermal cells in *Priapulus caudatus* are also given at the bottom of the table. Abbreviations are as follows: D, diameter; ELIXX, prefix of collection numbers (Early Life Institute, Northwest University, Xi'an, China); L, length; N, number of measured specimens; Np, number of pits; ns, number of sides; P, perimeter; Rt, ridges thickness.



Age	Clade	Species	Shape	Reticulation diameter (µm)	Relation to epidermis	Organism size	References
<b>FOSSIL</b>							
Earliest Cambrian	Scalidophora	unnamed	5-7 sided polygon	4-12	yes	Meiobenthos	this paper (SIR)
Earliest Cambrian	Scalidophora	unnamed	5-7 sided polygon	4-15	yes	Meiobenthos	this paper (SIF)
Earliest Cambrian	Scalidophora	unnamed	5-7 wrinkled sided polygon	5-19	yes	Meiobenthos	this paper (MIR)
Earliest Cambrian	Scalidophora	unnamed	5-7 wrinkled sided polygon with protuberances	5-15	yes	Meiobenthos	this paper (PIF)
Earliest Cambrian	Scalidophora	<i>Eopriapulites sphinx</i>	hexagonal pit/tubercle	8-13	nd	Meiobenthos	Shao et al., 2016
Early Cambrian	Priapulida	<i>Tabelliscolex hexagonus</i>	hexagonal pit/tubercle	25-40	nd	Macrobenthos	Han et al., 2003b
Early Cambrian	Priapulida	<i>Tabelliscolex chengliangensis</i>	hexagonal pit/tubercle	30	nd	Macrobenthos	Han et al., 2007c
Early Cambrian	Priapulida	<i>Cricocosmia jimringensis</i>	net-like	2-10	nd	Macrobenthos	Han et al., 2007c
Early Cambrian	Priapulida	<i>Tabelliscolex</i>	hexagonal pit/tubercle	20-30	nd	Macrobenthos	Steiner et al., 2012
Early Cambrian	Priapulida	<i>Cricocosmia</i>	hexagonal pit/tubercle	10-15	nd	Macrobenthos	Steiner et al., 2012
Early Cambrian	Priapulida	<i>Houscolex lepidotus</i>	platelet	2-5	nd	Meiobenthos	Zhang and Pratt, 1996
Early Cambrian	Priapulida	<i>Houscolex</i> sp.	platelet	1-2	nd	Meiobenthos	Zhang and Pratt, 1996
Early Cambrian	Priapulida	unnamed specimen	polygonal pit	2-3	nd	Meiobenthos	Zhang and Pratt, 1996
Early Cambrian	Priapulida	<i>Sahascolex labyrinthus</i>	labyrinthine structure	nd	nd	Meiobenthos	Zhang and Wrona, 2004, figs 9, 10
Middle Cambrian	Priapulida	<i>Austroscolex primitivus</i>	platelet	4-7	nd	Meiobenthos	Muller & Hinz-, 1993
Middle Cambrian	Priapulida	<i>Murrayascolex serratus</i>	platelet	4	nd	Meiobenthos	Muller & Hinz-, 1993
Middle Cambrian	Priapulida	<i>Rhomboscolex chaoticus</i>	rhombus	30-37	nd	Meiobenthos	Muller & Hinz-, 1993
Middle Cambrian	Priapulida	<i>Coraliscolex gravius</i>	coralliomorph surface	~20	nd	Meiobenthos	Muller & Hinz-, 1993
Late Cambrian	Priapulida	unnamed form - GMPKU2383	4-7 sided polygon	3-5	nd	Meiobenthos	Harvey et al., 2010
Late Cambrian	Priapulida	unnamed form - GMPKU2384	hexagon	3-6	nd	Meiobenthos	Harvey et al., 2010
Early Ordovician	Priapulida	<i>Palaoscolex piscatorum</i>	platelet	9-13	nd	Macrobenthos	Conway Morris, 1997
Middle Ordovician	Priapulida	<i>Wernia evimia</i>	hexagonal platelet	3-4	nd	Meiobenthos	Botting et al., 2012, figure 8
Middle Ordovician	Priapulida	<i>Radnoscolex bivalchi</i>	polygonal platelet	2-3	nd	Meiobenthos	Botting et al., 2012, figure 8
Middle Ordovician	Priapulida	<i>Aggeiscolex murichisoni</i>	hexagonal platelet	2.5-3	nd	Meiobenthos	Botting et al., 2012, figure 8
Middle Ordovician	Priapulida	<i>Ulexiscolex ornoradii</i>	polygonal platelet	1-4	nd	Meiobenthos	Botting et al., 2012, figure 8
Middle Ordovician	Priapulida	<i>Bullascolex inserere</i>	polygonal platelet	6-7	nd	Meiobenthos	Botting et al., 2012, figure 8
Middle Ordovician	Priapulida	<i>Plusscolex linearis</i>	polygonal platelet	5-15	nd	Meiobenthos	Botting et al., 2012, figure 8
Middle Ordovician	Priapulida	<i>Loriciscolex cuspidus</i>	polygonal microplate	1-2	nd	Meiobenthos	Botting et al., 2012, figure 8
<b>EXTANT</b>							
Recent	Priapulida	<i>Priapulius caudatus</i>	hexagon	nd	nd	Macrobenthos	Shapeiro, 1962, figure 2
Recent	Priapulida	<i>Priapulius caudatus</i>	scaly element	nd	nd	Macrobenthos	Hammond, 1970
Recent	Priapulida	<i>Priapulius caudatus</i>	hexagon	6-21	yes	Macrobenthos	this paper
Recent	Priapulida	<i>Hallicryptos spirulicus</i>	hexagon	4-12	nd	Macrobenthos	Oscogor & Janssen, 1991, figure 10
Recent	Loricifera	<i>Armoriforus</i> sp.	hexagon	0.6-1.6	nd	Meiobenthos	Kristensen & Gad, 2004, figure 14
Recent	Loricifera	<i>Nanaloricus</i> sp.	hexagon	0.4-2	nd	Meiobenthos	Bang-Berthelsen et al., 2013
Recent	Loricifera	<i>Nanaloricus givensae</i>	hexagon	0.8-1.6	nd	Meiobenthos	Bang-Berthelsen et al., 2013
Recent	Loricifera	<i>Nanaloricus</i> sp.	hexagon	0.3-0.8	nd	Meiobenthos	Bang-Berthelsen et al., 2013
Recent	Loricifera	<i>Nanaloricus</i> sp.	hexagon	0.8-1.1	nd	Meiobenthos	Bang-Berthelsen et al., 2013
Recent	Kinorhyncha	<i>Cateria</i> sp.	fusiform	0.6-2.8	nd	Meiobenthos	Neuhaus 2013
Recent	Kinorhyncha	<i>Pycnophyes dentatus</i>	polygon	2.6-4.3	nd	Meiobenthos	Neuhaus 2013

**Supplementary Table S2.** Measurements of reticulation in Cambrian-Ordovician and extant scalidophoran worms. Abbreviations are as follows: GMPKU, prefix of collection numbers (Geology department, Paleontological Collections, Peking University, Beijing, China); nd, no data.

Age	Clade	Species	Shape	Reticulation size (µm)			Relation to epidermis	Ecological category	References
				L	W	D			
<b>FOSSIL</b>									
Early Cambrian	Arthropoda	<i>Sanlangella xixiangensis</i>	polygon			10-25	nd	Epibenthos	Liu et al., 2008
Middle Cambrian	Arthropoda	<i>Pychnagnostus gibbus</i>	polygon			10-20	yes	Epi-or-Nektobenthos	Wilmot, 1990a
Middle Cambrian	Arthropoda	<i>Tuzoia</i>	polygon			1000-3000	nd	Nektobenthos	Vannier et al., 2007
Middle Cambrian	Arthropoda	? <i>Parahoulongdongella sp.</i>	microreticulation			7-10	no	Epi/Nektobenthos	Neil, 2006
Middle Cambrian	Arthropoda	? <i>Parahoulongdongella sp.</i>	macroreticulation			40-50	yes	Epi/Nektobenthos	Neil, 2006
Middle Cambrian	Arthropoda	<i>Zepaera sp.</i>	polygon with nodes			~10	nd	Epi/Nektobenthos	Neil, 2006
Late Cambrian	Arthropoda	<i>Homagnostus obesus</i>	polygon			10-15	yes	Epibenthos	Wilmot, 1990b
Late Cambrian	Arthropoda	<i>Olenus wahlenbergi</i>	polygon			10-15	yes	Epibenthos	Wilmot, 1990b
Late Cambrian	Arthropoda	<i>Olenus wahlenbergi</i>	elongated polygon	10	30		nd	Epibenthos	Wilmot, 1990b
Late Cambrian	Arthropoda	<i>Homagnostus obesus</i>	polygon			10-15	yes	Epibenthos	Wilmot, 1990a
Late Cambrian	Arthropoda	<i>Agnostus pisiformis</i>	polygon			10-20	yes	Epi/Nektobenthos	Muller and Walossek, 1987
Middle Ordovician	Arthropoda	<i>Asaphus raniceps</i>	polygonal network			6-7	yes	Epibenthos	Dalingwater, 1973
Silurian	Arthropoda	<i>Proetus concinnus</i>	polygon			5	nd	Epibenthos	Wilmot, 1990b
Silurian	Arthropoda (Ostracoda)	<i>Parabolbozea bohemica</i>	polygon			120-160	nd	Epibenthos	this paper, Perrier et al., 2019
Middle Devonian	Arthropoda	<i>Phacops rana</i>	polygon			15	yes	Epibenthos	Miller, 1976
Late Permian	Arthropoda	<i>Bulbocornigella quadrimodosa</i>	polygon			15-20	nd	Epibenthos	Jones, 2002
N-Middle Miocene	Arthropoda	<i>Hermanites glyphica</i>	microreticulation			4-11	no	Epibenthos	Neil, 2000
Q-Pleistocene	Arthropoda (Ostracoda)	<i>Bicomucythere bisanensis</i>	polygon			~60	yes	Epibenthos	Okada, 1981, 1982a
Early Cambrian	Lobopodia	<i>Microdictyon</i>	polygon with nodes			150-270	nd	Epibenthos	this paper
Early Cambrian	Lobopodia	<i>Tritonychus phanerosarkus</i>	polygon			6-11	yes	Epibenthos	Zhang et al., 2016
Early Cambrian	Lobopodia	<i>Microdictyon (plate type 1)</i>	hexagon with nodes			10-75	nd	Epibenthos	Topper et al., 2011
Early Cambrian	Lobopodia	<i>Microdictyon (plate type 2)</i>	hexagon with nodes			57-128	nd	Epibenthos	Topper et al., 2011
Early Cambrian	Lobopodia	<i>Microdictyon (plate type 3)</i>	hexagon with nodes			~195	nd	Epibenthos	Topper et al., 2011
Early Cambrian	Lobopodia	<i>Microdictyon (plate type 4)</i>	hexagon with nodes			32-90	nd	Epibenthos	Topper et al., 2011
Early Cambrian	Lobopodia	<i>Microdictyon (plate type 5)</i>	hexagon with nodes			58-136	nd	Epibenthos	Topper et al., 2011
Early Cambrian	Lobopodia	<i>Microdictyon (plate type 6)</i>	hexagon with nodes			11-81	nd	Epibenthos	Topper et al., 2011
Early Cambrian	Lobopodia	<i>Microdictyon effusum</i>	hexagon with nodes			10-130	nd	Epibenthos	Bengtson et al., 1986
Early Cambrian	Lobopodia	<i>Microdictyon rhomboidale</i>	hexagon with nodes			10-70	nd	Epibenthos	Bengtson et al., 1986
Early Cambrian	Lobopodia	<i>Microdictyon rabisoni</i>	hexagon with nodes			20-100	nd	Epibenthos	Bengtson et al., 1986
Early Cambrian	Lobopodia	<i>Microdictyon chinense</i>	hexagon with nodes			10-110	nd	Epibenthos	Zhang and Aldridge, 2007
Early Cambrian	Lobopodia	<i>Microdictyon jinshaense</i>	hexagon with nodes			10-150	nd	Epibenthos	Zhang and Aldridge, 2007
Early Cambrian	Lobopodia	<i>Microdictyon cf. effusum</i>	hexagon with nodes			10-160	nd	Epibenthos	Zhang and Aldridge, 2007
Early Cambrian	Lobopodia	<i>Microdictyon cf. rhomboidale</i>	hexagon with nodes			10-100	nd	Epibenthos	Zhang and Aldridge, 2007
Early Cambrian	Lobopodia	<i>Fusuconcharium typicum</i>	hexagon			5-70	nd	Epibenthos	Zhang and Aldridge, 2007
Early Cambrian	Lobopodia	<i>Quadratopora zhenbaensis</i>	hexagon			7-35	nd	Epibenthos	Zhang and Aldridge, 2007
Early Cambrian	Lobopodia	<i>Microdictyon sphaeroides</i>	hexagon with nodes			33-133	nd	Epibenthos	Hinz, 1987
Early Cambrian	Lobopodia	<i>Microdictyon fuchengense</i>	hexagon with nodes			25-180	nd	Epibenthos	Li and Zhu, 2001
Early Cambrian	Lobopodia	<i>Microdictyon depressum</i>	hexagon with nodes			10-130	nd	Epibenthos	Bengtson et al., 1990
Early Cambrian	Lobopodia	<i>Hallucigenia hongmeia</i>	net-like			~25	nd	Epibenthos	Stenier et al., 2012
Early Cambrian	Lobopodia	<i>Onychodictyon ferox</i>	net-like			20-30	nd	Epibenthos	Stenier et al., 2012
Early Cambrian	Lobopodia	<i>Quadratopora</i>	net-like			10-35	nd	Epibenthos	Stenier et al., 2012
Early Cambrian	Lobopodia	<i>Microdictyon sp.</i>	polygon with nodes			21.6-189	nd	Epibenthos	Pan et al., 2017
Early Cambrian	Lobopodia	<i>Microdictyon rozanovi</i>	polygon with nodes			30-90	nd	Epibenthos	Demidenko, 2006
Early Cambrian	Lobopodia	<i>Onychomicrodictyon spiniferum</i>	polygon			30-40	nd	Epibenthos	Demidenko, 2006
Late Cambrian	Lobopodia	<i>Orstenotubulus evamuelleriae</i>	hexagon			4.5-13	yes	Epibenthos	Maas et al., 2007
<b>EXTANT</b>									
Recent	Crustacea (Ostracoda)	<i>Bicomucythere bisanensis</i>	polygon			~60	yes	Epibenthos	Okada, 1981
Recent	Crustacea (Ostracoda)	<i>Calpodes ethlius</i>	polygon			3-15	yes	Epibenthos	Okada, 1981
Recent	Crustacea (Ostracoda)	<i>Anomoneura mori</i>	polygon			3-15	yes	Epibenthos	Okada, 1981
Recent	Crustacea (Ostracoda)	<i>Bicomucythere bisanensis</i>	polygon			~60	yes	Epibenthos	Okada, 1982a
Recent	Crustacea (Ostracoda)	<i>Baffinicythere</i>	polygon			40-80	yes	Epibenthos	Irizuki, 1994
Recent	Crustacea (Ostracoda)	<i>Polycopse reticulata</i>	small polygon			2.8-6.2		Epi/Meiobenthos	this paper
Recent	Crustacea (Ostracoda)	<i>Polycopse reticulata</i>	large polygon			30-60		Epi/Meiobenthos	this paper
Recent	Crustacea (Ostracoda)	<i>Conchoecia imbricata</i>	polygon			20-67		Pelagic	this paper
Recent	Crustacea (Isopoda)	<i>Hyloniscus beieri</i>	scaly microstructure	~31	14-19		yes	Terrestrial	Schmalzfuss, 1978
Recent	Crustacea (Isopoda)	<i>Cretoniscellus aegaeus</i>	polygon			12-19	yes	Terrestrial	Schmalzfuss, 1978
Recent	Crustacea (Isopoda)	<i>Haplophthalms montivagus</i>	polygon			12-33	yes	Terrestrial	Schmalzfuss, 1978
Recent	Crustacea (Isopoda)	<i>Oniscus asellus</i>	scaly microstructure			11-15	yes	Terrestrial	Schmalzfuss, 1978
Recent	Crustacea (Isopoda)	<i>Armadillo tuberculatus</i>	polygon			30-50	yes	Terrestrial	Schmalzfuss, 1978
Recent	Crustacea (Decapoda)	<i>Carcinus maenas</i>	polygon			10 to 12	yes	Epibenthos	Giraud-Guille, 1984
Recent	Insecta	<i>Anomoneura mori</i>	polygon			5 to 9	yes	Terrestrial	Waku, 1978
Recent	Insecta	<i>Calpodes ethlius</i>	polygon			16-17	yes	Terrestrial	Locke, 1966
Recent	Insecta	<i>Rhodnius</i>	polygon			12-15	yes	Terrestrial	Wigglesworth, 1973
Recent	Insecta	<i>Pteris rapae</i>	polygon			12-18	yes	Terrestrial	Honda et al., 2000
Recent	Myriapoda (Chilopoda)	<i>Clinopodes flavidus</i>	polygon			5-11	yes	Terrestrial	Fusco et al., 2000
Recent	Myriapoda (Chilopoda)	<i>Eupolybothrus grossipes</i>	polygon			9-14	yes	Terrestrial	Fusco et al., 2000
Recent	Myriapoda (Chilopoda)	<i>Lithobius muticus</i>	polygon			12-15	yes	Terrestrial	Fusco et al., 2000
Recent	Onychophora	<i>Metaperipatus inae</i>	hexagon			10-16.5	yes	Terrestrial	Maas et al., 2007
Recent	Onychophora	<i>Metaperipatus inae</i>	micro-polygon			0.7-2	/	Terrestrial	Maas et al., 2007
Recent	Tardigrada	<i>Echiniscus granulatus</i>	polygon			2-3	/	Terrestrial	Bertolani et al., 2009
Recent	Tardigrada	<i>Testechiniscus spitzbergensis</i>	polygon			3-3.5	/	Terrestrial	Biserov, 1996
Recent	Tardigrada	<i>Echiniscus wendti</i>	polygon			0.7-2	/	Terrestrial	Biserov, 1996

**Supplementary Table S3.** Measurements of reticulation in fossil and extant panarthropods. Abbreviations are as follows: D, diameter; L, length; W, width, Pg, Paleogene; N, Neogene; Q, Quaternary.

Age	Clade	Species	Shape	Reticulation size (µm)	Relation to epidermis	Ecological category	References
<b>FOSSIL</b>							
Pg-N	Nematomorpha	<i>Palaeochordodes protus</i>	columnar areole	4-5	yes	Parasite	Poinar, 1999
Early Cretaceous	Nematomorpha	<i>Cretachordodes brumitis</i>	diverse areole	3-5	nd	Parasite	Poinar and Buckley, 2006
<b>EXTANT</b>							
Recent	Nematomorpha	<i>Parachordodes tegonotus</i>	microareole	6.6-8.3	nd	Parasite	Poinar et al., 2004
Recent	Nematomorpha	<i>Parachordodes tegonotus</i>	areole	8.3-16.6	nd	Parasite	Poinaret al., 2004
Recent	Nematomorpha	<i>Parachordodes tegonotus</i>	megareole	16.6-26.6	nd	Parasite	Poinar et al., 2004
Recent	Nematomorpha	<i>Gordionus violaceus</i>	polygonal areole	8.5-20	nd	Parasite	Schmidt-Rhaesa, 2001c
Recent	Nematomorpha	<i>Gordionus wolterstorffii</i>	polygonal areole	10-17	nd	Parasite	Schmidt-Rhaesa, 2001c
Recent	Nematomorpha	<i>Gordius attoni</i>	polygonal areole	7-25	nd	Parasite	Schmidt-Rhaesa, 2003a
Recent	Nematomorpha	<i>Gordius difficilis</i>	polygonal areole	6-11	nd	Parasite	Schmidt-Rhaesa, 2003a
Recent	Nematomorpha	<i>Gordionus lineatus</i>	polygonal areole	8-13	nd	Parasite	Schmidt-Rhaesa, 2003a
Recent	Nematomorpha	<i>Neochordodes occidentalis</i>	polygonal areole	7-16	nd	Parasite	Schmidt-Rhaesa, 2003a
Recent	Nematomorpha	<i>Pseudochordodes gordioides</i>	polygonal microareole	2-6.5	nd	Parasite	Schmidt-Rhaesa, 2003a
Recent	Nematomorpha	<i>Acutogordius taiwanensis</i>	polygonal microareole	4-8	nd	Parasite	Chiu et al., 2017
Recent	Nematomorpha	<i>Pseudochordodes bediagae</i>	polygonal areole	17-30	nd	Parasite	De Villalobos & Restelli, 2001
Recent	Nematomorpha	<i>Gordionus diblastus</i>	columnal megareole	18-65	nd	Parasite	Poinar, 1991a
Recent	Nematomorpha	<i>Euchordodes nigramaculatus</i>	polygonal areole	16-29	nd	Parasite	Poinar, 1991a

**Supplementary Table S4.** Measurements of cuticular reticulation in fossil and extant nematomorphs. Abbreviations are as follows: Pg, Paleogene; N, Neogene.

## Supplementary references

- S1. Kier W.M. 2012 The diversity of hydrostatic skeletons. *The Journal of Experimental Biology* **215**, 1247-1257. (doi:10.1242/jeb.056549).
- S2. Vannier J., Martin E.L.O. 2017 Worm-lobopodian assemblages from the Early Cambrian Chengjiang biota: Insight into the “pre-arthropodan ecology”? *Palaeogeography, Palaeoclimatology, Palaeoecology* **468**, 373-387. (doi:10.1016/j.palaeo.2016.12.002).
- S3. Vannier J., Calandra I., Gaillard C., Žylińska A. 2010 Priapulid worms: Pioneer horizontal burrowers at the Precambrian-Cambrian boundary. *Geology* **38**(8), 711-714. (doi:10.1130/g30829.1).
- S4. Lemburg C. 1995 Ultrastructure of the introvert and associated structures of the larvae of *Halicryptus spinulosus* (Priapulida). *Zoomorphology* **115**, 11-29.
- S5. Zhang H.Q., Xiao S.H., Liu Y.H., Yuan X.L., Wan B., Muscente A.D., Shao T.Q., Gong H., Cao G.H. 2015 Armored kinorhynch-like scalidophoran animals from the early Cambrian. *Scientific Reports* **5**, 16521. (doi:10.1038/srep16521).
- S6. Han J., Zhang X.L., Zhang Z.F., Shu D.G. 2003 A new platy-armored worm from the early Cambrian Chengjiang Lagerstätte, South China. *Acta Geologica Sinica* **77**(1), 1-6.
- S7. Müller K.J., Hinz-Schallreuter I. 1993 Palaeoscolecid worms from the middle Cambrian of Australia. *Palaeontology* **36**(3), 549-592.
- S8. Steiner M., Hu S.X., Liu J., Keupp H. 2012 A new species of *Hallucigenia* from the Cambrian Stage 4 Wulongqing Formation of Yunnan (South China) and the structure of sclerites in lobopodians. *Bulletin of Geosciences*, 107-124. (doi:10.3140/bull.geosci.1280).
- S9. Wilmot N.V. 1990 Cuticular structure of the agnostine trilobite *Homagnostus obesus*. *Lethaia* **23**, 87-92.
- S10. Benson R.H. 1981 Form, function, and architecture of ostracode shells. *Annual Review of Earth and Planetary Sciences* **9**, 59-80.
- S11. Han J., Liu J.N., Zhang Z.F., Zhang X.L., Shu D.G. 2007 Trunk ornament on the palaeoscolecid worms *Cricocosmia* and *Tabelliscolex* from the Early Cambrian Chengjiang deposits of China. *Acta Palaeontologica Polonica* **52**(2), 423-431.
- S12. Botting J.P., Muir L.A., Van Roy P., Bates D., Upton C. 2012 Diverse middle Ordovician palaeoscolecidan worms from the Builth-Llandrindod Inlier of central Wales. *Palaeontology* **55**(3), 501-528. (doi:10.1111/j.1475-4983.2012.01135.x).
- S13. Zhang X.G., Pratt B.R. 1996 Early Cambrian palaeoscolecid cuticles from Shaanxi, China. *Journal of Paleontology* **70**(02), 275-279. (doi:10.1017/s0022336000023350).
- S14. Brusca R.C., Moore W., Shuster S.M. 2016 *Invertebrates*. Third ed, Sinauer Associates, Inc., Sunderland Massachusetts USA; 639-910 p.
- S15. Schmidt-Rhaesa A. 2007 *The Evolution of Organ Systems*, Oxford university press; 54-73 p.
- S16. Okada Y. 1982 Structure and cuticle formation of the reticulated carapace of the ostracode *Bicornucythere bisanensis*. *Lethaia* **15**, 85-101.
- S17. Giraud-Guille M.-M. 1984 Calcification initiation sites in the crab cuticle: The interprismatic septa- An ultrastructural cytochemical study. *Cell and Tissue Research* **236**, 413-420.
- S18. Fusco G., Brena C., Minell A. 2000 Cellular processes in the growth of lithobiomorph centipedes (Chilopoda: Lithobiomorpha). A cuticular view. *Zoologischer Anzeiger* **91**, 91-102.

- S19. Müller K.J., Walossek D. 1987 Morphology, ontogeny, and life habit of *Agnostus pisiformis* from the Upper Cambrian of Sweden. *Fossils and Strata* **19**, 1-12.
- S20. Okada Y. 1981 Development of cell arrangement in ostracod carapaces. *Paleobiology* **7**(2), 276-280.
- S21. Vannier J., Caron J.-B., Yuan J.L., Briggs D.E.G., Zhao Y.L., Zhu M.Y. 2007 *Tuzoia*: morphology and lifestyle of a large bivalved arthropod of the Cambrian seas. *Journal of Palaeontology* **81**(3), 445-471.
- S22. Hou X.G., Bergström J. 1997 Arthropods of the Lower Cambrian Chengjiang fauna, southwest China. *Fossils & Strata* **45**, 54-57.
- S23. Honda H., Tanemura M., Yoshida A. 2000 Differentiation of wing epidermal scale cells in a butterfly under the lateral inhibition model - Appearance of large cells in a polygonal pattern. *Acta Biotheoretica* **48**(2), 121-136.
- S24. Guillot C., Lecuit T. 2013 Mechanics of epithelial tissue homeostasis and morphogenesis. *Science* **340**(6137), 1185-1189.
- S25. Waku Y. 1978 Fine structure and metamorphosis of the wax gland cells in a psyllid insect, *Anomoneura mori* Schwartz (Homoptera). *Journal of Morphology* **158**, 243-274.
- S26. Maas A., Waloszek D., Haug J.T., Müller K.J. 2007 A possible larval roundworm from the Cambrian 'Orsten' and its bearing on the phylogeny of Cycloneuralia. *Memoirs of the Association of Australasian Palaeontologists* **34**, 499-519.
- S27. Ortega-Hernández J. 2015 Lobopodians. *Current Biology* **25**(19), R873-875. (doi:10.1016/j.cub.2015.07.028).
- S28. Smith M.R., Ortega-Hernández J. 2014 *Hallucigenia*'s onychophoran-like claws and the case for Tactopoda. *Nature* **514**(7522), 363-366. (doi:10.1038/nature13576).
- S29. Zhang X.G., Aldridge R.J. 2007 Development and diversification of trunk plates of the Lower Cambrian lobopodians. *Palaeontology* **50**(2), 401-415.
- S30. Demidenko Y.E. 2006 New Cambrian lobopods and chaetognaths of the Siberian Platform. *Paleontological Journal* **40**(3), 234-243. (doi:10.1134/s0031030106030026).
- S31. Smith M.R., Caron J.B. 2015 *Hallucigenia*'s head and the pharyngeal armature of early ecdysozoans. *Nature* **523**(7558), 75-78. (doi:10.1038/nature14573).
- S32. Maas A., Mayer G., Kristensen R.M., Waloszek D. 2007 A Cambrian micro-lobopodian and the evolution of arthropod locomotion and reproduction. *Chinese Science Bulletin* **52**(24), 3385-3392. (doi:10.1007/s11434-007-0515-3).
- S33. Neil J., Bell K. 2006 Microreticulation in Cambrian Ostracoda and its relation to similar patterns in tertiary and Recent Ostracoda. *Lethaia* **39**(1), 31-37.
- S34. Bertolani R., Altiero T., Nelson D.R. 2009 Tardigrada (Water Bears). *Invertebrates*, 443-456.
- S35. Müller K.J., Walossek D., Zakharov A. 1995 'Orsten' type phosphatized soft-integument preservation and a new record from the Middle Cambrian Kuonamka Formation in Siberia. *Neues Jahrbuch für Geologie und Paläontologie - Abhandlungen* **197**(1), 101-118.
- S36. Bertolani R., Grimaldi D. 2000 A new Eutardigrade (Tardigrada: Milnesiidae) in amber from the Upper Cretaceous (Turonian) of New Jersey. *Backhuys Publishers, Leiden*, 103-110.
- S37. Schmidt-Rhaesa A. 2013 *Handbook of zoology*. Germany, De Gruyter; 29-123 p.
- S38. Poinar G.J., Kerp H., Hass H. 2008 *Palaeonema phyticum* gen. n., sp. n. (Nematoda: Palaeonematidae fam. n.), a Devonian nematode associated with early land plants. *Nematology* **10**(1), 9-14.
- S39. Schmidt-Rhaesa A. 2014 *Handbook of Zoology*. Germany, De Gruyter; 5-12 p.

## 5.3 Palaeobiology of the Cambrian tubicolous ecdysozoan *Selkirkia*:

### New insights from the Chengjiang Lagerstätte

The Cambrian radiation gave rise to remarkable anatomical novelties and simultaneously to a great variety of lifestyles and strategies, that illustrate how animal life rapidly colonized new niches, adapted successfully to various environments and, eventually made marine ecosystems increasingly complex. Here I focused on palaeobiological and ecological aspects of scalidophoran worms. Although most of these worms seem to have been living within the sediment (burrowers), we know relatively little concerning their exact habitat, ecological niches, and role in the trophic webs.

This present study focuses on *Selkirkia* which differs markedly from all other known fossil and extant scalidophoran worms in that it secreted and lived within a conical tube open at both ends. Its aim was to better understand the nature and formation of this peculiar cuticular structure and to discuss its ecological implications. The submitted MS attached here presents two types of results: 1) concerning the autecology of *Selkirkia* and 2) the phylogeny of Scalidophora, including the relation of *Selkirkia* to other fossil and extant taxa. Phylogeny issues are discussed in details in the following chapter (Chapter 5.5).

Based on exceptionally preserved specimens from the Chengjiang Lagerstätte (ca 518 Ma), we re-explore the anatomy and lifestyle of *Selkirkia*, and more precisely the tube formation and relation to body. Fossil evidence indicate that the tube was probably secreted by trunk epithelial cells and renewed periodically via non-synchronous ecdysis. The tube of *Selkirkia* can be seen as a protective feature against physical damage and predation and may also have played a role in anchoring the animal to sediment. *Selkirkia* had a well-developed functional introvert that theoretically would have allowed it to move through muddy sediment like other scalidophoran worms. However, the tube is likely to have represented an extra-weight for the animal thus hindering or limiting its capacities to move through its environment, compared with non-tubicolous worms. The moulting process of *Selkirkia* implies that the worm could temporarily leave its tube and probably remained buried in sediment until the renewal of its cuticle. Although non-sedentary, *Selkirkia* probably had limited capacities for colonizing distant areas compared to other worms. This would be consistent the fossil occurrence of relatively dense concentrations of individuals found in some localities (possible gregarious habits).

We also found tiny brachiopod epibionts (only one per worm individual) invariably attached to the posterior end of the tube (Fig. 43F, G). We hypothesized that such brachiopods may have fed on tiny suspended organic particles released by feces through the posterior end of the tube of *Selkirkia sinica*, which would explain their preferential and exclusive location. Brachiopods would have gained benefits from their host which in return remained substantially unaffected by this interaction. These brachiopods whose feeding mode was probably generated by lophophoral cilia (as in all extant species) needed to be in constant contact with circulating water. These ecological constraints and the preferential location of brachiopods would suggest that *Selkirkia* probably lived relatively close to the water-sediment interface.

We also briefly revised other possible tubicolous Cambrian animals described in the literature, especially hemichordates, lobopodians, annelids (Fig. 43A-E) and other tubular

microfossils (e.g. cloudinids). The nature of the animal cloudinid and its relation to the tube are uncertain. However, it is unlikely to have affinities with ecdysozoans. In these hemichordates, lobopodians and annelids, it is unclear whether the tubular structure represents a constructed organic tube or simply a consolidated burrow coated with mucus. Thus, *Selkirkia* may appear as the oldest unambiguous tube-dwelling ecdysozoan. This evolutionary trait that offered the animal better protection and anchoring to sediment, may be seen as a possible adaptive response to increasing environmental or biological pressure in Cambrian marine ecosystems. The tube of *Selkirkia* well illustrates the capacities of ecdysozoans to secrete a remarkable variety of cuticular elements and appears as an early innovation within this group. However, *Selkirkia* became extinct by the mid-Cambrian (ca 508 Ma) and no other known scalidophoran worm seems to have adopted tubicolous lifestyles since then, except a single extant meiobenthic species (*Maccabeus tentaculatus*; see Fig. 50, the tube was not observed in these specimens). Other endobenthic strategies favouring faster locomotion and burrowing seem to have prevailed within the group.

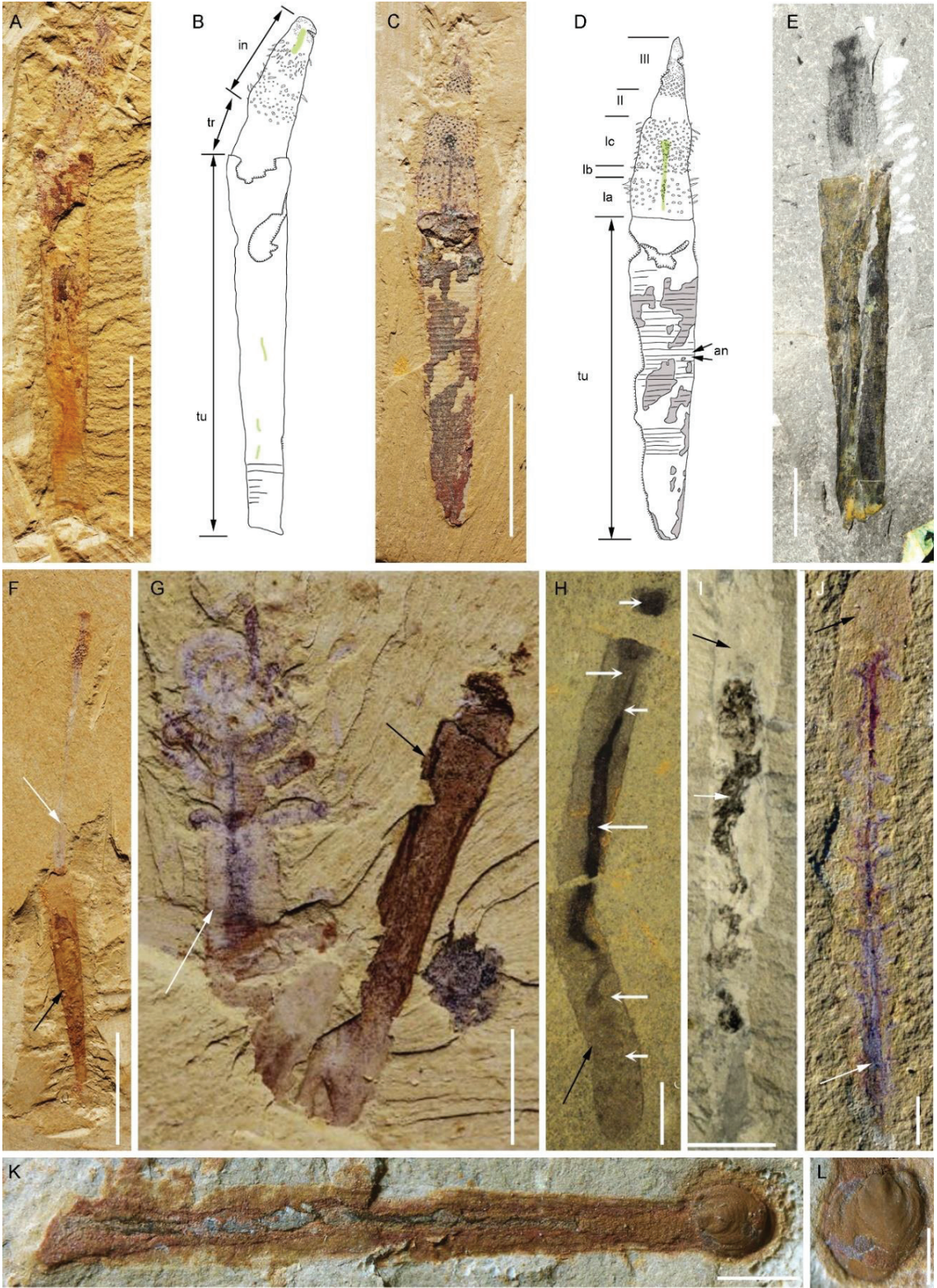




**Figure 43.** General body plan of *Selkirkia* and tubicolous habits in Cambrian animals. A, B. ELI-0002001, *Selkirkia sinica*, general view and line drawing. C, D. ELI-0000601, holotype, *Selkirkia transita* sp. nov., general view and line drawing. E. USNM 57624, *Selkirkia columbia*. F. *Selkirkia sinica* Luo and Hu in Luo et al., 1999 and Hou et al., 1999. G. *Facivermis yunnanicus* Hou and Sun, 1989b: stem-group of Onychophora. H. *Spartobranchus tenuis* Caron and Conway Morris, 2013: Hemichordata. I. *Oesia disjuncta* Nanglu et al., 2016: Hemichordata. J. *Dannychaeta tucolus* Chen et al., 2020: Annelida. White and black arrows indicate the trunk and tube, respectively. K, L. brachiopod symbiont of *Selkirkia sinica* in the early Cambrian Xiaoshiiba Lagerstätte. Abbreviations: an, annulation; in, introvert; tr, trunk; tu, tube. I, II, III represent divisions Zone I, Zone II, and Zone III of the introvert, respectively. Ia, Ib, Ic represent the subdivisions of Zone I. Green lines in b, d represent gut, grey areas in d represent inner surface of tube. Scale bars: 1 cm (J), 5 mm (A, C, E-I), 4 mm (K), 1 mm (L), 500  $\mu$ m (L). (G) from Howard et al. (2020). (H) from Caron and Conway Morris (2013). (I) from Nanglu et al. (2016). (J) from Chen et al. (2020). (K, L) from Yang et al. (submitted; see Chapter 5.4).

## SUBMITTED MANUSCRIPT

### Palaeobiology of the Cambrian tubicolous ecdysozoan *Selkirkia*: New insights from the Chengjiang Lagerstätte

Deng Wang<sup>1, 2</sup>, Jean Vannier<sup>2</sup>, Cédric Aria<sup>3</sup>, Jie Sun<sup>1</sup>, Jian Han<sup>1</sup>

<sup>1</sup> Shaanxi Key Laboratory of Early Life and Environments, State Key Laboratory of Continental Dynamics, Department of Geology, Northwest University, Xi'an 710069, PR China; e-mails: deng.wang@etu.univ-lyon1.fr, elihanj@nwu.edu.cn, shuibaobei@vip.qq.com

<sup>2</sup> Univ Lyon, Univ Lyon 1, ENSL, CNRS, LGL-TPE, F-69622, Villeurbanne, France; e-mail: jean.vannier@univ-lyon1.fr

<sup>3</sup> 27, rue des Têtes, 68000, Colmar, France; e-mail: cedric.aria@protonmail.com

#### Abstract

The radiation of ecdysozoans during the Cambrian gave rise to panarthropods and various groups of cycloneuralian worms among which scalidophorans have played an important role in early marine ecosystems. In this context, the palaeobiology and phylogenetic position of the tubicolous scalidophoran *Selkirkia* is re-explored and a new species, *Selkirkia transita* sp. nov., is erected based on new fossil specimens from the early Cambrian Chengjiang Lagerstätte (ca 518 Ma, China). We show that *Selkirkia* shared clear morphofunctional characteristics with the total-group Priapulida, including an introvert with tripartite subdivision, twenty-five longitudinal rows of scalids, possibly paired caudal appendages, and a pharynx lined with multi-spinose teeth. Our best phylogenetic model resolves *Selkirkia* as basal to total-group Priapulida. *Selkirkia* could move within its annulated tube which was secreted by trunk epithelial cells and renewed periodically via non-synchronous ecdysis. Its capacities to move were probably limited compared with non-tubicolous worms. Brachiopod epibionts attached to the posterior end of the tube suggest that *Selkirkia* probably lived buried in sediment close to the water sediment interface. The tubicolous habit of *Selkirkia* and other Cambrian animals such as some hemichordates, annelids and lobopodian panarthropods is therefore a widely convergent evolutionary trait that may have offered animals a better protection and anchoring to sediment during the Cambrian explosion.

Key words: Priapulida, Cambrian tubicolous worms, *Selkirkia*, Palaeobiology, Chengjiang Lagerstätte

#### Introduction

Scalidophora contains the Priapulida, Kinorhyncha and Loricifera (Lemburg 1995; Giribet and Edgecombe 2017) and constitutes a minor part of the global diversity of ecdysozoans (moulting invertebrates) that encompass millions of extant arthropod species. The diversity of extant scalidophorans is relatively low with less than 300 described species (Schmidt-Rhaesa 2013; Brusca et al. 2016), yet Priapulida, Kinorhyncha and Loricifera all have representatives

in the Cambrian (Conway Morris 1977; Han et al. 2003; Hou et al. 2017; Hu et al. 2013; Zhao 2011; Zhang et al. 2015; Peel 2010, b). Stem-group priapulids represent in fact the most abundant and diverse group of endobenthic worms of Cambrian marine ecosystems (Hou, et al. 2017; Fu et al. 2019; Conway Morris 1977). The evolutionary interest of scalidophorans therefore lies in the rich Cambrian fossil record which documents steps in the early assembly of the ecdysozoan body plan. Scalidophorans share a number of basic anatomical features such as an eversible introvert, a tubular annulated trunk, a relatively spacious blastocoelomic cavity and a well-developed network of longitudinal, circular and retractor muscles (Schmidt-Rhaesa 2013).

Although the body of scalidophorans is typically divided into two major regions—the trunk and the introvert—it is subject to significant morphological variations. For example, some priapulids have a differentiated neck between the trunk and the introvert (e.g. *Tubiluchus corallicola*; van der Land 1970). In other forms such as *Priapulus caudatus*, the trunk extends into a caudal appendage (van der Land 1970). Both loriciferans and kinorhynchs have a mouth cone and a system of plates along their trunk (abdomen). The trunk of adult kinorhynchs shows eleven external subdivisions, most of them bearing a dorsal (tergal) and paired ventral (sternal) plates (Brusca, et al. 2016). In loriciferans, the trunk is surrounded by a stiff cuticular structure (lorica) made up of 6 to 60 plates (Schmidt-Rhaesa 2013). A lorica is also found in the larval stages of priapulids (Wennberg et al. 2009).

Scalidophorans with diverse body plan have been reported from the lowermost Cambrian Kuanchuanpu Formation (ca. 535 Ma; Steiner et al. 2014; Sawaki et al. 2008) such as the phosphatized Small Shelly Fossils (SSFs) *Eokinorhynchus rarus* (Zhang et al. 2015), and *Eopriapulites sphinx* (Liu et al. 2014), and Burgess Shale-type scalidophorans from early to middle Cambrian (e.g. Chengjiang Lagerstätte, Hou, et al. 2017; Sirius Passet Lagerstätte, Conway Morris and Peel 2010; Burgess Shale Lagerstätten, Conway Morris 1977). The large body fossils can be grouped into six types including palaeoscolecids, priapulids, selkirkiids, sicyophoriids, corynetids and tylotitids (Han, et al. 2003; Han et al. 2004b; Han et al. 2004a; Ma et al. 2010; Hou, et al. 2017; Huang et al. 2004a, b). These groups differ from each other by their body subdivision and proportions, introvert shape and ornament, and also by the distribution pattern and morphology of various cuticular outgrowths (spines, sclerites, plates) that occur along the external surface of their trunk.

*Selkirkia* differs markedly from all other Cambrian scalidophoran worms in that they secreted and lived within a conical tube open at both ends (Conway Morris 1977). These tubicolous worms were first described from the Burgess Shale Lagerstätte (*Selkirkia columbia*, Walcott 1911 and Conway Morris 1977) but occur in other Burgess Shale localities (*Selkirkia* sp., Nanglu et al. 2020) and elsewhere on the North American continent (*Selkirkia spencei*, *Selkirkia willoughbyi* from the Spence Shale; Utah, Resser 1939; Conway Morris and Robison 1986). Selkirkiids have also been found in several Chinese Lagerstätten such as those of Chengjiang (*Paraselkirkia jinningensis* Hou et al., 1999 = *Selkirkia sinica* Luo et al. 1999), Xiaoshiba (Lan et al. 2015) and Kaili (Zhao 2011). Another genus of selkirkiids, *Sullulika*, was reported from the Sirius Passet Lagerstätte (Peel and Willman 2018; see Systematic palaeontology).

The nature of the selkirkiid tube has been discussed by several authors (Conway Morris 1977; Huang 2005; Maas et al. 2007) but major uncertainties remain concerning its structure, composition and ecological relation to the animal. Whether the tube was secreted by

epithelial cells or resulted from other processes (e.g. aggregation of external elements) has long been an open question. Equally unresolved is the capacity of selkirkiids to move within their tube and through their environment.

The present study focuses on early Cambrian representatives of selkirkiids from the Chengjiang Lagerstätte and aims to clarify their functional anatomy, tube secretion, lifestyles, and phylogenetic relationships to other scalidophoran groups (e.g. priapulids; Ma, *et al.* 2010; Wills *et al.* 2012; Huang 2005; Ma *et al.* 2014; Maas, *et al.* 2007). Our investigation is based on fossils with “soft body” preservation from the Chengjiang Lagerstätte that allowed new detailed exploration of the external and internal anatomy of selkirkiids, especially their introvert, pharynx, gut, tube and reproductive system (X.-Y Yang, personal communications).

## Material and methods

*Fossil data and observation.* Our fossil specimens (*Selkirkia sinica* and *Selkirkia transita* sp. nov.) come from several localities of the Chengjiang Lagerstätte (Yu’anshan Formation, equivalent of the Cambrian Series 2, Stage 3, ca 518 Ma; Steiner *et al.* 2020; Yang *et al.* 2018). They typically occur in strongly weathered laminated mudstones (Zhu *et al.* 2005). The twenty-two specimens of *S. sinica* studied here are from Yunlongsi (ELI-0002005), Shankou (ELI-0002004), Jianshan (ELI-0002001 to ELI-0002003, ELI-0002006 to ELI-0002009, ELI-0001405 and ELI-0002019 to ELI-0002021) and Erjie (ELI-0002010 to ELI-0002018). The six specimens of *Selkirkia transita* sp. nov. were collected from Erjie (ELI-0000601), Ercaicun (ELI-0000602) and Jianshan (ELI-0000603 to ELI-0000606). Details on the location and lithology of these localities are given in Hou *et al.* (1999) and Luo *et al.* (1999). All specimens are preserved as compressions. Details of their external (e.g. tube) and internal anatomy (e.g. ornamented proboscis, gut, oocytes) are typically highlighted by reddish and brownish iron oxides that sharply contrast with the surrounding beige or yellowish matrix.

Light photographs were taken with a Canon EOS 5DS R (Northwest University, Xi’an) and Canon EOS 5D Mark IV (University of Lyon 1, digital camera). Elemental mapping was performed with a FEI Quanta 250 FEG at CT $\mu$  (University Claude Bernard Lyon 1) and Micro X-ray Fluorescence ( $\mu$ -XRF; Northwest University, Xi’an). All specimens are deposited in the collections of the Shaanxi Key Laboratory of Early Life and Environments (SKLELE), Northwest University, Xi’an, China.

*Phylogenetic analyses.* Our cladistic investigation is based on discrete morphological data modified from Harvey *et al.* (2010) and Zhang *et al.* (2015), which focused on cycloneuralian relationships. *S. willoughbyi* and *S. spencei* were excluded due to a very large amount of uncertain coding (Conway Morris and Robison 1986). While revising this matrix, we realized that a lot of multistate characters lacked a corresponding “primary” or “sovereign” binary character (*sensu* Aria *et al.* 2015). The inclusion of an “absence” state in a multistate character is justified only if there are reasons to think that the presence of the character did not likely have a single origin; otherwise, the lack of a sovereign character represents an obvious loss of phylogenetic signal.

We therefore scrutinized the optimization of relevant character states with Mesquite v.3.61 (Maddison and Maddison 2019), but found that, in most cases, there was no strong homoplastic pattern justifying the omission of sovereign binary characters. The inclusion of such characters added important phylogenetic signal to the matrix, but also resulted in less-

resolved topologies in parsimony: this hints that the original matrix might have been “tailored” to increase the resolution of the strict consensus tree at the cost of a more representative but more conflicting coding of morphology, as was observed also in a panarthropod dataset (Caron and Aria 2017).

Although the goal of parsimony is to minimize transformational steps, homoplastic characters can still locally retain phylogenetic value (Congreve and Lamsdell 2016), which corrections based on secondary homology can remove—this is of course a more fundamental problem when using the same dataset for likelihood-based analyses. Unless true convergence can be demonstrated, instead of parallelism, any dataset thoroughly “optimized” in this way can provide spurious evolutionary reconstructions hidden behind fully-resolved and well-supported topologies.

Parsimony analyses were performed with TNT v.1.5 (Goloboff and Catalano 2016) as well as the R\* (R Team 2020) package TreeSearch v.0.4.3 (Smith 2018), which uses MorphyLib (Brazeau *et al.* 2017) to handle inapplicable data (Brazeau *et al.* 2019), and Bayesian analyses with MrBayes v.3.2.6 (Ronquist *et al.* 2012). *Lepidodermella squamata* (Gastrotricha) was chosen as the outgroup, and characters were unordered. In general, higher nodes are very poorly supported and reaching convergence in any method (except heuristic tree bisection reconnection (TBR)) required a greater-than-usual number of replications / generations for a dataset that size.

For parsimony, heuristic TBR was performed with 1,000 trees saved for 10 replications, because it yielded most parsimonious trees (MPTs) one step fewer than 10 trees saved for 1,000 replications. Tree search with new technology (TNT) used default parameters and 1,000 iterations of parsimony ratchet, 50 cycles of drifting, and 10 rounds of tree fusing. Owing to the lack of proper handling of inapplicable states by TNT or other common parsimony software (heuristic TBR and TNT treating here inapplicable entries as uncertainties), which could arguably be a significant issue in our matrix (inapplicability representing 17.6% of the data), we decided to also use the TreeSearch package in R\*, which makes use of the “scanning” algorithm proposed by Brazeau M. D. *et al.* (2019). Because an informed use of implied weighting was advocated to yield optimal trees when using parsimony as a conceptual basis (Smith 2019), we also computed a consensus of separate implied-weighting analysis from TreeSearch using concavity constants 3, 5 and 10, following the recommendations of Smith (2019). In each case, searches went through 2,000 iterations of ratchet.

Bayesian searches used an Mkv+ $\Gamma$  model (Lewis 2001) with 4 runs each with 4 chains for 10,000,000 generations and burn-in at 20%. In light of parsimony results (see Results), a backbone was also used to enforce a model with basal Loricifera + Kinorhyncha.

We used RogueNaRok (Aberer *et al.* 2013) to search for rogue taxa destabilizing the tree, but we found none having a significant impact.

## Preservation

*S. sinica* and *S. transitia* sp. nov. usually occur as isolated specimens and more rarely in relatively large concentration. Clusters of about four specimens (*S. sinica*) per cm<sup>2</sup> have been found on single bedding planes (e.g. Ercaicun Village; Fig. S1) and usually show directional polarity, suggesting that individuals were re-oriented by currents. The preservation of selkirkiids is identical to that of other associated fossils. Elemental mapping indicates the

presence of Al, Si, K and Mg in the matrix and infilled internal structures (here, intestinal), suggesting the presence of a magnesium aluminosilicate clay minerals. By contrast, fossil structures reveal concentrations of Fe, as a component of either oxidized pyrite or metamorphic clay phases (Figs 1M; 3I, M, O). Traces of C are found on the surface of fossilized tissues (here, gut and oocyte wall; Figs 2E; 6H), as is expected from BST preservation (Gaines *et al.* 2008). Most anatomical features are underlined by iron oxides which represent the weathered form of original pyrite microcrystals (pseudomorphosis; Hu 2005). For example, iron oxides faithfully replicate fine details of the introvert ornament (scalids, teeth) and occur in relatively large abundance over the external surface of the tube and within its wall structure (Figs 2E, F; 4G).

Numerous fossil specimens show extensive eversion of the whole pharyngeal structure (see also Figs 1A; 6A). This extreme state is not seen in living priapulids worms ((Vannier *et al.* 2010; Schmidt-Rhaesa 2013; personal observations) and may result from stress during escape reaction after burial. About 40% to 50% specimens of *S. sinica* and *S. transita* sp. nov. from the Chengjiang Lagerstätte have preserved soft parts. By comparison, *S. columbia* from the Burgess Shale (Canada) is overwhelmingly represented by vacant tubes (Conway Morris 1977).

## Terminology

Proboscis and introvert are very often used interchangeably in the scientific literature to designate the everted part of scalidophoran worms. According to Schmidt-Rhaesa (2013) the body of priapulids, kinorhynch and loriciferans is divided into a trunk region and an introvert defined as the body part which “*can be withdrawn completely into the trunk by the action of retractor muscles*” (Schmidt-Rhaesa 2013, p.147). The pressure exerted by trunk muscles on the fluid contained in the blastocoelomic cavity is responsible for the eversion of the introvert. In its fully everted state, the introvert generally exhibits, from proximal to terminal, a swollen and spiny region covered by scalids (spine-like cuticular structure) followed by the pharynx lined with teeth. In contrast, the term “proboscis” lacks a precise definition and is unspecific to invertebrates (Schmidt-Rhaesa, personal communication). For these reasons, we prefer to use “introvert” instead of “proboscis” in our morphological descriptions. We followed the terminology (Zones I to III) used by Conway Morris (1977) to describe the introvert of *Selkirkia* and added additional subdivisions.

## Systematic palaeontology

Phylum Priapulida Delage and Hérouard, 1897  
Order Selkirkiomorpha Adrianov & Malakhov, 1995  
Family Selkirkiidae Conway Morris, 1977

*Remark-* This family currently accommodates two genera: *Selkirkia* Walcott 1911 and *Sullulika* from the early Cambrian Sirius Passet Lagerstätte (Peel and Wilman 2018). However, *Sullulika* is an ill-defined genus, based on empty annulated tubes comparable with those of Chinese selkirkiids and the supposed presence of convex lappets around the large aperture of the tube (Peel and Wilman 2018; text-fig. 10), that do not occur in *Selkirkia*. The lack of information on its soft anatomy and uncertainties concerning these lappets makes the tentative placement of

*Sullulika* within Selkirkiidae uncertain. For these reasons, we find it premature to propose a diagnosis for this family.

Type genus: *Selkirkia* Walcott, 1911.

Genus included: Possibly, *Sullulika* Peel and Willman 2018.

#### Genus *Selkirkia* Walcott, 1911

*History of research.* *Selkirkia* was first erected by Walcott (1911) but it was not until the 1977 that its anatomy and phylogenetic position were analysed in details based on the extensive revision of a large number of exceptionally preserved specimens of *S. columbia* from the Burgess Shale (Conway Morris 1977). Two decades later, similar fossils were found in the Chengjiang Lagerstätte. Luo and colleagues assigned them to *Selkirkia sinica* (Luo, *et al.* 1999) and Hou and colleagues to *Paraselkirkia jinningensis* the same year (Hou *et al.* 1999). These tubicolous worms were later discovered in the Xiaoshiba Lagerstätte (Hongjingshao Formation, equivalent of Cambrian Series 2, Stage 3) and assigned to *Selkirkia sinica* (Lan, *et al.* 2015). *Paraselkirkia* was erected based on differences with *Selkirkia columbia* from the Burgess Shale (Table 1), such as the relatively smaller size and more complex introvert structure of *P. jinningensis* (Hou, *et al.* 1999). However, the present systematic revision reveals no major morphological differences between *Selkirkia columbia* and the Chengjiang selkirkiids that would justify maintaining two genera. To us, *Paraselkirkia* is a younger synonym of *Selkirkia* (Chen *et al.* 2002; Chen 2004) and *S. sinica* and *Selkirkia transita* sp. nov. both belong to *Selkirkia*.

Type species: *Selkirkia columbia* Conway Morris 1977.

Species included: *S. spencei* and *S. willoughbyi* Conway Morris and Robison, 1986, *S. sinica* Luo *et al.* 1999 and Hou *et al.* 1999, *S. transita* sp. nov.

*Diagnosis* (emended from Conway Morris, 1977). Selkirkiid worm (body length between 3 mm and 75 mm). Body divided into a spinose introvert and a trunk entirely covered with a tube. Conical introvert with three distinct zones (I to III from proximal to distal). Zone I with two ornamented subzones (Ia and Ic) separated by a smooth ring-like area (Subzone Ib). Fully everted specimens showing more or less developed, smooth area (Zone II) followed by elongated pharynx (Zone III) bearing multispinose or spinose teeth. Finely-annulated tube with low-angle conical shape, and openings at both ends.

#### *Selkirkia sinica* Lou *et al.*, 1999

Figures 1-4, S1, S2

1999 *Selkirkia sinica*, Luo *et al.*, p. 81-82, Pl. 20, Figs 4-6; Text-Fig. 30.

1999 *Paraselkirkia jinningensis*, Hou *et al.*, p. 63-64, Figs 73-76.

2002 *Selkirkia sinica*, Chen *et al.*, p. 195, Plate 18, Figs 4-5.

2004 *Paraselkirkia jinningensis*, Hou *et al.*, p. 71, Figs 12.4-12.5.  
2004 *Paraselkirkia sinica*, in Chen 2004., p. 180-181, Figs 271-272.  
2015 *Selkirkia sinica*, Lan *et al.*, p. 125-132, Figs 1-5.  
2017 *Paraselkirkia sinica*, in Hou *et al.* 2017, p.120-121, Fig. 17.5

*Stratigraphy and locality.* Yu'an-shan Formation (equivalent of Cambrian Series 2 Stage 3), *Eoredlichia-Wudingaspis* zone, Chengjiang Lagerstätte, Yunnan Province, China; Hongjingshao Formation, *Yunnanocephalus–Chengjiangaspis–Hongshiyanaspis* zone, Xiaoshiba Lagerstätte, Yunnan Province, China.

*Diagnosis* (emended from Luo *et al.*, 1999 and Hou *et al.*, 1999). *Selkirkia* with a relatively small size (< 20 mm long in average). Subzone Ia with spines arranged in irregular quincunxes. Subzone Ib well-developed. Subzone Ic with spines arranged in dense and regular quincunxes. Pharynx bearing numerous tiny, evenly spaced spinose teeth. Trunk possibly extending into two lobe-like caudal appendages. Oocytes concentrated within posterior half of body cavity on either side of gut. Tube bearing evenly spaced annulations (8 to 14 per millimetre).



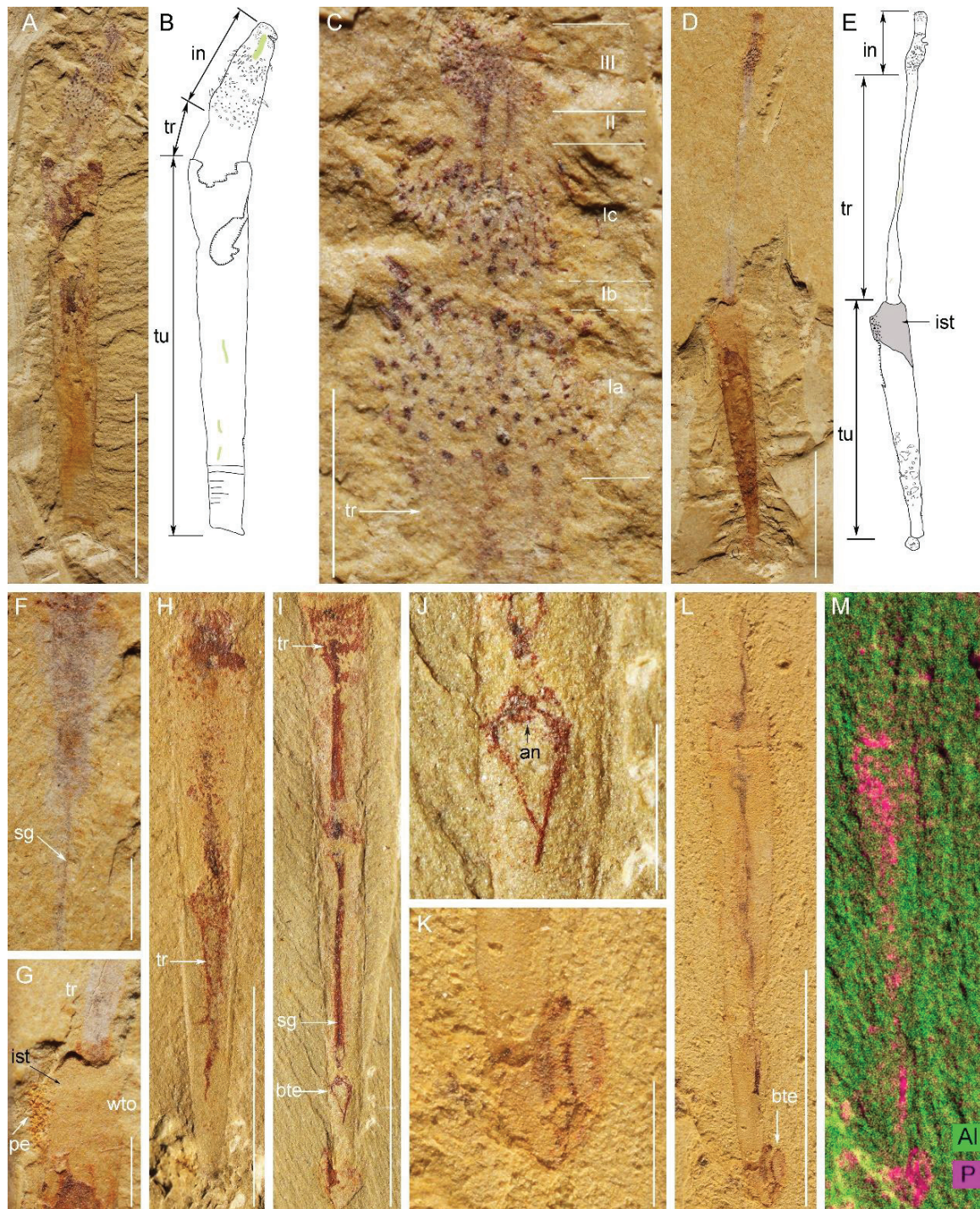


**FIGURE 1.** *Selkirkia sinica* from the early Cambrian Chengjiang Lagerstätte: morphology of introvert and trunk. A-C, ELI-0002001, showing fully everted introvert, general view with line drawing and details of introvert structure and ornament. D-G, ELI-0002002, showing the body almost entirely extracted from the tube, general view with line drawing and details of trunk (e.g. remains of gut tract). H, ELI-0002003, showing shrunk remains of trunk and a tapering trunk end. I, J, ELI-0002004, showing strongly shrunk trunk and bifurcating trunk ends and close up of corresponding structures. L, K, M, ELI-0002005, showing possible bifurcating structures at the posterior end of the trunk, general view, close-up and XRF image (note that bifurcating structures and trunk both have comparable elemental distribution). Abbreviations: an, anus; bte, possible bifurcated trunk ends; in, introvert; ist, inner surface of tube; pe, possible excrements; sg, straight gut; tr, trunk; tu, tube; wto, wide tube opening. Scale bars represent: 5 mm (A, D, H, I, L), 1 mm (C, F, G, J, K).

## Description

### Introvert

Fully everted introverts show three distinct spinose (Ia, Ib and III) and two smooth areas (Ib and II) (Figs 1A, B; 2A, D). The length of the best-preserved fully everted introvert is about 25% of total body length. Zone I is subdivided into three subzones termed Ia, Ib, Ic from proximal to distal. The boundary between the Zone I and Zone III (pharynx) is marked by a smooth, slightly constricted area (Zone II).

**Subzone Ia** (Fig. 1A-C). Its diameter is equal or slightly smaller than that of the anterior opening of the tube from which it protrudes. Its numerous, stout spines are distributed in discrete quincunx, directed backwards and decrease in size posteriorly. They form six circles, each of them lined with about 25 spines.

**Subzone Ib** (Fig. 1A-C). This obviously smooth area marks the boundary between Subzone Ia and Subzone Ic. Its length is one-third to one-fourth that of Subzone Ia.

**Subzone Ic** (Figs 1A-C; 2A, D; 3A). Characterized by relatively closely spaced, slender and long spines (N=ca 250) arranged in quincunx and directed backwards.

**Zone II** (Fig. 1A-C): This smooth area lies between Zone I and Zone III.

**Zone III** (Figs 1A-C; 2A, D; 3A). This ornamented zone represents the pharynx. Its morphology and length vary depending on the degree of eversion. In fully everted specimens, the pharynx appears as a slender conical structure bearing a large number (N> 200) of tiny teeth, all of virtually the same size (Fig. S3B, C, F). They arrange quincunxially as seen in the best-preserved specimens (Figs 3A; S3B). Their morphology is simple compared with that of the multi-cuspidate teeth seen in *S. columbia* (Conway Morris 1977; Smith, *et al.*, 2015; Fig. S3I, J). Some of our specimens show a bulbous structure at the distal end of the pharynx (Figs 1A-C; 2A, D).

### Trunk

A single specimen shows the body of the animal almost completely pulled out from its tube (Fig. 1D, E). The body is almost as long as the tube. Although faint traces of the gut are discernible, the external boundary of the trunk remains relatively featureless with no details of annulation and cuticular ornament. It does not seem to have suffered from severe decay as indicated by its consistent cylindrical shape and a relatively well-preserved introvert.

In other specimens, the distal part of the trunk slightly protrudes outside the large opening of the tube allowing the trunk cuticle to be observed (Fig. 3D). It is represented by a 20-30  $\mu\text{m}$  thick reddish layer (Figs 3D; 4A-G) approximately three times thinner than the tube wall (ca 100  $\mu\text{m}$ ; measured in empty tubes). Small, irregularly spaced protuberances are present around the protruding trunk (Figs 1A; 2A; 3D; 4H-K) and recall the papillae seen in the middle part of the trunk of *S. columbia* (Conway Morris 1977). However, they do not distribute in rows and may not have a biological origin.

Some specimens show a tiny gap between the tube and the external surface of the trunk (Fig. 4 B, D, I, J), which suggests that the body was free from the tube and could possibly move within it (see discussion part). In the vast majority of individuals, the trunk is some distance

away from the internal surface of the tube (e.g. posteriorly) although in contact with it locally (Fig. 1H, I). The exact morphology of the trunk end is unclear but may have borne a pair of relatively short caudal appendages that can be seen protruding outside the small opening of the tube (Fig. 1K, L) or in a more retracted position (Fig. 1I, J).



**FIGURE 2.** *Selkirkia sinica* from the early Cambrian Chengjiang Lagerstätte: gut tract and gut contents. A, ELI-0001405, showing fully everted introvert and basal part of trunk protruding beyond the tube opening. B, ELI-0002006, showing sinuous gut inside introvert. C, ELI-0002007, showing thin and straight gut tract and, posteriorly, two ovoid elements interpreted as possible unusually large pellets or undigested shells. D, ELI-0002008, showing fully everted introvert and 3D-preserved aligned pellet-like elements in gut. E, F, ELI-0002009, showing more randomly distributed pellet-like elements in gut (compared with D), elemental maps (see location in E). Abbreviations: gc, gut contents; sg, straight gut; sig, sinuous gut; tr, trunk; ue, undigested element (possibly shell). Scale bars represent: 5 mm (A, D, E), 2 mm (B, C), 200  $\mu$ m (F).

## Gut

The gut generally appears as a dark strip running from the everted pharynx to the trunk end. The anus seems to open close to the posterior opening of the tube (Figs 1; 2) and within the axial plane of the animal. The gut has an axial position and a straight outline although loops can be seen in some specimens (Fig. 2A, B). It is often filled with pellet-like elements aligned in rows or more irregularly distributed (Fig. 2D, E). These gut contents have a consistent ovoid shape (0.5-0.6 mm and 0.15-0.20 mm in length and width, respectively) and present a slight relief. Their relatively large number and local concentration suggest that the gut wall had the capacity to expand in order to accommodate food or undigested residues (Lan, *et al.* 2015; Peel 2016). SEM observations revealed no internal elements that may help characterize the worm diet. Two ovoid features of equal size occur near the posterior end of one specimen (Fig. 2C) and seem to be aligned within the gut tract. However, their size (1.5 mm long, 0.9 mm wide) is larger than that of the pellet-like elements usually found in a more anterior location within the gut. Their width is almost three times the gut diameter (0.5 mm in width). They may represent undigested shells (e.g. brachiopod), or unusually large pellets transiting through the digestive tract (Fig. 2E). Possible feces seen in a few specimens consist of shapeless coloured clusters of minerals such as mica and quartz grains (Figs 3P, Q; S2).

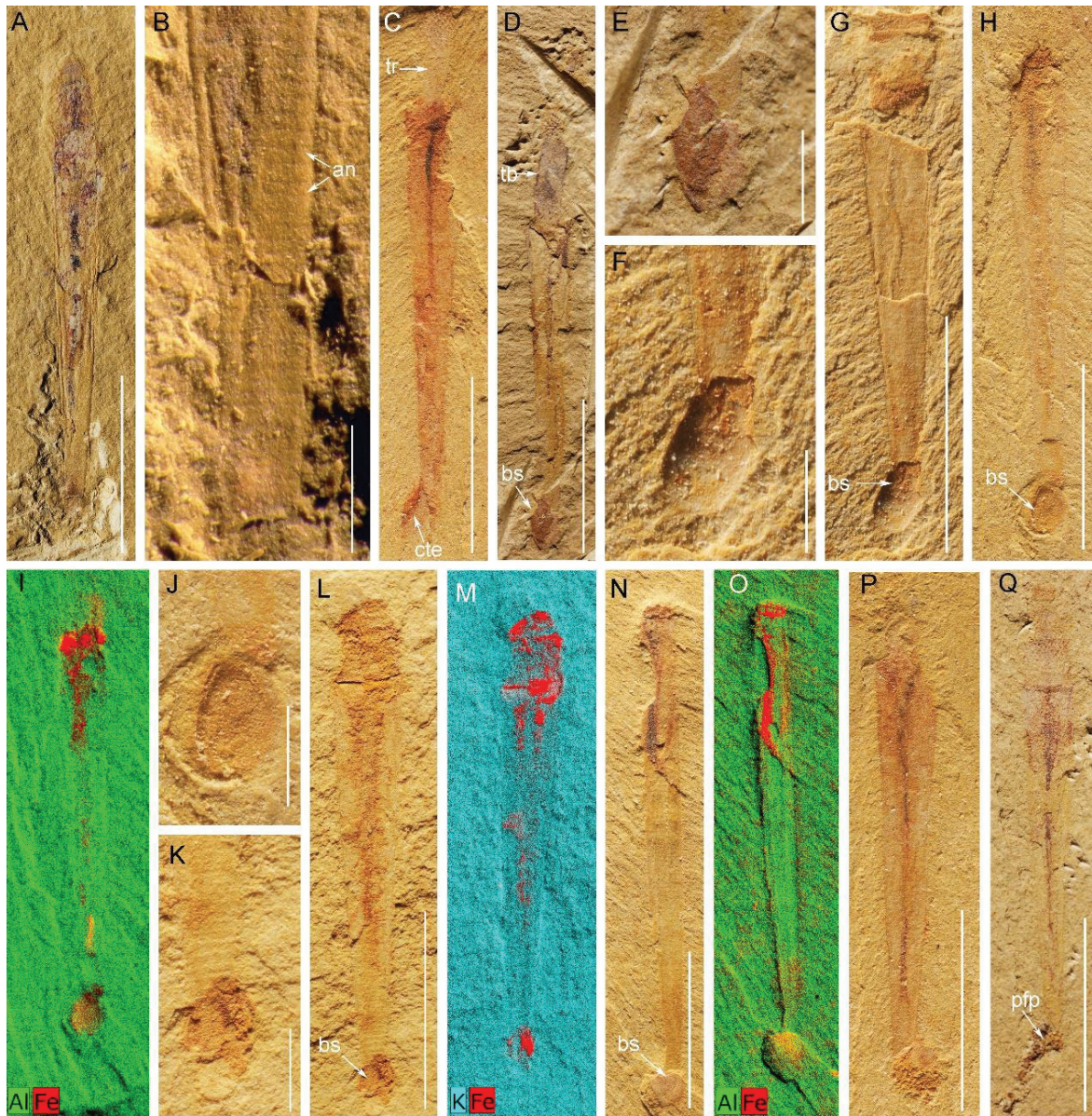


**FIGURE 3.** *Selkirkia sinica* from the early Cambrian Chengjiang Lagerstätte: annulations of tube, brachiopod epibionts and possible faecal pellets. A-B, ELI-0002010, showing annulations (tiny furrows) along the internal surface of the tube, general view and details. C, ELI-0002011, showing damaged posterior part of tube. D-E, ELI-0002012, showing protruding part of trunk and brachiopod shell near tube end. G, F, ELI-0002013, showing brachiopod attached near the posterior end of tube. H-J, ELI-0002014, showing brachiopod attached near the posterior end of tube. K-M, ELI-0002015, showing brachiopod attached to the tube and tube annulations. N, O, ELI-0002016, showing brachiopod fragment near the posterior end of tube. P, ELI-0002017 and Q, ELI-0002018, showing possible faecal pellets released from the posterior opening of the tube (e.g. undigested coarse sediment particles). I, M, O are XRF images to show elemental differences between tube and brachiopod. Abbreviations: an, annulations, bs, brachiopod shell; cte, cracked tube end; pfp, possible faecal pellets; tb, trunk boundary; tr, trunk; ttu, tapered tube end. Scale bars represent: 5 mm (A, C, D, G, H, L, N, P, Q), 1 mm (B, E, F, J, K).

### Tube

The tube forms a conical structure with a very low opening angle (ca 20°) and opens at both ends. Its length ranges from 6 to 13 mm long (N= 106) with the proximal opening being

approximately 2 mm wide. The external surface of the tube is regularly annulated with 8 to 14 tiny transverse ridges per millimetre (Fig. 3B) that faithfully correspond to comparable small furrows along the internal surface. The tube wall (ca 100 µm; Fig. 4B, D, G) is preserved in iron oxide (Fig. 4G) and does not show any ultrastructural details (e.g. cuticle layers). The posterior opening of the tube is relatively narrow and often broken (irregular margins) due to possible interactions with sediment or transportation (Figs 2A; 3C, P).

Brachiopods attached to the tube of *Selkirkia sinica* have been recently described from the Xiaoshiba Lagerstätte (Yang X.-Y, personal communications). Tiny ovoid features (size between 1 to 1.5 mm; Fig. 3D-O) found in our specimens from Chengjiang and seemingly attached near the posterior end of the tube are most probably similar brachiopod epibionts, although no growth lines are visible on their external surface.

*Remarks.* Our specimens do not show noticeable differences with the type specimens of *S. sinica* figured by Luo et al. (1999; Plate 20, figures 4-6) and Hou et al. (1999; Figs 73-76) and those more recently described from the Xiaoshiba Lagerstätte (Lan, *et al.* 2015); text-figure 1; Yang et al; in review). All display the same type of everted spinose introvert divided into two parts and elongated pharynx bearing teeth. Detailed observations of the arrangement, density and morphology of cuticular elements (scalids, pharyngeal teeth) did not reveal small-scale differences either (Table 1).

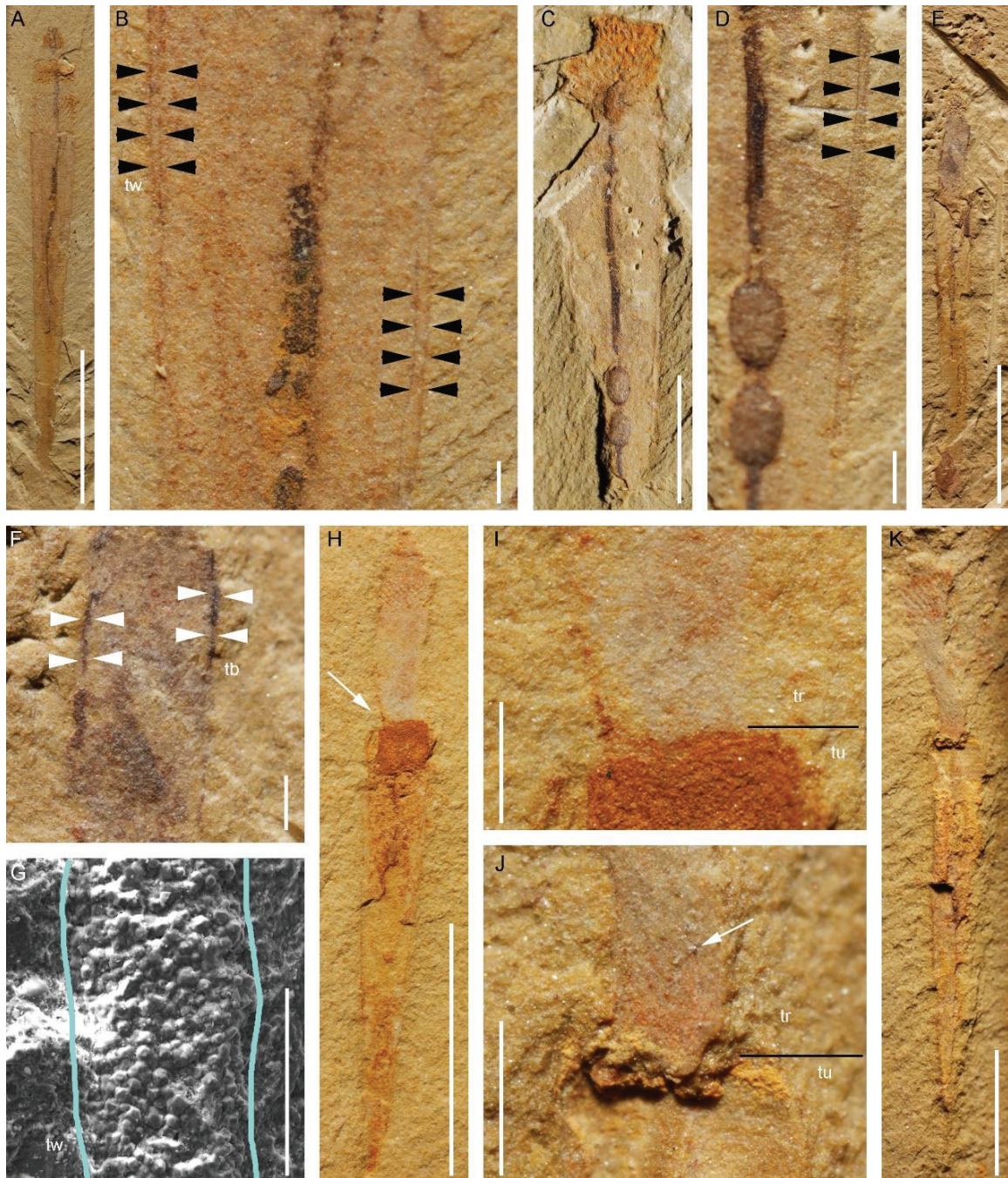


**FIGURE 4.** *Selkirkia sinica* from the early Cambrian Chengjiang Lagerstätte: relation between trunk and tube. A,B, ELI-0002019, showing tube wall (external and internal boundaries outlined by very thin coloured layers; see black arrows), general view and close-up. C,D, ELI-0002007, showing tube wall (as in A), general view and close-up. E-G, ELI-0002012, showing anterior part of trunk protruding outside the tube; trunk cuticle appears as a thin dark layer (white arrows), SEM image showing tube wall preserved in iron oxides. H-I, ELI-0002020, showing protruding trunk and distinct gap between trunk and tube (white arrow). K-J, ELI-0002021, showing protruding trunk with mineral grains (white arrow) and distinct gap between trunk and tube (black line). Abbreviations: tb, trunk boundary; tw, tube wall. Scale bars represent: 5 mm (A, E, H), 2 mm (C, K), 1 mm (D, I), 500  $\mu$ m (J), 400  $\mu$ m (F), 200  $\mu$ m (B), 100  $\mu$ m (G).

*Selkirkia transitia* sp. nov.

Figures 5-6

*Etymology.* From *transita* (Latin), alluding to resemblances with both *S. sinica* and *S. columbia*.

*Holotype:* ELI-0000601 (Fig. 5A)

*Paratype:* ELI-0000602, ELI-0000603 (Fig. 5F, I)

*Stratigraphy and locality.* Yu'anshan Formation (equivalent of Cambrian Series 2 Stage 3), *Eoredlichia-Wudingaspis* zone, Chengjiang Lagerstätte, Yunnan Province, China.

*Diagnosis.* *Selkirkia* with a relatively large size (> 20 mm in average). Subzone Ia with spines arranged in discrete quincunxes. Subzone Ib very narrow to virtually invisible. Subzone Ic with spines in dense and regular quincunxes. Pharynx bearing hundreds of multispinose teeth arranged quincunxially, pointing forwards and decreasing in size distally. Oocytes in the posterior half of body cavity and possibly arranged in two longitudinal rows. Tube bearing evenly spaced external annulations (5 to 9 per millimetre).

### *Description*

#### **Introvert**

**Subzone Ia** (Fig. 5A-C, G). It is the widest part of introvert. Spines distribute in discrete quincunxes with 6 circlets of about 25 spines arranged longitudinally. The distance between adjacent spines in diagonal is about 0.15 mm. Spines increase in size from proximal to distal part. The shortest and longest spines are 0.12 mm and 0.27 mm long (basis 0.10 mm and 0.12 mm), respectively.

**Subzone Ib** (Fig. 5B, D, G). Relatively narrow (ca 0.2 mm in longitudinal length), smooth and marks the boundary between Subzone Ia and Subzone Ic.

**Subzone Ic** (Fig. 5B, D, G). Slightly narrower than Subzone Ia and varies in length from 1.0 mm to 2.3 mm. Subzone Ic bears closely packed spines arranged in quincunx. Spines increase in size gradually from proximal to distal (the shortest and longest ones are 0.10 mm and 0.34 mm, respectively) and all point backwards. The basal width of spines is about 0.07 mm. Distal spines are three times longer than proximal ones.

**Zone II** (Fig. 5B, E, G). In specimens with a fully everted introvert, its length is 25% that of Subzone Ic and its diameter decreases distally.

**Zone III** (Fig. 5A, B, E-G, I). Corresponds to the pharynx and has a tapering shape especially well-marked in its terminal region. Bears numerous teeth arranged quincunxially and regularly decreasing in size distally. The most proximal ones (basal width between 0.05 and 0.11 mm) are clearly multispinose with one long central tip flanked with two smaller ones (Figs 8; S3E, G). The remaining spines appear as densely coloured dots of ca 0.02 mm in diameter with no visible details and point forwards.

#### **Trunk**

In one specimen, the broken part of the tube reveals details of the relation between trunk



and tube (Fig. 5F-H) with a gap between the cuticle and the internal surface of the tube (Fig. 5F-H). Paired retractor muscles (Fig. 5H) seem to be attached to the middle part of trunk.

## Tube

The conical tube of *Selkirkia transita* sp. nov. is 9 to 38 mm long and opens at both ends (Figs 5A, E, G, H; 6). As in *Selkirkia sinica*, it bears tiny low-elevated transverse ridges along its external surface that correspond to furrows along its internal wall (Figs 5H; 6A-C). Most ridges are regularly spaced (commonly 5 per mm) although local variations (from 5 to 9 per mm) may occur. Some ridges seem to fuse or bifurcate (Fig. 6E). Although often broken and damaged the posterior end of the tube seems to have a sharp ovoid opening with no additional cuticular features.

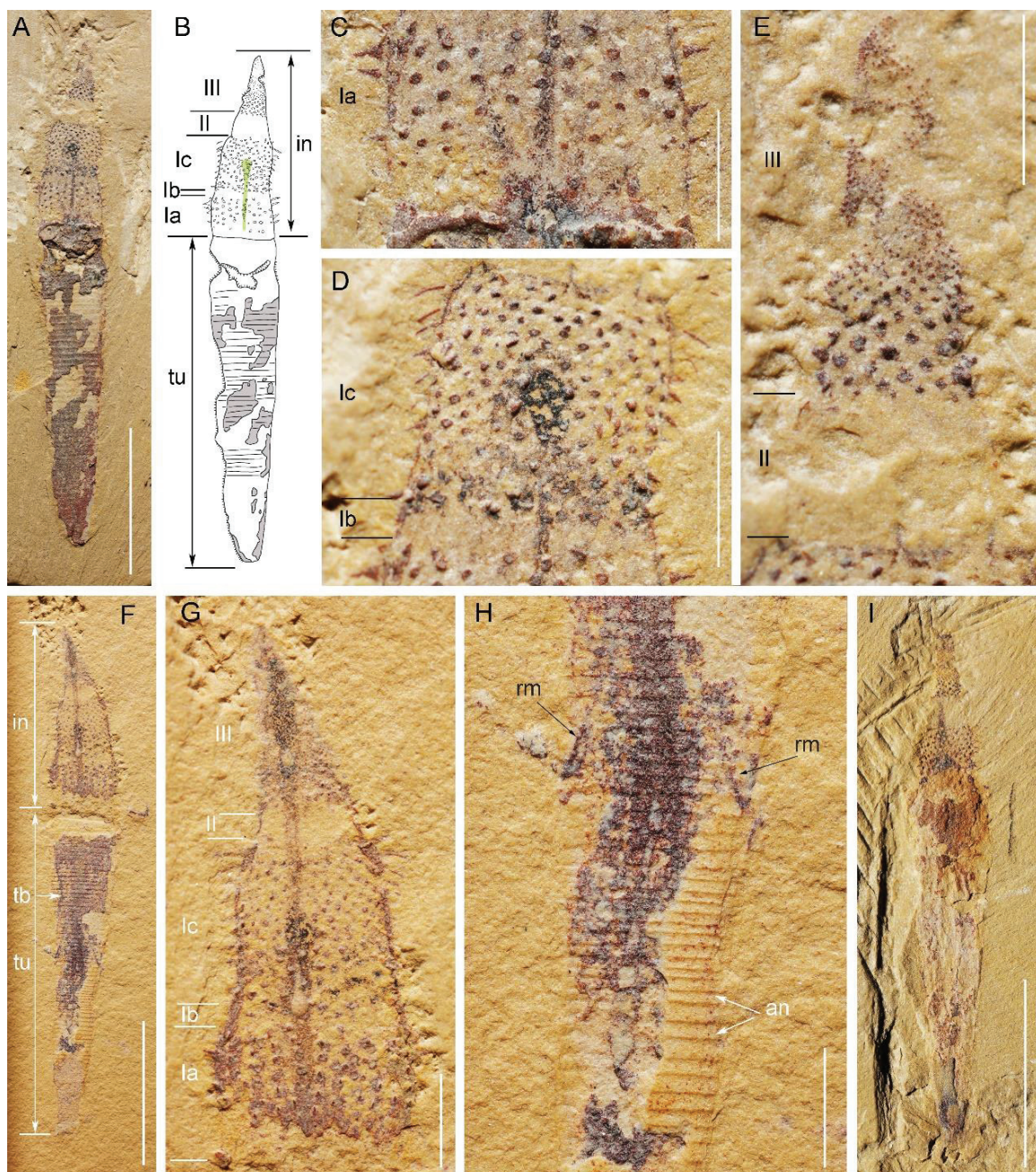


**FIGURE 5.** *Selkirkia transitia* sp. nov. from the early Cambrian Chengjiang Lagerstätte: general morphology. A-E, ELI-0000601, holotype, general view with line drawing and close-ups showing details of introvert structure. F-H, ELI-0000602, paratype, showing introvert, possible oblique retractor muscles and annulations along tube. I, ELI-0000603, paratype, showing part of introvert. Abbreviations: an, annulations; in, introvert; rm, possible retractor muscles; tb, trunk boundary; tu, tube. Scale bars represent: 5 mm (A, F, I), 1 mm (C-E, G, H).

## Gut

As seen in *S. sinica*, it appears as a narrow tube running from the tip of introvert to the anus and often contains pellets (Figs 4G; 5F).

## Reproductive system

Clusters of spherical elements (less than 30; diameter between 300 and 450  $\mu\text{m}$ ) found in the posterior part of the body cavity of *Selkirkia sinica* from the Xiaoshiba Lagerstätte have been recently interpreted as oocytes based on comparisons with extant priapulid worms (Yang X.-Y, personal communications). Similar features occur in a few specimens of *Selkirkia transitia* sp. nov. (Nmax= 14, diameter between 270 and 480  $\mu\text{m}$ ) and are highlighted by reddish iron oxides and small black patches (Fig. 6F-H). They form either a single cluster close to the inner wall of the body or irregular paired longitudinal rows on either side of the gut (Fig. 6G).

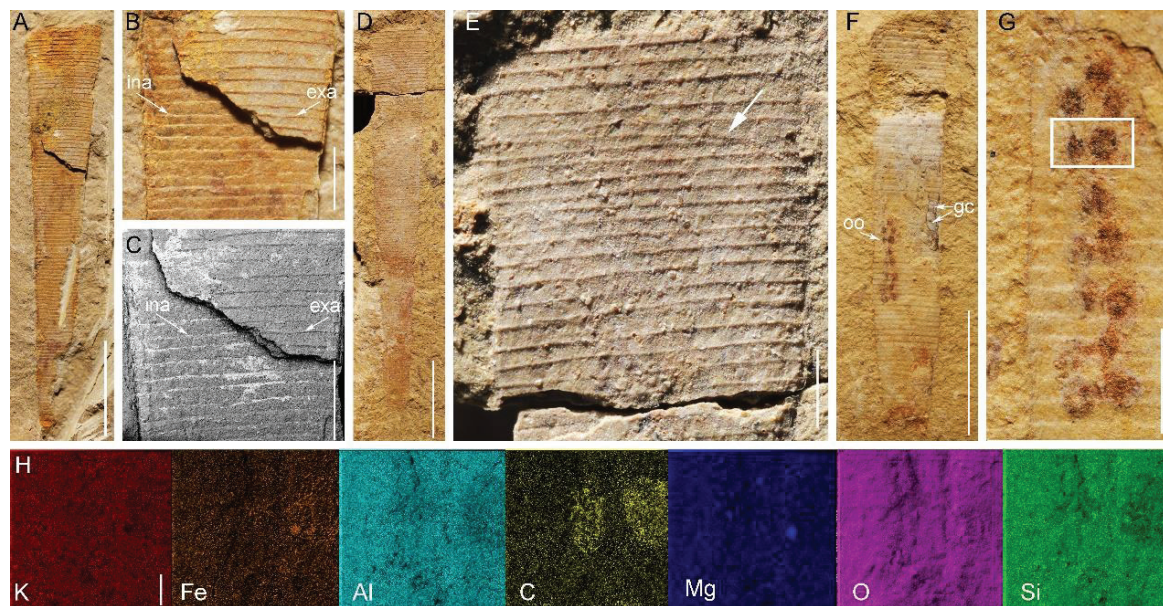


**FIGURE 6.** *Selkirkia transitia* sp. nov. from the early Cambrian Chengjiang Lagerstätte: tube and eggs. A-C, ELI-0000604, broken tube showing annulations along its external (ridges) and internal surface (furrows). D,E, ELI-0000605, showing annulations (tiny ridges) along the external surface of the tube; general view and close-up (note: irregularities in annulated pattern by white arrow). F-H, ELI-0000606, showing egg clusters (possibly oocytes, Yang X.-Y, personal communications) inside the tube; note marked differences with pellet-like gut contents; elemental maps of two eggs (see location in (G)); note enrichment in carbon). Abbreviations: exa, external annulation (ridges); gc, gut contents; ina, internal annulation (furrows); oo, possible oocytes. Scale bars represent: 5 mm (A, D, F), 1 mm (B, C, E, G), 100  $\mu\text{m}$  (H).

*Remarks.* *S. transitia* sp. nov. has an introvert and a stiff tube, that closely resemble those of *Selkirkia columbia* (Conway Morris 1977) but shows differences with other *Selkirkia* formerly described in the literature. In general, the size of *S. transitia* sp. nov. is larger than that of *S. sinica* but smaller than that of *S. columbia* (Conway Morris 1977; Luo, *et al.* 1999; Hou, *et al.* 1999). Subzone Ib of the introvert is poorly developed in *S. transitia* sp. nov., absent in *S. columbia* and instead well-marked in *S. sinica*. The most anterior spines of Subzone Ic point either outwards or backwards in *S. transitia* sp. nov. and *S. sinica*, but always forwards in *S. columbia*. Concerning the pharyngeal region, only one type of multispinose teeth part is present in *S. transitia* sp. nov., whereas two types occur in *S. columbia* (Smith *et al.* 2015). In contrast, *S. sinica* seems only to bear simple teeth. The tube bears about 40 annulations per mm in *S. columbia*, 8 to 14 in *S. sinica* and only 5 to 9 in *S. transitia* sp. nov. Altogether, *S. transitia* sp. nov. differs from *S. columbia* and *S. sinica* in several morphological characters, which justifies the erection of a new species (Table 1).

	<i>Selkirkia sinica</i>	<i>Selkirkia transitia</i> sp. nov.	<i>Selkirkia columbia</i>
Body size (mm)	8-19	15-40	20-50
Introvert subdivision	3 spinose and 2 smooth zones	3 spinose and 2 smooth zones	3 spinose and 1 smooth zones
Number of transverse circlets in Subzone Ia	5-6	5	12-13
Subzone Ib	well-defined	slightly visible	virtually absent
Direction of distal spines in Subzone Ic	backwards and outwards	backwards	forwards
Shape of Zone III	bulbous	blunt tip	tapering
Spines of Zone III	simple	one kind of multispinose teeth	two kinds of multispinose teeth
Trunk ornament	none	uncertain	twenty-six longitudinal rows papillae
Density of tube annulations	8-14/mm	5-9/mm	40/mm

Table 1. Comparisons between *S. sinica*, *S. transitia* sp. nov. and *S. columbia* using nine key characters.

## Phylogeny

Expectedly, our phylogenetic results differ considerably from those that were published before with the same original dataset (Zhang, *et al.* 2015; Liu, *et al.* 2014), owing to our extensive recoding and implementations of primary / sovereign characters (see Methods).

Heuristic TBR and TNT resolve similar topologies with extant priapulids forming a sister clade to *Selkirkia* and palaeoscolecids, and with Loricifera and Kinorhyncha branching off basally (Fig. S4A, B). By contrast, the unconstrained Bayesian runs converge on a basal *Selkirkia* sister group to Palaeoscolecida and Scalidophora (Fig. S5). In the unweighted TreeSearch analysis (Fig. S4C), Loricifera and Kinorhyncha are also resolved basally, but fossil groups all form a long stem to extant Priapulida, with *Selkirkia* and *Eximipriapulul* being their closest sister groups. When using implied weighting, consensus trees for individual concavity constants are well resolved, but they significantly differ from one another, leading to a polytomy if one combines these results (Fig. S4D). These topological discrepancies between concavity constants have been noted before (e.g. Aria, *et al.* 2015; Congreve and Lamsdell 2016), and, in practice, this means

that implied weighting is a method that may indeed be too inconsistent despite good performances with simulated data (Smith 2019). However, higher nodes in our topologies, regardless of the method, are poorly supported, and therefore, in our case, the loss of precision in the implied weighting consensus may also represent greater accuracy.

A basal position of Loricifera and Kinorhyncha with a large total-group Priapulida being consistently recovered in parsimony, we decided to test the strength of this model by enforcing a backbone on the Bayesian analysis. The resulting topology (Fig. 7) bears overall similarity with the unweighted TreeSearch topology and yields on average slightly better harmonic means than the unconstrained model (1,308.35 vs. 1,307.96, averaged over 8 runs). A better treatment of inapplicable states therefore helped parsimony converge with Bayesian likelihood, assuming a model with basal Loricifera and Kinorhyncha.

We therefore present the constrained Bayesian tree as the representative of the best evolutionary model for our data. In this scenario, most fossils are part of a populous stem within total-group Priapulida, with *Selkirkia* being closer to the crown than palaeoscolecids (Fig. 7). The crown of Priapulida includes the Carboniferous *Priapulites konecniorum*, and its immediate sister clade is composed of the early Cambrian *Paratubiluchus*, *Xiaoheiqingella* and *Yunnanpriapulidus*, with *Sicyophorus* branching off basally to this group. Two typical SSFs—*Eokinorhynchus* and *Eopriapulites*—are found here to constitute intermediate forms between *Sicyophorus* and *Selkirkia*. The Chengjiang fossil *Laojieella* is consistently retrieved as an early member of the *Selkirkia* clade, and Bayesian searches find that *Markuelia* is also a basal part of this clade.

Considering the weak support of higher nodes, the alternative topology retrieving *Selkirkia* outside of Scalidophora (Fig. S5) should not be too hastily discarded. It is more consistent with the findings of Ma *et al.* (2014) in the placement of *Eximipriapulidus*, but also implies that *Selkirkia*, palaeoscolecids and most fossil forms considered are instead part of the scalidophoran stem, although palaeoscolecids and other non-selkirkiid fossils also form a distinct clade. This scenario implies that the palaeoscolecids *sensu lato* and crown scalidophorans constituted two separate radiative lineages (Fig. S5), based on the morphology of the common ancestor shared with *Selkirkia*; this contrasts with the topology described above according to which the Cambrian fossil radiation was mostly linked to the build-up of the priapulid body plan.

### Palaeogeographical distribution

*Selkirkia* is represented by the following five species *Selkirkia columbia* from British Columbia, Canada (Conway Morris 1977), *Selkirkia spencei* and *Selkirkia willoughbyi* from Utah (Conway Morris and Robison 1986), *Selkirkia sinica* (Luo, *et al.* 1999; Hou, *et al.* 1999) and *Selkirkia transita* sp. nov. both from south China, and three undetermined species (*Selkirkia* sp.) from Spence Shale, Utah (Conway Morris and Robison 1986) and the Burgess Shale, British Columbia, Canada (Nanglu, *et al.* 2020; Smith, *et al.* 2015). Current paleogeographic reconstructions for the Cambrian (Torsvik and Cocks 2013, text-figures 2.7, 2.8, 2.9) place the South China plate separated from Laurentia by thousands of kilometres during the early to middle Cambrian interval (over 10 Ma). The presence of *Selkirkia* on two distant plates would imply faunal migration. Considering that *Selkirkia* had limited capacities for moving over long distances, egg or larval dispersion by currents seems to best explain their palaeogeographic

distribution. In modern endobenthic priapulids fertilization is external and followed by the development of hatching and loricate larvae that can be easily transported by currents. For example, *Priapulus caudatus* is found on either side of the Atlantic Ocean (Sweden, Wennberg, *et al.* 2009; USA, Trott 2017), the Pacific Ocean (Alaska; Shirley 1990), the White Sea in Russia (van der Land 1970) and Antarctic (Chile, van der Land 1970).

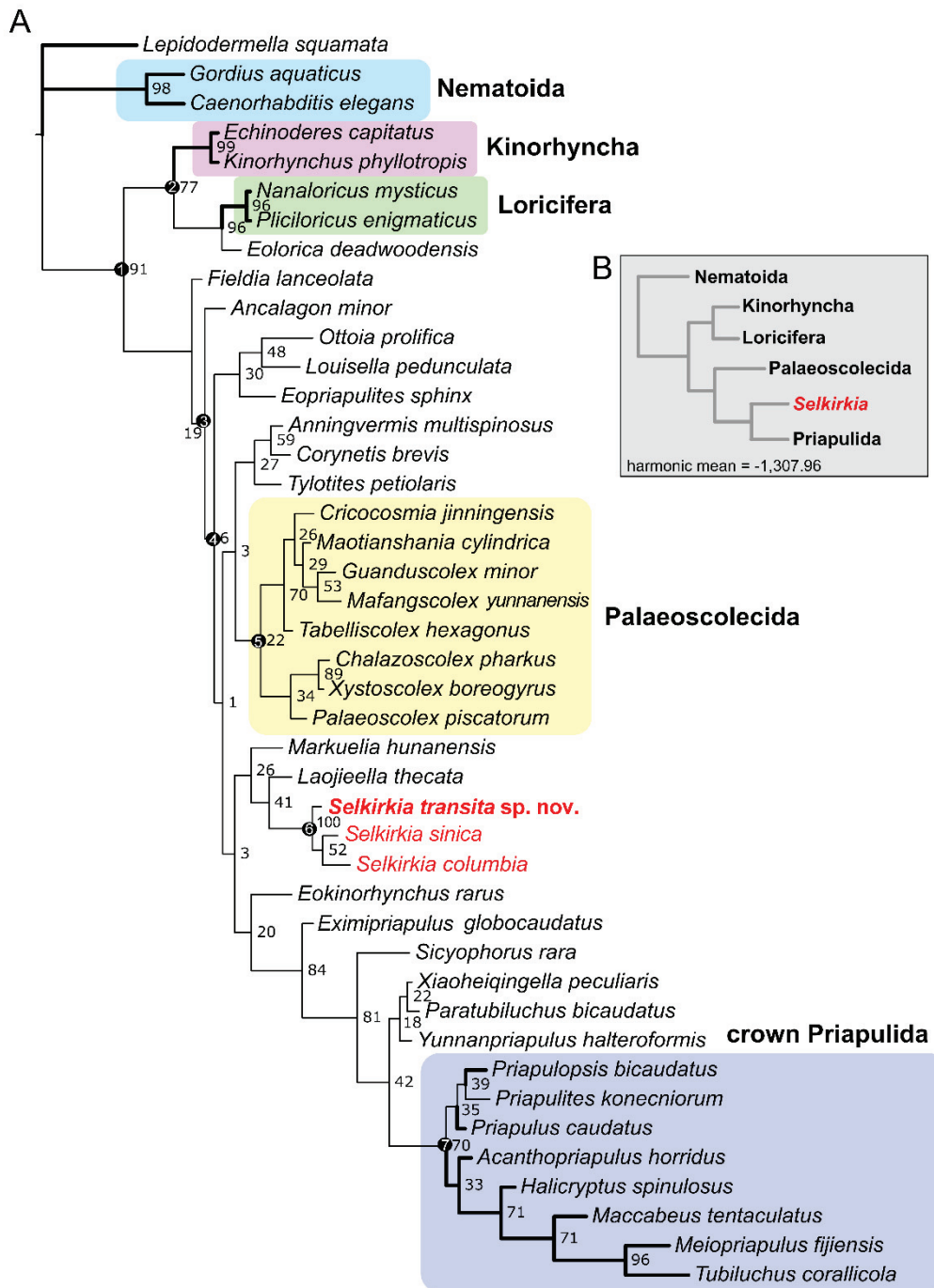


**FIGURE 7** Maximum clade compatibility tree from a Bayesian analysis using an Mk<sub>v</sub>+Γ model and a backbone enforcing basal Kinorhyncha and Loricifera. A. Full tree. Bold branches are extant species. Numbers next to node are posterior probabilities. Circled numbers at nodes are key apomorphic characters: 1, eversible introvert in adult. 2, mouth cone and oral stylets. 3, trunk annulations in adult. 4, circlets of pharyngeal teeth. 5, trunk plates with nodes, several rows plates in each annulation, posterior setae. 6, twenty-five longitudinal rows scalds arranged quincunxially (Fig. S6), cuticular and annulated tube and multi-subdivisions introvert. 7, unpaired

ventral nerve cord, pharyngeal nervous system. B. Simplified topology showing the position of *Selkirkia* and harmonic mean (-1,307.96).

## Discussion

### The introvert of *Selkirkia* and other Cambrian scalidophorans

The introvert of most Cambrian scalidophoran worms is subdivided into three distinct zones (I, II, III; see Conway Morris 1977) and a comparable subdivision is present in extant priapulids such as *Priapulidus*, *Halicryptus* and several meiobenthic representatives of the group (Schmidt-Rhaesa 2013). Based on recent fossil data and comparative studies with extant worms, we attempt here to homologize important features of the introvert (Fig. 8).

Zone I is recognized in *Ottoia*, *Cricocosmia*, *Louisella*, *Paratubiluchus* (Hou, et al. 2017; Conway Morris 1977; Han, et al. 2004a). It is characterized by various types of cuticular ornament such as hooks, spines and papillae and has direct equivalent in *Priapulidus* and *Halicryptus* (Conway Morris 1977); Figs 8).

Zone III is characterized by a distinct type of ornament made of mono- or multispinose teeth, pointing towards the tip of the introvert and more locally of spines (e.g. *Ottoia*, *Maotianshania*, *Anningvermis*). Comparatively oriented and distributed teeth occur along the everted pharynx of extant priapulids (Fig. S3M). Their role is to grasp prey or food particles and drawing them into the gut during the inversion process. Zone III can be confidently interpreted as the pharynx in fossil taxa, that is, a functional structure directly involved in feeding.

The transition between Zone I and III termed Zone II is often marked by a smooth area (e.g. *Tabelliscollex*, *Anningvermis*, *Maotianshania*; Huang 2005; Han, et al. 2003) or by a specific ornament such as a crown of long spines (e.g. *Louisella*, *S. columbia*, *Eopriapulites*, and *Ottoia*; Liu et al. 2014; Conway Morris 1977).

*Selkirkia* displays original features such as subdivisions (Ia, Ib and Ic) defined by the absence of ornament (Ib) or differences in the distribution of cuticular elements (Ia, Ic). These specific characters were first described in *Selkirkia columbia* (Conway Morris 1977, text-fig. 22) and are now recognized in the Chinese conspecific taxa (Figs 1A; 5A; 8). If our homologies are correct, then, *S. transita* sp. nov. characterized by a very narrow smooth Subzone Ib may appear as transitional between *S. sinica* (well-marked Subzone Ib) and *S. columbia* (Subzone Ib absent) (Fig. 8).

Comparative anatomy suggests that *Selkirkia* fits in with the body plan of extant and fossil scalidophorans, especially priapulids. The structure and micro-ornament of its introvert (Zone I-III) is not fundamentally different from those of typical Cambrian scalidophorans (e.g. *Ottoia*, *Eokinorhynchus*, Fig. 8) and extant priapulids (e.g. *Priapulidus*). What makes *Selkirkia* unique is mainly its conical and annulated tube that has no equivalent among fossil and extant scalidophorans.

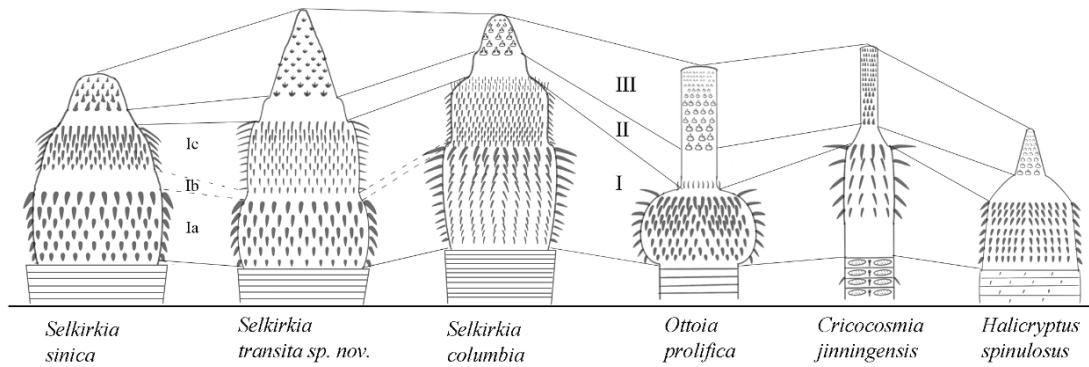


**FIGURE 8.** Possible homologies of introvert structure in selected Cambrian and extant (*Halicryptus spinulosus*) scalidophorans. For subdivisions in zones (I, II, III) and sub-zones (Ia, Ib, Ic), see explanations in text. *Selkirkia columbia* and *Ottoia prolifica* are modified from Conway Morris (1977).

### Phylogenetic position of *Selkirkia*

*Selkirkia* has long been assigned to priapulids based on overall similarities with extant priapulids, such as the introvert structure, pharyngeal teeth and trunk annulation (Ma, *et al.* 2010; Liu, *et al.* 2014; Wills, *et al.* 2012; Conway Morris 1977; Conway Morris and Whittington 1985; Luo, *et al.* 1999; Zhuravlev *et al.* 2011; Conway Morris 1997). Other authors have considered the tube of *Selkirkia* as a possible homologue of the lorica of extant priapulid larvae and loriciferans (Zhang *et al.* 2006), and advocated a position within scalidophorans without specifying to which group it may belong (Huang 2005; Zhang, *et al.* 2006; Maas, *et al.* 2007; Wills 1998; Ma, *et al.* 2014). *Selkirkia* clearly differs from extant Kinorhyncha and Loricifera, which both are characterized by the presence of a mouth cone and oral stylets (Heiner and Kristensen 2005). There are no such oral features in *Selkirkia* which instead has multispinose pharyngeal teeth arranged quincunxially as in numerous fossil and extant priapulid worms. Another major difference with these two groups is that the trunk of *Selkirkia* bears no external “segments” (the so-called zonites of kinorhynchs). Its finely annulated tube most probably secreted by the epidermal cells of the trunk (see below) has no equivalent in other groups.

Our main phylogenetic result (Fig. 7) finds that the *Selkirkia* clade is basal to Priapulida and its immediate stem, and therefore represents the onset of the priapulid radiation. The priapulid affinities of *Selkirkia* are supported by the following set of morphological characters shared with extant representatives of the group (Fig. 7): **(1)** the introvert of *Selkirkia* is subdivided in the same way as that of extant priapulids (i.e. Zone I, II, III) but clearly differs from that of kinorhynchs and loriciferans (Zone I, mouth cone); **(2)** Twenty-five longitudinal rows of scalids are found in *Selkirkia* and the vast majority of extant priapulids (except *Meiopriapulidus fijiensis*); **(3)** The pharynx of *Selkirkia* is lined with multispinose teeth as in extant (van der Land 1970) and Cambrian (Conway Morris 1977) priapulids; **(4)** The homology between the tube rings and the cuticular annulations seen in modern priapulids; **(5)** The possible paired caudal appendages of *Selkirkia* which have counterparts only in some extant (e.g. *Priapulidus*; van der Land 1970) and stem-group forms (e.g. *Paratubiluchus*; Han, *et al.* 2004a) priapulids.

An alternative phylogenetic scenario based on the same, but unconstrained, Bayesian analysis (Fig. S5) resolves *Selkirkia* in a basalmost position within a large stem-group

Scalidophora connecting this taxon to the origin of all non-nematoid cycloneuralians. Here, only a handful of fossils constitute the stem proper of Priapulida (e.g. *Paratubiluchus*, *Xiaoheiqingella*), most extinct forms documenting instead a parallel palaeoscolecid radiation (Fig. S5). In spite of being basal, the *Selkirkia* clade is only four nodes away from *Eximipriapulidus* (instead of two), and thus anatomical similarities with total-group Priapulida are still relevant.

### Tube formation, renewal and relation to body

Numerous invertebrate animals live within a tube. The membranous tube of some extant annelids (e.g. sabellids) is built from organic substances secreted by the collar (fold of peristomium) which cement sediment particles extracted from feeding currents (Brusca, *et al.* 2016). Serpulids secrete calcium carbonate crystals which, added to the organic matrix, form a thick and harder protective tube. In all cases, such annelids are able to move freely within their tube via slow peristaltic contractions and to withdraw quickly through the action of retractor muscles, part of the worm body remaining anchored to the inner wall of the tube (Brusca, *et al.* 2016). Siboglinids secrete chitinous tubes with relatively regularly spaced collared external morphologies whereas other annelids display smooth, granular or more or less irregularly corrugated or ringed tubes of various shapes (e.g. conical, cylindrical). Some elongate polyps (e.g. cerianthids) also live in tubes composed of fibrous material originating from mucus. *Maccabeus tentaculatus* (Por and Bromley 1974) is the only one example of an extant tubicolous priapulid worm. This less than three-mm-long priapulid lives within a cylindrical thin and flimsy tube open at both ends, apparently formed by plant fragments such as *Posidonia* agglutinated by stick substances secreted by glandular spines (Por and Bromley 1974). Tubicolous habits have appeared in early Cambrian annelids (*Dannychaeta*; Chen *et al.* 2020), lobopodian panarthropods (*Facivermis*; Howard *et al.* 2020) and middle Cambrian hemichordate (*Oesia*; Nanglu *et al.* 2016). The tube of *Oesia* was clearly made of intertwined collagen filaments (Nanglu *et al.* 2016). That of *Dannychaeta* (Chen *et al.* 2020) appears to be a burrow consolidated by adhering sediment and/or bioclasts and not a tube *sensu stricto*. *Facivermis* reveals no details of its tube structure and possible external ornament.

The tube of *Selkirkia* has been subject to various interpretations. It has been considered by some authors (Han 2002; Conway Morris 1977) to be a cuticular structure separated from the trunk by a gap, suggesting that the animal was free to move within its tube. Based on comparisons with *Maccabeus*, Conway Morris (1977) hypothesized that the tube of *S. columbia* was secreted by substances possibly emitted from hooks present around the proximal introvert (Zone Ia). Instead, other authors (e.g. Maas, *et al.* 2007; Huang 2005) suggested that the tube is an integral part of the trunk cuticle and that body and tube were inseparable elements. Our material shows that *Selkirkia* clearly had the capacity to protrude outside the large opening of the tube and even to leave the tube (Figs 1A, D; 2A; 3D; 4H, K). This configuration is unlikely to result from post-mortem displacement (e.g. decayed body detached from tube) and seems to indicate that the worm was free to move within its tube.

The tube of *Selkirkia* does not incorporate sediment or organic particles (e.g. *Maccabeus*). *Selkirkia* has neither specialized hooks nor visible secretion organs along its introvert and trunk that might indicate any excretion process as suggested by Conway Morris (1977). Instead, its tube bears regularly spaced parallel ridges which correspond internally to shallow furrows (Fig. 6A-C) thus resembling the annulations of non-tubicolous priapulids. This pattern most



probably resulted from the secretion of epithelial cells and the tube was renewed periodically via ecdysis, as in all scalidophorans.

For the formation of the tube and the moulting of the animal, we propose the following scenario, which integrates functional constraints related to locomotion, feeding and ecdysis (Fig. 9).

**(1)** The epithelial cells of the trunk secreted a cuticular layer that grew in thickness to eventually become and form a rigid tube. Sclerotization did not occur elsewhere, the introvert being lined with a thin and flexible cuticular layer.

**(2)** The sclerotized part of the tube split from the basal (non-sclerotized) layer of the cuticle (Lemburg 1998), thus creating a narrow gap between the tube and the body wall. At that stage, the whole worm body (introvert and trunk) was covered and protected by a flexible cuticular layer as in all non-tubicolous ecdysozoans (Fig. 9). Circular, longitudinal and retractor muscles allowed it to move within its tube and outside by exerting local pressure on the hydrostatic skeleton (Vannier and Martin 2017). This muscular system allowed the introvert to function as it does in extant scalidophorans (Vannier, *et al.* 2010). Contact between the body and the internal surface of the tube was made possible locally through the action of muscles (swelling of body cavity) thus creating anchoring features without which the animal could not have dragged its tube and carry it during locomotion (Fig. 10). *Selkirkia* most probably fed as most modern priapulids do (by using its pharyngeal teeth to catch food particles or preys and withdraw them into the gut).

**(3)** Just before moulting, the worm left its tube, discarded its exuvia and started renewing its cuticle as living ecdysozoans.

**(4)** A new tube formed around the trunk as the cuticle gradually became thicker and sclerotized.

If we consider the splitting of the sclerotized layer of the tube from the rest of the cuticle as the initial step of ecdysis, then the moulting process of *Selkirkia* differs from that of all other known scalidophorans in being non-synchronous, starting with the shedding of the tube and followed by the renewal of the whole cuticular layer. This moulting process has no equivalent in modern priapulids.

Other complex non-synchronous moulting processes seem to have occurred among Cambrian ecdysozoans groups. For example, the dorsal spines and claws of the mid-Cambrian lobopodian *Hallucigenia* display cone-in-cone features (Caron *et al.* 2013; Smith and Ortega-Hernández 2014).

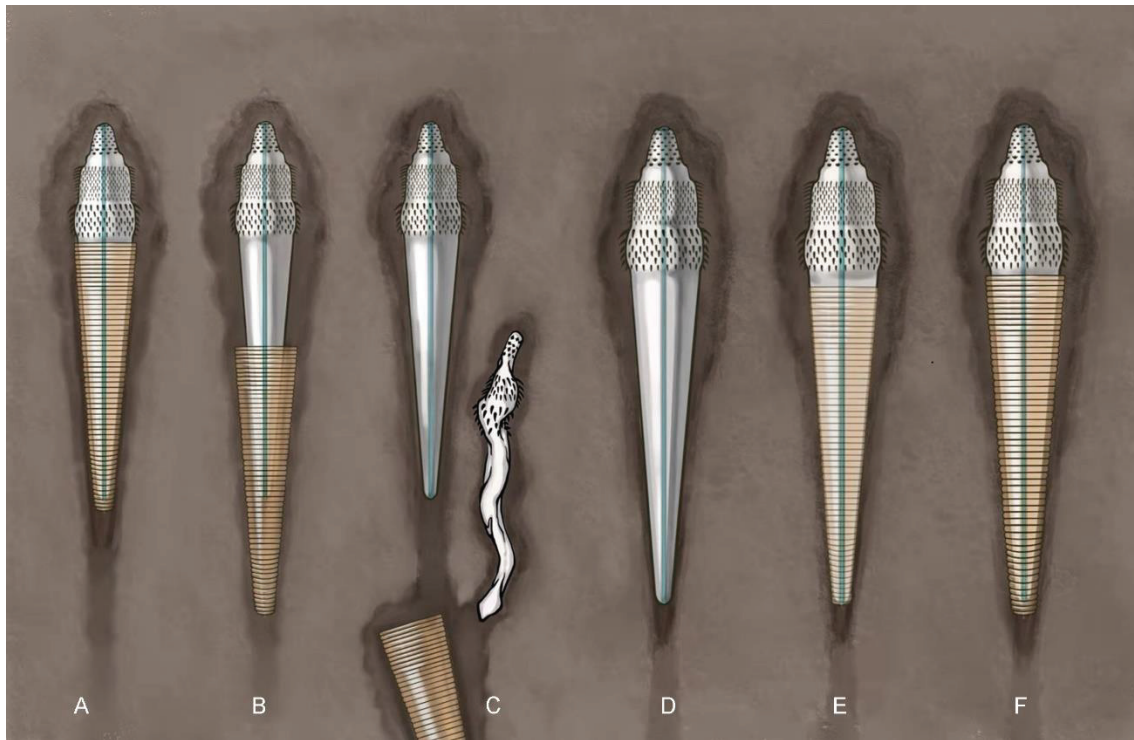


**FIGURE 9** Sequence diagram to explain the tube formation and moulting in *Selkirkia* (Cambrian). A. Worm within its tube at pre-moulting stage (whole body lined with thin cuticular layer; worm free from its tube). B, C. Worm getting rid of its old tube as moulting starts, then shedding its old cuticle over trunk, introvert, and pharynx (exuvia represented on right). D. Worm growing in size and rapidly secreting its new cuticle. E. Cuticle around trunk becoming thicker and sclerotized to eventually form a rigid tube around the trunk. F. Sclerotized layer (tube) splitting from the underlying cuticular layer around trunk (worm now free from its tube as in A). Ecdysis is seen here as a two-stage process.

### Brachiopod epibionts

The ovoid features that frequently occur near the posterior end of the tube of *S. columbia* and *S. sinica* have been interpreted as two flaps of unequal size (Conway Morris 1977; Lan, *et al.* 2015), implying that the tube had possible specialized posterior features (Lan, *et al.* 2015). Our fossil specimens (Fig. 3D-O), and those studied by X.-Y. Yang (personal communications) clearly show that these ovoid features are actually tiny brachiopods attached to the external surface of the tube and not tube flaps.

This interpretation is strongly supported by the presence of growth lines on the surface of some of brachiopod shells from the Xiaoshiba Lagerstätte (X.-Y. Yang, personal communications). Moreover, XRF images (Figs 1M; 3I, M) show that the chemical composition of brachiopod shells is different from that of the tube (e.g. presence of phosphorus in brachiopod shells). All studied specimens (X.-Y. Yang, personal communications and present paper) show no more than a single brachiopod always attached near the posterior opening of the tube. More detailed studies are needed to identify these brachiopods more precisely. However, they resemble tiny brachiopod epibionts such as *Inquilinus* (Zhang *et al.* 2010; Han, *et al.* 2004b) and *Kuangshanotreta* (Wang *et al.* 2012) that are found attached to various elements of the Chengjiang biota, such as larger brachiopods (*Diandongia*; Zhang, *et al.* 2010), algae-like organisms (*Malongitubus*; Wang, *et al.* 2012) and the palaeoscolecid *Cricocosmia*

(Han, *et al.* 2004b; Fig. S7). These brachiopods may have fed on tiny suspended organic particles released by feces through the posterior end of the tube (Fig. 3P, Q), which would explain their location in this preferential and exclusive area.

### **Tubicolous lifestyle**

The brachiopod feeding mode is generated by lophophoral cilia and requires constant contact with circulating water (Brusca *et al.* 2016). These ecological constraints and the preferential location of brachiopods near the posterior end of the worm tube would suggest that *Selkirkia* probably lived relatively close to the water-sediment interface, possibly lying in a subhorizontal or slightly tilted position, and maintaining contact with free water via the posterior tip of its tube. Extant scaphopod molluscs adopt a comparable infaunal lifestyle.

The tube of *Selkirkia* can be seen as a protective feature against physical damage and predation and may also have played a role in anchoring the animal to sediment. Numerous extant tubicolous animals as diverse as annelids (e.g. sabellids) and scaphopod molluscs live buried while maintaining contact with water-sediment interface (Brusca, *et al.* 2016). *Selkirkia* had a well-developed functional introvert that theoretically would have allowed it to move through muddy sediment like other scalidophoran worms (see above; Fig. 10). Locomotion was possibly achieved via **(1)** the eversion and anchoring of introvert (scalids) to sediment (Fig. 10A-C) and **(2)** the pressure exerted by the trunk on the tube wall (hydrostatic skeleton), that allowed the worm to drag its tube and move forwards (Fig. 10D, E). Clearly, the tube must have represented an extra weight for the animal thus hindering or limiting its capacities to move through its environment, compared with non-tubicolous worms.

The moulting process of *Selkirkia* (Fig. 9) implies that the worm temporarily left its tube and probably remained buried in sediment until the renewal of its cuticle. Although not sedentary, *Selkirkia* probably occupied a relatively restricted habitat with limited capacities for colonizing distant areas compared to other worms. This would be consistent with the relatively dense concentrations of individuals found in some localities and possibly indicating gregarious behaviour (Fig. S1). The pharyngeal teeth of *Selkirkia* suggest a feeding mechanism comparable with that of modern priapulid worms. Pellet-like elements found within its digestive tract seem to indicate that *Selkirkia* ingested a substantial amount of sediment mixed with food (possible meiobenthic prey or organic detritus). Finally, tubicolous lifestyles evolved separately in bilaterians (annelids, ecdysozoans, hemichordates) as a possible adaptive response to increasing environmental or biological pressure in Cambrian marine ecosystems.

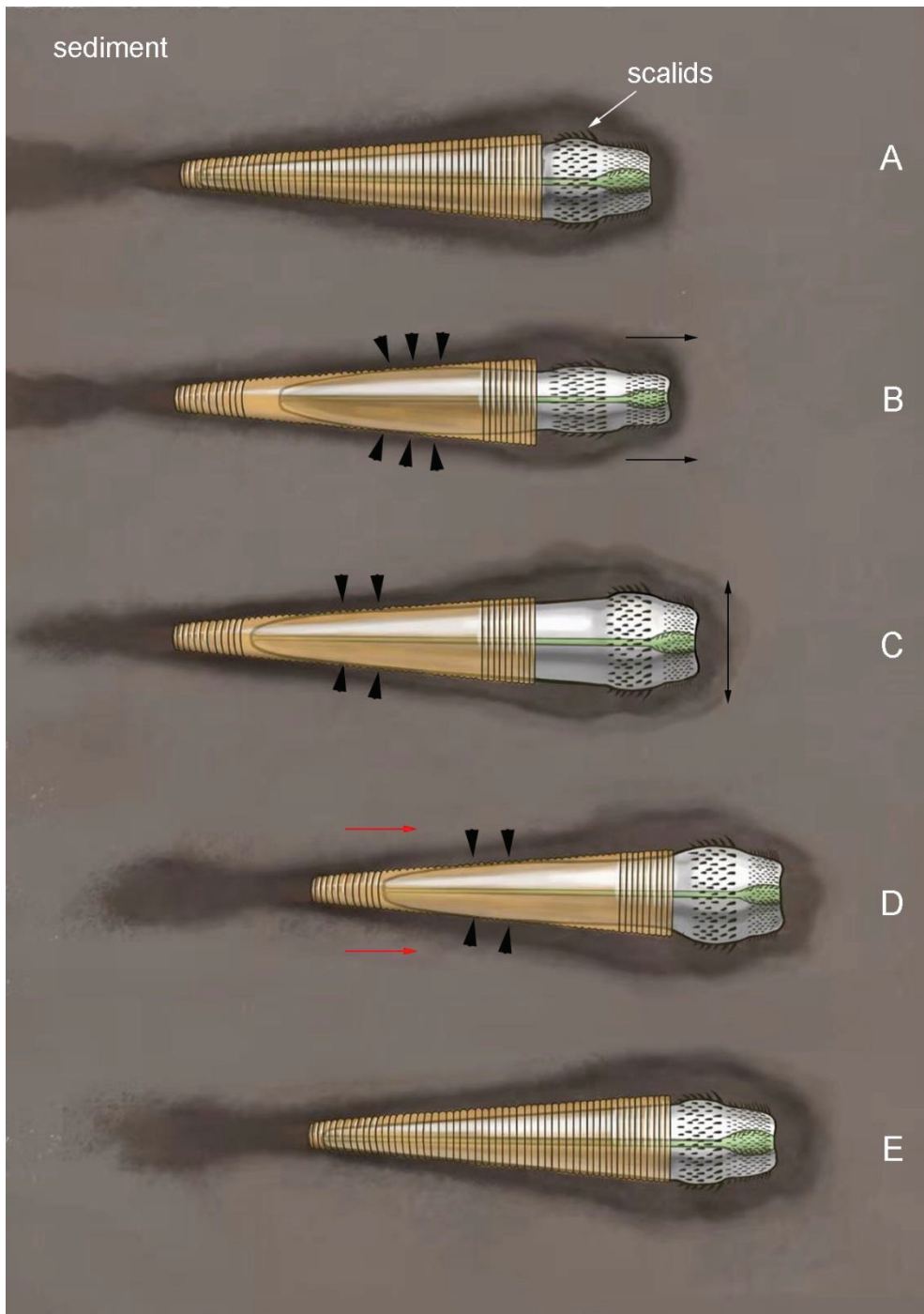


**FIGURE 10** Sequence diagram to explain locomotion in *Selkirkia* (Cambrian). A. Worm at rest within its tube (basal part of introvert protruding beyond tube opening). B. Eversion of introvert. C. Worm pushing its introvert into sediment and anchoring to it via scalids; medium part of trunk swollen (as the result of introvert tapering) and exerting pressure along the tube wall (black arrowheads). D. Double anchoring (trunk and scalids) allowing the worm to drag its tube and move forward (red arrows). E. Inversion of introvert leading to initial stage. Black thin arrows indicate introvert eversion/inversion. Muddy sediment in beige colour.

## Conclusions

The detailed study of *Selkirkia* presented here and based on new specimens from the Chengjiang Lagerstätte clarify key aspects of the palaeobiology and autecology of this

enigmatic Cambrian tubicolous worm. *Selkirkia* stands apart from other scalidophorans by having a cuticular tube, and we propose that the tube was renewed through non-synchronous ecdysis. Although this relatively thick and protective structure probably reduced its capacities to move fast through its environment, *Selkirkia* could slip within its tube and possibly escape from it. A single epibiotic brachiopod is frequently found attached to the posterior end of the tube. This in life association imposes constraints on the infaunal lifestyle of *Selkirkia* which probably lived close to the water-sediment interface. *Selkirkia* therefore adds to other Cambrian tubicolous animals such as hemichordates, annelids and panarthropods (lobopodians). In contrast with these unusual morphological and ecological features, *Selkirkia* closely resembles extant and Cambrian priapulids in the general organization and ornament of its introvert. The resolution of higher nodes in the cycloneuralian phylogeny remains a challenge, but we consistently found the *Selkirkia* clade to lie ancestrally close to the common ancestor of total-group Priapulida, with or without a separate radiation of Palaeoscolecida *sensu lato*.

**Acknowledgements.** We thank Z.-F Zhang and X.-Y Ren for XRF analysis of fossil specimens, J. Luo and M.-R Cheng (State Key Laboratory for Continental Dynamics, Northwest University, Xi'an, China) for assistance in both field and laboratory work, X.-Y Yang (Yunnan University, Kunming, China) for beneficial discussion. We also thank the Kristineberg Marine Station (Göteborg University, Sweden) and the Askö Laboratory (Stockholm University, Sweden) for assistance in collecting extant priapulid worms, J.-B Caron (Royal Ontario Museum, Canada) for providing images, the Centre Technologique des Microstructures (CT $\mu$ , Université Claude Bernard Lyon 1, France) for assistance and access to electronic microscopy, V. Perrier (Université Claude Bernard Lyon 1, France) for assistance with imaging, A. Schmidt-Rhaesa (Hamburg University, Germany) for discussions, and M. R. Smith (Cambridge University, UK) for discussion and help with the use of TreeSearch. This work was supported by the Strategic Priority Research Program of Chinese Academy of Science (grant no. XDB26000000), Natural Science Foundation of China (nos. 41621003, 41772010, 41672009, 41720101002), Ministry of Science and 111 project of Ministry of Education of China (no. D17013), the Most Special Fund from the State Key Laboratory for Continental Dynamics, Northwest University, China (BJ11060), the China Scholarship Council (CSC, grant no. 201806970013) for D.W.'s 2-year research stay at UCBL, the CNRS (France) and NSFC (China) for a PRC cooperation grant to J. Han and J. Vannier, the ASSEMBLE Program (grant to JV) and the Université Claude Bernard Lyon 1 and the Région Auvergne-Rhône-Alpes, PAI grant to JV).

**Authors' contributions.** JH conceived the project. DW prepared and photographed fossil material and assembled final figures. DW and JV compiled the character list and morphological dataset. CA ran the phylogenetic analyses and prepared the phylogeny figures. DW, JV and JH interpreted the fossil material, and all authors wrote the paper.

## References

- ABERER, A. J., KROMPASS, D. and STAMATAKIS, A. 2013. Pruning rogue taxa improves phylogenetic accuracy: an efficient algorithm and webservice. *Systematic Biology*, **62**, 162-6.
- ARIA, C., CARON, J.-B., GAINES, R. and ZHANG, X.-G. 2015. A large new leanchoilid from the

- Burgess Shale and the influence of inapplicable states on stem arthropod phylogeny. *Palaeontology*, **58**, 629-660.
- BRAZEAU M. D., GUILLERME T. and R., S. M. 2019 An algorithm for Morphological Phylogenetic Analysis with Inapplicable Data. *Systematic Biology*, **68**, 619–631.
- BRAZEAU, M. D., SMITH, M. R. and GUILLERME, T. 2017. MorphyLib: a library for phylogenetic analysis of categorical trait data with inapplicability.
- BRUSCA, R. C., MOORE, W. and SHUSTER, S. M. 2016. *Invertebrates*. Sinauer Associates, Inc., Sunderland Massachusetts USA, 639-910 pp.
- CARON, J. B. and ARIA, C. 2017. Cambrian suspension-feeding lobopodians and the early radiation of panarthropods. *BMC Evolutionary Biology*, **17**, 29.
- CARON, J. B., SMITH, M. R., and HARVEY, T. H. P. 2013. Beyond the Burgess Shale: Cambrian microfossils track the rise and fall of hallucigeniid lobopodians. *Proceedings of the Royal Society B*, **280**, 20131613.
- CHEN, H., PARRY, L. A., VINTHER, J., ZHAI, D., HOU, X. and MA, X. 2020. A Cambrian crown annelid reconciles phylogenomics and the fossil record. *Nature*, **583**, 249-252.
- CHEN, J. Y. 2004. *The Dawn of Animal World*. Jiangsu Science and Technology Press, Nanjing.
- CHEN, L., LUO, H., HU, S., YIN, J., JIANG, Z., WU, Z., LI, F. and CHEN, A. 2002. *Early Cambrian Chengjiang Fauna in eastern Yunnan China (in Chinese with English abstract)*. Yunnan Science and Technology Press.
- CONGREVE, C. R. and LAMSDELL, J. C. 2016. Implied weighting and its utility in palaeontological datasets: a study using modelled phylogenetic matrices. *Palaeontology*, **59**, 447-462.
- CONWAY MORRIS, S. 1977. Fossil priapulid worms. *Special Papers in Palaeontology*, **20**, 1-95.
- 1997. The cuticular structure of the 495-Myr-old type species of the fossil worm *Palaeoscolex*, *P. piscatorum* (?Priapulida). *Zoological Journal of the Linnean Society*, **119**, 69-82.
- CONWAY MORRIS, S. and PEEL, J. S. 2010. New palaeoscolecidan worms from the Lower Cambrian: Sirius Passet, Latham Shale and Kinzers Shale. *Acta Palaeontologica Polonica*, **55**, 141-156.
- CONWAY MORRIS, S. and ROBISON, R. A. 1986. Middle Cambrian priapulids and other soft-bodied fossils from Utah and Spain. *The University of Kansas Paleontological Contributions*, **117**, 1-22.
- CONWAY MORRIS, S. and WHITTINGTON, H. B. 1985. Fossils of the Burgess Shale, A nation treasure in Yoho National Park, British Columbia. *Geological survey of Canada*, **43**, 13-16.
- FU, D. J., TONG, G., DAI, T., LIU, W., YANG, Y., ZHANG, Y., CUI, L., LI, L., YUN, H., WU, Y., SUN, A., LIU, C., PEI, W., GAINES, R. R. and ZHANG, X. 2019. The Qingjiang biota-A Burgess Shale-type fossil Lagerstätte from the early Cambrian of South China. *Science*, **363**, 1338-1342.
- GAINES, R. R., BRIGGS, D. E. G. and YUANLONG, Z. 2008. Cambrian Burgess Shale-type deposits share a common mode of fossilization. *Geology*, **36**, 755.
- GIRIBET, G. and EDGECOMBE, G. D. 2017. Current understanding of Ecdysozoa and its internal phylogenetic relationships. *Integrative and Comparative Biology*, **57**, 455-466.
- GOLOBOFF, P. A. and CATALANO, S. A. 2016. TNT version 1.5, including a full implementation of phylogenetic morphometrics. *Cladistics*, **32**, 221-238.
- HAN, J. 2002. Introverta in Chengjiang Fauna (In Chinese with English abstract). Northwest University.

- HAN, J., SHU, D., ZHANG, Z. and LIU, J. 2004a. The earliest-known ancestors of Recent Priapulomorpha from the Early Cambrian Chengjiang Lagerstätte. *Chinese Science Bulletin*, **49**, 1860.
- HAN, J., ZHANG, X. L., ZHANG, Z. F. and SHU, D. G. 2003. A new platy-armored worm from the early Cambrian Chengjiang Lagerstätte, South China. *Acta Geologica Sinica*, **77**, 1-6.
- HAN, J., ZHANG, Z. and LIU, J. 2004b. Taphonomy and ecology of the introverts from the Chengjiang fauna (in Chinese with English abstract). *Journal of Northwest University (Natural Science Edition)*, **34**, 207-212.
- HEINER, I. and KRISTENSEN, R. M. 2005. Two new species of the genus Pliciloricus (Loricifera, Pliciloricidae) from the Faroe Bank, North Atlantic. *Zoologischer Anzeiger - A Journal of Comparative Zoology*, **243**, 121-138.
- HOU, X. G., BERGSTÖRM, J., WANG, H., FENG, X. and CHEN, A. 1999. *The Chengjiang Fauna - exceptional well-preserved animals from 530 million years ago (in Chinese with English summary)*. Yunnan Science and Technology Press, Yunnan.
- HOU, X. G., SIVETER, D. J., SIVETER, D. J., ALDRIDGE, R. J., CONG, P. Y., GABBOTT, S. E., MA, X. Y., PURNELL, M. A. and WILLIAMS, M. 2017. *The Cambrian Fossils of Chengjiang, China: The Flowering of Early Animal Life*. Wiley Blackwell, 98-270 pp.
- HOWARD, R. J., HOU, X., EDGEcombe, G. D., SALGE, T., SHI, X. and MA, X. 2020. A Tube-Dwelling Early Cambrian Lobopodian. *Current Biology*, **30**, 1-8.
- HU, S. 2005. *Taphonomy and Palaeoecology of the Early Cambrian Chengjiang Biota from Eastern Yunnan, China*. Berliner Paläobiologische Abhandlungen, Berlin.
- HU, S., ZHU, M., LUO, H., STEINER, M., ZHAO, F., LI, G., LIU, Q. and ZHANG, Z. 2013. *The Guanshan Biota*. Yunnan Publishing Group Co. Ltd. Yunnan Science and Technology Press, 1-204 pp.
- HUANG, D. 2005. Early Cambrian worms from SW China: morphology, systematics, lifestyles and evolutionary significance (unpublished PhD thesis). Université Claude Bernard Lyon 1, France.
- HUANG, D., VANNIER, J. and CHEN, J. 2004a. Anatomy and lifestyles of Early Cambrian priapulid worms exemplified by *Corynetis* and *Anningvermis* from the Maotianshan Shale (SW China). *Lethaia*, **37**, 21-33.
- 2004b. Recent Priapulidae and their Early Cambrian ancestors: comparisons and evolutionary significance. *Geobios*, **37**, 217-228.
- LAN, T., YANG, J., HOU, J. and ZHANG, X. 2015. The feeding behaviour of the Cambrian tubicolous priapulid *Selkirkia*. *Lethaia*, **48**, 125-132.
- VAN DER LAND, J. 1970. Systematic, Zoogeography and ecology of the Priapulida. *Zoologische Verhandelingen*, **112**, 4-104.
- LEMBURG, C. 1995. Ultrastructure of the introvert and associated structures of the larvae of *Halicryptus spinulosus* (Priapulida). *Zoomorphology*, **115**, 11-29.
- 1998. Electron microscopical localization of chitin in the cuticle of *Halicryptus spinulosus* and *Priapulid caudatus* (Priapulida) using gold-labelled wheat germ agglutinin: phylogenetic implications for the evolution of the cuticle within the Nemathelminthes. *Zoomorphology*, **118**, 137-158.
- LEWIS, P. O. 2001. A likelihood approach to estimating phylogeny from discrete morphological character data. *Systematic biology*. **50**(6), 913-925.
- LIU, Y. H., XIAO, S. H., SHAO, T. Q., BROCE, J. and ZHANG, H. Q. 2014. The oldest known

- priapulid-like scalidophoran animal and its implications for the early evolution of cycloneuralians and ecdysozoans. *Evolution & Development*, **16**, 155-65.
- LUO, H. L., HU, S., CHEN, L., ZHANG, S. and TAO, Y. 1999. *Early Cambrian Chengjiang Fauna from Kunming region China (In Chinese with English summary)*. Yunnan Science and Technology Press.
- MA, X., HOU, X. and BAINES, D. 2010. Phylogeny and evolutionary significance of vermiform animals from the Early Cambrian Chengjiang Lagerstätte. *Science China Earth Sciences*, **53**, 1774-1783.
- MA, X. Y., ALDRIDGE, R. J., SIVETER, D. J., SIVETER, D. J., HOU, X. G. and EDGECOMBE, G. D. 2014. A new exceptionally preserved Cambrian priapulid from the Chengjiang Lagerstätte. *Journal of Paleontology*, **88**, 371-384.
- MAAS, A., HUANG, D., CHEN, J., WALOSZEK, D. and BRAUN, A. 2007. Maotianshan-Shale nemathelminths — Morphology, biology, and the phylogeny of Nemathelminthes. *Palaeogeography, Palaeoclimatology, Palaeoecology*, **254**, 288-306.
- MADDISON, W. P. and MADDISON, D. R. 2019. Mesquite: a modular system for evolutionary analysis. Version 3.61.
- NANGLU, K., CARON, J.-B. and GAINES, R. R. 2020. The Burgess Shale paleocommunity with new insights from Marble Canyon, British Columbia. *Paleobiology*, **46**, 58-81.
- NANGLU, K., CARON, J. B., CONWAY MORRIS, S. and CAMERON, C. B. 2016. Cambrian suspension-feeding tubicolous hemichordates. *BMC Biology*, **14**, 56.
- PEEL, J. S. 2016. Mineralized gutfills from the Sirius Passet Lagerstätte (Cambrian Series 2) of North Greenland. *GFF*, **139**, 83-91.
- PEEL, J. S. and WILLMAN, S. 2018. The Buen Formation (Cambrian Series 2) biota of North Greenland. *Papers in Palaeontology*, **4**, 381-432.
- POR, F. D. and BROMLEY, H. J. 1974. Morphology and anatomy of *Maccabeus tentaculatus* (Priapulida : Seticoronaria). *Journal of Zoology*, **173**, 173-197.
- R TEAM 2020. R: A language and environment for statistical computing. R Foundation for Statistical Computing, Vienna, Austria.
- RESSER, C. E. 1939. The Spence Shale and its fauna. *Smithsonian Miscellaneous Collections*, **97**, 4-5.
- RONQUIST, F., TESLENKO, M., VAN DER MARK, P., AYRES, D. L., DARLING, A., HOHNA, S., LARGET, B., LIU, L., SUCHARD, M. A. and HUELSENBECK, J. P. 2012. MrBayes 3.2: efficient Bayesian phylogenetic inference and model choice across a large model space. *Systematic Biology*, **61**, 539-42.
- SAWAKI, Y., NISHIZAWA, M., SUO, T., KOMIYA, T., HIRATA, T., TAKAHATA, N., SANO, Y., HAN, J., KON, Y. and MARUYAMA, S. 2008. Internal structures and U–Pb ages of zircons from a tuff layer in the Meishucunian formation, Yunnan Province, South China. *Gondwana Research*, **14**, 148-158.
- SCHMIDT-RHAESA, A. 2013. Gastrotricha, Cycloneuralia and Gnathifera. *Handbook of zoology*. De Gruyter, Germany, 29-123 pp.
- SHIRLEY, T. C. 1990. Ecology of *Priapulidus caudatus* Lamarck, 1816 (Priapulida) in an Alaskan subarctic ecosystem. *Bulletin of Marine Science* **47**, 149-158.
- SMITH, M.R. 2018. TreeSearch: phylogenetic tree search using custom optimality criteria.
- SMITH, M. R. 2019. Bayesian and parsimony approaches reconstruct informative trees from simulated morphological datasets. *Biology Letters*, **15**, 20180632.



- SMITH, M. R., HARVEY, T. H. P., BUTTERFIELD, N. J. and KOUCHINSKY, A. 2015. The macro- and microfossil record of the Cambrian priapulid *Ottoia*. *Palaeontology*, **58**, 705-721.
- SMITH, M. R. and ORTEGA-HERNANDEZ J. 2014. *Hallucigenia*'s onychophoran-like claws and the case for Tactopoda. *Nature*, **514** (7522): 363-366.
- STEINER, M., QIAN, Y., LI, G. X., HAGADORN, J. W. and ZHU, M. Y. 2014. The developmental cycles of early Cambrian Olivooidea fam. nov. (?Cycloneuralia) from the Yangtze Platform (China). *Palaeogeography, Palaeoclimatology, Palaeoecology*, **398**, 97-124.
- STEINER, M., YANG, B., HOHL, S., ZHANG, L. and CHANG, S. 2020. Cambrian small skeletal fossil and carbon isotope records of the southern Huangling Anticline, Hubei (China) and implications for chemostratigraphy of the Yangtze Platform. *Palaeogeography, Palaeoclimatology, Palaeoecology*, **554**, 109817.
- TORSVIK, T. H. and COCKS, L. R. M. 2013. Chapter 2 New global palaeogeographical reconstructions for the Early Palaeozoic and their generation. *Geological Society, London, Memoirs*, **38**, 5-24.
- TROTT, T. J. 2017. Feeding by *Priapulid caudatus* (Cephalorhyncha: Priapulidae): observations of the effects of seasonal temperature change and molting. *Marine and Freshwater Behaviour and Physiology*, **50**, 55-65.
- VANNIER, J., CALANDRA, I., GAILLARD, C. and ŽYLIŃSKA, A. 2010. Priapulid worms: Pioneer horizontal burrowers at the Precambrian-Cambrian boundary. *Geology*, **38**, 711-714.
- VANNIER, J. and MARTIN, E. L. O. 2017. Worm-lobopodian assemblages from the Early Cambrian Chengjiang biota: Insight into the "pre-arthropodan ecology"? *Palaeogeography, Palaeoclimatology, Palaeoecology*, **468**, 373-387.
- WALCOTT, C. D. 1911. Middle Cambrian Annelids, Cambrian Geology and Paleontology II. *Smithsonian Miscellaneous Collections*, **57**, 110-144.
- WANG, H., ZHANG, Z., HOLMER, L. E., HU, S., WANG, X. and LI, G. 2012. Peduncular attached secondary tiering acrotretoid brachiopods from the Chengjiang fauna: Implications for the ecological expansion of brachiopods during the Cambrian explosion. *Palaeogeography, Palaeoclimatology, Palaeoecology*, **323-325**, 60-67.
- WENNERBERG, S. A., JANSSEN, R. and BUDD, G. E. 2009. Hatching and earliest larval stages of the priapulid worm *Priapulid caudatus*. *Invertebrate Biology*, **128**, 157-171.
- WILLS, M. A. 1998. Cambrian and recent disparity: the picture from priapulids. *Paleobiology*, **24**, 177-199.
- WILLS, M. A., GERBER, S., RUTA, M. and HUGHES, M. 2012. The disparity of priapulid, archaeopriapulid and palaeoscolecid worms in the light of new data. *Journal of Evolutionary Biology*, **25**, 2056-2076.
- YANG, C., LI, X.-H., ZHU, M., CONDON, D. J. and CHEN, J. 2018. Geochronological constraint on the Cambrian Chengjiang biota, South China. *Journal of the Geological Society*, **175**, 659-666.
- ZHANG, H. Q., XIAO, S. H., LIU, Y. H., YUAN, X. L., WAN, B., MUSCENTE, A. D., SHAO, T. Q., GONG, H. and CAO, G. H. 2015. Armored kinorhynch-like scalidophoran animals from the early Cambrian. *Scientific Reports*, **5**, 16521.
- ZHANG, X.-G., HOU, X.-G. and BERGSTRÖM, J. A. N. 2006. Early Cambrian priapulid worms buried with their lined burrows. *Geological Magazine*, **143**, 743-748.
- ZHANG, Z., HAN, J., WANG, Y., EMIG, C. C. and SHU, D. 2010. Epibionts on the lingulate brachiopod *Diandongia* from the Early Cambrian Chengjiang Lagerstätte, South China.

- Proceedings of the Royal Society B: Biological Sciences*, **277**, 175-81.
- ZHAO, Y. 2011. *Kali Biota-Ocean animals from 5.08 million years ago*. Guizhou Science and Technique Press, Guizhou Province.
- ZHU, M., BABCOCK, L. E. and STEINER, M. 2005. Fossilization modes in the Chengjiang Lagerstätte (Cambrian of China): testing the roles of organic preservation and diagenetic alteration in exceptional preservation. *Palaeogeography, Palaeoclimatology, Palaeoecology*, **220**, 31-46.
- ZHURAVLEV, A. Y., VINTANED, J. A. G. and LIÑÁN, E. 2011. The Palaeoscolecida and the evolution of the Ecdysozoa. *Palaeontographica Canadiana*, **31**, 177-204.

## Supplementary materials

### Palaeobiology of the Cambrian tubicolous ecdysozoan *Selkirkia*: New insights from the Chengjiang Lagerstätte

Deng Wang, Jean Vannier, Cédric Aria, Jie Sun, Jian Han



**Figure S1.** Large concentration of *Selkirkia sinica* on a bedding plane, ELI-0002022. White arrow indicates possible bradoriid or brachiopod shell. Scale bar represents 5 mm.

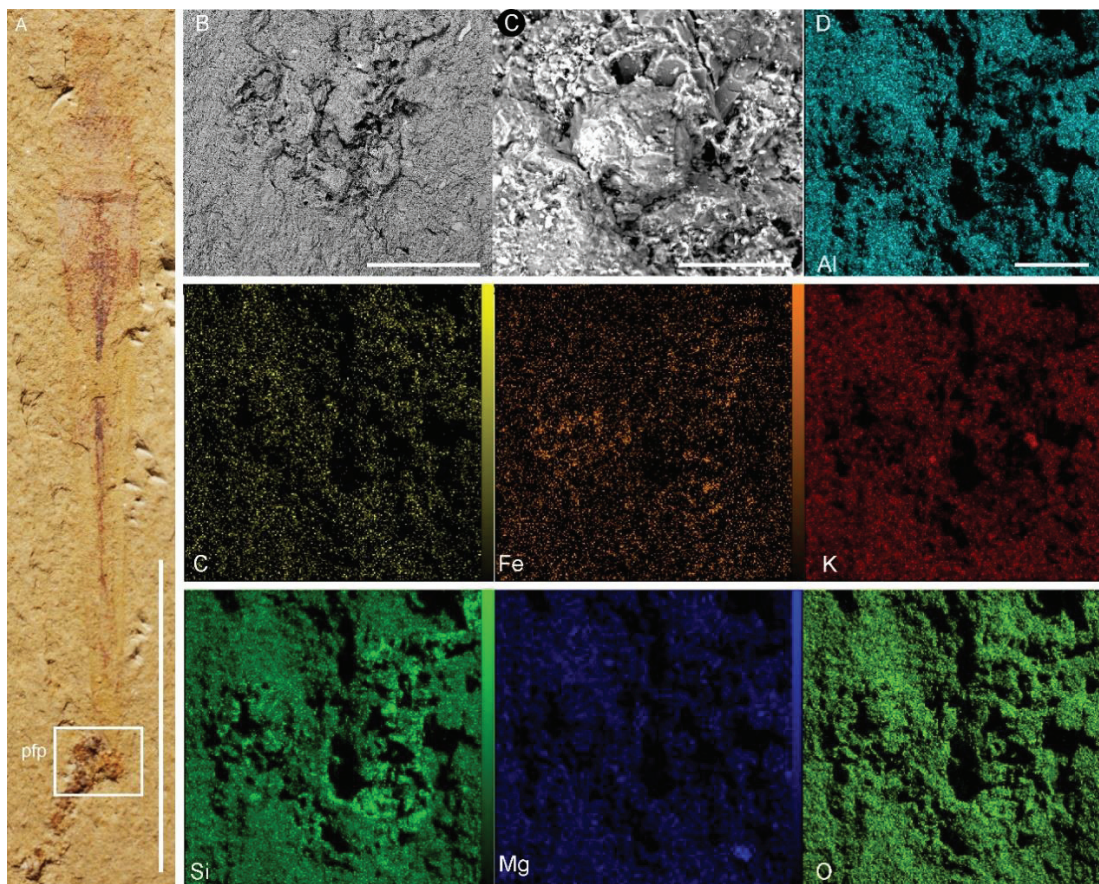


**Figure S2.** Assumed feces in *Selkirkia sinica*, ELI-0002018. A, general view, light photograph. B-D, close ups (SEM images; see location in A) and elemental mapping (same location). Abbreviation: pfp, possible feces pellets. Scale bars represent: 5 mm (A), 500  $\mu\text{m}$  (B), 200  $\mu\text{m}$  (D), 50  $\mu\text{m}$  (C).

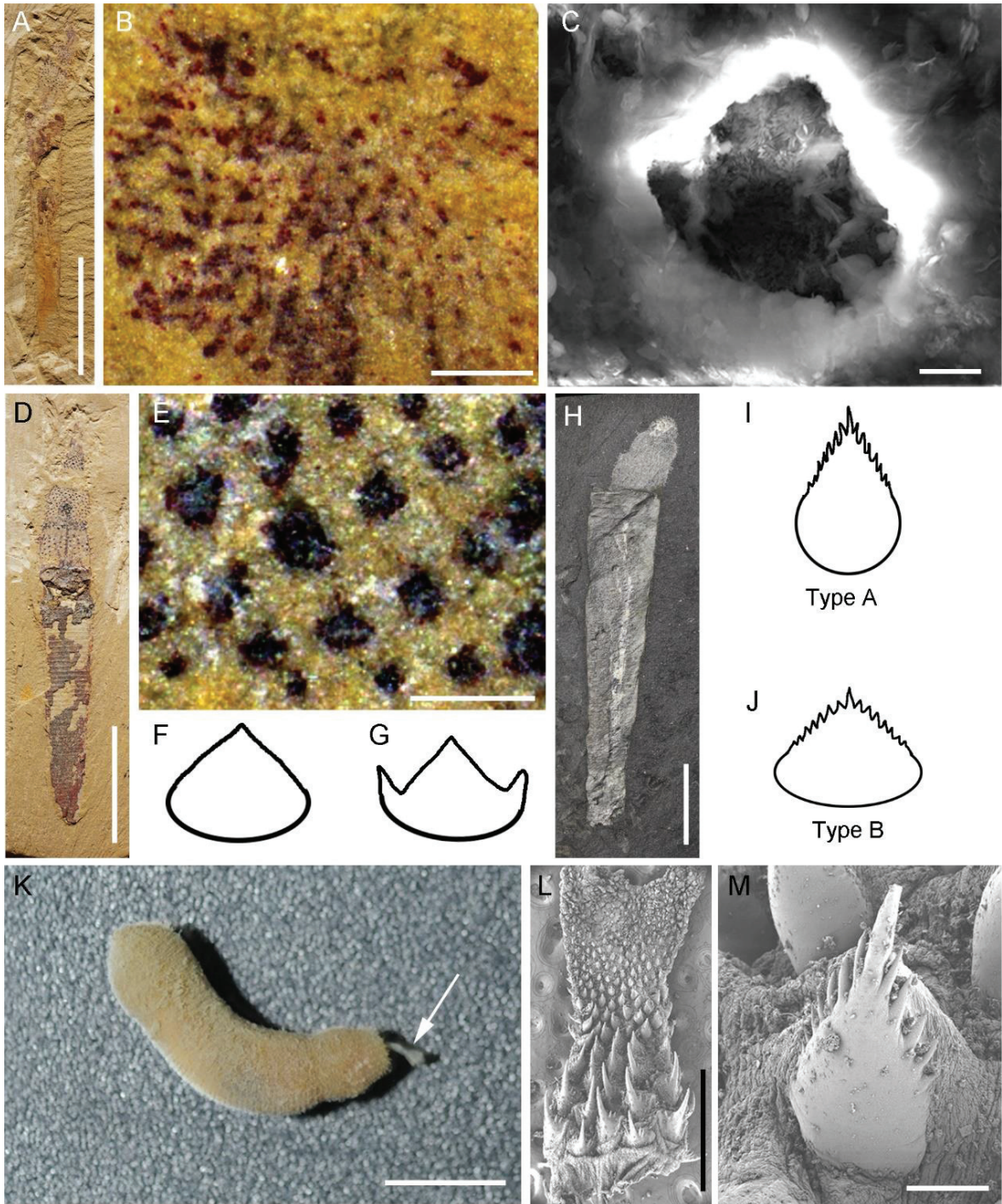


**Figure S3.** Pharyngeal teeth types in *Selkirkia* and extant priapulid. (A-C, F), *Selkirkia sinica*, general view of ELI-0002001, close-up of everted pharynx, SEM image of pharyngeal tooth (from B), and outline. (D, E, G), *Selkirkia transita* sp. nov., general view of ELI-000601, close-up of everted pharyngeal teeth, outline of pharyngeal tooth (from E). (H-J), *Selkirkia columbia*, general view of USNM 83941a (courtesy Jean-Bernard Caron), outline of two types of pharyngeal teeth, modified from Smith et al. (2015). (K-M), *Halicryptus spinulosus*, general view (white arrow indicates the everted pharynx) and SEM image showing everted pharynx and tooth. Scale bars represent: 1 cm (H), 5 mm (A, D, K), 1 mm (L), 200  $\mu$ m (B, E), 50  $\mu$ m (M), 2  $\mu$ m (C).

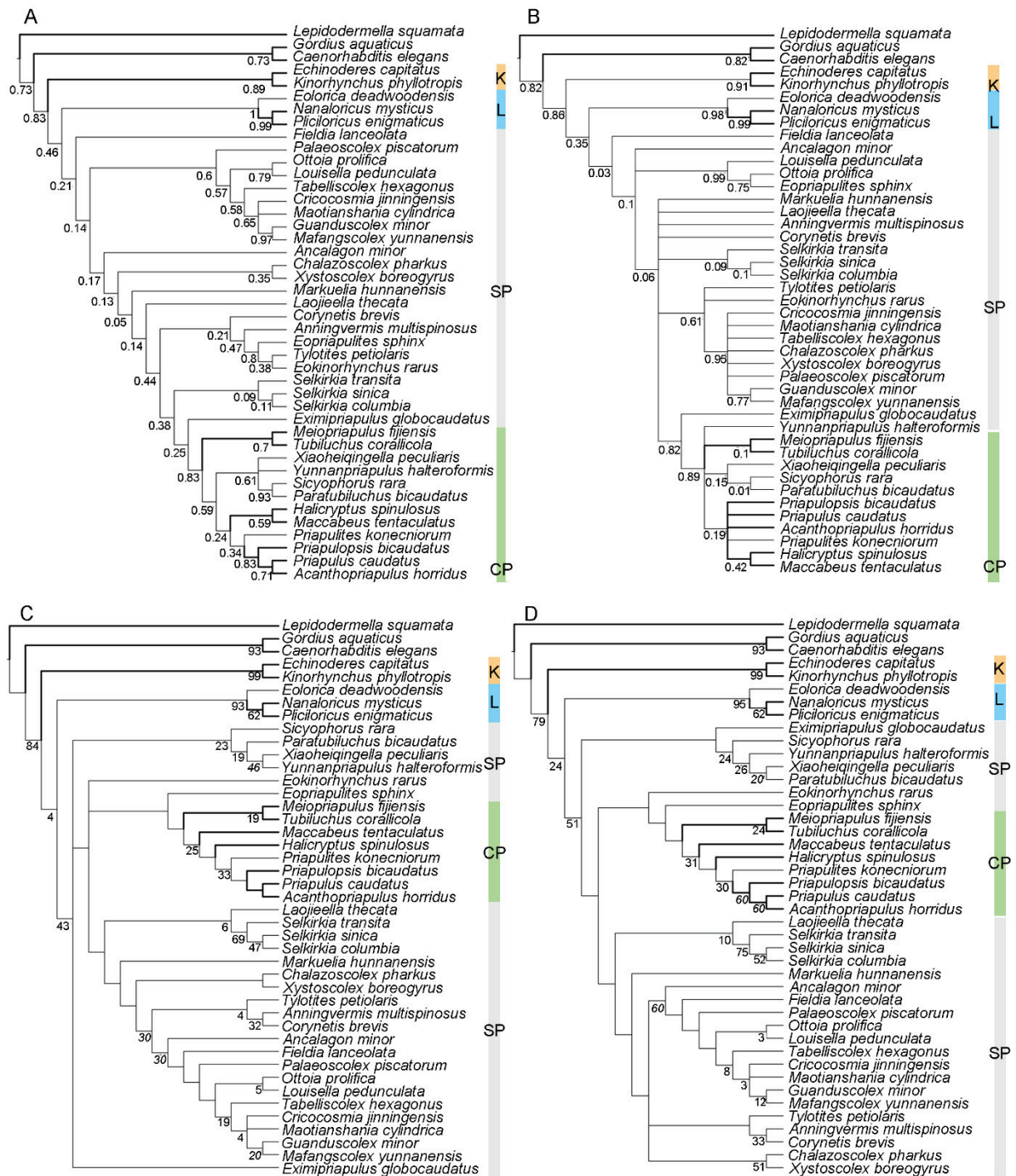


**Figure S4.** Consensus cladograms of parsimony. A. Heuristic Tree Bisection Reconnection, 12 Most Parsimonious Trees (MPTs), 307 steps. B. Tree search using new technology (TNT), including Ratchet and Drifting, 5 MPTs, 307 steps. C. Unweighted analysis using TreeSearch, 26 MPTs, 317 steps. D. Consensus of TreeSearch analyses using implied weighting for  $k=(3, 5, 10)$ . Bold branches are extant. Numbers at nodes are jackknifed support values; italicized numbers at nodes in A and B are frequencies of occurrence for nodes not present in all MPTs.

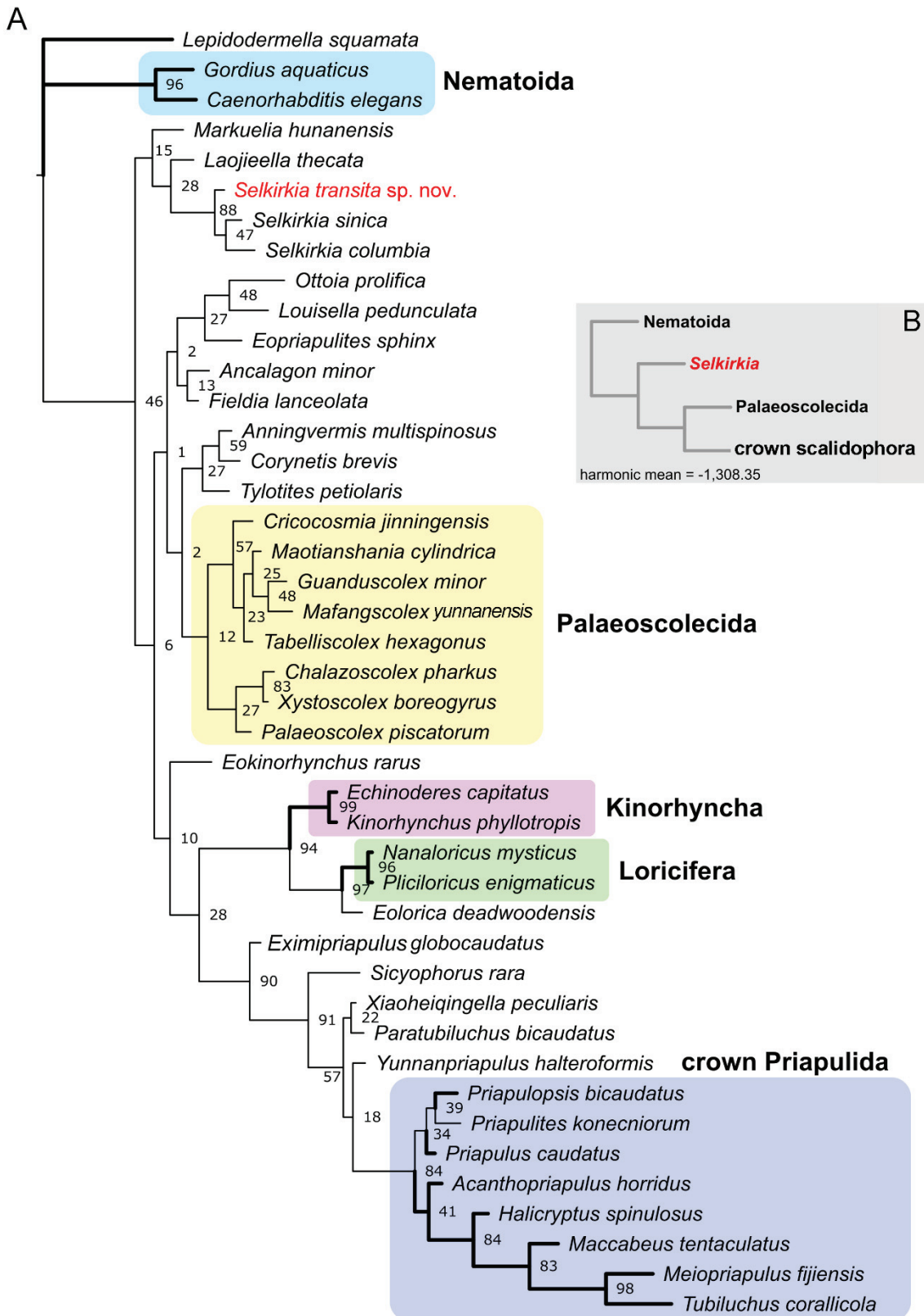


**Figure S5.** Maximum clade compatibility tree from a Bayesian analysis using an Mkv+ $\Gamma$  model and not a backbone used. A, Full tree. *Selkirkia* is at the basal position of stem-scalidophorans. Bold branches are extant species. Numbers next to node are posterior probabilities. B. Simplified topology showing the position of *Selkirkia* and harmonic mean (-1,308.35).

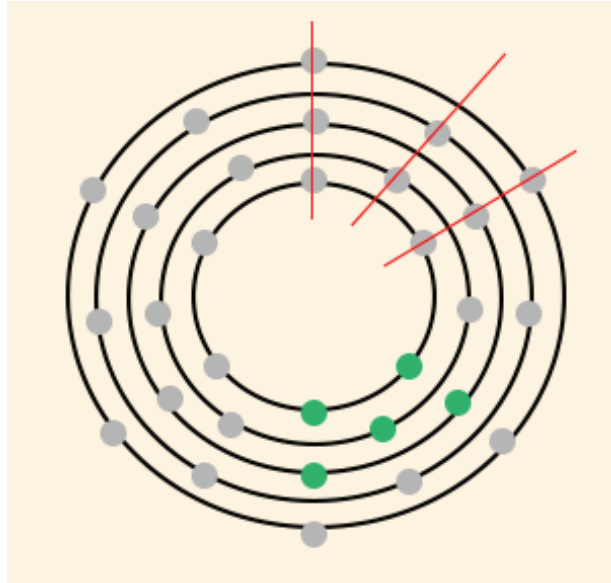


**Figure S6.** Polar-coordinate diagram showing the quincunxes distribution of scalids (green dots) as in *Selkirkia*, palaeoscoleoids and extant priapulids.



**Figure S7.** Trunk of *Cricocosmia* with attached brachiopod shell from the Chengjiang Lagerstätte. Scale bars represent: 2 mm.



## 5.4 Cambrian priapulid worms with oocytes shed light on the early evolution of reproductive systems

This study is also based on *Selkirkia* (see Chapter 5.3) and was made possible through a collaboration project with a research team based in Kunming (Yunnan University). The first author (Ms. Xiaoyu Yang) of this submitted MS is a PhD-candidate, like me.

This study goes far beyond the systematic description of *Selkirkia* and addresses the important question of the reproductive organs and strategies of early animals. The fossil material was collected by Ms Yang and her co-workers from the Xiaoshiba Lagerstätte (Stage 4; ca 514 Ma). Despite significant advances on vital aspects of the biology of early animals, many issues concerning the reproduction and developmental modes of Cambrian animals are still unresolved. Exceptionally preserved fossils from Cambrian Lagerstätten (e.g. Chengjiang and the Burgess Shale) have revealed exquisite details about the functional anatomy, development, lifestyles and behaviour of a great variety of animals but rarely shed light on their reproduction organs.

Eggs and embryos found in Cambrian rocks provide key information about the embryonic development of early animals but tell us nothing about the younger steps of their reproduction cycle (gonads, eggs, fertilization). Some shrimp-like, bivalved waptiid arthropods from the Burgess Shale and Chengjiang Lagerstätten (Caron and Vannier, 2016; Duan et al., 2014; Ou et al., 2020; Fig. 44F-H) show well-preserved egg clusters that were carried symmetrically on either side the female's body, thus indicating that different types of brood care (evolutionary trade-off; see Ou et al., 2020) were used by such ancient animals. We describe here eggs preserved in situ within the internal cavity of early Cambrian scalidophoran worms (*Selkirkia*, Fig. 44A-D) and interpreted as oocytes (non-fertilized eggs) rather than early embryos.

The cohesive appearance of some of the oocyte clusters seen in *Selkirkia* (Fig. 44A-D) suggests that they were maintained within a single or more complex ovarian structure before being released outside through the urogenital ducts, as observed in modern priapulids. We based our interpretations on modern analogues seen in both macrobenthic (e.g. *Priapulid*, collected in Sweden; see Chapter 5.1) and meiobenthic (e.g. *Meiopriapulid fijiensis*, Higgins and Stroch, 1991; *Maccabeus tentaculatus*; Fig. 50). The relatively large size (possible yolk-rich) and low number of oocytes suggest that the reproductive strategy of *Selkirkia* was comparable with that of modern meiobenthic priapulids and that energy invested by this Cambrian scalidophoran worm was possibly oriented towards quality rather than quantity (i.e., evolutionary trade-off concerning waptiid arthropods; Ou et al., 2020; Fig. 44E).

Our study also indicates that the general organization of female gonads in scalidophoran worms has remained virtually unchanged since the early Cambrian. Our findings provide, for the first time, key information on the reproductive organs and pre-embryonic development of Scalidophora. Whether the last common ancestor of Ecdysozoa possessed comparable paired organs and reproductive modes remains an open question which needs to be examined cautiously. Modern priapulids teach us that ecological factors may greatly influence reproductive strategies (microbenthic species tend to have a large number of small eggs in contrast with meiobenthic ones). Having that in mind, the reproductive system of *Selkirkia* may not represent the ancestral condition of scalidophorans but could simply result from its peculiar lifestyle (see Chapter 5.3).

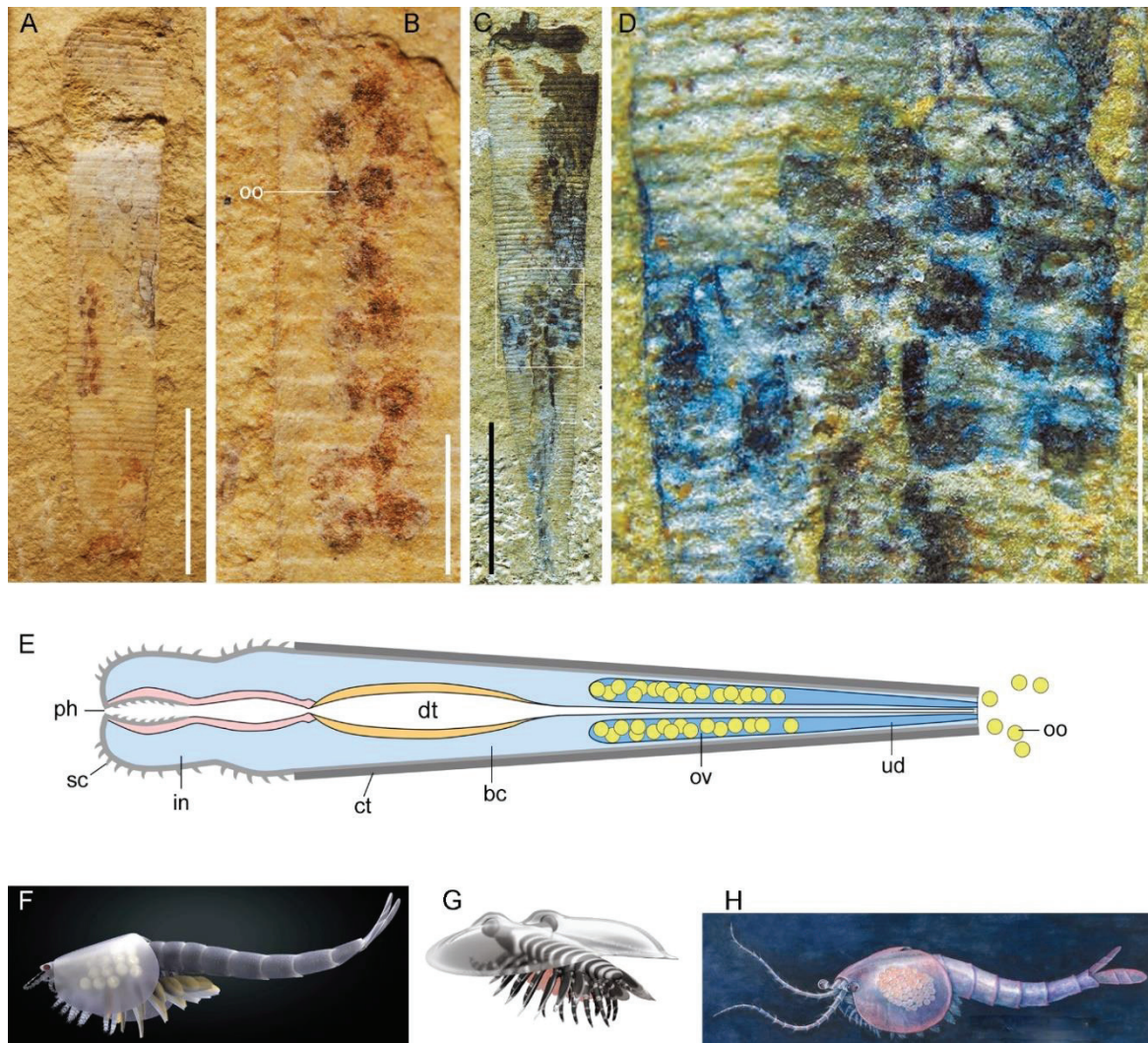


**Figure 44.** Reproductive system of Cambrian Ecdysozoa. A, B. *Selkirkia transita* sp. nov. from the Chengjiang Lagerstätte, showing longitudinal rows of oocytes, close-up. C, D. *Selkirkia sinica* from the Xiaoshiba Lagerstätte, showing oocyte clusters. E. diagram showing the reproductive system of *Selkirkia* (oocytes in yellow). F. *Waptia fieldensis* Walcott, 1912 from the mid-Cambrian Burgess Shale, with eggs brooded between the inner surface of the carapace and the body (reconstruction). G. *Kunmingella douvillei* Duan et al., 2014 from early Cambrian, with eggs attached to endopods and gathered ventrally (reconstruction). H. *Chuandianella ovata* Li, 1975 from early Cambrian, with eggs brooded between the inner surface of the carapace and the body. Abbreviations: bc, body cavity; ct, cuticular tube; dt, digestive tract; in, introvert; oo, oocyte; ov, ovary; ph, pharynx; sc, scalid; ud, urogenital duct. Scale bars: 5 mm (A), 4 mm (C), 1 mm (B, D). (C, D) from Yang et al. (submitted). (E-G) courtesy J. Vannier. (H) from Ou et al. (2020).

## SUBMITTED MANUSCRIPT

### Cambrian priapulid worms with oocytes and the evolution of reproductive systems in early Ecdysozoa

Xiao-yu Yang,<sup>1</sup> Jean Vannier,<sup>2</sup> Jie Yang,<sup>1</sup> Deng Wang,<sup>2,3</sup> and Xi-guang Zhang<sup>1,\*</sup>

<sup>1</sup>Key Laboratory for Paleobiology, MEC International Joint Laboratory for Paleoenvironment, Yunnan University, Chenggong Campus, Kunming 650500, China.

<sup>2</sup>Univ Lyon, Univ Lyon 1, ENSL, CNRS, LGL-TPE, F-69622, Villeurbanne, France.

<sup>3</sup>Shaanxi Key Laboratory of Early Life and Environments, State Key Laboratory of Continental Dynamics, Department of Geology, Northwest University, Xi'an 710069, China.

\*Correspondence: xgzhang@ynu.edu.cn (X.G.Z.)

#### SUMMARY

Although recent discoveries have brought to light vital aspects of the anatomy and embryonic development of Cambrian animals, their reproductive organs have long remained enigmatic. We describe here *in situ* oocyte clusters in the priapulid worm *Paraselkirkia sinica* from the Cambrian Stage 3 Xiaoshiba Lagerstätte (ca 514 Ma, S. China). These oocytes were less than 30 per individual, relatively large, and accommodated within paired tubular ovaries located in the posterior half of the blastocoelomic cavity as in modern meiobenthic priapulid worms, thus indicating that the general organization of female tubular gonads in priapulid worms has remained virtually unchanged for half a billion years. Our findings provide, for the first time, key information on the reproductive organs and pre-embryonic development of basal ecdysozoans. Comparative analysis on the reproductive strategies of *Paraselkirkia* and modern meiobenthic priapulids also reveals the possible influence of environment and ecology on the diversification of reproductive systems in early Cambrian animals.

**Keywords:** Priapulida, reproductive system, paleoecology, evolution, Burgess Shale-type preservation, China

Despite significant advances on vital aspects of the biology of early animals, many issues concerning their reproduction and developmental modes are still unresolved. Exceptionally preserved fossils from Lagerstätten such as that of the Burgess Shale and Chengjiang reveal exquisite details about the functional anatomy, lifestyles and behaviour of early animals but amazingly do not shed light on their reproductive organs. Fossilized eggs from the Palaeozoic Era are rare and limited to a few cases of isolated strands (Middle Pennsylvanian from Illinois [1]) or clusters laid by undetermined animals (Middle Cambrian Kaili Lagerstätte from China [2]) and to clutches carried or brooded by Cambrian arthropods [3–5]. In contrast, secondarily phosphatized embryos found in Cambrian Orsten-type deposits from China and Siberia [6–10] provide detailed information about the embryonic development of early animals but tell us nothing about the younger steps of their reproduction cycle (gonads, eggs, fertilization).

As shown by their rich fossil record, ecdysozoan worms were abundant and diverse throughout the Cambrian and are likely to have played a significant role in early benthic

ecosystems, as bioturbators [11,12], predators and recyclers [13]. They are well represented in several Cambrian Lagerstätten such as those of the Burgess Shale [14], Chengjiang [15] and Qingjiang [16]. Recent studies of *in situ* brooded eggs found in bivalved shrimp-like arthropods from these exceptional fossil localities showed that extended investment in offspring survivorship and possible evolutionary trade-offs related to brood care [3,4], possibly developed soon after the Cambrian emergence of animals. Exceptionally well-preserved embryos from the early Cambrian to the Early Ordovician have provided key information on the embryonic development of ecdysozoan worms. More precisely, synchrotron-radiation X-Ray-tomographic microscopy (SRXTM) has revealed three-dimensional aspects of the development of *Markuelia* [10], a worm comparable to living scalidophorans, but the reproductive organs and oogenesis of this animal still remain unknown.

We describe *in situ*-preserved oocytes in *Paraselkirkia sinica* Luo and Hu, 1999 [17], a priapulid worm from the Cambrian Stage 3 Xiaoshiba Lagerstätte (ca 514 Ma; east suburb of Kunming, Yunnan Province, China [18, 19]). This finding fills an important gap of knowledge concerning the reproduction of early priapulid worms. Detailed comparison with the reproductive system of modern meiobenthic priapulids leads to considering possible interactions between ecology and reproduction in the early evolution of the group.

## RESULTS

*Paraselkirkia sinica* is a typical element of the Chengjiang biota. This selkirkiid worm is about 15 mm long with a maximum length of 36 mm, and shares important morphological features with extant (e.g. priapulans [20]) and fossil scalidophoran worms, such as an eversible introvert lined with scaldid rows and a circum-oral pharyngeal structure bearing teeth (Figs. 1A,C,D, 2I and S1A). Its most distinctive, possibly derived character is the conical tube that encases the whole trunk. This protective tube is opened at both ends, bears numerous, evenly spaced rings (Figs. 1 and 2) and presumably represents a cuticular structure secreted by underlying epidermal tissues. *P. sinica* occurs in many early Cambrian localities in China and is frequently found in dense aggregations [21]. Selkirkiids are represented by two other Cambrian genera, namely *Selkirkia* from North America [22] and *Sullulika* from the Buen Formation of North Greenland [23]. Selkirkiids are often regarded as having close affinities with Priapulida and may belong to its stem group [51, 52].

Our study is based on about 200 specimens of *Paraselkirkia sinica*, all collected from the early Cambrian Stage 3 Xiaoshiba Lagerstätte (Kunming, eastern Yunnan Province, China). Like most fossils from this locality and those from the Chengjiang and Qingjiang Lagerstätten [15,16], *P. sinica* occurs as two-dimensional compressions [18,24], except its pellet-like gut contents (Figs. 1A, 2B,I and S1F) which retain some relief (see Micro-CT analysis; movie S1). Both internal (e.g. gut tract) and cuticular (e.g. introvert, pharynx, tube) features are underlined by brownish, reddish or yellowish iron oxides and locally by remains of organic matter. These oxides resulted from the weathering of both primary and secondary pyrite deposited on organic tissues through the action of sulphate-reducing bacteria under anaerobic conditions. This taphonomic scenario is common to other Cambrian Lagerstätten such as that of the Cambrian (Stage 3) Chengjiang [25,26], China and the Ordovician (Tremadocian) Fezouata Shale, Morocco [27].

Ovoid elements—usually no more than 30 pieces aggregated in clusters—were found in 11 specimens. They invariably occur below the transverse midline of the trunk, have a relatively sharp, rounded outline and often appear as conspicuous dark spots (Figs. 1, 2F,G and S1B–I). Their diameter ranges between 300 and 450  $\mu\text{m}$ . Some of them clearly lie on top of the intestine and are overprinted by the annulated pattern of the tube (Fig. 1G), indicating that they were located within the interspace between the digestive tract and the inner body wall (Fig. S1B–I) (blastocoelomic cavity as in extant priapulans; see Figs. 3 and 4). They do not seem to be scattered randomly within the internal cavity but instead form relatively coherent clusters (Fig. 1C–G). In a few specimens, they seem to spread as elongated, possibly paired clusters on either side of the gut (Figs. 1H,I and S1F,G). In others, clusters occur on a single side of the body (Fig. S1B–E,H,I). Their consistent location, shape and size all suggest that these rounded objects are eggs *sensu lato* (i.e. fertilized or not) carried by female individuals. No visible features suggest that these rounded bodies were attached to soft tissues as internal parasitic bodies normally do, or to the tube. Marked differences with the elongated pellet-like elements found within the gut (Figs. 1A and S1F) also invalidate the hypothesis that these ovoid structures might have been extruded gut contents. As revealed by elemental mapping (EDS), these eggs mainly contain C, Al and Si, with small amounts of Fe and P (Fig. S2). Comparable elemental composition was found in the brooded eggs of Cambrian bivalved arthropods such as *Waptia* and *Chuandianella* from the Burgess Shale [3] and Chengjiang Lagerstätten [4], respectively). C is likely to represent underlying thin carbon films of organic origin. Whereas micro-CT analysis revealed exquisite details of scalds and digestive tract (Fig. 2I and movie S1), it failed to provide insight into the detailed morphology of eggs (Fig. 2F–H). This might be due to their extreme flattening or their chemical composition such as a low concentration in iron oxides compared with other anatomical features.

Fluorescence imaging of one egg cluster (Fig. 1E) allowed to distinguish a possible external envelope (weak fluorescence) with sharp external margins from a brighter inner core which appears to be detached from the peripheral structure. This core shows no internal differentiation and may represent either a nucleus or the retracted remains of other material of biological origin (e.g. yolk).

Twenty-two of our specimens reveal a remarkable faunal association with lingulate and kutorginate [28] brachiopods (Fig. 2A–E). In each case, a single brachiopod is attached to one side of the posterior end of the tube of *Paraselkirkia*. Although brachiopod epibionts are frequent in various animal groups from other Cambrian localities [29,30], they were found in no other species from the Xiaoshiba Lagerstätte. Brachiopods are attached to selkirkiids with preserved internal organs, which suggest that both animals possibly formed a mutualistic association.

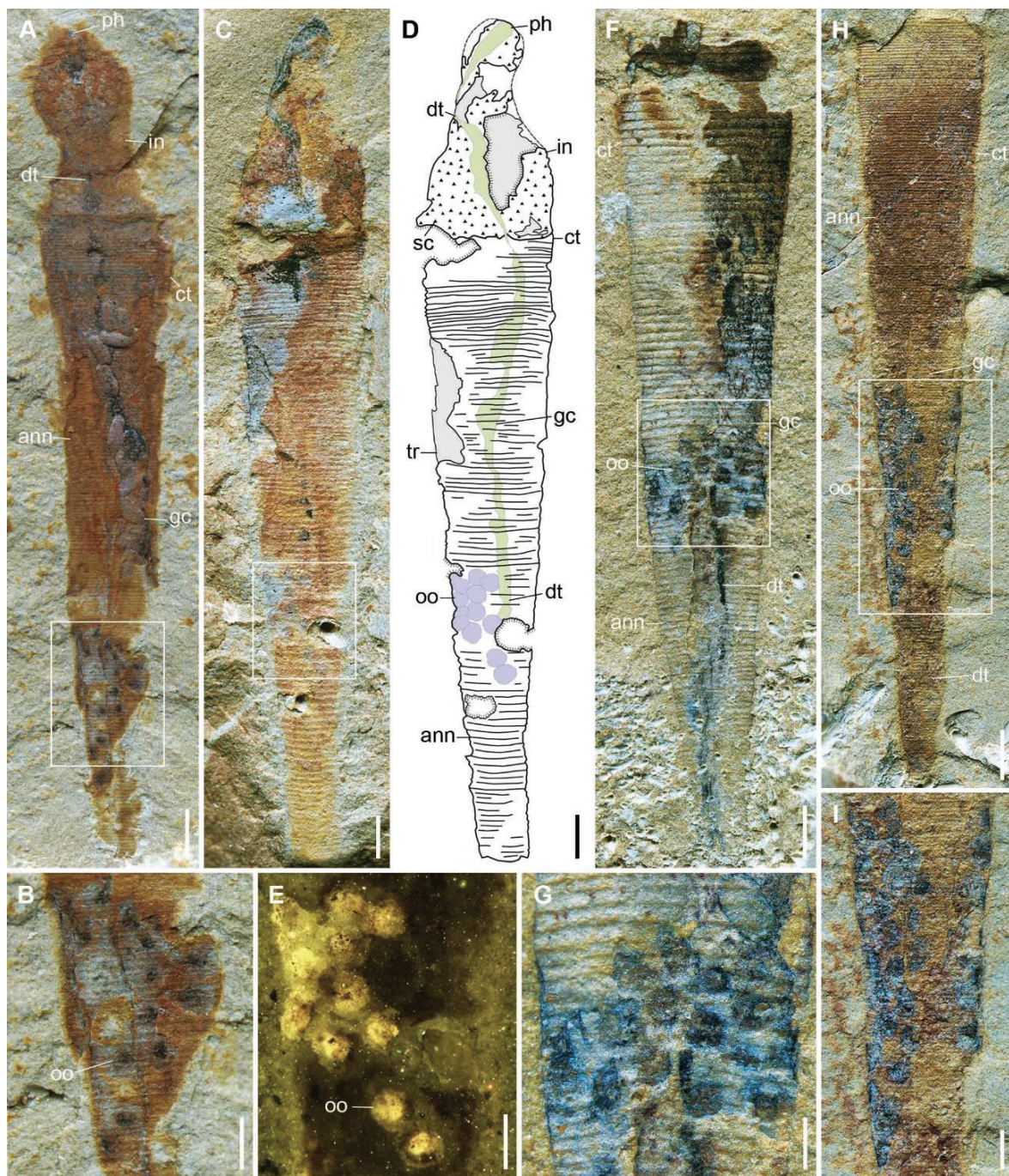


**Figure 1.** Oocyte-bearing *Paraselkirkia sinica* from the Cambrian Stage 3 Xiaoshiba Lagerstätte. (A,B) YKLP 12089: (A) incomplete specimen showing partly preserved introvert, digestive tract and oocytes; (B) Close-up (see location in A) showing oocytes within possible tubular ovaries. (C–E) YKLP 12350: (C) nearly complete specimen showing partly preserved introvert; (D) interpretative drawing; (E) fluorescence image of close-up (see location in C) showing oocytes. (F,G) YKLP 12351: (F) incomplete specimen (introvert missing) with oocytes within the tube; (G) close-up (see location in F) showing the egg cluster. (H,I) YKLP 12352: (H) complete tube showing oocytes; (I) close-up (see location in H) showing up to 30 eggs seemingly organized in longitudinal rows. Abbreviations: ann, annulation; ct, cuticular conical tube; dt, digestive tract; gc, gut contents; in, introvert; oo, oocytes; ph, pharynx; sc, scalid; tr, trunk. Scale bars: 1 mm (A,C,D,F,H) and 500  $\mu$ m (B,E,G,I).

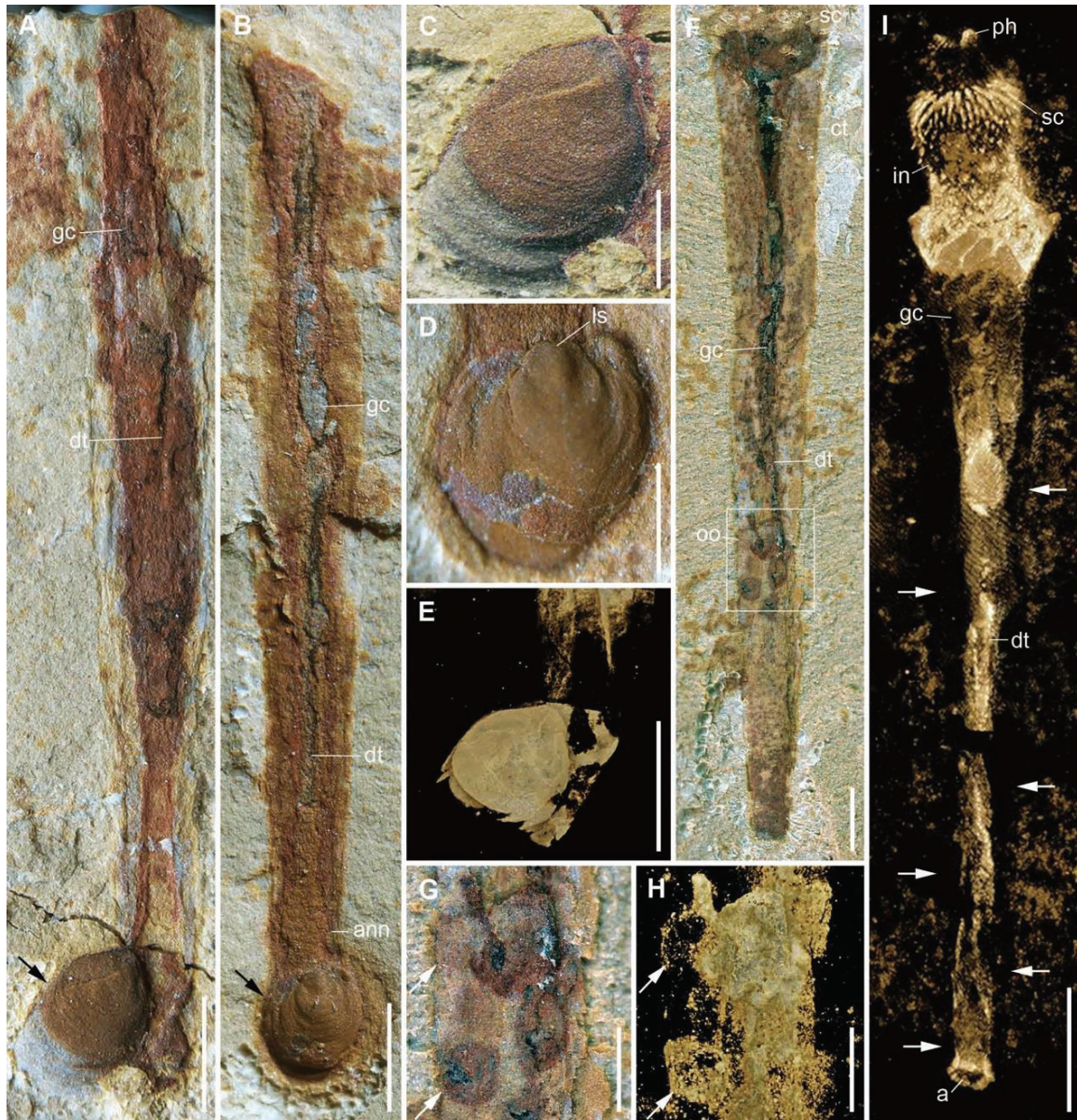


**Figure 2.** *Paraselkirkia sinica* from the Cambrian Stage 3 Xiaoshiba Lagerstätte: general morphology and brachiopod symbiont. (A,C,E) YKLP 12353: (A) a lingulate brachiopod (arrowed) attached close to the posterior opening of the tube; (C) close-up of the brachiopod; (E) dorsal perspective from a micro-CT scan. (B and D) YKLP 12354: (B) similar attachment by a kutorginate brachiopod (arrowed); (D) close-up of the brachiopod. (F–H) YKLP 12355, specimen with complete tube showing egg cluster: (F) general view; (G) close-up (see location in F) with the left three oocytes (arrowed); (H) micro-CT image showing poorly survived outlines of the oocytes (arrowed). (I) YKLP 12085, micro-CT image showing a complete, well-pyritized specimen showing detailed structures of introvert and digestive tract, and the boundary between the tube wall and the matrix is visible (arrowed). Abbreviations: ls, lower shell; others as in Fig. 1. Scale bars: 2 mm (I), 1 mm (A,B,F), and 500  $\mu$ m (C-E,G,H).

## Discussion

### *Reproduction in Paraselkirkia*

Extant priapulid worms provide key information essential to the understanding of the reproductive system of *Paraselkirkia*. The gonads of extant priapulids (females and males bear ovaries and testes, respectively [20]) are paired structures located in the posterior part of the

trunk as seen in *Priapulius caudatus* (dissected specimen; Fig. 3A, B) and *Maccabeus tentaculatus* (Fig. 3F-H). *Meiopriapulius fijiensis* with a single ovary seems to be an exception [31]. Priapulids are dioecious animals and reported cases of hermaphroditism are uncertain [32]. Gonads can reach a relatively large size especially in macrobenthic species such as *Priapulius caudatus* (Fig. 3A, B) and often occupy a major part of the blastocoelomic cavity in mature females. Observations and experiments [32,33] have shown that fertilization is external in macrobenthic species (*P. caudatus*) with females and males spawning their gametes slightly asynchronously into the water, most probably at or near the water-sediment interface although this phenomenon requires confirmation. In *Priapulius*, thousands of mature oocytes are released outside the body through paired urogenital ducts that open on either side of the anus [20,34,35]. External sexual dimorphism is absent in extant priapulids, except for *Tubiluchus* in which males differ from females in bearing numerous setae along their ventral side [34,36]. Internal fertilization in *Tubiluchus* is based on indirect evidence such as dimorphic features [37], the atypical morphology of spermatozoa [20], and occasional findings of spermatozoa embedded into the epithelium of the urogenital duct of female individuals of *T. philippinensis* [38]. The assumed internal fertilization of *Meiopriapulius fijiensis* is based on the observation of a single embryo that, questionably, seems to have been released from the female urogenital pore [39].

In macrobenthic species such as *Priapulius caudatus* and *Halicryptus spinulosus*, ovaries consist of a large number of ovarian sacs suspended between the gonoduct and a muscular strand [34,40], and usually contain thousands of oocytes (Figs. 3C-F and 4A) with a maximum diameter ( $D_o$ ) of 80 and 60  $\mu\text{m}$ , respectively [20]. In contrast, the vast majority of meiobenthic species have simple tubular ovaries that can only produce a small number of oocytes (Fig. 4B) during the breeding season. For example, *Meiopriapulius fijiensis* has fewer ( $N_o = 8$ ) but much larger oocytes ( $D_o = 250 \mu\text{m}$ ) [39] than in macrobenthic species. Similar reproduction modes are known in other meiobenthic species such as *Tubiluchus corallicola* ( $D_o = 80 \mu\text{m}$ ;  $N_o = 20$ ) [41] and *Maccabeus tentaculatus* ( $D_o = 100 \mu\text{m}$ ;  $N_o = 8$ ; [42] and see Fig. 3F-H)

*Paraselkirkia sinica* does not show any external sexual dimorphism or mechanism that would convincingly support internal fertilization. The fertilization and embryonic development (either direct or indirect) most probably took place outside the animal. In such a case, the relatively large ovoid elements ( $D_o = 300\text{--}450 \mu\text{m}$ ) of *P. sinica* should be interpreted as oocytes (non-fertilized eggs) rather than early embryos. Their relatively low number ( $N_o < 30$ ) and large size indicate marked differences with extant macrobenthic priapulids (table S1) and, instead, strong similarities with meiobenthic representatives of the group such as *Meiopriapulius fijiensis* ( $D_o = 250 \mu\text{m}$ ) and *Maccabeus tentaculatus* (Fig. 3G-H). Several specimens of *P. sinica* (Figs. 1H,I and S1B-I) have paired oocyte clusters and were possibly aligned within a tubular structure (Fig. 1A,B) as seen in *Tubiluchus corallicola* [41] and *Maccabeus tentaculatus* (Fig. 3G-H).

The cohesive appearance of some of the oocyte clusters (Fig. 1C-G) suggests that they were maintained within a single (e.g. tubular; *Maccabeus tentaculatus*, Fig. 3G-H) or more complex (e.g. *Priapulius*, Fig. 3A-D) ovarian structure before being released outside through the urogenital ducts, as observed in modern priapulids. In extant macrobenthic priapulids mature oocytes bulge into the coelomic cavity although tightly maintained by the ovarian basal lamina [20,34]. Such very thin supporting structures are prone to rapid decay after death (autolysis). If present in *Paraselkirkia*, they may have limited the dispersal of oocytes within the



blastocoelomic cavity, as observed in our fossil specimens (Fig. 1C–G). The relatively large internal structures observed within the oocytes of *Paraselkirkia* (fluorescence images, Fig. 1E) are comparable in size with the nucleus of oocytes in *Priapulid caudatus* (ca 40% of oocyte diameter) [40] and may therefore be interpreted as such.

Our study suggests that the general organization of the female reproductive system of priapulid worms with paired tubular ovaries, has remained virtually unchanged since the early Cambrian. Macrobenthic priapulid worms such as palaeoscoleoids are extremely abundant in Cambrian Lagerstätten (e.g. Chengjiang, Burgess Shale) and often display remarkably fine details of their anatomy. However, none of the thousands of specimens available in collections show any trace of eggs or embryos unlike other animal groups such as bivalved arthropods (e.g. *Waptia* and *Chuanodianella* with well-preserved brooded embryos [3,4]). One possible reason for this may be that the eggs of Cambrian macrobenthic priapulids were relatively small as in their modern counterparts (e.g. diameter between 60 and 80  $\mu\text{m}$ ), and had therefore very low potential to survive decay processes. If correct this hypothesis would imply that two types of reproductive mode may have coexisted among Cambrian priapulids, one in macrobenthic species (numerous small eggs) and the other in smaller forms such as *Paraselkirkia* (large eggs in much smaller number). The differentiation seen in extant priapulids may therefore have a very ancient origin.

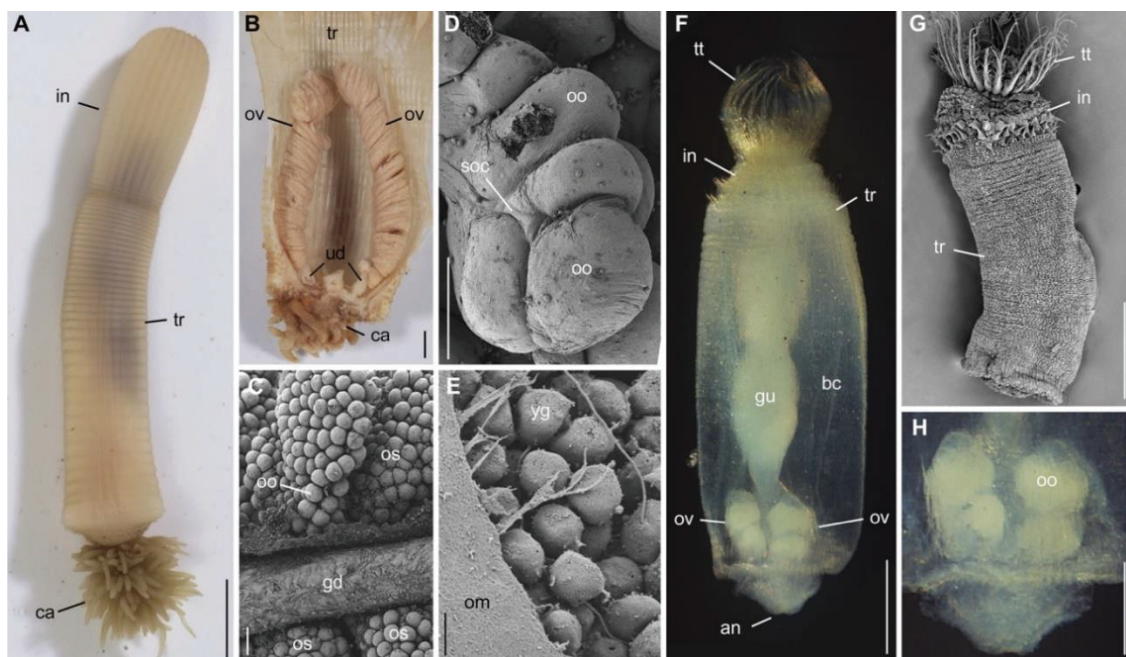


**Figure 3.** Female reproductive organs and oocytes in extant microbenthic and meiobenthic priapulid worms. (A–E) *Priapulid caudatus*. (A) Live specimen (in sea water). (B) Dissected specimen showing paired ovaries in the posterior part of the trunk. (C, D) Ovarian sacs bearing numerous oocytes and supporting structure. (E) Yolk spherules inside the oocyte (oocyte membrane removed). (F–H) *Maccabeus tentaculatus*. (F, H) Specimen bearing paired oocyte clusters (seen in transmitted light, under alcohol). (G) General view showing introvert crowned with tentacles (specialized scalids). (C–E, G) are SEM images. Abbreviations; an, anus; bc, blastocoelomic cavity; ca, caudal appendage; gd, gonoduct; in, introvert; om, oocyte membrane; oo, oocyte; os, ovarian sac; ov, ovary; soc, supporting ovarian cells; tr, trunk; tt, trichoscalids tentacles; ud, urogenital duct; ys, yolk spherule. A, B from the Gullmarsfjord, Sweden; C–E from the White Sea, Russia) and F–H from Cyprus. Scale bars: 1 cm (A), 2 mm (B); 100  $\mu\text{m}$  (C, D, G, H) and 2  $\mu\text{m}$  (E).

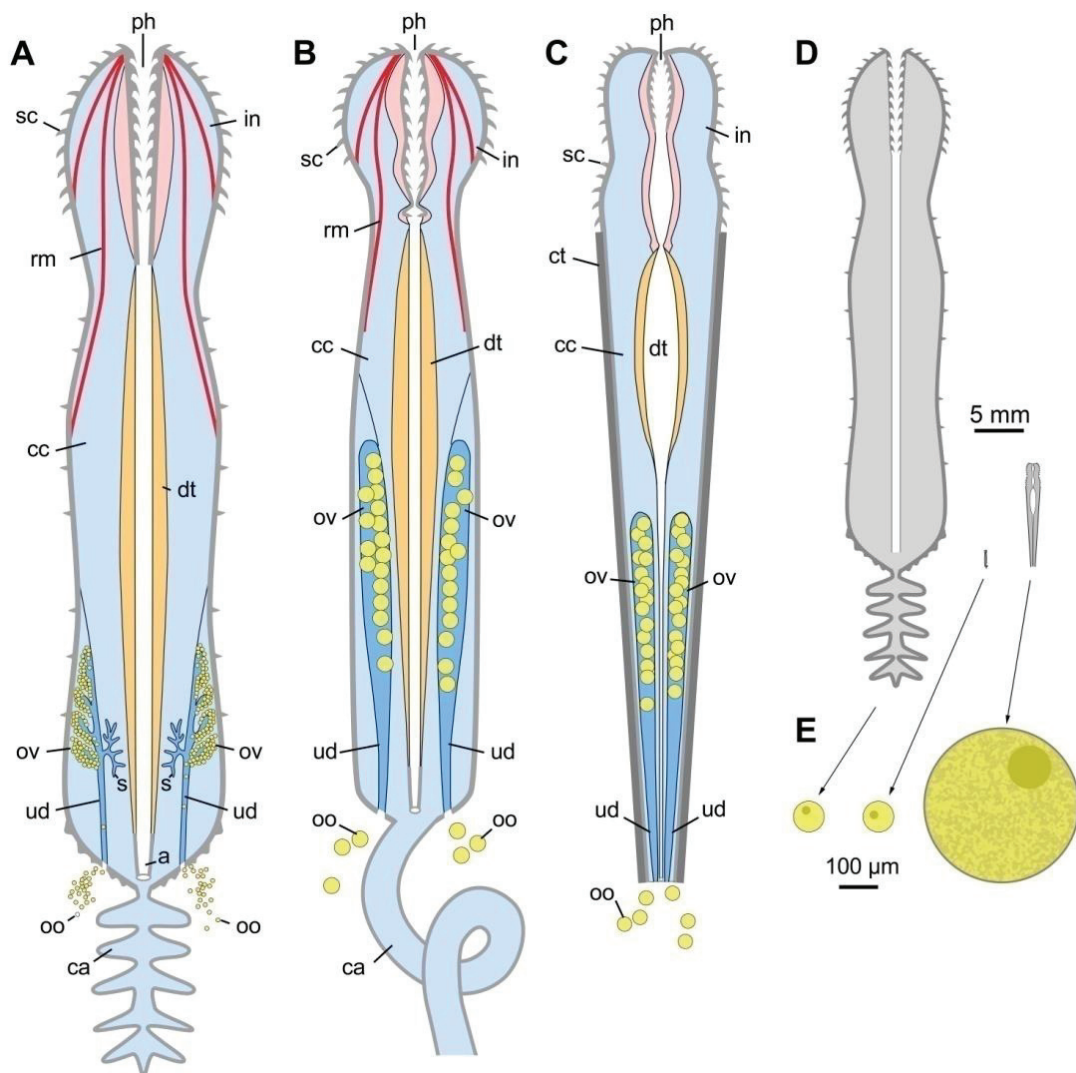


**Figure 4.** Comparative diagrams showing female reproductive organs in extant priapulans and early Cambrian *Paraselkirkia*. (A) Macrobenthic priapulans *Priapululus caudatus* (simplified after [20]). (B) Meiobenthic priapulans *Tubiluchus corallicola* (simplified after [41]). (C) Early Cambrian *Paraselkirkia sinica*. (simplified reconstruction). (D) Outline of the three forms represented at the same scale (from left to right: *Priapululus*, *Tubiluchus* and *Paraselkirkia*). (E) Mature oocytes of the three forms at the same scale. Coelomic cavity in light blue, ovaries in dark blue, oocytes in yellow, muscular tissues in light red (around pharynx), digestive tissues in light orange, cuticle in gray. Retractor muscles may be present in *Paraselkirkia* but are not represented. Abbreviations: a, anus; ca, caudal appendage; cc, coelomic cavity; ct, cuticular conical tube; dt, digestive tract; in, introvert; oo, oocytes; ov, ovary; ph, pharynx; rm, retractor muscle; s, solenocytes; sc, scalid; ud, urogenital duct.

### Lifestyle

Selkirkiids have been interpreted as burrowers that possibly lived vertically embedded in sediment [15,22], or alternatively as epibenthic tubicolous worms [43] based on the argument that a worm encased within a rigid tube is unable to move through sediment and cannot have an endobenthic lifestyle. Although selkirkiids may have relatively limited capacities to move through their environment, compared with non-tubicolous forms, their introvert was well-developed, eversible and most likely able to penetrate soft sediment. Scalids (introvert) and

the close contact of the trunk with the internal surface of the tube both represent potential anchoring features essential to locomotion. Numerous extant tubicolous animals as diverse as annelids (e.g. sabellids) and scaphopod molluscs live buried in sediment. Their tube plays an important protective and anchoring role, irrespective of its secretion mode (e.g. agglutinated of particles, calcified shell, cuticle). A permanent epibenthic lifestyle [43] would have probably exposed selkirkiids to predation and removal by bottom currents. It seems more realistic to consider them as benthic animals living close to the water-sediment interface. Association with brachiopods provides additional support to this interpretation. The brachiopods found in association with *Paraselkirkia* are all relatively small (ca 1 mm in length), lack a long pedicle and are always attached to the posterior end of the tube (Fig. 2A–E). Ovoid features previously interpreted as caudal outgrowths [21] more likely represent brachiopod valves. The brachiopod feeding mode is generated by lophophoral cilia and requires constant contact with circulating water. These ecological constraints and the preferential location of brachiopods along the tub, both suggest that *Paraselkirkia* lived relatively close to the water-sediment interface (Fig. 5), possibly maintaining contact with it via the posterior tip of its tube, as seen in modern scaphopod molluscs. Importantly, its assumed position in sediment would be consistent with gametes being released at or very close to the water-sediment interface, thus facilitating external fertilization. Brachiopod epibionts are likely to have colonized their host for only part of its life cycle (e.g. between successive moulting stages)

#### ***Relation between reproduction mode and ecology***

The reproduction mode of *Paraselkirkia* differs from that of extant macrobenthic priapulids (e.g. *Priapulidus*; large number of small oocytes) and instead shares close similarities with meiobenthic forms (e.g. *Meiopriapulidus fijiensis* [39], *Tubiluchus corallicola* [41] and *Maccabeus tentaculatus*) that inhabit interstitial benthic environments and typically produce a small number of large oocytes (e.g. compare Fig. 1F, G and Fig. 3F–H). This raises the question of the possible relation between ecology and reproductive mode in extant and early priapulids. In meiobenthic priapulids, optimal offspring survivorship seems to be achieved through a small number of yolk-rich embryos that presumably develop within a protective interstitial environment, suggesting that energy investment is oriented towards quality rather than quantity. Each fertilized embryo has a relatively high probability of surviving to adulthood (e.g. as in K-selected species). By releasing thousands of gametes presumably outside, macrobenthic species, on the contrary, seem to rely on a different reproductive strategy. Their embryos are likely to develop in a less protective environment, comparatively more exposed to predation and physical damage than in interstitial species, in which the important loss of offspring is offset by high fecundity (e.g. as in r-selected species). The reproductive strategy of both Cambrian selkirkiids and modern meiobenthic priapulids may result from shared ecological features and constraints, such as a relatively small size, infaunal habits and limited mobility. Selkirkiids might provide a rare example of the possible impact of ecology on the reproductive strategies of early Cambrian animals.

The reproductive mode of selkirkiids may not represent the ancestral condition for priapulids but more likely a derived state largely constrained by ecological factors (e.g. tubicolous lifestyle, low mobility). Similarly, *Facivermis*, a lobopodian from the early Cambrian [44] offers another example of highly specialized and tube dwelling animal with a derived position within the onychophoran stem-group and a lifestyle radically different from all other lobopodians.

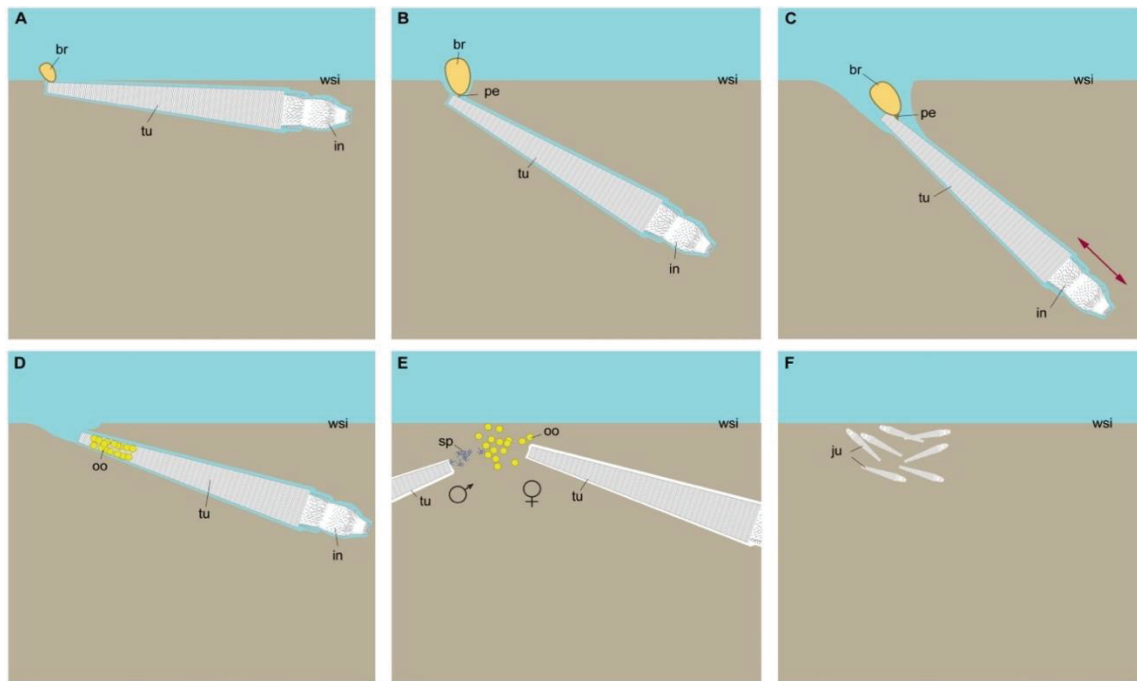


**Figure 5.** Lifestyle and reproduction in *Paraselkirkia* inferred from fossil evidence. (A–C) *Paraselkirkia* living close the water-sediment interface; juvenile brachiopod attached to the posterior end of the tube, which grows in size; worm represented in an assumed tilted position within sediment; locomotion and feeding achieved via the eversion/inversion of introvert (red arrows) and muscular contractions. (D–F) Reproduction cycle showing oocytes in ovaries, release of oocytes and spermatozooids near the water-sediment interface, external fertilization and juveniles in sediment. Abbreviations: br, brachiopod; in, introvert; ju, juveniles; oo, oocytes; pe, pedicle; sp, spermatozooids; tu, tube; wsi, water-sediment interface.

### **Early evolution of reproductive systems**

Present-day metazoans display a huge variety of asexual and sexual reproduction modes that include aspects related to the formation of gametes and gonads, fertilization processes and embryonic development. Gonads are either tubular organs or more complex sac-like structures often arranged in symmetrical pairs. The development mode of gonads is diverse and suggests that they probably evolved independently within various metazoan groups [45]. Fertilization occurs externally or internally via copulation or other methods such as the deposition of spermatophores. Diverse brood care behaviours accompany the embryonic development of numerous extant species (e.g. crustaceans). The reproductive behaviour of early animals has remained largely enigmatic because of the lack or scarcity of information on their reproductive organs and strategies. However, exceptional fossils from lower Palaeozoic Lagerstätten provide key elements that shed light on the evolution of the reproductive systems of a particular group, the ecdysozoans which stand as a major element of early animal life (Fig. 6). First, paired ovaries and external fertilization seem to characterize basal scalidophorans exemplified here by *Paraselkirkia*; 2) Brood care is known from two groups of lower Palaeozoic euarthropods, the Cambrian waptiids [3,4] and Ordovician ostracods [46]. In waptiids, egg clusters are carried symmetrically on either side the female's body suggesting that they were released from paired gonads as in *Paraselkirkia*; 3) Copulatory organs known in early Silurian myodocope ostracods from the Hereforshire Lagerstätte [47] (ca 425 Ma) indicate that copulation and internal fertilization have a very ancient origin among euarthropods. Although

fragmentary and limited to a single clade, these few examples suggest that at least four of the most essential features of bilaterian reproduction (paired gonads, external and internal fertilization, copulation) had already evolved through various ecdysozoan lineages during the early Palaeozoic.

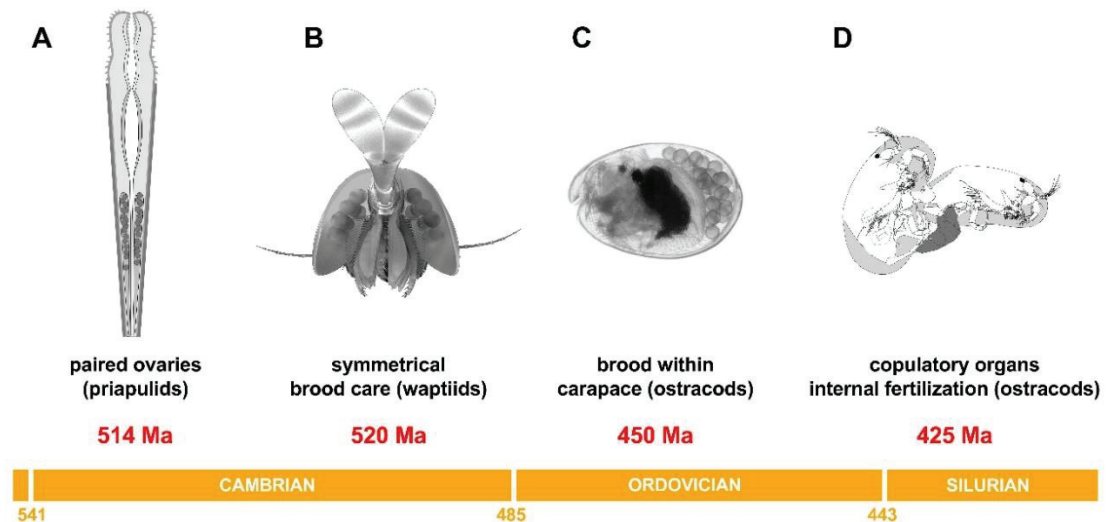


**Figure 6.** Key reproductive features in early ecdysozoan animals (oldest fossil occurrence in red). (A) Paired ovaries in early Cambrian priapulid worms (this paper). (B) Brood care in Cambrian shrimp-like waptiid euarthropods (egg clusters on either side of the female’s body, protected by carapace flaps [3,4]). (C) Brood care in Ordovician ostracod (Crustacea) euarthropods [46]. (D) Copulatory organ in Silurian ostracod euarthropods [47]. B is from an animated reconstruction [49]; C is an extant myodocope ostracod [3] brooding eggs in a manner identical to its Ordovician ancestors [46]; D represents the copulating behaviour of extant ostracods [50]; copulatory organs found in Silurian ostracods suggest comparable copulatory behaviour in ancestral representatives of the group.

## ACKNOWLEDGMENTS

This study was supported by the National Natural Science Foundation of China (41730318) to X.G.Z. and J.Y., the Innovative Research Fund for Graduate Students of Yunnan University (2019228) to X.Y.Y., the ASSEMBLE, PRC (CNRS, France and NSFC, China) and PAI (Univ. Lyon 1, Région Auvergne Rhône Alpes) grants to J.V. We thank T. Lan, J.-B. Hou, K.-S. Du, J.-F. He and K.-R. Li for assistance with field work, Q. Ou for help with literature search, H.-J. Mai for assistance with micro-CT analysis, the staff of the Kristineberg Marine Station (Sweden) for assistance in collecting extant priapulans, A. Chipman (Hebrew University of Jerusalem, Israel) for the loan of Maccabeus specimens from Cyprus, the Centre Technologique des Microstructures (CTμ, Univ. Lyon 1, France) and C. Aria for linguistic corrections and insightful remarks.

## AUTHOR CONTRIBUTIONS

J.Y. collected the material and provided the geological information; X.Y.Y., X.G.Z. and J.V. designed the study; X.Y.Y., J.V., J.Y. and X.G.Z. performed the investigation; X.Y.Y., J.V. and X.G.Z. wrote the manuscript with input from other authors; J.Y. prepared all fossils for photography; X.Y.Y. and X.G.Z. produced the fossil figures, D.W. and J.V. studied extant priapulans and produced the relevant figures and drawings, and X.Y.Y. designed and operated the elemental map analysis.

## DECLARATION OF INTERESTS

The authors declare no competing interest.

## METHODS

All studied specimens are from the early Cambrian Stage 3 (local Canglangpuan) Hongjingshao Formation at the Xiaoshiba section near Kunming, eastern part of Yunnan Province (ca 3.7 km SE of Ala village [18]). They are deposited in the collections of the Key Laboratory for Paleobiology, Yunnan University (<http://www.yklp.ynu.edu.cn/>). Fossils were prepared manually with fine needles under high a Nikon SMZ800 or 1500 stereomicroscope, imaged using a Leica DFC 500 digital camera mounted on a Leica M205-C Stereoscope under bright-field illumination, a Leica DFC7000 T monochrome digital camera attached to a Leica M205 FA fluorescence stereomicroscope and a FEI Quanta 650 Scanning Electron Microscope (SEM) under low vacuum (including elemental mapping). Extant priapulids from Sweden, Russia and Cyprus were fixed with glutaraldehyde or formaldehyde, dried in a Leica critical point dryer and observed under a Zeiss Merlin Compact SEM. Digital photographs were processed with Adobe Photoshop CS6 and CorelDRAW X8, diagrams with Adobe Illustrator CS6. Selected specimens were scanned using *X-ray computed microtomography* (Zeiss Xradia 520) to explore potential internal structures, and the data were processed with Drishti (Version 2.6.4) software, resulting in a suite of the 3D-projection images representing thin sections of the examined specimens (e.g. Fig. 2E,H,I, scanning resolution was 3.56 $\mu$ m, 3.96  $\mu$ m and 4.92  $\mu$ m, respectively).

## REFERENCES

1. Godfrey, S.J. (1992). Fossilized eggs from Illinois. *Nature* 356, 21.
2. Lin, J.-P., Scott, A.C., Li, C.-W., Wu, H.-J., Ausich, W.I. Zhao, Y.-L., and Hwu, Y.-K. (2006). Silicified egg clusters from a Middle Cambrian Burgess Shale-type deposit, Guizhou, south China. *Geology* 34, 1037–1040.
3. Caron, J.-B., and Vannier, J. (2016). *Waptia* and the diversification of brood care in early arthropods. *Curr. Biol.* 26, 69–74.
4. Ou, Q., Vannier, J., Yang, X.-F., Chen, A.-L., Mai, H.-J., Shu, D.-G., Han, J., Fu, D.-J., Wang, R., and Mayer, G. (2020). Evolutionary trade-off in reproduction of Cambrian arthropods. *Sci. Adv.* 6, eaaz3376.
5. Duan, Y.-H., Han, J., Fu, D.-J., Zhang, X.-L., Yang, X.-G., Komiya, T., and Shu, D.-G. (2014). Reproductive strategy of the bradoriid arthropod *Kunmingella douvillei* from the Lower Cambrian Chengjiang Lagerstätte, South China. *Gondwana Res.* 25, 983–990.
6. Zhang, X.-G., and Pratt, B.R. (1994). Middle Cambrian arthropod embryos with blastomeres. *Science* 266, 637–639.
7. Bengtson, S., and Yue, Z. (1997). Fossilized metazoan embryos from the earliest Cambrian. *Science* 277, 1645–1648.
8. Conway Morris, S. (1998). Eggs and embryos from the Cambrian. *BioEssays* 20, 676–682.
9. Dong, X.-P., Donoghue, P.C.J., Cheng, H., and Liu, J.-B. (2004). Fossil embryos from the Middle and Late Cambrian period of Hunan, south China. *Nature* 427, 237–240.

10. Donoghue, P.C.J., Bengtson, S., Dong, X.-P., Gostling, N.J., Hultgren, T., Cunningham, J.A., Yin, C.-Y., Yue, Z., Peng, F., and Stampanoni, M. (2006). Synchrotron X-ray tomographic microscopy of fossil embryos. *Nature* 442, 680–683.
11. Kesidis, G., Slater, B.J., Jensen, S., and Budd, G.E. (2019). Caught in the act: priapulid burrowers in early Cambrian substrates. *Proc. R. Soc. B* 286, 20182505.
12. Vannier, J., Calandra, I., Gaillard, C., and Żylińska, A. (2010). Priapulid worms: Pioneer horizontal burrowers at the Precambrian-Cambrian boundary. *Geology* 38, 711–714.
13. Vannier, J. (2012). Gut contents as direct indicators for trophic relationships in the Cambrian marine ecosystem. *PLoS ONE* 7, e52200.
14. Briggs, D.E.G., Erwin, D.H., and Collier, F.J. (1994). *The Fossils of the Burgess Shale* (Washington and London: Smithsonian Institution Press).
15. Hou, X.-G., Siveter, D.J., Siveter, D.J., Aldridge, R.J., Cong, P.-Y., Gabbott, S.E., Ma, X.-Y., Purnell, M.A., and Williams, M. (2017). *The Cambrian Fossils of Chengjiang, China: The Flowering of Early Animal Life* (Chichester: Wiley Blackwell).
16. Fu, D.-J., Tong, G.-H., Dai, T., Liu, W., Yang, Y.-N., Zhang, Y., Cui, L.-H., Li, L.-Y., Yun, H., and Wu, Y. et al. (2019). The Qingjiang biota—a Burgess Shale-type fossil Lagerstätte from the early Cambrian of South China. *Science* 363, 1338–1342.
17. Luo, H.-L., Hu, S.-X., Chen, L.-Z., Zhang, S.-S., and Tao, Y.-H. (1999). *Early Cambrian Chengjiang Fauna from Kunming Region, China* (Kunming: Yunnan Science & Technology Press).
18. Yang, J., Ortega-Hernández, J., Legg, D.A., Lan, T., Hou, J.-B., and Zhang, X.-G. (2018). Early Cambrian fuxianhuiids from China reveal origin of the gnathobasic protopodite in euarthropods. *Nat. Commun.* 9, 470.
19. Hou, J.-B., Yang, J., Zhang, X.-G., Hughes, N.C., and Lan, T. (2019). Trilobite-based biostratigraphy of the Xiaoshiba Lagerstätte. *Fossils and Strata*, 173–191.
20. Schmidt-Rhaesa, A. (2013). Priapulida. In *Handbook of Zoology. Gastrotricha, Cycloneuralia and Gnathifera*, A. Schmidt-Rhaesa, ed. (Berlin, Germany: Walter de Gruyter GmbH), pp. 147–180.
21. Lan, T., Yang, J., Hou, J.-B., and Zhang, X.-G. (2015). The feeding behaviour of the Cambrian tubiculous priapulid *Selkirkia*. *Lethaia* 48, 125–132.
22. Conway Morris, S. (1977). Fossil priapulid worms. *Spec. Pap. Palaeontol.* 20, 1–95.
23. Peel, J.S., and Willman, S. (2018). The Buen Formation (Cambrian Series 2) biota of North Greenland. *Pap. Palaeontol.* 4, 381–432.
24. Yang, J., Ortega-Hernández, J., Butterfield, N.J., and Zhang, X.-G. (2013). Specialized appendages in fuxianhuiids and the head organization of early euarthropods. *Nature* 494, 468–471.
25. Gabbott, S.E., Hou, X.-G., Norry, M.J., and Siveter, D.J. (2004). Preservation of Early Cambrian animals of the Chengjiang biota. *Geology* 32, 901–904.
26. Zhu, M.-Y., Babcock, L.E., and Steiner, M. (2005). Fossilization modes in the Chengjiang Lagerstätte (Cambrian of China): testing the role of organic preservation and diagenetic alteration in exceptional preservation. *Palaeogeogr. Palaeoclimatol. Palaeoecol.* 220, 31–46.
27. Kouraiss, K., El Hariri, K., El Albani, A., Azizi, A., Mazurier, A., and Vannier, J. (2018). X-ray microtomography applied to fossils preserved in compression: Palaeoscolecoid worms

- from the Lower Ordovician Fezouata Shale. *Palaeogeogr. Palaeoclimatol. Palaeoecol.* 508, 48–58.
28. Holmer, L.E., Zhang, Z.-F., Topper, T.P., Popov, L., and Claybourn, T.M. (2018). The attachment strategies of Cambrian kutorginate brachiopods: the curious case of two pedicle openings and their phylogenetic significance. *J. Paleontol.* 92, 33–39.
  29. Zhang, Z.-F., Han, J., Wang, Y., Emig, C.C., and Shu, D.-G. (2010). Epibionts on the lingulate brachiopod *Diandongia* from the Early Cambrian Chengjiang Lagerstätte, South China. *Proc. R. Soc. B* 277, 175–181.
  30. Topper, T.P., Strotz, L.C., Holmer, L.E., and Caron, J.-B. (2015). Survival on a soft seafloor: life strategies of brachiopods from the Cambrian Burgess Shale. *Earth-Sci. Rev.* 151, 266–287.
  31. Storch, V., Higgins, R.P., and Morse, M.P. (1989). Internal anatomy of *Meiopriapulidus fijiensis* (Priapulida). *Trans. Am. Microsc. Soc.* 108, 245–261.
  32. Wennberg, S.A. (2008). Aspects of priapulid development, *Ph.D. Thesis*. Uppsala University.
  33. Wennberg, S.A., Janssen, R., and Budd, G.E. (2009). Hatching and earliest larval stages of the priapulid worm *Priapulidus caudatus*. *Invertebr. Biol.* 128, 157–171.
  34. van der Land, J. (1975). Priapulida. In *Reproduction of Marine Invertebrates*, A. Giese, and J.S. Pearse, eds. (New York: Academic Press), pp. 55–65.
  35. Storch, V. (1991). Priapulida. In *Microscopic Anatomy of Invertebrates*. Aschelminthes, F.W. Harrison, and E.E. Ruppert, eds. (New York: Wiley-Liss), pp. 333–350.
  36. Schmidt-Rhaesa, A., Rothe, B.H., and Martínez, A.G. (2013). *Tubiluchus lemburgi*, a new species of meiobenthic Priapulida. *Zool. Anz.* 253, 158–163.
  37. van der Land, J. (1970). Systematics, zoogeography, and ecology of the Priapulida. *Zool. Verh.* 112, 1–118.
  38. Alberti, G., and Storch, V. (1988). Internal fertilization in a meiobenthic priapulid worm: *Tubiluchus philippinensis* (Tubiluchidae, Priapulida). *Protoplasma* 143, 193–196.
  39. Higgins, R.P., and Storch, V. (1991). Evidence for direct development in *Meiopriapulidus fijiensis* (Priapulida). *T. Am. Microsc. Soc.* 110, 37–46.
  40. Nørrevang, A., and van der Land, J. (1983). Priapulida. In *Reproductive Biology of Invertebrates. Oogenesis, Oviposition, and Oosorption*, K.G. Adiyodi, and R.G. Adiyodi, eds. (Chichester: John Wiley & Sons), pp. 269–282.
  41. Kirsteuer, E., and van der Land, J. (1970). Some notes on *Tubiluchus corallicola* (Priapulida) from Barbados, West Indies. *Mar. Biol.* 7, 230–238.
  42. Por, F.D., and Bromley, H.J. (1974). Morphology and anatomy of *Maccabeus tentaculatus* (Priapulida: Seticoronaria). *J. Zool.* 173, 173–197.
  43. Maas, A. Huang, D.-Y., Chen, J.-Y., Waloszek, D., and Braun, A. (2007). Maotianshan-Shale nemathelminthes—morphology, biology, and the phylogeny of Nemathelminthes. *Palaeogeogr. Palaeoclimatol. Palaeoecol.* 254, 288–306.
  44. Howard, R.J., Hou, X.-G., Edgecombe, G.D., Salge, T., Shi, X.-M., and Ma, X.-Y. (2020). A tube-dwelling early Cambrian lobopodian. *Curr. Biol.* 30, 1529–1536.
  45. Schmidt-Rhaesa, A. (2007). *The Evolution of Organ Systems* (Oxford and New York: Oxford University Press).
  46. Siveter, D.J., Tanaka, G., Farrell, Ú.C., Martin, M.J., Siveter, D.J., and Briggs, D.E.G. (2014). Exceptionally preserved 450-million-year-old ordovician ostracods with brood care. *Curr. Biol.* 24, 801–806.



47. Siveter, D.J., Sutton, M.D., Briggs, D.E.G., and Siveter, D.J. (2003). An ostracode crustacean with soft parts from the Lower Silurian. *Science* 302, 1749–1751.
48. dos Reis, M., Thawornwattana, Y., Angelis, K., Telford, M.J., Donoghue, P.C.J., and Yang, Z.-H. (2015). Uncertainty in the timing of origin of animals and the limits of precision in molecular timescales. *Curr. Biol.* 25, 2939–2950.
49. Vannier, J., Aria, C., Taylor, R.S., and Caron, J.-B. (2018). *Waptia fieldensis* Walcott, a mandibulate arthropod from the middle Cambrian Burgess Shale biota. *R. Soc. open sci.* 5, 172206.
50. Smith, R.J., and Kamiya, T. (2007). Copulatory behaviour and sexual morphology of three *Fabaeformiscandona* Krstić, 1972 (Candoninae, Ostracoda, Crustacea) species from Japan, including descriptions of two new species. *Hydrobiologia* 585, 225–248.
51. Budd, G.E., and Jensen, S. (2000). A critical reappraisal of the fossil record of the bilaterian phyla. *Biol. Rev.* 75, 253–295.
52. Smith, M.R., Harvey, T.H.P., and Butterfield, N.J. (2015). The macro- and microfossil record of the Cambrian priapulid *Ottoia*. *Palaeontology* 58, 705–721.

## **Supplementary materials**

### **Cambrian priapulid worms with oocytes and the evolution of reproductive systems in early Ecdysozoa**

Xiao-yu Yang, Jean Vannier, Jie Yang, Deng Wang, and Xi-guang Zhang



**Figure S1.** *Paraselkirkia sinica* (Priapulida) from the Cambrian Stage 3 Xiaoshiba Lagerstätte. (A) YKLP 12356, complete specimen showing body and remains of tube to which a poorly preserved lingulate brachiopod is attached (arrowed). (B and C) YKLP 12357, nearly complete specimen, general view and close-up (see location in B) showing oocyte cluster (see explanation in text) along one side of the body between the digestive tract and the inner body wall. (D and E) YKLP 12358, nearly complete specimen, general view and close-up (see location in D) on a few visible eggs. (F and G) YKLP 12359, incomplete specimen, general view (note bradoriid valve, arrowed) and close-up (see location in F) showing paired oocyte clusters. (H and I) YKLP 12360, part and counterpart, respectively, general view and close-up (see location in H) showing a few oocytes. Abbreviations as in Fig 1. Scale bars: 1 mm (A, B, D, F and H) and 500  $\mu$ m (C, E, G and I).

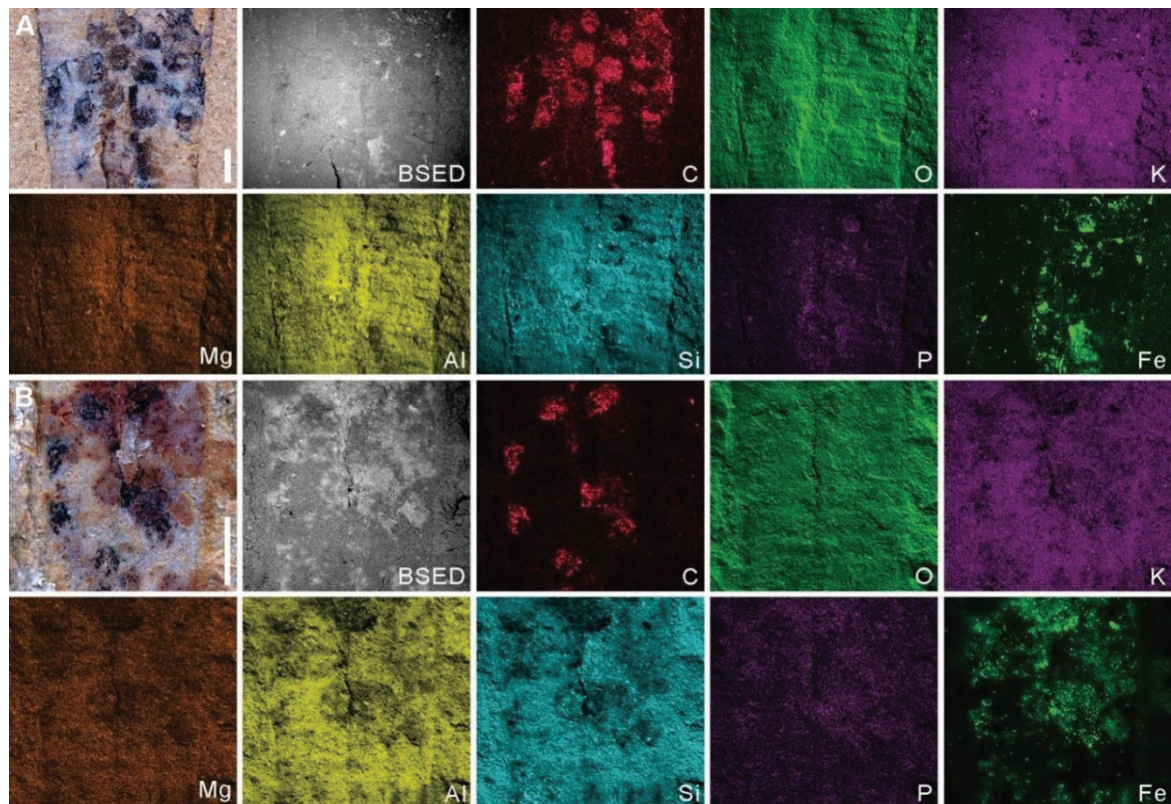


**Figure S2.** Elemental maps of egg clusters in *Paraselkirkia sinica* from the Cambrian Stage 3 Xiaoshiba Lagerstätte. (A) YKLP 12351; (B) YKLP 12361. Note enrichment in carbon in oocytes of both specimens. Abbreviation: BSED, Back-scattered Electron Detector. Scale bars: 500  $\mu\text{m}$  (A and B).

Species	L (mm)	Do ( $\mu\text{m}$ )	No	Do/L (%)	ovaries	external dimorphism	lifestyle	refs
<i>Priapulius caudatus</i>	100	80	thousands	0.08	complex, tree-shaped	none	macrobenthic	Schmidt-Rhaesa 2013
<i>Halicrytus spinulosus</i>	40	60	thousands	0.15	complex, tree-shaped	none	macrobenthic	Schmidt-Rhaesa 2013
<i>Tubiluchus corallicola</i>	2.5	80	20	3.2	simple, tubular	setae on male abdomen	meiobenthic ?	Kirsteuer & van der Land 1970
<i>Maccabeus tentaculatus</i>	2.85	80	8	2.8	simple, tubular	none	meiobenthic	Por & Bromley 1974
<i>Metopriapulius fijiensis</i>	2.15	250	6	11.6	simple, tubular	none	meiobenthic	Higgins & Storch 1991
<i>Paraselkirkia sinica</i>	15	450	30	3.0	probably tubular	none	macrobenthic	this paper

**Table S1.** Measurements of *Paraselkirkia sinica* (Cambrian) and extant macrobenthic and meiobenthic priapulids. Do, diameter of oocytes; L, approximate adult body length; No, approximate number of oocytes.

## 5.5 Phylogeny of scalidophorans

### 5.5.1 Previous work

Attempts to reconstruct the phylogeny of Scalidophora (Priapulida, Kinorhyncha, Loricifera) have been made by several authors, based on the analysis of either anatomical characters (Ax, 1996; Nielsen, 2012; Schmidt-Rhaesa, 1998) or molecular data (Laumer et al., 2019; Webster et al., 2006). Some of these phylogenies integrate morphological data obtained from fossils (Liu et al., 2014; Zhang et al., 2015). The eversible introvert bearing various types of scalids is often seen as the principal synapomorphy of Scalidophora (Bang-Berthelsen et al., 2013; Neuhaus, 2013; Schmidt-Rhaesa, 2013). However, the phylogenetic relationships between and among scalidophoran groups are still unsolved. The presence of a loricate larva in both Priapulida and Loricifera has led authors (Ax, 2003; Lemburg, 1999) to consider these two groups (grouped under the term Vincitplicata) as the sister group to Kinorhyncha. Some molecular phylogenies indicate that Priapulida is the sister group of Kinorhyncha plus Loricifera (Dunn et al., 2008). Others instead suggest that Loricifera is the sister group of Nematomorpha (Park et al., 2006; Sørensen et al., 2008; Fig. 6G) or that Priapulida is the sister group to the remaining seven ecdysozoan phyla (Laumer et al., 2019; Petrov and Vladychenskaya, 2005; Webster et al., 2006; Fig. 6G).

This apparent inconsistency may be attributed to the limited sampling of scalidophoran taxa (Giribet and Edgecombe, 2017) and to analyses based on single datasets (e.g. 18S rRNA, Park et al., 2006). Recent studies reconsidered the significance of anatomical data (Annapurna et al., 2017; Herranz et al., 2019; Schmidt-Rhaesa and Freese, 2019) and gave a more appropriate balance between molecular and morphological data obtained from extant species (Hogvall et al., 2019; Martín-Durán and Hejnol, 2015; Yamasaki et al., 2015). In this context, palaeontology (e.g. Cambrian taxa) plays an essential role in providing critical information on the ancestral traits of scalidophorans and the early evolutionary history of the group.

Over the last decades a huge amount of high-resolution morphological data has been obtained from several early Palaeozoic Lagerstätten that yielded a great variety of “priapulid-like” worms (Conway Morris, 1977a; Hou et al., 2017; Kimmig et al., 2019; Whitaker et al., 2020), kinorhynchs (Fu et al., 2019), loriciferans (Maas et al., 2009; Peel, 2010a, b) and many stem species with uncertain affinities (Table 1). These fossil data have been integrated by various authors (Dong et al., 2004; Harvey et al., 2010; Ma et al., 2014a; Wills et al., 2012; Zhang et al., 2015; Fig. 45) who proposed scalidophoran phylogenies and tried to establish phylogenetic relations between early scalidophorans and the modern representatives of the group.

Other fossil data obtained more recently (Dong et al., 2018; Harvey and Butterfield, 2017; Peel and Rahman, 2017; Whitaker et al., 2020; Yang et al., 2020; Yang et al., 2017; Yang and Zhang, 2016a, b) had also been integrated into updated cladistic analyses. This was one the objective of my thesis i.e., expand the scalidophoran database, reassess morphological characters used by previous authors and perform new cladistic analyses by using different methods.

Some scalidophoran species found in the Cambrian can be confidently assigned to loriciferans and kinorhynchs because they clearly display morphological features typical of

modern representatives, such as oral stylets and lorica for loriciferans (see Bang-Berthelsen et al., 2013; Harvey and Butterfield, 2017; Peel, 2010a, b) and segmented body and oral styles for kinorhynchs (Brusca et al., 2016; Fu et al., 2019; Neuhaus, 2013). In contrast, the vast majority of Cambrian scalidophorans are uneasy to relate to any particular scalidophoran subgroup. For example, the phylogenetic affinities of palaeoscolecids, *Selkirkia*, *Fieldia* and *Sicyophorus* have often appeared as controversial or uncertain (Harvey et al., 2010; Wills et al., 2012). Previous authors have considered *Xiaoheiqingella* and *Paratubiluchus* as potential crown-group priapulids based on a suite of characters recognized in modern priapulids, such as three-fold introvert, 25 longitudinal rows of scalids (Conway Morris, 1977a; Han et al., 2004a), an eversible pharynx lined with pentaradial multi-spinose teeth (Huang, 2005; Schmidt-Rhaesa, 2013), and caudal appendages (Han et al., 2004a; Huang et al., 2004b).

Some authors suggested that the aforementioned features may be plesiomorphic characters of scalidophorans, cycloneuralians even ecdysozoans (Budd, 2001, 2003; Huang, 2005; Ma et al., 2014a; Maas, 2013; Zhang et al., 2006). Palaeoscolecids are important elements of the early Cambrian-to late-Silurian marine fauna (Harvey et al., 2010; Yang, 2016; Table 4.1) but there is no real consensus concerning their affinities. They have been alternatively assigned to the stem-group Priapulida (Conway Morris, 1977a; Harvey et al., 2010), Nematomorpha (Hou and Bergstrom, 1994), Ecdysozoa (Budd, 2003; Conway Morris and Peel, 2010), and even considered as priapulid-like ancestors of Onychophora and Tardigrada (Dzik and Krumbiegel, 1989). The interpretation of certain morphological features has also led to controversial placements. For example, some authors (Zhang et al., 2006) interpreted the tube of *Selkirkia* as the equivalent and a possible homologue of the lorica of extant priapulid larvae and loriciferans, and therefore suggested that *Selkirkia* should be affiliated to either Priapulida or Loricifera. Detailed studies on *Selkirkia* presented here help in clarifying some of these uncertainties (see Chapter 5.3).

Previous phylogenetic analyses have often been performed by single analysis algorithm. This method may not be adequate for taking into account the effect of homoplastic characters (Congreve and Lamsdell, 2016). I found it better to process the data by using various algorithms. Results may differ depending on the cladistic method chosen for processing morphological data (Fig. 45). The detailed study of *Selkirkia* (see Chapter 5.3) gave me the opportunity to revise the phylogeny of scalidophorans.

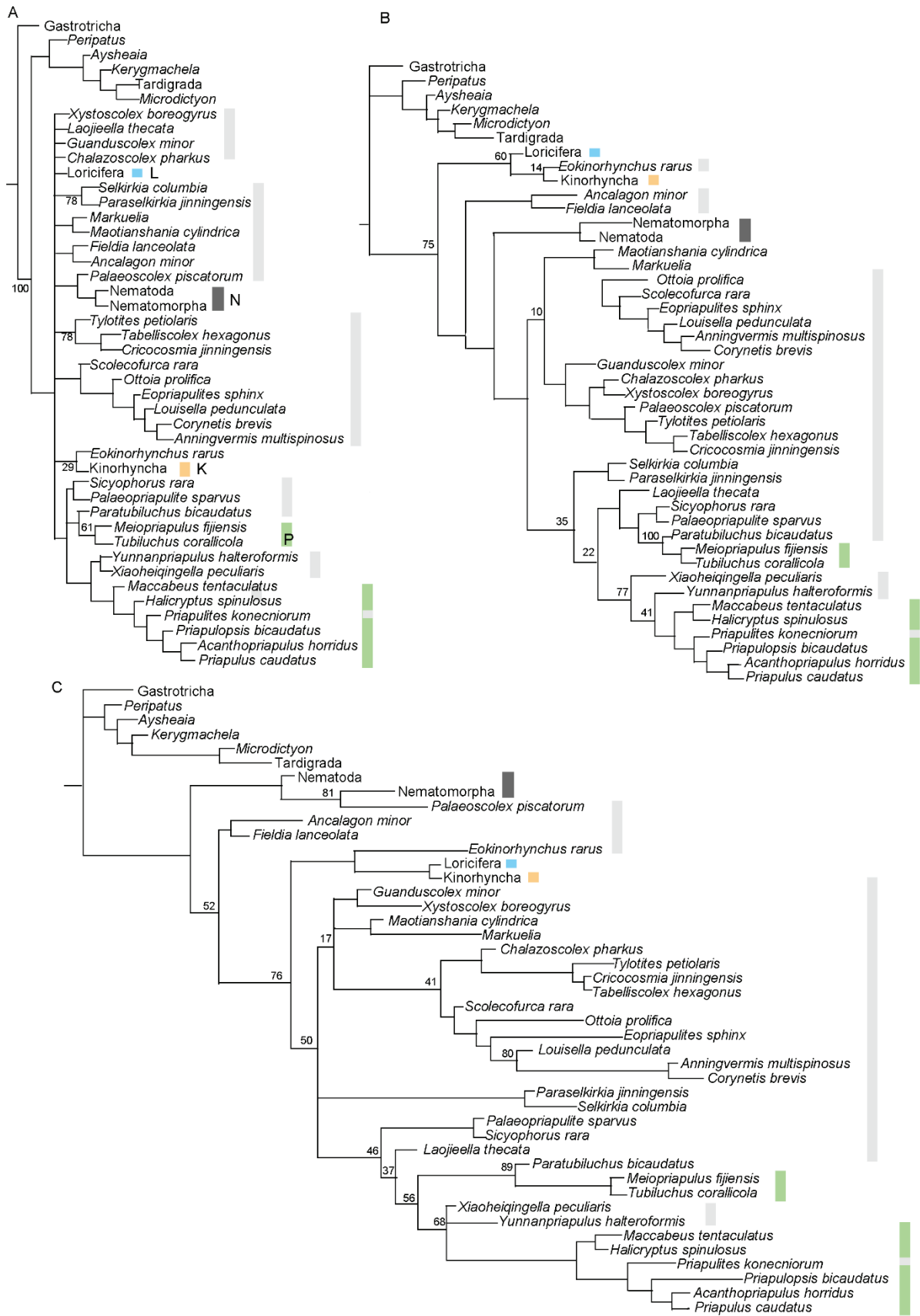


**Fig. 45.** Scalidophoran dataset from Zhang et al. (2015) processed by three different algorithms. Note that the same dataset performed by different methods leads to different results. A. 50% majority rule tree of TNT (maximum parsimony). B. consensus tree of Bayesian inference. C. consensus tree of IQTREE (maximum likelihood). Abbreviations: N, Nematoida; K, Kinorhyncha; L, Loricifera; P, Priapulida. Colour bars represent different animal groups. Nematoida in dark grey, Kinorhyncha in yellow, Loricifera in blue, Priapulida in green. Cambrian and Carboniferous fossil scalidophorans represent by light grey bars. Numbers close to taxa are bootstrap values.

## 5.5.2 New phylogenetic analysis of Scalidophora

### 5.5.2.1 New dataset and methods

Our cladistic investigation is based on discrete morphological data modified from Harvey et al. (2010) and Zhang et al. (2015), which focused on cycloneuralian relationships. *S. willoughbyi* and *S. spencei* were excluded due to a very large amount of uncertain coding (Conway Morris and Robison, 1986). While revising this matrix, we realized that a lot of multistate characters lacked a corresponding “primary” or “sovereign” binary character (*sensu* Aria et al., 2015). The inclusion of an “absence” state in a multistate character is justified only if there are reasons to think that the presence of the character did not likely have a single origin; otherwise, the lack of a sovereign character represents an obvious loss of phylogenetic signal.

We therefore scrutinized the optimization of relevant character states with Mesquite (Maddison and Maddison, 2019), but found that, in most cases, there was no strong homoplastic pattern justifying the omission of sovereign binary characters. The inclusion of such characters added important phylogenetic signal to the matrix, but also resulted in less-resolved topologies in parsimony: this hints that the original matrix might have been “tailored” to increase the resolution of the strict consensus tree at the cost of a more representative but more conflicting coding of morphology, as was observed also in a panarthropod dataset (Caron and Aria, 2017).

Although the goal of parsimony is to minimize transformational steps, homoplastic characters can still locally retain phylogenetic value (Congreve and Lamsdell, 2016), which corrections based on secondary homology can remove — this is of course a more fundamental problem when using the same dataset for likelihood-based analyses. Unless true convergence can be demonstrated, instead of parallelism, any dataset thoroughly “optimized” in this way can provide spurious evolutionary reconstructions hidden behind fully-resolved and well-supported topologies.

Parsimony analyses were performed with TNT (Goloboff and Catalano, 2016) as well as the R\* (R Team, 2020) package TreeSearch (Smith, 2018), which uses MorphyLib (Brazeau et al., 2017) to handle inapplicable data (Brazeau et al., 2019), and Bayesian analyses with MrBayes (Ronquist et al., 2012). *Lepidodermella squamata* (Gastrotricha) was chosen as the outgroup, and characters were unordered. In general, higher nodes are very poorly supported and reaching convergence in any method (except heuristic tree bisection reconnection (TBR))



required a greater-than-usual number of replications / generations for a dataset that size.

For parsimony, heuristic TBR was performed with 1,000 trees saved for 10 replications, because it yielded most parsimonious trees (MPTs) one step fewer than 10 trees saved for 1,000 replications. Tree search with new technology (TNT) used default parameters and 1,000 iterations of parsimony ratchet, 50 cycles of drifting, and 10 rounds of tree fusing. Owing to the lack of proper handling of inapplicable states by TNT or other common parsimony software (heuristic TBR and TNT treating here inapplicable entries as uncertainties), which could arguably be a significant issue in our matrix (inapplicability representing 17.6% of the data), we decided to also use the TreeSearch package in R\*, which makes use of the “scanning” algorithm proposed by (Brazeau et al., 2019). Because an informed use of implied weighting was advocated to yield optimal trees when using parsimony as a conceptual basis (Smith, 2019), we also computed a consensus of separate implied-weighting analysis from TreeSearch using concavity constants 3, 5 and 10, following the recommendations of Smith (2019). In each case, searches went through 2,000 iterations of ratchet.

Bayesian searches used an Mkv+ $\Gamma$  model (Lewis, 2001) with 4 runs each with 4 chains for 10,000,000 generations and burn-in at 20%. In light of parsimony results (see Results), a backbone was also used to enforce a model with basal Loricifera + Kinorhyncha.

The maximum-likelihood tree search was conducted in IQ-TREE, and support was assessed using the ultrafast phylogenetic bootstrap replication method to run 300,000 replicates (Nguyen et al., 2015).

We used RogueNaRok (Aberer et al., 2013) to search for rogue taxa destabilizing the tree, but we found none having a significant impact.

### 5.5.2.2 General results

Our results differ considerably from those that were published before with the same original dataset (Liu et al., 2014; Zhang et al., 2015), owing to our extensive recoding and implementations of primary / sovereign characters (see above).

Heuristic TBR and TNT resolve similar topologies with extant priapulids forming a sister clade to *Selkirkia* and palaeoscolecids, and with Loricifera and Kinorhyncha branching off basally (Fig. 48C, D). By contrast, the unconstrained Bayesian runs converge on a basal *Selkirkia* sister group to Palaeoscolecida and Scaldiphora (Fig. 47). In the unweighted TreeSearch analysis (Fig. 48A), Loricifera and Kinorhyncha are also resolved basally, but fossil groups all form a long stem to extant Priapulida, with *Selkirkia* and *Eximipriapulidus* being their closest sister groups. When using implied weighting, consensus trees for individual concavity constants are well resolved, but they significantly differ from one another, leading to a polytomy if one combines these results (Fig. 48B). These topological discrepancies between concavity constants have been noted before (e.g. Aria et al., 2015; Congreve and Lamsdell, 2016), and, in practice, this means that implied weighting is a method that may indeed be too inconsistent despite good performances with simulated data (Smith, 2019). However, higher nodes in our topologies, regardless of the method, are poorly supported, and therefore, in our case, the loss of precision in the implied weighting consensus may also represent greater accuracy.

A basal position of Loricifera and Kinorhyncha with a large total-group Priapulida being consistently recovered in parsimony, we decided to test the strength of this model by enforcing a backbone on the Bayesian analysis. The resulting topology (Fig. 46) bears overall similarity

with the unweighted TreeSearch topology and yields on average slightly better harmonic means than the unconstrained model (1,308.35 vs. 1,307.96, averaged over 8 runs). A better treatment of inapplicable states therefore helped parsimony converge with Bayesian likelihood, assuming a model with basal Loricifera and Kinorhyncha.

I therefore present the constrained Bayesian tree as the representative of the best evolutionary model for our data. In this scenario, most fossils are part of a populous stem within total-group Priapulida, with *Selkirkia* being closer to the crown than palaeoscolecid (Fig. 46). The crown of Priapulida includes the Carboniferous *Priapulites konecniorum*, and its immediate sister clade is composed of the early Cambrian *Paratubiluchus*, *Xiaoheiqingella* and *Yunnanpriapulidus*, with *Sicyophorus* branching off basally to this group. Two typical SSFs—*Eokinorhynchus* and *Eopriapulites*—are found here to constitute intermediate forms between *Sicyophorus* and *Selkirkia*. The Chengjiang fossil *Laojieella* is consistently retrieved as an early member of the *Selkirkia* clade, and Bayesian searches find that *Markuelia* is also a basal part of this clade.

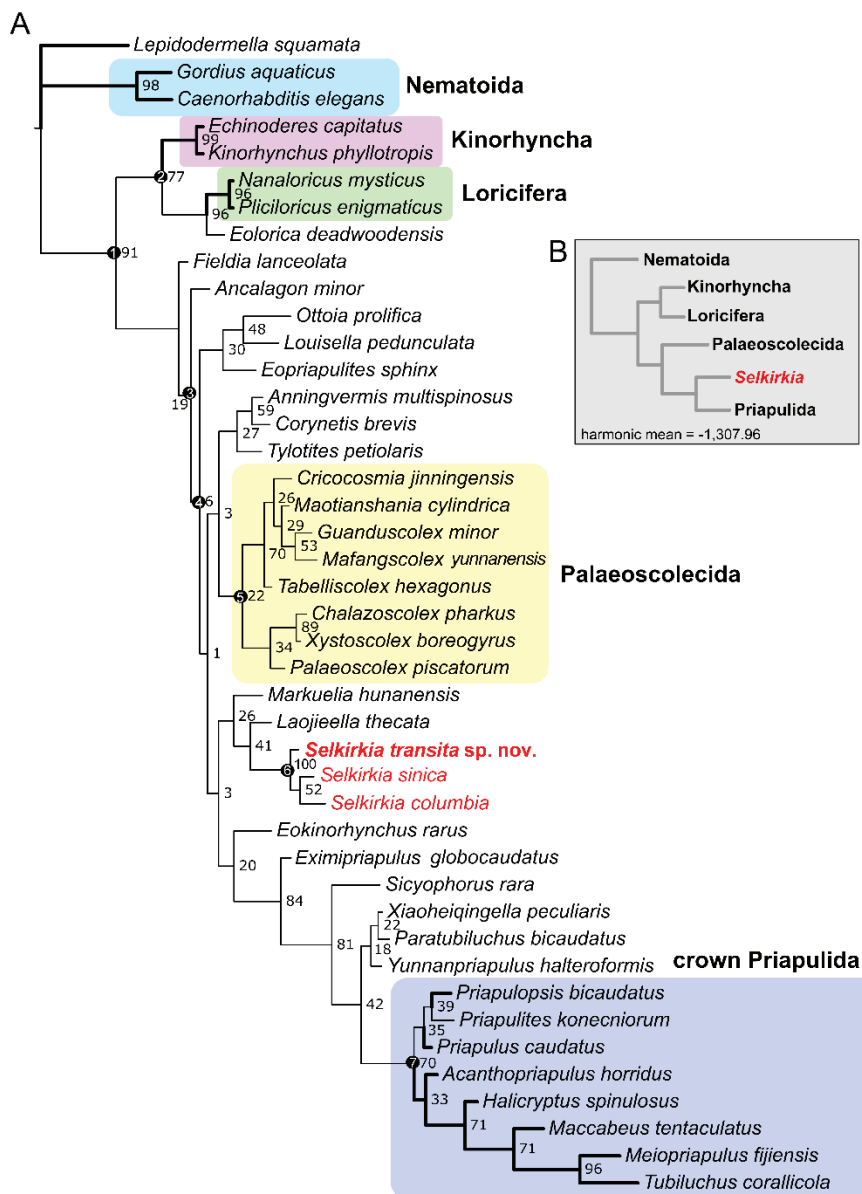


**Figure 46.** Maximum clade compatibility tree from a Bayesian inference (BI) using an Mkv+ $\Gamma$  model and a backbone enforcing basal Kinorhyncha and Loricifera. A. Full tree. Bold branches are extant species. Numbers next to node are posterior probabilities. Circled numbers at nodes are key apomorphic characters: 1, eversible introvert in adult. 2, mouth cone and oral stylets. 3, trunk annulations in adult. 4, circlets of pharyngeal teeth. 5, trunk plates with nodes, several rows plates in each annulation, posterior setae. 6, twenty-five longitudinal rows scalids arranged quincunxially (Fig. S6), cuticular and annulated tube and multi-subdivisions introvert. 7, unpaired ventral nerve cord, pharyngeal nervous system. B. Simplified topology showing the position of *Selkirkia* and harmonic mean (-1,307.96).

Considering the weak support of higher nodes, the alternative topology retrieving *Selkirkia* outside of Scalidophora (Fig. 47) should not be too hastily discarded. It is more consistent with the findings of (Ma et al., 2014a) in the placement of *Eximipriapulius*, but also implies that *Selkirkia*, palaeoscolecids and most fossil forms considered are instead part of the scalidophoran stem, although palaeoscolecids and other non-selkirkiid fossils also form a distinct clade. This scenario implies that the palaeoscolecids *sensu lato* and crown scalidophorans constituted two separate radiative lineages (Fig. 47), based on the morphology of the common ancestor shared with *Selkirkia*; this contrasts with the topology described above according to which the Cambrian fossil radiation was mostly linked to the build-up of the priapulid body plan.

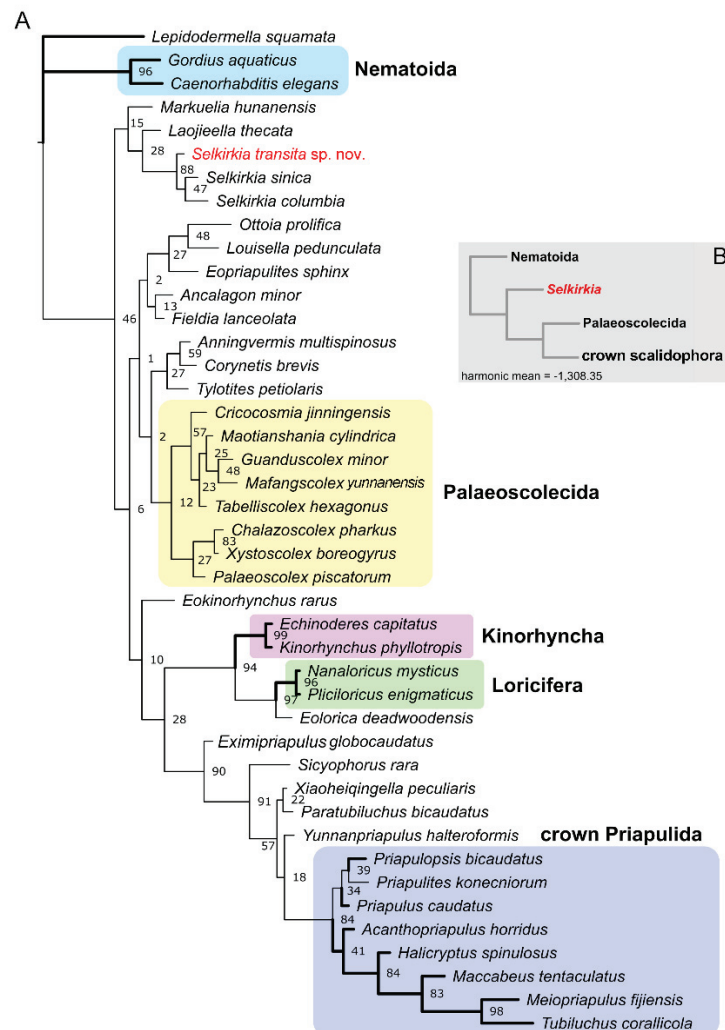


**Figure 47.** Maximum clade compatibility tree from a Bayesian analysis using an Mk<sub>v</sub>+ $\Gamma$  model and not a backbone used. A. Full tree. *Selkirkia* is at the basal position of stem-scalidophorans. Bold branches are extant species. Numbers next to node are posterior probabilities. B. Simplified topology showing the position of *Selkirkia* and harmonic mean (-1,308.35).

### 5.5.2.3 Discussion

#### *Selkirkia*

*Selkirkia* has long been assigned to priapulids based on overall similarities with extant priapulids, such as the introvert structure, pharyngeal teeth (Conway Morris, 1977a, 1997; Han et al., 2004a; Huang, 2005) and trunk annulation (Conway Morris, 1977a; Wills et al., 2012; Zhuravlev et al., 2011). Other authors have considered the tube of *Selkirkia* has the equivalent and a possible homologue of the lorica of extant priapulid larvae and loriciferans (Zhang et al., 2006), and advocated a position within scalidophorans without specifying to which group it may belong (Huang, 2005; Ma et al., 2014a; Maas et al., 2007; Wills, 1998; Zhang et al., 2006). *Selkirkia* clearly differs from extant Kinorhyncha and Loricifera, which are both characterized by the presence of a mouth cone and oral stylets (Heiner and Kristensen, 2005). *Selkirkia* lacks such oral configuration and, instead, has multispinose pharyngeal teeth arranged quincunxially as in numerous other taxa. *Selkirkia* bears no external “segments” (the so-called zonites of kinorhynchs). Although most probably secreted by the epithelial cells of the trunk (see Chapter 5.3), its finely annulated tube has no equivalent in other scalidophoran groups.

The main phylogenetic result (Fig. 46) finds that the *Selkirkia* clade is basal to Priapulida and its immediate stem, and therefore represents the onset of the priapulid radiation. The priapulid affinities of *Selkirkia* are supported by the following set of morphological characters shared with extant representatives of the group (Fig. 41): **(1)** Introvert subdivided in the same way as that of extant priapulids (i.e. Zone I, II, III) and clearly different from that of kinorhynchs and loriciferans (Zone I, mouth cone); **(2)** Twenty-five longitudinal rows of scalids are found in *Selkirkia* and the vast majority of extant priapulids (except *Meiopriapulid fijiensis*); **(3)** Pharynx lined with multispinose teeth as in extant priapulids (van der Land, 1970) and Cambrian priapulids (Conway Morris, 1977a); **(4)** Probable homology between the tube rings and the cuticular annulations seen in modern priapulids; **(5)** Possible paired caudal appendages as in extant (e.g. *Priapulid*; van der Land, 1970) and stem-group forms (e.g. *Paratubiluchus* and see Han et al., 2004a) priapulids; **(6)** Probable paired tubular ovaries as in extant female priapulids (*Priapulid*, Schmidt-Rhaesa, 2013; see Chapter 5.4).

An alternative phylogenetic scenario based on the same, but an unconstrained Bayesian analysis (Fig. 47) resolves *Selkirkia* in a basalmost position within a large stem-group Scalidophora connecting this taxon to the origin of all non-nematoid cycloneuralians. Here, only a handful of fossils constitute the stem proper of Priapulida (e.g. *Paratubiluchus*, *Xiaoheiqingella*), most extinct forms documenting instead a parallel palaeoscolecid radiation (Fig. 47). In spite of being basal, the *Selkirkia* clade is only four nodes away from *Eximipriapulid* (instead of two), and thus morphofunctional similarities with the total-group Priapulida are still relevant.

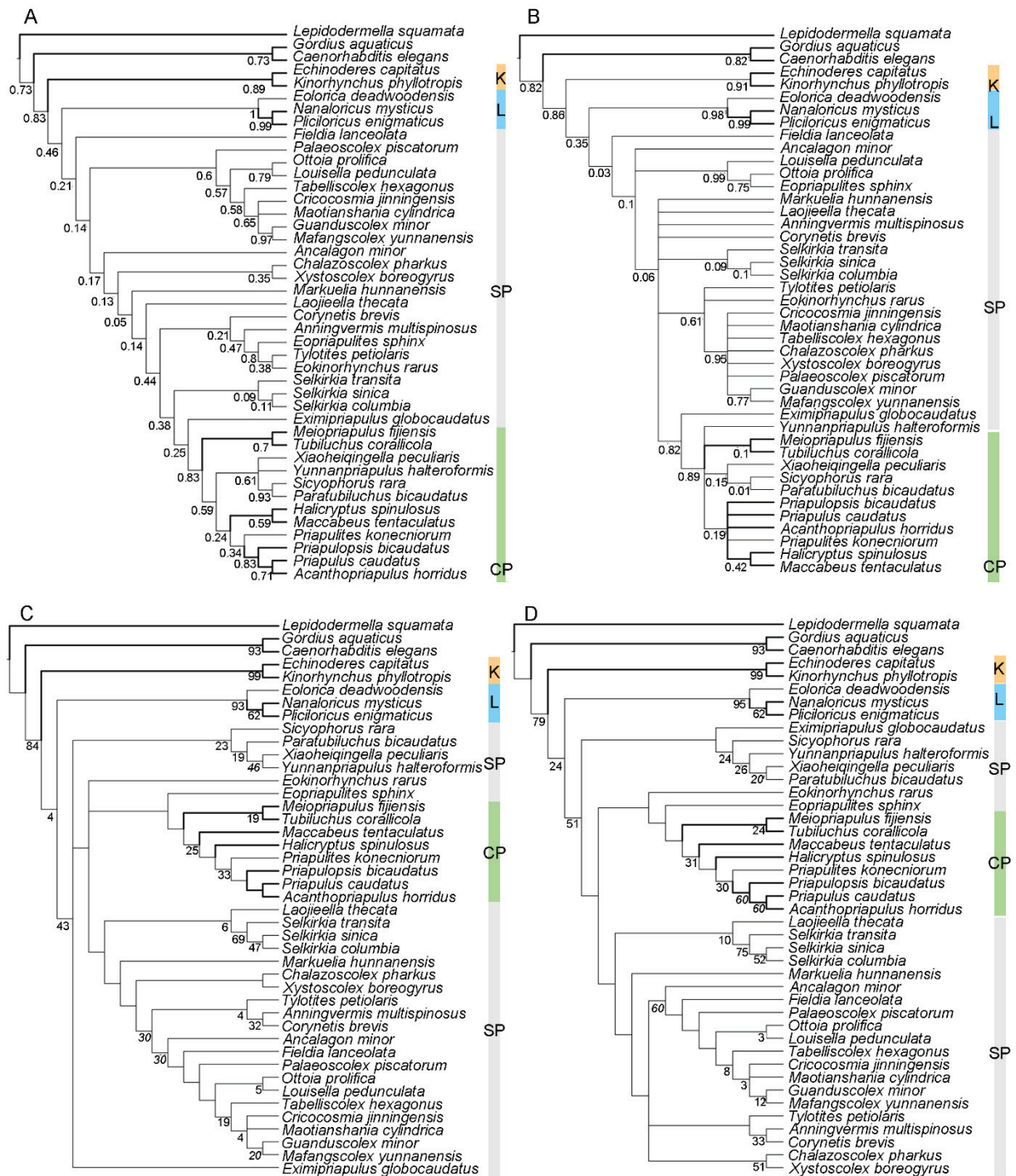


**Figure 48.** Consensus cladograms of maximum parsimony (MP). A. unweighted analysis using TreeSearch, 26 MPTs, 317 steps. B. Consensus of TreeSearch analyses using implied weighting for  $k = (3, 5, 10)$ . C. Heuristic Tree Bisection Reconnection, 12 Most Parsimonious Trees (MPTs), 307 steps. D. Tree search using new technology (TNT), including Ratchet and Drifting, 5 MPTs, 307 steps. Abbreviations: K, Kinorhyncha. L, Loricifera. CP, crown Priapulida. SP, stem Priapulida. Colour bars represent different animal groups. Kinorhyncha in yellow, Loricifera in blue, Priapulida in green, Cambrian and Carboniferous fossil scalidophorans in light grey. Bold branches are extant. Numbers at nodes are jackknifed support values; italicized numbers at nodes in C and D are frequencies of occurrence for nodes not present in all MPTs.

### ***Xiaoheiqingella*, *Yunnanpriapul* and *Paratubiluchus***

These three taxa share a series of common features such as an introvert, a neck, and a trunk with paired caudal appendages. Their introvert bears 25 longitudinal rows of scalids, and their pharynx is armed with pentaradial teeth (Figs 29A; 32). *Xiaoheiqingella*, *Yunnanpriapul* and *Paratubiluchus* form a well-defined clade in our phylogenetic trees, which resolve them as the closest stem-group priapulids both by Bayesian inference (BI; Figs 46, 47; posterior probabilities > 40) and maximum likelihood (ML; Fig. 49; bootstrap value is 58), whereas they were resolved as the members of crown priapulids by TreeSearch based on maximum parsimony (MP; Fig. 48A, B; bootstrap values > 82). These results are consistent with phylogenies proposed by previous authors (Liu et al., 2014; Zhang et al., 2015).

### ***Sicyophorus***

*Sicyophorus* has a rather unusual morphology characterized by a gourd-shape body, a scalid-bearing introvert, a neck and trunk encased within a lorica (Figs 29D; 33B). Pharyngeal teeth seem to be arranged in a pentaradial manner (Cheng 2019). Our phylogenetic results resolve *Sicyophorus* as a very close position to crown-group of priapulids both by Bayesian inference (Figs 46, 47; posterior probabilities > 90) and maximum likelihood (ML; Fig. 49; bootstrap value is 76), whereas it is resolved as the member of crown priapulids by TreeSearch based on maximum parsimony (Fig. 48A, B; bootstrap values > 60). These results are consistent with phylogenies proposed by previous authors (Liu et al., 2014; Zhang et al., 2015; Ma et al., 2014; Fig. 45A).

### ***Tyloites*, *Anningvermis*, and *Corynetis***

*Tyloites* is characterized by an introvert with scalids, a trunk with numerous spines, and possible paired caudal hooks (Han et al., 2007b; Figs 29C; 31I-L). Our results (BI, Fig. 46; MP, Fig. 48B-D; ML, Fig. 49) resolve *Tyloites* as a sister group of palaeoscolecids within stem-group of priapulids, although the support value is low (<30). These results support former analysis (e.g. Harvey et al., 2010).

*Corynetis* and *Anningvermis* both bear an introvert, a spinose trunk and a caudal appendage or projection (Fig. 33C, D). The basal part of their introvert is devoid of scalids. They bear a circlet of elongated spines in a circumoral position. Their pharynx is slim and armed with numerous teeth (Fig. 33C, D). Former phylogenetic analyses (MPTs, Ma et al., 2014a; Wills et al., 2012) placed both taxa in the sister group of palaeoscolecids and within stem or crown-group Scalidophora. In the phylogenies proposed by Liu et al. (2014) and Zhang et al. (2015) (Fig. 45B, C), *Corynetis* and *Anningvermis* have the sister relationships with *Louisella*, *Eopriapulites*, and appear within the stem-group Priapulida. Our trees show that *Corynetis* and *Anningvermis* appear within stem-group Priapulida and have the sister relationships with *Tyloites* (BI, posterior probability is 27, Fig. 46; HTBR, frequency value is 4, Fig. 48C; ML, bootstrap value is 85, Fig. 49) rather than *Louisella* and *Eopriapulites*.

### **Palaeoscolecids *sensu stricto***

Palaeoscolecids *sensu stricto* are characterized by tessellating plates along their trunk (Fig. 30) including *Chalazoscolex*, *Xystoscolex*, *Palaeoscolex*, *Guanduscolex*, and *Mafanguscoelx* (Harvey et al., 2010). Former phylogenies used to place them within the stem-group Priapulida (Harvey et al., 2010) thus refuting the opinion that palaeoscolecids *sensu stricto* may belong to Nematomorpha (Hou and Bergstrom, 1994), stem-group Cycloneuralia (Maas et al., 2007; Budd, 2001), or to stem-group Ecdysozoa (Budd 2003; Conway Morris and Peel, 2010).

However, our results based on ML and BI show that palaeoscolecids *sensu stricto* also contain *Tabelliscolex*, *Cricocosmia*, *Maotianshania* which are without tessellating plates (see Chapter 4.3.1.3) (BI, posterior probability is 12, Figs 46, 47; ML, bootstrap value is 47, Fig. 49). Results from MP are very unstable (Fig. 48). These phylogenetic results suggest that tessellating plates may be not the only diagnosis to define palaeoscolecids *sensu stricto*. Most of our results resolve the palaeoscolecids *sensu stricto* as the stem-group Priapulida but they branch off relatively distally from crown-group Priapulida (Figs 46, 48, 49).

### ***Eokinorhynchus* and *Eopriapulites***

These two forms are among the oldest known scalidophoran worms and both come from the 535-million-year-old Kuanchuanpu Formation (*Eokinorhynchus*, Zhang et al., 2015; *Eopriapulites*, Liu et al., 2014; Fig. 25A, B). They bear an introvert with scalids and a trunk with small and large sclerites. Former studies assigned *Eopriapulites* and *Eokinorhynchus* to the stem-group Priapulida and Kinorhyncha, respectively (Fig. 45). We consider that the macroannulations of *Eokinorhynchus* differ markedly from the so-called “segments” seen in extant kinorhynchs, thus making possible affinities with kinorhynchs questionable. Instead, these macroannulations are comparable with the trunk annulations seen in other scalidophoran worms from the Kuanchuanpu Formation (Fig. 25D-H).

Our results show that *Eokinorhynchus* is either close to the crown-group Priapulida (BI, Fig. 46, posterior probability is 20; MP, Fig. 48D) or far away from the crown-group Priapulida (MP, Fig. 48A-C, bootstrap values < 40; ML, Fig. 49, bootstrap value is 88) but still within total Priapulida. *Eokinorhynchus* also is resolved as the stem-group Scalidophora under unconstraint Bayesian inference (Fig. 47) with a very low posterior probability (10). Most of our phylogenetic results support *Eokinorhynchus* as a member of stem-group Priapulida rather than stem-group Kinorhyncha.

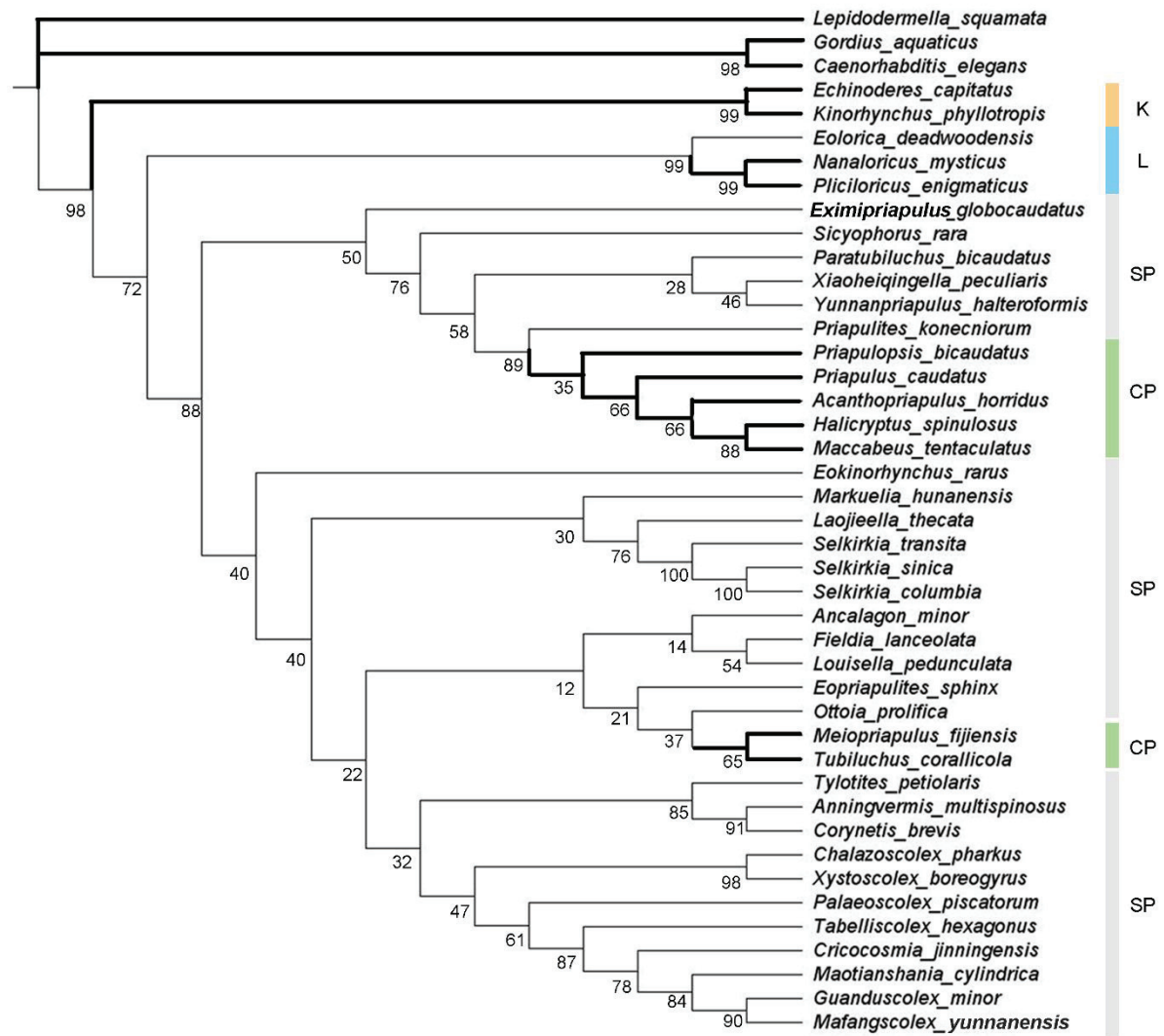


**Figure 49.** Consensus cladogram of maximum likelihood (ML). Tree inferred in IQ-TREE. K, Kinorhyncha (yellow colour). L, Loricifera (blue colour). CP, crown Priapulida (green colour). SP, stem Priapulida (grey colour). Bold branches are extant. Numbers close to taxa are bootstrap values.

*Eopriapulites* bears scalids and pharyngeal teeth along the introvert arranged in a hexaradial manner (Fig. 25A) thus contrasting with the typical pentaradial symmetry of fossil and extant priapulids (e.g. *Selkirkia*, *Xiaoheiqingella*, *Priapululus*; Liu et al., 2014; Han et al., 2004a; Schmidt-Rhaesa, 2013). *Eopriapulites* was successively interpreted as a member of the stem-group Priapulida (Liu et al., 2014), stem-group Scalidophora (Shao et al., 2015), and more recently stem-group Cycloneuralia (Shao et al., 2019). Shao et al. (2019) suggested that body size of *Eopriapulites* might have reached more than one centimetre based on a supposed length-to-width ratios (10-15) estimated from trunk fragments. Shao et al. (2019) hypothesized that the morphology of *Eopriapulites* was close to that of the last common ancestor of Cycloneuralia/Ecdysozoa predicted by Budd (2001). These assumptions lack strong support.

Our phylogenetic results strongly support the affinity of *Eopriapulites* with stem-group Priapulida. It lies close to *Ottoia* but is quite distant from crown-group Priapulida (BI, posterior probability is 30, Fig. 46; MP, bootstrap value is 75, Fig. 48B; ML, bootstrap value is 21, Fig. 49). They are supported by the following features: 1) *Eopriapulites* bears a circlet of coronal scalids



pointing forward at the bottom of Zone II (circumoral area), which resembles the long spines of *Louisella pedunculata*, *Ottoia prolifica*, *Selkirkia columbia* (Conway Morris, 1977a), *Mafangsolex* cf. *yunnanensis* (Yang et al., 2020) and extant priapulid *Maccabeus tentaculatus* (Por, 1983; Por and Bromley, 1974; Fig. 50A). 2) The eversible trunk end of *Eopriapulites* (Shao et al., 2019) resembles that of *Ottoia* (Conway Morris, 1977a) and the extant priapulid *Maccabeus* (Salvini-Plawen, 1974) Fig. 50C). 3) The trunk of *Eopriapulites* lacks sclerotized structures such as plates, sclerites, spines, and bears naked annulated ridges and furrows (Fig. 25A) that are almost identical with those of the extant priapulid *Maccabeus* (Fig. 50C).

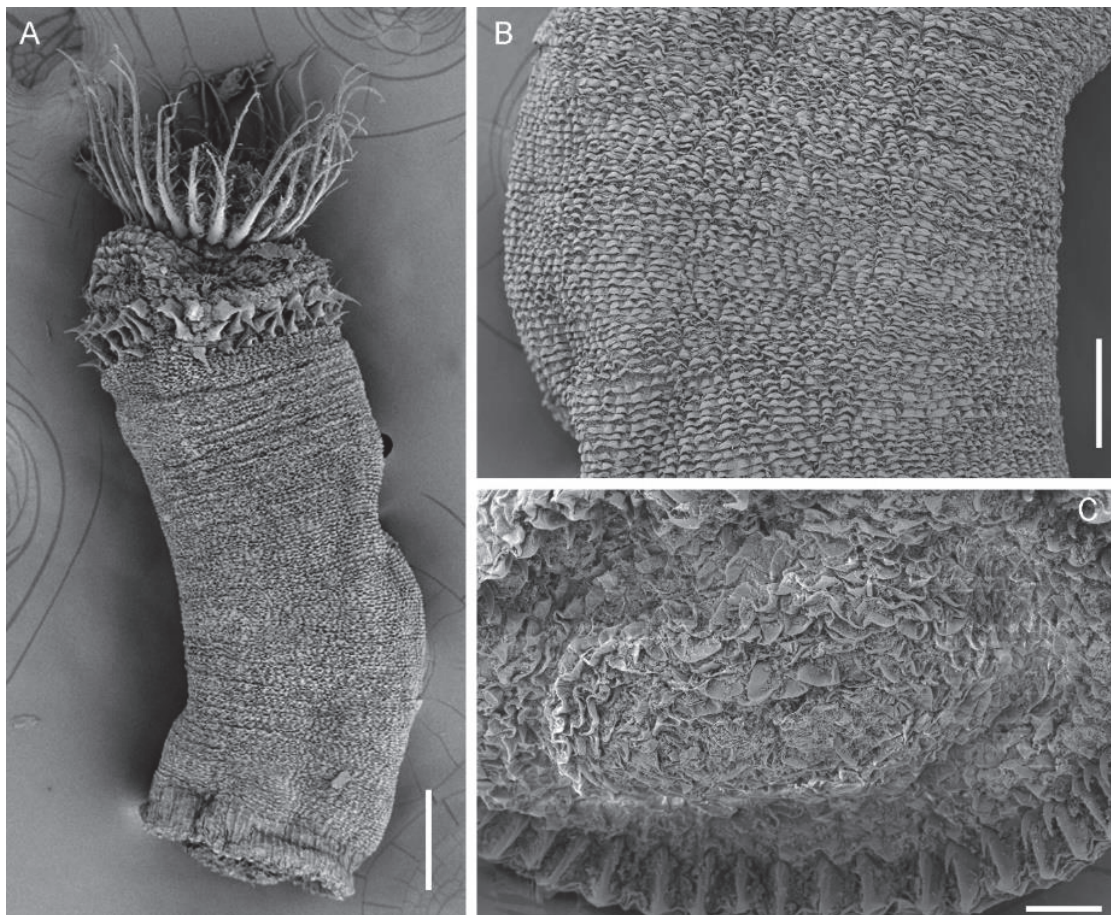


**Figure 50.** *Maccabeus tentaculatus* Por and Bromley, 1974, an extant meiobenthic priapulid from Cyprus. A. General view. B. Trunk cuticle. C. Posterior end (anal area). Scale bars: 100  $\mu\text{m}$  (A), 50  $\mu\text{m}$  (B), 20  $\mu\text{m}$  (C).

In summary, our phylogenetic study based on an expanded matrix and different cladistic methods (ML, MP, BI) show that most Cambrian scalidophorans are members of the stem-group Priapulida (Figs 46, 48, 49). These results differ from former studies, which assigned forms such as palaeoscolecids *sensu lato*, *Markuelia*, *Selkirkia* to stem- or crown-group scalidophorans (Dong et al., 2004; Wills et al., 2012; Ma et al., 2014a; Zhang et al., 2015; Shao et al., 2019). Our study (Fig. 46, node 7) indicates that the possible crown-group Priapulida (including *Xiaoheiqingella*, *Yunnanpriapulidus*, *Paratubiluchus*, and *Sicyophorus*) is supported by two important morphological characters: 25 longitudinal rows of scalids along the introvert and pentaradial pharyngeal teeth (Schmidt-Rhaesa, 2013). Our results also show that palaeoscolecids may be not only defined by presence tessellating plates since other forms (e.g. *Maotianshania*, *Cricocosmia*) that lack this feature have their full place (well supported by

different methods) within the group. Our studies do not support *Tylotites*, *Anningvermis*, and *Corynetis* as palaeoscolecids and shows that *Eokinorhynchus* and *Eopriapulites* from the Kuanchuanpu Formation (ca 535 Ma) have closer affinities with the stem-group Priapulida than with any other group (e.g. stem-group Kinorhyncha or stem-group Scalidophora/Cycloneuralia).

# Chapter 6 Conclusions and prospects

## 6.1 Conclusions

Ecdysozoans have a very long evolutionary history with diverse groups abundantly represented in the early Cambrian. In the present state of knowledge, the earliest-known ecdysozoans are scalidophoran worms from the 535-million-year-old Kuanchuanpu Formation (Cambrian Fortunian Stage; China). However, the origin of the group is to be found in the Precambrian as indicated by trace fossils made by vermiform (possibly ecdysozoan) animals. The aim of my thesis was to study new aspects the early evolutionary history of scalidophorans from fossil evidence obtained from the basal (Terreneuvian; Fortunian) and early (Series 2; Stage 3 and 4) Cambrian (Kuanchuanpu Formation, ca 535 Ma; Chengjiang and Xiaoshiba Lagerstätten, ca 518 and 514 Ma, respectively).

These ancestral scalidophorans are strikingly similar to their modern representatives in their overall body plan, cuticular structure and ornament, cuticle formation, moulting process, locomotion, feeding, and reproduction mode. We have seen that their moulting process was almost identical with that of modern priapulids which implies that complex mechanical and physical processes involved in ecdysis had already evolved in the early Cambrian and were controlled by specific genes. However, we lack information on the exact biochemical pathway used by modern priapulids and their possible Cambrian ancestors. The fine reticulated network seen over the external surface of early Cambrian scalidophorans appears as a faithful replica of their original underlying cellular pavement. As in extant priapulids such as *Priapulidus* and *Halicryptus*, their epithelial cells played a crucial role in making a new cuticle after the exuvia had been discarded. Both ecdysis and cuticle formation seem to have been acquired very early in the evolution of scalidophorans and conserved through to the present day. However, some of these ancestral scalidophorans have no exact counterparts among modern worms. This is the case for *Selkirkia*, a very unusual scalidophoran worm that lived encased with a protective conical tube. We have seen that this tube probably formed by non-synchronous ecdysis. The tube formation appears as an early innovation within the group. However, *Selkirkia* became extinct by the mid-Cambrian (ca 508 Ma) and no other known scalidophoran worm seems to have adopted tubicolous lifestyles since then, except a single extant meiobenthic species (*Maccabeus tentaculatus*). Other endobenthic strategies favouring faster locomotion and burrowing seem to have prevailed within Scalidophora.

Since most scalidophoran worms were endobenthic animals, their cuticular ornament is likely to have played a crucial role in locomotion (scalids), protection (spines, plates, loricae, and tube) and feeding (pharyngeal teeth). The oldest known scalidophorans (Kuanchuanpu Formation; ca 535 Ma) had already acquired a complex cuticular system with annuli, different types of spiny sclerites and pharyngeal teeth. Their relatively small size has led most authors to consider them as meiobenthic (interstitial) animals. Younger early Cambrian Lagerstätten reveal a much greater diversity within scalidophorans and a huge variety of cuticular ornament. These worms are much larger and characterized by various spines, plates along their trunk, and even more specialized cuticular elements such as lorica or a tube (e.g. *Selkirkia*). Particularly relevant is the development of tessellating plates along the elongated body of palaeoscolecids. This 'explosion' of cuticular features may be a response to environmental

pressure such as a need for better protection and anchoring to sediment, and a more efficient locomotion. Predation on soft-bodied animals such as worms is likely to have increased during the Cambrian radiation, especially after arthropods became a major element of marine ecosystems. Perhaps the relative simplicity of ornamented features seen in scalidophorans from the basal Cambrian results from a lower level of evolutionary pressure. Scalidophoran worms such as *Selkirkia* have also told us how early ecdysozoans reproduced – i.e., via oocytes formed in paired ovaries within the internal cavity, that were released outside through urogenital ducts. Again, comparisons with modern priapulids were particularly useful for interpreting their reproductive strategies. The large size and small number of oocytes suggest that energy invested by these Cambrian ecdysozoan worms in reproduction was possibly oriented towards quality rather than quantity. This strategy is that of modern meiobenthic priapulids whereas macrobenthic members of the group such as *Priapulid* use an alternative reproductive mode (numerous small eggs). In extant scalidophorans, ecological factors play an important role in favouring one strategy over another. This seems to have been true in the Cambrian, too, as exemplified by *Selkirkia*. The way cuticular elements distribute around the cylindrical body of early scalidophorans often highlight specific symmetry modes. For example, scalids distribute either pentaradially (e.g. *Eokinorhynchus* and *Xiaoheiqingella*) or hexaradially (e.g. *Eopriapulites*). A comparable diversity is seen in the arrangement of pharyngeal teeth with an octaradial, hexaradial and pentaradial symmetry in *Eokinorhynchus*, *Eopriapulites* and *Paratubiluchus*, respectively. This contrasts with the dominant pentaradial symmetry of modern priapulids. Similarly, other groups of early Cambrian animals such as cnidarians (Han et al., 2016a; Wang et al., 2020) exhibit diverse symmetry modes whereas modern representatives retained a single type (e.g. tetramerous symmetry of jellyfish; Brusca et al., 2016). Which type of symmetry prevailed in the most ancestral scalidophorans cannot be determined in the current state of knowledge.

There was a need for updating the phylogeny of scalidophorans. That's what we did by expanding the date base, reassessing the morphological characters and testing different cladistic methods. Our phylogenetic trees indicate that most Cambrian scalidophorans are stem-group priapulids. *Selkirkia* occupies a position close to the crown-group Priapulida. The twenty-five longitudinal rows of scalids and the pentaradial pharyngeal teeth appear as important apomorphies of Priapulida. Some Cambrian forms such as *Sicyophorus*, *Xiaoheiqingella*, and *Paratubiluchus* may belong to the crown-group Priapulida or lie close to it, as proposed by previous authors. Our phylogenies also suggest that the lorica may have evolved independently in separate groups such as *Sicyophorus* and loriciferans. The position of palaeoscolecids is far away from the crown-group Priapulida. Some "atypical" forms such as *Maotianshan* were resolved as members of palaeoscolecids *sensu stricto*, suggesting that the status of palaeoscolecids *sensu stricto* is unstable.

The last common ancestor of Ecdysozoa (LCAE) has been reconstructed as a large worm-like form with annulated trunk, small sclerites on the trunk, and a terminal mouth (Budd, 2001; Telford et al., 2008; Giribet and Edgecombe, 2017). However, this model remains hypothetical partly because of the lack of detailed fossil evidence from potential Precambrian ancestors. I would like to make some brief comments on this important issue although it is clearly out of the scope of my thesis and requires further detailed studies. Modern scalidophorans (e.g. priapulids) are capable of moving on or burrowing into soft sediment. They have a network of circular and longitudinal muscles that exert selective pressure on their hydrostatic skeleton

(internal cavity filled with a fluid), and a nervous system to coordinate muscular action. The introvert plays a key role in locomotion -i.e., projected forward by internal pressure and withdrawn by retractor muscles. Early scalidophorans (e.g. Kuanchuanpu, Chengjiang) seem to have been equipped with such muscle system, hydrostatic skeleton, and introvert. The morphology of numerous trace-fossils found across the Cambrian-Precambrian boundary (e.g. treptichnids) or deeper into the Precambrian suggest that their makers could move through soft sediment via peristaltic contractions that would imply an extensive muscular network with both circular and longitudinal muscles.

Extant nematodes and nematomorphs lack circular muscles and their fluid-filled blastocoelom is relatively reduced. Their cuticle consists of collagen instead of chitin as in scalidophorans. Some authors have suggested that nematodes and nematomorphs had lost their circular muscles in the course of evolution but provide no clear explanation concerning this supposed secondary loss. For example, Schmidt-Rhaesa (2007), speculated that the loss of circular muscles could be explained by the poor ability of collagen cuticular structure to deform. In the absence of circular muscles around their body, nematoids are unable to perform peristaltic burrowing, thus contrasting with scalidophorans. Nematodes typically move through their environment (e.g. soil, water) via contractions of longitudinal muscles and produce a whiplike undulatory motion (Brusca et al., 2016). No trace fossils indicate that such a locomotion mode may have occurred in the Precambrian.

We propose here that the ancestral ecdysozoan may have been a worm with a network of both longitudinal and circular muscles. Whether this hypothetical animal had a functional introvert or not is uncertain. Scalidophoran worms from the Kuanchuanpu Formation such as *Eokinorhynchus* have trunk annulation along the anterior part of their introvert, in contrast with all other extant and fossil scalidophorans. This would suggest that the introvert evolved through the differentiation of the anterior trunk. However, this hypothesis requires testing from more fossil material. In summary, the ancestral ecdysozoan animal would be seen as an animal with a cylindrical body, a blastocoelomic cavity, an extensive network of circular and longitudinal muscles, a chitinous cuticle, but no differentiated introvert. The introvert might have been a key innovation that dramatically increased the burrowing power of these vermiform animals with important implications on their capacity to exploit food sources. Whether the ancestral ecdysozoan was a naked vermiform or ornamented animal is matter of speculation. Anchoring features are essential to modern vermiform animals moving through sediment. Pharyngeal teeth are equally important for grasping food. For these reasons, it is probable that cuticular ornament (possibly various types of spiny outgrowths) occurred in ancestral ecdysozoans (Fig. 51).

The idea of scalidophorans arising from leg-bearing ecdysozoans (Zhuravlev et al., 2011) lack strong support from fossil evidence (both body and trace fossils) and molecular data (Telford et al. 2008; Eriksson et al., 2003; Laumer et al., 2019). How appendages evolved from a supposed vermiform ancestor remains a fascinating research topic. Hints could be found in the study of lobopodians from the basal Cambrian and the genetical pathways responsible for the development of legs (Budd, 2001; Giribet and Edgecombe, 2017; Oliveira et al., 2019).

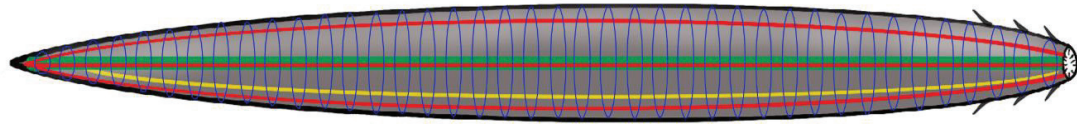


**Figure 51.** Hypothetical reconstruction of the last common ancestor of Ecdysozoa (LCAE). Red, blue, green, and yellow lines represent longitudinal muscles, circular muscles, alimentary, and unpaired ventral nerve cord, respectively.

## 6.2 Future research and prospects

### 6.2.1 Postdoctoral research

A few months ago, I applied to the Alexander von Humboldt Foundation for a postdoctoral research position in Germany (in Georg Mayer's lab, Kassel University). This project entitled "Origin and evolution of Ecdysozoa (moulting animals): a molecular and palaeontological approach" is a direct follow-up to my thesis and is summarized below.

#### ***Shedding light on the origin and evolution of moulting using a molecular approach***

All ecdysozoans share a common feature, that of renewing their cuticle periodically via a complex process called ecdysis that involves neuro-endocrine system and specific molecular pathways. A genomic and transcriptomic study (Schumann et al., 2018) has recently shed new light on the molecular pathways involved in the moulting process of ecdysozoans leading to the formulation of a possible evolutionary scenarios (Fig. 52). Likewise, we discovered exuviae in ancient scalidophoran worms from the early Cambrian of China (ca. 535 Ma; Wang et al., 2019) and have shown that ecdysis had a remote ancestry and was possibly one of the key innovations that led to the remarkable diversification of ecdysozoans and particularly the rise of arthropods. However, unanswered questions remain concerning the origin of ecdysis. While it is evident that steroid hormones such as ecdysone (E) and 20-hydroxyecdysone (20E), play a pivotal role in the moulting process of extant panarthropods, their involvement in ecdysis has not been demonstrated outside the panarthropod clade. In the first part of my project, I will therefore inject E and 20E into the body cavity of specimens of the priapulid species *Priapulus caudatus*. In addition, I will perform similar injection experiments with the dafachronic acid (DA), another sterol-derived hormone, which has been identified as a moulting hormone in the nematode *Caenorhabditis elegans* (Markov et al., 2009). This will help to clarify whether the ecdysteroid E and 20E or rather the steroid DA induce moulting in priapulids and whether the ecdysteroid or the dafachronic acid pathway controlled ecdysis in the last common ancestor of Ecdysozoa. I will also attempt to characterize the whole genetic pathway responsible for moulting in priapulids by analysing the available genomic and transcriptomic data from the priapulid *P. caudatus*. The results of this study will shed light on the successive genetic innovations and changes that have led to the evolution of ecdysis.

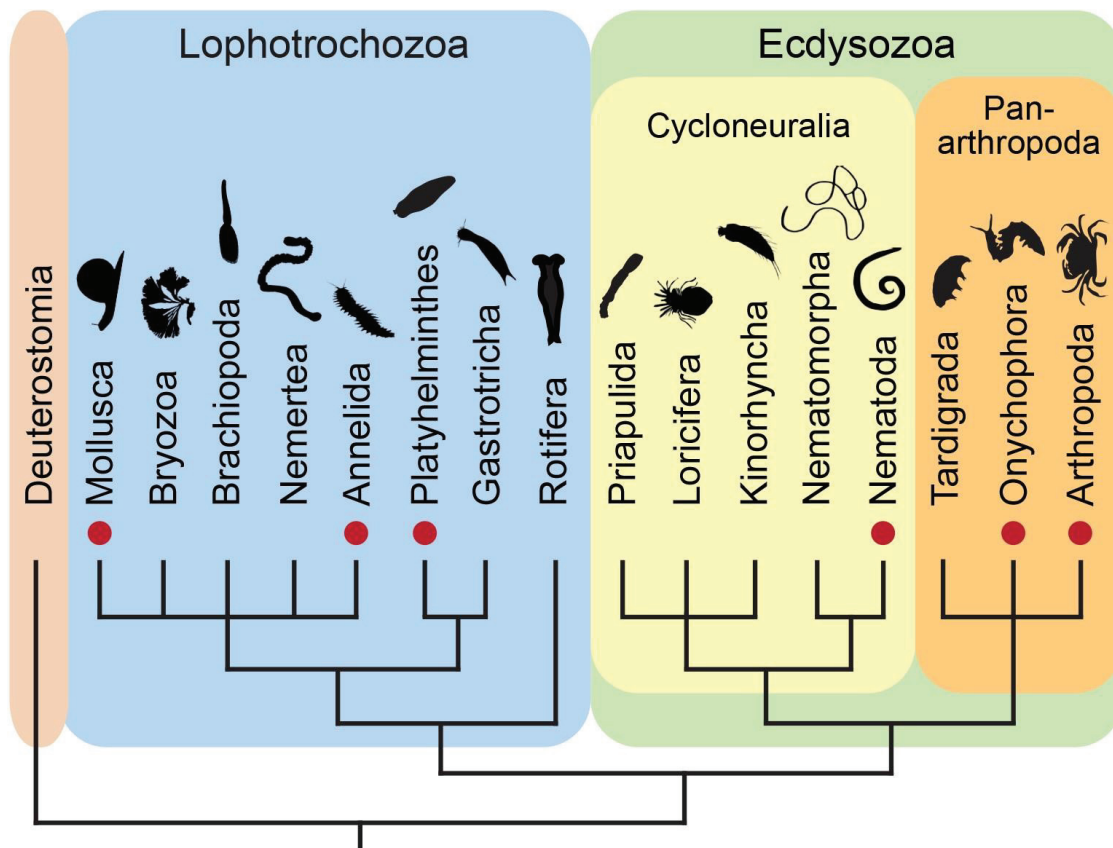


**Figure 52.** Identified occurrence of 20-hydroxyecdysone (indicated by red dots) in protostomes. Note that this hormone is not only found in ecdysozoans but also in other protostomes, including molluscs, annelids and platyhelminths. Courtesy G. Mayer.

### ***Elucidating the emergence of arthropods using a paleontological approach***

Ecdysozoans have a rich fossil record covering the lower Palaeozoic biodiversification events (“Cambrian Explosion” and “Great Ordovician Biodiversification Event”) and were present at virtually all levels of the early trophic webs, from sediment feeders (e.g. scalidophoran worms) to giant predators (e.g. anomalocaridids) (Hou et al., 2017). Phylogenomic analyses generally support the placement of panarthropods, scalidophorans and nematoids within Ecdysozoa, but the phylogenetic relationship between the individual clades is still unresolved. In particular, the monophyly of Cycloneuralia and the position of Tardigrada are still discussed controversially (Martin et al., 2017; Fig. 53). Besides, functional morphological aspects of the body plan of ancestral scalidophoran worms and panarthropods are still far from being understood.

The aim of the second part of my project is therefore to analyse exceptionally preserved fossil specimens from the basal Cambrian Kuanchuanpu Formation and especially two faunal elements: the scalidophoran worms which may represent one of the most ancestral ecdysozoan body plans, and the so-called lobopodians, which may be intermediate forms between worm-like organisms and arthropods.

(i) The scalidophoran worms from the Kuanchuanpu Formation are the earliest known scalidophorans represented by five species and, twelve indeterminate forms (Wang et al., 2019), but they are also abundant in unstudied material from collections (Fig. 54A–D). These

worms have a relatively simple anatomy with a large body cavity, an eversible introvert with cuticular spiny outgrowths and an unarmed annulated trunk (Liu et al., 2014).

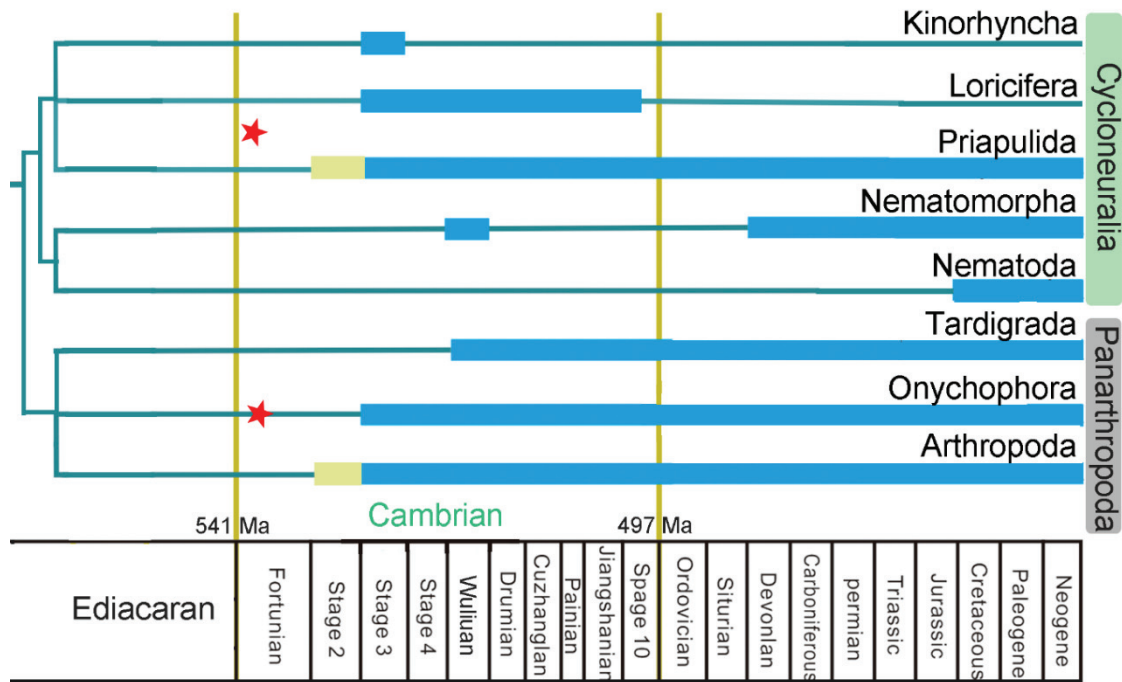


**Figure 53.** Diagram showing discrepancy between fossil and molecular clock estimates in early ecdysozoan evolution. Topology and molecular data modified from Schumann et al. (2018), fossil modified from Wang et al. (2020). Blue bars represent fossil record, yellow bars represent the predicted appearance of groups (molecular data), red stars represent unpublished occurrence of lobopodian and scalidophoran fossils.

(ii) Fossil lobopodians (e.g. *Luolishania longicuris*, *Paucipodia inermis* and *Hallucigenia fortis*) form an enigmatic group of animals (Fig. 54J–L), some of which resemble extant onychophorans. They are currently considered as stem-lineage representatives of panarthropods (Smith and Ortega-Hernández, 2014) and more precisely as possible stem-group onychophorans (Yang et al., 2015). It has been suggested that arthropods evolved from worm-like, legless ancestors via possible intermediate forms with soft legs exemplified by lobopodians. However, this transitional scenario still lacks solid fossil evidence. Unpublished lobopodian material from the Kuanchuanpu Formation (Fig. 54E, F) will be studied to provide insights into the early evolution of lobopodians.

Taken together, the study of fossils from the earliest Cambrian Kuanchuanpu Formation has the potential to provide key information on the composition of the ecdysozoan fauna before the Cambrian reached its peak, and to clarify the divergence time of the ecdysozoan clades and the appearance of arthropods. I will use this exceptional source of information to clarify these questions. Comparisons with scalidophorans and lobopodians from younger Cambrian deposits (e.g. Chengjiang biota, ca. 518 Ma; Fig. 54G–L) will be carried out to characterize possible evolutionary trends within the group. The apparent and remarkable lack of arthropod remains in the Kuanchuanpu Formation will be tested (ecological/taphonomic bias versus evolutionary absence). Anatomical comparison with extant onychophorans and tardigrades, which are extensively studied and available in the host laboratory, will be highly beneficial to my project.



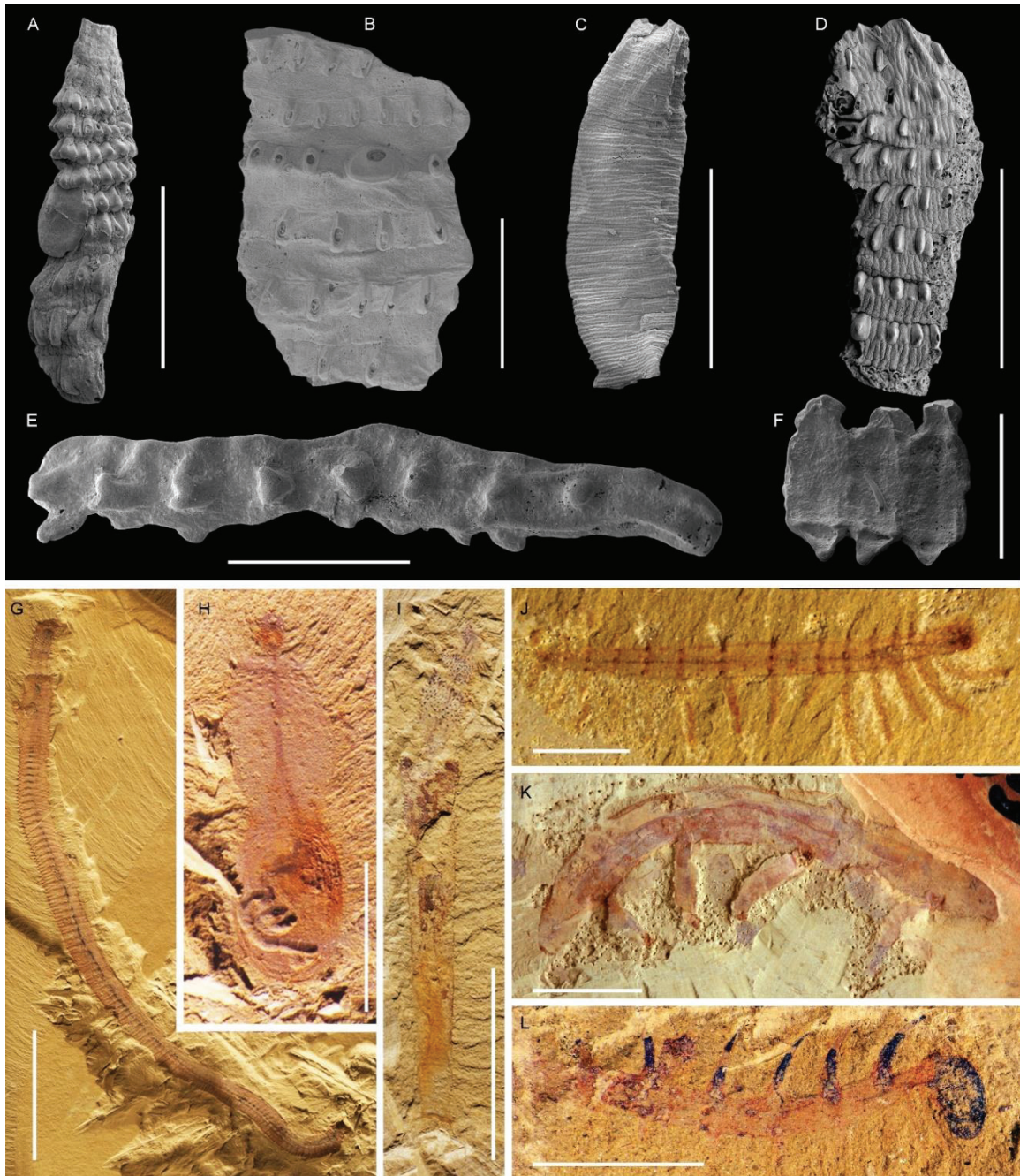


**Figure 54.** Ecdysozoan fossils. A–F. Micro-ecdyszoans from Kuanchuanpu Formation (ca. 535 Ma). A–D. Scalidophoran worms. E, F. Lobopodians. G–L. Ecdysozoans from Chengjiang biota (ca. 518 Ma). G–I. Scalidophoran worms. J–L. Lobopodians. (A, B, D, E, F) unpublished material deposited at Northwest University, Xi’an.

## Material and Methods

### *Collection of extant specimens*

Living specimens of the priapulid *Priapulius caudatus* will be collected at the Kristineberg Marine Research Station in Sweden. Living onychophorans (the peripatopsid *Euperipatoides rowelli* and the peripatid *Principapillatus hitoyensis*) and tardigrades (*Hypsibius exemplaris*) are cultured in the laboratory at the University of Kassel in Germany and will be available for

molecular and anatomical studies.

### *Collection and preparation of fossil specimens*

Cambrian scalidophorans and lobopodians will be obtained from Small Shelly Fossils (SSF) assemblages already extracted from rocks (Kuanchuanpu Formation, Southern Shaanxi Province, China) and housed in the collections of the Shaanxi Key Laboratory of Early Life and Environments, Northwest University, Xi'an, China. They will be available for the present project. These microfossils are preserved three-dimensionally (via early phosphatization of their cuticular and soft tissues) and will be extracted from rocks by using standard techniques (diluted acetic acid as described in Wang et al., 2020). They will be analysed using a Hitachi S-4000 field emission Scanning Electron Microscope (SEM; Hitachi High-Technologies Europe GmbH, Krefeld, Germany) for observing the external morphology and Synchrotron radiation-based X-ray micro-computed tomography (SR- $\mu$ CT) for exploring internal structures. Three-dimensional (3D) reconstruction will be performed with VG STUDIO MAX 3.2 (Volume Graphics, Heidelberg, Germany).

### *Molecular studies*

Specimens of the priapulid *P. caudatus* will be induced to moult by injecting the steroid hormones E, 20E and, DA. The RNA will be isolated from tissues with TRIzol<sup>®</sup> Reagent (Invitrogen, Carlsbad, CA) and RNeasy MinElute Cleanup Kit (Qiagen, Hilden, Germany). Fragments of selected genes (see Schumann *et al.* 2018) will be amplified using specific primers and cloned into the pJet 1.2/blunt vector system (Thermo Scientific, Waltham, MA, USA). Functional analyses will be performed by RNA interference (RNAi) to knock out selected genes of the moulting pathway identified in nematodes and insects (Schumann *et al.* 2018).

## **6.2.2 Future research in China and international cooperation**

In the future, I want to get a position in China because there are a large number of Cambrian fossil sites to be exploited. Fundamental research (e.g. Palaeontology) is developing fast in China and is strongly supported by our government. Interdisciplinary approaches (e.g. biology, chemistry, physical, and artificial intelligence) applied to palaeontology are emphasised. I want to use my experience abroad for developing international cooperation with top laboratories and cutting-edge technologies.

## References

- Aberer, A. J., Krompass, D., and Stamatakis, A., 2013, Pruning rogue taxa improves phylogenetic accuracy: an efficient algorithm and webservice: *Systematic Biology*, v. 62, no. 1, p. 162-166.
- Adrianov, A. V., and Malakhov, V. V., 2001, Symmetry of Priapulids (Priapulida). 1. Symmetry of Adults: *Journal of Morphology*, v. 247, p. 99-110.
- Aguinaldo, A. M. A., Turbeville, J. M., Linford, L. S., Rivera, M. C., Garey, J. R., Raff, R. A., and Lake, J. A., 1997, Evidence for a clade of nematodes, arthropods and other moulting animals: *Nature*, v. 387, no. 6632, p. 489-493.
- Ahrlrichs, W., 1995, Ultrastruktur und Phylogenie von *Seison nebaliae* (Grube 1859) und *Seison annulatus* (Claus 1876). Hypothesen zu phylogenetischen Verwandtschaftsverhältnissen innerhalb der Bilateria., Göttingen, Cuvillier Verlag.
- Allison, P. A., and Briggs, D. E. G., 1993, Exceptional fossil record: distribution of soft-tissue preservation through the Phanerozoic: *Geology*, v. 21, p. 527-530.
- Annapurna, C., Vijaya Bhanu, C., Srinivasa Rao, M., Sheeja, C., Sanjeevi, P., Naveen Babu, M., Satyanarayana, A., and Ambedkar, A., 2017, Loricifera, an under known phyla: first record of higgins larva of *Armorloricus* (Loricifera: Nanaloricidae) from Indian waters: *Indian Journal of Geo Marine Sciences*, v. 46, no. 2, p. 317-321.
- Aria, C., Caron, J.-B., Gaines, R., and Zhang, X.-G., 2015, A large new leancoiliid from the Burgess Shale and the influence of inapplicable states on stem arthropod phylogeny: *Palaeontology*, v. 58, no. 4, p. 629-660.
- Attout, T., Martin, C., Babayan, S. A., Kozek, W. J., Bazzocchi, C., Oudet, F., Gallagher, I. J., Specht, S., and Bain, O., 2008, Pleural cellular reaction to the filarial infection *Litomosoides sigmodontis* is determined by the moulting process, the worm alteration, and the host strain: *Parasitology International*, v. 57, no. 2, p. 201-211.
- Ax, P., 1996, *Multicellular Animals*, Springer-Verlag Berlin Heidelberg GmbH, The phylogenetic System of the Metazoa, 1-41 p.:
- Ax, P., 2003, *Multicellular Animals: Order in Nature-System Made by Man*, Springer-Verlag Berlin Heidelberg GmbH, 1-41 p.:
- Babcock, L. E., Zhang, W. T., and Leslie, S. A., 2001, The Chengjiang biota: record of the early Cambrian diversification of life and clues to exceptional preservation of fossils: *GSA Today*, v. 11, p. 4-9.
- Bang-Berthelsen, I. H., Schmidt-Rhaese, A., and Møbjerg, K., 2013, *Handbook of zoology, Germany, De Gruyter, Gastrotricha, Cycloneuralia and Gnathifera*, 29-123 p.: Volume 1: Nematomorpha, Priapulida, Kinorhyncha, Loricifera: Loricifera, 349-370 p.
- Bengtson, S., and Yue, Z., 1997, Fossilized metazoan embryos from the earliest Cambrian: *Science*, v. 277, no. 12, p. 1645-1648.
- Bengtson, S., Conway Morris, S., and Cooper, B., 1990, Early Cambrian fossils from south Australia, *Association of Australasian Palaeontologists*, 1-364 p.
- Bennet-Clark, H. C., 1971, The cuticle as a template for growth in *Rhodnius prolixus*: *Journal of Insect Physiology*, v. 17, p. 2421-2434.
- Bereiter-Hahn, J., Matoltsy, A. G., and Richards, K. S., 1984, *Biology of the Integument*, Springer-Verlag, Invertebrates.

- Bergström, J., and Hou, X.-G., 2001, Cambrian Onychophora or Xenusians: *Zoologischer Anzeiger*, v. 240, no. 3-4, p. 237-245.
- Berner, R. A., 1970, Sedimentary pyrite formation: *American Journal of Science*, v. 268, p. 1-23.
- Berner, R. A., 1984, Sedimentary pyrite formation: an update: *Geochimica et Cosmochimica Acta*, v. 48, p. 605-615.
- Bertolani, R., Altiero, T., and Nelson, D. R., 2009, Tardigrada (Water Bears): *Invertebrates*, p. 443-456.
- Bhattacharya, D., Yoonb, H. S., Hedgesc, S. B., and Hackettd, J. D., 2009, Eukaryotes (Eukaryota), in Hedges, S. B., and Kumar, S., eds., *The Timetree of Life*, Oxford University Press Inc., New York, p. 116-120.
- Billings, E., 1872, On some fossils from the primordial rocks of Newfoundland: *Canadian Naturalist and Quarterly Journal of Science*, v. 6, p. 465-479.
- Blair, J. E., 2009, Animals (Metazoa), in Hedges, S. B., and Kumar, S., eds., *The Timetree of Life*, Oxford University Press Inc., New York, p. 223-230.
- Blair, S. S., 2008, Segmentation in animals: *Current Biology*, v. 18, no. 21, p. R991-995.
- Borner, J., Rehm, P., Schill, R. O., Ebersberger, I., and Burmester, T., 2014, A transcriptome approach to ecdysozoan phylogeny: *Molecular Phylogenetics and Evolution*, v. 80, p. 79-87.
- Botos, S., 2015, Life on a hydrothermal vent.
- Brazeau, M. D., Guillerme, T., and Smith, M. R., 2019 An algorithm for Morphological Phylogenetic Analysis with Inapplicable Data: *Systematic Biology*, v. 68, no. 4, p. 619-631.
- Brazeau, M. D., Smith, M. R., and Guillerme, T., 2017, MorphoLib: a library for phylogenetic analysis of categorical trait data with inapplicability, Zenodo.
- Briggs, D. E. G., 2003, The role of decay and mineralization in the preservation of soft-bodied fossils: *Annual Review of Earth and Planetary Sciences*, v. 31, no. 1, p. 275-301.
- Briggs, D. E. G., Erwin, D. H., and Collier, F. J., 1994, *The Fossils of the Burgess Shale*, Smithsonian Institution Press, 115 p.
- Brusca, R. C., Moore, W., and Shuster, S. M., 2016, *Invertebrates*, Sinauer Associates, Inc., Sunderland Massachusetts USA, 639-910 p.: Ecdysozoa.
- Bruton, D. L., 2001, A death assemblage of priapulid worms from the Middle Cambrian Burgess Shale: *Lethaia*, v. 34, p. 163-167.
- Buatois, L. A., and Gabriela Mángano, M., 2016, Ediacaran Ecosystems and the Dawn of Animals, in Gabriela Mángano, M., and Buatois, L. A., eds., *The Trace-Fossil Record of Major Evolutionary Events, Volume 1: Precambrian and Paleozoic*, Springer, p. 1-126.
- Budd, G. E., 1993, A Cambrian gilled lobopod from Greenland: *Nature*, v. 364, p. 709-711.
- Budd, G. E., 1998, The morphology and phylogenetic significance of *Kerygmachela kierkegaardii* Budd (Buen Formation, Lower Cambrian, N Greenland): *Transactions of the Royal Society of Edinburgh: Earth Sciences*, v. 89, p. 249-290.
- Budd, G. E., 1999, A nektaspid arthropod from the Early Cambrian Sirius Passet fauna, with a description of retrodeformation based on functional morphology: *Palaeontology*, v. 42, no. 1, p. 99-122.
- Budd, G. E., 2001, Why are arthropods segmented?: *Evolution & Development*, v. 3, no. 5, p. 332-342.
- Budd, G. E., 2003, Arthropods as Ecdysozoans: the fossil evidence.

- Budd, G. E., and Telford, M. J., 2009, The origin and evolution of arthropods: *Nature*, v. 457, no. 7231, p. 812-817.
- Campbell, N. A., 1996, *Biology*, The benjamin/cummings publishing company, Inc.
- Caron, J. B., and Aria, C., 2017, Cambrian suspension-feeding lobopodians and the early radiation of panarthropods: *BMC Evolutionary Biology*, v. 17, no. 1, p. 29.
- Caron, J. B., and Aria, C., 2020, The Collins' monster, a spinous suspension-feeding lobopodian from the Cambrian Burgess Shale of British Columbia: *Palaeontology*, v. 63, no. 6, p. 979-994.
- Caron, J. B., and Vannier, J., 2016, *Waptia* and the diversification of brood care in early arthropods: *Current Biology*, v. 26, no. 1, p. 69-74.
- Caron, J. B., Conway Morris, S., and Cameron, C., 2013, Tubicolous enteropneusts from the Cambrian period: *Nature* v. 495, p. 503-506.
- Caron, J.-B., Smith, M. R., and Harvey, T. H. P., 2013, Beyond the Burgess Shale: Cambrian microfossils track the rise and fall of hallucigeniid lobopodians: *Proceedings of the Royal Society B*, v. 280, no. 1767, p. 20131613.
- Chang, E. S., and Mykles, D. L., 2011, Regulation of crustacean molting: a review and our perspectives: *General and Comparative Endocrinology*, v. 172, no. 3, p. 323-330.
- Chapman, R. F., 2013, *The Insects-Structure and function*, Cambridge University Press, 463-498 p.
- Chen, A. L., Feng, H. Z., Zhu, M. Y., Ma, D. S., and Li, M., 2003a, A new vetulicolian from the early Cambrian Chengjiang fauna in Yunnan of China: *Acta Geologica Sinica*, v. 77, no. 3, p. 281-287.
- Chen, H., Parry, L. A., Vinther, J., Zhai, D., Hou, X., and Ma, X., 2020, A Cambrian crown annelid reconciles phylogenomics and the fossil record: *Nature*, v. 583, no. 7815, p. 249-252.
- Chen, J. Y., and Zhou, G. Q., 1997, *Biology of the Chengjiang fauna*: *Bulletin of the National Museum of Natural Science*, v. 10, p. 11-106.
- Chen, J. Y., Hou, X. G., and Lu, H. Z., 1989, Early Cambrian netted scale-bearing worm-like sea animal: *Acta Palaeontologica Sinica*, v. 28, no. 1, p. 1-20.
- Chen, J. Y., Huang, D. Y., Peng, Q. Q., Chi, H. M., Wang, X. Q., and Feng, M., 2003b, The first tunicate from the Early Cambrian of South China: *Proceedings of the National Academy of Sciences*, v. 100, no. 14, p. 8314-8318.
- Chen, J. Y., Zhou, G. Q., and Ramsköld, L., 1995, A new Early Cambrian onychophoran-like animal, *Paucipodia* gen. nov., from the Chengjiang fauna, China: *Transactions of the Royal Society of Edinburgh: Earth Sciences*, v. 85, no. 04, p. 275-282.
- Chen, J. Y., Zhou, G. Q., Zhu, M. Y., and Yeh, K. Y., 1996, *The Chengjiang Biota. A unique window of the Cambrian explosion.*, Taiwan, National Museum of Natural Science.
- Chen, L., Luo, H., Hu, S., Yin, J., Jiang, Z., Wu, Z., Li, F., and Chen, A., 2002, Early Cambrian Chengjiang Fauna in eastern Yunnan China (in Chinese with English abstract), Yunnan Science and Technology Press.
- Chen, Z., Zhou, C., Xiao, S., Wang, W., Guan, C., Hua, H., and Yuan, X., 2014, New Ediacara fossils preserved in marine limestone and their ecological implications: *Scientific Reports*, v. 4, p. 4180.
- Chen, Z., Zhou, C., Yuan, X., and Xiao, S., 2019, Death march of a segmented and trilobate bilaterian elucidates early animal evolution: *Nature*, v. 573, no. 7774, p. 412-415.

- Cheng, J. L., 2019, Restudy of the gourd-shaped priapulids from the Cambrian Chengjiang biota and their phylogeny [Master: Yunnan University.
- Cong, P., Daley, A. C., Edgecombe, G. D., and Hou, X. G., 2017, The functional head of the Cambrian radiodontan (stem-group Euarthropoda) *Amplectobelua symbrachiata*: BMC Evolutionary Biology, v. 17, no. 1, p. 1-23.
- Cong, P., Ma, X., Hou, X., Edgecombe, G. D., and Strausfeld, N. J., 2014, Brain structure resolves the segmental affinity of anomalocaridid appendages: Nature, v. 513, no. 7519, p. 538-542.
- Congreve, C. R., and Lamsdell, J. C., 2016, Implied weighting and its utility in palaeontological datasets: a study using modelled phylogenetic matrices: Palaeontology, v. 59, no. 3, p. 447-462.
- Conway Morris, S., 1977a, Fossil priapulid worms: Special Papers in Palaeontology, v. 20, p. 1-95.
- Conway Morris, S., 1977b, A new metazoan from the Cambrian Burgess Shale of British Columbia: Palaeontology, v. 20, no. 3, p. 623-640.
- Conway Morris, S., 1997, The cuticular structure of the 495-Myr-old type species of the fossil worm *Palaeoscolex*, *P. piscatorum* (?Priapulida): Zoological Journal of the Linnean Society, v. 119, p. 69-82.
- Conway Morris, S., and Peel, J. S., 2010, New palaeoscolecidan worms from the lower Cambrian: Sirius Passet, Latham Shale and Kinzers Shale: Acta Palaeontologica Polonica, v. 55, no. 1, p. 141-156.
- Conway Morris, S., and Robison, R. A., 1986, Middle Cambrian priapulids and other soft-bodied fossils from Utah and Spain: The University of Kansas Paleontological Contributions, v. 117, p. 1-22.
- Conway Morris, S., Peel, J. S., Higgins, A. K., Soper, N. J., and Davis, N. C., 1987, A Burgess shale-like fauna from the Lower Cambrian of North Greenland: Nature, v. 362, p. 181-183.
- Cui, L., Liu, W., and Zhang, X., 2020, Phosphatized microbial fossils from the lowest Cambrian of South China and their ecological and environmental implications for the Kuanchuanpu biota: Precambrian Research, v. 338, p. 105560.
- Cunningham, J. A., Liu, A. G., Bengtson, S., and Donoghue, P. C. J., 2017, The origin of animals: Can molecular clocks and the fossil record be reconciled?: Bioessays, v. 39, no. 1, p. 1-12.
- Cuvier, G., 1817, Le Règne animal, distribué d'après son organization pour servir de base à l'histoire naturelle des animaux et d'introduction à l'anatomie comparée, Deterville, Paris.
- Daley, A. C., and Antcliffe, J. B., 2019, Evolution: The battle of the first animals: Current Biology, v. 29, no. 7, p. R257-R259.
- Daley, A. C., and Drage, H. B., 2016, The fossil record of ecdysis, and trends in the moulting behaviour of trilobites: Arthropod Structure & Development, v. 45, no. 2, p. 71-96.
- Daley, A. C., and Legg, D. A., 2015, A morphological and taxonomic appraisal of the oldest anomalocaridid from the Lower Cambrian of Poland: Geological Magazine, v. 152, no. 05, p. 949-955.
- Daley, A. C., Budd, G. E., Caron, J. B., Edgecombe, G. D., and Collins, D., 2009, The Burgess Shale anomalocaridid *Hurdia* and its significance for early euarthropod evolution: Science, v. 323, no. 5921, p. 1597-1600.
- Dong, C. Z., Hu, S. X., and Zhao, F. c., 2018, Occurrence of *Sicyophorus* from the early Cambrian Guanshan biota: Acta Palaeontologica Sinica, v. 57, no. 4, p. 424-428.

- Dong, X. P., Donoghue, P. C., Cheng, H., and Liu, J. B., 2004, Fossil embryos from the Middle and Late Cambrian period of Hunan, south China: *Nature*, v. 427, no. 6971, p. 234-240.
- Dong, X. P., Donoghue, P. C., Cunningham, J. A., Liu, J. B., and Cheng, H., 2005, The anatomy, affinity, and phylogenetic significance of *Markuelia*: *Evolution & Development*, v. 7, no. 5, p. 468-482.
- Drage, H. B., Holmes, J. D., García-Bellido, D. C., and Daley, A. C., 2018, An exceptional record of Cambrian trilobite moulting behaviour preserved in the Emu Bay Shale, South Australia: *Lethaia*, v. 51, no. 4, p. 473-492.
- Duan, Y., Han, J., Fu, D., Zhang, X., Yang, X., Komiya, T., and Shu, D., 2014, Reproductive strategy of the bradoriid arthropod *Kunmingella douvillei* from the Lower Cambrian Chengjiang Lagerstätte, South China: *Gondwana Research*, v. 25, no. 3, p. 983-990.
- Dunn, C. W., Giribet, G., Edgecombe, G. D., and Hejnol, A., 2014, Animal Phylogeny and Its Evolutionary Implications: *Annual Review of Ecology, Evolution, and Systematics*, v. 45, no. 1, p. 371-395.
- Dunn, C. W., Hejnol, A., Matus, D. Q., Pang, K., Browne, W. E., Smith, S. A., Seaver, E., Rouse, G. W., Obst, M., Edgecombe, G. D., Sorensen, M. V., Haddock, S. H., Schmidt-Rhaesa, A., Okusu, A., Kristensen, R. M., Wheeler, W. C., Martindale, M. Q., and Giribet, G., 2008, Broad phylogenomic sampling improves resolution of the animal tree of life: *Nature*, v. 452, no. 7188, p. 745-749.
- Dzik, J., 2003, Early Cambrian lobopodian sclerites and associated fossils from Kazakstan: *Palaeontology*, v. 46, no. 1, p. 93-112.
- Dzik, J., and Krumbiegel, G., 1989, The oldest 'onychophoran' *Xenusion*: a link connecting phyla?: *Lethaia*, v. 22, p. 169-181.
- Edgecombe, G. D., 2009, Palaeontological and molecular evidence linking arthropods, onychophorans, and other Ecdysozoa: *Evolution: Education and Outreach*, v. 2, no. 2, p. 178-190.
- Elder, H. Y., and Hunter, R. D., 1980, Burrowing of *Priapulus caudatus* (Vermes) and the significance of the direct peristaltic wave: *Journal of Zoology*, v. 191, p. 333-351.
- Eriksson, B. J., Tait, N. N., and Budd, G. E., 2003, Head development in the onychophoran *Euperipatoides kanangrensis* with particular reference to the central nervous system: *Journal of Morphology*, v. 255, no. 1, p. 1-23.
- Evans, S. D., Droser, M. L., and Gehling, J. G., 2015, *Dickinsonia* liftoff: evidence of current derived morphologies: *Palaeogeography, Palaeoclimatology, Palaeoecology*, v. 434, p. 28-33.
- Fänge, R., and Mattisson, A., 1961, Function of the caudal appendage of *Priapulus caudatus*: *Nature*, v. 190, p. 1216-1217.
- Farris, J. S., 1970, Methods for Computing Wagner Trees: *Systematic Zoology*, v. 19, no. 1, p. 83.
- Fitch, W. M., 1971, Toward defining the course of evolution: minimum change for a specific tree topology: *Systematic Zoology*, v. 20, no. 4, p. 406-416.
- Fu, D. J., Zhang, X. L., Budd, G. E., Liu, W., and Pan, X. Y., 2014, Ontogeny and dimorphism of *Isoxys auritus* (Arthropoda) from the early Cambrian Chengjiang biota, South China: *Gondwana Research*, v. 25, no. 3, p. 975-982.

- Fu, D., Tong, G., Dai, T., Liu, W., Yang, Y., Zhang, Y., Cui, L., Li, L., Yun, H., Wu, Y., Sun, A., Liu, C., Pei, W., Gaines, R. R., and Zhang, X., 2019, The Qingjiang biota-A Burgess Shale-type fossil Lagerstätte from the early Cambrian of South China: *Science*, v. 363, no. 6433, p. 1338-1342.
- Gabbott, S. E., Xian-guang, H., Norry, M. J., and Siveter, D. J., 2004, Preservation of Early Cambrian animals of the Chengjiang biota: *Geology*, v. 32, no. 10, p. 901.
- Gad, G., 2005, A parthenogenetic, simplified adult in the life cycle of *Pliciloricus pedicularis* sp. n. (Loricifera) from the deep sea of the Angola Basin (Atlantic): *Organisms Diversity & Evolution*, v. 5, p. 77-103.
- Gaines, R. R., Briggs, D. E. G., and Zhao, Y. L., 2008, Cambrian Burgess Shale-type deposits share a common mode of fossilization: *Geology*, v. 36, no. 10, p. 755.
- García-Bellido, D. C., Paterson, J. R., and Edgecombe, G. D., 2013, Cambrian palaeoscoleids (Cycloneuralia) from Gondwana and reappraisal of species assigned to *Palaeoscolex*: *Gondwana Research*, v. 24, no. 2, p. 780-795.
- Garey, J. R., 2001, Ecdysozoa: The Relationship between Cycloneuralia and Panarthropoda: *Zoologischer Anzeiger - A Journal of Comparative Zoology*, v. 240, no. 3-4, p. 321-330.
- Gibson, M. C., Patel, A. B., Nagpal, R., and Perrimon, N., 2006, The emergence of geometric order in proliferating metazoan epithelia: *Nature*, v. 442, no. 7106, p. 1038-1041.
- Gibson, W. T., and Gibson, M. C., 2009, Cell topology, geometry, and morphogenesis in proliferating epithelia: *Current Topics in Developmental Biology*, v. 89, p. 87-114.
- Giribet, G., and Edgecombe, G. D., 2017, Current understanding of Ecdysozoa and its internal phylogenetic relationships: *Integrative and Comparative Biology*, v. 57, no. 3, p. 455-466.
- Glaessner, M. F., 1958, New fossils from the base of the Cambrian in South Australia: *Transactions of the Royal Society of South Australia*, v. 81, p. 185-188.
- Glaessner, M. F., 1979, Lower Cambrian Crustacea and annelid worms from Kangaroo Island, South Australia: *Alcheringa: An Australasian Journal of Palaeontology*, v. 3, no. 1, p. 21-31.
- Goloboff, P. A., and Catalano, S. A., 2016, TNT version 1.5, including a full implementation of phylogenetic morphometrics: *Cladistics*, v. 32, p. 221-238.
- Golubic S., P. R. D., Lukas K. J., 1975, *The study of trace fossils*, Heidelberg, Germany, Springer, Boring microorganisms and microborings in carbonate substrates.
- Guillerme, T., Brazeau, M. D., and Smith, M. R., 2018, Inapp: Reconstruction of Inapplicable Discrete Characters on Phylogenetic Trees (Version v0.4.1): Zenodo.
- Hammond, R. A., 1970, The Surface of *Priapulius caudatus* (Lamarck, 1816): *Zeitschrift für Morphologie der Tiere*, v. 68, p. 255-268.
- Han, J. Zhang, X. L., Zhang, Z. F., and Shu, D. G., 2003, A new platy-armored worm from the early Cambrian Chengjiang Lagerstätte, South China: *Acta Geologica Sinica-English Edition*, v. 77, no. 1, p. 1-6.
- Han, J., 2002, *Introverta in Chengjiang Fauna* (In Chinese with English abstract) [Doctor of Philosophy: Northwest University, 15-80 p.
- Han, J., and Hu, S., 2006, Response to "Discussion on the systematic position of the early Cambrian priapulomorph worms": *Chinese Science Bulletin*, v. 51, no. 2, p. 250-256.
- Han, J., Hu, S., Cartwright, P., Zhao, F., Ou, Q., Kubota, S., Wang, X., and Yang, X., 2016b, The earliest pelagic jellyfish with rhopalia from Cambrian Chengjiang Lagerstätte: *Palaeogeography, Palaeoclimatology, Palaeoecology*, v. 449, p. 166-173.



- Han, J., Kubota, S., Li, G., Ou, Q., Wang, X., Yao, X., Shu, D., Li, Y., Uesugi, K., Hoshino, M., Sasaki, O., Kano, H., Sato, T., and Komiya, T., 2016a, Divergent evolution of medusozoan symmetric patterns: Evidence from the microanatomy of Cambrian tetrameric cubozoans from South China: *Gondwana Research*, v. 31, p. 150-163.
- Han, J., Kubota, S., Uchida, H.-o., Stanley Jr., G. D., Yao, X., Degan, S., Li, Y., Li, and Yasui, K., Yasui, 2010, Tiny sea anemone from the Lower Cambrian of China: *PLoS One*, v. 5, no. 10, p. e13276.
- Han, J., Liu, J. N., Zhang, Z. F., Zhang, X. L., and Shu, D. G., 2007a, Trunk ornament on the palaeoscolecid worms *Cricocosmia* and *Tabelliscolex* from the Early Cambrian Chengjiang deposits of China: *Acta Palaeontologica Polonica*, v. 52, no. 2, p. 423-431.
- Han, J., Shu, D., Zhang, Z., and Liu, J., 2004a, The earliest-known ancestors of Recent Priapulomorpha from the Early Cambrian Chengjiang Lagerstätte: *Chinese Science Bulletin*, v. 49, no. 17, p. 1860.
- Han, J., Yao, Y., Zhang, Z. F., Liu, J., and Shu, D., 2007b, New observation on the palaeoscolecid worm *Tylotites petiolaris* from the Cambrian Chengjiang Lagerstätte south China: *Paleontological Research*, v. 11, no. 1, p. 59-69.
- Han, J., Zhang, X. L., Zhang, Z. F., and Shu, D. G., 2006, A new theca-bearing Early Cambrian worm from the Chengjiang Fossil Lagerstätte, China: *Alcheringa: An Australasian Journal of Palaeontology*, v. 30, p. 1-10.
- Han, J., Zhang, Z. F., and Liu, J. N., 2007d, The trace fossils of priapulids from the Early Cambrian Chengjiang deposits and implications for their locomotory styles: *Journal of China University of Geoscience*, v. 18, special issue, p. 392-393.
- Han, J., Zhang, Z., and Liu, J., 2004b, Taphonomy and ecology of the introverts from the Chengjiang fauna (in Chinese with English abstract): *Journal of Northwest University (Natural Science Edition)*, v. 34, no. 2, p. 207-212.
- Han, J., Zhang, Z., Liu, J., and Shu, D., 2007c, Evidence of priapulid scavenging from the early Cambrian Chengjiang deposits, southern China: *Palaios*, v. 22, no. 6, p. 691-694.
- Harvey, T. H. P., and Butterfield, N. J., 2017, Exceptionally preserved Cambrian loriciferans and the early animal invasion of the meiobenthos: *Nature Ecology & Evolution*, v. 1, no. 3, p. 22.
- Harvey, T. H., Dong, X., and Donoghue, P. C., 2010, Are palaeoscolecids ancestral ecdysozoans?: *Evol Dev*, v. 12, no. 2, p. 177-200.
- He, T. G., and Xie, Y. S., 1989, Some problematic small shelly fossils from the Meishucunian of the Lower Cambrian in the western Yangtze region: *Acta Micropalaeontologica Sinica*, v. 6, no. 2, p. 111-127.
- He, Y. X., and Yang, X. H., 1986, Early Cambrian coelenterates from Nanjiang, Sichuan: *Bulletin of the Chengdu Institute of Geology and Mineral Resources*, v. 7, p. 31-43 (In Chinese with English abstract).
- Heiner, I., and Kristensen, R. M., 2005, Two new species of the genus *Pliciloricus* (Loricifera, Pliciloricidae) from the Faroe Bank, North Atlantic: *Zoologischer Anzeiger - A Journal of Comparative Zoology*, v. 243, no. 3, p. 121-138.
- Hejnol, A., Obst, M., Stamatakis, A., Michael, O., Rouse, G. W., Edgecombe, G. D., Martinez, P., Baguna, J., X. B., Jondelius, U., and al., e., 2009, Assessing the root of bilaterian animals with scalable phylogenomic methods: *Proceedings of the Royal Society B*, v. 276, no. 4261-4270.

- Herranz, M., Leander, B. S., Pardos, F., and Boyle, M. J., 2019, Neuroanatomy of mud dragons: a comprehensive view of the nervous system in *Echinoderes* (Kinorhyncha) by confocal laser scanning microscopy: *BMC Evolutionary Biology*, v. 19, no. 1, p. 86.
- Higgins, R. P., and Stroch, V., 1991, Evidence for direct development in *Meiopriapulidus fijiensis* (Priapulida): *Transactions of the American Microscopical Society*, v. 110, no. 1, p. 37-46.
- Hogvall, M., Vellutini, B. C., Martin-Duran, J. M., Hejnol, A., Budd, G. E., and Janssen, R., 2019, Embryonic expression of priapulid Wnt genes: *Development Genes and Evolution*, v. 229, no. 4, p. 125-135.
- Hopkins, P. M., 2001, Limb regeneration in the fiddler crab, *Uca pugilator*: hormonal and growth factor control: *American Zoologist*, v. 41, no. 3, p. 389–398.
- Hou, X. G., 1987, Three new large arthropods from lower Cambrian, Chengjiang, eastern Yunnan: *Acta Palaeontologica Sinica*, v. 26, p. 272–285. (In Chinese with English abstract).
- Hou, X. G., and Bergström, J., 1997, Arthropods of the Lower Cambrian Chengjiang fauna, southwest China: *Fossils & Strata*, v. 45, p. 54-57.
- Hou, X. G., and Chen, J. Y., 1989a, Early Cambrian arthropod-annelid intermediate sea animal, *Luolishania* gen. nov. from Chengjiang, Yunnan: *Acta Palaeontologica Sinica*, v. 28, no. 2, p. 207-214.
- Hou, X. G., and Chen, J. Y., 1989b, Early Cambrian tentacled worm-like animals (*Facivermis* gen. nov.) from Chengjiang, Yunnan: *Acta Palaeontologica Sinica*, v. 28, no. 1, p. 32-43.
- Hou, X. G., and Sun, W. G., 1988, Discovery of Chengjiang fauna, Meishucun, Jinning, Yunnan, v. 27, no. 1, p. 1-16.
- Hou, X. G., Ramskold, L., and Bergstrom, J., 1991, Composition and preservation of the Chengjiang fauna -a Lower Cambrian soft-bodied biota: *Zoologica Scripta*, v. 20, no. 4, p. 395-411.
- Hou, X. G., Siveter, D. J., Siveter, D. J., Aldridge, R. J., Cong, P. Y., Gabbott, S. E., Ma, X. Y., Purnell, M. A., and Williams, M., 2017, *The Cambrian Fossils of Chengjiang, China: The Flowering of Early Animal Life*, Wiley Blackwell, 98-270 p.:
- Hou, X., Bergström, J., Wang, H., Feng, X., and Chen, A., 1999, The Chengjiang Fauna-exceptional well-preserved animals from 530 million years ago (in Chinese with English summary), Yunnan, Yunnan Science and Technology Press.
- Hou, X.-g., and Bergstrom, J., 1994, Palaeoscolecoid worms may be nematomorphs rather than annelids: *Lethaia*, v. 27, p. 11-17.
- Hou, X.-g., and Bergström, J., 1995, Cambrian lobopodians—ancestors of extant onychophorans?: *Zoological Journal of the Linnean Society* v. 114, p. 3-19.
- Howard, R. J., Edgecombe, G. D., Shi, X., Hou, X., and Ma, X., 2020b, Ancestral morphology of Ecdysozoa constrained by an early Cambrian stem group ecdysozoan: *BMC Evolutionary Biology*, v. 20, no. 1, p. 156.
- Howard, R. J., Hou, X., Edgecombe, G. D., Salge, T., Shi, X., and Ma, X., 2020a, A tube-dwelling early Cambrian lobopodian: *Current Biology*, v. 30, p. 1-8.
- Hu, S., 2005, *Taphonomy and Palaeoecology of the Early Cambrian Chengjiang Biota from Eastern Yunnan, China*, Berlin, Berliner Paläobiologische Abhandlungen.
- Hu, S., Zhu, M., Luo, H., Steiner, M., Zhao, F., Li, G., Liu, Q., and Zhang, Z., 2013, *The Guanshan Biota*, Yunnan Publishing Group Co. Ltd. Yunnan Science and Technology Press, 1-204 p.
- Huang, D., 2005, Early Cambrian worms from SW China: morphology, systematics, lifestyles and evolutionary significance [Doctor: Université Claude Bernard Lyon 1, 19-234 p.

- Huang, D., Chen, J., and Vannier, J., 2006, Discussion on the systematic position of the Early Cambrian priapulomorph worms: Chinese Science Bulletin, v. 51, no. 2, p. 243-249.
- Huang, D., Chen, J., Zhu, M., and Zhao, F., 2014, The burrow dwelling behavior and locomotion of palaeoscolecid worms: New fossil evidence from the Cambrian Chengjiang fauna: Palaeogeography, Palaeoclimatology, Palaeoecology, v. 398, p. 154-164.
- Huang, D., Vannier, J., and Chen, J., 2004a, Anatomy and lifestyles of Early Cambrian priapulid worms exemplified by *Corynetis* and *Anningvermis* from the Maotianshan Shale (SW China): Lethaia, v. 37, no. 1, p. 21-33.
- Huang, D., Vannier, J., and Chen, J., 2004b, Recent Priapulidae and their Early Cambrian ancestors: comparisons and evolutionary significance: Geobios, v. 37, no. 2, p. 217-228.
- Huelsenbeck, J. P., and Ronquist, F., 2001, MRBAYES: Bayesian inference of phylogenetic trees: Bioinformatics v. 17, p. 754-755.
- Ivantsov, A. Y., and Wrona, R., 2004, Articulated palaeoscolecid sclerite arrays from the Lower Cambrian of eastern Siberia: Acta Geologica Polonica, v. 54, no. 1, p. 1-22.
- Ivantsov, A. Y., Malakhovskaya, Y. E., and Serezhnikova, E. A., 2004, Some problematic fossils from the Vendian of the southeastern White Sea Region: Paleontological Journal, v. 38 no. 1, p. 1-9.
- Ivantsov, A. Y., Zhuravlev, A. Y., Leguta, A. V., Krassilov, V. A., Melnikova, L. M., and Ushatinskaya, G. T., 2005, Palaeoecology of the Early Cambrian Sinsk biota from the Siberian Platform: Palaeogeography, Palaeoclimatology, Palaeoecology, v. 220, no. 1-2, p. 69-88.
- Jiang, Z., 1980, Monoplacophorans and gastropods fauna of the Meishucun Stage from the Meishucun section, Yunnan: Acta Geologica Sinica, v. 2, p. 112-123.
- Kesidis, G., Slater, B. J., Jensen, S., and Budd, G. E., 2019, Caught in the act: Priapulid burrowers in early Cambrian substrates: Proceedings of the Royal Society B, v. 286, no. 1894, p. 20182505.
- Kimmig, J., Strotz, L. C., Kimmig, S. R., Egenhoff, S. O., and Lieberman, B. S., 2019, The Spence Shale Lagerstätte: an important window into Cambrian biodiversity: Journal of the Geological Society, v. 176, no. 4, p. 609-619.
- Kirstensen, R. M., 1983, Loricifera, a new phylum with Aschelminthes characters from the meiobenthos: Zeitschrift für zoologische Systematik und Evolutionsforschung, v. 21, no. 3, p. 163-180.
- Kirstensen, R. M., 1991, Loricifera, in Harrison, F. W., and Ruppert, E. E., eds., Microscopic Anatomy of Invertebrates, Volume 4: New York, Wiley-Liss, p. 351-375.
- Kirsteuer, E., and van der Land, J., 1970, Some notes on *Tubiluchus corallicola* (Priapulida) from Barbados, West Indies: Marine Biology, v. 7, p. 230-238.
- Knaust, D., 2020, Invertebrate coprolites and cololites revised: Papers in Palaeontology, v. 6, no. 3, p. 385-423.
- Kouraiss, K., El Hariri, K., El Albani, A., Azizi, A., Mazurier, A., and Vannier, J., 2018, X-ray microtomography applied to fossils preserved in compression: Palaeoscolecid worms from the Lower Ordovician Fezouata Shale: Palaeogeography, Palaeoclimatology, Palaeoecology, v. 508, p. 48-58.
- Kristensen, R. M., 2002, An introduction to Loricifera, Cyclophora, and Micrognathozoa: Integrative and comparative biology, v. 42, p. 641-651.

- Laflamme, M., Gehling, J. G., and Droser, M. L., 2018, Deconstructing an Ediacaran frond: three-dimensional preservation of *Arborea* from Ediacara, South Australia: *Journal of Paleontology*, v. 92, no. 3, p. 323-335.
- Lan, T., Yang, J., Hou, J., and Zhang, X., 2015, The feeding behaviour of the Cambrian tubicolous priapulid *Selkirkia*: *Lethaia*, v. 48, no. 1, p. 125-132.
- Laumer, C. E., Bekkouche, N., Kerbl, A., Goetz, F., Neves, R. C., Sorensen, M. V., Kristensen, R. M., Hejnol, A., Dunn, C. W., Giribet, G., and Worsaae, K., 2015, Spiralian phylogeny informs the evolution of microscopic lineages: *Current Biology*, v. 25, no. 15, p. 2000-2006.
- Laumer, C. E., Fernandez, R., Lemer, S., Combosch, D., Kocot, K. M., Riesgo, A., Andrade, S. C. S., Sterrer, W., Sorensen, M. V., and Giribet, G., 2019, Revisiting metazoan phylogeny with genomic sampling of all phyla: *Proceedings of the Royal Society B*, v. 286, no. 1906, p. 20190831.
- Lemburg, C., 1995, Ultrastructure of the introvert and associated structures of the larvae of *Halicryptus spinulosus* (Priapulida): *Zoomorphology*, v. 115, p. 11-29.
- Lemburg, C., 1998, Electron microscopical localization of chitin in the cuticle of *Halicryptus spinulosus* and *Priapulus caudatus* (Priapulida) using gold-labelled wheat germ agglutinin: phylogenetic implications for the evolution of the cuticle within the Nemathelminthes: *Zoomorphology*, v. 118, p. 137-158.
- Lemburg, C., 1999, Ultrastrukturelle untersuchungen an den larven von *Halicryptus spinulosus* und *Priapulus caudatus*. Hypothesen zur phylogenie der Priapulida und deren dedeutung für die evolution der Nemathelminthen., Göttingen, Cuvillier Verlag.
- Lewis, P. O., 2001, A likelihood approach to estimating phylogeny from discrete morphological character data: *Systematic biology*, v. 50, no. 6, p. 913-925.
- Li, Y. W., 1975, On the Cambrian ostracodes with new material from Sichuan, Yunnan and Shaanxi, China: *Professional Papers on Stratigraphy and Palaeontology*, v. 2, p. 37-72. Geological Publishing House, Beijing (in Chinese with English abstract).
- Li, Z. P., 1984, The discovery and its significance of early Cambrian small shell fossils in Hexi area Xixiang Shaanxi: *Geology of Shaanxi*, v. 2, no. 1, p. 73-78. (in Chinese with English abstract).
- Liu, J. N., Shu, D. G., Han, J., Zhang, Z. F., and Zhang, X. L., 2006, A large xenusiid lobopod with complex appendages from the lower Cambrian Chengjiang Lagerstätte: *Acta Palaeontologica Polonica*, v. 51, no. 2, p. 215-222.
- Liu, J., Shu, D., Han, J., Zhang, Z., and Zhang, X., 2007, Morpho-anatomy of the lobopod *Magadictyon cf. haikouensis* from the Early Cambrian Chengjiang Lagerstätte, South China: *Acta Zoologica*, v. 88, no. 4, p. 279-288.
- Liu, J., Steiner, M., Dunlop, J. A., Keupp, H., Shu, D., Ou, Q., Han, J., Zhang, Z., and Zhang, X., 2011, An armoured Cambrian lobopodian from China with arthropod-like appendages: *Nature*, v. 470, no. 7335, p. 526-530.
- Liu, Y. H., Qin, J. C., Wang, Q., Maas, A., Duan, B. C., Zhang, Y. N., Zhang, H., Shao, T. Q., Zhang, H. Q., and Zhang, X. G., 2018, New armoured scalidophorans (Ecdysozoa, Cycloneuralia) from the Cambrian Fortunian Zhangjiagou Lagerstätte, South China: *Papers in Palaeontology*, p. 1-20.
- Liu, Y. H., Xiao, S. H., Shao, T. Q., Broce, J., and Zhang, H. Q., 2014, The oldest known priapulid-like scalidophoran animal and its implications for the early evolution of cycloneuralians and ecdysozoans: *Evolution & Development*, v. 16, no. 3, p. 155-165.

- Luo, H. L., and Zhang, S. S., 1986, Early Cambrian vermes and trace fossils from Jinning-Anning region, Yunnan: *Acta Palaeontologica Sinica*, v. 25, no. 3, p. 307-313.
- Luo, H. L., Jiang, Z. W., Wu, X. C., Song, X. L., and Ou-Yang, L., 1982, The Sinian-Cambrian boundary in eastern Yunnan, China: The People's Press of Yunnan, p. 163-215.
- Luo, H., Hu, S., Chen, L., Zhang, S., and Tao, Y., 1999, Early Cambrian Chengjiang Fauna from Kunming region China (In Chinese with English summary), Yunnan Science and Technology Press.
- Ma, X. Y., Aldridge, R. J., Siveter, D. J., Siveter, D. J., Hou, X. G., and Edgecombe, G. D., 2014a, A new exceptionally preserved Cambrian priapulid from the Chengjiang Lagerstätte: *Journal of Paleontology*, v. 88, no. 2, p. 371-384.
- Ma, X., Edgecombe, G. D., Legg, D. A., and Hou, X., 2014b, The morphology and phylogenetic position of the Cambrian lobopodian *Diania cactiformis*: *Journal of Systematic Palaeontology*, v. 12, no. 4, p. 445-457.
- Ma, X., Hou, X., and Baines, D., 2010, Phylogeny and evolutionary significance of vermiform animals from the Early Cambrian Chengjiang Lagerstätte: *Science China Earth Sciences*, v. 53, no. 12, p. 1774-1783.
- Maas, A., 2013, Handbook of zoology, Germany, De Gruyter, Gastrotricha, Cycloneuralia and Gnathifera, 29-123 p.: Volume 1: Nematomorpha, Priapulida, Kinorhyncha, Loricifera: The fossil record, 11-28 p.
- Maas, A., Braun, A., Dong, X.-P., Donoghue, P. C. J., Müller, K. J., Olempska, E., Repetski, J. E., Siveter, D. J., Stein, M., and Waloszek, D., 2006, The 'Orsten'—More than a Cambrian Konservat-Lagerstätte yielding exceptional preservation: *Palaeoworld*, v. 15, no. 3-4, p. 266-282.
- Maas, A., Huang, D., Chen, J., Waloszek, D., and Braun, A., 2007a, Maotianshan-Shale nemathelminths-Morphology, biology, and the phylogeny of Nemathelminthes: *Palaeogeography, Palaeoclimatology, Palaeoecology*, v. 254, no. 1-2, p. 288-306.
- Maas, A., Mayer, G., Kristensen, R. M., and Waloszek, D., 2007b, A Cambrian micro-lobopodian and the evolution of arthropod locomotion and reproduction: *Chinese Science Bulletin*, v. 52, no. 24, p. 3385-3392.
- Maas, A., Waloszek, D., Haug, J. T., and Muller, K. J., 2009, Loricated larvae (Scalidophora) from the Middle Cambrian of Australia: *Memoirs of the Association of Australasian Palaeontologists* v. 37, p. 281-302.
- Maddison, W. P., and Maddison, D. R., 2019, Mesquite: a modular system for evolutionary analysis. Version 3.61.
- Markov, G.V., Tavares, R., Dauphin-Villemant, C., Demeneix, B.A., Baker, M.E., Laudet, V., 2009, Independent elaboration of steroid hormone signaling pathways in metazoans: *Proceedings of the National Academy of Science*, v. 106, p. 11913-11918.
- Martin, C., Gross, V., Hering, L., Tepper, B., Jahn, H., Oliveira, I.S., Stevenson, P.A. & Mayer, G., 2017, The nervous and visual systems of onychophorans and tardigrades: learning about arthropod evolution from their closest relatives: *Journal of Comparative Physiology A*, v. 203, p. 565-590.
- Martín-Durán, J. M., and Hejnol, A., 2015, The study of *Priapulius caudatus* reveals conserved molecular patterning underlying different gut morphogenesis in the Ecdysozoa: *BMC Biology*, v. 13, p. 29.

- Martín-Durán, J. M., Passamaneck, Y. J., Martindale, M. Q., and Hejnol, A., 2016, The developmental basis for the recurrent evolution of deuterostomy and protostomy: *Nature Ecology Evolution*, v. 1, no. 1, p. 5.
- Mayer, G., Martin, C., Rudiger, J., Kauschke, S., Stevenson, P. A., Poprawa, I., Hohberg, K., Schill, R. O., Pflugger, H. J., and Schlegel, M., 2013, Selective neuronal staining in tardigrades and onychophorans provides insights into the evolution of segmental ganglia in panarthropods: *BMC Evolutionary Biology*, v. 13, p. 230.
- McLean, N., 1984, Amoebocytes in the lining of the body cavity and mesenteries of *Priapulid* *Priapulid* (*Priapulida*): *Acta Zoology*, v. 65, p. 75-78.
- McLoughlin, N., Brasier, M. D., Wacey, D., Green, O. R., and Randall, S. P., 2007, On biogenicity criteria for endolithic microborings on Early Earth and beyond: *Astrobiology*, v. 7, p. 10-26.
- Missarzhevsky, V. V., 1973, Conodont-shaped organisms from Precambrian-Cambrian boundary strata of the Siberian Platform and Kazakhstan: *Trudy Instituta Geologii i Geofiziki SO AN SSSR*, v. 49, p. 53-57 (In Russian with English abstract).
- Müller, K. J., 1962, Aus der Praxis-Ein einfacher behelf für die listungstechnik: *Paläontologische Zeitschrift*, v. 36, p. 265-267.
- Müller, K. J., 1979, Phosphatocopine ostracodes with preserved appendages from the Upper Cambrian of Sweden: *Lethaia*, v. 12, no. 1, p. 1-27.
- Müller, K. J., Walossek, D., and Zakharov, A., 1995, 'Orsten' type phosphatized soft-integument preservation and a new record from the Middle Cambrian Kuonamka Formation in Siberia: *Neues Jahrbuch für Geologie und Paläontologie - Abhandlungen*, v. 197, no. 1, p. 101-118.
- Muller, M. C., and Schmidt-Rhaesa, A., 2003, Reconstruction of the muscle system in *Antygomonas* sp. (Kinorhyncha, Cyclorhagida) by means of phalloidin labeling and cLSM: *Journal of Morphology*, v. 256, no. 2, p. 103-110.
- Murdock, D. J. E., Gabbott, S. E., Mayer, G., and Purnell, M. A., 2014, Decay of velvet worms (Onychophora), and bias in the fossil record of lobopodians: *BMC Evolutionary Biology*, v. 14, p. 222.
- Naimark, E. B., and Ivantsov, A. Y., 2009, Growth variability in the late Vendian problematic *Parvancorina* Glaessner: *Paleontological Journal*, v. 43, no. 1, p. 12-18.
- Nanglu, K., Caron, J. B., Conway Morris, S., and Cameron, C. B., 2016, Cambrian suspension-feeding tubicolous hemichordates: *BMC Biology*, v. 14, p. 56.
- National Commission on Stratigraphy of China, 2015, *Stratigraphic Guide of China and China Stratigraphic Guide Manual*, Beijing, Geological Publishing House.
- Neuhaus, B., 1994, Ultrastructure of alimentary canal and body cavity, ground pattern, and phylogenetic relationships of the Kinorhyncha: *Microfanua Marina*, v. 9, p. 61-156.
- Neuhaus, B., 2013, *Handbook of zoology, Germany, De Gruyter, Gastrotricha, Cycloneuralia and Gnathifera*, 29-123 p.: Volume 1: Nematomorpha, Priapulida, Kinorhyncha, Loricifera: Kinorhyncha, 181-348 p.
- Neuhaus, B., and Higgins, R. P., 2002, Ultrastructure, biology, and phylogenetic relationships of Kinorhyncha: *Integrative and Comparative Biology*, v. 42, p. 619-632.
- Neves, R. C., Bailly, X., Leasi, F., Reichert, H., Sørensen, M. V., and Kristensen, R. M., 2013, A complete three-dimensional reconstruction of the myoanatomy of Loricifera: comparative morphology of an adult and a Higgins larva stage: *Frontiers in Zoology* v. 10, p. 19.

- Nguyen, L. T., Schmidt, H. A., Von Haeseler, A., and Minh, B. Q., 2015, IQ-TREE: a fast and effective stochastic algorithm for estimating maximum-likelihood phylogenies: *Molecular biology and evolution*, v. 32, no. 1, p. 268-274.
- Nielsen, C., 1995, *Animal Evolution: Interrelationships of the Living Phyla*, Oxford university press, Oxford.
- Nielsen, C., 2012, *Animal Evolution: Interrelationships of the Living Phyla*, Oxford university press, Oxford, 238-310 p.
- Nijhout, H. F., 2013, *Arthropod Biology and Evolution*, in Minelli, A., Boxshall, G., and Fusco, G., eds., *Arthropod Developmental Endocrinology*, Springer, p. 123-148.
- Ødegaard, F., 2000, How many species of arthropods? Erwin's estimate revised: *Biological Journal of the Linnean Society*, v. 71, no. 4, p. 583–597.
- Oeschger, R., and Janssen, H. H., 1991, Histological studies on *Halicyrtus spinulosus* (Priapulida) with regard to environmental hydrogen sulfide resistance: *Hydrobiologia*, v. 222, p. 1-12.
- Oliveira, I. S., Schaffer, S., Kvartalnov, P. V., Galoyan, E. A., Palko, I. V., Weck-Heimann, A., Geissler, P., Ruhberg, H., and Mayer, G., 2013, A new species of *Eoperipatus* (Onychophora) from Vietnam reveals novel morphological characters for the South-East Asian Peripatidae: *Zoologischer Anzeiger*, v. 252, no. 4, p. 495-510.
- Oliveira, I.S., Kumerics, A., Jahn, H., Müller, M., Pfeiffer, F. & Mayer, G., 2019, Functional morphology of a lobopod: Case study of an onychophoran leg: *Royal Society Open Science*, v. 6, p. 191200.
- Orr, P. J., Benton, M. J., and Briggs, D. E. G., 2003, Post-Cambrian closure of the deep-water slope-basin taphonomic window: *Geology*, v. 31, p. 769–772.
- Ortega-Hernandez, J., 2015, Homology of head sclerites in Burgess Shale euarthropods: *Current Biology*, v. 25, no. 12, p. 1625-1631.
- Ortega-Hernández, J., 2016, Making sense of 'lower' and 'upper' stem-group Euarthropoda, with comments on the strict use of the name Arthropoda von Siebold, 1848: *Biological Reviews*, v. 91 no. 1, p. 255–273.
- Ou, Q., 2020, Cambrian lobopodians: confusion and consideration: *Earth Science Frontiers*, v. 27, no. 6, p. 47-66.
- Ou, Q., and Mayer, G., 2018, A Cambrian unarmoured lobopodian, *Lenisambulatrix humboldti* gen. et sp. nov., compared with new material of *Diania cactiformis*: *Scientific Reports*, v. 8, no. 1, p. 13667.
- Ou, Q., Conway Morris, S., Han, J., Zhang, Z. F., Liu, J. N., Chen, A. L., Zhang, X. L., and Shu, D. G., 2012, Evidence for gill slits and a pharynx in Cambrian vetulicolians: implications for the early evolution of deuterostomes: *BMC biology*, v. 10, no. 1, p. 81.
- Ou, Q., Liu, J., Shu, D., Han, J., Zhang, Z., Wan, X., and Lei, Q., 2011, A rare onychophoran-like lobopodian from the Lower Cambrian Chengjiang Lagerstätte, southwestern China, and its phylogenetic implications: *Journal of Paleontology*, v. 85, no. 3, p. 587-594.
- Ou, Q., Vannier, J., Yang, X. F., Chen, A. L., Mai, H. J., Shu, D. G., Han, J., Fu, D. J., Wang, R., and Mayer, G., 2020, Evolutionary trade-off in reproduction of Cambrian arthropods: *Science Advances*, v. 6, no. 18, p. eaaz3376.
- Ou, Q., Xiao, S., Han, J., Sun, G., Zhang, F., Zhang, Z., and Shu, D., 2015, A vanished history of skeletonization in Cambrian comb jellies: *Science Advances*, v. 1, no. 6, p. e1500092.

- Park, J. K., Rho, H. S., Kristensen, R. M., Kim, W., and Giribet, G., 2006, First molecular data on the phylum Loricifera: an investigation into the phylogeny of Ecdysozoa with emphasis on the positions of Loricifera and Priapulida: *Zoological Science*, v. 23, no. 11, p. 943-954.
- Paterson, J. R., Edgecombe, G. D., and Lee, M. S. Y., 2019, Trilobite evolutionary rates constrain the duration of the Cambrian explosion: *Proceedings of the National Academy of Science*, v. 116, p. 4394-4399.
- Paterson, J. R., García-Bellido, D. C., Jago, J. B., Gehling, J. G., Lee, M. S., and Edgecombe, G. D., 2016, The Emu Bay Shale Konservat-Lagerstätte: a view of Cambrian life from East Gondwana: *Journal of the Geological Society*, v. 173, no. 1, p. 1-11.
- Paxton, H., 2005, Molting polychaete jaws – ecdysozoans are not the only molting animals: *Evolution & Development*, v. 7, no. 4, p. 337–340.
- Peel, J. S., 2010a, A corset-like fossil from the Cambrian Sirius Passet Lagerstätte of North Greenland and its implications for cycloneuralian evolution: *Journal of Paleontology*, v. 84, no. 2, p. 332-340.
- Peel, J. S., 2010b, Articulated hyoliths and other fossils from the Sirius Passet Lagerstätte (early Cambrian) of North Greenland: *Bulletin of Geosciences*, p. 385-394.
- Peel, J. S., 2017, Feeding behaviour of a new worm (Priapulida) from the Sirius Passet Lagerstätte (Cambrian Series 2, Stage 3) of North Greenland (Laurentia): *Palaeontology*, v. 60, no. 6, p. 795-805.
- Peel, J. S., Stein, M., and Kristensen, R. M., 2013, Life cycle and morphology of a Cambrian stem-lineage loriciferan: *PLoS One*, v. 8, no. 8, p. e73583.
- Peng, J. I. N., Huang, D., Zhao, Y., and Sun, H., 2015, Palaeoscoleids from the Balang Fauna of the Qiandongian (Cambrian Series 2), Guizhou, China: *Geological Magazine*, v. 153, no. 3, p. 438-448.
- Petrov, N. B., and Vladychenskaya, N. S., 2005, Phylogeny of molting protostomes (Ecdysozoa) as inferred from 18S and 28S rRNA gene sequences: *Molecular Biology*, v. 39, no. 4, p. 503–513.
- Philippe, H., Lartillot, N., and Brinkmann, H., 2005, Multigene analyses of bilaterian animals corroborate the monophyly of Ecdysozoa, Lophotrochozoa, and Protostomia: *Molecular biology and evolution*, v. 22, no. 5, p. 1246-1253.
- Pilato, G., Binda, M. G., Biondi, O., D’Urso, V., Lisi, O., Marletta, A., Maugeri, S., Nobile, V., Rappazzo, G., Sabella, G., Sammartano, F., Turrise, G., and Viglianisi, F., 2005, The clade Ecdysozoa, perplexities and questions: *Zoologischer Anzeiger*, v. 244, no. 1, p. 43-50.
- Piper, R., 2013, *Animal Earth: the amazing diversity of living creatures*. London, Thames & Hudson, 1-320 p.
- Por, F. D., 1983, Class Seticoronaria and phylogeny of the Phylum Priapulida: *Zoologica scripta*, v. 12, no. 4, p. 267-272.
- Por, F. D., and Bromley, H. J., 1974, Morphology and anatomy of *Maccabeus tentaculatus* (Priapulida: Seticoronaria): *Journal of Zoology*, v. 173, p. 173-197.
- Purves, W. K., Sadava, D., Orians, G. H., and Heller, H. C., 2004, *Life: the science of biology*, Sunderland, MA: Sinauer Associates, 641-654 p.
- Qian, Y., 1977, Hyolitha and some problematica from the Lower Cambrian Meishucun Stage in central and S.W. China: *Acta Palaeontologica Sinica*, v. 16, p. 225-275. (in Chinese with English abstract).



- Qian, Y., 1999, Taxonomy and biostratigraphy of small shelly fossils in China, Beijing, Science Press.
- Qian, Y., Chen, M. e., He, T., Zhu, M., Yin, G., Feng, W., Xu, J., Jiang, Z., Liu, D., Li, G., Ding, L., Mao, Y., and Xiao, B., 1999, Taxonomy and biostratigraphy of Small Shelly Fossils in China, Science Press.
- R Team, 2020, R: A language and environment for statistical computing. R Foundation for Statistical Computing, Vienna, Austria.
- Rigby, J. K., and Hou, X. G., 1995, Lower Cambrian demosponges and hexactinellid sponges from Yunnan, China: *Journal of Paleontology*, v. 69, p. 1009-1019.
- Robson, E. A., 1964, The cuticle of *Peripatopsis moseleyi*: *Journal of Cell Science*, v. 105, p. 281-299.
- Ronquist, F., Teslenko, M., van der Mark, P., Ayres, D. L., Darling, A., Höhna, S., Larget, B., Liu, L., Suchard, M. A., and Huelsenbeck, J. P., 2012, MrBayes 3.2: efficient Bayesian phylogenetic inference and model choice across a large model space: *Systematic Biology*, v. 61, no. 3, p. 539-542.
- Rota-Stabelli, O., Daley, A. C., and Pisani, D., 2013, Molecular timetrees reveal a Cambrian colonization of land and a new scenario for ecdysozoan evolution: *Current Biology*, v. 23, no. 5, p. 392-398.
- Rožanov, A. Y., Missarzhevsky, V. V., Volkova, N.A., Voronova, L.G., Krylov, I.N., Keller, B.M., Korolyuk, I.K., Lenzion, K., Mikhnyar, R., Pykhova, N.G., and Sidorov, A.D., 1969, Tommotskiu jarus i problema nizhney granisty kembriya: *Trudy Geoligske Institut Leningrad*, v. 206, p. 1-379 (In Russian with English abstract).
- Runnegar, B., 1985, Shell microstructures of Cambrian molluscs replicated by phosphate: *Alcheringa* v. 9, p. 245–257.
- Salvini-Plawen, L. V., 1974, Zur Morphologie und Systematik der Priapulida: *Chaetostephanus praeposteriens*, der Vertreter einer neuen Ordnung Seticoronaria: *Zeitschrift Zoologie Systematik Evolutionsforschung*, v. 12, p. 31-54.
- Sansom, R. S., 2016, Preservation and phylogeny of Cambrian ecdysozoans tested by experimental decay of *Priapulid*: *Scientific Reports*, v. 6, p. 32817.
- Sawaki, Y., Nishizawa, M., Suo, T., Komiya, T., Hirata, T., Takahata, N., Sano, Y., Han, J., Kon, Y., and Maruyama, S., 2008, Internal structures and U–Pb ages of zircons from a tuff layer in the Meishucunian formation, Yunnan Province, South China: *Gondwana Research*, v. 14, no. 1-2, p. 148-158.
- Schmidt-Rhaesa, A., 1996, The nervous system of *Nectonema munidae* and *Gordius aquaticus*, with implications for the ground pattern of the Nematomorpha: *Zoomorphology*, v. 116, p. 133-142.
- Schmidt-Rhaesa, A., 1998, Phylogenetic relationships of the Nematomorpha - A discussion of current hypotheses: *Zoologischer Anzeiger*, v. 236, no. 4, p. 203-216.
- Schmidt-Rhaesa, A., 2007, *The Evolution of Organ Systems*, Oxford university press, 1-73 p.:
- Schmidt-Rhaesa, A., 2013, *Handbook of zoology, Germany, De Gruyter, Gastrotricha, Cycloneuralia and Gnathifera: Volume 1: Nematomorpha, Priapulida, Kinorhyncha, Loricifera: 29-180 p.*
- Schmidt-Rhaesa, A., 2014, *Handbook of Zoology, Germany, De Gruyter, Gastrotricha, Cycloneuralia and Gnathifera: Volume 2: Nematoda, 5-12 p.*

- Schmidt-Rhaesa, A., and Freese, M., 2019, Microscopic priapulid larvae from Antarctica: *Zoologischer Anzeiger*, v. 282, p. 3-9.
- Schmidt-Rhaesa, A., and Rothe, B. H., 2006, Postembryonic development of longitudinal musculature in *Pycnophyes kielensis* (Kinorhyncha, Homalorhagida): *Integrative and comparative biology*, v. 46, p. 144–150.
- Schmidt-Rhaesa, A., Bartolomaeus, T., Lemburg, C., Ehlers, U., and Garey, J. R., 1998, The position of the Arthropoda in the phylogenetic system: *Journal of Morphology*, v. 238, p. 263–285
- Schmidt-Rhaesa, A., Panpeng, S., and Yamasaki, H., 2017, Two new species of *Tubiluchus* (Priapulida) from Japan: *Zoologischer Anzeiger*, v. 267, p. 155-167.
- Schumann, I., Kenny, N., Hui, J., Hering, L., and Mayer, G., 2018, Halloween genes in panarthropods and the evolution of the early moulting pathway in Ecdysozoa: *Royal Society Open Science*, v. 5, no. 9, p. 180888.
- Shao, T. Q., Liu, Y. H., Wang, Q., Zhang, H. Q., Cao, X., He, H. H., Zhang, Y. N., Li, Y., Zheng, P. L., Zhu, C. Y., and Hu, J. X., 2015, New small shelly fossils (*Acanthocassis* and *Xinlispina* gen. nov.) from the Fortunian stage (early Cambrian) in southern China: *Acta Geologica Sinica (English Edition)*, v. 89, no. 5, p. 1470-1481.
- Shao, T. Q., Liu, Y. H., Wang, Q., Zhang, H. Q., Tang, H. H., and Li, Y., 2016, New material of the oldest known scalidophoran animal *Eopriapulites sphinx*: *Palaeoworld*, v. 25, no. 1, p. 1-11.
- Shao, T. Q., Qin, J. C., Shao, Y., Liu, Y. H., Waloszek, D., Maas, A., Duan, B. C., Wang, Q., Xu, Y., and Zhang, H. Q., 2019, New macrobenthic cycloneuralians from the Fortunian (lowermost Cambrian) of South China: *Precambrian Research*, p. 105413.
- Shao, T. Q., Wang, Q., Liu, Y. H., Qin, J. C., Zhang, Y. N., Liu, M. J., Shao, Y., Zhao, J. Y., and Zhang, H. Q., 2020, A new scalidophoran animal from the Cambrian Fortunian Stage of South China and its implications for the origin and early evolution of Kinorhyncha: *Precambrian Research*, v. 349, p. 105616.
- Shu, D. G., and Han, J., 2020, The core value of Chengjiang fauna: the information of animal kingdom and the birth basic human organs: *Earth Science Frontiers*, v. 27, p. 1-32.
- Shu, D. G., Conway Morris, S., Han, J., Chen, L., Zhang, X. L., Zhang, Z. F., Liu, H. Q., Li, Y., and Liu, J. N., 2001, Primitive deuterostomes from the Chengjiang Lagerstätte (Lower Cambrian, China): *Nature*, v. 414 no. 6862, p. 419–424.
- Shu, D. G., Luo, H. L., Conway Morris, S., Zhang, X. L., Hu, S. X., Chen, L., Han, J., Zhu, M., Li, Y., and Chen, L. Z., 1999, Lower Cambrian vertebrates from south China: *Nature*, v. 402, no. 6757, p. 42.
- Skovsted, C., Brock, G., and Paterson, J., 2006, Bivalved arthropods from the Lower Cambrian Mernmerna Formation of South Australia and their implications for the identification of Cambrian 'small shelly fossils': *Association of Australasian Palaeontologists Memoirs*, v. 32, p. 7–41.
- Smith, M. R., 2018, TreeSearch: phylogenetic tree search using custom optimality criteria.
- Smith, M. R., 2019, Bayesian and parsimony approaches reconstruct informative trees from simulated morphological datasets: *Biology Letters*, v. 15, no. 2, p. 20180632.
- Smith, M. R., and Caron, J. B., 2015, *Hallucigenia*'s head and the pharyngeal armature of early ecdysozoans: *Nature*, v. 523, no. 7558, p. 75-78.

- Smith, M. R., and Ortega-Hernández, J., 2014, *Hallucigenia's* onychophoran-like claws and the case for Tactopoda: *Nature*, v. 514, no. 7522, p. 363-366.
- Smith, M. R., Harvey, T. H. P., Butterfield, N. J., and Kouchinsky, A., 2015, The macro- and microfossil record of the Cambrian priapulid *Ottoia*: *Palaeontology*, v. 58, no. 4, p. 705-721.
- Sørensen, M. V., Hebsgaard, M. B., Heiner, I., Glenner, H., Willerslev, E., and Kristensen, R. M., 2008, New data from an enigmatic phylum: evidence from molecular sequence data supports a sister-group relationship between Loricifera and Nematomorpha: *Journal of Zoological Systematics and Evolutionary Research*, v. 46, no. 3, p. 231-239.
- Srivastava, M., Begovic, E., Chapman, J., Putnam, N. H., Hellsten, U., Kawashima, T., Kuo, A., Mitros, T., Salamov, A., Carpenter, M. L., Signorovitch, A. Y., Moreno, M. A., Kamm, K., Grimwood, J., Schmutz, J., Shapiro, H., Grigoriev, I. V., Buss, L. W., Schierwater, B., Dellaporta, S. L., and Rokhsar, D. S., 2008, The *Trichoplax* genome and the nature of placozoans: *Nature*, v. 454, p. 955-960.
- Steiner, M., Li, G. X., Qian, Y., and Zhu, M. Y., 2004, Lower Cambrian Small Shelly Fossils of northern Sichuan and southern Shaanxi (China), and their biostratigraphic importance: *Géobios*, v. 37, no. 2, p. 259-275.
- Steiner, M., Li, G., Qian, Y., Zhu, M., and Erdtmann, B.-D., 2007, Neoproterozoic to Early Cambrian small shelly fossil assemblages and a revised biostratigraphic correlation of the Yangtze Platform (China): *Palaeogeography, Palaeoclimatology, Palaeoecology*, v. 254, no. 1-2, p. 67-99.
- Steiner, M., Qian, Y., Li, G. X., Hagadorn, J. W., and Zhu, M. Y., 2014, The developmental cycles of early Cambrian Olivooidea fam. nov. (?Cycloneuralia) from the Yangtze Platform (China): *Palaeogeography, Palaeoclimatology, Palaeoecology*, v. 398, p. 97-124.
- Steiner, M., Wallis, E., Erdtmann, B.-D., Zhao, Y. L., and Yang, R. D., 2001, Submarine-hydrothermal exhalative ore layers in black shales from South China and associated fossils: insights into a Lower Cambrian facies and bio-evolution: *Palaeogeography, Palaeoclimatology, Palaeoecology*, v. 169, p. 165-191.
- Steiner, M., Yang, B., Hohl, S., Zhang, L., and Chang, S., 2020, Cambrian small skeletal fossil and carbon isotope records of the southern Huangling Anticline, Hubei (China) and implications for chemostratigraphy of the Yangtze Platform: *Palaeogeography, Palaeoclimatology, Palaeoecology*, v. 554, p. 109817.
- Steiner, M., Zhu, M. Y., Zhao, Y. L., and Erdtmann, B. D., 2005, Lower Cambrian Burgess Shale-type fossil associations of South China: *Palaeogeography, Palaeoclimatology, Palaeoecology*, v. 220, p. 129-152.
- Storch, V., 1991, Priapulida, in Harrison, F. W., and Ruppert, E. E., eds., *Microscopic Anatomy of Invertebrates*: New York, Wiley-Liss, p. 333-350.
- Storch, V., Higgins, R. P., and Morse, M. P., 1989, Ultrastructure of the body wall of *Meiopriapulid fijiensis* (Priapulida): *Transactions of the American Microscopical Society*, v. 108, no. 4, p. 319-331.
- Sun, W. G., and Hou, X. G., 1987, Early Cambrian worms from Chengjiang, Yunnan, China: *Maotianshania* gen. nov.: *Acta Palaeontologica Sinica*, v. 26, no. 3, p. 299-307.
- Telford, M. J., Bournat, S. J., Economou, A., Papillon, D., and Rota-Stabelli, O., 2008, The evolution of the Ecdysozoa: *Philosophical Transactions Royal Society B*, v. 363, no. 1496, p. 1529-1537.

- Torsvik, T. H., and Cocks, L. R. M., 2013, New global palaeogeographical reconstructions for the Early Palaeozoic and their generation: Geological Society, London, Memoirs, v. 38, no. 1, p. 5-24.
- Trott, T. J., 2017, Feeding by *Priapulius caudatus* (Cephalorhyncha: Priapulidae): observations of the effects of seasonal temperature change and molting: Marine and Freshwater Behaviour and Physiology, v. 50, no. 1, p. 55-65.
- Tunnicliffe, V., 1991, The biology of hydrothermal vents: ecology and evolution: Oceanography and Marine Biology, v. 29, p. 319-407.
- Valentine, J. W., and Collins, A. G., 2000, The significance of moulting in ecdysozoan evolution: Evolution & Development, v. 2, no. 3, p. 152-156.
- van der Land, J., 1968, A new aschelminth, probably related to the Priapulida: Zoologische Mededelingen v. 42, no. 22, p. 237-250.
- van der Land, J., 1970, Systematic, Zoogeography and ecology of the Priapulida: Zoologische Verhandlungen, v. 112, p. 4-104.
- Van Roy, P., Daley, A. C., and Briggs, D. E., 2015, Anomalocaridid trunk limb homology revealed by a giant filter-feeder with paired flaps: Nature, v. 522, no. 7554, p. 77-80.
- Vannier, J., 2012, Gut contents as direct indicators for trophic relationships in the Cambrian marine ecosystem: PLoS One, v. 7, no. 12, p. e52200.
- Vannier, J., and Chen, J., 2002, Digestive system and feeding mode in Cambrian naraoiid arthropods: Lethaia, v. 35, p. 107-120.
- Vannier, J., and Martin, E. L. O., 2017, Worm-lobopodian assemblages from the Early Cambrian Chengjiang biota: Insight into the “pre-arthropodan ecology”? Palaeogeography, Palaeoclimatology, Palaeoecology, v. 468, p. 373-387.
- Vannier, J., Aria, C., Taylor, R. S., and Caron, J. B., 2018, *Waptia fieldensis* Walcott, a mandibulate arthropod from the middle Cambrian Burgess Shale: Royal Society Open Science, v. 5, no. 6, p. 172206.
- Vannier, J., Calandra, I., Gaillard, C., and Żylińska, A., 2010, Priapulid worms: Pioneer horizontal burrowers at the Precambrian-Cambrian boundary: Geology, v. 38, no. 8, p. 711-714.
- Vannier, J., Caron, J.-B., Yuan, J. L., Briggs, D. E. G., Zhao, Y. L., and Zhu, M. Y., 2007, *Tuzoia*: morphology and lifestyle of a large bivalved arthropod of the Cambrian seas: Journal of Palaeontology, v. 81, no. 3, p. 445-471.
- Vannier, J., Liu, J., Lerosey-Aubril, R., Vinther, J., and Daley, A. C., 2014, Sophisticated digestive systems in early arthropods: Nature Communications, v. 5, p. 3641.
- Vinther, J., Stein, M., Longrich, N. R., and Harper, D. A., 2014, A suspension-feeding anomalocarid from the Early Cambrian. Nature, v. 507, no. 7493, p. 496-499.
- Vogel, K., and Marincovich Jr., L., 2004, Paleobathymetric implications of microborings in Tertiary strata of Alaska, USA: Palaeogeography, Palaeoclimatology, Palaeoecology, v. 206, p. 1-20.
- Voronova, L. G., and Missarzhevsky, V. V., 1969, Finds of algae and worm tubes in the Precambrian-Cambrian boundary beds of the northern part of the Siberian Platform: Doklady AN SSSR, v. 184, p. 207-210 (In Russian with English abstract).
- Walcott, C. D., 1911, Middle Cambrian Annelids, Cambrian Geology and Paleontology II: Smithsonian Miscellaneous Collections, v. 57, no. 5, p. 110-144.

- Walcott, C. D., 1912, Middle Cambrian Branchiopoda, Malacostraca, Trilobita and Merostomata: Cambrian Geology and Paleontology II. Smithsonian Miscellaneous Collections, v. 57, p. 145-228.
- Wang, D., Vannier, J., Schumann, I., Wang, X., Yang, X. G., Komiya, T., Uesugi, K., Sun, J., and Han, J., 2019, Origin of ecdysis: fossil evidence from 535-million-year-old scalidophoran worms: Proceedings of the Royal Society B, v. 286, no. 1906, p. 20190791.
- Wang, D., Vannier, J., Yang, X. G., Sun, J., Sun, Y. F., Hao, W. J., Tang, Q. Q., Liu, P., and Han, J., 2020, Cuticular reticulation replicates the pattern of epidermal cells in lowermost Cambrian scalidophoran worms: Proc Biol Sci, v. 287, no. 1926, p. 20200470.
- Wang, X., 2018, Diversification of early cnidarians: exceptionally preserved microfossils from the Kuanchuanpu Formation (lower Cambrian; 535 Ma), Shaanxi Province, China [Doctor of Philosophy 53-57]: Université de Lyon.
- Wang, X., Han, J., Vannier, J., Ou, Q., Yang, X. G., Uesugi, K., Sasaki, O., Komiya, T., and Sevastopulo, G., 2017, Anatomy and affinities of a new 535-million-year-old medusozoan from the Kuanchuanpu Formation, South China: Palaeontology, v. 60, no. 6, p. 853-867.
- Wang, X., Vannier, J., Yang, X., Kubota, S., Ou, Q., Yao, X., Uesugi, K., Sasaki, O., Komiya, T., Han, J., and Smith, A., 2020, An intermediate type of medusa from the early Cambrian Kuanchuanpu Formation, South China: Palaeontology, v. 63, no. 5, p. 775-789.
- Wang, Y. F., Peng, J., Wang, Q., Wen, R., Zhang, H., Du, G., and Shao, Y., 2020, Moulting in the Cambrian oryctocephalid trilobite *Arthricocephalites xinzhaiheensis* from Guizhou Province, South China: Lethaia.
- Webster, B. L., Copley, R. R., Jenner, R. A., Mackenzie-Dodds, J. A., Bourlat, S. J., Rota-Stabelli, O., Littlewood, D. T. J., and Telford, M. J., 2006, Mitogenomics and phylogenomics reveal priapulid worms as extant models of the ancestral Ecdysozoan: Evolution & Development, v. 8, no. 6, p. 502-510.
- Wennberg, S. A., Janssen, R., and Budd, G. E., 2009, Hatching and earliest larval stages of the priapulid worm *Priapulius caudatus*: Invertebrate Biology, v. 128, no. 2, p. 157-171.
- Whitaker, A. F., Jamison, P. G., Schiffbauer, J. D., and Kimmig, J., 2020, Re-description of the Spence Shale palaeoscolecid in light of new morphological features with comments on palaeoscolecid taxonomy and taphonomy: PalZ, v. 94, no. 4, p. 661-674.
- Whittard, W.F., 1953, *Palaeoscolex piscatorum* gen et sp. nov., a worm from the Tremadocian of Shropshire: Quarterly Journal of the Geological Society of London, v. 109, p. 125-135.
- Whittington, H. B., 1978, The lobopod animal *Aysheaia pedunculata* Walcott, Middle Cambrian, Burgess Shale, British Columbia: Philosophical Transactions of the Royal Society of London: Biological Sciences, v. 284, p. 165-197.
- Wigglesworth, V. B., 1973, The role of the epidermal cells in moulding the surface pattern of the cuticle in *Rhodnius* (Hemiptera): Journal of cell science, v. 12, p. 683-705.
- Wills, M. A., 1998, Cambrian and recent disparity: the picture from priapulids: Paleobiology, v. 24, no. 2, p. 177-199.
- Wills, M. A., Gerber, S., Ruta, M., and Hughes, M., 2012, The disparity of priapulid, archaeopriapulid and palaeoscolecid worms in the light of new data: Journal of Evolutionary Biology, v. 25, no. 10, p. 2056-2076.
- Wolfe, J.M., 2017, Metamorphosis is ancestral for crown Euarthropods, and evolved in the Cambrian or earlier: Integrative and Comparative Biology, v. 57, p. 499-509.

- Won, J. Y., 2006, Deep-sea hydrothermal vents: ecology and evolution: *Journal ecological field biology*, v. 29, no. 2, p. 175-183.
- Xiao, S. H., and Knoll, A. H., 1999, Fossil preservation in the Neoproterozoic Doushantuo phosphorite Lagerstätte, South China: *Lethaia*, v. 32, no. 3, p. 219-238.
- Yamasaki, H., Fujimoto, S., and Miyazaki, K., 2015, Phylogenetic position of Loricifera inferred from nearly complete 18S and 28S rRNA gene sequences: *Zoological Lett*, v. 1, p. 18.
- Yang, C., Li, X.-H., Zhu, M., Condon, D. J., and Chen, J., 2018, Geochronological constraint on the Cambrian Chengjiang biota, South China: *Journal of the Geological Society*, v. 175, no. 4, p. 659-666.
- Yang, J., Ortega-Hernandez, J., Butterfield, N. J., and Zhang, X. G., 2013, Specialized appendages in fuxianhuides and the head organization of early euarthropods: *Nature*, v. 494, no. 7438, p. 468-471.
- Yang, J., Ortega-Hernández, J., Gerber, S., Butterfield, N. J., Hou, J.-b., Lan, T., and Zhang, X.-g., 2015, A superarmored lobopodian from the Cambrian of China and early disparity in the evolution of Onychophora: *Proceedings of the Academy of Natural Sciences of the United States of America*, v. 112, no. 28, p. 8678-8683.
- Yang, J., Smith, M. R., Zhang, X.-g., and Yang, X.-y., 2020, Introvert and pharynx of *Mafangscplex*, a Cambrian palaeoscolecoid: *Geological Magazine*, v. 157, no. 12, p. 2044-2050.
- Yang, X. G., Han, J., Wang, X., Schiffbauer, J. D., Uesugi, K., Sasaki, O., and Komiya, T., 2017, Euendoliths versus ambient inclusion trails from Early Cambrian Kuanchuanpu Formation, South China: *Palaeogeography, Palaeoclimatology, Palaeoecology*, v. 476, p. 147-157.
- Yang, X. H., and He, T. G., 1984, New small shelly fossils from Lower Cambrian Meishucun stage of Nanjiang area, northern Sichuan: *Professional Papers of Stratigraphy and Palaeontology*: v. 13, p. 35-48.
- Yang, X. H., He, Y. X., and Deng, S. H., 1983, On the Sinian–Cambrian boundary and the small shelly fossil assemblages in Nanjiang Area, Sichuan: *Bulletin of the Chengdu Institute of Geology and Mineral Resources, The Chinese Academy of Geological Sciences*, p. 91-110.
- Yang, X., 2018, Microbial fossils and micro-structures from the Early Cambrian Kuanchuanpu Biota [Doctor of Philosophy: Northwest University].
- Yang, Y. N., 2016, Taxonomy and evolution of Cambrian priapulids from South China [Doctor of Philosophy: Northwest University, 188 p.
- Yang, Y. N., and Zhang, X. L., 2016a, The Cambrian palaeoscolecoid *Wronascolex* from the Shipai fauna (Cambrian Series 2, Stage 4) of the Three Gorges area, South China: *Papers in Palaeontology*, v. 2, no. 4, p. 555-568.
- Yang, Y. N., and Zhang, X. L., 2016b, Distinctive scleritome with marginal tubercles of a new palaeoscolecoid worm from the Shipai Fauna (Cambrian Epoch 2) at Three Gorges, South China: *Acta Geologica Sinica*, v. 90, no. 3, p. 807–817.
- Yang, Y., Zhang, X., Zhao, Y., Qi, Y., and Cui, L., 2017, New palaeoscolecoid worms from the early Cambrian north margin of the Yangtze Platform, South China: *Journal of Paleontology*, v. 92, no. 01, p. 49-58.
- Yue, Z., and Bengtson, S., 1999, Embryonic and post-embryonic development of the Early Cambrian cnidarian *Olivoooides*: *Lethaia*, v. 32, no. 2, p. 181-195.
- Zeng, H., Zhao, F., Niu, K., Zhu, M., and Huang, D., 2020, An early Cambrian euarthropod with radiodont-like raptorial appendages: *Nature*, 1-5 p.

- Zhang, H. Q., Maas, A., and Waloszek, D., 2018, New material of scalidophoran worms in Orsten-type preservation from the Cambrian Fortunian Stage of South China: *Journal of Paleontology*, v. 92, no. 01, p. 14-25.
- Zhang, H. Q., Xiao, S. H., Liu, Y. H., Yuan, X. L., Wan, B., Muscente, A. D., Shao, T. Q., Gong, H., and Cao, G. H., 2015, Armored kinorhynch-like scalidophoran animals from the early Cambrian: *Scientific Reports*, v. 5, p. 16521.
- Zhang, T., Lei, D., Wang, B., Niu, B., Yang, X., and Han, J., 2019, Artificial intelligence identification of microfossils from the lower Cambrian Kuanchuanpu Formation in southern Shaanxi, China: *Acta Palaeontologica Sinica*, v. 58, no. 2, p. 141-151.
- Zhang, W. T., 1950. *Eoredlichia*. Annual Meeting of Chinese Society of Paleontology, v. 2, no. 1, p. 10.
- Zhang, X. L., Liu, W., Isozaki, Y., and Sato, T., 2017, Centimeter-wide worm-like fossils from the lowest Cambrian of South China: *Scientific Reports*, v. 7, no. 1, p. 14504.
- Zhang, X. L., Shu, D. G., and Erwin, D. H., 2007, Cambrian naraoiids (Arthropoda): morphology, ontogeny, systematics, and evolutionary relationships: *Journal of Paleontology*, v. 81, no. sp68 p. 1-52.
- Zhang, X., Liu, W., and Zhao, Y., 2008, Cambrian Burgess Shale-type Lagerstätten in South China: Distribution and significance: *Gondwana Research*, v. 14, no. 1-2, p. 255-262.
- Zhang, X.-G., Hou, X.-G., and Bergström, J. A. N., 2006, Early Cambrian priapulid worms buried with their lined burrows: *Geological Magazine*, v. 143, no. 5, p. 743-748.
- Zhang, Z., Holmer, L. E., Popov, L., and Shu, D., 2011, An obolellate brachiopod with soft-part preservation from the early Cambrian Chengjiang Fauna of China: *Journal of Paleontology*, v. 85, no. 3, p. 460-463.
- Zhao, F. C., Smith, M. R., Yin, Z. J., Zeng, H., Hu, S. X., Li, G. X., and Zhu, M. Y., 2015, First report of *Wiwaxia* from the Cambrian Chengjiang Lagerstätte: *Geological Magazine*, v. 152, no. 2, p. 378-382.
- Zhao, Y., 2011, *Kali Biota-Ocean animals from 5.08 million years ago, Guizhou Province, Guizhou Science and Technique Press.*
- Zhao, Y., Vinther, J., Parry, L. A., Wei, F., Green, E., Pisani, D., Hou, X., Edgecombe, G. D., and Cong, P., 2019, Cambrian sessile, suspension feeding stem-group ctenophores and evolution of the comb jelly body plan: *Current Biology*, v. 29, no. 7, p. 1112-1125 e1112.
- Zheng, Y. J., Yao, X. Y., Han, J., and Guo, J. F., 2017, Microscopic fossils with multi-level tetrad cell structures from the Cambrian Kuanchuanpu Formation in south Shaanxi: *Acta Palaeontologica Sinica*, v. 56, no. 4, p. 1-9.
- Zhu, M. Y., Yang, A. H., Yuan, J. L., Li, G. X., Zhang, J. M., Zhao, F. C., Ahn, S. Y., and Miao, L. Y., 2019, Cambrian integrative stratigraphy and timescale of China.: *SCIENTIA SINICA Terrae*, v. 49, no. 1, p. 26-65 (in Chinese with English abstract).
- Zhu, M. Y., Zhang, J. M., and Li, G. X., 2001, Sedimentary environments of the early Cambrian Chengjiang biota: sedimentology of the Yu'an-shan Formation in Chengjiang County, eastern Yunnan. In: Zhu Mao-yan, Van Iten, H., Peng Shan-chi & Li Guo-xiang (eds), *The Cambrian of South China.*: *Acta Palaeontologica Sinica*, v. sp40, p. 80-105.
- Zhu, M., Babcock, L. E., and Steiner, M., 2005, Fossilization modes in the Chengjiang Lagerstätte (Cambrian of China): testing the roles of organic preservation and diagenetic alteration in exceptional preservation: *Palaeogeography, Palaeoclimatology, Palaeoecology*, v. 220, no. 1-2, p. 31-46.

Zhuravlev, A. Y., Vintaned, J. A. G., and Liñán, E., 2011, The Palaeoscolecida and the evolution of the Ecdysozoa: *Palaeontographica Canadiana*, v. 31, p. 177-204.



# Appendices

## Appendix 1- Fixation techniques

### 1 Preparing Chemicals

#### 1.1 Buffer PBS solution

Put one tablet of PBS (Phosphate buffered saline) in 200 ml of deionized water. Keep the solution in a bottle in room temperature.

#### 1.2 Glutaraldehyde 25% EM-quality-solution

Mix 10 ml of glutaraldehyde with 90 ml of buffer solution to get 100 ml of solution for fixing animals. Keep this solution in a small bottle in the fridge. Use thin gloves.

#### 1.3 Ethanol

Use 100% ethanol and prepare 30, 50 and 70% ethanol.

### 2 How to fix animals

Use small vials and plastic disposable pipettes (label the pipette for glutaraldehyde).

2.1 Drop specimen(s) in PBS solution (15 minutes). Remove liquid and do it gain (15 minutes). Remove liquid.

2.2 Add glutaraldehyde solution. Keep in the fridge at least 4 hours or more (if it is a large specimen). For meiofauna, 4 hours is probably enough.

2.3 Remove glutaraldehyde solution and replace by PBS solution (glutaraldehyde was cycled, because it is not good for environment). Leave specimens in PBS 15 minutes. Remove liquid and rince again in PBS for 15 minutes. Remove liquid.

2.4 Put 30% ethanol. Leave 15-30 minutes. Remove ethanol.

2.5 Put 50% ethanol. Leave 15-30 minutes. Remove ethanol.

2.6 Put 70% ethanol.

## Appendix 2- Updated morphological characters of fossil and extant Cycloneuralia

### Characters description

#### General body plan

##### 1. Body shape:

- (0) cylindrical,
- (1) gourd-like,

##### 2. External subdivision of adult body:

- (0) body with no visible subdivision,
- (1) introvert, neck and trunk
- (2) introvert and trunk
- (3) introvert, neck, thorax and loricate abdomen

**Note: Status (0), a head appears of Nematoida and Gastrotrich which cannot everted and overall is no boundary with trunk but bearing a few cuticular elements (Brusca et al., 2016). Head in Nematoida can be considered as Zone I which is defined in Scalidophora.**

##### 3. Terminal mouth opening:

- (0) simple
- (1) with stiff cilia,
- (2) with amphids,
- (3) with mouth cone.
- (4) none.

##### 4. Percentage of animal length taken up by introvert:

- (0) 0% (no introvert),
- (1) between 1% and 30%,
- (2) 31 to 50%.

##### 5. Body cavity in adults:

- (0) absent
- (1) present.

##### 6. Body cavity:

- (0) largely filled by mesenchyme and organs,
- (1) forms a blastocoel cavity

##### 7. Body musculature:

- (0) only longitudinal muscles,
- (1) longitudinal and circular muscles.

## **Introvert**

### **8. Introvert in adults:**

- (0) absent,
- (1) present.

### **9. Degree to which the introvert or head can be invaginated:**

- (0) not invaginable at all,
- (1) partially invaginable,
- (2) completely invaginable into the trunk.

### **10. Zone I: overall shape**

- (0) cylindrical,
- (1) swollen.

### **11. Zone I: number of subdivisions**

- (0) 1
- (1) 2
- (2) 3.

**Note:** The introvert of scalidophoran worms can be divided into three parts named (from proximal to distal): Zone I (with scalids), Zone II (a smooth area between Zone I and Zone II), and Zone III corresponding to the everted pharynx (Conway Morris, 1977).

### **12. Zone I: internal structure of scalids**

- (0) composed exclusively of cuticle,
- (1) cuticle limited to a thin outer covering.

**Note:** Nematoida does not bear eversible introvert instead of head. Here scalids present corresponding structures of Nematoida's head.

### **13. Zone I: scalids distributed along longitudinal ridges**

- (0) absent
- (1) present

### **14. Zone I: annulations**

- (0) absent
- (1) present

### **15. Proximal part of Zone I: distribution pattern of cuticular elements**

- (0) no visible regular pattern,
- (1) discrete parallel longitudinal rows,
- (2) quincunx.

**Note:** "Proximal part of Zone I" is defined as "Subzone Ia" in main text.

**16. Proximal part of Zone I: radial distribution of cuticular elements**

- (0) pentaradial,
- (1) hexaradial.

**17. Proximal part of Zone I: morphology of cuticular elements**

- (0) papillae,
- (1) simple spines,
- (2) hooks or spinose hooks,
- (3) conical scalids,
- (4) telescopiform scalids,
- (5) curved scalids and dentoscalids,
- (6) complex scalids,
- (7) glandular scalids, trifold spines, sensory spines,
- (8) scalids with pectinate hood,
- (9) spinoscalids and trichoscalids.

**18. Proximal part of Zone I: number of trichoscalids**

- (0) 0,
- (1) 6,
- (2) 14.

**19. Proximal part of Zone I: number of longitudinal rows of elements along introvert**

- (0) 6-19,
- (1) 20,
- (2) 24,
- (3) 25,
- (4) > 25.

**20. Proximal part of Zone I: sequence of scalids**

- (0) elements organized in a single series,
- (1) elements organized in two or more series.

**21. Proximal part of Zone I: basal circlet**

- (0) no constriction or longitudinal or circular muscles,
- (1) marked by a constriction, longitudinal or circular muscles.

**22. Middle part of Zone I: length**

- (0) almost invisible
- (1) narrow
- (2) wide

**Note: Here the "Middle part of Zone I" is defined as "Subzone Ib" in main text.**

**23. Distal part of Zone I: morphology of cuticular ornament**

- (0) papillae,
- (1) simple spines,
- (2) hooks or spinose hooks,
- (3) conical scalids,
- (4) telescopiform scalids,
- (5) curved scalids,
- (6) complex scalids,
- (7) double tentaculite scalids,
- (8) scalids with pectinate hood,
- (9) spinoscalids and clavoscalids

**Note: “Distal part of Zone I” is defined as “Subzone Ic” in main text.**

**24. Distal part of Zone I: number of clavoscalids**

- (0) 0,
- (1) 6,
- (2) 8.

**25. Distal part of Zone I: distribution of cuticular elements**

- (0) no visible regular pattern,
- (1) discrete parallel longitudinal rows,
- (2) quincunx.

**26. Distal part of Zone I: radial distribution of cuticular elements:**

- (0) pentaradial,
- (1) hexaradial
- (2) octradial.

**27. Distal part of Zone I: number of longitudinal rows of elements**

- (0) 7-19,
- (1) 20,
- (2) 24,
- (3) 25,
- (4) > 25.

**28. Zone II: cuticular ornament**

- (0) none,
- (1) few cuticular elements (e.g. tiny spines, papillae).

**29. Zone II: elongate basal spines/coronal scalids**

- (0) absent,
- (1) present.

## **Pharyngeal teeth**

### **30. Zone III: cuticular elements**

- (0) spines,
- (1) multispinose,
- (2) hooks,
- (3) conical with a fringe of spines,
- (4) sclerotized trabeculae,
- (5) pectinate.

### **31. Zone III: circlets of cuticular elements**

- (0) absent
- (1) present.

### **32. Zone III: number of circlets cuticular elements**

- (0) 1-4,
- (1) 5-16,
- (2) >16.

### **33. Pharyngeal lumina**

- (0) round,
- (1) triradiate
- (2) triradiate in the distal and hexagonal in the proximal region.

### **34. Mouth cone: oral stylets**

- (0) absent,
- (1) present.

### **35. Mouth cone: number of outer oral stylets:**

- (0) 4,
- (1) 6,
- (2) 8,
- (3) 9.

**Note: Here "Mouth cone" is only for Kinorhyncha and Loricifera. It may be equal to Zone II plus Zone III of Priapulida. Inferred to Character 3 state (3).**

### **36. Zone III: number of elements in basal circlet**

- (0) 5
- (1) 6-9
- (2) >=10.

**37. Zone III: number of basal, pentagonal circlets**

- (0) none,
- (1) four,
- (2) five,
- (3) six,
- (4) seven,
- (5) two.

**38. Zone III: morphology of distal part**

- (0) blunt tip or tapering gradually,
- (1) bulbous
- (2) tube.

**39. Zone III: eversibility**

- (0) completely eversible,
- (1) incompletely eversible, but eversible beyond the proximal teeth,
- (2) normally eversible only as far as the proximal teeth.

**40. Zone III: size evenness of cuticular elements from proximal to distal**

- (0) approximately equal size,
- (1) decrease,
- (2) increase,
- (3) first increase and then decrease.

**Neck- (trunk-introvert boundary)**

**41. Neck:**

- (0) absent,
- (1) present.

**42. Neck cuticular ornament:**

- (0) cuticular plates (as in larvae/juveniles),
- (1) cuticular plates + scalids,
- (2) transverse wrinkles with cuticular spines,
- (3) cuticular scalids or papillae.

**43. Placids:**

- (0) absent,
- (1) present.

**44. Number of placids:**

- (0) 8,
- (1) 16.

## **Trunk**

### **45. Trunk length to width ratio in adult:**

- (0) <10,
- (1) between 10 and 20,
- (2) >20.

### **46. Annulations in adults:**

- (0) absent,
- (1) present.

### **47. Number of trunk annulations in adults:**

- (0) 12-29,
- (1) 30-60,
- (2) 61-139,
- (3) 140 or more.

### **48. Trunk segmentation:**

- (0) absent,
- (1) present.

### **49. Trunk segment 1:**

- (0) ring-like,
- (1) with 3 sternal + 1 tergal plates.

### **50. Cuticular elements in adults:**

- (0) absent,
- (1) present.

### **51. Trunk cuticular elements in adults: morphology**

- (0) sclerites,
- (1) spines,
- (2) round or oval plates,
- (3) longitudinal arranged plates/plicae
- (4) single extremely large plate.

### **52. Small nodes/tubercles on trunk cuticular elements in adult:**

- (0) absent,
- (1) present.



**53. Number of transverse rows of cuticular elements present in each annulation or in lorica:**

- (0) 1,
- (1) 2,
- (2) 3,
- (3) 4,
- (4) between 7 and 8,
- (5) 6 or 22.

**54. Trunk papillae in adults:**

- (0) absent,
- (1) present.

**55. Trunk papillae in adults: morphology**

- (0) simple,
- (1) extremely long.

**56. Trunk tumuli:**

- (0) absent,
- (1) present.

**57. Trunk tubuli:**

- (0) absent,
- (1) present.

**58. Trunk tubercles:**

- (0) absent,
- (1) present.

**59. Trunk flosculi, N-flosculi or sensory spots:**

- (0) absent,
- (1) flosculi present (between 7 and 16 petals).

**60. Trunk clavulae:**

- (0) absent,
- (1) present.

**Trunk-Posterior region**

**61. Arc or ring of posterior spines or hooks:**

- (0) absent,
- (1) present.

**62. Posterior ring papillae:**

- (0) absent,
- (1) present.

**63. Eversible bursa:**

- (0) absent,
- (1) present.

**64. Posterior tubulae or setae:**

- (0) absent,
- (1) present.

**65. Posterior tubulae or setae or hooks: arrangement**

- (0) unpaired pattern,
- (1) paired pattern,
- (2) radial pattern.

**66. Terminal posterior adhesive tube:**

- (0) absent,
- (1) present.

**67. Posterior warts:**

- (0) absent,
- (1) present.

**68. Posterior warts: size**

- (0) 1% to 5% of trunk diameter,
- (1) 6% to 10% of trunk diameter.

**69. Caudal appendage(s):**

- (0) absent,
- (1) present.

**70. Caudal appendage(s): length**

- (0) less than the length of the body,
- (1) up to three times the length of the body.

**71. Caudal appendage(s): number and position**

- (0) single and positioned terminally,
- (1) single and positioned dorso-medially,
- (2) bicaudal.

**72. Caudal appendage(s): morphology**

- (0) undivided,
- (1) pseudosegmented (external).

**73. Caudal appendage: surface**

- (0) smooth,
- (1) vesiculate,
- (2) bearing hooks,
- (3) bearing transverse wrinkles or striations.

**74. Position of the anus:**

- (0) terminal, whether within bursa or otherwise,
- (1) in posterolateral or posteroventral surface of abdomen.

**75. Polythyridium:**

- (0) absent,
- (1) present.

**Tube**

**76. Tube:**

- (0) absent,
- (1) present.

**77. Tube morphology:**

- (0) composed of agglutinated debris,
- (1) cuticular and annulated.

**78. Tube: average number of annulations per millimeter**

- (0) 0 (no annulation),
- (1) <10,
- (2) between 11 and 19,
- (3) >20.

**Nervous system**

**79. Unpaired ventral nerve cord throughout its length:**

- (0) absent,
- (1) present.

**80. Ventral nerve cords merging caudally:**

- (0) absent,
- (1) present.

**81. Unpaired dorsal nerve cord:**

- (0) absent,
- (1) present.

**82. Circumpharyngeal brain:**

- (0) absent,
- (1) present.

**83. Brain with antero-posterior sequence (perikarya-neuropil-perikarya):**

- (0) absent,
- (1) present.

**84. Apical part of brain composed of perikarya:**

- (0) absent,
- (1) present.

**85. Pharyngeal nervous system:**

- (0) absent,
- (1) present.

**86. Two rings of introvert retractors passing through the collar-shaped brain:**

- (0) absent,
- (1) present.

**Larval and Developmental characters**

**87. Developmental type:**

- (0) direct,
- (1) biphasic.

**88. Loricata larval stage:**

- (0) absent,
- (1) present.

**89. Cuticle of the larva/juvenile dorso-ventrally flattened (at least in older stages), with six lateral plates in-folded and accordion like:**

- (0) absent,
- (1) present.

**90. Cuticles of the annuli divided into plates, especially in late juveniles or adults:**

- (0) absent,
- (1) present.

**91. Six long pharynx retractor muscles in larvae/juveniles:**

- (0) absent,
- (1) present.

**92. Differentiated introvert in larva/juvenile:**

- (0) absent,
- (1) present.

## **Reproductive system**

### **93. Cloaca in both sexes:**

- (0) absent,
- (1) present.

### **94. Protonephridia:**

- (0) absent,
- (1) present.

### **95. Protonephridia: relation with gonad**

- (0) do not flow into the gonoduct and are not integrated into the gonad,
- (1) flow into the gonoduct and/or are integrated into the gonad.

### **96. Urogenital system attached to the body wall by a ligament:**

- (0) absent,
- (1) present.

### **97. Spermatozoa with a flagellum:**

- (0) absent,
- (1) present.

### **98. Perigenital setae:**

- (0) absent or reduced,
- (1) prominent.

## **Cuticle**

### **99. Cuticle predominantly containing collagen:**

- (0) absent,
- (1) present.

### **100. Cuticle containing chitin:**

- (0) absent,
- (1) present.

### **101. Distribution of chitin in cuticle:**

- (0) predominantly within the middle cuticle layer (exocuticle),
- (1) predominantly within the lowermost cuticle layer (endocuticle).

### **102. Cuticle with homogeneous layer at surface/beneath epicuticle:**

- (0) absent,
- (1) present.

**103. Exocuticle:**

- (0) Homogenous,
- (1) Heterogenous.

**104. Exocuticle: radially striated or vertical canal:**

- (0) absent,
- (1) present.

**105. Crisscrossed fibres in cuticle:**

- (0) absent,
- (1) present.

**106. Large helicoidal fibres in cuticle:**

- (0) absent,
- (1) present and composed of unpaired fibrils.

## Appendix 3- Updated matrix and operation commands

### 3.1 Updated matrix

<i>Lepidodermella_squamata</i>	0	0	1	0	0	-	1	0	-	-	-	-	-	-	-	-	-	-	-
-	-	-	-	-	-	-	-	-	-	-	-	-	-	-	-	1	-	-	-
-	-	-	-	0	-	0	-	0	0	-	0	-	0	-	-	0	-	0	0
0	0	0	0	0	0	0	-	1	0	-	0	-	-	-	0	0	0	-	-
0	0	0	0	0	0	0	-	0	0	-	-	0	0	0	1	0	0	1	0
0	-	0	0	-	0	0													
<i>Gordius_aquaticus</i>	0	0	4	0	1	0	0	0	-	0	-	0	0	0	0	0	?	-	-
-	-	?	?	-	1	-	?	?	?	-	-	-	-	-	0	-	-	-	-
-	-	0	-	0	-	2	0	-	0	-	0	-	-	-	0	-	0	0	0
0	0	0	0	0	-	0	0	-	0	-	-	-	-	1	0	0	-	-	0
0	1	1	1	0	0	1	0	-	0	0	1	1	0	-	0	0	0	1	0
1	0	-	1	0															
<i>Caenorhabditis_elegans</i>	0	0	2	0	1	1	0	0	-	0	-	0	0	0	0	0	0	?	-
-	-	-	?	?	-	1	-	?	?	?	-	-	-	-	-	1	-	-	-
-	-	-	0	-	0	-	2	0	-	0	-	0	-	-	-	0	-	0	0
0	0	0	0	0	0	-	0	0	-	0	-	-	-	-	0	0	0	-	-
1	1	1	1	1	0	0	0	0	-	0	0	0	1	0	-	0	0	0	1
1	1	1	1	1	1														
<i>Echinoderes_capitatus</i>	0	1	3	1	1	1	1	1	2	0	0	1	0	0	2	0			
9	1	4	0	1	-	9	0	2	0	4	0	0	-	0	-	0	1	3	-
2	0	0	1	0	1	1	0	0	-	1	0	1	1	0	0	0	-	0	0
0	0	0	0	0	0	-	0	0	-	0	-	-	-	-	0	0	0	-	-
1	0	1	1	1	0	1	0	0	-	1	0	1	0	1	0	0	1	0	0
0	1	1	0	0	0														
<i>Kinorhynchus_phyllotripsis</i>	0	1	3	1	1	1	1	1	2	0	0	1	0	0	2				
0	9	2	4	0	1	-	9	0	2	0	4	0	0	-	0	-	0	1	3
-	2	0	0	1	0	1	0	0	0	-	1	1	1	1	0	0	0	-	0
0	0	0	0	0	0	0	-	0	0	-	0	-	-	-	-	0	0	0	-
0	1	0	1	1	1	0	1	0	0	-	1	0	1	0	1	0	0	1	0
1	0	1	1	0	0	0													
<i>Nanaloricus_mysticus</i>	1	3	3	1	1	1	1	1	2	0	0	1	0	0	2	?			
9	0	4	0	1	-	9	2	2	2	4	0	0	-	0	-	2	1	2	-
2	1	0	1	1	0	-	0	0	-	0	-	1	3	0	5	0	-	0	0
1	0	0	0	0	0	-	0	0	-	0	-	-	-	-	0	0	0	-	-
0	0	1	1	1	0	1	1	1	0	0	0	1	0	1	1	1	1	0	0
1	1	1	0	0	0														

<i>Pliciloricus_enigmaticus</i>	1	3	3	1	1	1	1	1	2	0	0	1	0	0	2	?				
9	0	4	0	1	-	9	2	2	2	4	0	0	-	0	-	2	1	0	-	-
2	1	0	1	1	0	-	0	0	-	0	-	1	3	0	5	0	-	0	0	0
1	0	0	0	0	0	-	0	0	-	0	-	-	-	-	0	0	0	-	-	0
0	0	1	1	1	0	1	1	1	0	0	0	1	0	1	1	1	1	0	0	1
1	1	?	0	0	0															
<i>Eolorica_deadwoodensis</i>	1	?	?	2	?	?	?	1	2	?	0	1	0	0	2	?				
9	?	4	?	?	-	9	1	2	1	4	?	?	?	?	-	?	1	1	-	-
?	?	?	?	?	0	-	0	0	-	0	-	1	3	0	5	0	-	0	0	0
0	0	0	0	0	0	-	0	0	-	0	-	-	-	-	0	0	0	-	-	?
?	?	?	?	?	?	?	?	1	?	0	?	1	?	?	?	?	?	?	?	?
?	?	?	?	?	?															
<i>Meiopriapulius_fijiensis</i>	0	2	0	1	1	1	1	1	2	1	0	1	0	0	2	0				
8	-	4	0	0	-	8	-	0	0	4	1	0	5	1	2	0	0	-	1	0
0	2	0	0	-	0	-	1	1	3	0	-	0	-	-	-	0	-	0	1	1
1	0	1	0	0	0	-	0	0	-	0	-	-	-	-	0	1	0	-	-	1
0	0	1	1	0	1	1	0	0	-	-	-	1	0	1	1	1	1	0	0	?
?	?	?	?	1	0															
<i>Tubiluchus_corallicola</i>	0	1	0	1	1	1	1	1	2	1	0	1	0	0	1	0				
6	-	3	0	0	-	6	-	1	0	3	1	0	5	1	2	0	0	-	2	0
0	2	0	1	3	0	-	1	1	3	0	-	0	-	-	-	0	-	1	1	0
1	1	0	0	0	0	-	0	0	-	1	1	0	0	0	1	1	0	-	-	1
0	0	1	1	0	1	1	1	1	0	0	1	1	0	1	1	1	1	1	0	?
?	?	?	?	?	0															
<i>Halicryptus_spinulosus</i>	0	2	0	1	1	1	1	1	2	0	0	1	1	0	1	0				
5	-	3	0	0	-	5	-	1	0	3	1	0	1	1	1	0	0	-	0	3
0	2	1	0	-	0	-	0	1	2	0	-	0	-	-	-	1	0	0	1	0
0	0	0	1	0	1	2	0	1	0	0	-	-	-	-	1	0	0	-	-	1
0	0	1	1	1	1	1	1	1	1	0	1	1	0	1	1	1	1	0	0	1
1	1	1	1	0	0															
<i>Maccabeus_tentaculatus</i>	0	2	0	1	1	1	1	1	2	0	0	1	0	0	1	0				
0	7	-	3	0	0	-	7	-	1	0	3	1	1	4	1	1	0	0	-	0
3	0	2	0	0	-	0	-	0	1	3	0	-	0	-	-	-	0	-	0	1
1	0	0	1	0	0	1	0	0	0	-	0	-	-	-	-	0	0	1	0	0
1	0	0	1	1	1	1	1	1	1	1	0	1	1	0	1	1	1	1	0	0
?	?	?	?	?	?	0														
<i>Priapulopsis_bicaudatus</i>	0	2	0	2	1	1	1	1	2	1	0	1	1	0	1	0				
4	-	3	1	0	-	4	-	1	0	3	1	0	1	1	2	0	0	-	1	2
0	2	1	0	-	0	-	0	1	1	0	-	0	-	-	-	1	0	1	0	0
0	0	0	1	0	0	-	0	0	-	1	0	2	0	1	1	0	0	-	-	1
0	0	1	1	1	1	1	1	1	1	0	1	1	0	1	1	1	1	0	0	?
?	?	?	?	?	?															



<i>Priapulus_caudatus</i>	0	2	0	2	1	1	1	1	2	1	0	1	1	0	1	0	3				
-	3	1	0	-	3	-	1	0	3	1	0	1	1	2	0	0	-	0	4	0	
2	1	0	-	0	-	0	1	1	0	-	0	-	-	-	1	0	0	0	0	0	
0	0	1	0	0	-	0	1	1	1	0	1	1	1	1	0	0	-	-	1	0	
0	1	1	1	1	1	1	1	1	0	1	1	0	1	1	1	1	0	0	1	1	
1	1	0	0	0																	
<i>Acanthopriapulus_horridus</i>	0	1	0	2	1	1	1	1	2	0	0	1	0	0	1	0	0	1			
0	3	-	3	0	0	-	3	-	1	0	3	1	0	1	?	?	0	0	-	0	
1	0	2	1	0	-	0	-	0	1	1	0	-	0	-	-	-	1	0	0	0	
0	0	0	0	1	0	0	-	0	0	-	1	0	1	1	(12)	1	0	0	-	-	
1	0	0	1	1	1	1	1	1	1	1	0	1	1	0	1	1	1	1	1	0	0
?	?	?	?	?	?	?	0														
<i>Sicyophorus_rara</i>	1	1	0	2	1	1	?	1	2	1	1	?	1	0	-	-	-				
-	-	-	-	-	1	-	1	0	1	1	0	0	1	0	?	0	-	2	0	0	
2	1	1	2	0	-	0	0	-	0	-	1	3	0	-	0	-	0	0	0	0	
0	0	0	0	0	-	0	0	-	0	-	-	-	-	1	0	0	-	-	?	?	
?	?	?	?	?	?	?	?	1	0	-	?	?	?	?	?	?	?	?	?	?	
?	?	?	?	?																	
<i>Xiaoheiqingella_peculiaris</i>	0	1	0	2	1	1	?	1	?	1	?	1	1	?	1	0	-				
-	-	-	-	-	-	-	1	-	1	0	3	0	0	1	1	?	?	0	-	2	
?	0	2	?	1	2	0	-	0	1	3	0	-	0	-	-	-	1	0	0	0	
0	0	0	0	1	0	0	-	0	0	-	1	0	2	0	0	1	0	0	-	-	
?	?	?	?	?	?	?	?	?	?	?	?	0	?	?	?	?	?	?	?	?	
?	?	?	?	?	?	?															
<i>Yunnanpriapulus_halteroformis</i>	0	1	0	2	1	1	?	1	?	1	?	1	1	?	1	1	0				
-	-	-	-	-	-	-	1	-	1	0	3	0	0	1	1	?	?	0	-		
2	5	?	2	?	1	2	0	-	0	1	?	0	-	0	-	-	-	1	0	0	
0	0	0	0	0	1	0	0	-	0	0	-	1	0	0	1	0	1	0	0	-	
-	?	?	?	?	?	?	?	?	?	?	?	0	?	?	?	?	?	?	?	?	
?	?	?	?	?	?	?	?														
<i>Paratubiluchus_bicaudatus</i>	0	1	0	2	1	1	?	1	?	1	?	1	1	?	1	0	-				
-	-	-	-	-	-	-	1	-	1	0	3	0	0	1	1	?	?	0	-	?	
?	0	2	?	1	2	0	-	0	0	-	0	-	0	-	-	-	1	0	0	0	
0	0	0	0	?	0	0	-	0	0	-	1	0	2	0	3	1	0	0	-	-	
?	?	?	?	?	?	?	?	?	?	?	?	0	?	?	?	?	?	?	?	?	
?	?	?	?	?	?	?															
<i>Priapulites_konecniorum</i>	0	2	0	1	1	?	?	1	?	1	?	1	0	?	1	0	1				
0	3	-	1	1	0	-	3	-	1	0	1	?	?	?	?	?	0	-	?		
?	?	?	?	0	-	0	-	0	1	1	0	-	0	-	-	-	1	0	0	0	
0	0	0	0	1	0	0	-	0	0	-	1	0	2	0	?	?	0	0	-	-	
?	?	?	?	?	?	?	?	?	?	?	?	0	?	?	?	?	?	?	?	?	
?	?	?	?	?	?	?															

<i>Markuelia_hunanensis</i>	0	?	?	?	?	?	?	?	1	?	0	0	1	0	0	2	2			
1	-	0	0	0	-	1	-	2	2	0	?	?	?	?	?	0	-	?	?	
?	?	?	0	-	0	-	?	1	?	0	-	?	?	?	?	?	?	?	?	
?	?	1	0	0	0	-	0	0	-	0	-	-	-	0	0	0	-	-	?	
?	?	?	?	?	?	?	?	0	0	-	?	?	1	?	?	?	?	?	?	
?	?	?	?	?	?															
<i>Eximipriapulus_globocaudatus</i>	0	1	0	1	1	?	?	1	?	1	?	1	0	?	?	?	0			
2	0	3	-	?	0	0	-	1	-	2	0	?	0	0	0	1	?	?	0	-
2	?	0	2	?	1	3	0	-	0	1	2	0	-	1	1	-	-	1	0	0
0	0	0	0	0	1	0	0	-	0	0	-	0	-	-	-	-	0	0	0	-
-	?	?	?	?	?	?	?	?	?	?	?	?	?	?	?	?	?	?	?	?
?	?	?	?	?	?	?	?													
<i>Ottoia_prolifica</i>	0	2	0	1	1	1	?	1	2	1	0	?	0	0	2	0	2	-		
4	0	0	-	2	-	2	0	4	1	1	3	1	2	?	0	-	2	0	1	0
1	0	-	0	-	0	1	2	0	-	0	-	-	-	0	-	0	0	0	0	0
1	0	1	0	-	0	0	-	0	-	-	-	-	0	0	0	-	-	1	0	?
?	?	?	?	?	?	?	?	0	?	?	?	?	?	?	?	?	?	?	?	?
?	?	?	?																	
<i>Ancalagon_minor</i>	0	2	0	1	?	?	?	?	1	0	0	0	?	0	0	2	?	2		
-	?	0	0	-	2	-	2	?	?	0	0	2	?	?	?	0	-	1	0	0
?	?	0	-	0	-	1	1	3	0	-	1	1	0	0	0	-	0	0	0	0
0	0	0	0	0	-	0	0	-	0	-	-	-	-	0	0	0	-	-	?	?
?	?	?	?	?	?	?	?	?	0	?	?	?	?	?	?	?	?	?	?	?
?	?	?	?	?																
<i>Fieldia_lanceolata</i>	0	2	0	1	?	?	?	?	1	?	0	0	?	0	0	?	?	2		
-	?	0	0	-	2	-	?	?	?	0	0	0	?	?	?	0	-	2	0	?
?	?	0	-	0	-	2	0	-	0	-	1	1	0	-	0	-	0	0	0	0
0	0	0	0	0	-	0	0	-	0	-	-	-	-	0	0	0	-	-	?	?
?	?	?	?	?	?	?	?	?	?	?	?	?	?	?	?	?	?	?	?	?
?	?	?	?	?																
<i>Louisella_pedunculata</i>	0	2	0	1	?	?	?	?	1	1	0	0	?	0	0	2	0			
0	-	0	0	0	-	0	-	2	0	0	1	1	0	1	2	?	0	-	2	0
1	0	1	0	-	0	-	2	0	-	0	-	1	(12)?	?	?	1	1	0	0	0
0	0	0	0	1	0	-	0	0	-	0	-	-	-	-	0	0	0	-	-	?
?	?	?	?	?	?	?	?	?	?	?	0	?	?	?	?	?	?	?	?	?
?	?	?	?	?	?															
<i>Laojiella_thecata</i>	0	2	0	1	?	?	?	?	1	?	0	0	?	0	0	2	?	1		
-	(12)0	0	-	1	-	2	?	(12)0	0	0	1	2	?	0	-	1	0	0		
0	1	0	-	0	-	2	1	?	0	-	1	4	0	-	0	-	0	0	0	0
0	0	0	0	0	-	0	0	-	1	0	2	0	0	0	0	0	-	-	?	?
?	?	?	?	?	?	?	?	?	?	?	?	?	?	?	?	?	?	?	?	?
?	?	?	?	?																

<i>Anningvermis_multispinosus</i>	0	2	0	1	?	?	?	1	?	0	0	?	0	0	-	-	-				
-	-	-	-	-	-	-	-	-	-	0	1	1	1	2	?	0	-	2			
5	0	0	1	0	-	0	-	1	1	1	0	-	1	1	0	0	0	0			
0	0	0	0	0	0	0	-	0	0	-	1	0	0	0	0	0	0	-	-		
?	?	?	?	?	?	?	?	?	?	?	0	?	?	?	?	?	?	?	?		
?	?	?	?	?	?	?	?														
<i>Corynetis_brevis</i>	0	2	0	1	?	?	?	1	2	0	0	?	0	0	-	-	-				
-	-	-	-	-	-	-	-	-	0	1	0	1	2	?	0	-	2	?	0		
0	0	0	-	0	-	1	1	1	0	-	1	1	0	0	1	0	0	0	0		
0	0	1	0	0	-	0	0	-	1	0	0	0	0	0	0	-	-	?	?		
?	?	?	?	?	?	?	?	?	0	?	?	?	?	?	?	?	?	?	?		
?	?	?	?	?																	
<i>Tylotites_petiolaris</i>	0	2	0	1	?	?	?	1	?	0	1	?	0	0	-	-	-				
-	-	-	-	-	2	-	1	0	0	0	0	1	?	?	0	-	?	?	0		
0	3	0	-	0	-	1	1	1	0	-	1	1	0	0	0	-	0	0	0		
0	0	0	0	1	1	0	0	-	1	0	0	1	0	0	0	-	-	?	?		
?	?	?	?	?	?	?	?	?	0	?	?	?	?	?	?	?	?	?	?		
?	?	?	?	?																	
<i>Cricocosmia_jinningensis</i>	0	2	0	1	?	?	?	1	2	0	1	?	0	0	-	-	-				
-	-	-	-	-	-	-	2	-	1	0	0	0	0	1	1	2	?	0	-	0	
5	0	0	1	0	-	0	-	2	1	2	0	-	1	2	1	0	0	-	0	0	
0	0	0	0	0	0	1	1	0	0	-	0	-	-	-	-	0	0	0	-	-	
?	?	?	?	?	?	?	?	?	?	?	0	?	?	?	?	?	?	?	?	?	
?	?	?	?	?	?	?															
<i>Maotianshania_cylindrica</i>	0	2	0	1	?	?	?	1	2	0	1	?	0	0	-	-	-				
-	-	-	-	-	-	-	2	-	1	0	0	0	0	0	1	2	?	0	-	?	
?	1	0	1	0	-	0	-	2	1	2	0	-	1	2	1	4	0	-	0	0	
0	0	0	0	0	0	1	1	0	0	-	0	-	-	-	-	0	0	0	-	-	
?	?	?	?	?	?	?	?	?	?	?	0	?	?	?	?	?	?	?	?	?	
?	?	?	?	?	?	?															
<i>Guanduscolex_minor</i>	0	2	0	1	?	?	?	1	?	0	1	?	0	0	-	-	-				
-	-	-	-	-	-	-	2	-	1	0	0	0	0	0	1	1	?	0	-	2	0
1	0	2	0	-	0	-	1	1	2	0	-	1	2	1	2	0	-	0	0	0	
0	0	0	0	0	1	1	0	0	-	0	-	-	-	-	0	0	0	-	-	?	
?	?	?	?	?	?	?	?	?	?	?	0	?	?	?	?	?	?	?	?	?	
?	?	?	?	?	?																
<i>Tabelliscolex_hexagonus</i>	0	2	0	1	?	?	?	1	?	0	0	?	0	0	?	?					
?	-	?	?	0	-	2	-	?	?	?	0	0	?	1	?	?	0	-	?	?	
1	?	?	0	-	0	-	2	1	2	0	-	1	2	1	0	0	-	0	0	0	
0	0	0	0	0	1	1	0	0	-	0	-	-	-	-	0	0	0	-	-	?	
?	?	?	?	?	?	?	?	?	?	?	0	?	?	?	?	?	?	?	?	?	
?	?	?	?	?	?																

<i>Chalazoscolex_pharkus</i>	0	2	0	1	?	?	?	1	?	0	0	?	0	0	0	?				
1	-	?	?	0	-	2	-	0	?	?	?	?	?	1	?	?	0	-	?	?
0	0	?	0	-	0	-	1	1	3	0	-	1	2	?	2	0	-	0	0	0
0	0	0	0	1	?	?	0	0	-	0	-	-	-	-	0	0	0	-	-	?
?	?	?	?	?	?	?	?	?	?	0	?	?	?	?	?	?	?	?	?	?
?	?	?	?	?	?															
<i>Xystoscolex_boreogyrus</i>	0	2	0	1	?	?	?	1	?	0	0	?	0	0	0	?				
1	-	?	?	0	-	2	-	0	?	?	?	?	?	1	?	?	0	-	?	?
0	0	?	0	-	0	-	1	1	3	0	-	1	2	?	2	0	-	0	0	0
0	0	0	0	0	?	?	0	0	-	0	-	-	-	-	0	0	0	-	-	?
?	?	?	?	?	?	?	?	?	?	0	?	?	?	?	?	?	?	?	?	?
?	?	?	?	?	?															
<i>Mafangscoclex_yunnanensis</i>	0	2	0	1	?	?	?	1	2	0	1	?	0	0	-					
-	-	-	-	-	-	-	2	-	1	0	0	0	0	0	1	1	?	0	-	1
0	1	0	?	0	-	0	-	2	1	3	0	-	1	2	1	3	1	0	0	0
0	0	0	0	0	0	1	1	0	0	-	0	-	-	-	-	?	0	0	-	-
?	?	?	?	?	?	?	?	?	?	?	0	?	?	?	?	?	?	?	?	?
?	?	?	?	?	?															
<i>Palaeoscolex_piscatorum</i>	0	2	?	1	?	?	?	1	?	0	0	?	0	0	?					
?	?	-	?	?	0	-	?	-	?	?	?	?	?	?	?	?	0	-	?	
?	?	0	?	0	-	0	-	2	1	3	0	-	1	2	1	1	0	-	0	0
0	0	0	0	0	0	0	-	0	0	-	0	-	-	-	-	0	0	0	-	-
?	?	?	?	?	?	?	?	?	?	?	0	?	?	?	?	?	?	?	?	?
?	?	?	?	?	?															
<i>Eopriapulites_sphinx</i>	0	2	0	1	1	1	?	1	?	0	0	1	0	0	2	1	3			
-	0	0	0	-	3	-	2	1	0	1	1	0	1	0	0	0	-	2	0	?
?	1	0	-	0	-	1	1	3	0	-	0	-	-	-	0	-	0	0	0	0
0	0	0	?	0	-	0	0	-	0	-	-	-	-	0	?	0	-	-	?	?
?	?	?	?	?	?	?	?	?	?	?	?	?	?	?	?	?	?	?	?	?
?	?	?	?	?																
<i>Eokinorhynchus_rarus</i>	0	2	0	1	?	?	?	1	2	0	1	1	0	1	2	0				
3	-	0	0	0	-	3	-	2	0	3	0	0	0	1	0	?	0	-	2	0
?	?	1	0	-	0	-	0	1	0	0	-	1	0	0	0	0	-	0	0	0
0	0	0	0	0	1	1	0	0	-	0	-	-	-	-	0	?	0	-	-	?
?	?	?	?	?	?	?	?	?	?	0	?	?	?	?	?	?	?	?	?	?
?	?	?	?	?	?															
<i>Selkirkia_transita</i>	0	2	0	1	?	?	?	1	1	0	2	?	0	0	2	0	1			
-	3	0	0	1	1	-	2	?	3	0	0	1	1	2	?	0	-	2	0	0
0	1	0	-	0	-	1	?	?	0	-	0	-	-	-	?	?	?	?	?	?
?	?	?	?	?	?	0	?	?	?	?	?	?	?	0	0	1	1	1	?	?
?	?	?	?	?	?	0	0	-	-	?	1	?	?	?	?	?	?	?	?	?
?	?	?	?	?																

<i>Selkirkia_sinica</i>	0	2	0	1	?	?	?	1	1	0	2	?	0	0	2	0	1	-			
3	0	0	2	1	-	2	?	3	0	0	1	1	1	?	0	-	2	0	0	0	
0	0	-	0	-	1	?	?	0	-	0	-	-	-	0	-	0	0	0	0	0	
0	0	0	0	-	0	0	-	1	0	2	0	?	0	0	1	1	2	?	?	?	
?	?	?	?	?	0	0	-	-	?	1	?	?	?	?	?	?	?	?	?	?	
?	?	?	?																		
<i>Selkirkia_columbia</i>	0	2	0	1	?	?	?	1	1	0	1	?	0	0	1	0	1				
-	3	0	0	0	1	-	2	?	3	0	0	1	1	1	?	0	-	2	0	0	
0	1	0	-	0	-	1	?	?	0	-	0	-	-	-	1	0	0	0	0	0	
0	?	?	?	?	?	0	?	?	?	?	?	?	?	?	0	0	1	1	3	?	?
?	?	?	?	?	?	?	?	?	?	?	?	?	?	?	?	?	?	?	?	?	?
?	?	?	?	?																	

### 3.2 Dataset format and commands for MrBayes

Begin data;

```
dimensions ntax=43 nchar=106;  
format datatype=standard gap=- missing=?;  
matrix
```

Updated matrix

;

end;

BEGIN MRBAYES;

SET autoclose=yes nowarn=yes;

LOG START filename=new4uc.output;

OUTGROUP Lepidodermella\_squamata;

LSET rates=gamma coding=variable;

CONSTRAINT Root = 9-;

PRSET topologypr = CONSTRAINT (

Root

);

MCMCP temp=0.1 samplefreq=1000 printfr=10000 nruns=4 nchain=4 relburnin=yes  
burninfrac=0.20;

MCMCP savebrlens=yes filename=new4uc;

SHOWMOVES;

MCMC ngen=10000000;

SUMT filename=new4uc contype=allcompat relburnin=yes burninfrac=0.20;

SUMP filename=new4uc relburnin=yes burninfrac=0.20;

end;

Note: Updated matrix see 3.1.

### 3.3 Dataset format and commands for TNT

```
xread  
43 106  
Updated matrix  
;
```

Commands: All characters were unordered and weighted equally. Gap mode was treated as missing, collapse rule 1 was adopted (default collapse rule in TNT), and TNT memory was set to 10,000 trees. The data set was analyzed under traditional search (commands: heuristic search with 1000 random addition sequences, 1 random seed and holding 10 trees to save per replication, followed by TBR branch-swapping).

Note 2: Updated matrix see 3.1.

### 3.4 Dataset format and commands for IQTREE

```
43 106  
Updated matrix  
;
```

Commands: -s filename.phy -m MK+ASC -o *Lepidodermella\_squamata* -nt AUTO -bb 300000.

Note: Updated matrix see 3.1.